METEOR-BERICHTE
Nr. 93-4

NORDATLANTIK 92

Reise Nr. 21
16. März - 31. August 1992

Herausgegeben von:
Olaf Pfannkuche, Jan C. Duinker, Gerd Graf,
Rüdiger Henrich, Hjalmar Thiel, Bernt Zeitzschel

Redaktionelle Bearbeitung:
Ingrid Rogge, Keiko D. Kähler-Mähl
Institut für Meereskunde an der Universität Kiel

Leitstelle METEOR
Institut für Meereskunde der Universität Hamburg

1993

Inhaltsverzeichnis

		Seite
Zusammenfassung		vii
Abstract		viii
1	Forschungsthemen	1
2	Fahrtteilnehmer	6
3	Forschungsprogramm	15
	3.1 BIO-C-FLUX	15
	3.2 JGOFS-Programme	16
	3.2.1 Physikalische Ozeanographie	16
	3.2.2 Spurenelementchemie	19
	3.2.3 Organische Spurenstoffchemie	19
	3.2.4 CO_2-Chemie	20
	3.2.5 Meeresoptik	20
	3.2.6 Planktologie	21
	3.2.7 Marine Mikrobiologie	23
	3.3 Sonderforschungsbereich 313 (SFB 313)	24
4	Ablauf der Reise	25
	4.1 Erster Fahrtabschnitt	25
	4.2 Zweiter Fahrtabschnitt	31
	4.3 Dritter Fahrtabschnitt	33
	4.4 Vierter Fahrtabschnitt	36
	4.5 Fünfter Fahrtabschnitt	43
	4.6 Sechster Fahrtabschnitt	46
5	Preliminary results	50
	5.1 Physical oceanography	50

5.1.1 Hydrography at 47°N, 20°W (JGOFS)
(S. Podewski, U. Beckmann,P. Kähler, R. Link) 50
5.1.2 Large-scale CTD section along 20°W during M 21/3 (JGOFS)
(S. Podewski) 65

5.2 Chemical oceanograghy 69
5.2.1 Trace element geochemistry (JGOFS)
(U. Schüßler, R. Bruhn, G. Lippert) 69
5.2.2 Organic trace compounds (JGOFS) 75
5.2.2.1 Biomarker substances (J. Maassen, A. Körtzinger,
U. Lundgreen, D.D. Schulz-Bull) 75
5.2.2.2 Chlorinated Biphenyls
(G. Petrick, D. Schulz-Bull) 76
5.2.3 CO_2 Chemistry 77
5.2.3.1 CO_2 partial pressure measurements (JGOFS)
(B. Schneider) 77
5.2.3.2 Alkalinity, total carbonate, pH, and organics (JGOFS)
(L. Mintrop, A. Korves) 78
5.2.4 Nutrients and dissolved oxygen (T. Körner) 79
5.2.5 The CO_2 System of the North Altantic Ocean (JGOFS)
(K. Pegler, S. Kempe) 79
5.2.6 Biogeochemical sediment investigations at 47°N, 20°W
(BIO-C-FLUX) (A. Dolle) 88
5.2.7 Air chemistry 95
5.2.7.1 Biogeochemical and atmospheric investigations
by the International Air-Sea Exchange Group
(M.O. Andreae, D. Amouroux, T.W. Andreae,
O. Donard, D. Meyerdierks, S. Rapsomanikis,
C. Thiel, G. Uher) 95
5.2.7.2 Dimethyl sulfide, dimethyl sulfoniopropionate,
and phytoplankton in seawater
(T.W. Andreae, D. Meyerdierks, C. Thiel) 95
5.2.7.3 Sea-to-air flux of dimethylsulfide and the
atmospheric sulfur cycle
(M.O. Andreae, T.W. Andreae) 96
5.2.7.4 Nitrous oxide and methane in seawater and the
overlying atmosphere (S. Rapsomanikis) 97
5.2.7.5 Photochemical production of carbonyl sulfide
in seawater (G. Uher) 97
5.2.7.6 Formation and variabitity of hydrogen
peroxide (H_2O_2) (O.F.X. Donard, D. Amouroux) 98

5.3 Biological Oceanography 100

5.3.1 Planktological investigations during the Winter-Spring-Summer transition at 47°N, 20°W (JGOFS) (W. Koeve, S. Podewski, F. Pollehne, B. Zeitzschel, F. Jochem, P. Kähler, A. Dettmer, M. Deckers, O. Haupt, S. Reitmeier, S. Böhm, P. Fritsche, R. Werner, C. Sellmer) 100

5.3.1.1 Overview (W. Koeve, B. Zeitzschel) 100

5.3.1.2 Standing stocks of plant nutrients and chlorophyll-a (W. Koeve, S. Podewski, R. Werner, P. Fritsche, S. Böhm, S. Reitmeier) 105

5.3.1.3 Productivity regime and phytoplankton size structure (F. Jochem) 108

5.3.1.4 Quantitative and qualitative measurements of pico-and nanoplankton fy flow cytometry and epifluorescence microscopy (A. Detmer) 113

5.3.2 Dissolved organic carbon (DOC) (JGOFS, SFB 313) (P. Kähler, A. Antia, O. Haupt, C. Sellmer) 115

5.3.3 Microbiology of the upper mixed layer (B. Karrasch, A. Carstensen, J. de Wall) 117

5.3.4 Population dynamics of planktic Foraminifera (JGOFS) (C. Hemleben, J. Bijma, H. Gminder, S. Heller, B. Hiller, W. Kamleiter) 120

5.3.5 Deep-sea zooplankton and micronekton (BIO-C-FLUX) (R. Koppelmann) 126

5.3.6 Benthopelagic nekton and megafauna (BIO-C-FLUX) (B. Christiansen) 127

5.3.7 Benthic investigations (BIO-C-FLUX) (O. Pfannkuche) 128

5.3.8 Differentation between biologically degradable and non-degradable compounds of sedimentary particulate organic matter (BIO-C-FLUX) (S. Scheibe) 134

5.3.9 Small-scale variability of sedimentary biochemical indicators of biological abundance and activity in the NE Atlantic (T. Soltwedel) 136

5.3.10 Microbial enzyme activity in deep-sea sediments (BIO-C-FLUX) (A. Boetius) 137

5.3.11 Experiments on microbial breakdown of organic matter (BIO-C-FLUX) (K. Lochte, A. Boetius) 139

5.3.12 Microbiology of deep-sea sediments at 47°N, 20°W (BIO-C-FLUX) (K. Poremba) 140

5.3.13 Vertical particle flux - recovery and redeployment of the moorings NB6/NB7 and OG5/OG6 (SFB 313) (B. von Bodungen) 144

5.3.14 Near-bottom particle flux (SFB 313) (G. Graf, P. Linke, W. Ritzrau, W. Queisser) 144
5.3.15 Microbiology of sediments (SFB 313) (M. Ehmcke-Kasch, M. Hollinde, M. Köster, L.-A. Meyer-Reil) 147
5.3.16 Porifera communities along shelf-basin transects in the Norwegian and Greenland Sea (SFB 313) (J. Reitner, S. Müller-Wille) 150
5.3.17 Benthic communities of the Greenland Island and Norwegian Sea (SFB 313) (A. Brandt, K.v. Juterzenka, S. Müller-Wille, D. Piepenburg, J. Reitner, U. Witte) 155
5.3.18 Mammals and Seabirds at 47°N, 20°W (BIO-C-FLUX) (B. Christiansen, O. Pfannkuche) 159

5.4 Marine geosciences 160
5.4.1 Geophysical investigation of the sea floor (SFB 313) (J. Mienert, M. Bobsien, J. Chi, F.-J. Hollender, T. Bergmann) 160
5.4.2 Analysis of sediment sections and preliminary paleoceanographic results: Norwegian-Greenland Sea deep-sea records (SFB 313) 162
5.4.2.1 Aegir Ridge, Barents Sea continental margin and northern Knipovitch Ridge (T. Wagner, M. Antonow, B. Schlünz, K. Michels, S. Schulz, P. Goldschmidt, R. Henrich) 162
5.4.2.2 Norwegian Sea, south eastern Greenland and Iceland Sea (SFB 313) (S. Locker, T. Bohlen, B. Brunssen, S. Jing, A. Kohly, U. Struck) 169
5.4.3 Near-bottom sediment transport and areas of high Holocene sediment accumulation rates (SFB 313) (J. Rumohr, F. Blaume, H. Beese, M. Seiß) 173
5.4.4 Cold water shelf carbonates and lag deposits and associated living benthic communities: Spitsbergen Bank (SFB 313) (R. Henrich, J. Reitner, A. Wehrmann) 176
5.4.5 Marine versus terrigenous organic matter fluxes: first considerations from sediment cores along the polar front in the Barent Sea (SFB 313) (T. Wagner, B. Schlünz, R. Henrich) 181

5.5 Actuopaleontological studies of living plankton communities in the North Atlantic and Norwegian-Greenland Sea and their distribution in sediments (K.-H. Baumann, A. Schröder, A. Kohly, S. Locker) 181

5.6 Marine optics (R. Reuter, S. Determann) 188

6 Bericht der Bordwetterwarte 194

6.1 Erster Fahrtabschnitt (D. von Bargen) 194

6.2 Zweiter Fahrtabschnitt (E. Röd) 195

6.3 Dritter Fahrtabschnitt (C. Knaack) 196

6.4 Vierter Fahrtabschnitt (C. Knaack) 197

6.5 Fünfter Fahrtabschnitt (R. Hartig) 199

6.6 Sechster Fahrtabschnitt (R. Hartig) 199

7 Lists 201

7.1 Station lists leg M 21/1 201
7.1.1 List of benthic sampling stations (BIO-C-FLUX) 201
7.1.2 List of water stations (JGOFS) 202
7.1.3 List of benthiopelagic nekton and megafauna sampling stations (BIO-C-FLUX) 203
7.1.4 $1m^2$-MOCNESS-hauls during M 21/1 204

7.2 Station lists leg M 21/2 206
7.2.1 List of benthic sampling stations (BIO-C-Flux) 206
7.2.2 List of water station (JGOFS) 207

7.3 Station list leg M 21/3 211
7.3.1 General list of sampling stations 211
7.3.2 List of water station (JGOFS) 213
7.3.3 List of benthic sampling stations (BIO-C-FLUX) 214

7.4 Station list leg M 21/4 215

7.5 Station list leg M 21/5 229

7.6 Station list leg M 21/6 237
7.6.1 List of water station (JGOFS) 237
7.6.2 List of benthic sampling stations (BIO-C-FLUX) 239

7.6.3 List of benthopelagic nekton and megafauna sampling stations (BIO-C-FLUX) 240
7.6.4 $1m^2$ double-MOCNESS-hauls during M 21/6 241
7.6.5 $10m^2$-MOCNESS-hauls during M21/6 242

7.7 Kernbeschreibungen M 21/4 und M 21/5 (SFB 313) 243

8 Schlußbemerkung 274

9 Literatur 275

Zusammenfassung

Die 21. Forschungsreise vom FS METEOR führte das Schiff in den östlichen Nordatlantik. Die Forschungsvorhaben wurden zwischen Madeira und Spitzbergen durchgeführt. Die Reise war in 6 Fahrtabschnitte untergliedert. Ein Hauptziel war auf 4 Fahrtabschnitten im Seegebiet zwischen Madeira und Island die Untersuchung des ozeanischen Kreislaufs von klimarelevanten Gasen im Rahmen deutscher Joint Global Ocean Flux Study (JGOFS) - Vorhaben. Die Beobachtungen liefern Daten für die Entwicklung und Verifizierung von Modellen zur Klimaveränderung. Die physikalischen, chemischen und biologischen Meßprogramme von JGOFS konzentrieren sich auf einen Untersuchungsabachnitt entlang des 20. Längengrades und auf eine Zeitserienstation im BIOTRANS-Gebiet bei 47° N, 20° W. Untersuchungsschwerpunkte waren der Gasaustausch zwischen der ozeanischen Deckschicht und der Atmosphäre, die biologische Fixierung und der Kreislauf von Kohlendioxid im Epipelagial sowohl der Fluß von sedimentiertem partikulären Kohlenstoff im Bereich der Bodengrenzschicht.

Den zweiten Forschungsschwerpunkt bildeten auf 2 Fahrtabschnitten im Bereich der Norwegen-, Grönland- und Barentssee die Arbeiten des Sonderforschungsbereiches 313 der Universität Kiel. Neben Untersuchungen zum vertikalen, durch pelagische Prozesse bestimmten Partikelfluß konzentrierten sich die Arbeiten auf den lateralen Partikeltransport sowie auf die Prozesse in der bodennahen Nepheloidschicht und auf die Stoffflüsse in der benthischen Grenzschicht. Aufbauend auf den Erkenntnissen zur rezenten Sedimentbildung und teilweise analog zu diesen Untersuchungen soll die Geschichte der marinen Umwelt rekonstruiert werden.

Der vorliegende Bericht enthält eine Zusammenfassung der Forschungsziele, Berichte zum Fahrtverlauf und Darstellungen vorläufiger, an Bord gewonnener Ergebnisse. Die Texte werden ergänzt durch Tabellen, die Beobachtungen und Stationslisten zusammenfassen. Die Darstellung der vorläufigen Forschungsergebnisse erfolgt in Englisch. Weitere Textteile (Zusammenfassungen) sowie die Abbildungs- und Tabellenlegenden sind in deutscher oder englischer Sprache verfaßt.

Abstract

The 21st expedition of RV METEOR led into the eastern North Atlantic. Research was carried out between Madeira and the Svalbard Archipelago. The expedition was divided into 6 legs. The main objective on four legs which concentrated on the area between Madeira and Iceland was the investigation of the oceanic flux of greenhouse gases. The investigations carried out by the German groups of the Joint Global Ocean Flux Study (JGOFS) will provide data for the creation and verification of models for climatic changes. Physical, chemical, and biological investigations were concentrated to a transect along 20° W and to a time series station in the BIOTRANS area at 47° N, 20° W. The investigations focussed on the fluxes of greenhouse gases between the ocean's upper mixed layer and the atmosphere, the chemical and biological carbon dioxide fixation on the cycling of carbon in the epipelagial as well as the flux of sedimented particulate organic carbon in the deep-sea benthic boundary zone.

Two legs were restricted to investigatons in the Norwegian, Greenland and Barents Sea. The programmes were carried out by the Sonderforschungsbereich 313 of the Kiel University. Apart from investigations on the vertical particle flux influenced by pelagic processes, station work focussed on studies of the lateral particle transport, on processes in the bottom near nepheloid layer, and on fluxes in the benthic boundary layer. On the basis of already available data on recent sediment formation processes and partly in analogy with these investigations, it is intended to reconstruct the history of the marine environment.

The present report summarizes the research objectives, cruise narratives and preliminary results which were already obtained during the expedition. The text is supplemented by tables summarizing the investigations and by station lists. The chapter "Preliminary Results" is exclusively written in English. Other chapters (abstract) as well as the legends of figures and tables are written either in German or English.

1 Forschungsthemen

Die METEOR-Expedition Nr. 21 führte in den östlichen Nordatlantik. Sie verband Forschungsvorhaben aller großen ozeanographischen Fachdisziplinen, die sich mit dem Themenkomplex des Einflusses von Klimaveränderungen auf das ozeanische Ökosystem befassen:

- BIO-C-FLUX (Biologischer Kohlenstoffffluß in der bodennahen Wasserschicht des küstenfernen Ozeanes),
- die Arbeitsgruppen des deutschen JGOFS (Joint Global Ocean Flux Study),
- Sonderforschungsbereich 313 (SFB 313) an der Universität Kiel (Veränderung der Umwelt: der nördliche Atlantik).

Die Arbeiten von BIO-C-FLUX und der deutschen JGOFS-Gruppen waren als Prozeßstudien im Rahmen der Untersuchungen des internationalen JGOFS-Programmes an den Stationen der JGOFS-Pilotstudie (1989, METEOR-Reise Nr. 10) geplant. Ziel der Untersuchungen ist eine Quantifizierung der chemischen und biologischen Kohlenstoffixierung und die Bestimmung der Flüsse kohlenstoffhaltiger Verbindungen und biologisch relevanter chemischer Elemente im Nordatlantik. Dabei kam den Untersuchungen der ozeanischen Deckschicht und der Bodengrenzschicht, in denen neben den physikalischen und chemischen auch eine Intensivierung biologischer Prozesse stattfindet, eine besondere Bedeutung zu. Weiterhin sollte die Wechselwirkung zwischen Ozean und Atmosphäre in bezug auf das CO_2-System studiert werden.

Der SFB 313 setzte seine laufenden Untersuchungen im Europäischen Nordmeer fort, wobei auch einige JGOFS-Arbeitsgruppen integriert wurden.

Die Nordatlantik 92-Expedition schloß sich unmittelbar an die Ostatlantik 91/92-Expedition (METEOR-Reise Nr. 20) an, die am 13.03.1992 in Las Palmas endete. Der Fahrtabschnitt M 21/1 begann am 16.03.1992 in Las Palmas. Die Untersuchung des Systems der Bodengrenzschicht durch die BIO-C-FLUX Arbeitsgruppe, in der die Situation vor Beginn der Sedimentation der Frühjahrsblüte untersucht werden sollte, bildete den Schwerpunkt dieses Fahrtabschnittes. Die Stationsarbeiten konzentrierten sich hauptsächlich auf die "BIOTRANS-Station" bei 47°N, 20°W. Auf der Anfahrt in das Gebiet wurden auch Sedimentproben auf der Madeira Tiefsee-Ebene bei 34°N, 20°W genommen, die dem Vergleich mit den Arbeiten aus dem Jahr 1990 (METEOR-Reise Nr. 12/3) dienen. Die Planktologen von BIO-C-FLUX untersuchten die Verteilung des benthopelagischen Planktons und Nektons in der bodennahen Wasserschicht. Die Arbeiten in der oberen Deckschicht für JGOFS wurden hauptsächlich mit treibenden Sinkstoffallen und einer begleitenden Aufnahme der Wassersäule (CTD, Nährstoffe, Primärproduktion) durchgeführt. Weitere JGOFS-Projekte untersuchten das CO_2-System (Alkalinität, gesamter organischer Kohlenstoff, pH) (siehe auch Abschnitte M 21/3 und M 21/6). Ferner wurden die Populationsdynamik von planktischen Foraminiferen und ihr Einfluß auf die Exportproduktion und Sedimentbildung untersucht. Diese Arbeiten wurden auf allen Fahrtabschnitten durchgeführt.

Am Ende des 1. Fahrtabschnittes, auf der Anreise nach Dublin, wurde eine Jahresverankerung für die britischen JGOFS-Untersuchungen auf dem Porcupine Abyssal Plain (49°N, 17°W) ausgebracht. Der Fahrtabschnitt M 21/1 endete am 09.04.1992 in Dublin.

Der Abschnitt M 21/2, der am 12.04.1992 in Dublin begann, führte wiederum ins Arbeitsgebiet bei 47°N, 20°W. Es wurden hauptsächlich Prozeßstudien zur Entwicklung der Phytoplanktonblüte durchgeführt, bei denen treibende Sinkstoffallen eingesetzt wurden. Neben planktologischen Arbeiten wurden wieder Benthosproben genommen. Einen weiteren Schwerpunkt des Abschnittes M 21/2 stellten luftchemische Messungen der biologisch wichtigen Spurengase Dimethylsulfid (DMS) und Dimethylsulfoniopropionat (DMSP) in der Grenzschicht Wasser/Atmosphäre dar. Der Fahrtabschnitt M 21/2 endete am 06.05.1992 in Funchal.

Der Fahrtabschnitt M 21/3 begann am 09.05.1992 in Funchal. Den Schwerpunkt bildeten die Untersuchung chemischer Parameter sowie Verankerungsarbeiten im Rahmen des deutschen Beitrages zu JGOFS. Die Fahrt führte entlang eines meridionalen Schnittes auf 20°W von Funchal bis Reykjavik und ermöglichte so eine interdisziplinäre Aufnahme zahlreicher Parameter in verschiedenen Klimazonen des Nordostatlantiks. Es wurden insgesamt 9 Stationen zwischen 33°N und 60°N angefahren, auf denen Vertikalprofile der Wassersäule bezüglich chemischer Parameter wie Spurenelemente, organische Spurenstoffe, Meßgrößen des CO_2-Systems, Isotopenzusammensetzung des Karbonatkohlenstoffes, biologischer Parameter wie Biomasse, Planktonabundanz, Chlorophyll und physikalischer Parameter wie Temperatur und Salzgehalt erhalten wurden. Ein Großteil der Stationsarbeiten wurde für die Ausbringung von Verankerungen zur Messung des vertikalen Partikelflusses mit Hilfe von Sinkstoffallen benötigt.

Auf den Fahrtabschnitten zwischen den Stationen wurde mit Hilfe des "Kieler Pumpsystems" kontinuierlich das Wasser der Deckschicht beprobt. Auch diese Proben dienten schwerpunktmäßig der Bestimmung chemischer Parameter, vor allem im suspendierten partikulären Material (SPM).

An dem Fahrtabschnitt nahmen drei meereschemische Arbeitsgruppen teil, welche sich primär mit der Untersuchung partikulärer Spurenstoffe bzw. mit dem ozeanischen Karbonatsystem befaßten. Die Verteilung des gelösten organischen Kohlenstoffes bzw. Stickstoffes wurde durch die Kieler Planktologen untersucht, weitere benthische Probennahmen wurden durch die BIO-C-FLUX- Arbeitsgruppe durchgeführt. Die mikrobiologischen Arbeiten des Abschnittes M 21/2 wurden fortgeführt. Geologische Fragestellungen wurden von zwei Arbeitsgruppen aus Kiel und Tübingen behandelt. Physikalisch-optische Untersuchungen wurden von einer JGOFS-Arbeitsgruppe aus Oldenburg durchgeführt. Der Fahrtabschnitt endete am 02.06.1992 in Reykjavik.

Die Abschnitte M 21/4 und M 21/5 von Reykjavik (05.06.1992) nach Trondheim (28.06.1992) und zurück nach Reykjavik (01.07.-23.07.1992) dienten den Arbeiten des Sonderforschungsbereiches 313 an der Universität Kiel. Neben Untersuchungen zum vertikalen, durch pelagische Prozesse bestimmten Partikelfluß konzentrierten sich die Arbeiten auf den lateralen Partikeltransport sowie auf die Prozesse in der bodennahen Nepheloidschicht und auf die Stoffflüsse in der benthischen Grenzschicht.

Aufbauend auf den Erkenntnissen zur rezenten Sedimentbildung und teilweise analog zu diesen Untersuchungen soll die Geschichte der marinen Umwelt rekonstruiert werden. Seismische Untersuchungen an Sedimentprofilen, paläoökologische Untersuchungen der pelagischen und benthischen Mikrofossiliengruppen sowie die Aufnahme der physikalischen und chemischen Eigenschaften der Sedimente dienen der flächendeckenden Darstellung der Geschichte der Biosphäre und der Zirkulation sowie der Erfassung der tatsächlichen Zeitspannen von Klimaabläufen.

Das Auftreten von eisbedeckten und warmen Wassermassen in unmittelbarer Nachbarschaft im nördlichen Nordatlantik bestimmten die regionalen Arbeitsschwerpunkte. Die Untersuchungen konzentrierten sich auf das Vöring Plateau, den Kontinentalhang und die angrenzenden Tiefseegebiete der Barentssee sowie auf die Eisrandzone im Ostgrönlandstrom.

Das Hauptgewicht des letzten Fahrtabschnittes M 21/6, der am 26.07.1992 in Reykjavik begann, bildeten wiederum die Untersuchungen von BIO-C-FLUX. Nach den bisherigen Ergebnissen der METEOR-Reisen Nr. 3/1 und Nr. 10/4 war zu dieser Zeit (Juli/August) mit dem Auftreten von Phytodetritus zu rechnen, der nach der Sedimentation der Frühjahrsplanktonblüte am Meeresboden aggregiert. Unter derartigen Bedingungen kommt es zu einer deutlichen Steigerung der Umsatzprozesse am Meeresboden. Parallel dazu untersuchten die Planktologen der JGOFS-Arbeitsgruppe die Produktionsverhältnisse dieser Nachblütensituation in der oberen Deckschicht.

Mit dem planmäßigen Einlaufen von METEOR am 31.08.1992 in ihrem Heimathafen Hamburg endete die Reise M 21.

Tab.1: Fahrtabschnitte u. Fahrtleiter der METEOR-Reise Nr. 21
Legs and chief scientist of METEOR cruise no. 21

Fahrtabschnitt/Leg M 21/1
16.03.-09.04. 1992, Las Palmas - Dublin
Prof. Dr. H. Thiel (Fahrtleiter/chief scientist)

Fahrtabschnitt/Leg M 21/2
12. 04. - 06. 05. 1992, Dublin - Funchal
Prof. Dr. B. Zeitzschel (Fahrtleiter/chief scientist)

Fahrtabschnitt/Leg M 21/3
09. 05. - 02. 06. 1992, Funchal - Reykjavik
Prof. Dr. J.C. Duinker (Fahrtleiter/chief scientist)

Fahrtabschnitt/Leg M 21/4
05. 06. - 28. 06. 1992, Reykjavik - Trondheim
Dr. R. Henrich (Fahrtleiter/chief scientist)

Fahrtabschnitt/Leg M 21/5
01. 07. - 23. 07. 1992, Trondheim - Reykjavik
Prof. Dr. G. Graf (Fahrtleiter/chief scientist)

Fahrtabschnitt/Leg M 21/6
26. 07. - 31. 08. 1992, Reykjavik - Hamburg
Dr. O. Pfannkuche (Fahrtleiter/chief scientist)

Koordination/Coordination: Dr. O. Pfannkuche

Kapitäne/Masters (F/S METEOR): Kapitän A. Müller
Kapitän J. Wagener

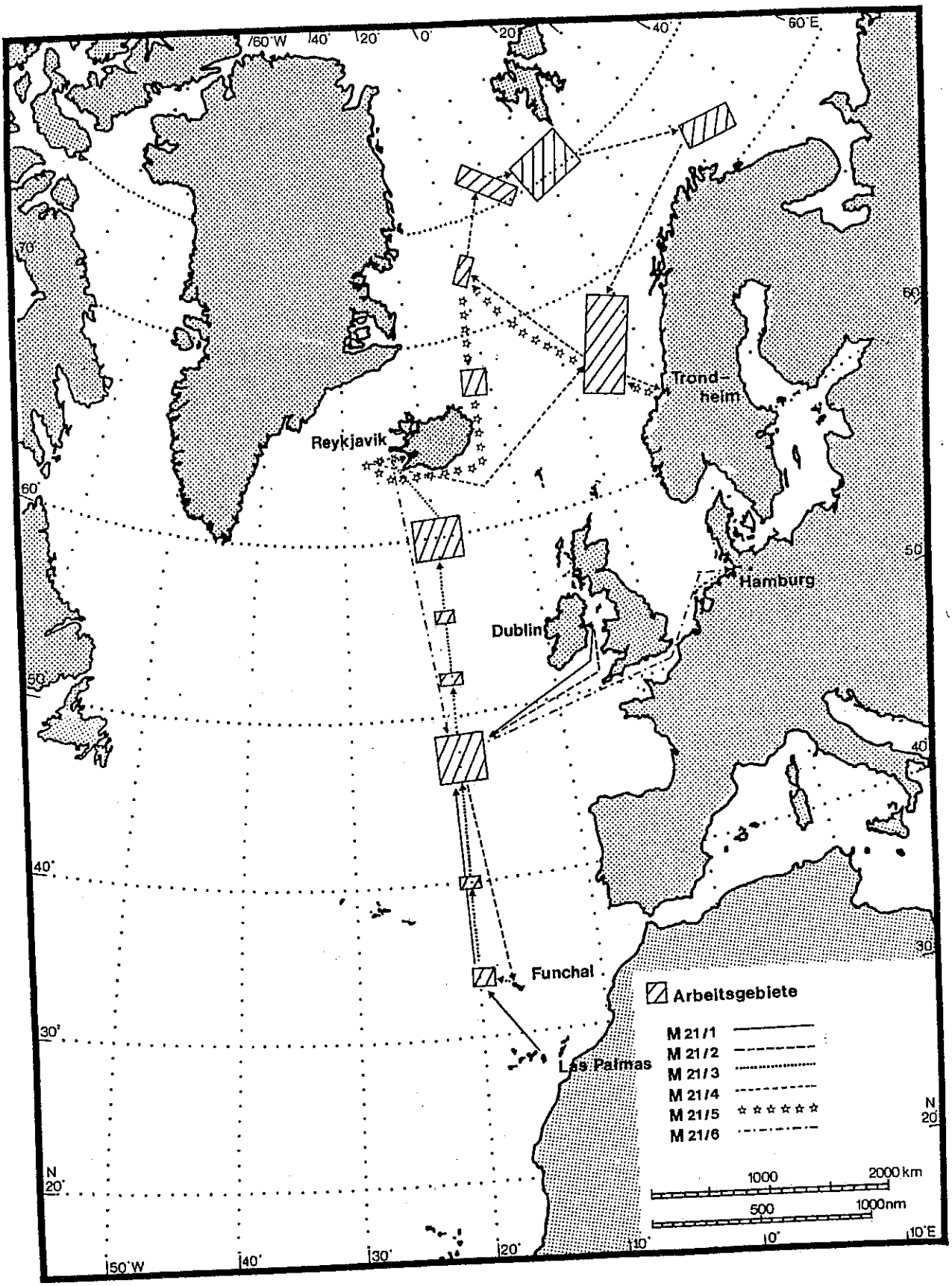

Abb. 1: Fahrtrouten der METEOR-Reise Nr. 21

Fig. 1: Tracks of METEOR cruise no. 21

2 Teilnehmer

Die Fahrtteilnehmer sind in Tabelle 2 nach Fahrtabschnitten geordnet aufgelistet. Die beteiligten Institutionen sind in Tabelle 3 aufgeführt.

Tab. 2: Fahrtteilnehmer der METEOR-Reise Nr. 21
Participants of METEOR cruise no. 21

Fahrtabschnitt M 21/1

Name	Fachrichtung	Institut
Thiel, Hjalmar, Prof. Dr., Fahrtleiter	Benthosbiologie	IHF
Bargen v., Dieter, Dipl.-Met.	Meteorologie	DWD
Boetius, Antje, Stud.	Benthosbiologie	IHF
Buschmann, Frank, Stud.	Benthosbiologie	IHF
Christiansen, Bernd, Dr.	Planktologie	IHF
Deckers, Monica, Dipl.-Biol.	Planktologie	IFM
Dolle, Antje, Stud.	Geochemie	IHF
Groß, Onno, Dipl.-Biol.	Benthosbiologie	IHF
Fölling, Peter, Stud.	Meereschemie	IBM
Hemleben, Christoph, Prof. Dr.	Paläontologie	GPT
Hiller, Birgit, Dipl.-Biol.	Paläontologie	GPT
Jeskulke, Karen, T.A.	Mikrobiologie	IFM
Körtzinger, Arne, Dipl.-Chem.	Meereschemie	IFM
Koppelmann, Rolf, Dipl.-Biol.	Planktologie	IHF
Lendt, Ralph, Stud.	Biogeochemie	IBM
Nuppenau, Volker, Dipl.-Ing.	Elektronik	IHF
Ochsenhirt, Wolf-Thilo, T.A.	Funkwettertechnik	DWD
Peter, Sabine, T.A.	Benthosbiologie	IHF
Petersen, Johannes, T.A.	Meereschemie	IFM
Podewski, Sigrid, Dipl.-Oz.	Meeresphysik	IFM
Poremba, Knut, Dr.	Mikrobiologie	IFM
Reitmeier, Sven, Dipl.-Biol.	Planktologie	IFM
Scheibe, Stephan, Dipl.-Biol.	Benthosbiologie	IHF
Sellmer, Claudia, Stud.	Planktologie	IFM
Soltwedel, Thomas, Dipl.-Biol.	Benthosbiologie	IHF
Steffani, Nina, Stud.	Benthosbiologie	IHF
Tempelmann, Annette, Stud.	Planktologie	IHF
Uthicke, Sven, Stud.	Planktologie	IHF
Werner, Rolf, T.A.	Planktologie	IFM
White, David, T.A.	Elektronik	IOS

Fahrtabschnitt M 21/2

Name	Fachrichtung	Institut
Zeitzschel, Bernt, Prof. Dr., Fahrtleiter	Planktologie	IFM
Amouroux, David, Dipl.-Chem.	Chemie	CUB
Andreae, Meinrat, Prof. Dr.	Luftchemie	MPC
Andreae, Tracy W., Dipl.-Biol.	Luftchemie	MPC
Beckmann, Uwe, T.A.	Meeresphysik	IFM
Bijma, Jelle, Dr.	Paläontologie	GPT
Böhm, Sonja, T.A.	Planktologie	IFM
Carstensen, Anett, T.A.	Mikrobiologie	IFM
Deckers, Monica, Dipl.-Biol.	Planktologie	IFM
Detmer, Andrea, Dipl.-Biol.	Planktologie	IFM
De Wall, Jürgen, Dipl.-Biol.	Mikrobiologie	IFM
Donard, Olivier, Prof. Dr.	Chemie	ESA
Fritsche, Peter, T.A.	Planktologie	IFM
Jochem, Frank, Dr.	Planktologie	IFM
Kähler, Paul, Dr.	Planktologie	IFM
Karrasch, Bernhard, Dipl.-Biol.	Mikrobiologie	IFM
Koeve, Wolfgang, Dipl.-Biol.	Planktologie	IFM
Nuppenau, Volker, Dipl.-Ing.	Elektronik	IHF
Matschulat, Anja, Stud.	Benthosbiologie	IHF
Meyerdierks, Doris, Dipl.-Biol.	Planktologie	BUB
Michalek, Kirsten, T.A.	Benthosbiologie	IHF
Ochsenhirt, Wolf-Thilo, T.A.	Wetterfunktechnik	DWD
Pfannkuche, Olaf, Dr.	Benthosbiologie	IFM
Podewski, Sigrid, Dipl.-Biol.	Planktologie	IFM
Pollehne, Falk, Dr.	Planktologie	IFM
Rapsomanikis, Spyridon, Dr.	Luftchemie	MPC
Röd, Erhard, Dipl.-Met.	Meteorologie	DWD
Rödiger, Bodo, T.A.	Paläontologie	GPT
Thiel, Cornelia, Dipl.-Biol.	Planktologie	BUB
Uher, Günther, Dipl.-Chem.	Luftchemie	MPC

Fahrtabschnitt M 21/3

Name	Fachrichtung	Institut
Duinker, Jan C., Prof. Dr., Fahrtleiter	Chemie	IFM
Baumann, Karl-Heinz, Dipl.-Geol.	Planktologie	GPK
Bruhn, Regina, Stud.	Chemie	IFM
Carstensen, Annett, T.A.	Mikrobiologie	IFM
Determann, Stephan, Dipl.-Phys.	Optik	POL
Haupt, Olaf, Dipl.-Biol.	Planktologie	IFM
Heller, Stefan, Stud.	Paläontologie	GPT
Janßen, Silke, T.A.	Benthosbiologie	IFM
Kähler, Paul, Dr.	Planktologie	IFM
Karrasch, Bernhard, Dipl.-Biol.	Mikrobiologie	IFM
Körner, Thomas, T.A.	Chemie	IFM
Körtzinger, Arne, Dipl.-Chem.	Chemie	IFM
Korves, Anette, T.A.	Chemie	IFM
Link, Rudolf, T.A.	Chemie	IFM
Lippert, Gabriele, T.A:	Chemie	IFM
Lundgreen, Ulrich, Dipl.-Chem.	Chemie	IFM
Mintrop, Ludger, Dr.	Chemie	IFM
Morak, Anja, T.A.	Chemie	IFM
Pegler, Kay, Dipl.-Geol.	Biogeochemie	IBM
Petersen, Johannes, T.A.	Chemie	IFM
Petrick, Gert, T.A.	Chemie	IFM
Podewski, Sigrid, Dipl.-Oz.	Planktologie	IFM
Reuter, Rainer, Prof. Dr.	Optik	POL
Schüßler, Uwe, Dipl.-Chem.	Chemie	IFM
Scheibe, Stephan, Dipl.-Biol.	Benthosbiologie	IHF
Schulz-Bull, Detlef, Dr.	Chemie	IFM
Viergutz, Thomas, T.A.	Chemie	IFM

Fahrtabschnitt M 21/4

Name	Fachrichtung	Institut
Henrich, Rüdiger, Dr., Fahrtleiter	Geologie/Sedimentologie	GOM
Anders, Tanja, Stud.	Paläontologie	SFB
Antonow, Martin, Dr.	Geologie	GPF
Bassek, Dieter, T.A.	Wetterfunktechnik	DWD
Beese, Helmut, T.A.	Elektronik	SFB
Blaume, Frank, Dr.	Sedimentologie	SFB
Bobsin, Michael, Dipl.-Geol.	Geophysik	SFB
Chi, Jian, Dipl.-Geol.	Geophysik	SFB
Franke, Christoph, Stud.	Gerätetechnik	SFB
Geminder, Hilke, T.A.	Paläontologie	GPT
Goldschmidt, Peter, Dipl.-Geol.	Sedimentologie	SFB
Hemleben, Chrisoph, Prof. Dr.	Paläontologie	GPT
Juterzenka v., Karen, Dipl.-Biol.	Benthosbiologie	SFB
Kaiser, Frank, Stud.	Biogeochemie	IBM
Knaack, Christian, Dipl.-Met.	Meteorologie	DWD
Lendt, Ralf, Stud.	Biogeochemie	IBM
Michels, Klaus, Dipl.-Geol.	Sedimentologie	SFB
Mienert, Jürgen, Dr.	Geophysik	GOM
Müller-Wille, Stephan, Dipl.-Geol.	Paläontologie	GPT
Reitner, Joachim, Dr.	Paläontologie	IPB
Rheder, Wilma, T.A.	Geologie	GPK
Rumohr, Jan, Dr.	Sedimentologie	GOM
Schlünz, Birger, Stud.	Sedimentologie	SFB
Schröder, Andrea, Dipl.-Geol.	Paläontologie	SFB
Schulz, Susanne, T.A.	Geologie	SFB
Seiss, Maren, T.A.	Sedimentologie	SFB
Steen, Eric, T.A.	Paläontologie	SFB
Wagner, Thomas, Dipl.-Geol.	Geologie	GPM
Wehrmann, Achim, Dipl.-Geol.	Paläontologie	SFB
Witte, Ursula, Dipl.-Biol.	Benthosbiologie	

Fahrtabschnitt M 21/5

Name	Fachrichtung	Institut
Graf, Gerhard, Prof. Dr., Fahrtleiter	Benthosbiologie	GOM
Antia, Avan N., Dr.	Planktologie	IFM
Bassek, Dieter, T.A.	Meteorologie	DWD
Beese, Helmut, T.A.	Elektronik	SFB
Bergmann, Tim, Stud.	Geophysik	SFB
Bohlen, Thomas, Stud.	Geologie	SFB
Bodungen v., Bodo, Prof. Dr.	Planktologie	IFM
Brandt, Angelika, Dr.	Benthosbiologie	SFB
Brunssen, Bernd, Stud.	Geologie	SFB
Ehmcke-Kasch, Maren, T.A.	Mikrobiologie	SFB
Fölling, Peter, Stud.	Biogeochemie	IBM
Hartig, Rüdiger, Dipl.-Met.	Meteorologie	DWD
Hollender, Franz-Josef, Dipl.-Geol.	Geophysik	SFB
Hollinde, Michael, Dipl.-Biol.	Mikrobiologie	IFM
Jung, Simon, Dipl.-Geol.	Geologie	SFB
Juterzenka v., Karen, Dipl.-Biol.	Benthosbiologie	SFB
Kähler, Paul, Dr.	Planktologie	IFM
Kamleiter, Wilfried, T.A.	Paläontologie	GPT
Kohly, Alexander, Dipl.-Geol.	Geologie	SFB
Köster, Marion, Dr.	Mikrobiologie	SFB
Linke, Peter, Dr.	Benthosbiologie	SFB
Locker, Sigurd, Dr.	Paläoozeanographie	SFB
Maassen, Jörg, Dipl.-Chem.	Meereschemie	SFB
Pegler, Kay, Dipl.-Geol.	Biogeochemie	IBM
Piepenburg, Dieter, Dr.	Benthosbiologie	IPÖ
Queisser, Wolfgang, T.A.	Benthosbiologie	GOM
Ritzrau, Will, Dipl.-Biol.	Benthosbiologie	GOM
Struck, Ulrich, Dr.	Geologie	SFB
Willamowski, Claudia, Stud.	Meereschemie	SFB
Witte, Ursula, Dipl.-Biol.	Benthosbiologie	SFB

Fahrtabschnitt M 21/6

Name	Fachrichtung	Institut
Pfannkuche, Olaf, Dr., Fahrtleiter	Benthosbiologie	IFM
Bassek, Dieter, T.A.	Wetterfunktechnik	DWD
Boetius, Antje, Stud.	Benthosbiologie	IHF
Christiansen, Bernd, Dr.	Planktologie	IHF
Dolle, Antje, Stud.	Benthosbiologie	IHF
Dölle, Martina, Stud.	Benthosbiologie	IHF
Drüke-Wams, Barbara, Stud.	Planktologie	IHF
Eardly, Donal, Dr.	Mikrobiologie	UCG
Fischer, Uwe, Stud.	Paläontologie	GPT
Hartig, Rüdiger, Dipl.-Met.	Meteorologie	DWD
Hiller, Birgit, Dipl.-Biol.	Paläontologie	GPT
Hupe, Axel, Stud.	Meereschemie	IBM
Jeskulke, Karen, T.A.	Mikrobiologie	IFM
Kähler, Paul, Dr.	Planktologie	IFM
Koppelmann, Rolf, Dipl.-Biol.	Planktologie	IHF
Lampe, Katrin, T.A.	Planktologie	IHF
Link, Rudolf, T.A.	Meereschemie	IFM
Lochte, Karin, Dr.	Mikrobiologie	AWI
Lundgren, Ulrich, Dipl.-Chem.	Meereschemie	IFM
Matschulat, Anja, Stud.	Benthosbiologie	IHF
Martin, Bettina, Stud.	Planktologie	IHF
Moore, Heather, M. Sci.	Benthosbiologie	IHF
Nuppenau, Volker, Dipl.-Ing.	Elektronik	IHF
Pachleitner, Alexander, Stud.	Meereschemie	IBM
Peter, Sabine, T.A.	Benthosbiologie	IHF
Petersen, Johannes, T.A.	Meereschemie	IFM
Poremba, Knut, Dr.	Mikrobiologie	IFM
Sablotny, Burkhard, Dipl.-Ing.	Elektronik	IHF
Scheibe, Stephan, Dipl.-Biol.	Benthosbiologie	IHF
Sellmer, Claudia, Stud.	Planktologie	IFM

Tab. 3: An der METEOR-Reise Nr. 21 beteiligte Institutionen
Participating institutions

AWI	Alfred-Wegener-Institut für Polar- und Meeresforschung, Postfach 12 01 61 27568 Bremerhaven, Germany
BUB	Fachbereich 2, Meeresbotanik, Universität Bremen, Postfach 33 04 40 28334 Bremen, Germany
CUB	Groupe d'Océanographie Physico- Chimique, Université de Bordeaux I, Talence, France
DWD	Deutscher Wetterdienst, Seewetteramt Hamburg, Bernhard-Nocht-Str. 78, 20359 Hamburg, Germany
ESA	School of Environmental Sciences University of East Anglia, Norwich, NR4 7TJ, United Kingdom
GOM	GEOMAR Forschungszentrum für Marine Geowissenschaften, Universität Kiel, Wischhofstr. 1-3, 24148 Kiel, Germany
GPF	Geologisch-Paläontologisches Institut, Bergakademie Freiberg 71691 Freiberg, Germany

Tab. 3: **Fortsetzung/continued**

GPK	Geologisch-Paläontologisches Institut und Museum, Christian-Albrechts-Universität, Olshausenstr. 40, 24118 Kiel, Germany
GPM	Geologisch-Paläontologisches Institut, Universität Marburg, 35037 Marburg, Germany
GPT	Institut und Museum für Geologie und Paläontologie, Universität Tübingen, Sigwartstr. 10 72076 Tübingen, Germany
IBM	Institut für Biogeochemie und Meereschemie, Universität Hamburg, Bundestr. 55, 20146 Hamburg, Germany
IFM	Institut für Meereskunde an der Universität Kiel, Düsternbrooker Weg 20, 24105 Kiel, Germany
IHF	Institut für Hydrobiologie und Fischereiwissenschaft, Universität Hamburg, Zeiseweg 9, 22765 Hamburg, Germany

Tab. 3: **Fortsetzung/continued**

IOS	Institute of Oceanographic Sciences, Deacon Laboratory, Brook Road, Wormley/Godalming, Surrey GU8 5UB, United Kingdom
IPB	Institut für Paläontologie, Freie Universität Berlin, Malteser Str. 76-100, 12249 Berlin, Germany
IPÖ	Institut für Polarökologie Universität Kiel, Olshausenstr. 40 24118 Kiel, Germany
MPC	Max-Planck-Institut für Chemie, Abteilung Biogeochemie, Postfach 3060, 55020 Mainz, Germany
POL	Fachbereich Physik Universität Oldenburg, Postfach 2503, 26111 Oldenburg, Germany
SFB	Sonderforschungsbereich 313 Christian-Albrechts-Universität, Olshausenstr. 40, 24118 Kiel, Germany
UCG	University of Galway, Galway, Ireland

3 Forschungsprogramm

3.1 BIO-C-FLUX

Das vom Bundesminister für Forschung und Technologie geförderte Projekt BIO-C-FLUX untersucht den Kohlenstoffumsatz in der küstenfernen Tiefsee. BIO-C-FLUX stellt zwar einen eigenständigen Forschungsansatz zum biologischen Kohlenstoffffluß in der Tiefsee dar, ist aber sowohl inhaltlich als auch räumlich mit den Vorhaben der internationalen und deutschen JGOFS-Programme gekoppelt.

BIO-C-FLUX wird von einer gemeinsamen Arbeitsgruppe des Institutes für Hydrobiologie und Fischereiwissenschaft der Universität Hamburg und des Institutes für Meereskunde an der Universität Kiel, Abteilung Marine Mikrobiologie, durchgeführt.

Auf der METEOR-Reise Nr. 21 sollte zum ersten Mal für die küstenferne Tiefsee der Versuch unternommen werden, innerhalb einer Produktionsperiode des Planktons die Wechselbeziehungen zwischen der oberen Deckschicht und der Bodengrenzschicht (BGS) zu verfolgen. Ergebnisse aus verschiedenen Monaten der Jahre 1985 bis 1989 (PFANNKUCHE 1992, 1993) gaben deutliche Hinweise auf eine Saisonalität in der Biomasseproduktion der kleineren Größenklassen des Benthos und in der Respirationsrate der Infauna, die mit Sedimentationsereignissen von Phytodetritus gekoppelt war.

Die geplanten Arbeiten schlossen die bodennahe Wasserschicht (entspricht etwa der Bodentrübungsschicht bis 500 m über dem Boden), das Sedimentkontaktwasser (20 cm über dem Boden), die Sedimentoberfläche und verschiedene Sedimenthorizonte bis zu 50 cm Tiefe ein. Da die bodennahe Wasserschicht und die oberen Sedimenthorizonte ein vielfach miteinander vernetztes biologisches System darstellen, werden sie als Bodengrenzschicht (BGS) zusammengefaßt. Der Untersuchung der Organismen in der BGS kommt eine besondere Bedeutung zu, da in dieser Zone die wichtigsten biologischen Umsetzungen innerhalb des Systems der Tiefsee stattfinden. Die Arbeiten schlossen die Untersuchungen der Infauna (Bakterien, Nano-, Meio-, Makro- und Megabenthos), des Zooplanktons und der verschiedenen Größenklassen des benthopelagischen Nektons ein. BIO-C-FLUX beschränkt sich auf die Untersuchungen der biologischen Umsetzung des sedimentierenden partikulären organischen Kohlenstoffes (POM) und verfolgt das Ziel, die Wege des organischen Kohlenstoffflusses in der benthischen Grenzschicht zu beschreiben und zu quantifizieren. Die Arbeiten zielten hauptsächlich auf die Beantwortung folgender Fragen:

- Wie wirkt sich die Sedimentation von im Epipelagial gebildetem POM auf die Organismen der BGS aus?
- Gibt es eine direkte pelago-benthische Kopplung?
- Tritt Saisonalität in der Sedimentation von POM in der BGS auf?

- Welche Zusammensetzung und Quantität hat das partikuläre organische Material auf dem und im Sediment?
- Welches sind die wesentlichen Regionen des Abbaues organischer Substanz in der BGS (z.B. Bodentrübungsschicht, Bodenkontaktwasser, bestimmte Sedimenthorizonte)?
- Welche bodennahen vertikalen Gradienten existieren in der Menge und Zusammensetzung des benthopelagischen Planktons und Nektons?
- Welche Nahrungsbeziehungen bestehen in der BGS?
- Welche Wechselbeziehungen bestehen zwischen POM-Sedimentation und metabolischen Aktivitätsraten des Benthos?
- Wie hoch sind die Umsatzraten an sedimentiertem partikulären organischen Kohlenstoff (POC) in der Lebensgemeinschaft der benthischen Grenzschicht (Abbau von organischem Kohlenstoff, Respiration, Biomasseproduktion)?

3.2 JGOFS-Programme

Die Arbeiten im Rahmen des deutschen JGOFS-Programmes haben das Verständnis des Kohlenstoffkreislaufes im Ozean als übergeordnetes Ziel. Dabei wurden während der Abschnitte M 21/1, M 21/2, M 21/3 und M 21/6 Prozeßstudien zur Quantifizierung der biologischen C-Fixierung und zur Bestimmung der Flüsse kohlenstoffhaltiger Verbindungen sowie biologisch relevanter chemischer Elemente im Nordatlantik durchgeführt, wobei der ozeanischen Deckschicht eine besondere Bedeutung zukam. Weiterhin wurde die Wechselwirkung zwischen Ozean und Atmosphäre in bezug auf das CO_2-System studiert.

3.2.1 Physikalische Ozeanographie

Die Untersuchungen der hydrographischen Arbeitsgruppe während der Fahrtabschnitte M 21/1-3 und M 21/6 waren eng an die Probennahmestrategien der biologischen und chemischen Arbeitsgruppen an Bord von METEOR angelehnt. Die planktologischen Untersuchungen während der ersten beiden und des letzten Abschnittes sollten schwerpunktmäßig die biologisch/chemischen Prozesse in der oberen Wassersäule mit saisonaler zeitlicher Auflösung im Hauptarbeitsgebiet der deutschen Beteiligung an der internationalen JGOFS-Studie bei 47°N, 20°W erfassen. Die CTD-Stationsdichte war während der Abschnitte 1, 2 und 6 abhängig von der vorhandenen Stationszeit und den Wetterverhältnissen, so daß sich unterschiedliche Auflösungen ergaben, die den Stationskarten und -listen zu entnehmen sind.

Das Hauptarbeitsgebiet der JGOFS-Studie liegt im westeuropäischen Becken zwischen der Azorenfront und der subarktischen Front im Einflußbereich des Nordatlantischen Stromes (NAC). Frühere Untersuchungen über den Verlauf des mittleren NAC führten teilweise zu gegensätzlichen Beschreibungen der Zirkulation. Zum Beispiel beschrieben DIETRICH et al.

(1975), daß sich der NAC im Bereich des Mittelatlantischen Rückens (MAR) in verschiedene Strombänder aufspaltete, die sich größtenteils östlich des Rückens fortsetzten, während WORTHINGTON (1976) postulierte, daß ein großer Teil des NAC bereits westlich des MAR rezirkuliert. Diese offenen Fragen führten dazu, daß internationale Projekte, wie NOAMP (Nordostatlantisches Monitoring Programm) und TOPOGULF, initiiert wurden. Diese Projekte führten zum einen quasi-synoptische CTD-Messungen westlich und östlich des MAR zu unterschiedlichen Jahreszeiten durch. Zum anderen wurden Strommesserverankerungen im Bereich des Rückens und westlich und östlich davon ausgelegt, die die kurz- und langperiodischen Strömungssignale in den verschiedenen Tiefenniveaus zu beiden Seiten des Rückens aufzeichneten. Zentrale offene Fragen waren z.B., ob der NAC den MAR als breites Stromband überquert oder sich in diverse Strombänder aufteilt, welcher Anteil des NAC bereits westlich des Rückens rezirkuliert, und wie sich die mittlere Zirkulation östlich des MAR entwickelt (KUPFERMANN et al., 1986; MITTELSTAEDT, 1987; HARVEY und ARHAN, 1988; SY, 1988; ARHAN et al., 1989; SCHAUER, 1989; COLIN DE VERDIERE et al., 1989; ARHAN, 1990; SY et al., 1992).

Die Untersuchungen von HARVEY und ARHAN (1988) und ARHAN (1990) ergaben, daß mindestens zwei Strombänder des NAC den MAR überqueren, was sich auch deutlich in Temperaturfronten widerspiegelte. Die Autoren beschrieben eine südliche Front bei 48°N und eine nördliche Front bei 52°N, die sie zusammen mit den damit verbundenen sog. nördlichen und südlichen Strombändern des NAC als permanente Strukturen der Region westlich von 25°W ansahen. Diese beiden permanenten Strombänder des NAC mäandern um die o.a. Breitengrade und ARHAN et al. (1989) schließen aus direkten Strommessungen, daß das südlichste Stromband ca. 150 km um seine zentrale Position oszilliert. Nach Analysen von SY (1988) und SY et al. (1992) spaltet sich der NAC westlich der MAR auf. Ein großer Teil des Stromes überquert danach den MAR im Bereich der GIBBS-Bruchzone bei ca. 52°N und bildet die permanente subarktische Front, während südlich dieser Region bis ca. 45°N je nach Jahreszeit und mit zwischenjährlicher Variabilität eine unterschiedliche Anzahl von Strombändern des NAC (ca. 100 km Horizontalskala) den MAR überqueren.

Den einzelnen Strombändern konnten charakteristische Temperatur-/Salzgehaltverteilungen zugeordnet werden. Östlich des MAR, im Bereich der Position der JGOFS-Zeitserienuntersuchung, wurde starke mesoskalige Variabilität vorgefunden (KRAUSS und KÄSE, 1984). Die Bildung und Entwicklung einzelner mesoskaliger Wirbelstrukturen konnte aufgezeichnet werden, die zum Teil in enger Wechselwirkung mit einem mäandrierenden Stromband des NAC in Verbindung gebracht werden konnten (KUPFERMANN et al., 1986;, MITTELSTAEDT, 1987; SCHAUER, 1989). CTD-Trübungsmessungen zeigten, daß die Wirbelsignale teilweise bis zum Boden reichten (NYFFELER und GODET, 1986). Diese Beobachtung spiegelte sich in den direkten Strommessungen der Verankerungen als kurzperiodische Stromsignale mit relativ hohen Geschwindigkeiten beim Überströmen der Verankerungspositionen wieder (COLIN DE VERDIERE et al., 1989).

Während der JGOFS-Pilotstudie 1989 wurden im Untersuchungsgebiet 47°N, 20°W und nördlich dieser Position Wirbelstrukturen mit unterschiedlichen Horizontalskalen vorgefunden (ROBINSON et al., 1993), die einen starken Einfluß auf die chemisch/biologische Entwicklung im Gebiet hatten. Dieser Einfluß mesoskaliger Strukturen auf die Entwicklung der Planktonblüte zeigte sich auch deutlich in den U.K. Biogeochemical Ocean Flux Study-(BOFS) Untersuchungen in 1990, die u.a. von SAVIDGE et al. (1992) beschrieben wurden. Die hydrographischen Untersuchungen der ersten beiden Fahrtabschnitte dieser Expedition hatten deshalb zum Ziel, die zu erwartenden meso- und submesoskaligen Strukturen in den oberen ca. 1000 m der Wassersäule aufzulösen, und den Einfluß dieser hydrographischen Strukturen auf die Frühjahrsentwicklung der Phytoplanktonblüte zu dokumentieren.

Während M 21/1-2 wurden quasi Lagrang'sche Drifter ausgesetzt, die aus einer Argos-Oberflächenboje, Auftriebskugeln und einer Sinkstoffalle, die unterhalb der durchmischten Schicht hing, bestanden. Die Einsatztiefen der Sinkstoffallen variierten entsprechend der kontinuierlichen Verflachung der Deckschicht in den ersten 2 Monaten der Expedition (siehe unten). Der Einsatz der treibenden Sinkstoffallen diente der quantitativen und qualitativen Erfassung sinkender Partikel. Die Drifterfallen sollten im 'Idealfall' mit dem Wasserkörper treiben, um die zeitliche Entwicklung der biologisch/chemischen Variablen als Funktion der Prozesse in der oberen Wassersäule aufzuzeichnen. Die Erfahrungen vergangener Experimente haben jedoch gezeigt, daß die Art der eingesetzten Driftsysteme aufgrund der auftretenden Stromscherungen zwischen der Deckschicht und den darunterliegenden hydrographischen Strukturen, aber auch durch den direkten Windeinfluß auf die Argosboje, häufig nicht Lagrange treiben (KOEVE et al., 1993; PODEWSKI et al., 1993; SAVIDGE et al., 1992). Aus diesem Grund wurde bei den Langzeitdriftern kurz unterhalb der Sinkstoffalle ein Aanderaa-Strömungsmesser eingesetzt, der die Temperatur sowie die relativen Stromgeschwindigkeiten und -richtungen in den entsprechenden Tiefen in 10minütigen Meßintervallen aufzeichnete. Wir hoffen, durch den zusätzlichen Einsatz dieser Strömungsmesser eine Verbesserung der Beurteilung des Driftverhaltens zu erhalten. Würde das Driftersystem Lagrange treiben, wäre zu erwarten, daß die registrierten Strömungsgeschwindigkeiten im Bereich der Meßgenauigkeit des Strömungsmessers liegen und keine bevorzugten Stromrichtungen auftreten. Abbildung 9 gibt die Driftertrajektorien der 4 Driftexperimente während der Fahrtabschnitte M 21/1-3 wieder.

Während des dritten Abschnittes wurde ein großskaliger Schnitt im Bereich des Längengrades 20°W gefahren. Neben oberflächennahen Registrierungen der Temperatur und des Salzgehaltes wurden an ausgewählten Positionen CTD-Messungen durchgeführt, die Aufschlüsse über die Kopplung der Wassermassenverteilungen mit biologisch/chemischen Variablen geben soll. Abbildung 10 gibt die Positionen der CTD-Stationen wieder.

Während der Experimente wurden die Temperatur- und Salzgehaltsdaten (T/S) des kontinuierlich registrierenden Thermosalinographen (aus ca. 6 m Tiefe) aufgenommen, die einen Überblick über die Variabilität in der Deckschicht vermitteln. Direkte Strommessungen in den oberen 300 m der Wassersäule (ADCP-Daten) wurden mittels des bordeigenen

"Acoustic Doppler Current Profiler" (ADCP) aufgezeichnet. Die UV- und Globalstrahlungsdaten sowie die meteorologischen Daten wurden ebenso wie die T/S-Daten dem bordeigenen Datenverteilungssystem entnommen und gespeichert.
Im Verlauf der genannten Fahrtabschnitte wurden vier unterschiedliche CTD-O_2-Sonden eingesetzt. Bei den Fahrtabschnitten M 21/2-3 und /6 war außerdem ein Rückstreufluoreszenzsensor mit dem jeweiligen CTD-O_2-System gekoppelt. Es ist zu beachten, daß bei den in diesem Fahrtbericht dargestellten CTD-Daten bzw. -Analysen bisher noch nicht geeichte Daten verwendet wurden. Dies gilt auch für die mit Chlorophyllproben geeichten Fluoreszenzdaten (im folgenden in vivo Chlorophyll genannt).

3.2.2 Spurenelementchemie

Ein fundamentales Problem in der chemischen Ozeanographie ist die Aufklärung des Phänomens der auffallend niedrigen Konzentrationen von im Meerwasser gelösten Elementen wie Al, Cd, Co, Cu, Fe, Mn, V, Zn u.a.. Die geringen Gehalte dieser sog. Spurenelemente lassen sich weder durch mangelnde Salzzufuhr einer seit geologischen Zeiträumen ablaufenden Kontinentalerosion noch durch die Sättigungskonzentrationen ihrer schwerlöslichen Verbindungen im Meerwasser erklären. Es muß angenommen werden, daß die ozeanische Verteilung dieser Elemente bzw. ihre Entfernung aus der Wassersäule von den sedimentierenden, überwiegend in der Oberflächenschicht gebildeten biogenen Partikeln gesteuert wird. Der vertikale Partikelfluß dieser Spurenelemente sollte in verschiedenen Klimagebieten des Nordatlantiks näher untersucht werden.

Ein Hauptziel der Experimente war die Quantifizierung des Spurenelementflusses und damit die Notwendigkeit zur Erfassung seiner kurzfristigen, saisonalen und langfristigen Veränderungen. Eine weitere wichtige Zielsetzung der Untersuchungen war das Sammeln von Informationen über Zusammenhänge zwischen den partikulären Spurenelementflüssen und dem vertikalen Kohlenstofftransport bzw. den in der ozeanischen Deckschicht ablaufenden "Ereignissen". Ferner sollte versucht werden herauszufinden, ob die Aufnahme der Elemente in die organischen Partikel biologisch gesteuert wird, wie schnell ihre Remineralisierung in der Wassersäule verläuft und ob Rückschlüsse auf die Existenz metallorganischer Bindungen anhand der gleichzeitig gemessenen organischen Substanzen bzw. Stoffklassen möglich sind.

3.2.3 Organische Spurenstoffchemie

Die Bildung und der Transport von natürlichen partikulären organischen Stoffen ("Biomarker") und von an Partikel gebundenen Kohlenwasserstoffen anthropogenen Ursprunges ("Tracer") sollten in der Wassersäule über längere Zeiträume und in verschiedenen Klimazonen des Atlantiks untersucht werden. Als "Biomarker" sind Verbindungen definiert (z.B. n-Alkane, Fettsäuren, Sterole und vor allem acyclische und polycyclische Isoprenoide),

die hinreichend große Anteile ihrer ursprünglichen chemischen Struktur bewahrt haben, um als modifizierte Version einer biogenen Quellverbindung erkannt zu werden. Vom sedimentären "record" kann nur unzureichend auf die pelagische Organismengemeinschaft geschlossen werden, z.B. können C_{org}-reiche Horizonte sowohl auf erhöhtem marinen oder terrigenen "input" als auch auf größerer Persistenz beruhen.

Hauptziel der Untersuchungen war, Informationen über den Einfluß biologischer Prozesse auf die chemische Zusammensetzung zu erhalten und den Auf- und Abbau dieser sedimentierenden organischen Stoffe sowie zur Quantifizierung ihres vertikalen Partikelflusses und damit über die Notwendigkeit, seine kurzfristigen, saisonalen und langfristigen Veränderungen zu erfassen.

Ferner sollte versucht werden, das geochemische Verhalten von anthropogenen Spurenstoffen näher zu untersuchen. Es wird vermutet, daß speziell der Nordatlantik die wichtigste Senke für schlecht abbaubare Verbindungen ist.

3.2.4 CO_2-Chemie

Während des Fahrtabschnittes M 21/3 sollten die vier meßtechnisch zugänglichen Größen des ozeanischen Karbonatsystems (CO_2-Partialdruck/ pCO_2, Gesamtkarbonat, Alkalinität, pH-Wert) gemessen werden. Durch diese Überbestimmung des Systems ist es möglich, die thermodynamische Konsistenz der durchgeführten Messungen zu überprüfen. Einen Schwerpunkt bildeten die Partialdruckmessungen, da diese Größe die treibende Kraft für den Austausch mit der Atmosphäre darstellt. Zusammenhänge mit der biologischen Produktion sollten durch die parallele Aufnahme der Nährstoff- und Chlorophylldaten ermittelt werden.

Auf den Stationen sollten die genannten Parameter sowie Sauerstoffgehalte und DOC-Konzentrationen (DOC-Dissolved Organic Carbon) in der Wassersäule aufgenommen werden. Ziel dieser Untersuchungen war es, den nicht durch anthropogenes CO_2 beeinflußten Ozean zu beschreiben.

Weiterhin sollte ein methodisches Problem untersucht werden: Berechnungen des pCO_2 auf der Grundlage von Alkalinitätstitrationen weichen zum Teil erheblich von direkt gemessenen Werten ab. Ob und in welchem Umfang diese Diskrepanzen durch organische Säuren im Meerwasser bedingt sind, war ebenfalls Gegenstand der Untersuchungen.

3.2.5 Meeresoptik

Organische Substanzen im Meerwasser bilden eine wichtige Komponente des marinen Kohlenstoffkreislaufes und lassen sich mit Hilfe der Fluoreszenzspektroskopie empfindlich und

teilweise auch spezifisch untersuchen. Die Fluoreszenz des Chlorophylls, der Carotinoide, aromatischer Aminosäuren und des Gelbstoffes sind bekannte Beispiele. Quellen des Gelbstoffes können sowohl Festlandabflüsse als auch biologische Aktivität im Meer sein.

Den bisherigen Befunden über die Fluoreszenz des Gelbstoffes und der aromatischen Aminosäuren (DETERMANN et al., 1993; HAYASE et al., 1988; CHEN and BADA, 1992) sollte weiter nachgegangen werden, um somit die Aussagekraft der Fluoreszenzspektroskopie an partikulärem und gelöstem Material im offenen Ozean zu verifizieren (YENTSCH and PHINNEY, 1985). Das Verfahren soll einen neuen und wesentlichen Beitrag zur Analyse des ozeanischen Kohlenstoffkreislaufes und insbesondere der Wechselwirkung zwischen partikulärem und gelöstem organischem Material liefern.

3.2.6 Planktologie

Im gesamten planktologischen Teil der Studie sollte der pelagische Stoffkreislauf im Hinblick auf den Verlust an organischem Material aus der euphotischen Zone untersucht werden. Ziel der planktologisch/hydrographischen Arbeitsgruppe während der Reise war die Beschreibung der biologischen Umsätze beim Übergang von einer Situation mit tiefer winterlicher Durchmischung zu einem System zunehmender Schichtung der oberen Wassersäule und Verflachung der Deckschicht. Diese Veränderung der Deckschichttiefe bildet die Grundlage für den Übergang, der von einem biologisch wenig produktiven Wintersystem in die hochproduktive Frühjahrssituation führt. In dieser Zeit treten in der Folge der biologischen Prozesse auch die größten Veränderungen des vertikalen Partikelflusses im Jahresverlauf auf.

Planktologische Arbeiten sollten auf den Fahrtabschnitten 1 bis 3 (Frühjahrssystem) und 6 (Sommersystem) insbesondere im BIOTRANS-Gebiet durchgeführt werden. Den Schwerpunkt der Arbeiten bildete hierbei der zweite Fahrtabschnitt, in dessen Zentrum eine planktologische Prozeßstudie mit driftenden Sinkstoffallen und einer Vielzahl von Feldmessungen und Experimenten stand. Treibende Sinkstoffallen unterhalb der durchmischten Schicht wurden darüberhinaus auch auf dem ersten Fahrtabschnitt und im Übergang vom zweiten zum dritten Fahrtabschnitt eingesetzt.
Während des ersten Fahrtabschnittes wurde im Rahmen der Verankerungsgruppe der Kieler Meereschemie eine Kurzzeitverankerung bei 47°N, 20°W mit Sinkstoffallen in 500, 1000 und 3500 m Tiefe gesetzt, die über den Elementfluß in größeren Tiefen Aufschluß geben wird. Auf dem dritten Fahrtabschnitt wurden von dieser Arbeitsgruppe weitere Verankerungen bei 47°N, 20°W und 54°N, 21°W gesetzt.

Wir erwarteten während des ersten Abschnittes ein Vorherrschen der winterlichen Situation. Die Untersuchungen dieses Abschnittes sollte damit die Grundlage für die Zeitserienuntersuchung der Frühjahrsblüte während des 2. Abschnittes dieser Expedition bilden. Es wurden hier insbesondere strukturelle Untersuchungen zum Plankton- und Elementbestand in der

Wassersäule durchgeführt. Im Einzelnen wurden Messungen der Nährstoffkonzentrationen (NO_3, NH_4, SiO_2 und PO_4), des Sauerstoffgehaltes und der Chlorophyll-a-Bestände direkt an Bord durchgeführt. Proben zur Messung des Gehaltes an partikulärem organischen Kohlenstoff und Stickstoff (POC/N) bzw. partikulärem Silikat (PSi) sowie Utermöhlproben für die mikroskopische Phytoplanktonanalyse und Filtrationsproben zur Pigmentanalytik (HPLC-Technik) wurden genommen, um später im Labor aufgearbeitet zu werden.

Während des zweiten Abschnittes wurde das biologische Programm intensiviert. Nach Erreichen des Arbeitsgebietes wurde ein mesoskaliges Grid mit kontinuierlichen vertikalen CTD- und Fluoreszenz-Profilen und diskreten Nährstoff- und Chl-a-Messungen abgefahren. Auf ausgewählten Stationen dieses Grids wurden auch Inkubationsexperimente zur neuen Produktion des Phytoplanktons durchgeführt.

Im weiteren Verlauf des Fahrtabschnittes wurde ein Driftexperiment mit treibenden Sinkstofffallen durchgeführt. Dazu wurden zwei Driftsysteme mit Sinkstoffallen in 120 m (Doppelfalle fixiert-unfixiert, Tagesdrifter) bzw. 185 m (Automatikfalle, Langzeitdrifter) ausgesetzt. Jeweils am frühen Morgen vor der Dämmerung wurde die Wassersäule in der Nähe des Tagesdrifters mit der CTD-Fluoreszenz-Rosette beprobt. Hierbei wurden die oberen 150 m für verschiedene Bestandsparametermessungen beprobt (Nährstoffe, Sauerstoff, Chlorophyll-a, Pigment-HPLC-Analytik, POC/N, PSi, Utermöhlproben, Piko- und Nanoplanktonproben (Flow Cytometer)). Proben zur Messung der Primärproduktion (^{14}C-DIC Aufnahme, ^{15}N-NO_3-Aufnahme) wurden aus den oberen 60-80 m entnommen und in situ am Tagesdrifter für ca. 12 Stunden inkubiert. Nach der Wassersäulenbeprobung wurde der Tagesdrifter aufgenommen, die Fallengläser gewechselt und der Drifter wieder ausgebracht. Die Beprobung der Bestandsparameter wurde an einigen Tagen zur Abendzeit wiederholt. Darüberhinaus wurde eine Reihe von tiefen CTD-Profilen aufgenommen, entlang derer diskrete Proben zur Messung ausgewählter Bestandsparameter genommen wurden. Zusätzliche Planktonfänge wurden regelmäßig mit verschiedenen Netzen durchgeführt (Apstein-Netz: 20 µm Maschenweite; Ring-Netz: 200 µm Maschenweite).

Neben den nachfolgend aufgelisteten verschiedenen Standardbestandsparametern (Sauerstoff, Nährstoffe [NO_3, NO_2, NH_4, SiO_4, PO_4], Chl-a, Phaeopigmente, partikulärer organischer Kohlenstoff und Stickstoff [POC/PON], partikuläres anorganisches Silizium [PSi]) wurden an verschiedenen Stationen während des zweiten Fahrtabschnittes Proben zur genaueren Beschreibung der Phytoplanktonzusammensetzung genommen. Neben Utermöhlproben zur Zählung insbesondere der Mikroplanktonfraktion wurden im Flow Cytometer Proben zur genaueren Klassifizierung der Piko- und Nanoplanktonfraktion gemessen (siehe unten). Weitere Proben zur Messung der Pigmentzusammensetzung werden an Land mittels der HPLC-Technik untersucht. Diese Messungen versprechen sowohl weitere Informationen über die Phytoplanktonzusammensetzung als auch über die Bedeutung heterotropher, remineralisierender Prozesse in der Wassersäule.

In Zusammenarbeit mit der DOC-Arbeitsgruppe und der Mikrobiologischen Arbeitsgruppe (siehe unten) wurden zusätzlich Tankexperimente durchgeführt. In $1m^3$-Tanks wurden dazu Proben aus der Oberflächenschicht des Ozeans an Deck inkubiert. Bei diesen Tankexperimenten wird die in situ Planktonentwicklung im wesentlichen simuliert. Aus den Tanks wurden Proben entnommen, mindestens einmal am Tag für Nährstoffe, Chl-a, POC/N und PSi und in regelmäßigen Abständen zusätzlich für Utermöhl- und Flow Cytometer-Untersuchungen. Da die überwiegende Zahl der Tankproben erst an Land ausgewertet werden, wird im Ergebnisteil nicht weiter auf diese Experimente eingegangen.

Auf dem dritten und sechsten Fahrtabschnitt sollte ein stark eingeschränktes Probennahmeprogramm durchgeführt werden, das sich auf wenige Bestandsparameter (O_2, Nährstoffe, Chl-a, POC/N und teilweise HPLC) beschränkte. Insbesondere der DOC-Arbeitsgruppe (P. Kähler und anderen) sei an dieser Stelle für die Unterstützung bei der Probennahme gedankt.

3.2.7 Marine Mikrobiologie

Das Driftexperiment auf dem Fahrtabschnitt M 21/2 konzentrierte sich auf die Messung der Abundanz und Biomasse der Bakterien, Pikocyanobakterien und heterotrophen Nanoflagellaten, der partikulären DNA-Konzentration sowie der mikrobiellen Netto-Sekundärproduktion mit Hilfe der ^{3}H-Methyl-Thymidin- und ^{3}H-Leucin-Methode. Aus diesen Parametern läßt sich der Umfang des Stoffumsatzes sowie die Nährsalzfreisetzung innerhalb des 'microbial loop' ableiten. Zusätzlich zu diesen Untersuchungen sollten die Dynamik des PON- und DON-Pools (PON-Particulate Organic Nitrogen, DON-Dissolved Organic Nitrogen) mit Hilfe der Messung der mikrobiellen extrazellulären Enzymaktivität erfaßt, mikroautoradiographische Untersuchungen zur Ermittlung der aktiven Bakterienpopulation durchgeführt sowie Proben für molekularbiologische Untersuchungen der Stickstoffixierung durch Pikocyanobakterien genommen werden.

Auf dem Fahrtabschnitt M 21/3 wurden unter den gleichen konzeptionellen und methodischen Gesichtspunkten die mikrobiellen Biomassevariablen sowie die bakterielle Produktivität und der extrazelluläre enzymatische Abbau organischen Materiales in Vertikalprofilen von der Wasseroberfläche bis zum Sediment verfolgt. Des weiteren wurden in Zusammenarbeit mit der DOC-Arbeitsgruppe gemeinsame Inkubationsexperimente zum DOC-Abbau und zur Ökodynamik pelagialer Systeme durchgeführt.

3.3 Sonderforschungsbereich 313 (SFB 313)

In seiner dritten Antragsphase untersucht der SFB 313 der Universität Kiel die Abbildung der Veränderlichkeit der Lebensbedingungen im nördlichen Nordatlantik, insbesondere wie sie sich in verschiedenen Skalen von Raum und Zeit in den Sedimentfolgen dokumentiert. Während der Fahrtabschnitte M 21/4 und M 21/5 konzentrierten sich die Aktivitäten auf die Untersuchung der Abbildung der pelagischen Prozesse am Kontinentalhang und den angrenzenden Tiefseeregionen. Schwerpunktmäßig wurde überprüft, wie weit sich der Einfluß der Schelfgebiete in die Tiefsee hinein verfolgen läßt und wie hierdurch die pelagischen Signale überprägt und modifiziert werden. Aus diesem Grund mußten neben dem vertikalen, durch pelagische Prozesse bestimmten Partikelfluß auch die lateralen bodennahen Partikeltransporte untersucht werden. Letztere können durch verschiedene Prozesse, wie z.B. Winterwasserkaskaden, zum Aufbau von Hochakkumulationszonen an spezifischen Schelfhanglokationen oder über "topographischen Fallen" im Tiefseebereich führen. Ein besonderer Vorteil dieser Hochakkumulationsgebiete ist die vorzügliche Auflösung ozeanographischer und klimatologischer Signale, die lediglich mit der von Eiskernen verglichen werden kann.

Während des Fahrtabschnittes M 21/4 sind die Sedimentationsprozesse in derartigen Hochakkumulationszonen durch verschiedene in situ-Experimente (Aufzeichnungen von Bodenstrommessern sowie Unterwasservideoaufzeichnungen) an zwei Lokationen, dem nördlichen Vöring Plateau Escarpment und der Kveiteholarinne vor der Bäreninsel, aufgezeichnet worden. Die Vernetzung derartiger Lateraladvektionsprozesse mit den saisonal geprägten pelagischen Partikelflüssen ist vor allem in der nordöstlichen Region des Europäischen Nordmeeres von außerordentlich großer Bedeutung, ein Seegebiet, in dem METEOR während des 4. Fahrtabschnittes überwiegend operierte.

Der Barentsschelf, insbesondere seine ausgedehnten Flachwassergebiete, wie beispielsweise die Spitzbergenbank, bilden nicht nur ein wichtiges Reservoir für in die Tiefsee abströmende dichte Schelfwässer, die durch winterlichen Meereiszuwachs entstehen, sondern sie stellen auch spezifische Biotope dar, die unterschiedlichen, an arktische Bedingungen adaptierten Flachwasser-Benthosökosystemen einen geeigneten Siedlungsraum bieten. Die Erforschung der ökofaziellen Struktur sowie der benthischen Nahrungsketten arktischer Flachwasserbiozönosen wurde von benthosbiologischen Arbeitsgruppen des SFB 313 sowie von Arbeitsgruppen des DFG-Schwerpunktprogrammes "Globale und regionale Steuerungsprozesse in der biogenen Sedimentation" verfolgt.

Im Gegensatz zu Fahrtabschnitt 4 lag der Schwerpunkt des 5. Abschnittes im Bereich des Kaltwasserausstromes des Europäischen Nordmeeres auf der grönländischen Seite. Die Anreise von Trondheim wurde dabei genutzt, um die auf dem Vöring Plateau begonnenen Zeitreihen fortzusetzen, einen Ost-West-Transekt durch die verschiedenen Wassermassen aufzunehmen und die seit 1985 permanent betriebene Verankerung im Lofotbecken auszuwechseln.

Das Sedimentationsgeschehen im Bereich des Ostgrönlandstromes ist durch die Nähe zur Eiskante geprägt, an der sich starke Diatomeenblüten entwickeln können, die ihrerseits deutliche Sedimentationspulse auslösen. Erstmals wurde in diesem Gebiet auf der METEOR-Reise Nr. 10/3 grüner "Fluff" auf dem Meeresboden gefunden. Ziel dieser Reise war es, die Abbildung solcher Ereignisse im Sediment und die Auswirkung auf die Besiedlungsmuster unter den besonderen Bedingungen des Kontinentalhanges, an dem die Prozesse durch laterale Advektion verstärkt werden, zu untersuchen.

Auf der Heimreise ergab sich die Gelegenheit, nordöstlich von Island auf dem Island-Färoer-Rücken Sedimentkerne zu nehmen. An diesem Material soll analysiert werden, wie sich die Wassermassen, die das Europäische Nordmeer verlassen, im Sediment dokumentieren und die quartären Ausstromverhältnisse rekonstruiert werden.

4 Ablauf der Reise

4.1 Erster Fahrtabschnitt

METEOR war, von ihrer 20. Reise aus dem Südostatlantik kommend, am 13.03.1992 in Las Palmas eingelaufen. Am 15.03., schifften sich die Arbeitsgruppen für den ersten Fahrtabschnitt der Reise Nr. 21 ein. Am 16.03. wurden 2 Transport-Container, 1 Kaltlabor-Container, 1 Isotopenlabor, 1 Chemieabfall-Container und 1 Radiosonden-Container übernommen und weitere 3 Transport-Container an der Pier entladen. Außerdem wurde ein 6 mm kunststoffummantelter Spezialdraht für spurenchemische Untersuchungen auf die Winde W3 aufgespult. Wegen unsachgemäßer Aufspulung auf die Transporttrommel durch die Lieferfirma riß der Draht bei der Übernahme auf die W3, so daß von den 5000 m nur etwa 3100 m, eine ausreichende Länge für die zunächst geplanten Arbeiten, übernommen werden konnten.

Am Nachmittag wurden etwa 80 Studenten des Faches Meereskunde von der Universidad de Las Palmas de Gran Canaria, Facultad de Ciencias del Mar, unter der Leitung von Dr. Santiago Torres Curbelo, die Ziele der Forschungsreise erläutert und in vier Gruppen das Schiff gezeigt. Dr. Torres hatte 1989 an der METEOR-Reise Nr. 10 teilgenommen und seither Kontakte zur BIO-C-FLUX-Arbeitsgruppe aufrecht erhalten.

Um 18.30 Uhr verließ METEOR den Hafen von Las Palmas und nahm Kurs auf die erste Station NW von Madeira auf 34°N, 20°W, die am Morgen des 18.03. erreicht wurde (Abb. 2). Zum Einsatz kamen eine CTD, u.a. um Tiefenwasser für die später durchzuführenden biochemischen Analysen und mikrobiologischen Versuche zu erhalten, sowie zwei Multinetze und zwei Multicorer. Trotz stark verringerter Gewichte drang der Multicorer so tief in das Sediment ein, daß die Proben nicht verwendbar waren. Die Suche nach geeignetem Sediment

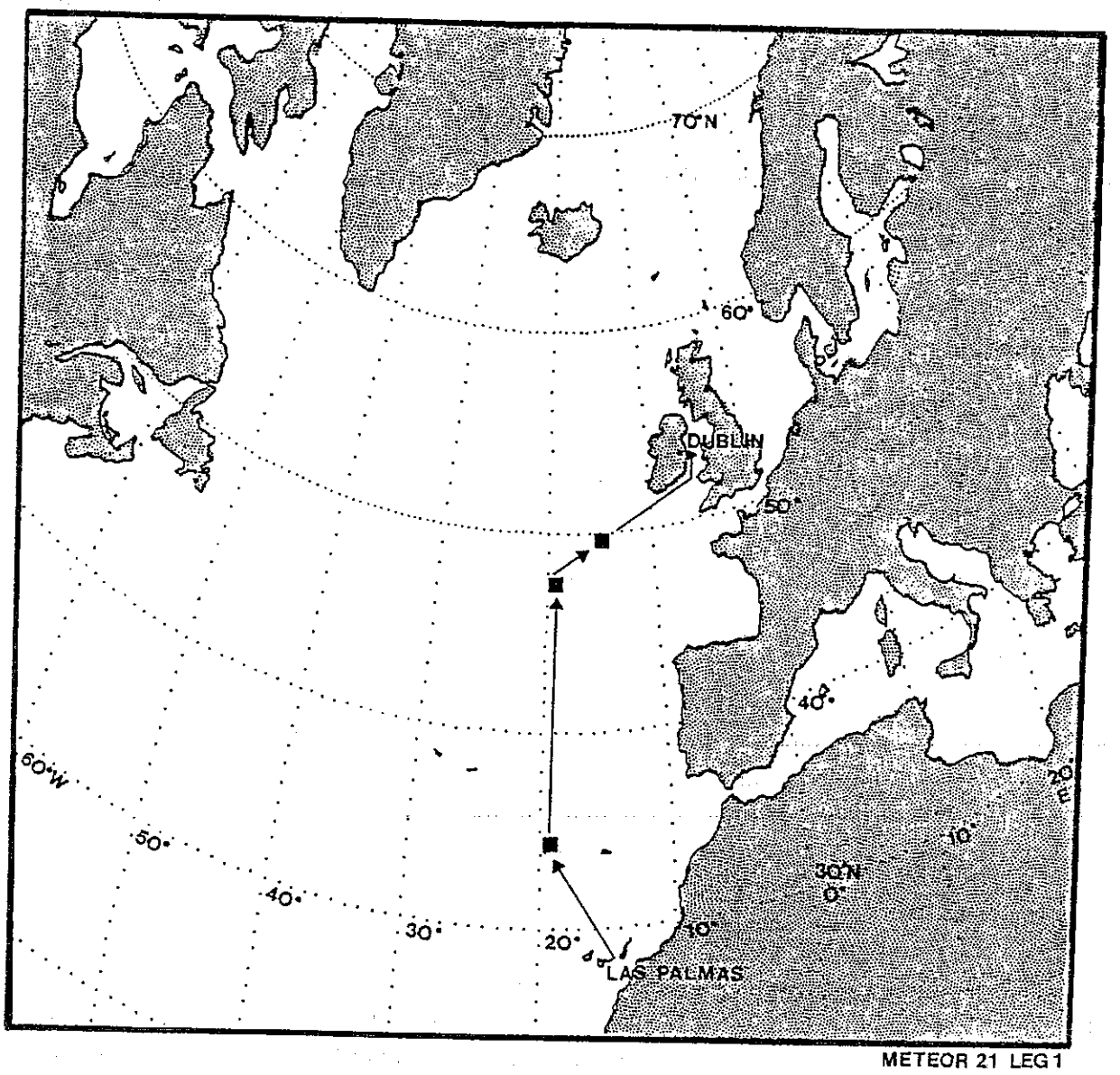

Abb. 2: Fahrtrouten und Untersuchungsstationen des ersten Fahrtabschnittes
Fig. 2: Cruise tracks and areas of investigation during leg 1

erschien aus zeitlichen Gründen mit großem Risiko behaftet, so daß die Station nach 17 Stunden abgebrochen und die Anreise zum Hauptarbeitsgebiet fortgesetzt wurde.

Für die nächsten zwei Wochen konzentrierten sich die Arbeiten im BIOTRANS-Gebiet nahe der JGOFS-Position 47°N, 20°W, in dem Benthos- und Tiefseeplankton-Untersuchungen schon seit 1984 und Oberflächenplankton-Arbeiten im Rahmen von JGOFS seit 1989 durchgeführt wurden. Die geplanten Arbeiten waren durch bestimmte Vorgaben zum Teil zeitlich und räumlich festgelegt. Die Benthos-Arbeiten sollten vorwiegend im Zentrum eines auszulegenden Transponderfeldes genommen werden, für das Mikro- und Makroplankton sollten Tag- und Nachtfänge außerhalb der Dämmerungszeiten gesammelt werden, und die Oberflächenplankton- und Hydrographiestationen sollten möglichst regelmäßig vormittags und im Nahbereich einer auszusetzenden Driftstation mit einer Sinkstoffalle gefahren werden. Weiterhin kam es in der Stationsplanung darauf an, eine optimale Reihenfolge für alle Projekte und Mitarbeiter zu finden. Die Wartezeit von etwa 1.5 Stunden zwischen dem Auslösen von Freifallgeräten und ihrem Erscheinen an der Oberfläche mußte genutzt werden, die Probensammlung für die Untersuchungen am Plankton, der Chemie und Hydrographie durften nicht während oder gleich nach der Bearbeitung von Bodenproben an Deck erfolgen, und die laborseitige Aufarbeitung der Sedimentproben war so aufwendig und mußte für die biochemischen Arbeiten so schnell geschehen, daß nur eine begrenzte Zahl von Multicorer- und Kastengreifereinsätzen in direkter Folge gefahren werden konnte. Diese zeitlichen und räumlichen Vorgaben erschienen zunächst recht zeitaufwendig. Die Verluste an Schiffszeit konnten jedoch in Grenzen gehalten werden.

Am 21.03. hatte METEOR die Sollposition gegen Abend erreichen können. Da es für die Transpondernavigation erforderlich war, die Dichtestruktur der Wassermassen zu kennen, die Plankton-Hydrographie-Station jedoch erst am nächsten Morgen gefahren werden sollte, wurden die Einsätze von zwei Geräten vorgezogen. Für geologische Untersuchungen bestand Interesse an Proben aus dem sogenannten "Lysoloch", dessen Sedimente bei über 4900 m Tiefe unterhalb der Lysokline liegen (während der Arbeiten 1986 zuerst beprobt und so benannt). Die Position 40 sm südlich der Ansteuerungsposition mußte bei der Anreise überlaufen werden, und so bot es sich an, dort auf dem Anmarsch einen Multicorer einzusetzen. Ohne Zeitverluste wurde das Lysoloch gefunden und am Nachmittag beprobt. Der Multicorer mit 6 großen Rohren (71 cm^2) und 4 kleinen Rohren (25 cm^2) brachte genügend Material, so daß zusätzlich auch biochemische Analysen durchgeführt werden konnten. Während der weiteren Anreise wurde das 1 m^2-MOCNESS-Netz (Multiple Opening Closing Net and Sensing System) für Mikro- und Makroplankton sowie Nekton eingesetzt, das bei nördlichen Winden in Richtung auf die Sollposition in Tiefen zwischen 1650 m und 400 m geschleppt werden und 8 Proben aus verschiedenen Tiefenstufen bringen konnte.

Auf der Sollposition im BIOTRANS-Gebiet, 47°10'N, 19°35'W, gleichzeitig die Position des Transponders A, wurde am 22.03. eine große Plankton-Hydrographie-Station gefahren, die regulär aus dem Einsatz von 2 Multisonden (CTD) bis 200 m und 4000 m, 3 Multischließ-

netzen bis 100 m, 700 m und 2000 m, 4 Apsteinnetzen bis 250 m und dem Einsatz der Secchischeibe bestand.

Anschließend wurden 4 Navigationstransponder (A-C) in einem Quadrat mit 3000 m Kantenlänge ausgelegt, und das Transponderfeld wurde vermessen. Dabei zeigte sich, daß Transponder B, 3000 m östlich von A, keine sinnvollen Werte lieferte und sogar die Navigation mit Hilfe der übrigen Transponder störte. Die Aufnahme von B wurde jedoch verschoben, da diese nachts nicht geschehen sollte und am nächsten Morgen die Sinkstoffallenkette 40 sm nördlich ausgesetzt werden sollte.

Bei weiterhin nördlichen Winden konnte beim Anlaufen der Aussetzposition wieder das MOCNESS eingesetzt werden. Das Aussetzen der Sinkstoffallenkette nahm am Vormittag des 23.03. zunächst 3.5 Stunden in Anspruch. Abschließend sollte das Abtauchen der Kopfboje beobachtet werden. Als diese jedoch nach 1.5 Stunden vom Grundgewicht nicht in die Tiefe gezogen worden war, war sicher, daß die Kette gerissen sein mußte. Der an der Oberfläche treibende Teil wurde wieder aufgenommen und dann entschieden, daß die Auslösung des unteren Teiles erst am nächsten Morgen um 6.00 Uhr erfolgen sollte. Dieser Teil ohne jegliche über die Meeresoberfläche hinausragende Markierung und mit nur 20 kg Restauftrieb konnte bei seiner tiefen Lage in der Wasseroberfläche in der kurzen noch hellen Zeit und bei 2.5 m hoher See nicht sicher aufgefunden werden. Die Nacht wurde wieder zum Fang von Plankton mit dem MOCNESS verwendet.

Am Morgen des 24.03. wurde die Restkette gegen 6.00 Uhr ausgelöst und um 7.30 Uhr an der Oberfläche erwartet. Die akustische Positionsmessung blieb - auch während der folgenden Stunden - erfolglos, vermutlich weil der Abstrahlungswinkel des in der Oberfläche treibenden Transponders im Restsystem so ausgerichtet war, daß der Empfänger unter dem Schiff die Signale nicht empfangen konnte. Vormittags und bis in den frühen Nachmittag wurde die Restkette für 5.5 Stunden mit zahlreichen Personen auf der Brücke und einem Ausguck auf der Plattform erfolglos gesucht. Dann wurde der Beschluß gefaßt, den oberen Teil der Kette mit nur zwei Fallen wieder auszusetzen. Kurz vor Beendigung der vorbereitenden Arbeiten wurde die Restkette doch noch gesichtet, aufgenommen und mit dem oberen Teil zusammen in der ursprünglich geplanten Konfiguration ausgesetzt. Das Abtauchen der Kopfboje erfolgte um 19.30 Uhr.

Während der anschließenden Rückfahrt zum Transponderfeld wurden keine Geräteeinsätze vorgenommen, um den nicht funktionsfähigen Transponder möglichst bald auszutauschen und mit der erneuten Vermessung des Transponderfeldes zu beginnen. Nach dem Auslösen wurde während der Wartezeit bis zum Erscheinen des Transponders an der Oberfläche ein flacher Einsatz mit dem MOCNESS (0 m-400 m) gefahren. Mit Hilfe seines Blinklichtes wurde der Transponder schnell gesichtet, aufgenommen, und der Ersatztransponder konnte sofort zu Wasser gelassen werden. Die anschließende Vermessung des Transponderfeldes wurde innerhalb von 4.5 Stunden erfolgreich abgeschlossen.

Nach Beendigung dieser vorbereitenden Arbeiten konnte das Routineprogramm zur Probensammlung beginnen. Dazu gehörten die Entnahme von Sedimentproben mit Multicorer und Kastengreifer, die Sammlung von Wasserproben mit einer Multisonde, der Fang von Plankton mit Multinetz und Apsteinnetz, die Beobachtung der Sichttiefe mit der Secchischeibe, der Fang von tieflebendem Mikro- und Makrozooplankton und Nekton mit dem $1m^2$-MOCNESS sowie der Fang von benthopelagischen Carnivoren und Aasfressern mit beköderten Fallen.

In Ergänzung der regelmäßig eingesetzten Geräte wurden andere nur gelegentlich verwendet: Expandable Bathythermographs (XBT) wurden auf längeren Fahrtstrecken im Bereich um das BIOTRANS-Gebiet abgeworfen, um die hydrographische Struktur genauer zu erfassen. Eine driftende Sinkstoffalle wurde am 01.04. im NO des Transponderfeldes ausgesetzt und am 03.04. im SO wieder aufgenommen. Dieses mit Hilfe von Satellitentelemetrie zu ortende System wurde am 04.04. erneut ausgesetzt, um während des 2. Fahrtabschnittes verfolgt und aufgenommen zu werden. Das Freifall-Greifer-Respirometer wurde ebenfalls am 04.04. in der Nähe des Transponderfeldes ausgesetzt, um den Sauerstoffverbrauch der benthischen Lebensgemeinschaft zu messen. Es wurde auf dem 2. Fahrtabschnitt wieder aufgenommen.

Erfolglos blieben alle Versuche, die Tiefsee-Videoanlage zum Einsatz zu bringen. Mit großem Zeitaufwand wurde die Anpassung des Systems an das Tiefseekabel vorgenommen. Beim ersten Einsatz am 01.04. mit dem Fototrawl zeigte sich jedoch, daß das 18 mm Koaxialkabel nicht mehr brauchbar war. Nachdem bereits über 3000 m Länge ausgesteckt waren, wurde festgestellt, daß zahlreiche äußere Kardele des Kabels beim Laufen über die Friktion brachen. Das Gerät wurde mit großer Vorsicht wieder an Deck gehievt. Versuche, die Videoanlage allein über die 9 mm und 6 mm Koaxialkabel zu fahren, scheiterten ebenfalls, da das Videosignal von ihnen nicht übertragen wurde. Diese Kabelmängel haben die Arbeiten über das Megabenthos erheblich zurückgeworfen.

Während der gesamten Reise wurde über einen Ansaugstutzen im Lotschacht aus dem Niveau des Schiffsbodens Wasser für chemische Analysen angesogen. Sie dienten der Erfassung des Kohlendioxidsystems über die kontinuierliche Bestimmung des gesamten Kohlendioxides, der Alkalinität, des pH-Wertes und der Salinität.

Die Arbeiten wurden im BIOTRANS-Gebiet zweimal durch Sturm unterbrochen. Am 28.03. mußten abends die weiteren Probennahmen bis zum 31.03. mittags eingestellt werden. Der Sturm erreichte Stärken von 9-10 Bft, in Böen bis 12 Bft. Bei Windstärken um 9 Bft mußten die Arbeiten in den frühen Morgenstunden des 03.04. noch einmal unterbrochen werden, so daß von der insgesamt schon knappen Arbeitszeit insgesamt 3 Tage ausgefallen sind.

Nach der akustischen Auslösung der Meßplattform im Respirometer am Abend des 04.04. lief METEOR mit NO-Kurs aus dem BIOTRANS-Gebiet ab und schleppte dabei das MOCNESS-Netz über eine Strecke von 20 sm. Die einzelnen Netze wurden in 300 m bis 500 m über

Grund ausgelöst, entsprechend Wassertiefen von 4150 m bis 3950 m. Am Ende der Schleppstrecke wurde noch eine ausführliche Plankton-Hydrographie-Station gefahren.

Im Rahmen der EG-Forschungsförderung wird durch die Marine Science and Technology (MAST I und II) Programme zur Zeit ein Tiefseevorhaben finanziert: "Natural Variability and the Prediction of Changes in a Deep-sea Benthic Environment". Ein zweites befindet sich in Vorbereitung: "OMEX - Ocean Margin Experiment". An beiden Programmen ist das Institut für Hydrobiologie und Fischereiwissenschaft der Universität Hamburg beteiligt, und einige, wenig Zeit in Anspruch nehmende Arbeiten waren an je einer Station im Anschluß an die Arbeiten im BIOTRANS-Gebiet bei der Anreise nach Dublin vorgesehen.

METEOR erreichte die erste der beiden Stationen, in der Porcupine Abyssal Plain (48°51'N, 16°29'W) am Morgen des 06.04., wo noch während der Dunkelheit ein Multicorer erfolgreich in über 4800 m Wassertiefe gefahren werden konnte. Anschließend wurden für die britischen Projektpartner vom Institute of Oceanographic Sciences Deacon Laboratory Geräte aufgenommen bzw. ausgesetzt. Kurz vor 6.00 Uhr wurde eine Freifallkamera ausgelöst, die im Mai 1991 ausgesetzt worden war. Ursprünglich sollte diese im Oktober 1991 durch R.V. CHARLES DARWIN aufgenommen werden, jedoch wurde dieses durch ungünstiges Wetter verhindert. Das Kamerasystem erreichte kurz nach 7.00 Uhr die Oberfläche und war bereits vor 8.00 Uhr an Deck genommen. Anschließend wurde eine zweite Station (48°57'N, 16°19'W) in 12 sm Entfernung angelaufen, wo eine weitere Kamera und in deren Nähe 3 Sinkstoffallen in einer Kette mit einem Strömungsmesser und einer Sinkstoffkamera ausgesetzt wurden. Diese Arbeiten waren kurz nach Mittag abgeschlossen.

Bei achterlichem Wind mit Stärken bis zu 9 Bft lief METEOR zur nächsten Station auf dem Goban Spur (49°30'N, 13°10'W), um dort am 07.04. als Vorbereitung für das OMEX-Programm 3 Multicorereinsätze zu fahren.

Mit der Station auf dem Goban Spur waren die wissenschaftlichen Arbeiten des 1. Fahrtabschnittes dieser Expedition abgeschlossen, und METEOR trat die Reise nach Dublin an, wo sie am 09.04. um 9.00 Uhr fest war. Am selben Tag verließen die wissenschaftlichen Arbeitsgruppen das Schiff, bis auf diejenigen Personen, die auch am 2. Fahrtabschnitt teilnehmen sollten. Die neuen Gruppen reisten am 10. und 11.04. an.

Am Abend des 11.04. wurde ein Empfang an Bord der METEOR ausgerichtet, an dem der Landwirtschaftsminister der Republik Irland, offizielle Vertreter der Hafenbehörden und des Meteorologischen Dienstes sowie Wissenschaftler aus der Republik Irland und aus Nordirland teilnahmen.

4.2 Zweiter Fahrtabschnitt

METEOR lief planmäßig am 12.04.1992 von Dublin aus. Bedingt durch einen lokalen Streik in Dublin mußten die beiden aufzunehmenden Container nach Cork umgeleitet werden, wo sie am nächsten Tag ohne Probleme übernommen werden konnten, so daß METEOR am Abend des 13.04. die Reise fortsetzen konnte.

Nach zwei Probestationen am 15.04. wurde am 16.04. der Langzeitdrifter, der zum Ende des Fahrtabschnittes M 21/1 ausgelegt worden war, geborgen. Er war mit einer automatischen Sinkstoffalle und einem Aanderaa-Strommesser bestückt.

Mit einem Stationsabstand von 13 sm wurde dann ein hydrographischer Schnitt ins BIOTRANS-Gebiet bei 47°N und 20°W gefahren (Abb. 3). In dem während M 21/1 ausgelegten Transponderfeld von 3000 x 3000 m wurden am 17.04. drei Multicorer-Beprobungen erfolgreich durchgeführt und danach das ebenfalls auf dem vorigen Fahrtabschnitt verankerte Respirometer aus 4500 m Wassertiefe geborgen.

In den nächsten 36 Stunden wurde in einem Quadrat mit 46 sm Kantenlänge die hydrographische Struktur untersucht. Anhand der Ergebnisse der Schnittfahrten wurde die Ausgangsposition der Driftstudie ausgewählt und am Ostersonntag, dem 19.04., die Auslegung des Tages- und Langzeitdrifters (14 Tage) vorgenommen. Am Ostermontag wurde zusätzlich zu den bereits durchgeführten chemischen Analysen der Luft mit der international verabredeten Beprobung der Wassersäule begonnen und eine Reihe von Laborexperimenten gestartet.

Die Arbeiten an der Driftstation bei 47°N, 20°W wurden nach einem Standardprogramm durchgeführt:

- Nach einer morgendlichen CTD-Station bis 1000 m Wassertiefe wurde der Tagesdrifter aufgenommen und die Sammelgläser, in denen sich das absinkende Material angereichert hatte, ausgewechselt. Eine Doppelfalle wurde gleich danach wieder für 24 Stunden ausgelegt - zusätzlich wurde während des Tages ein Inkubationsrigg zur in situ-Messung der Primärproduktion angebracht.
- Danach wurden verschiedene Schließnetze in unterschiedlichen Tiefen gefahren - abgelöst von weiteren CTD-Fluoreszenzprofilen. Wasserproben wurden mit einer Rosette mit 24 x 10-Liter-Wasserschöpfern an Deck gebracht. In den Labors wurden die meisten Analysen des Wassers und der Luft gleich durchgeführt, um die Ergebnisse für die Meßstrategie zu nutzen. Außerdem wurde eine Reihe von Experimenten mit Hochseeplankton durchgeführt.

Am 23.04. gegen Abend mußten die Stationsarbeiten bis zum 26.04. eingestellt werden. Bei Sturm zwischen 8 und 10 Bft hatte sich eine rauhe See aufgebaut, die durch eine unangenehme hohe Dünung ca. 45 Grad zur Windrichtung noch verstärkt wurde.

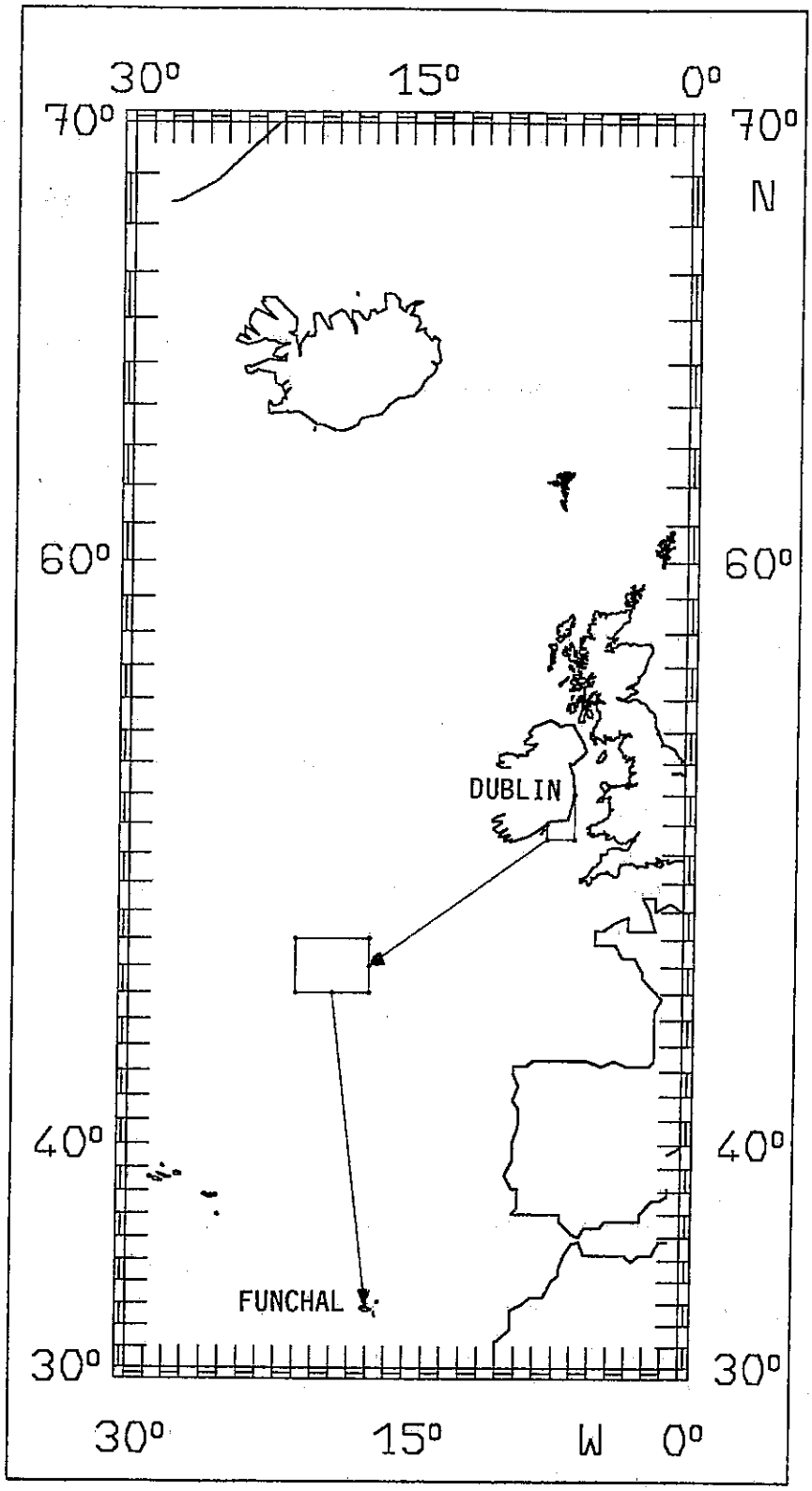

Abb. 3: Fahrtrouten und Untersuchungsstationen des Fahrtabschnittes M 21/2
Fig. 3: Cruise tracks and areas of investigations during leg 2

Am 28.04.1992 wurden im Transponderfeld erfolgreich drei Multicorer gefahren. Nachdem das Schiff zum Tagesdrifter zurückgekehrt war, wurden dort die JGOFS-Untersuchungen zur Charakterisierung der biogeochemischen Prozesse in der Wassersäule bis zum 02.05. fortgesetzt. Am gleichen Tag wurde der Langzeitdrifter am Morgen geborgen, neu programmiert und am Nachmittag wieder ausgelegt. Er sollte während des nächsten Abschnittes (M 21/3) wieder geborgen werden. Gegen 19.00 Uhr wurden die Stationsarbeiten am 02.05. beendet und METEOR nahm Kurs auf das ca. 900 sm entfernte Funchal/Madeira.

Im Madeira Becken wurden am 04.05. die drei an Bord befindlichen CTD-Sonden noch einmal bis zum Boden eingesetzt, um ihre Eichung zu überprüfen.

METEOR lief planmäßig am 06.05.1992 morgens in Funchal ein. Damit war der Fahrtabschnitt M 21/2 beendet.

4.3 Dritter Fahrtabschnitt

METEOR verließ am Sonnabend, den 09.05. um 10.00 Uhr den Hafen von Funchal und erreichte am 10.05. um 13.00 Uhr das Arbeitsgebiet im Madeira Becken (34°N, 22°W, Hauptstation 1) (Abb. 4).

Auf der Anreise wurde das "Kieler Pumpsystem" im hydrographischen Schacht zur kontinuierlichen Entnahme von Oberflächenwasserproben eingebaut.

Im Rahmen von BIO-C-FLUX wurden im Madeira Becken zweimal Oberflächensedimente mit einem Multicorer genommen. Da die Länge des auf der W12-Winde vorhandenen 18 mm Drahtes für die Wassertiefe (5400 m) nicht ausreichte, der im Laderaum vorhandene, längere Draht für den Einsatz der 400-Liter-Schöpfer aber nicht wünschenswert erschien, wurde für diese Station eine Notlösung mit einem Vorläufer gefunden.
Die Untersuchungen der Wassersäule wurden mit der CTD/Rosette begonnen, gefolgt von Multischließnetzen der Tübinger Planktologen auf 100, 500 und 2500 m. Von den Kieler Chemikern wurden 400-Liter-Schöpfer aus Edelstahl für die Analyse organischer Stoffe, 30-Liter-GoFlo-Schöpfer für Spurenelemente und eine Serie von neuentwickelten Pumpen für die in situ-Filtration und Adsorption von organischen Stoffen aus dem Wasser an XAD-Harzen eingesetzt. Am Anfang ergaben sich noch Schwierigkeiten mit den computergesteuerten Pumpen, aber mit Hilfe der Schiffselektroniker konnten Anpassungen an Hardware und Software erfolgreich vorgenommen werden. Die Testphase dieser neuen Systeme kann als abgeschlossen betrachtet werden, die in situ-Pumpen sind bis zu einer Tiefe von 6000 m und bis zu 14 Stunden einsetzbar (extrahiertes Volumen 600 Liter bez. für 24 Stunden und 1000 l). Am Ende der Stationsarbeiten wurden noch ein Multischließnetz in 100 und 500 m und zweimal der Multicorer eingesetzt.

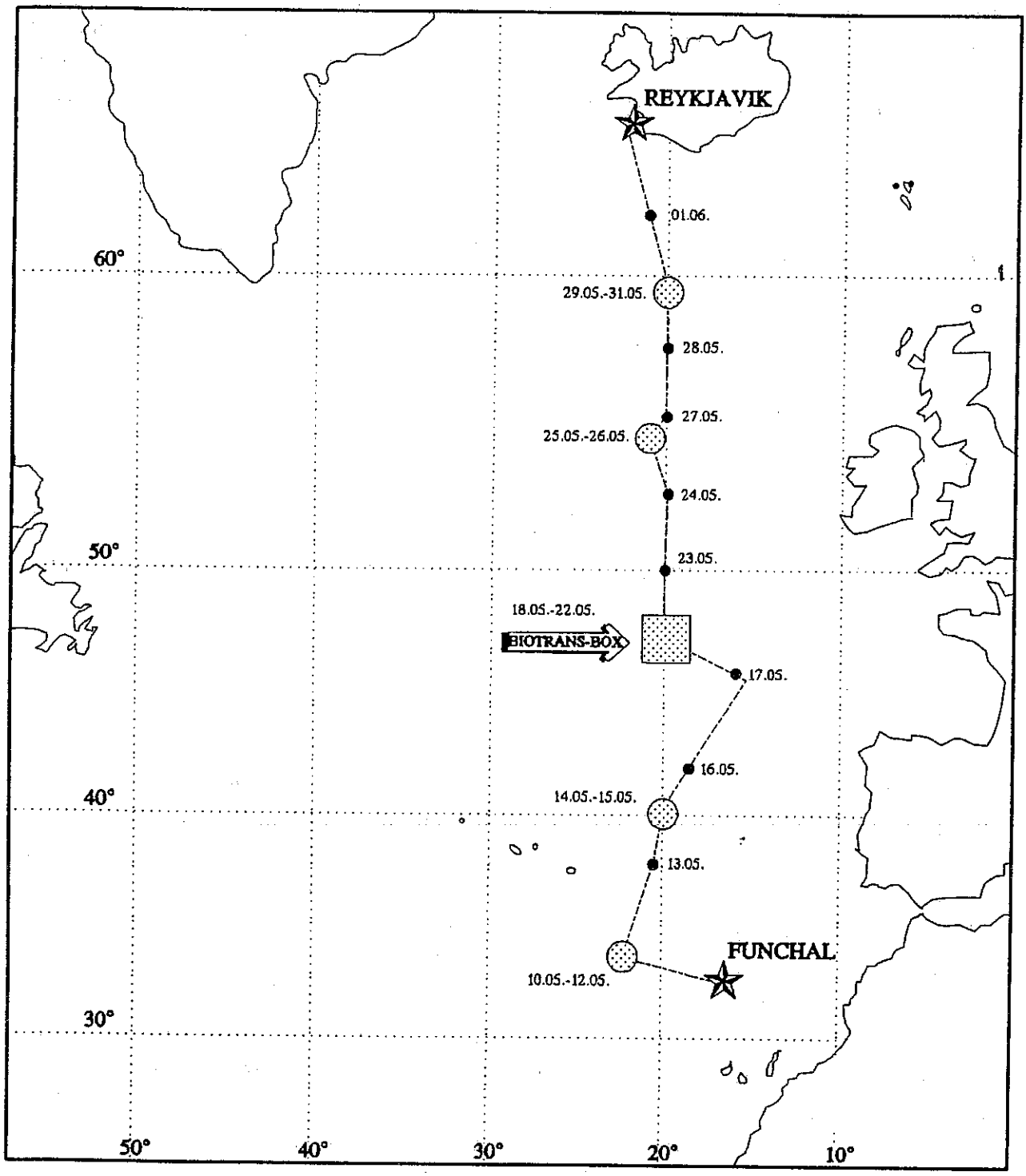

Abb. 4: Fahrtrouten und Untersuchungsstationen des Fahrtabschnittes M 21/3
Fig. 4: Cruise tracks and areas of investigations during leg 3

Die Arbeiten auf 34°N, 21°W wurden am 12.05. um 14.00 Uhr beendet. Die zweite Hauptstation (40°N, 20°W) wurde am 14.05. um 7.00 Uhr erreicht. Der Ablauf fand nach demselben Muster wie an der ersten Hauptstation statt. Die in situ-Pumpen wurden über Nacht eingesetzt, um die anderen Arbeiten möglichst bei Tageslicht durchführen zu können. Zusätzlich wurden Tiefenwasserproben mit dem GoFlo-Schöpfer für die Bestückung der Sedimentfalle am nächsten Tag genommen. In einer Tiefe von 1000 m wurde der einzusetzende Auslöser getestet. Am 15.05. um 21.00 Uhr wurde diese Station beendet.

Die auf dem Abschnitt M 21/2 ausgebrachte Drifterfalle wurde am 17.05. um 7.30 Uhr bei günstigen Windverhältnissen auf 44°52.40'N, 15°46.98'W geborgen.

Auf der Strecke zur dritten Hauptstation (47°N, 20°W) wurde, wie auch während der sonstigen Fahrtstrecken, das "Kieler Pumpsystem" benutzt, um größere Wassermengen für die Analysen in der Oberflächenschicht sammeln zu können. Im BIOTRANS-Gebiet wurde ein verlängertes Standardprogramm durchgeführt. Es wurde am 18.05. eine Verankerung mit Sinkstoffallen ausgelegt. Leider sank die Kopfboje wegen eines Bruches der Kevlar-Verbindung bei 2500 m nicht ab. Der größte Teil der Verankerung wurde trotzdem geborgen. Obwohl der Auslöser dieser Verankerung wahrscheinlich funktioniert, ließ er sich nicht ansprechen. Bis spät abends wurde am 19.05. sowie auch am 20.05. bis 12.00 Uhr nach den Resten der Verankerung erfolglos gesucht. Eine Sinkstoffalle und fünf Auftriebskugeln müssen daher als verloren betrachtet werden. Trotz der Verluste wurde die Verankerung L2-92-B mit 4 Sinkstoffallen unverändert am 20.05. auf 47°47.60'N, 19°47.00'W ausgelegt. Eine mit physikalischen Meßgeräten bestückte Verankerung (L2-92-PH) wurde am 19.05. auf 47°43.8'N, 19°54.3'W ausgelegt. Mit drei Multicorer-Einsätzen im Transponderfeld wurden die Arbeiten im Bereich 47°N, 20°W am 22.05. um 16.00 Uhr beendet.

Am 23.05. wurde, hauptsächlich zur Aufnahme eines pCO_2-Profils, auf 50°N, 20°W eine CTD-Station gefahren, anschließend folgte ein flaches Multischließnetz. Ein ähnliches Programm fand am 24.05. auf 52°30'N, 20°W statt, gefolgt von einer Tiefenwasser-Probenahme mit dem GoFlo-Schöpfer für die Füllung der Probenflaschen in den auszulegenden Sinkstoffallen.

Am 25.05. wurde eine mit vier Sinkstoffallen bestückte Verankerung (L3-92) auf 54°32.0'N, 21°04.4'W und am 26.05. eine mit physikalischen Meßgeräten bestückte Verankerung (L3-92-PH) auf 54°42'N, 21°14'W ausgelegt. Daneben wurde das Standardmeßprogramm durchgeführt (Hauptstation 5, 3000 m Wassertiefe, 25.05., 5.00 Uhr bis 28.05., 22.00 Uhr). Am Morgen des 28.05. wurden Multischließnetz, Planktonnetz (Paläontologie/ Planktologie, Kiel), CTD und in situ Pumpen gefahren. Die Arbeiten auf Hauptstation 5 wurden um 22.00 Uhr beendet.

Am 29.05. wurde die letzte Station (59°30'N, 20°W, Hauptstation 6) erreicht. Mit jeweils zwei Multicorern, in situ-Pumpen, Multischließnetz, CTD, hochauflösenden pCO_2-Messungen in

der Oberflächenschicht und anschließend einmal GoFlo-Schöpfern und Planktonnetz wurde allen Wünschen der Teilnehmer bei schönem Wetter während fast der gesamten Fahrt nachgekommen. METEOR verließ die letzte Station am 01.06. um 0.00 Uhr und beendete den Fahrtabschnitt M 21/3 in Reykjavik am 02.06. um 6.00 Uhr.

4.4 Vierter Fahrtabschnitt

Infolge umfangreicher Verladearbeiten und hohem Zeitaufwand für das Umspulen des Tiefseedrahtes liefen wir mit einer zeitlichen Verzögerung am 05.06.1992 um 18.10 Uhr UTC in Reykjavik aus. Beim Versegeln mit Südostkurs pickten wir südlich von Island etwas rauhere See und frischen Wind auf, der sich in der Folge auf Windstärken zwischen 7 und 8 Bft einpendelte, ein erster Test der Seetauglichkeit des Wissenschaftlerteams. Nach dem Durchzug der Front verbesserte sich die Wetterlage erheblich, so daß die Arbeiten auf der ersten Station an der Südflanke des Island-Färöer-Rückens Sonntagnacht 3.10 Uhr UTC, 07.06.92 programmgemäß mit einer Probennahme und Messungen in der Wassersäule (CTD/KWS, Multinetz, Radiolariennetz) begonnen werden konnten (Abb. 5). Anschließend erfolgte eine Beprobung der oberflächennahen Sedimentschichten mit dem Großkastengreifer (GKG). Während des Transektes zum Barentsseehang wurde in den folgenden Tagen (Montag, 08.06.92 bis Freitag, 12.06.92) ein gleichartiges Meß- und Beprobungsprogramm auf Stationen am Nordrand des Island-Färöer-Rückens (M 21/224, 225), dem Südhang des Norwegischen Beckens (M 21/226), der Ostflanke des Ägirrückens (M 21/227), im Lofotbecken (M 21/228, 229) und am Hang des Barentssee-Sedimentfächers durchgeführt. Generell konnten die Arbeiten ohne größere technische Schwierigkeiten durchgeführt werden. Probleme ergaben sich bei den CTD-Messungen. Nach längerer Fehlersuche wurde festgestellt, daß ein falscher Codierfile von der Herstellerfirma installiert worden war. Durch Umschreiben entsprechender Teile des Meßprogrammes konnte der Fehler behoben und die erhobenen Grunddaten gesichert werden. Die erfolgreiche Lösung des CTD-Problemes ist ein gutes Fallbeispiel für die generell sehr gute Zusammenarbeit zwischen Schiffsführung, Besatzung und Wissenschaftlerteam.

Auf den vier Stationen zwischen Ägir-Rücken und Zentralstation im Lofotbecken zeigten sich deutliche Unterschiede in der Zonierung der Wassersäule. Südlich des Island-Färöer-Rückens war in 50 m Tiefe eine Thermokline ausgebildet, gekoppelt mit einem Chlorophyll-Maximum zwischen 40 m und 60 m. Die CO_2-Werte in der Wassersäule, die ständig parallel von der CO_2-Gruppe gemessen wurden, waren jedoch recht hoch und sprachen nicht für eine Blütensituation. Es wurde ein hoher Anteil atlantischer Warmwasserfauna beobachtet. Im Bereich der nördlichen Flanke des Island-Färöer-Rückens lag die Thermokline in der gleichen Tiefe. Große Anreicherungen von Diatomeen (*Rhizosolenia spp.*) korrespondierten hier mit einem CO_2-Minimum in den oberen 40 m. Weiter nördlich im Bereich des Ägir-Rückens lag die Thermokline wesentlich höher (10-15 m). In den oberen 20 m wurden ebenfalls große Mengen von Diatomeen (*Rhizosolenia spp.*) und zudem *Phaeocystis spp.* beobachtet (geringe

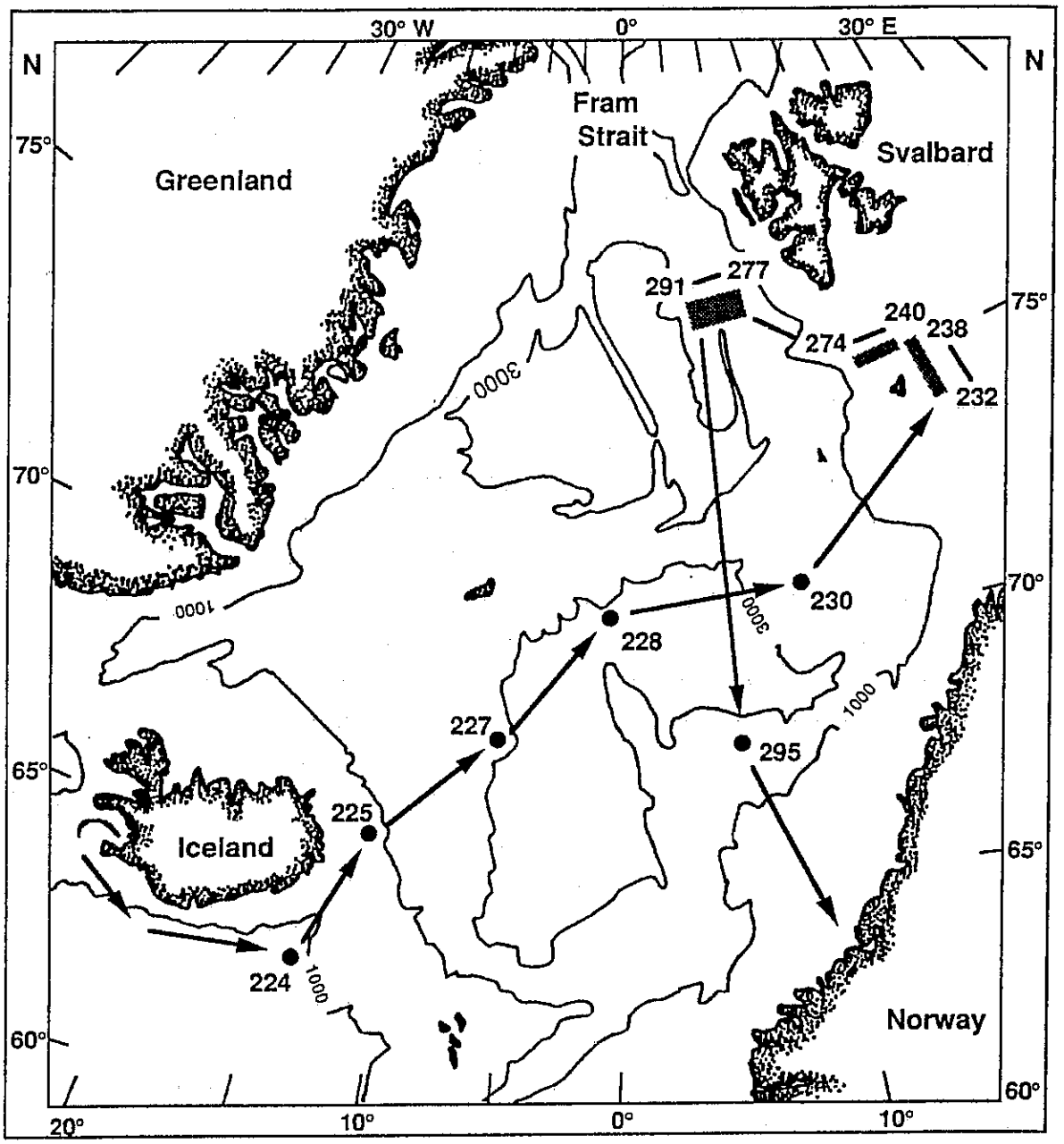

Abb. 5: Fahrtrouten und Untersuchungsstationen des Fahrtabschnittes M 21/4

Fig. 5: Cruise tracks and areas of investigations during leg 4

CO_2-Werte). Im unteren Bereich dominierten Phytodetritus und Pellets sowie deren Produzenten. Zudem waren Phaeodarien in großen Mengen in der Fauna vorhanden. Auf der Zentralstation im Lofotbecken lag die Thermokline wieder bei 50 m Wassertiefe, und Phytoplankton war nur in sehr geringen Mengen vorhanden. Auffällig waren hingegen die enormen Mengen von Copepoden. Die CO_2-Messungen ergaben hohe Werte.

Auf der Station am Ägir-Rücken (M 21/227) wurde im Anschluß an eine ausführliche 3.5 kHz/Hydrosweep/Parasound-Vorerkundung die Sedimentsäule mit GKG und KAL beprobt. Der GKG-Einsatz erbrachte ein ungestörtes Profil der postglazialen und holozänen Abfolge mit der Einschaltung einer markanten Aschenlage, bei der es sich um die auf 10.6 ka datierte Vedde-Asche handelt, die somit einen sehr guten stratigraphischen Marker darstellt. Außerdem wird das holozäne Klimamaximum durch einen hellen, 5 cm mächtigen, karbonatreichen Horizont deutlich abgebildet. Die Basis des GKG bei 50 cm endet in Eisdriftsedimenten mit zahlreichen Sand-Dropstones. Das 4.75 m lange KAL Profil beprobt eine Schichtfolge der Isotopenstadien 1-6 in der für dieses Seegebiet typischen Ausbildung. Besonders auffällig sind dunkelolivgraubraune Diamikthorizonte, die vermutlich in die in das Isotopenstadium 6 einzustufende Schichtfolge eingeschaltet sind. Diese Horizonte enthalten hohe Konzentrationen von bis zu mehreren cm-großen Gesteinsdropstones und zahlreiche vom Eis verfrachtete Schlammklasten. Als weiteres charakteristisches Merkmal fällt der hohe Anteil an Kohlefragmenten auf. An der Basis des Kernes ist eine Rutschmasse angeschnitten. Ein 0,4 m mächtiger Bereich im mittleren Abschnitt des Kernes ist durch Hangkriechen leicht deformiert worden. Zusätzlich wurden Agassiztrawl-Einsätze am Nordhang des Island-Färöer-Rückens (M 21/226) bei 2200 m und in der Tiefsee-Ebene des Lofotbeckens (M 21/229) gefahren. Die AGT-Einsätze erbrachten an Station M 21/226 eine reiche Fisch- und Kieselschwammausbeute, sowie an Station M 21/229 ein typisches Weichboden-Tiefseebenthos mit irregulären Seeigeln, kleinen Kieselschwämmen (*Thenea abyssorum, Cladorhiza, Clathria*), zahlreichen cm-großen Seegurken, Meerasseln sowie einigen kleinen Pecten und Schnecken.

METEOR lief das erste Hauptarbeitsgebiet (Bäreninseltrog, Leirdjupet und Kveitehola-Trog) am 13.06.92, an. Die Meeresgebiete im Westabschnitt der Spitzbergenbank und der angrenzenden Tröge gehören mit Sicherheit zu den interessantesten Schelfregionen des Europäischen Nordmeeres. Die Gründe sind vielfältig. Es handelt sich um eines der potentiellen Gebiete, in denen sich über flachen Schelfbänken dichte Winterwässer bilden, die in die angrenzenden Tiefseegebiete durch Zufuhrkanäle abströmen. Die Kaltwasserkarbonatvorkommen am Top und oberen Hang der Spitzbergenbank sind in ihrer Dimension und Genese von grundsätzlicher Bedeutung für das Phänomen "Karbonatanreicherung in hohen Breiten". Entlang der ozeanischen Front atlantischer Wassermassen und des kalten Hopen-Spitzbergenstromes entwickelt sich am Rand der Spitzbergenbank eine Hochproduktionszone.
Um Beiträge zu den o.a. Themenkomplexen zu liefern, wurden in der Zeit von Samstag, den 13.06., bis Mittwoch, den 17.06.92, (Stationen M 21/232-274) neben einer umfangreichen geologischen und benthosbiologischen Beprobung auch Video- und Unterwasserphotosurveys der oberen Hangregionen der Spitzbergenbank und CTD-Trübemessungen in der Kveite-

holarinne, einer der potentiellen Zufuhrkanäle für dichte Winterwässer, durchgeführt. In der Kveiteholarinne wurde eine ausführliche 3.5 kHz/Parasound/Hydrosweep-Kartierung, aufbauend auf den Ergebnissen früherer Ausfahrten, fertiggestellt. Die typische asymmetrische Sedimentverteilung in der Kveiteholarinne, mit randlichen mächtigen holozänen Sedimentkissen und geringmächtigen Rinnenfüllungen, weist eine unterschiedliche benthische Besiedlung auf. Der Auslaß des Kveiteholas zeigt typische Restsedimentdecken über glaziomarinen Sedimenten.

Im Leirdjupet, einer morphologisch ähnlichen Zufuhrrinne am Abfall der Spitzbergenbank in den Bäreninseltrog wie die Kveiteholarinne, wurde ein 7.57 m mächtiges KAL-Profil gewonnen, das für Fragen der Herkunft und Variation des organischen Materiales außerordentlich interessant erscheint. Neben resuspendierten Schwarzschieferfragmenten kommt eine autochthone C_{org}-Komponente an der Hochproduktionszone im Randbereich der Spitzbergenbank hinzu. In der Wassersäule fanden wir eine sehr starke Anreicherung von Phytodetritus sowie Larven von Flachwasserbenthos (benthische Foraminiferen, Echinoiden etc.).

Der Videosurvey entlang zweier Profile von 150 m Wassertiefe zum Top der Spitzbergenbank bei 40 m Wassertiefe war für uns alle ein erster Höhepunkt. Die Bildqualität war durchweg vorzüglich, und durch Beschweren des Videogestelles mit Bleigewichten waren die Absetzmanöver sehr gut und kontrolliert durchführbar. Auf den 120 m, 100 m und 80 m Stationen beobachteten wir eine sehr dichte Besiedlung von Geröllfeldern (Restsedimentdecken, die fast ausschließlich aus den im Untergrund anstehenden jurassischen Schwarzschiefern bestehen) in Verzahnung mit Schalenanreicherungen (überwiegend frühholozäne *Mya truncata*). Der Bewuchs (Balaniden, dickästige Bryozoen, Hydrozoen, Weichkorallen) war abschnittweise so dicht, daß regelrechte Wälder aufgebaut waren. Lokal fanden wir dichte Ansiedlungen von *Chlamys islandica* mit riffartigen Aufwüchsen auf den Dorsalklappen. In den Flachwasserstationen nahm die Strömungsenergie sehr stark zu, und es herrschten Schill- und Karbonatsandböden vor. Am Top der Bank fegte ein Unterwassersturm Sandfahnen vorbei.

Die Kveiteholarinne weist in ihrem Mittelabschnitt eine asymmetrische Sedimentfüllung auf, mit einem bis zu 40 m mächtigen holozänen Sedimentkissen in Leeposition und einer geringmächtigen Folge im Prallhang der Rinne. Abhängig von den unterschiedlichen Substraten variierte auch das Benthos. Die weichen, dunkelgraugrünen Schlicke in Leeposition weisen einen sehr dichten Besatz von bis zu 20 cm langen Wurmröhren auf. Bereits in einer Korntiefe von einigen wenigen cm setzt Sulfatreduktion ein. Die wesentlich geringer mächtigen Prallhangsedimente enthalten sandige Lagen und führen horizontweise Anreicherungen von Muschelklappen und Karbonatdetritus, der vom Top und höheren Hang der Spitzbergenbank eingetragen wurde. Eine nach Norden zum Top der Spitzbergenbank verlaufende Seitenrinne des Kveiteholas, die möglicherweise einen Hauptzufuhrkanal für ablaufende dichte Wassermassen von der Bank darstellt, wurde genau vermessen, mit Unterwasservideo und Bodenkamera erkundet und beprobt. Die in den 3.5 kHz/Parasound-Profilierungen aufgezeichnete

Sedimentverteilung in dieser Seitenrinne bestätigte diese Vermutung. Im Einlaufbereich der Seitenrinne in den Kveitehola wurden bis zu 15 m mächtige holozäne Schlicke kartiert. Nach Norden dünnt die Sedimentdecke aus und geht in Geröll- und Sandflächen über.

Am Ausgang der Kveiteholarinne wurde am 15.06.92 in 900 m Wassertiefe (Station M 21/247) eine Beprobung der Oberflächensedimente für benthosbiologische Fragestellungen durchgeführt, anschließend ein Einsatz der Bodenkamera, Aufnahme eines CTD-Meßprofiles und Beprobung der Wassersäule mit Multinetz und KWS. Wichtigste Fragestellungen waren die Erfassung von abströmenden dichten bodennahen Wassermassen und Untersuchungen der Planktongemeinschaften, speziell Tiefenwanderungsrhythmen planktischer Foraminiferen im Lunarzyklus. Anschließend versetzen wir zu einer Position im Tiefwasserbereich (2000 m Wassertiefe) des Barentssee-Sedimentfächers, um einen ersten Testeinsatz des im Teilprojekt (TP) B1 des SFB 313 neu entwickelten OBS-Systems durchzuführen. Das Gerätesystem besteht aus einem Hydrophon, das mit einem Bodengewicht am Meeresboden abgesetzt wird, und einem tiefgeschleppten Senderfisch. Beim Test wurde zunächst der unbeschwerte Empfänger ausgesetzt, seine Schwimmeigenschaften geprüft und das Anpeilen des Ortungssenders überprüft. Anschließend wurde das kombinierte Gerätesystem einschließlich des Bodengewichtes über den Heckgalgen ausgesetzt, um die Auslöser zwischen Fisch und Empfänger einerseits, und Empfänger und Bodengewicht andererseits unter realistischen Einsatzbedingungen in 2000 m Wassertiefe zu testen. Beim Ausfahren des Heckgalgens holte das Schiff über einen Wellenberg. Dabei konnte der Heckgalgen den aufgebauten Druck unverständlicherweise nicht halten, so daß er mit einem starken Schlag ein Stück frei durchfiel und mit seinem Gewicht den Stempel auf Backbordseite zerfetzte sowie die Zentralhydraulik lahmlegte. Nach Abklemmen des Heckgalgens von der Zentralhydraulik konnten die Stationsarbeiten fortgeführt werden. Alle Funktionstests des OBS-Systems verliefen erfolgreich und störungsfrei. Nach dem Versegeln wurden Suchprofile über die in den nächsten Tagen geplante OBS-Station gefahren und das Arbeitsprogramm in der Kveiteholarinne fortgesetzt. Der zweite Einsatz des OBS-Systems in einem Sedimentwellengebiet am Barentsseehang in 1400 m Wassertiefe mußte am 16.06. wegen zu starken Seeganges abgebrochen werden. Deshalb wurden die Arbeiten in der Kveitehola fortgesetzt, die am 17.06. mit einem Video- und Bodenkamerasurvey von der Seitenrinne des Kveiteholas zum Top der Spitzenbergenbank abgeschlossen werden konnten (Stationen M 21/263-271). Noch am gleichen Abend versegelten wir zum zweiten Hauptarbeitsgebiet, mit Kurs auf den nördlichen Knipovitchrücken.

Am 18.06. wurde ein umfangreiches Kernentnahmeprogramm auf verschiedenen Seitenkuppen des Knipovitchrückens zwischen 76°N und 77°N begonnen (Stationen M 21/277-291). In den folgenden 4 Tagen (Donnerstag, 18.06. bis Montag, 22.06.92) wurden insgesamt 7 ungestörte GKG und KAL-Sedimentkerne von 5 m-7 m Länge gezogen. Zusätzlich wurde die Wassersäule mit der CTD/KWS-Sonde, dem Multinetz und dem Radiolariennetz untersucht und beprobt. Die Festlegung der Kernentnahmepunkte erfolgte durch 3.5 kHz/ Parasound/Hydrosweep-Profilierungen entlang vorher, aufgrund von morphologischen Kriterien ausgewählter Transekte. Dabei zeigte sich, daß die existierenden bathymetrischen Karten oft

ein stark verzerrtes Bild der Topographie wiedergeben, das durch Hydrosweepkartierungen entlang der Transekts erheblich verbessert werden konnte. Trotz seiner intensiven Gliederung weist das untersuchte Segment des Knipovitchrückens meist eine mächtige Sedimentbedeckung auf, die sich in einer maximalen Eindringungstiefe von 60 m - 80 m auf einigen Kuppen dokumentiert. Lithologisch ist die Schichtfolge durch den Wechsel pastellfarbener mächtiger (Meterbereich) glaziomariner Ablagerungen mit Einschaltungen dunkler Diamikthorizonte und geringmächtiger (Dezimeterbereich) brauner, interglazialer, karbonatreicher Foraminiferenschlämme charakterisiert. Eine Serie mächtiger Diamikthorizonte in den Kernprofilen konnte mit starken Reflektoren in den 3.5 kHz/Parasound-Aufzeichnungen korreliert werden. Ähnliche Sediment- und Reflektorabfolgen wurden an nahezu allen Kernentnahmepositionen beobachtet, so daß eine zumindest regional einheitliche Verbreitung der Diamikte angenommen werden kann. Anhand des jetzt vorhandenen Kernmateriales wird es möglich sein, Randzonen und Wirbel des Atlantikwassers in seiner Interferenz mit den arktischen Wassermassen paläozeanographisch im Detail zu erfassen und die Geschichte der Karbonatlysokline entlang bathymetrischer Transekte zu studieren. In diesem Zusammenhang sind die Ergebnisse der planktologischen Untersuchungen in der Wassersäule von besonderem Interesse. Während sich auf der Ostflanke des Knipovitchrückens der ungebremste Einfluß atlantischer Oberflächenwassermassen in hohen Anteilen subpolarer planktischer Foraminiferen manifestierte, wurden auf der Westseite des Rückens, trotz der dem Atlantikwasser entsprechenden Temperaturen und Salinitäten, lediglich eine von *N. pachyderma* dominierte Population beobachtet.

Auf einer Kuppe mit besonders gut ausgebildeter und mächtiger Reflektorenfolge (Station M 21/287) wurde das OBS-System erneut eingesetzt. Der OBS-Einsatz wurde zunächst mit dem gekoppelten System durchgeführt, d.h. Senderfisch, OBS und Bodengewicht waren miteinander verbunden und konnten über Auslöser entkoppelt werden. Das Aussetzen des Gerätes erfolgte über das Heck mit Hilfe des Beiholerkranes, da der Heckgalgen nach wie vor defekt war. Beim Fieren konnte in 80 m Wassertiefe infolge eines Bruches im Einleiterkabel keine Signalübertragung mehr erreicht werden. Bei einem zweiten Versuch trat der gleiche Defekt in 1700 m Wassertiefe auf. Als das Gerät an Deck kam, stellte sich heraus, daß das Einleiterkabel direkt am Fisch abgedreht war. Dies wurde vermutlich durch ein ständiges Trudeln des Gerätes beim Fieren verursacht. Daher wurden keine weiteren Versuche unternommen, das kombinierte Gerätesystem in dieser Form einzusetzen. Stattdessen wurde das OBS mit Bodengewicht nur mit Hilfe der Beiholerwinde über die Seite zu Wasser gelassen, ausgeklinkt und zum Meeresboden abgesenkt. Anschließend wurden die genaue Position des OBS durch Kreuzpeilungen ermittelt und mehrere Kurse mit eingeschaltetem Parasound über die Position gefahren. Nach dem Auslösen konnte der Weg des OBS zur Wasseroberfläche durch Abstandspeilungen gut verfolgt werden, das Gerät nach dem Auftauchen sofort geortet und an Deck genommen werden.

Nach Abschluß der Arbeiten am 22.06. versetzen wir kurz vor Mitternacht erneut mit Kurs auf den Barentssee-Sedimentfächer, um dort noch ausstehende benthosbiologische/ plankto-

logische (Station M 21/292) und seismische (Station M 21/293) Untersuchungen durchzuführen. Der Besatz der Weichböden des Barentssee-Sedimentfächers erwies sich als relativ spärlich und wurde von kleinwüchsigen Kieselschwämmen der Art *Thena abyssorum* dominiert. Besonderes Interesse verdienen hauchdünne Kieselschwammkrusten auf der Sedimentoberfläche, die erheblich zur Stabilisierung der Weichböden beitragen. Anschließend versegelten wir zur nächsten Station, einem Sedimentwellenfeld, wo ein Einsatz des OBS-Systems geplant war.

Am 24.06. wurde für die genaue Positionierung der OBS-Station eine Traverse von 3.5 kHz und Parasound-Suchprofilen über ein bereits vorher bekanntes Sedimentwellenfeld gelegt und das Areal topographisch mit Hydrosweep kartiert. Im Laufe der Profilierung stellte sich heraus, daß das Sedimentwellenfeld weitflächig von Rutschungen unterlagert wurde und somit für einen OBS-Einsatz nicht geeignet war. Daher wurde die Profilierung in benachbarten Gebieten fortgesetzt und ein weitflächig topographisch sehr ruhiges Areal mit einer deutlichen Reflektorfolge und einer Eindringung von 20 m-30 m für eine Positionierung des OBS ausgewählt. Um 3.50 Uhr UTC wurde das OBS-System, bestehend aus Senderfisch, OBS-Empfänger und Bodengewicht, bei idealen Witterungsbedingungen (Sonne, gute Sicht und ruhige See) zu Wasser gelassen. Über Grund wurden die Funktionen des Senderfisches sowie die Ansprechbarkeit der Auslösesysteme und des Abstandsmessers erneut getestet und der Fisch vom OBS einschließlich Bodengewicht durch Auslösen getrennt. Danach wurden zwei Meßkurse über die OBS-Station mit dem Senderfisch gefahren. Um 8.40 Uhr UTC war der Senderfisch wieder an Deck. Nunmehr wurde der akustische Auslöser zur Entkoppelung von OBS und Bodengewicht aktiviert. Das Auslösegerät zeigte die Auslösung an, und auch die ersten Abstandspeilungen vermittelten den Eindruck, daß das OBS auf dem Weg nach oben sei. Nach dem Einschalten des bordseitigen Peilempfängers wurde mit der Suchfahrt begonnen. Weitere Abstandspeilungen legten den Verdacht nahe, daß das Gerät trotz anfänglicher gegenteiliger Anzeige doch nicht freigesetzt worden war. Dies bestätigte sich durch Kreuzpeilungen der Abstände von verschiedenen Positionen. Die genaue Position des Gerätes konnte hieraus ermittelt werden. Beim Überlaufen der Position zeigte der Abstandsmesser konstant die exakte Wassertiefe an diesem Punkt an, ein sicherer Hinweis dafür, daß das Gerät nach wie vor auf Grund lag. Nachdem trotz wiederholter Auslöseversuche keine Änderungen in den Abstandspeilungen auftraten, beschlossen wir nach kurzer Beratung mit der Schiffsleitung zu dredgen. Dazu wurden 9000 m Draht in einem offenen Kreiskurs um die Position des OBS ausgelegt und anschließend der Draht durch Einhieven über Grund gezogen, um das Gerät freizusetzen und zum Aufschwimmen zu bringen. Zusätzlich wurden Beobachtungswachen mit einem stündlichen Ablösungsmodus auf dem Peildeck gegangen, um auch bei einem Auftauchen des OBS mit defektem Sender das Gerät sichten und bergen zu können. Um 17.07 Uhr UTC kam das leere Suchgeschirr wieder an Deck. Ein zweiter Dredgeversuch mußte wegen des schlechten Zustandes des Tiefseedrahtes aufgegeben werden. Anschließend wurde nochmals zur Position des OBS versegelt, wo das Gerät mit genau 2531 m Abstand entsprechend der Wassertiefe direkt unter dem Schiff geortet werden

konnte. Trotz mehrfacher erneuter Auslöseversuche blieben die Abstandsmessungen weiter konstant, gleichbedeutend mit einer nach wie vor unveränderten Lage auf dem Meeresboden.

Als mögliche Ursachen für das nicht erfolgte Auftreiben des OBS halten wir einen Schaden der Auftriebskugeln oder ein zu tiefes Eindringen des Gerätes in den Schlick als wahrscheinlicher als ein Versagen beider Auslösesysteme. Anschließend versegelten wir unverrichteter Dinge von der OBS-Station mit Kurs auf unser letztes Hauptarbeitsgebiet, das nördliche Vöring Plateau.

Nach einer eintägigen Transitstrecke liefen am Freitag, dem 26.06.92, die Stationsarbeiten im Hochakkumulationsgebiet am nördlichen Vöring Plateau Escarpment mit dem Ziehen von 5 RL und 1 KAL-Kernen entlang eines Profiles im Ostsektor des Hochakkumulationsgebiete (Stationen M 21/294-298) an. Anschließend wurden in den Nachtstunden 3.5 kHz/Parasound-Profilkurse zur Vervollständigung von vorhandenen Kartierungen im Hochakkumulationsgebiet gefahren. Während des Tages wurde am 27.06. eine Serie von insgesamt 13 CTD/Transmissiometer-Messungen entlang zweier Nord-Süd-Transekte über das Zentrum des Hochakkumulationsgebietes gelegt, mit dem Ziel einer genauen Erkundung der BNL. An allen Stationen wurde eine gut ausgebildete BNL angetroffen, die z.T. bis zu 200 m über den Meeresboden entwickelt war. Die Stationsarbeiten wurden am 28.06.92 um 1.00 Uhr UTC beendet.

Anschließend liefen wir mit Kurs auf Trondheim. Infolge starken Gegenwindes und abschnittweise unruhiger See konnten wir über weite Strecken nur mit reduzierter Fahrt dampfen. Ein Teil der Verspätung wurde jedoch später wieder eingeholt. Mit lediglich 2 Stunden Verzug machten wir am Montag, dem 29.06.92, um 11.15 Uhr UTC an der Pier fest.

4.5 Fünfter Fahrtabschnitt

Fahrtabschnitt 5 begann in Trondheim mit einer 32stündigen Verzögerung, denn zunächst sollte der Heckgalgen repariert und ein neuer Tiefseedraht aufgetrommelt werden. Beim Heckgalgen stellte sich heraus, daß er vor Ort nicht in angemessener Zeit wiederhergestellt werden konnte. Daher wurden beide Druckzylinder ausgebaut und der Galgen in der achterlichsten Stellung fixiert.

Am Donnerstag, dem 02.07.1992, legten wir schließlich um 18.15 Uhr ab und erreichten nach 25 Stunden unser erstes Einsatzgebiet auf dem Vöring Plateau (Abb. 6). Diese Zentralstation (Station 317), die seit 1985 regelmäßig angelaufen wird, diente für die meisten als Teststation. Die Fahrtplanung der ersten Woche orientierte sich überwiegend an den Stationswünschen der Geologen, die einen Transekt vom Vöring Plateau (Station 315) zur Fallenposition im Norwegischen Becken intensiv untersuchten, um die Abbildung pelagischer Organismen, die fossil erhaltbar sind, erstmals synoptisch zu erfassen. Am 07.07. wurde die Station der

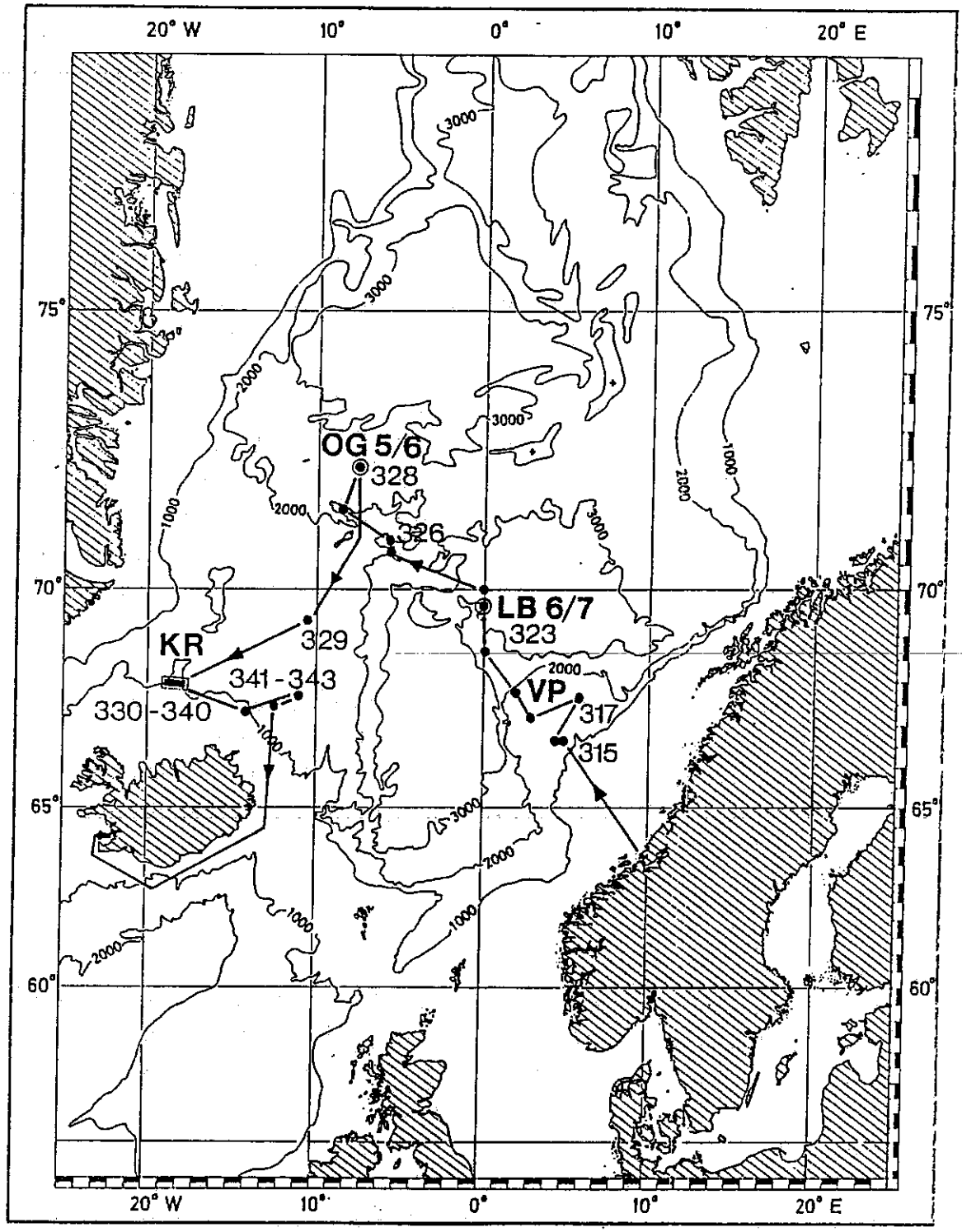

Abb. 6: Fahrtrouten und Untersuchungsstationen des Fahrtabschnittes M 21/5

Fig. 6: Cruise tracks and areas of investigations during leg 5

Langzeitverankerung (LB 6/7, Station 323) im Lofotbecken erreicht. In der zweiten Woche wurde das Ost-West-Profil durch das Europäische Nordmeer fortgesetzt und an der nordwestlichsten Position, bei der Ostgrönland-Verankerung (OG 5, Station 328), abgeschlossen. Die Sinkstoffallen konnten ebenso problemlos geborgen und wieder ausgesetzt werden wie zuvor im Lofotbecken. Auf der Anreise wurde durch intensive Suchfahrten mit dem tiefgeschleppten SideScanSonar versucht, die vermißte NB4-Verankerung zu finden. Unmittelbar in Nähe der Position des 1989 ausgesetzten Grundgewichtes konnten Objekte sichtbar gemacht werden, die der Größe von Verankerungsteilen entsprachen. Leider scheiterte der anschließende Versuch, die Verankerung zu dredgen.

Bereits während der Anfahrt zur Ostgrönland-Verankerung konnten in der Ferne erste Eisschollen beobachtet werden. Die Westgrenze des Treibeises befand sich etwa bei 10°W, so daß die in dieser Gegend geplanten Profilfahrten der Geophysiker ausfallen mußten. Auch das Arbeitsgebiet für die benthosbiologischen Untersuchungen wurde nach Süden in den Bereich des Kolbeinsey-Rückens verlegt.

Am 10.07. wurde eine Station (326) bearbeitet, die schon auf früheren Reisen durch ihren Reichtum an benthischen Großforaminiferen (Hyperaminen) aufgefallen war.

Auf der Anreise zum Kolbeinsey-Rücken, die von einer weiteren Kernentnahmestation auf dem nördlichen Island Plateau unterbrochen wurde (Station 329), hatten wir das Glück, sehr nah an der Insel Jan Mayen vorbeizukommen, und konnten den Beerenberg in voller Schönheit in der Sonne bewundern.

Am 16.07. trafen wir, wie vereinbart, den Coast Guard Eisbrecher "POLAR SEA", um einen Kollegen, Herrn Will Ritzrau, überzusetzen, der an der amerikanischen Expedition in die Nord-Ost-Polynia teilnehmen sollte. Fahrtleiter und Seniorwissenschaftler nutzten die Begegnung zu einer Besichtigung des Eisbrechers und einem kurzen Gespräch mit den amerikanischen Kollegen.

Das Hauptarbeitsgebiet der Woche lag auf dem südlichen Kolbeinsey-Rücken bei etwa 67°55'N, nördlich von Island. Dieser Rücken trennt den Ost-Grönlandstrom vom Ost-Islandstrom, so daß innerhalb kürzester Entfernung zwei sehr verschiedene Wassermassen und Sedimentationsmuster untersucht werden konnten (Stationen 330-340). Der Schwerpunkt lag bei den benthosbiologischen Untersuchungen.

Die letzten 48 Stunden der Arbeitszeit wurden für die Beprobung des Arbeitsgebietes 7 (Stationen 341-343) nordöstlich von Island genutzt, in dem noch einige Schwerelote und Kastengreifer gewonnen wurden, an Hand derer der Einstrom des Nordatlantiks in das Europäische Nordmeer untersucht werden soll. Leider wurde das Wetter bei diesen letzten Einsätzen sehr rauh. Am Dienstag, dem 21.07., um etwa 10.00 Uhr wurden die Stationsarbeiten

beendet und Kurs auf Reykjavik genommen, wo wir am 23.07.1992 um circa 8.30 Uhr einliefen.

4.6 Sechster Fahrtabschnitt

Am 26.07. verließ METEOR um 10.00 Uhr Reykjavik, nachdem zuvor die Reparatur der A-Galgenhydraulik erfolgreich abgeschlossen worden war, und nahm Kurs auf das erste Arbeitsgebiet auf 59°16'N, 21°W (Abb. 7). Dieses Gebiet wurde schon während des JGOFS North Atlantic Bloom Experiments 1989 (METEOR-Reise Nr. 10) beprobt. An der Station wurde vom 27.07. bis zum 29.07. gearbeitet. CTD/Rosette, Multischließnetz und Multicorer sowie ein Tiefsee-Ottertrawl kamen zum Einsatz. Während der Stationsarbeiten herrschten Windstärken um 7 Bft, so daß der geplante Einsatz des neu beschafften $1m^2$-Doppel-MOCNESS abgesetzt werden mußte.

Am 29.07. verließ METEOR das Arbeitsgebiet und nahmen Kurs auf das BIOTRANS-Gebiet auf 47°N, 20°W. Auf der Anreise wurden 2 Stationen des dritten Fahrtabschnittes erneut mit CTD/Rosette und Multischließnetzen beprobt. (Positionen: 55°N, 20°W, 52°30'N, 20°W). Während der Anfahrt herrschten Windstärken zwischen 6 und 7 Bft aus südwestlicher Richtung, die die Anreise deutlich verlangsamten.

Am 02.08. um 4.00 Uhr morgens wurde das BIOTRANS-Gebiet erreicht und mit den Arbeiten im Transponderfeld (Zentralstation) der BIO-C-FLUX-Gruppe, das auf dem ersten Fahrtabschnitt an dieser Position installiert worden war, begonnen. Sedimentproben wurden mit dem Kastengreifer und dem Multicorer genommen, wobei das Benthosprogramm der Fahrtabschnitte 1, 2 und 3 fortgesetzt wurde. Auf dem Meeresboden wurde in einer fleckenhaften Verteilung eine bis zu 1 cm starke Auflage von weißlichem Phytodetritus ("Fluff") gefunden. Die Farbe des Phytodetritus deutet auf ein Sedimentationsereignis hin, das schon im Juli stattgefunden haben mußte. An Freifallgeräten wurden die Reusenkette und der mikrobiologische Freifall-Inkubator verankert.

Da alle Winden mit den maximalen Drahtlängen ausgestattet waren, konnte die BIO-C-FLUX-Arbeitsgruppe alle geschleppten Tiefseesysteme optimal einsetzen, u.a. gelang ein Hol mit dem Ottertrawl in 4560 m Tiefe, für den 10500 m Tiefseedraht ausgesteckt wurden. Das $10m^2$-MOCNESS zum Fang von Mikronekton und das $1m^2$-Doppel-MOCNESS wurden erfolgreich mit maximalen Fangtiefen von 4550 m eingesetzt. Das neu beschaffte Tiefsee-Beobachtungssystem mit einer Videokamera und einer Kamera für Einzelbilder lieferte uns zum ersten Mal faszinierende Direktbilder vom Meeresboden in unserem Arbeitsgebiet. Das Tiefsee-Beobachtungssystem wurde sowohl zur Beobachtung des Transponderfeldes als auch für einen Transekt über den "Großen Dreizack", einem Tiefseeberg, der sich 700 m über die umgebende Ebene erhebt, eingesetzt.

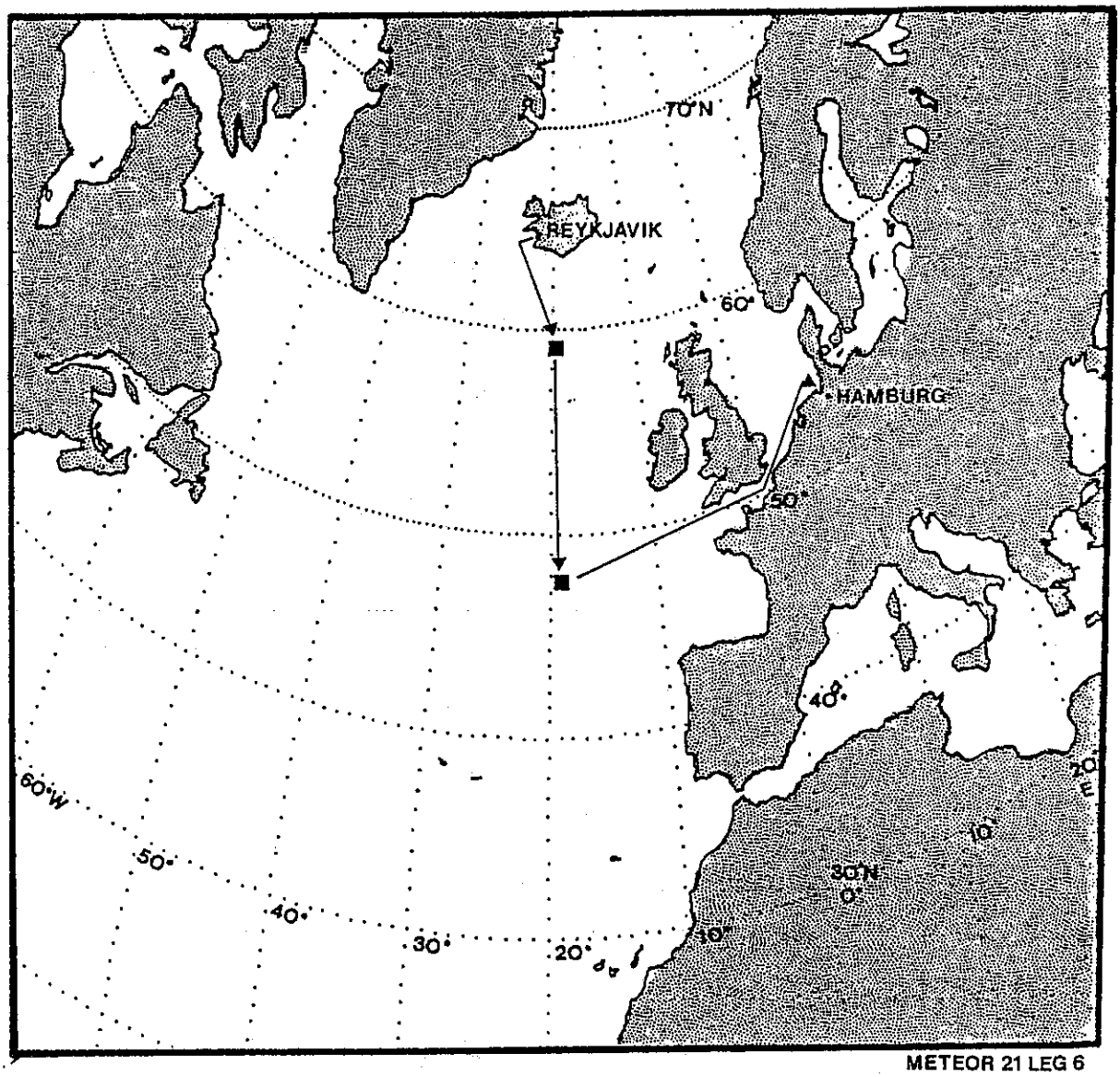

Abb. 7: Fahrtrouten und Untersuchungsstationen des Fahrtabschnittes M 21/6

Fig. 7: Cruise tracks and areas of investigations during leg 6

Die Planktologen und Chemiker des IFM Kiel setzten in regelmäßigen Abständen eine kombinierte CTD/Schöpferrosette ein. Die Chemiker des IFM Kiel setzten am 03.08. eine treibende Sinkstoffalle 25 sm westlich des Tranponderfeldes aus. Die Hamburger CO_2-Gruppe nahm während der gesamten Reise Wasserproben mit einem im Lotschacht installierten Schnorchelsystem. Die Tübinger Mikropaläontologen nahmen regelmäßige Multischließnetzfänge bis in 2500 m Tiefe.

Durch den dauernden Durchzug von Tiefausläufern gestaltete sich das Wetter sehr wechselhaft. Die Windstärken lagen maximal bei 8 Bft. Hohe Dünung querab zur Windrichtung bewirkte an einem Arbeitstag ein starkes Krängen des Schiffes und verursachte durch Überholen mehrere vorzeitige Auslösungen des Multicorers.

Am 13.08. setzte die BIO-C-FLUX-Gruppe zum ersten Mal den epibenthischen Schlitten mit Videokamerabestückung in 4500 m Tiefe ein. Nach unserem Erachten war dies der erste Einsatz eines videogesteuerten Tiefseetrawls. Das Gerät zeigte sich sowohl in der Wassersäule als auch am Boden außerordentlich lagenstabil und konnte so gefahren werden, daß das W12-Kabel nie den Boden berührte. Der Einsatz konnte somit auch zeigen, daß auch Grundschleppgeräte gefahrlos an Kabeln gefahren werden können.

Da für das am 02.08. ausgesetzte Driftfallensystem der Kieler Meereschemiker nur eine Positionsmeldung der Argosboje vom 05.08. vorlag, wurde, da die Satellitenortung offensichtlich defekt war, am 15.08. bei relativ ruhiger See ein Suchraster gefahren. Dabei wurde versucht, die Boje mit dem Nahpeilsender zu orten. Leider blieb die Suchfahrt erfolglos, so daß nur noch eine geringe Chance bestand, die Auslegung zu bergen. Die Peilversuche mit dem Nahpeilsystem wurden jedoch wärend der gesamten Aufenthaltszeit im BIOTRANS-Gebiet kontinuierlich fortgesetzt.

Für die Kieler Planktologen und Meereschemiker wurde am 15./16.08. ein großflächiges CTD/Rosetten-Stationsraster von 10 Stationen verteilt auf 40 sm^2 gefahren. Am 16.08. mußten die Stationsarbeiten am Nachmittag für einige Stunden unterbrochen werden, da ein Leck an der Zentralleitung der Hydraulikanlage beseitigt werden mußte.

Am 17.08. verließ METEOR die Zentralstation, um einen weiteren Suchkurs für das Driftfallensystem zu fahren. Am Ende der Suchaktion, die wiederum erfolglos blieb, nahmen wir Kurs auf 47°50'N, 19°39'W, um eine von den Chemikern des IFM Kiel auf dem ersten Fahrtabschnitt ausgelegte Verankerung mit Sedimentfallen zu bergen. Die Verankerungsposition lag ca. 40 sm nördlich des Transponderfeldes. Beim Auslöseversuch der Grundgewichte wurde kein Kommunikationssignal vom Releasetransponder ("OCEANO RT 661") empfangen. Daraufhin wurde ein Dreieckskurs um die mutmaßliche Auslegeposition gefahren und versucht, den Transponder aus verschiedenen Richtungen auszulösen, wobei 3 verschiedene Bordeinheiten verwendet wurden (2x "OCEANO TT-201", 1x "OCEANO TT-301"). Der Releasetransponder gab bei allen Versuchen keine Antwort, weder auf Auslösesignale noch

auf die Kommandos "Enable" und "Disable". Da es erfahrungsgemäß auch zu Auslösungen ohne positive Rückantwort kommen kann, wurde nach einer Wartezeit von zwei Stunden nach der letzten Auslösung ein Suchraster gefahren. Auch dieser Versuch blieb erfolglos, so daß davon ausgegangen werden mußte, daß die Verankerung nicht ausgelöst wurde. Daraufhin wurde beschlossen, die Auslegung zu dredgen. Die erfolglosen Dredgeversuche (4x) wurden am Vormittag des 19.08. eingestellt. Da in der Nähe zwei weitere Jahresverankerungen der gleichen Zusammenstellung und mit den gleichen Releasetranspondern während M 21/3 ausgebracht worden waren, wurde versucht, diese mit den Kommandos "Enable" und "Disable" anzutriggern. Auch diese Versuche blieben erfolglos, so daß davon ausgegangen werden mußte, daß bei allen drei Verankerungen ein Systemfehler am Releasetransponder vorlag.

Am 21.08. wurde von der BIO-C-FLUX-Gruppe zum ersten Mal ein Freifall-Amphipoden-Respirometer eingesetzt. Das System wurde 5 m über dem Boden verankert und lockt nekrophage Organismen, hauptsächlich Amphipoden, in beköderte Meßkammern, in denen nach dem Schließen der Eingangsreuse der Sauerstoffverbrauch der Organismen in situ kontinuierlich registriert wird. Da die Köder in speziellen Nebenkammern aufbewahrt werden, die verschließbar sind, können die Messungen wahlweise an Tieren nach oder ohne Nahrungsaufnahme durchgeführt werden.

Am 23.08. wurde mit der Aufnahme der Markierungstransponder das Transponderfeld abgebaut. In der Nacht vom 25.08. auf den 26.08. wurden um 2.00 Uhr nach einem Fototrawleinsatz und einer abschließenden CTD/Multischließnetz-Station die Stationsarbeiten der Reise METEOR Nr. 21 eingestellt und mit der Heimfahrt nach Hamburg begonnen. Am 31.08. machte METEOR frühmorgens am Schuppen 27b in Hamburg fest und beendete ihre 21. Expeditionsreise.

5 Preliminary results

5.1 Physical oceanography

5.1.1 Hydrography at 47°N, 20°W (JGOFS)

(S. Podewski, U. Beckmann, P. Kähler, R. Link)

Leg 1

During late winter or early spring the mixed layer dynamic is the dominating process for the development of the phytoplankton bloom. Due to the increase in atmospheric warming, the deep winter mixed layer is shallowing and the seasonal thermocline starts to develop. During this time of the year and especially within the area of investigation, phases with increasing stratification of the upper water column are interrupted by stormy periods during which the mixed layer may deepen again due to turbulence and cooling.

Derived from historical CTD data sets (ROBINSON et al., 1979; LEVITUS, 1982; WOODS, 1984; GLOVER and BREWER, 1988), calculated mixed layer depths are ranging from 200 to 500 m in the area of investigation during March. The variability of calculated mixed layer depths derived from historical data seems partly to be due to interannual variability but also depending on the mixed layer criterium choosen and the quality and quantity of the available CTD data.

Figure 8 shows a selection of temperature profiles measured during M 21/1 in March 1992. After reaching the BIOTRANS area on 22 March, CTD measurements showed an unexpected actual mixed layer depth of approximately 70 m (see profile 4 in Figure 8). The seasonal thermocline below the mixed layer was relatively pronounced already. Approximately 40 km to the north of this station an even shallower mixed layer depth of 50 m was detected (see profile 5 in Figure 8), whereas the temperature within the mixed layer was up to 1°C cooler and the seasonal thermocline was not as well established as in the southern area. The start of the phytoplankton bloom was already detectable which is described in detail by KOEVE et al. (this volume, chapter 5.3.1).

During the first leg of this cruise, originally designed to study late winter processes in the area, we were already able to document submesoscale differences in the development of the seasonal stratification and the resulting mixed layer depths. These observations were manifested at the beginning of the second leg. An interesting question to answer during further experiments and to explain by models is to what extend these differences were due to advection and/or the result of stormy events during this period of the year. Turbulence and cooling during storm events seemed to play a major role because of entrainment due to mixing with water masses below the mixed layer. A storm with windforcing up to 12 Bft. occuring between 27 and 31 March induced dramatic changes. The mixed layer depth increased from 40 m to about 240 m (see Figure 8, profiles 10 and 11) before and after the

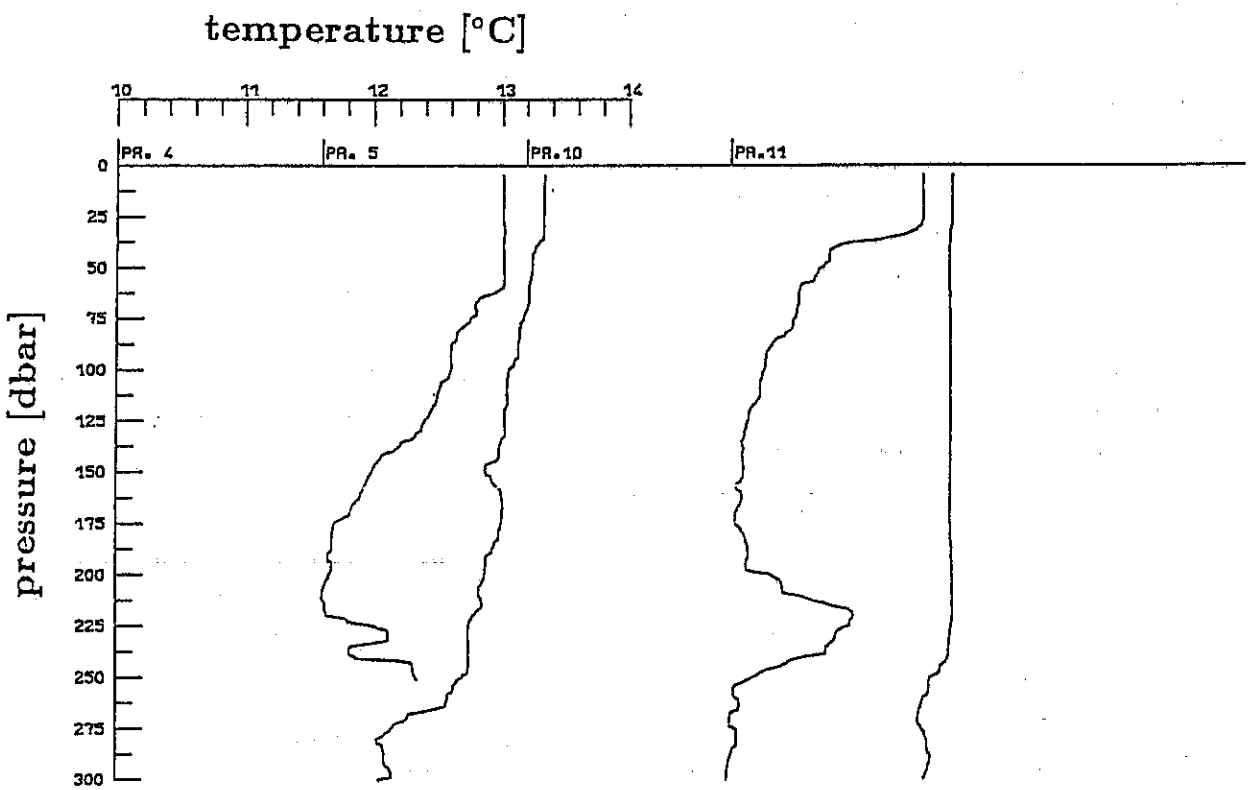

Fig. 8: Selected temperature profiles measured during M 21/1

storm according to CTD profiles taken at nearly the same position. The deepening was correlated with a decrease in the mixed layer temperature and an increase in the nutrient concentrations.

The pre-storm observations indicated that a much earlier start of the phytoplankton bloom than previously expected can occur, if the weather conditions allow an early stabilization of the upper water column for some period, while storms in contrast are interrupting the accumulation of phytoplankton within the mixed layer.

After the stormy event we conducted a drift experiment for two days. The drifter trajectory is shown in Figure 9.

Leg 2

Pre-survey

At the end of the first leg we launched a drifter rig which was successfully recovered after 11 days at the beginning of the second leg. The drifter trajectory shown in Figures 10 a and b already indicated that the rig may have been trapped within an anticyclonic hydrographic feature after some days of deployment. This anticyclonic structure (meander or eddy) was sampled along the first CTD section (see Figure 10, profiles 21 to 30) and can be identified by the decrease and increase of the isotherms between profiles 21 to 24 presented in Figure 11. The mixed layer temperature increased along the above mentioned east-west section from about 12°C to 13.5°C (see also Figure 12 a). The phytoplankton distribution varied strongly at the stations of the pre-survey. This showed up immediately on board by looking at the fluorescence profiles. As an example Figure 12 b presents all fluorescence profiles taken along the east-west section. The fluorescence profiles 21 to 26 seemed to be more scattering and more spiky than the relatively smooth profiles 27 to 30 taken in the western part of the section. In general, the variance of a fluorescence signal allows a preliminary qualitative interpretation of the phytoplankton size classes occurring. Smooth profiles are always indicating that relatively small size fractions of phytoplankton are dominating while scattering and spiky profiles give an indication that bigger size classes are apparent. This observation was verified on board by DECKERS and POLLEHNE (pers. comm.) who microscoped water column samples. They found diatoms dominating in the eastern part of the section and dinoflagellates and smaller plankton dominating in the western part.

The horizontal distribution of temperature (Figure 13 a) and in vivo chlorophyll (Figure 13 b) in 15 dbar depth derived from all CTD stations of the pre-survey grid are indicating distinct differences in the principle course of the gradients. There it seemed to have existed only a relatively weak correlation between in vivo chlorophyll concentration and temperature within the mixed layer. Besides this observation the horizontal distribution of in vivo chlorophyll and in vivo chlorophyll standing stock integrated between 0 to 200 m depth (see Figure 14 b) seemed to be strongly correlated with the dynamic of the deeper layers represented by the

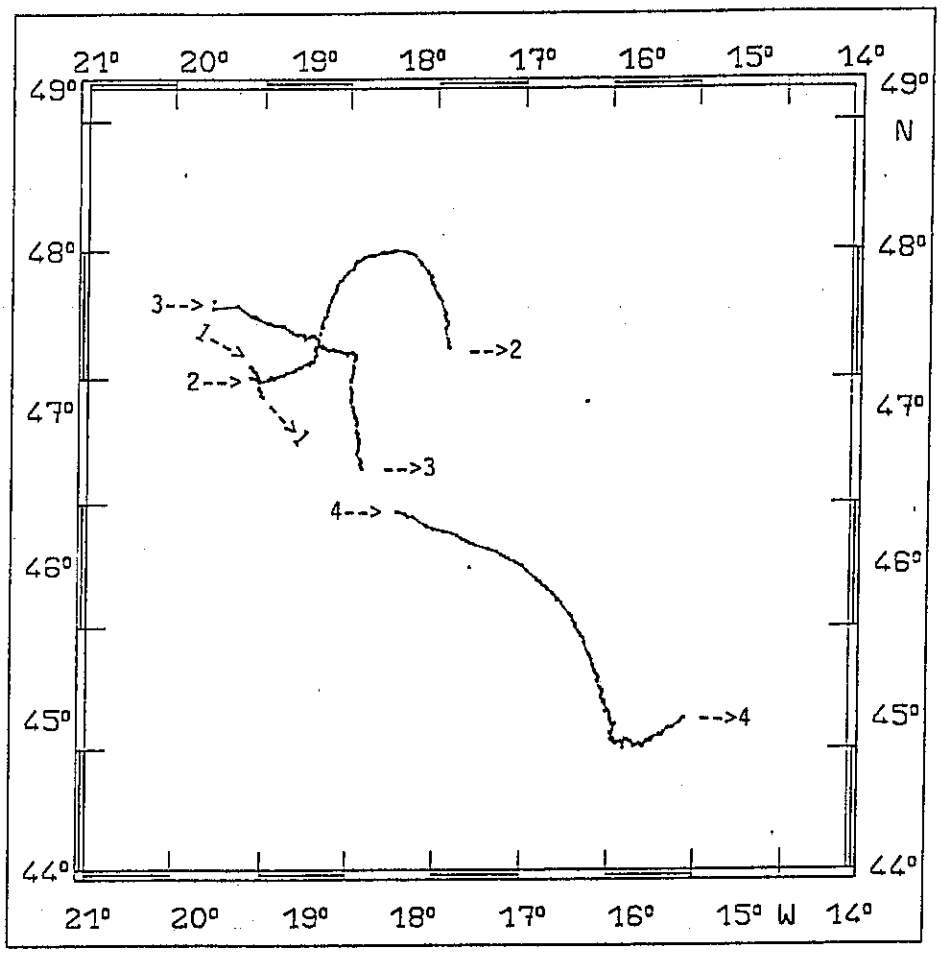

Fig. 9: Trajectories of the drifter rigs during M 21/1-3.
Periods of deployment:

1: 01.04. to 03.04.
2: 04.04. to 16.04.
3: 19.04. to 02.05. (so-called Long-Term Drifter)
4: 02.05. to 17.05.

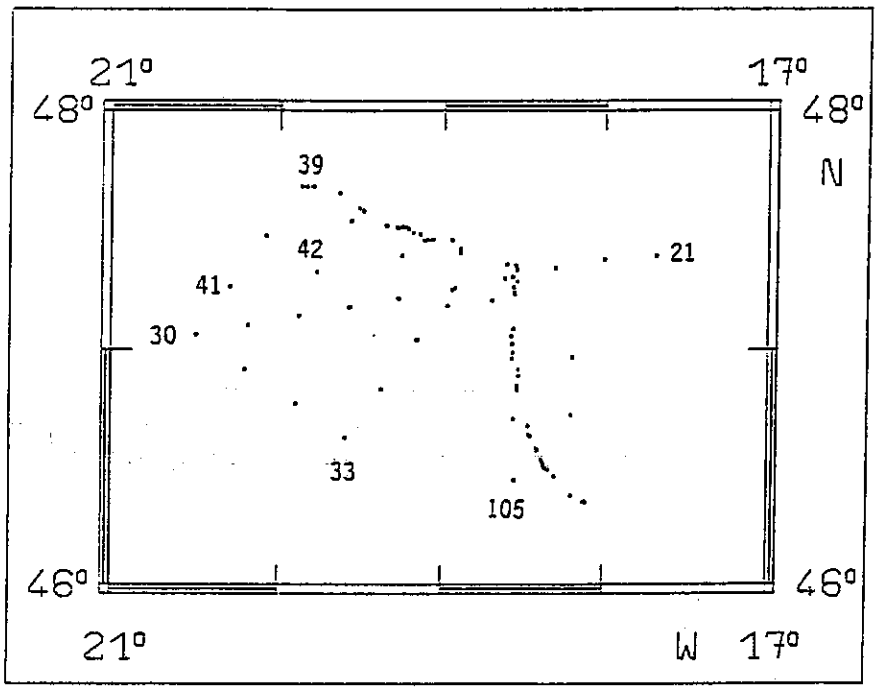

a

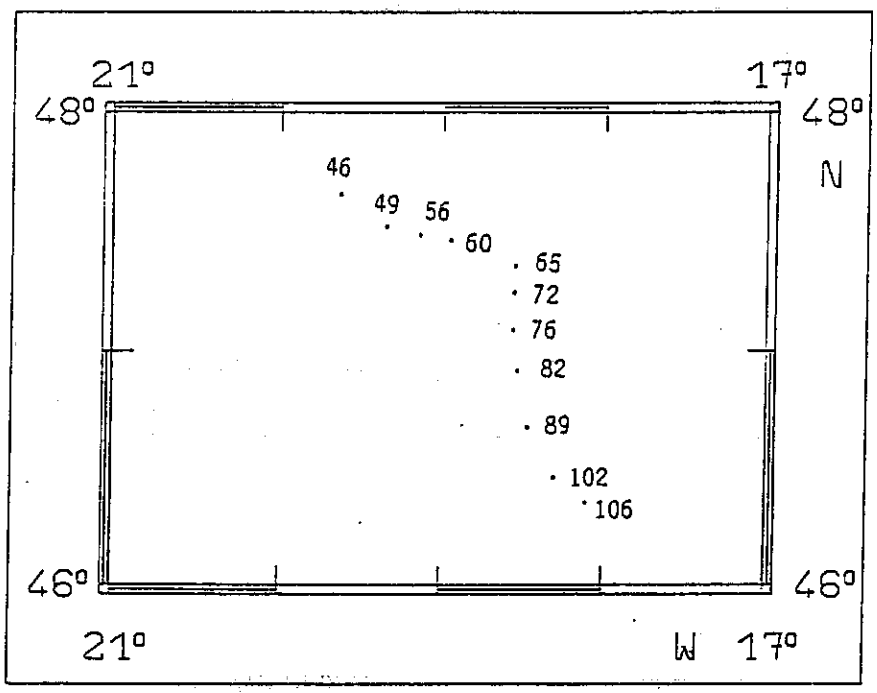

b

Fig. 10: a) Positions of the CTD profiles during M 21/2.
Profiles 21 to 42 were taken during the pre-survey.

b) As in Fig. 10 a) but along the Day Drifter trajectory

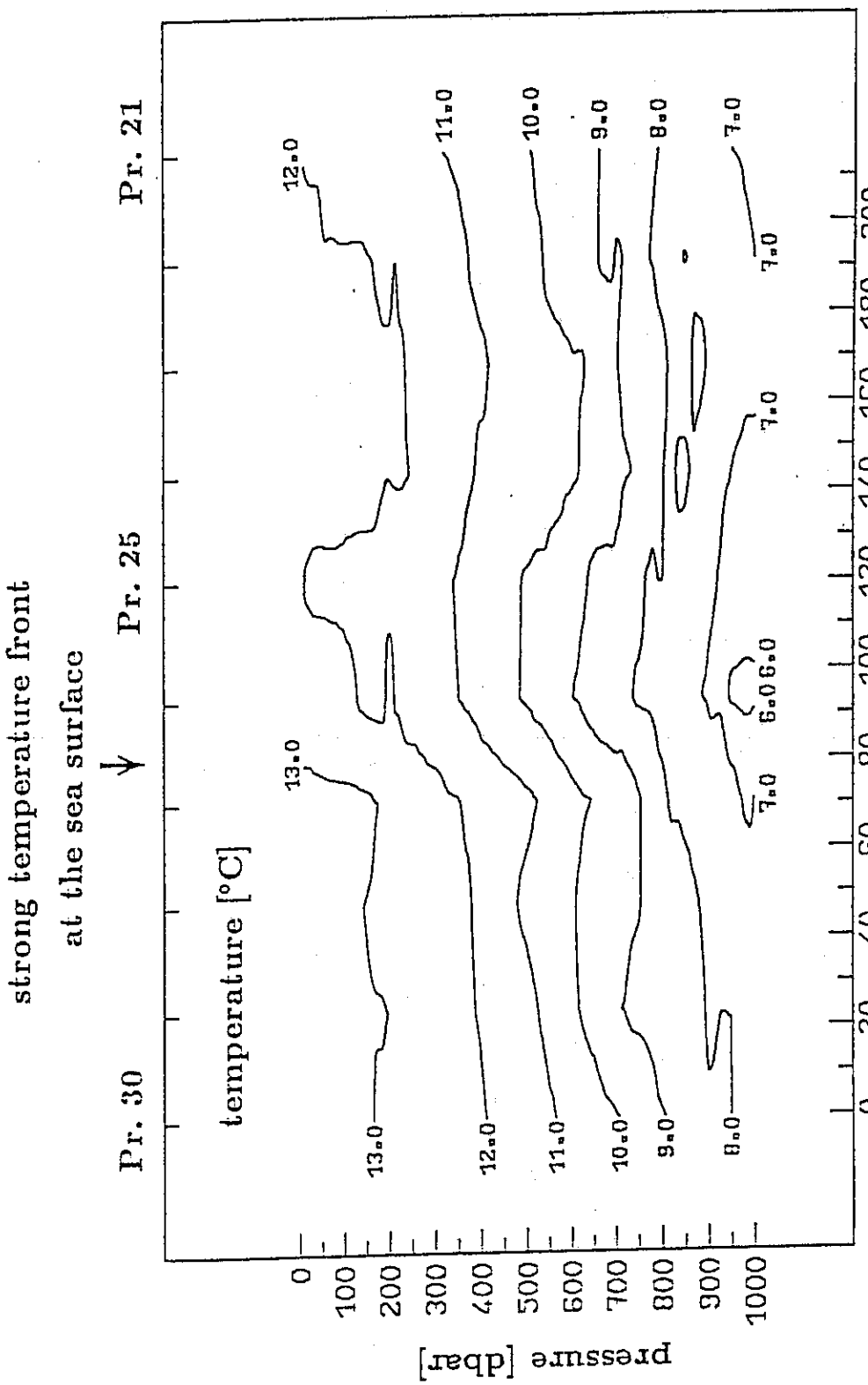

Fig. 11: Distribution of temperature along the east-west section of the pre-survey (M 21/2)

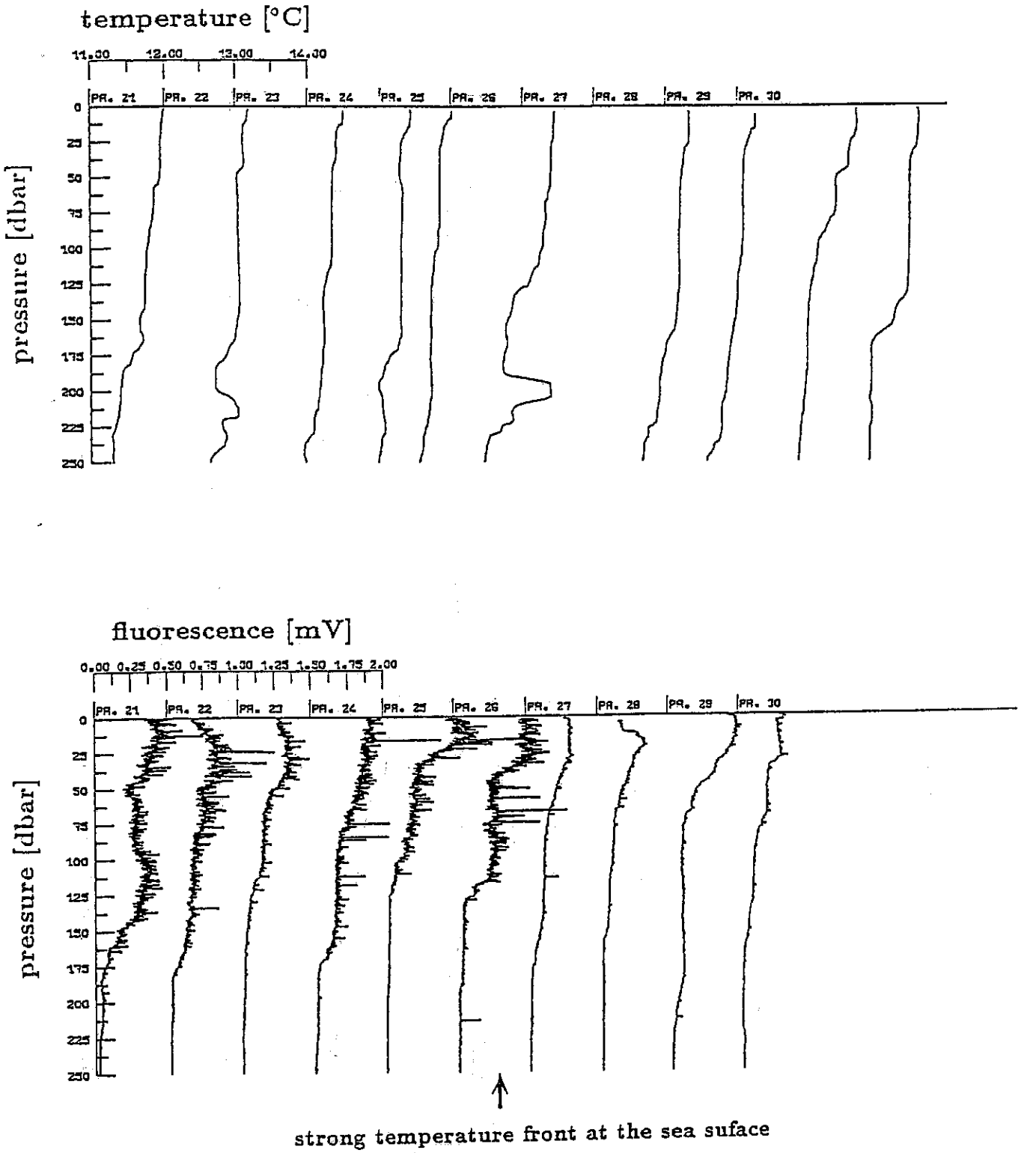

Fig. 12: a) Temperature and b) fluorescence profiles along the east-west section of the pre-survey (M 21/2)

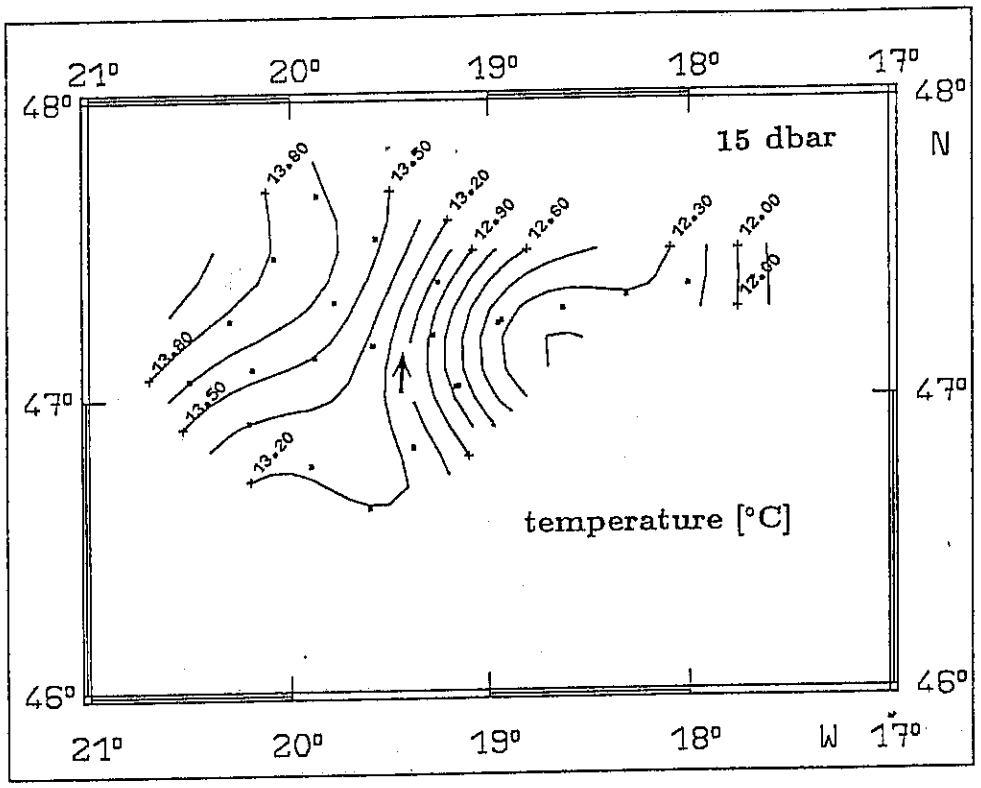

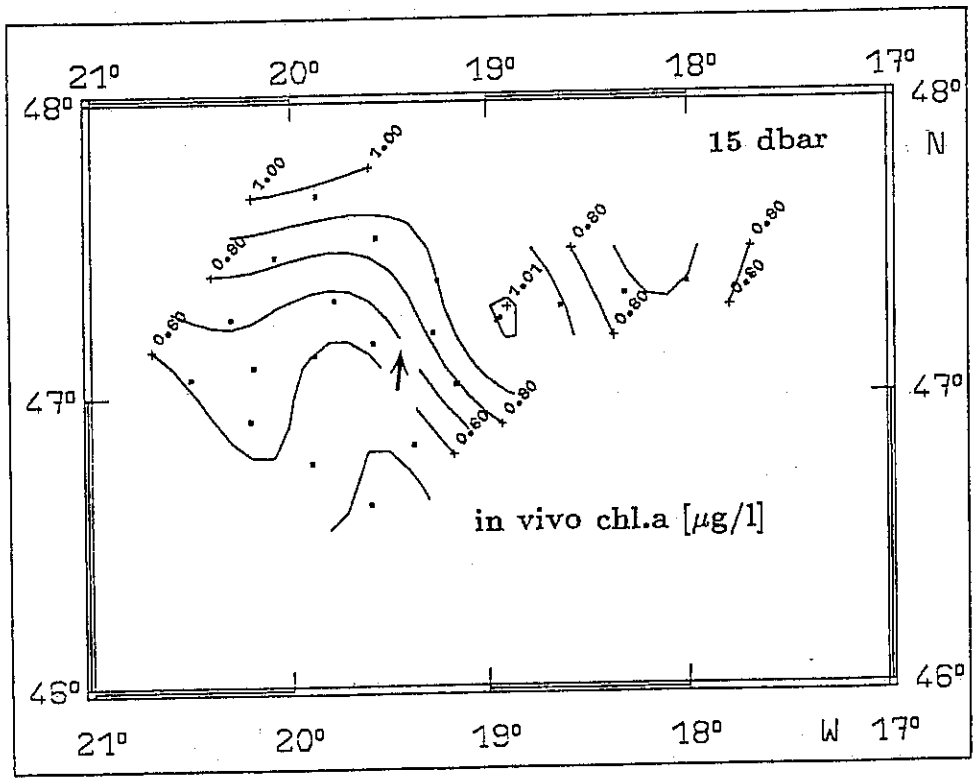

Fig. 13: a) Horizontal distribution of temperature and
b) in vivo chlorophyll in 15 dbar

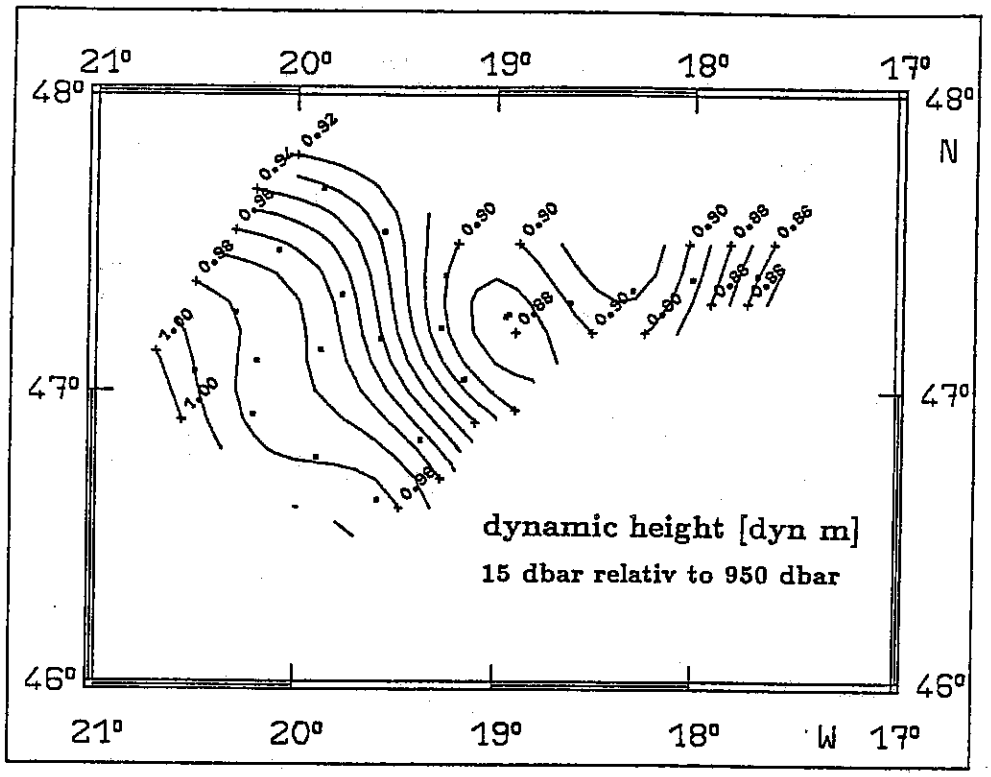

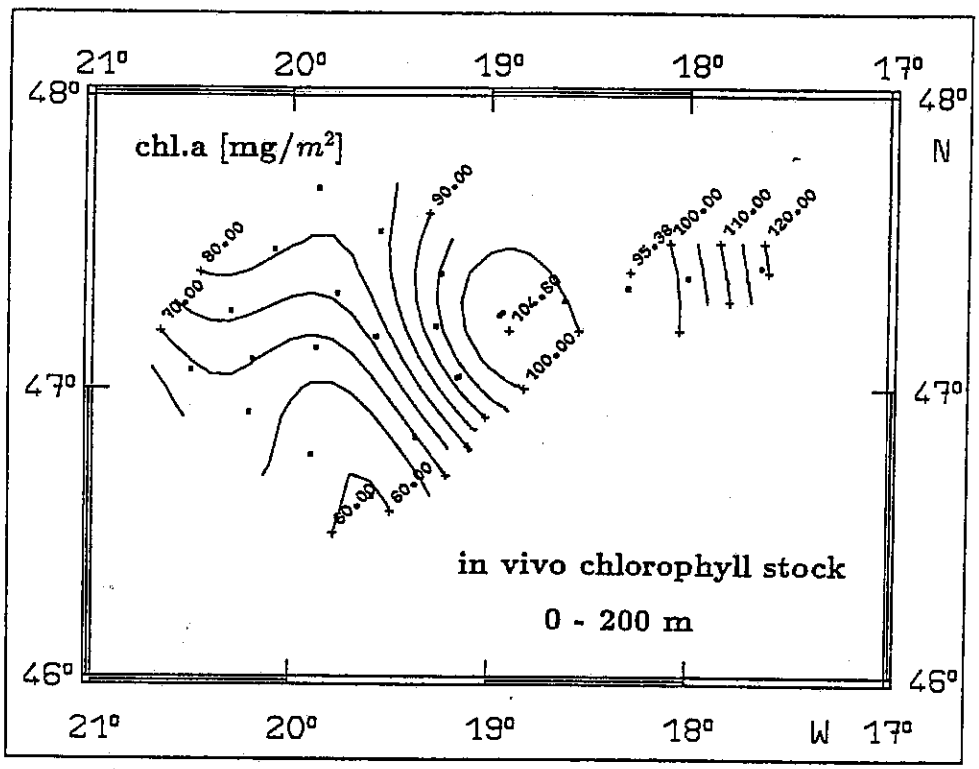

Fig. 14: a) Dynamic topography in 15 dbar relative to 950 dbar and
b) in vivo Chlorophyll standing stock (integrated from the surface down to 200 m) calculated with the CTD profiles of the pre-survey (M 21/2)

dynamic topography in 15 dbar relative to 950 dbar (Figure 14 a). The maximum values of in vivo chlorophyll and in vivo chlorophyll standing stock were concentrated in the central part of a cold cyclonic structure.

Drift experiment

After the launching of the so-called "Day and Long-Term Drifter", the CTD measurements were performed along the drifter trajectory of the Day Drifter. Figure 10 a shows the trajectory of the Day Drifter which can be identified by the increased number of CTD stations. The trajectory of the Long-Term Drifter is shown in Figure 10. Both drifters moved quasi parallel, except at the end of the experiment when the Day Drifter moved to the southeast while the Long-Term Drifter maintained its southerly component. The recovery of the Day Drifter took place at profile 106 and that of the Long-Term Drifter at profile 105 (Figure 10).

During some nights we got available station time to conduct CTD fluorescence measurements in some distance from the drifters. Nevertheless, the spatial resolution was much lower than during the pre-survey. A storm between 23 and 26 April increased the mixed layer depths again but less distinctly than during the first leg at the end of March. The temperature profiles at the morning drift stations (Figure 15 a) showed a deepening of the mixed layer from approximately 80 m down to 150 m just after the storm, but the actual turbulent mixed layer was already shallower. This was much better derivable from the fluorescence profile (Figure 15, profile 65) than to deduce from the CTD profile alone, because the already established gradients were very weak at that time. The increase in the scatter signal of the fluorescence profiles after the stormy event reflected the stronger importance of diatoms and gave a first indication that the drifter had moved into a significant different hydrographical/biological system after the storm. This was correlated with a sudden change in the drifter trajectories after the wind had died away.

The CTD fluorescence profiles taken after the storm until the end of the experiment showed a distinct division of the upper water column. Caused by increased warming of the atmosphere after the storm, the stabilization of the seasonal thermocline started again very quickly. At the end of the drift experiment, mixed layer depths of 30 m at the morning stations and even shallower during the day were measured. The "old" mixed layer signal induced during the storm was furthermore recognizable as quasi homogenous signals over some vertical distance within the CTD fluorescence profiles. While there was a relatively distinct accumulation of biomass within the more and more shallowing mixed layer, phytoplankton biomass was left behind within the seasonal thermocline.

Figure 16 shows the temperature and in vivo chlorophyll distribution along the trajectory of the Day Drifter. The rise of the 12°C isotherm from about 250 m to 125 m validate the above formulated statement that the rigs had drifted into a different hydrographic system after the storm.

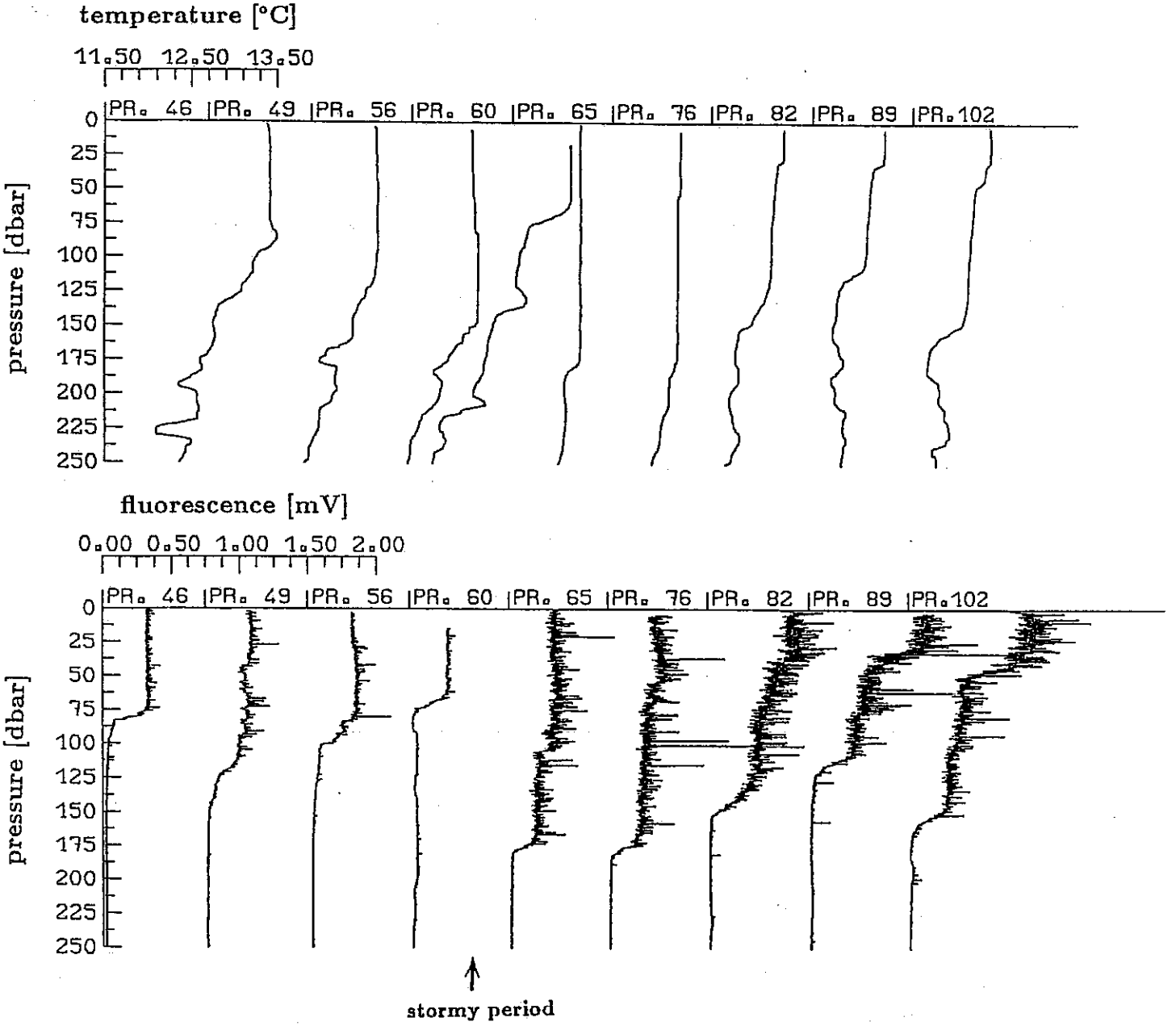

Fig. 15: a) Temperature and b) fluorescence profiles at the positions of the morning stations during the drift experiment (M 21/2)

An interesting aspect of the sedimentation process, most probably hydrographically induced, is shown in Figure 17. Below distinctive fluorescence minima deep fluorescence maxima at about 100 m down to 250 m occurred showing very low but significant relative values.

Fluorometrically measured chlorophyll values within these peaks showed significant but low concentrations in the order of 0.1µg/l. These fluorescence peaks seemed to be biological indicators of "old" mixed layer signals transported down to these depths and, therefore, seemed to be not coupled directly with the history of the upper water column above. The occurring temperature intrusions within these depth intervals are indicators for frontal processes which were most probably responsible for the transport of relatively fresh biogenic material down to greater depths (see for example the temperature intrusion showing up between profiles 82 to 102 in Figure 16 a).

Leg 3

A fluorescence maximum was found within the upper 25 m within the mixed layer (Figure 18, see profile 116). This observation was an early indication that the mixed layer was not at all nutrient depleted as could have been expected at the end of the second leg 18 days earlier. As a result a subsurface fluorescence maximum would have shown up. Nutrient measurements validated this a priori guess (see chapter Chemical Oceanography). The analyses of samples taken from the snorcle system will allow a much better description of the spatial variability within the mixed layer in the investigation area. The available station time did not allow to take more than one shallow CTD fluorescence profile.

The general division of the upper water column observed during the second leg occurred again indicating the history of the seasonal stratification. This holds for the occurrence of a deep fluorescence peak at 150 m down to 175 m depth.

Leg 6

Nutrient depletion within the mixed layer and distinct subsurface fluorescence maxima occurred at the upper part of the strongly developed seasonal thermocline, reflecting a typical summer situation within the area. Because of the relatively low spatial resolution of CTD fluorescence stations, further analyses will concentrate on possible submeso-scale and small-scale horizontal variability.

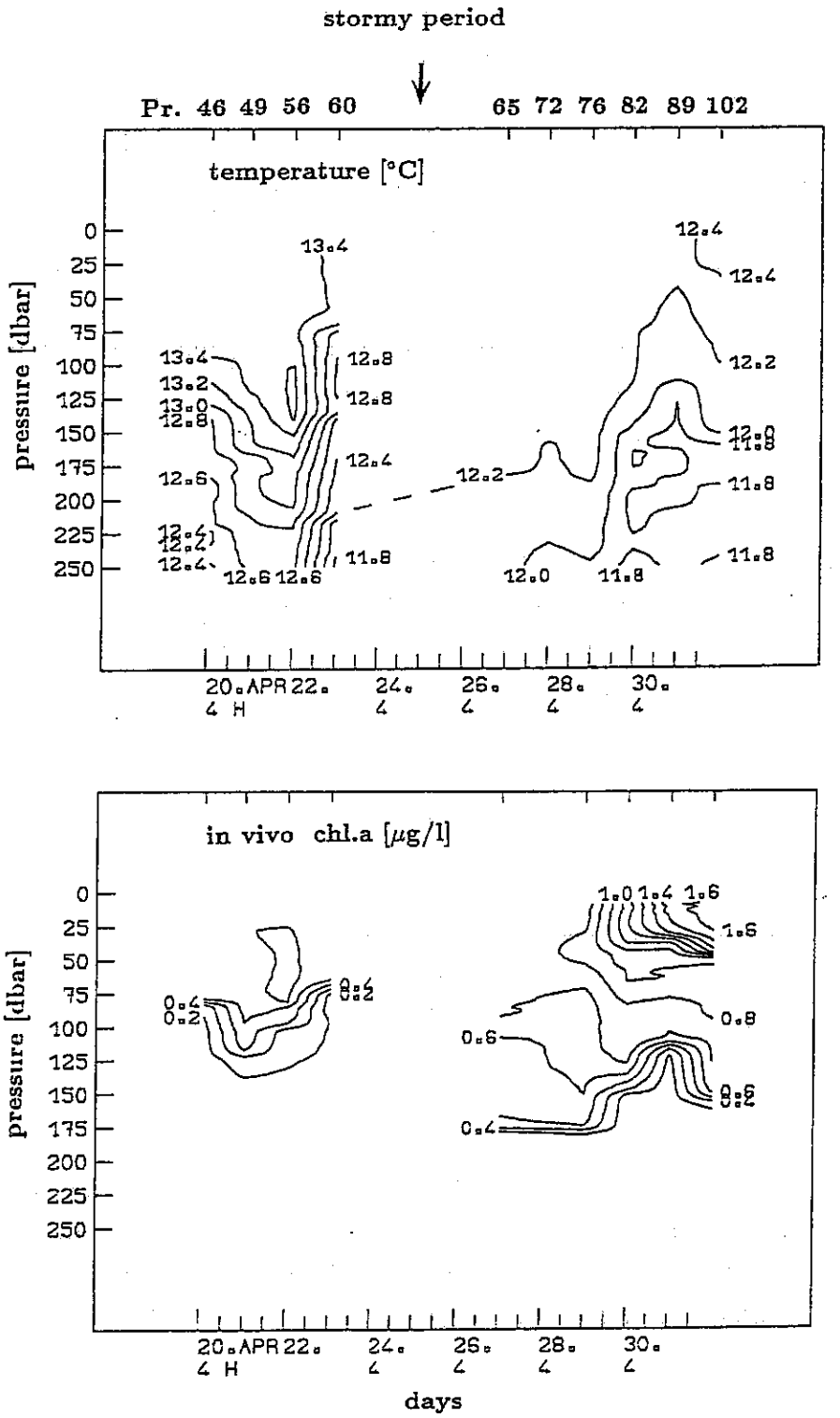

Fig. 16: Vertical distribution of temperature and in vivo chlorophyll along the trajectory of the Day Drifter (M 21/2).

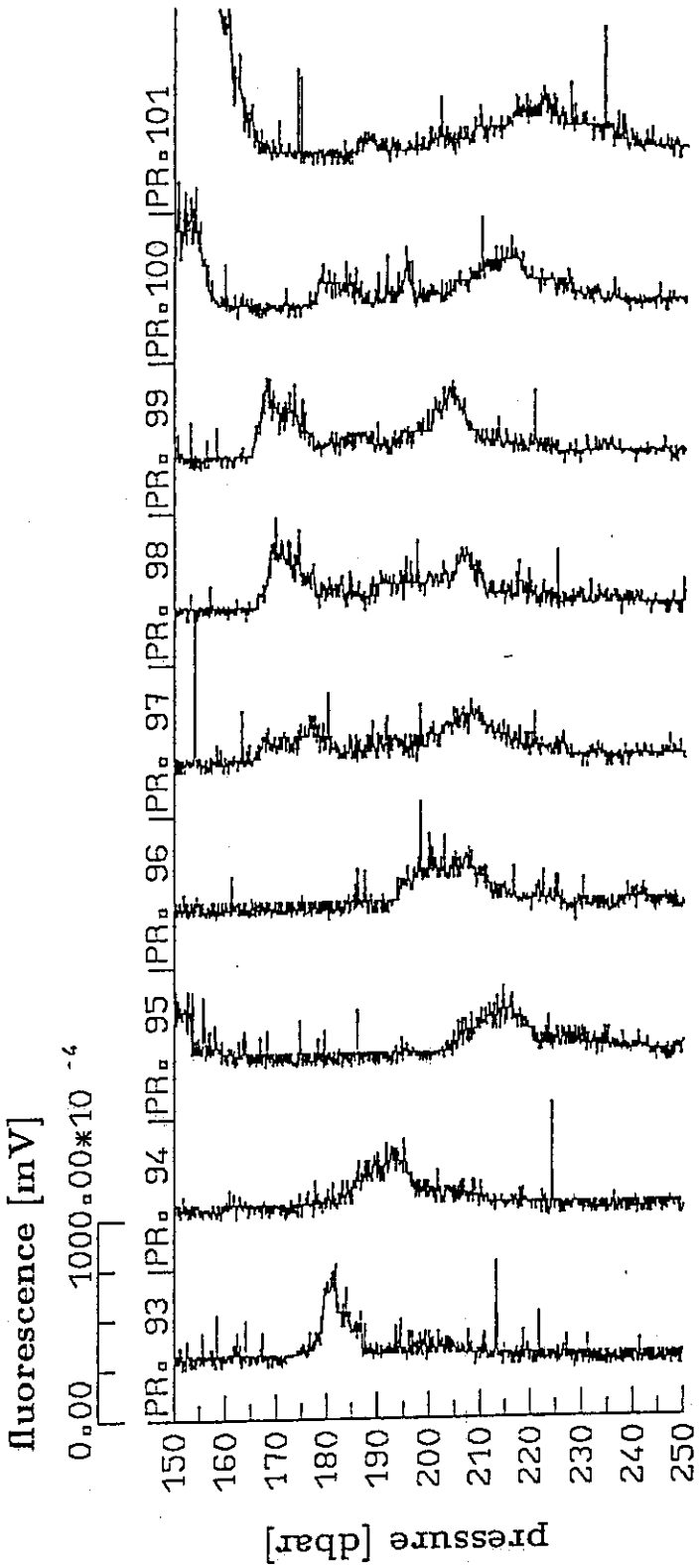

Fig. 17: Fluorescence profiles measured in a jojo mode during one night at the end of the drift experiment (M 21/2)

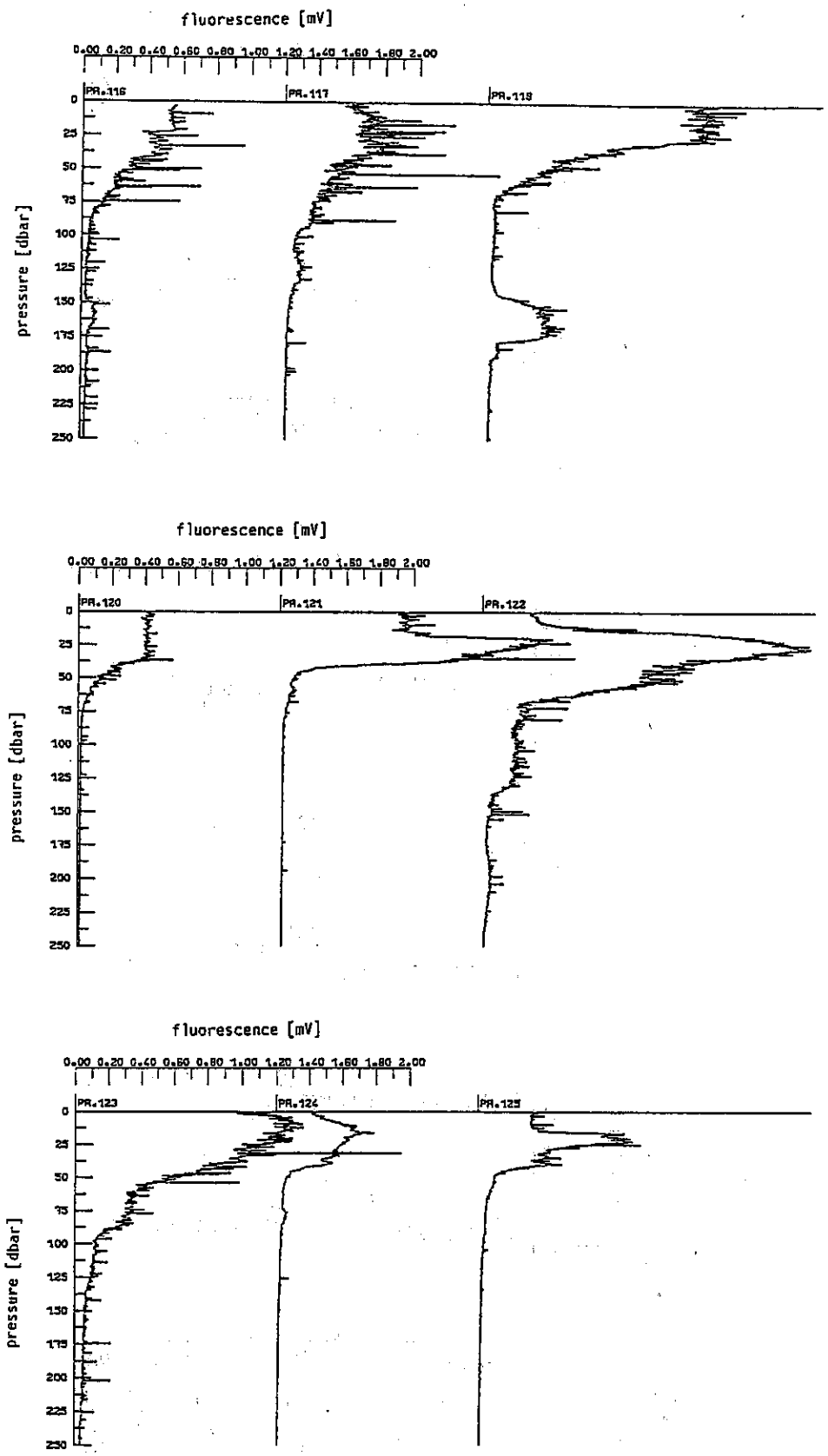

Fig. 18: Fluorescences profiles measured during M 21/3

5.1.2 Large-scale CTD section along 20°W during M 21/3 (JGOFS) (S. Podewski)

A large-scale CTD survey between 34°N and 20°W was carried out during leg M 21/3 (Fig. 19).

The diagrams of potential temperature versus salinity (θ/S diagrams) of all CTD profiles (110-125) taken during the third leg are presented in Figure 20 a, whereas the corresponding profiles are shown in Figure 21. The influence of Mediterranean Water (MW) at about 600 m down to 2000 m was most obvious within the profiles 110 to 112 taken between latitude 34°N and 40°N along the section. Profile 112 at 40°N showed maximum salinity values and the course of the profile seemed to indicate that the profile was possibly taken within a mediterranean eddy (a so-called MEDDY). Profiles 110/111 at 34°N showed distinct staircase structures occurring below the salinity maxima indicating actual salt-fingering.

Figure 20 b summarized the θ/S diagrams of profiles 114-125 taken between latitude 47°N and 59°N. Included within the presentation are the definition areas of pure North Atlantic Central Water (NACW), Subarctic Intermediate Water (SAIW) and the θ/S-point of Labrador Sea Water (LSW) at the particular places of origin of each characteristic water mass discussed by HARVEY and ARHAN (1988) and ARHAN (1990). The straight line leading from the base of "pure" NACW to the θ/S-point of LSW has no particular physical significance but shall separate waters which are mostly influenced by SAIW (deviation to the left of the line) or mostly by MW (deviation to the right of the line).

Obviously no pure NACW was found north of 47°N but instead so-called modified NACW was evident which is characterized by mixtures of NACW and SAIW (HARVEY and ARHAN, 1988). According to these observations profiles 114 to 118 should have been situated north of the southernmost branch of the NAC which is defined as the northern limit of "pure" NACW by HARVEY and ARHAN (1988). The θ/S variability at potential density values less than 27.3 (density level of the upper boundary of SAIW) and close to the lower boundary of pure NACW may indicate diapycnal mixing between NACW and SAIW.

Similarly HARVEY and ARHAN (1988) defined the northern NAC branch as the southern limit of outcropping SAIW (subarctic front).

Profiles 120/121 taken at 54°N at the positions of the annual moorings showed the most pronounced SAIW influence along the section north of 47°N. The domination of pure SAIW described by ARHAN (1990) for the region north of the northernmost branch of the NAC north of 52°N was not evident within our data set. This was mainly due to the fact that our stations were lying far more to the east of the region analyzed by ARHAN (1990).

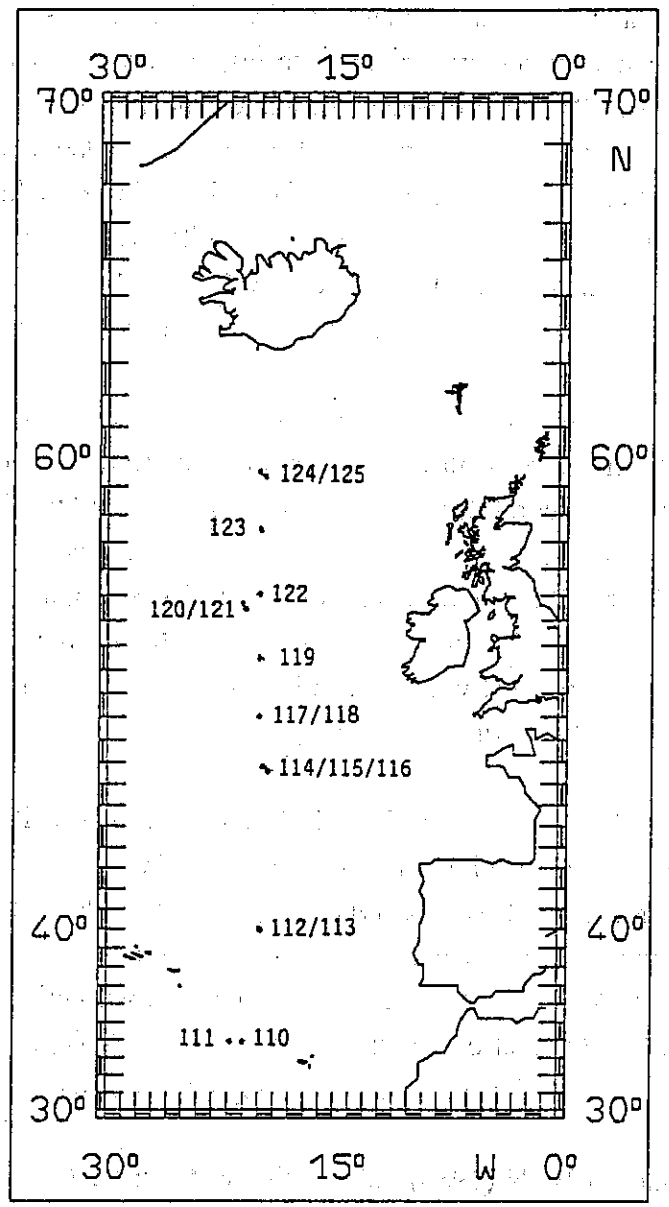

Fig. 19: Positions of the CTD profiles during M 21/3

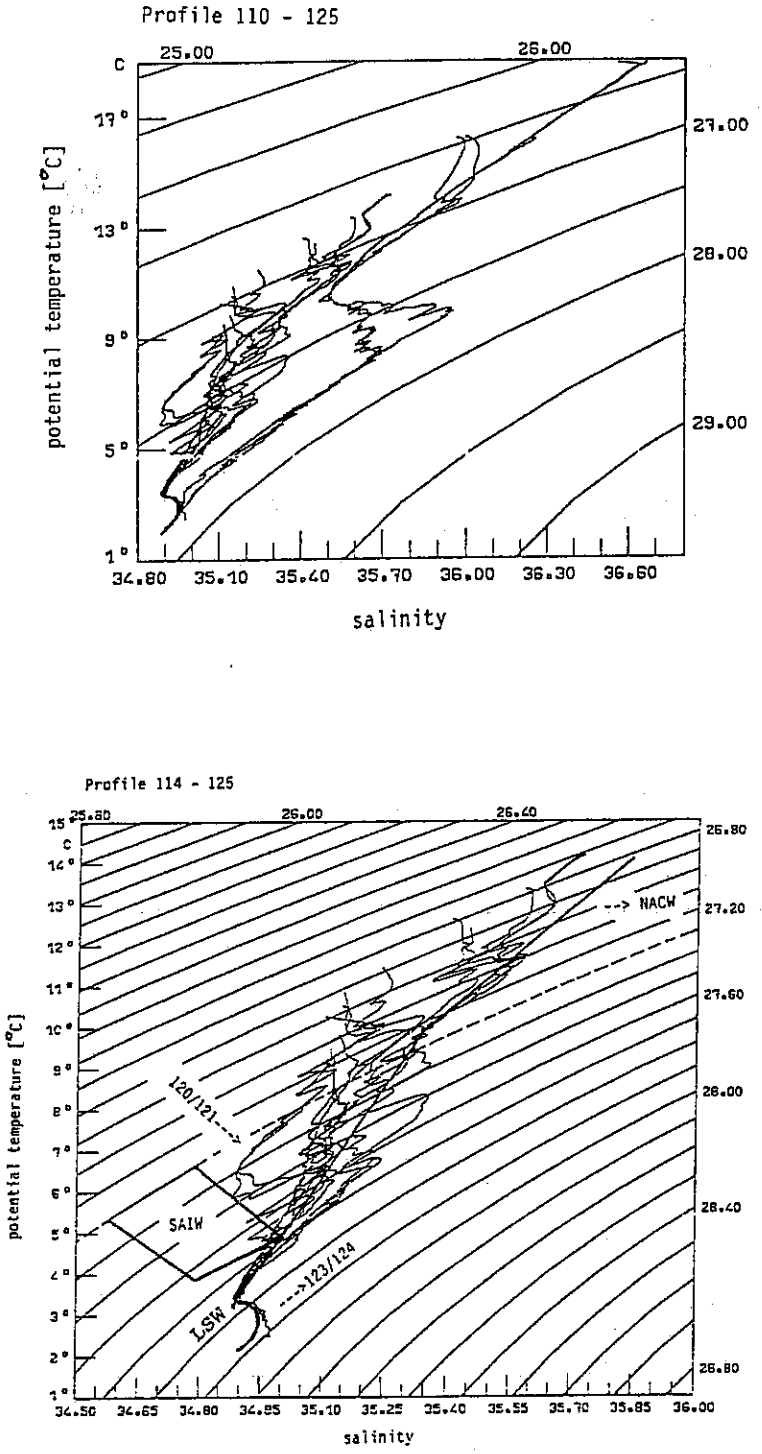

Fig. 20: a) θ/S diagrams of CTD profiles 110 to 125 measured during M 21/3
b) As in Figure 20 a), but for CTD profiles 114 to 125

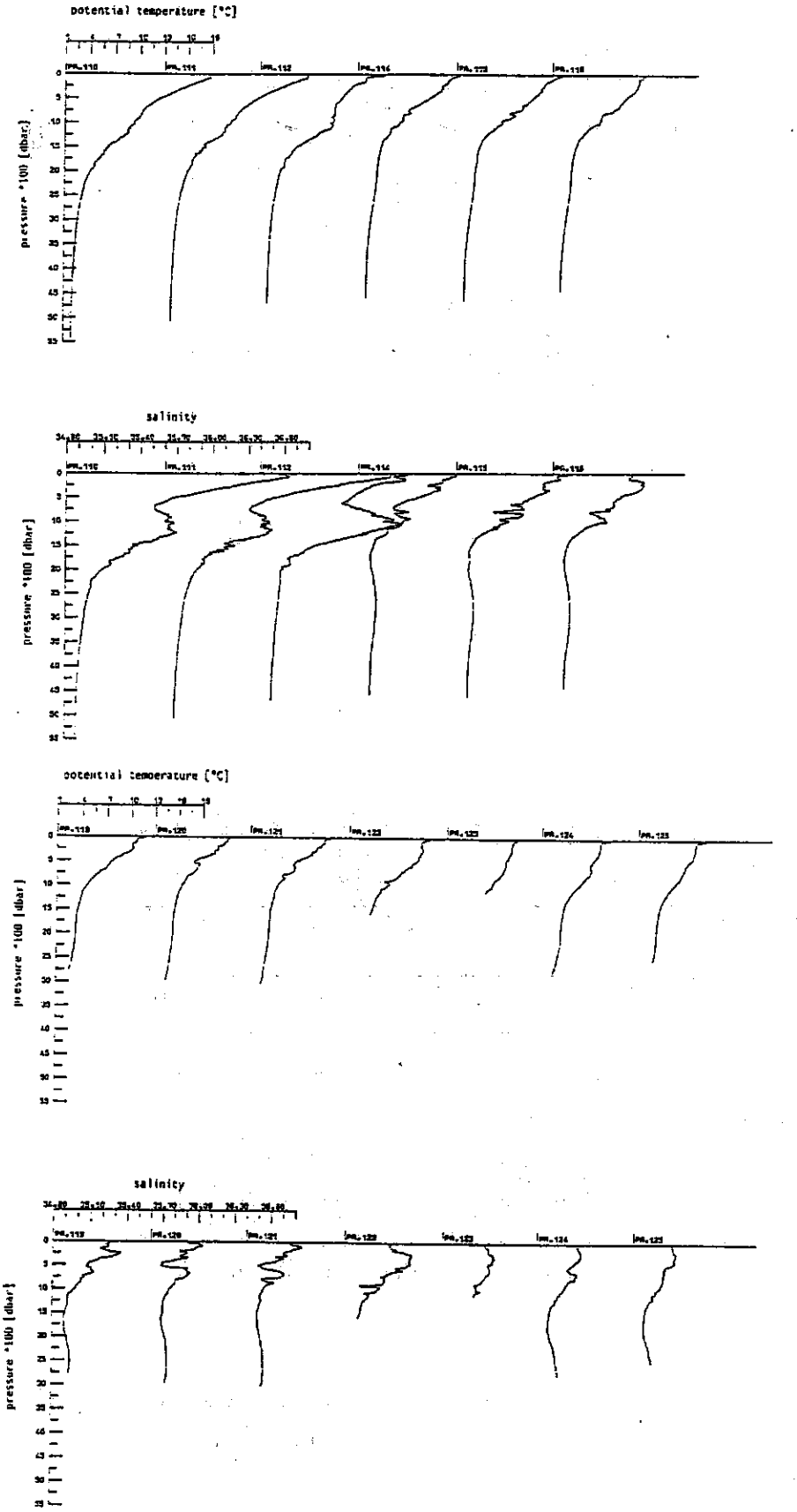

Fig. 21: a) Potential temperature and salinity profiles 110-118 (M 21/3)
b) As in Figure 21 a), but for profiles 119-125.

Below LSW the θ/S relations were lying within the definition area of North Atlantic Deep Water (NADW). The occurrence of relatively unmixed salty Iceland-Scotland Overflow Water (ISOW) was reflected in the θ/S diagrams of profiles 123/124 north of 57°30'N.

The fluorescence profiles taken between latitudes 47°N and 60°N are shown in Figure 18 indicating biological variability along these latitudes in May. Please note that profiles taken during the day light phase always show a fluorescence minimum in the upper 10 to 15 m due to the process of photoinhibition (see profiles 117, 122, 123 to 125). This process induced apparent subsurface fluorescence maximum values which have to be analyzed very carefully in conjunction with CTD measurements and fluorometrically analyzed chlorophyll values.

The influence of physical processes on the spatial variability of the phytoplankton distribution within the euphotic zone shall be discussed here for profiles 120/121. Both profiles were taken at early sun rise (when the influence of photoinhibition was neglectable) at the positions of the annual moorings 24 hours apart with a station distance of approximately 15 km. Profile 120 showed a classical spring phytoplankton maximum within the mixed layer whereas a subsurface maximum occured in profile 121. This was understandable while looking at the temperature profile 121 (Figure 22). A slightly warmer actual mixed layer with a fluorescence minimum was found overlying slightly colder water which had a fluorescence maximum. Because the mixed layer within the area was not nutrient depleted advection seemed to be responsible for such a configuration. There is some indication that this process was also occurring at profile 125.

The occurrence of deep fluorescence peaks much below the euphotic zone was already described in detail in chapter 5.1.1. During this leg the most pronounced deep fluorescence peak occurred within profile 119 at about 150 m down to 180 m in conjunction with a distinctively lower temperature above and below this depth interval. The deep fluorescence peak showed values up to one third of the maximum value within the mixed layer indicating that the deep peak represented relatively fresh biogenic material which could not have been transported out of the euphotic zone for a long time. This was also reflected in the continuously measured oxygen profile showing maximum values within the depth of the fluorescence peak.

5.2 Chemical oceanography

5.2.1 Trace element geochemistry (JGOFS) (U. Schüßler, R. Bruhn, G. Lippert)

The geochemical trace element studies presented here have been performed as part of the joint Chemistry-Planktology-Programme within the German contribution to JGOFS ("Short- and long-term variabilty of particulate fluxes in the Northeast Atlantic"). Many of the field activities were carried out in close cooperation with the group on "Organic Trace

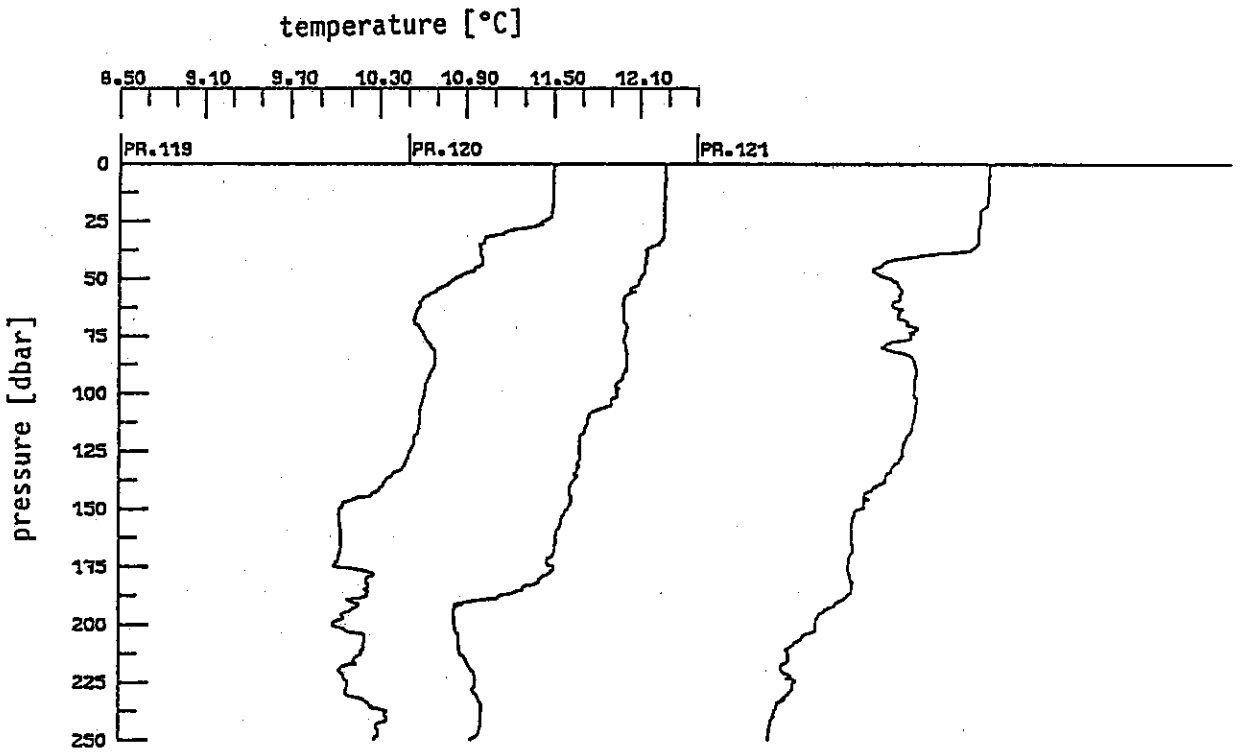

Fig. 22: Temperature profiles 119 to 121 measured during M 21/3

Compounds" (see there), also with our colleagues of the Planktology Department, all of Institut für Meereskunde Kiel.

The marine geochemistry of trace elements was investigated during cruise legs M 21/1, /3, and /6.

Field work may be divided into two different categories, reflecting some of the main goals of our joint programme. First, the vertical flux of particle-bound trace elements was investigated (sediment trap studies). The second part of shipboard activities concerned the elemental composition of both suspended and sinking material (sample collections in various depths by different means).

Three moorings with sediment traps were deployed at the 47°N, 20°W site during cruise leg M 21/1 in March 1992. These traps were scheduled for a sampling period of ca. 4 months during summer 1992 with high temporal resolution. The traps, as well as those deployed during cruise leg M 21/3 (see below), were preconditioned for marine trace element analyses. The rigid cleaning procedures for the traps and a special design of the mooring array were intended to suppress contamination of the samples and thus enable analyses of chemically unbiased samples.

Upon recovery of the moorings, the trap samples were immediately transported to the Kiel laboratory, where all analyses were to be performed under clean room conditions.

Two similar mooring arrays were deployed during cruise leg M 21/3 at 47°N, 20°W and 54°N, 21°W. Each string contained a set of four traps, scheduled for an annual sampling interval (June 1992 to June 1993).

Using both the short-term and the annual trap moorings will give us the opportunity to achieve temporal resolution on different time scales.

Sampling of suspended particulate matter (SPM) was done by two different methods.

Large volume samples of surface particulates (from 8-20m^3 water each) were collected from the cruising ship by high-speed centrifugation using the "Kiel Pumping System" (SCHÜSSLER and KREMLING, 1993). The system consists of a steel shaft with an inner high density polyethylene tube, submerged below the ship's hull, a membrane pump, and several sampling facilities onboard ship (e.g. clean benches, filtration units, and the above mentioned centrifuge). These devices can be supplied with uncontaminated seawater, thus enabling clean surface water sampling techniques required for marine trace constituent investigations.

In addition, water column sampling of particulate matter was done with in situ pumps (see chapter 5.2.2) while working on station. Similar to bottle casts, the pumps were operated while attached to a hydrowire.

In addition, samples were collected for the analysis of dissolved trace element species, particulate organic carbon, particulate organic nitrogen, chlorophyll-a, nutrients, and salinity at 49 stations along the M 21/3 cruise track (Fig. 23). Salinity was measured on board. The remaining parameters as well as data evaluation are subject to onshore analysis.

Salinity decreased along the nearly meridional transect from south to north (Fig. 24), ranged from ca. 36.6 psu down to ca. 35.1 psu around 60°N. From these preliminary data, there appears to be a large (hydrographic) variability in surface waters along the transect. This is in accordance with previously published results (SY, 1988). Similar variability can be shown in the chlorophyll-a data, though, in general, as a function of latitude along the cruise track M 21/3. Crosses denote individual sampling locations. The meridional gradient is opposite to that of salinity. South of about 42°N, there were low chlorophyll-a concentrations (Fig. 25). They tended to substantially higher values further north, but also exhibited strong variability on comparatively small scales (all data shown are preliminary data).

The analyses of the other parameters mentioned above as well as final data analysis are currently dealt with.

Between Madeira and Iceland a total of 12 SPM samples was obtained, transecting different surface water regimes of the Northeast Atlantic (Fig. 23). Optical inspection of the samples qualitatively revealed different features throughout the transect. Apparently low SPM concentrations were found in the southernmost samples from the subtropical NE Atlantic. Amounts of particulate matter of biogenic origin being retained in the centrifuge increased progressively while steaming further north. This is in agreement with the preliminary chlorophyll-a data presented above.

A total of 12 samples of suspended matter for trace element analysis was collected from greater depths with the in situ pumps. All SPM samples were deep-frozen on board, chemical analyses of the samples will be performed onshore. Elements to be analyzed will be Ca, Mg, Sr, Ti, V, Fe, Co, Ni, Zn, Cd, Al, P, and others. Major components of the vertical material fluxes will be determined in cooperation with the other two groups of the joint JGOFS Chemistry/Planktology project.

Both trace element fluxes and the element composition of oceanic suspended matter are important for the description and quantification of the processes affecting trace elements in the ocean's interior. The combination of the element composition of surface SPM (as a precursor of sinking particles) with particle-associated trace element fluxes within the water column will give more detailed insight into marine biogeochemical cycles of trace elements.

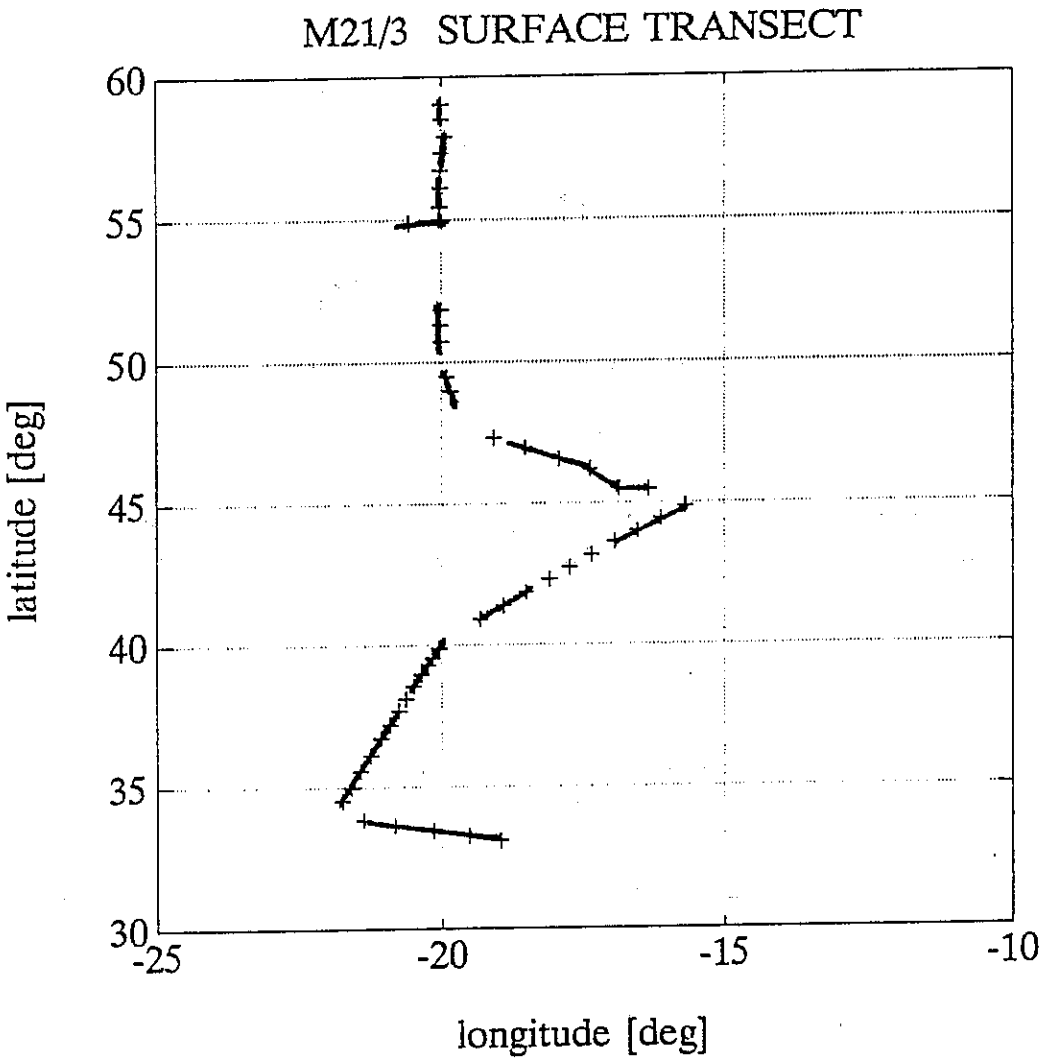

Fig. 23: Sampling locations during M 21/3. Bars indicate distance integrated collection of centrifuge samples. Crosses denote locations of individual spot samples.

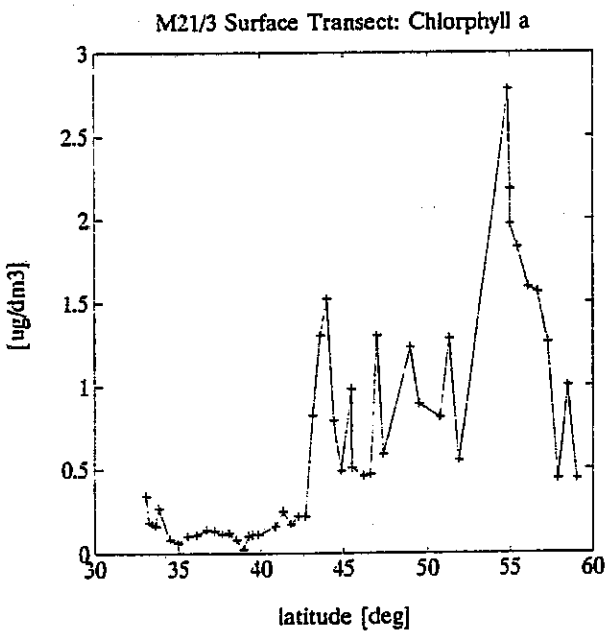

Fig. 24: Plot of surface salinity (given in psu, ca. 7 m depth, preliminary data) as a function of latitude along the cruise track M 21/3. Crosses denote individual sampling locations.

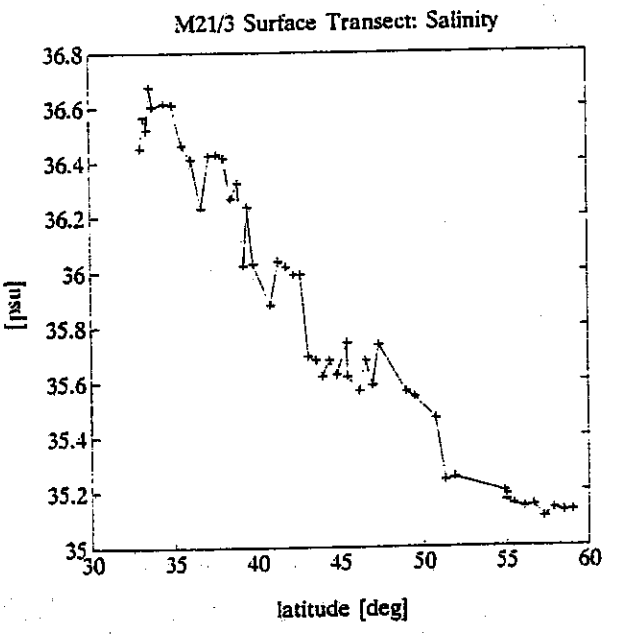

Fig. 25: Plot of surface chlorophyll-a (given in $\mu g/dm^3$, ca. 7 m depth, preliminary data) as a function of latitude along the cruise track M 21/3. Crosses denote individual sampling locations.

5.2.2 Organic trace compounds (JGOFS)

5.2.2.1 **Biomarker substances** (J. Maassen, A. Körtzinger, U. Lundgreen, D.E. Schulz-Bull)

Quantitative and qualitative characterization of sinking and suspended particulate matter in the water column and the upper sediment layers is crucial in understanding more about production and modification of organic material in the ocean. Lipid class biomarkers like isoprenoids, fatty acids and wax esters have proven to be useful tools for providing additional information on the source and fate of particles.

Isoprenoid analysis

During cruise leg M 21/5 water column samples were taken at three stations (318, 323, 328) along a transect from the Vöring Plateau to the East Greenland Sea, and six stations (330, 332, 333, 335, 338, 339) at Kolbeinsey Ridge. Samples from the water-sediment interface and the upper sediment levels were taken from multicorer casts at each site. Suspended particulate matter samples obtained from Whatman GF/F-filtration of casts with a 400-liter stainless steel Gerard sampler and from a newly developed in situ pumping system will be compared as check for consistency. In cooperation with the working group of G. Graf, the near-bottom nepheloid layer was sampled by means of a deep-sea bottom water sampler in four horizons at all stations on Kolbeinsey Ridge.

Sediment samples were centrifuged and stored at -20°C until final processing in the home laboratory after removal of pore water by filtration. All filters were extracted with organic solvents on board. Chemical characterization was carried out by WCOT gaschromatography/ flame ionization detection.

Chromatograms of extracts of suspended particles and preextracted sediments show characteristic features in the chemical composition. Sharp concentration gradients were observed in the nepheloid layer. The compositions of bottom water from both sides of Kolbeinsey Ridge showed differences. Identification of selected compounds of the very complex mixtures had to be done onshore.

Fatty acid/wax esters

During cruise leg M 21/3 the main focus was put on sampling of suspended particulate matter by different means. Water from the "Kiel Pumping System" (snorkel at app. 7 m depth) was filtered through GF/F filters while steaming. At the same time suspended particulate matter was sampled by underway ultracentrifugation along the transects. Water samples from 400-liter stainless steel Gerard samplers were filtered for suspended particulate matter from different horizons of the water colum (50 to 3800 m). Profiles of fatty acid composition in suspended matter will be generated from samples drawn with in situ pumps (GF/F filters) which were deployed at up to 5 different depths at the same time. The consistency of large

volume water samplers and in situ pumping systems for collection of suspended particulate matter was another point of interest.

In addition, the upper 15 cm of the sediment from 3 multicorer casts (stations 200, 209, 217 close to mooring positions) were divided into 2 cm slices for the analysis of the contents and distribution patterns of fatty acids.

All samples were extracted with different organic solvents on board. Analyses are now carried out using multidimensional capillary column gaschromatography (MD-GC) and gaschromatography-mass spectrometry (GC-MS) after cleanup.

Amino acids
The main objective was to monitor the temporal variation of vertical concentration profiles of amino acids at the central JGOFS station (47°N, 20°W) over a six months period (cruise legs M 21/1, /3, and /6).

Samples were drawn from shallow and deep CTD rosette casts (depths range from 10 m to 4500 m) and processed immediately. In order to distinguish between dissolved and particulate amino acids, samples were filtered through 0.4 µm polycarbonate membrane filters. Treatment of filtered particles and filtrates for analysis of particulate hydrolyzable amino acids (PHAA), dissolved free amino acids (DFAA) and total dissolved hydrolyzable amino acids (TDHAA) was carried out on board. Samples were then stored at -20°C until final analysis in the home laboratory. The analytical method involves high performance liquid chromatography (HPLC) of ortho-phthaldialdehyde derivatives. A total of 200 samples from 23 water casts was taken.

A second objective was to assess concentration levels of amino acids in the underlying sediment at 47°N, 21°W. Therefore 20 samples of the upper sediment levels (0-15 cm) were taken from 2 multicorer casts. Samples were centrifugated and frozen at -20°C until further processing in the home laboratory.

5.2.2.2 **Chlorinated Biphenyls** (G. Petrick, D. Schulz-Bull)

Samples were taken from the "Kiel Pumping System" during 9 periods while the ship was steaming, and at various (between 3 and 6) depths from 20 m below the surface to 50 m above the sediment at the stations 206, 211, 215, 216, 219 and 221, by means of in situ pumps described below. The samples were extracted, subjected to a clean up procedure, and analysed by single column GC-ECD on board. Concentrations of individual chlorobiphenyls were between 0.1 and 0.5 pg/l. Further details on the composition of the complex mixtures are now analysed by multidimensional GC-ECD in the home laboratory.

A newly developed in situ pumping system was used for the first time in open ocean waters. The system allows in situ filtration of up to 1000 liter seawater and simultaneous extraction of the dissolved species onto a resin. The high pressure at depth does not affect the resin. The entire procedure of starting and ending the water flow, regulating and maintaining the pumping velocity and battery voltage, is controlled by a built-in microcomputer. Initial problems with the brand-new software could be solved with the help of the electronics department of METEOR and programme details received from Kiel via satellite communication.

The pumping system worked properly, allowing accurate analyses of extremely low concentrations of organics in seawater at various depths, contamination problems being practically eliminated.

5.2.3 CO_2 Chemistry

5.2.3.1 CO_2 partial pressure measurements (JGOFS) (B. Schneider)

The CO_2 partial pressure in surface water (pCO_2) was measured continuously with an equilibrator/infrared system. Measurements were interrupted once daily to measure the atmospheric CO_2 concentration and twice daily to calibrate the infrared spectrometer.

At the beginning of the expedition, water was pumped into the equilibrator with a dedicated pumping system; later on it was supplied by a membrane pump. Due to the higher capacity of this pump, the difference between measured and in situ temperature was reduced to 1°C. Therefore, only minor temperature corrections were required.

The pCO_2 was relatively stable at 310 µatm between 34°N and 42°N. In the same region, low chlorophyll-a concentrations (<0.5 µg/L) and nutrient data close to the detection limits were found.

These results indicate that the spring bloom had ceased in this region and pCO_2 was rising due to seasonal warming and exchange with the atmosphere. North of 42°N, pCO_2 decreased quickly by about 20 µatm and fluctuated between 270 µatm and 340 µatm. The significant correlation between chlorophyll-a concentrations and pCO_2 (r=0.73) allows the conclusion that pCO_2 is controlled by the primary biomass production in this region. A coefficient $d(pCO_2)/d(\text{chl-a}) = 20$ µatm $dm^3/\mu g$ was determined by linear regression. A coefficent of 17 µatm $dm^3/\mu g$ was determined on an earlier expedition in the South Atlantic during the southern spring (November).

These results indicate an important discovery, paralleling the attempt to recognize large-scale, biologically influenced CO_2 changes using satellite observations of the chlorophyll-a

distribution. The variability of primary production and the pCO_2 distribution on scales between 10 and 100 km is mainly due to physical factors, as there is a negative correlation between pCO_2 and temperature on a regional basis. The average CO_2 concentration in the atmosphere was 358 ppm(v). This corresponds to a partial pressure difference between ocean and atmosphere of about 56 µatm north of 42°N and -30 µatm south. Calculations with a global circulation model for the expedition area and time period (E. Maier-Reimer and K. Kurz, Max Planck Institut für Chemie Hamburg) showed a partial pressure difference of only 10 to 15 µatm, underestimating the biological effect on the pCO_2 distribution.

The strong undersaturation of surface water and the resulting transport of CO_2 into the ocean was reflected by changes in CO_2 concentrations in the lower atmosphere. Sometimes, atmospheric CO_2 concentrations measured were up to 8 ppm lower than average values.

5.2.3.2 Alkalinity, total carbonate, pH, and organics (JGOFS)

(L. Mintrop, A. Korves)

During M 21/3 samples were taken from the hydrocast (12 to 16 depths) at 9 locations in order to determine alkalinity, total carbonate concentration, and pH by potentiometric titration (GOYET and POISSON, 1989; JOHNSON et al., 1987). Additionally, surface samples (44 in total) were drawn about every 30 nm using the "Kiel Pumping System". Titrations were carried out immediately after sample collection. The possibility of systematic errors associated with the method of potentiometric determination of total carbonate (as described in literature) was to be examined.

Alkalinity and total carbonate in surface water

A clear trend towards increasing alkalinity and total carbonate values with decreasing temperature was observed. The correlation is quite good for total carbonate, resulting in an effect of -13 µmol/°C. This is mainly explained by the higher solubility of CO_2 in cold water. The correlation is not as good for alkalinity: the effect reduces to -3 µeq/°C. These findings correlate well with those of CHEN (1982) (-12 µmol/°C and -4 µeq/°C, respectively).

Vertical profiles

The vertical profiles showed generally higher values in the oceanic surface layer, lower values at intermediate depths (mainly arising from salinity variations) and increasing values in the deep water towards the sediment, as a result of enhanced dissolution of biogenic carbonate. Mediterranean water is characterized by higher values (salinity effect). Vertical profiles of total carbonate showed good correlation with nutrients (nitrate, phosphate), indicating that organic tissue remineralization contributed more to the increase of total carbonate than dissolution of biogenic carbonate.

Methods comparison

A preliminary comparison of total carbonate values with the coulometer data shows a very good match between the horizontal transect and the vertical profiles. Absolute values differ at about 5-10 µmol/kg. Differences of comparable magnitude also arise from different mathematical assays (nonlinear regression, using 3 or 4 variables, GRAN method) used to fit the same titration data. However, the calculations, especially those for the comparison of titration data, are not finished yet.

Organic acids

The extracts of surface water samples have been processed in the meantime, split into humic and fulvic acids, and the free acids (after THURMAN and MALCOLM, 1981). Mean concentrations, as calculated from the extracted seawater volume and the weight of the isolated extracts, range from 50 to 300 µg/l. The assumed composition $(CH_2O)_{106}$ $(NH_3)_{16}$ H_3PO_4 leads to a mean concentration between 2 and 8 µmol C/l.

5.2.4 **Nutrients and dissolved oxygen** (T. Körner)

Samples for nutrient analyses were taken at all 15 stations of M 21/3 throughout the water column. An autoanalyser was used to determine nitrate, phosphate, silicate, and ammonia on board. Ammonia determinations were less successful in the first part of the cruise; in all cases accurate values were obtained by the additional hand method (Hitachi photometer, 5 cm cell, calibration with deep water).

Nutrients were also determined in samples taken from the "Kiel Pumping System" along the transects from Madeira to Reykjavik. The large number of data are now analysed in the home laboratory. All water samples were analysed for dissolved oxygen concentrations according to the Winkler method. The results agree well with the data obtained with the CTD probe, at least in a qualitative sense.

Characteristic features of the measurements are shown in Figures 26 to 28.

5.2.5 **The CO_2 System of the North Atlantic Ocean (JGOFS)** (K. Pegler, S. Kempe)

On five M 21 legs (no. 1, 3, 4, 5, and 6) total alkalinity (TA), total dissolved inorganic carbon (TC) and salinity were measured. These data are used to calculate the partial pressure of carbon dioxide (pCO_2), the carbon dioxide concentration (CO_2) and the pH of seawater.

On 78 CTD profiles a total of 794 seawater samples was taken with a multiple seawater sampler (24 x 10dm3 Niskin bottles) and analysed soon after the sampling (see table below). Underway, a total of 540 surface samples from ca. 7m water depth supplied by a continual

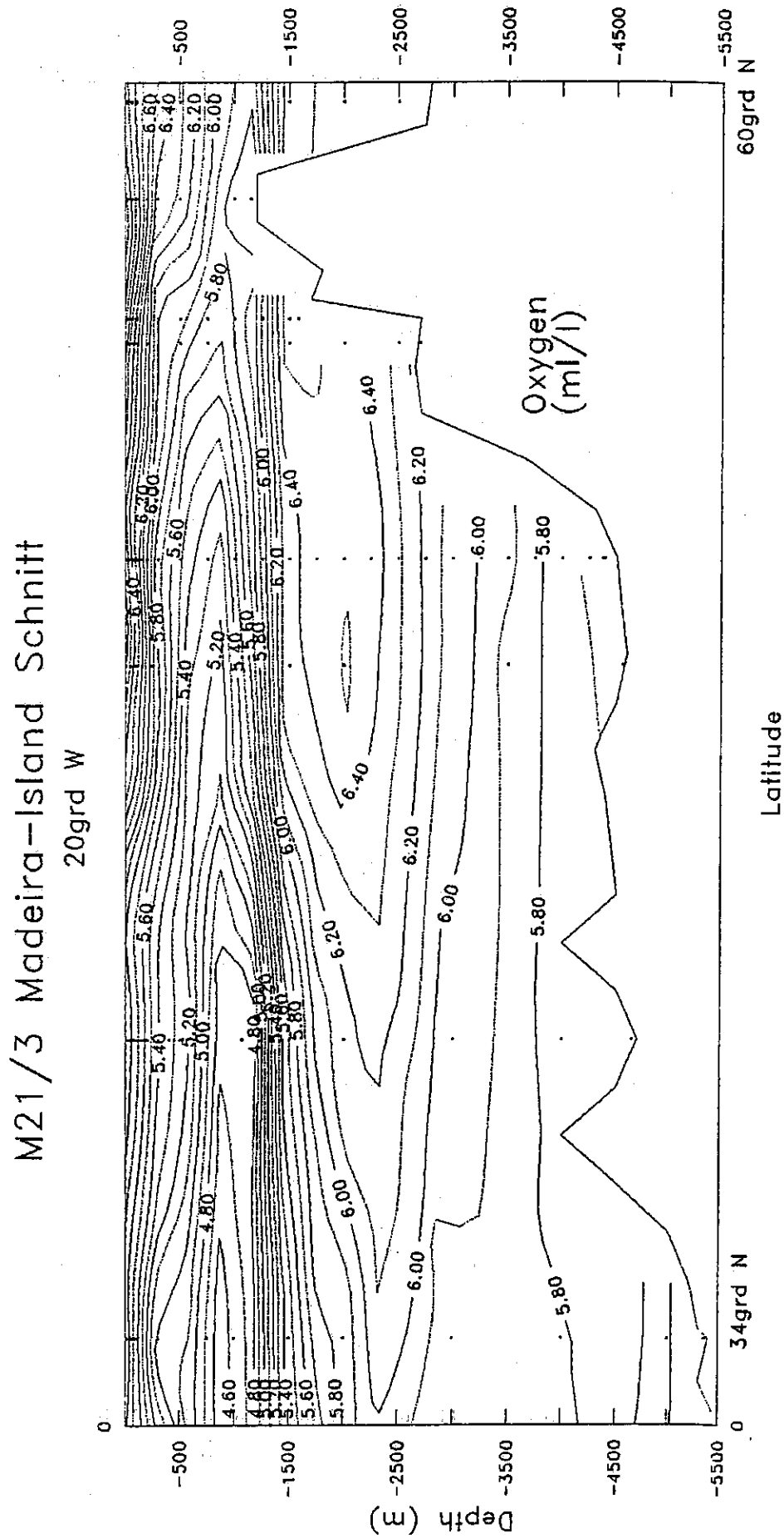

Fig. 26: Concentrations of phosphate (PO_4, in µmol/l), nitrate (NO_3, in µmol/l), and silicate (SiO_4, in µmol/l) from underway samples (pump system) at ca. 7 m water depth. Cross section of dissolved oxygen along 20°W.

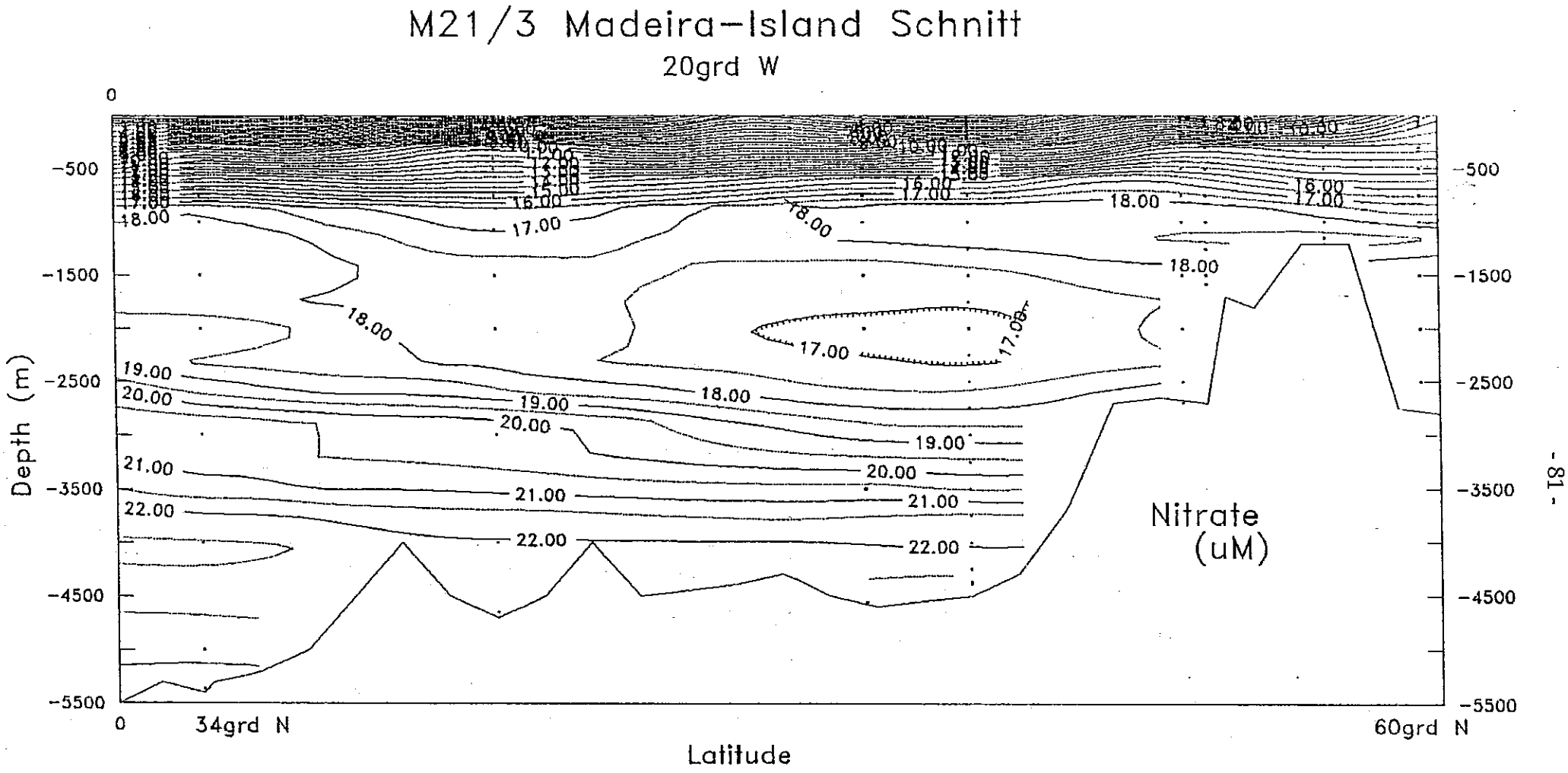

Fig. 27: Concentrations of phosphate (PO_4, in µmol/l), nitrate (NO_3, in µmol/l), and silicate (SiO_4, in µmol/l) from underway samples (pump system) at ca. 7 m water depth. Cross section of NO_3 concentration along 20°W.

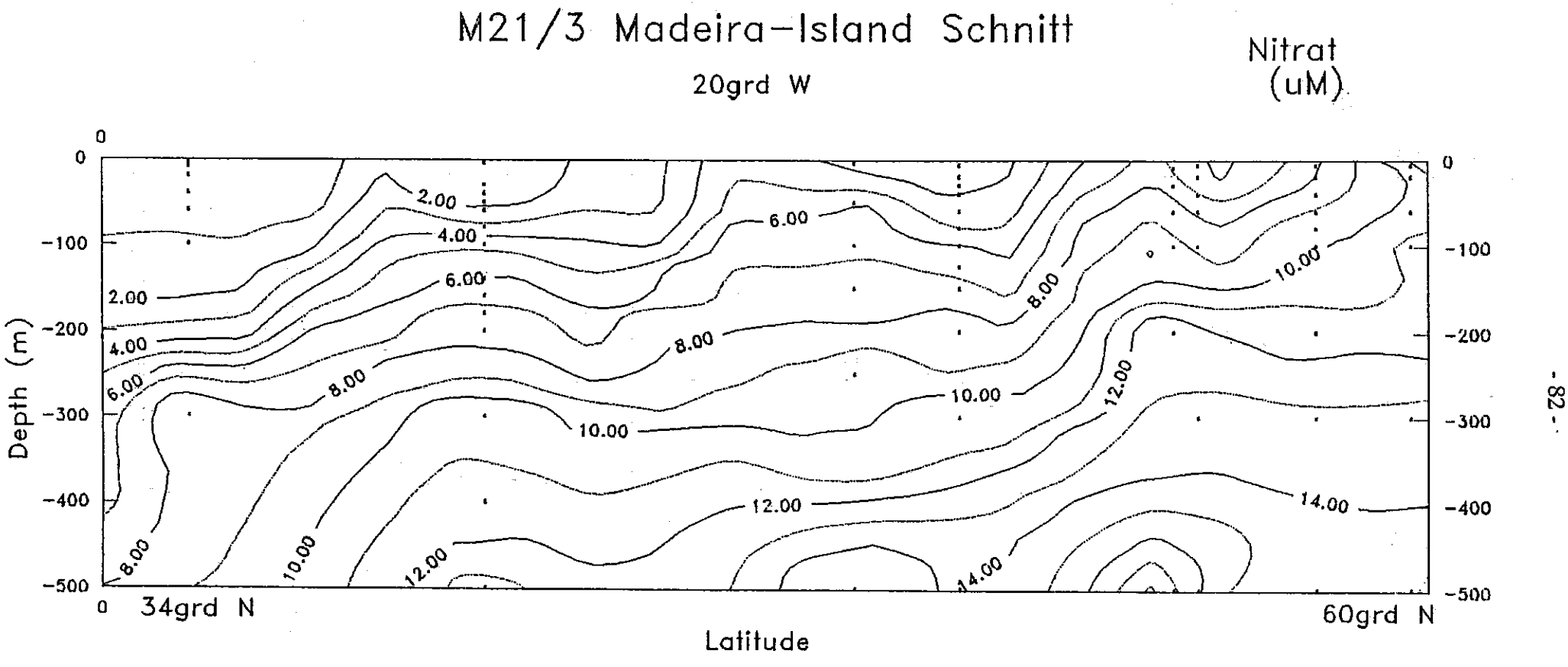

Fig. 28: Concentrations of phosphate (PO_4, in µmol/l), nitrate (NO_3, in µmol/l), and silicate (SiO_4, in µmol/l) from underway samples (pump system) at ca. 7 m water depth. Cross section of NO_3 concentration in the surface layer along 20°W.

seawater pump system (on M 21/1 and M 21/4 to 6 by IBM Hamburg, on M 21/3 comp. SCHÜSSLER and KREMLING, 1993) was measured every two to three hours (UW = underway samples). Additionally, during leg M 21/5 24 samples were taken with a bottom water sampler (= BWS; by G. Graf and P. Linke/SFB 313) on six stations across the Kolbeinsey Ridge north of Iceland. On one cast, the BWS collects four samples from 10, 15, 30, and 45 cm above seafloor (Table 4).

Table 4: List of samples analysed for CO_2 measurements

Cruise legs	CTD samples	Niskin samples	UW samples	BWS samples
M 21/1	9	109	125	-
M 21/3	12	133	57	-
M 21/4	17	198	159	-
M 21/5	18	159	70	24
M 21/6	22	195	129	-
Total	78	794	540	24

On board TA and TC analyses were carried out using a potentiometric precision titration method (see e.g. DICKSON, 1981; DICKSON and GOYET, 1991; ALMGREN et al., 1983). The evaluation of the titration curves occurred ashore. In addition to the potentiometric titration method the TC concentrations of three to four replicates were measured applying a complete CO_2 extraction combined with a coulometric detector (TC coulometry as described by ROBINSON and WILLIAMS, 1991; see also DICKSON and GOYET, 1991).

The preliminary results of the potentiometric titrations (TA and TC), of the coulometric TC analysis, and of the calculated pCO_2, pH, and CO_2 concentrations of leg M 21/3 will be discussed. The final results of all expeditions are available from March 1993.

Concerning the samples taken with the continual pump system, the TA of the seawater surface decreased from the south (beginning at 34°N: > 2400 µeq/kg) to the north (up to 60°N: < 2350 µeq/kg) together with decreasing salinity (ca. 37-35.3 psu) and temperature (17-8°C) (Fig. 29). Therefore, TA behaved conservatively to salinity. In comparison to that, the potentiometrically measured TC (from 2070 µmol/kg at 34°N to > 2100 µmol/kg at 60°N) as well as the coulometrically measured TC (generally by 25 µmol/kg lower as the potentiometric TC) increased towards the north (Fig. 29). This TC increase was due to the uptake of atmospheric CO_2 by the cooling of the North Atlantic Surface Water (NASW). The calculated pCO_2 with approximately 300 µatm suggests that the northern Atlantic was a CO_2 sink in May and June 1992.

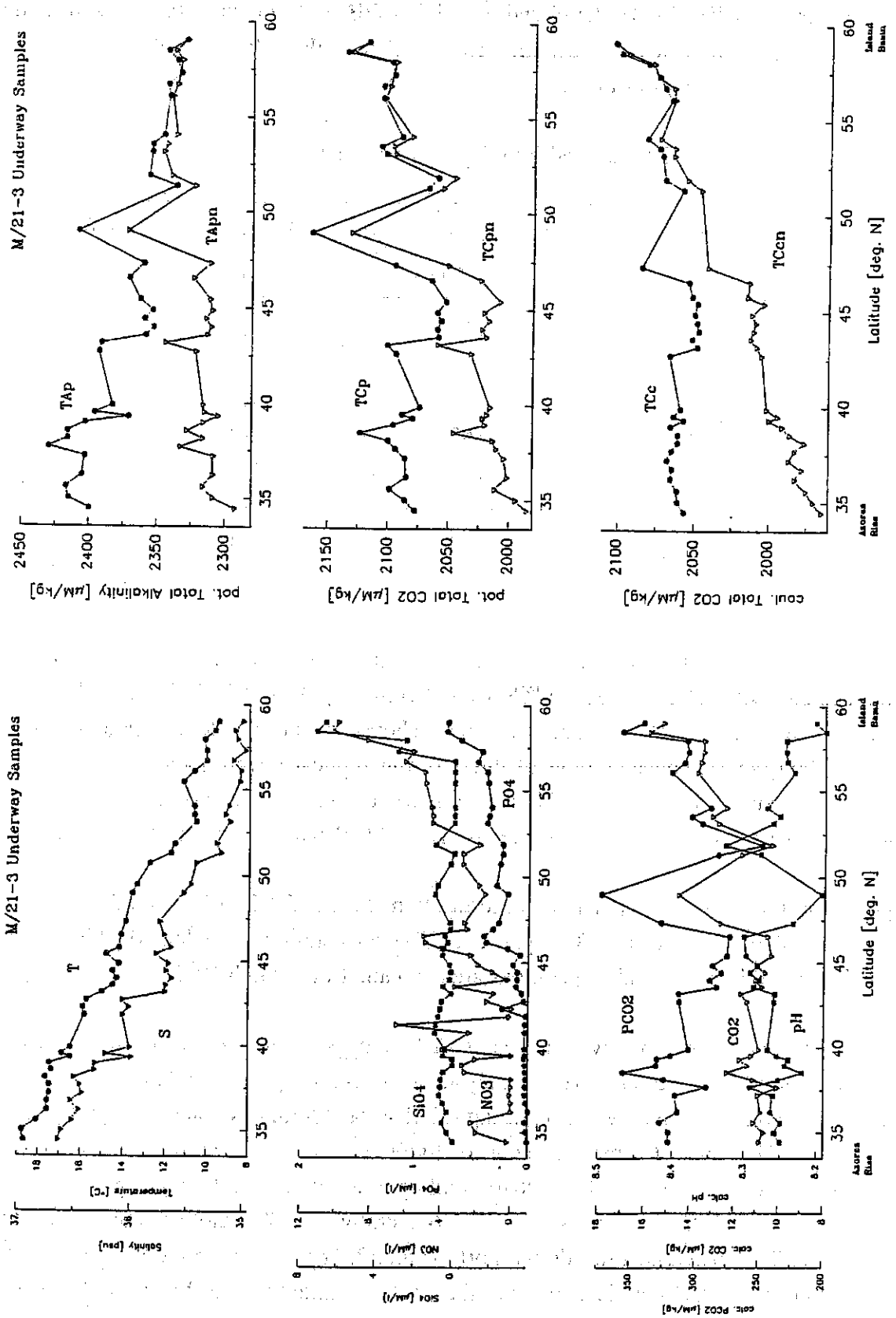

Fig. 29: Underway transects during M 21/3 between 34° and 60°N

The physically dissolved CO_2 in the mixing zone is contrasted by the fixation/release of CO_2 by biological processes. Between 34° and 47°N the PO_4 content at the surface was near to 0 µmol/dm^3, while fluctuating NO_3 concentrations of 0-5 µmol/dm^3 referred to local phytoplankton blooms (Fig. 29) (nutrient measurements by T. Körner/IFM Kiel). From 47° up to 60°N nutrient concentrations slowly increased (0.2-0.5 µmol PO_4/dm^3 and 2-8 µmol NO_3/dm^3) (Fig. 29). Remineralization of nutrients in a quantity of 0.2 µmol PO_4/dm^3 and 5 µmol NO_3/dm^3 by the destruction of organic matter - which had a C:N:P element ratio of 105:15:1 - can release about 20 µmol TC/kg. In contrast, photosynthesis will fix this amount of TC. The difference between a biologically caused short-termed TC maximum and minimum equals with 40 µmol/kg the CO_2 uptake through the cooling of the NASW on the way to the north. Therefore, biogenically implied fluctuations in the marine CO_2 system are seasonally and locally very important.

By definition, TA and TC change proportionally to salinity (e.g. BROECKER and PENG, 1982). The influence of the salt content upon TA and TC is eliminated when these parameters are normalized to a salinity of 35 psu (TAn and TCn). The potentiometrically determined TCn increases from 1980 µmol/kg at 34°N to > 2100 µmol/kg at 60°N (Fig. 29). The coulometrically determined TCn is about 25 µmol/kg lower (Fig. 29). Therefore, the temperate and cold surface differs by 150 µmol TCn/kg which is three times the difference of the unnormalized TC. Obviously, the northward increase of TCn of the NASW is driven by enhanced atmospheric CO_2 dissolution when loosing heat rather than by biological processes.

In comparison to the bulk surface TAn and TCn concentrations of the GEOSECS programme (e.g. BROECKER and PENG, 1982) and the TTO programme (e.g. BREWER et al., 1986), our measurements do not show any deviations. Therefore, the annual pCO_2 increase of 1-1.5 µatm is not traceable with our TC measurements in mixed layer samples.

From the relation of TAn and TCn of the M 21/3 CTD stations one can deduce that the formation ratios of calcium carbonate (Cc) and organic carbon (C_{org}) by marine organisms (i) in the mixed layer of 34° to 47°N is equal to 2:3, and (ii) in the mixed layer of 50° to 60°N equal to 1:3 (Fig. 30). Figure 30 distinguishes between two different water masses and/or different biological activities (e.g. the extraction of $CaCO_3$ by coccolithophorides and foraminifers). So does the TAn record from underway samples (Fig. 29). Following the regression of all TAn and TCn results (surface and deep-sea samples together) of the CTD stations, the Cc/Corg input ratio is 1:4 (Fig. 31). This agrees well with the results of BROECKER and PENG (1982, Fig. 2-9). Therefore, formation and destruction of particles (Cc and Corg) change the TA/TC ratio. The proportion to which cooling of NASW and the organic and inorganic particle flux contributes to the CO_2 export to the NADW (North Atlantic Deep Water) still remains unclear.

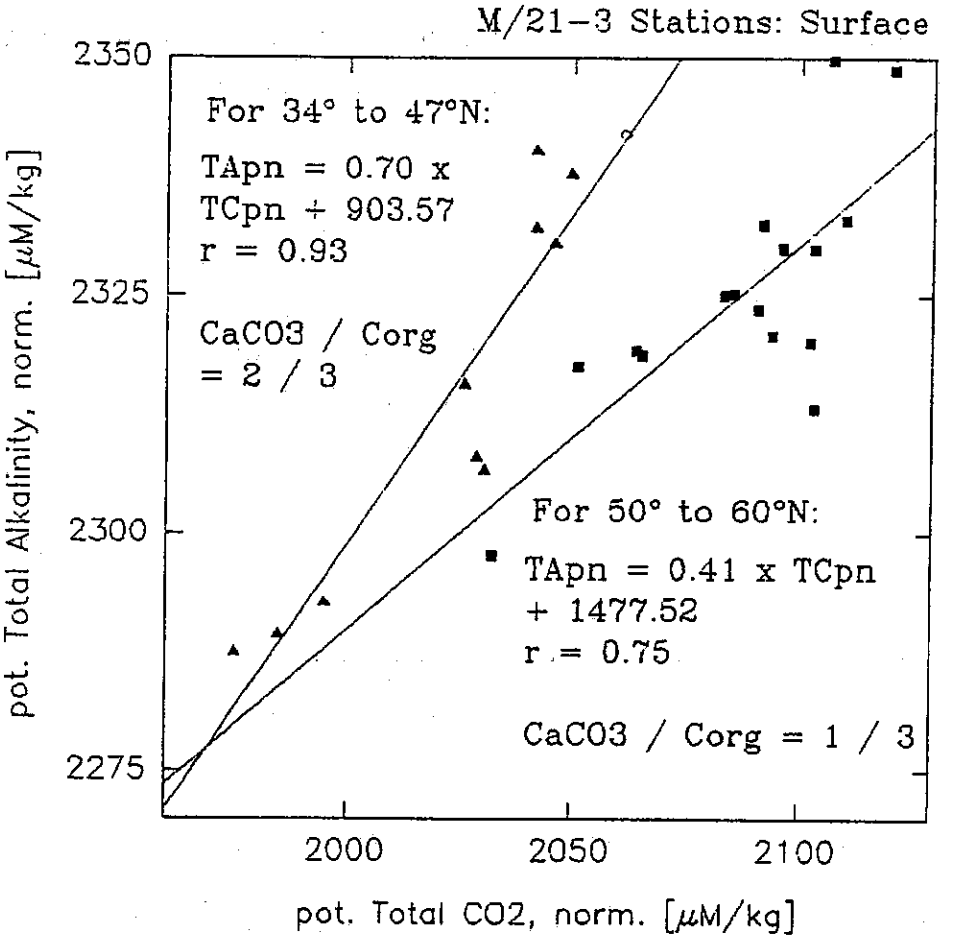

Fig. 30: TA-TC-diagram showing the results from water samples of CTD stations (only mixed layer), with potentiometric total alkalinity normalized to 35 psu salinity (TA_{pn}, in µeq/kg) and potentiometric total dissolved inorganic carbon normalized to 35 psu salinity (TC_{pn}, in µmol/kg).

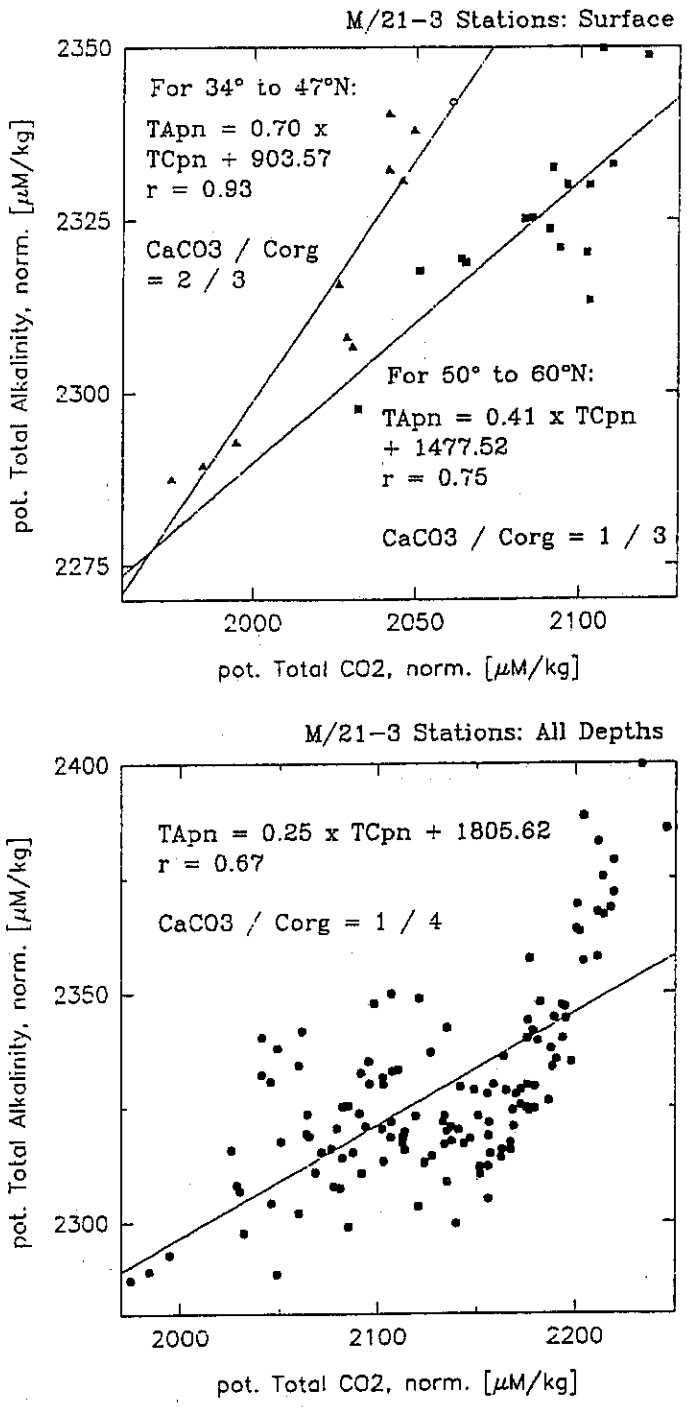

Fig. 31: TA-TC-diagram showing the results from water samples of CTD stations (all water depths), with potentiometric total alkalinity normalized to 35 psu salinity (TA_{pn}, in µeq/kg) and potentiometric total dissolved inorganic carbon normalized to 35 psu salinity (TC_{pn}, in µmol/kg).

5.2.6 Biogeochemical sediment investigations at 47°N, 20°W (BIO-C-FLUX)

(A. Dolle)

Sediment samples from the multiple corer were analyzed during legs M 21/1 and 6 for nutrient contents in the pore water, grain size, and water content. Additionally, some experiments were conducted on changes in contents of ammonia, nitrite and nitrate under different pressure.

Nutrients

Our main interest focussed on the contents of nitrite, nitrate, ammonia, and silicate in different depths of sediment cores taken at ten different stations. Each core from 0 to 21 cm was devided into layers of variable thickness. The first 2 cm were devided into layers of 0.5 cm, the next 3 cm from 2 to 5 cm into layers of 1 cm and down to 21 cm into layers of 2 cm. The sediment of each layer was split up onto 4 test tubes, centrifuged for 1 hour under in situ temperature of 2°C. To avoid erratic effects of particles and bacteria, the overlaying pore water was filtered through a 2 micron syringe filter. In total, a maximum of 60 test tubes was centrifugated depending on the water content of each layer.

The contents of nitrite, silicate, and ammonia were determined after GRASSHOFF (1976). The nitrate contents were later determined at the IHF laboratory in Hamburg. The concentrations were measured photometrically at a wavelength of 810 nm for silicate, 540 nm for nitrite, and 630 nm for ammonia.

Experiments

The following experiments were carried out in cooperation with K. Poremba (BIO-C-FLUX) and aimed at the study of nitrification processes under different pressure conditions. The upper 10 cm of sediment from 10 multiple corer cores were used for the first experiment. The sediment was cut into layers of 1 cm. Samples of the same depths were mixed, split and filled into plastic bags sealed afterwards.

One half of the sediment was incubated under a pressure of 450 bar and the second half under atmospherical pressure, both sets at a temperature of 2°C. For this first experiment a time scale of 0, 4.5, 7, and 12.5 days was applied. After each time interval the pore water was gained from the subsamples as described above. The content of ammonia, nitrite, and nitrate was measured. The different pressure conditions caused an immense increase of ammonia under atmospherical pressure (Fig. 32), and of nitrate under a pressure of 450 bar (Fig. 35). The increase of nitrate under atmospherical pressure was lower, but in comparison to the amounts of the starting values obviously high (Fig. 34). This increase was a result of nitrification initiated by previous increase of ammonia (Fig. 32 and 33) caused by bacterial degradation of proteins. The amount of the increase under atmospherical pressure and a pressure of 450 bar indicated different intrification rates, which were definitely higher under

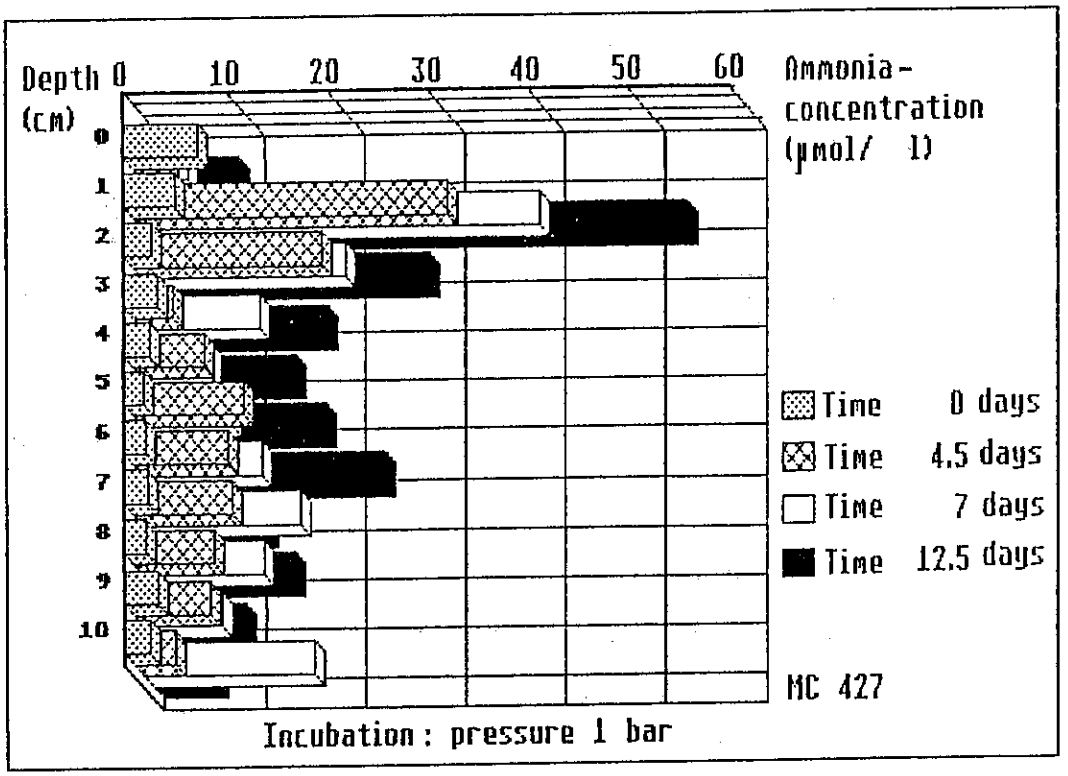

Fig. 32: Increase of ammonia concentration during 12.5 days. Incubation at a pressure of 1 bar.

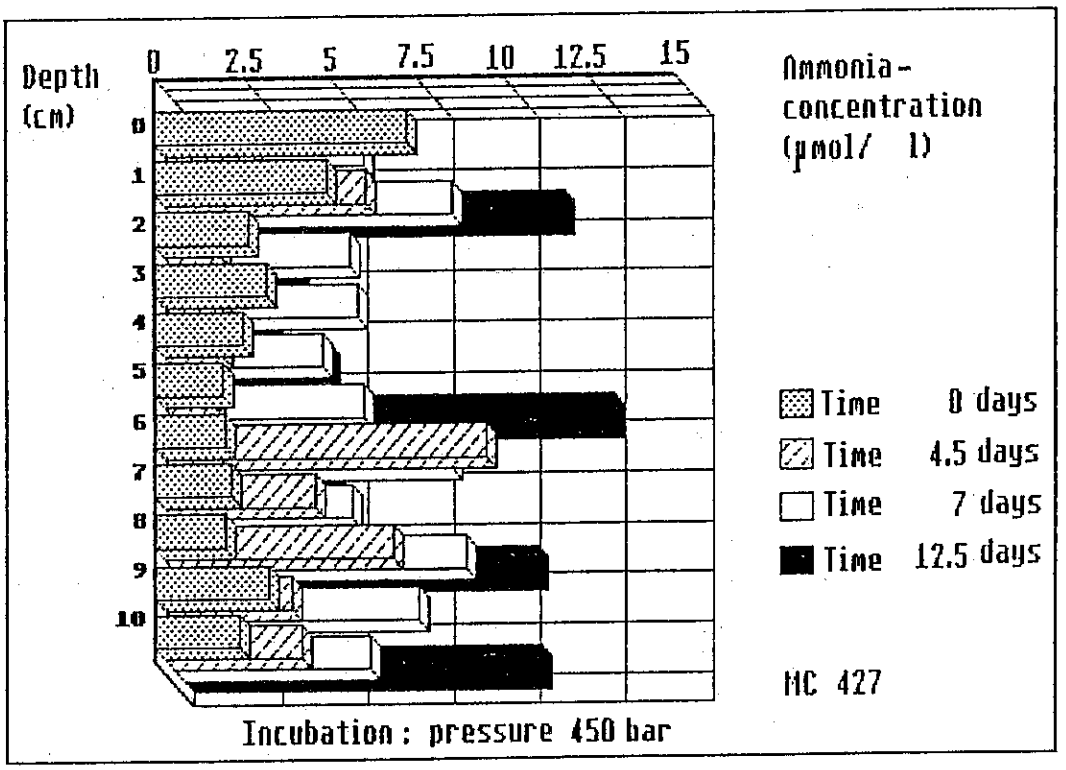

Fig. 33: Increase of ammonia concentration during 12.5 days. Incubation at a pressure of 450 bar.

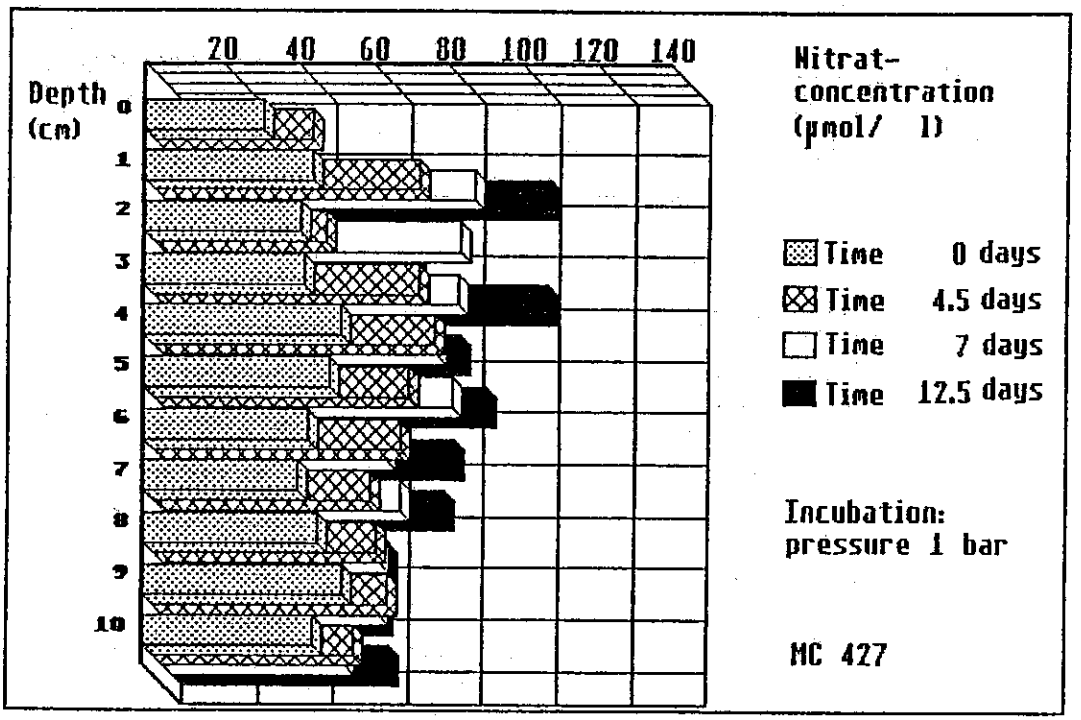

Fig. 34: Increase of nitrate concentration during 12.5 days. Incubation at pressure of 1 bar.

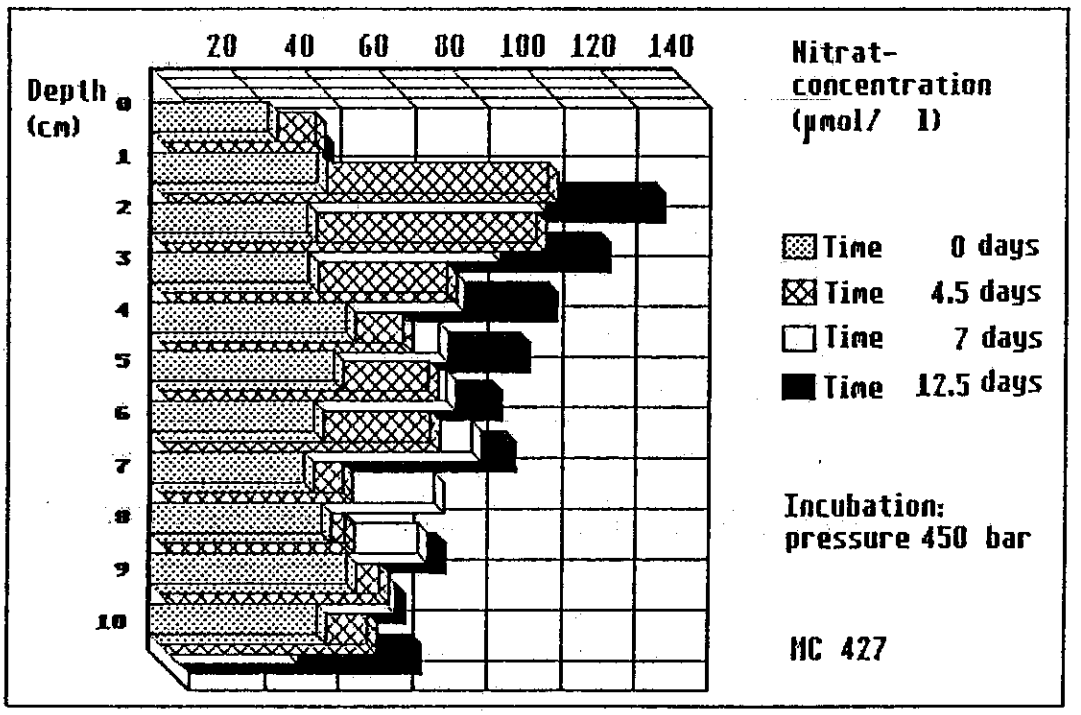

Fig. 35: Increase of nitrate concentration during 12.5 days. Incubation at pressure of 450 bar.

450 bar. This experimental work pointed out the importance of pressure for turnover processes in the deep-sea.

Description of the sediments

To characterize the sediments of the sampled cores some additional parameters like grain size and pore water, carbonate, and organic content were determined. For the determination of pore water content, different layers of sediment were dried at 105°C. The results were calculated from dry and wet weight values.

The results showed a typical gradient of the pore water content in this area (Fig. 36). The first half centimeter contained the highest amount of water which decreased to a minimum at 5 to 9 cm depth and increased below this layer to the deepest layer of the core. The pore water nitrification initiated by a previous increase of ammonia (Fig. 32 and 33) caused by bacterial degradation of proteins. The amount of the increase under atmospherical pressure and a pressure of 450 bar indicated different nitrification rates, which were definitely higher under content at all stations reached in the deepest layers very high values, an indication for the possible presence of a turbidite.

To compare the biological and geological way of determination, two temperatures were used. Whereas in biological work the mainly used temperature is 60°C, in geological surveys 105°C is more common. The results showed an expected decrease of dry weight at 105°C drying temperature and indicated a loss of free and fixed water. Only the free water was dried out at 60°C.

Carbonate content was determined using a closable tube combined with a barometer. The dried samples were devided into two fractions (> 63 µm, < 63 µm) and 1 g of each fraction was used in the procedure. A dried sample of 1 g weight was mixed with an adequate amount of HCl (10%), and the pressure resulting from the formation of CO_2 was calculated to carbonate values.

Dried samples left from pore water analysis were used for the calculation of the organic content in the sediment. Each sample was heated at 500°C for 24 hours. Calculations were done on the basis of dry weight and weight after heating. For some samples the organic content was calculated from sediment dried at temperatures of 60°C or 105°C. First results showed a deviation of nearly 15% between these two temperatures.

Porosity of sediments

To study the porosity of the sediments, several laboratory experiments were set up. First, sampled cores in tubes were fixed in a rack hanging 10 cm above the ground. The lower ends of the tubes were closed with a net, below the cores funnels ending in test tubes with a highly differentiated scale were fitted. A fixed volume of overlying water (204,3 ml) was left in each core. After a definite time, the water which had flown through the sediment core was

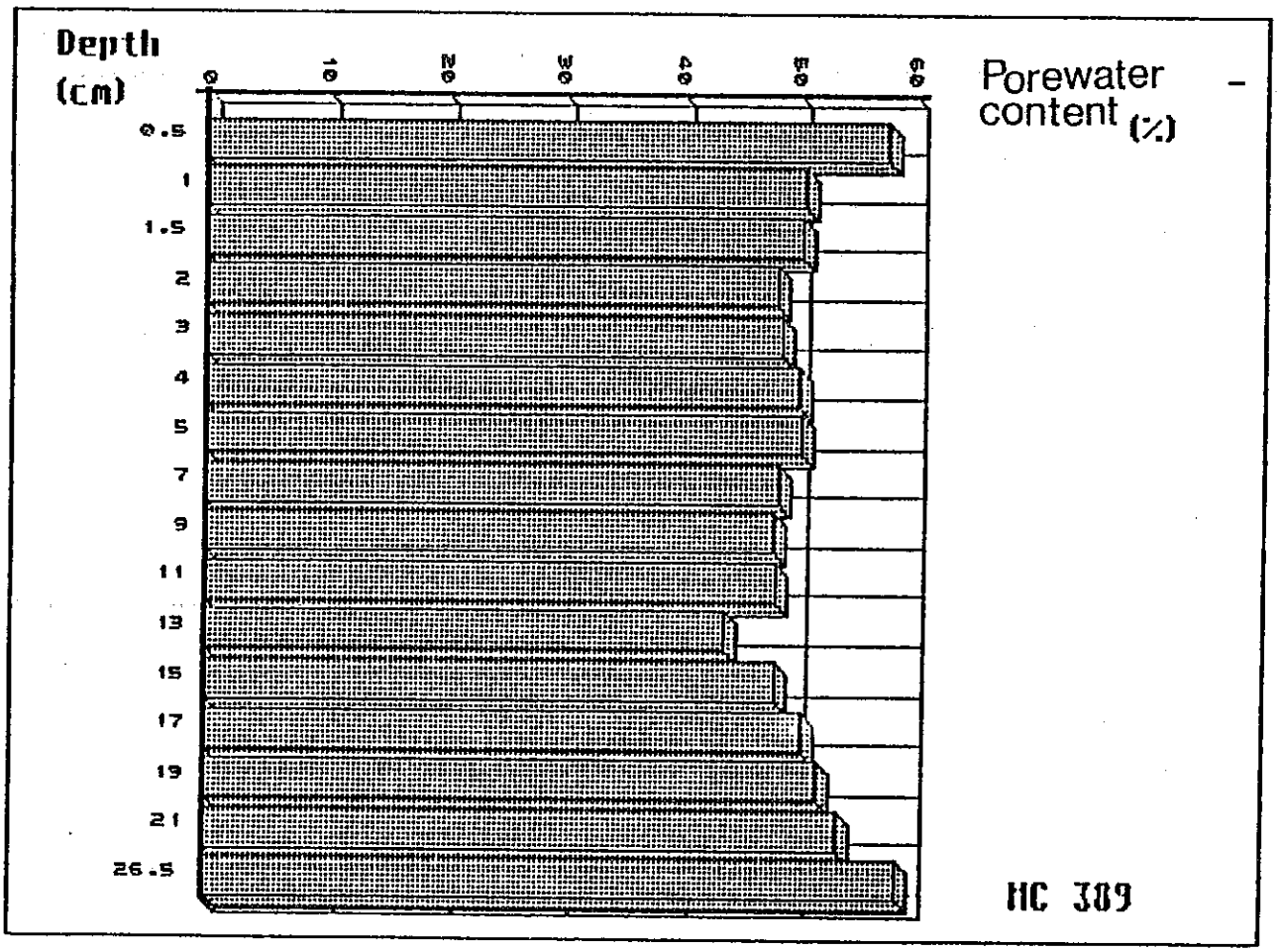

Fig. 36: Pore water contents (%) from a MC sediment core of 26.5 cm length

measured. The results showed that the sediments were less pervious down to the maximal sampling depth of multiple corer cores (30-35 cm).

Then fresh cores were compared with frozen ones. The results showed a clear difference between the natural cores and the previously frozen ones. As demonstrated in Figure 37, the amount of pore water flowing through the prefrozen cores was much higher than through the untreated ones. As seawater freezes in a rather irregular way, i.e. water freezes out first, hypersalinic rest water remains and freezes only at temperatures well below 0°C, the widening of pore space between grains by growing ice crystals or still fluid hypersalinic rest water may be an explanation.

Enrichment of nutrients in the sediment

To understand the diffusive processes which are partly responsible for the enrichment of nutrients in the sediment, a free fall bottom landing incubator ("Freifallinkubator") was used in an in situ experiment to find out how much time nutrients need to penetrate into the sediment by diffusion. This gear resembles the multiple corer but can be left on the deep-sea floor for several days. The main part of it are plastic tubes connected with syringes. These were filled with fluorescein, which was used as a dye. When the gear reaches the bottom and the plastic tubes are half filled with sediment, the syringes are closed with a lid during closing the tubes. Figure 37 demonstrates this process. Thus the overlying water mixes with the dye and is sealed off the surrounding water by the lid. The incubator is equipped with two releases and weights which can be left on the bottom. The buoyancy is received from floats.

After three days the experiment was finished and the weights were released by a hydrophone. The way to the sea surface took one hour and nearly 15 minutes. After recovery of the samples, the concentration of fluorescein was analysed in the overlying water and in different depths of the sediment. The cores were devided into layers of 0.5 cm down to a depth of 3 cm. Fluorescein could be determined down to this depth.

In comparison to this experiment under in situ conditions another experimental work was started on three tubes from the multiple corer in the ship`s laboratory. The tubes were filled with sediment and overlying water. Similar to the in situ experiment the overlying water was mixed with three different concentrations of fluorescein. An incubation time of 5 days was applied. After splitting the samples into different layers and centrifuging the sediment, fluorescein could be determined down to a depth of 2 cm.

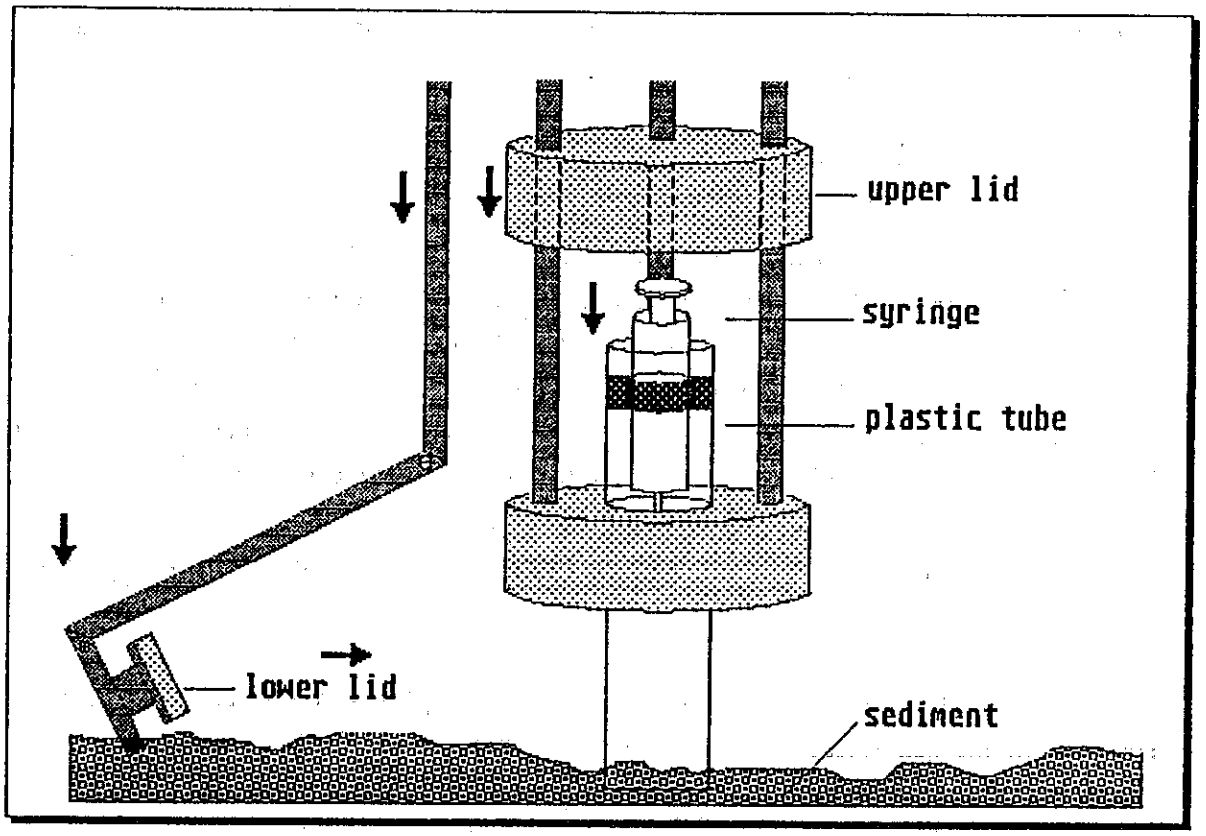

Fig. 37: Closing mechanism of the incubator "Freifallinkubator"

5.2.7 Air chemistry

5.2.7.1 Biogeochemical and atmospheric investigations by the International Air-Sea Exchange Group (M.O. Andreae, D. Amouroux, T.W. Andreae, O. Donard, D. Meyerdierks, S. Rapsomanikis, C. Thiel, G. Uher)

The interrelationships between plankton dynamics on one hand and the production of organic sulfur compounds, carbonyl sulfide (COS), nitrous oxide (N_2O), methane (CH_4), hydrogen peroxide (H_2O_2), and photochemically active substances in seawater on the other were the focus of the biogeochemical investigations by the Air-Sea Exchange Group during leg 2. These studies were accompanied by measurements of the atmospheric concentrations of the trace gases, dimethyl sulfide (DMS), COS, N_2O, CH_4, and ozone (O_3), and of the chemical and physical properties of the atmospheric aerosol. Preliminary results are presented in the following sections which have been contributed by the responsible investigators.

5.2.7.2 Dimethyl sulfide, dimethyl sulfoniopropionate, and phytoplankton in seawater (T.W. Andreae, D. Meyerdierks, C. Thiel)

DMS was determined by gas stripping of seawater, followed by cryogenic trapping, gas chromatographic separation and detection by flame photometry. Dissolved DMSP was measured by addition of NaOH to a degassed seawater sample, followed by determination of the DMS produced from the alkaline hydrolysis of DMSP. Particulate (intracellular) DMSP was determined by filtration (Whatman GF/C glass fiber filters) of seawater, treatment of the filter residue with NaOH, and measurement of the evolved DMS by GC/FPD. For the determination of chlorophyll-a, seawater samples were filtered on glass fiber filters (Whatman GF/C), the filters extracted with acetone, and the extract analyzed by fluorometry. Cell density and phytoplankton species composition will be determined after the cruise from 220 ml subsamples preserved with neutralized formaldehyde solution.

Surface seawater samples for the determination of DMS, DMSP, and chlorophyll were taken every four hours during the transit periods to and from the area of investigations as well as during the drift station. Samples for vertical profiles through the upper 250 m of the water column were taken from 9 CTD casts at the drift station. The diurnal variation in particulate DMSP in surface seawater was followed over a 28 hour time period by hourly sampling at the drift station.

Analysis of the surface water samples showed low concentrations of DMS (ca. 0.5-1.1 nM [nmol/l]), DMSP (diss.) (ca. 3-10 nM) and DMSP (part.) (ca.10-40 nM) in spite of relatively high levels of phytoplankton biomass (ca. 1-2 µg Chl-/l) at the drift station. Higher values were only observed during the approach to the BIOTRANS area, and especially just south of this area of investigation (up to 6 nM DMS and 25 nM DMSP (diss.)). The low DMS/DMSP-

to-biomass ratios observed are typical for early bloom situations, where diatoms and other species with low DMSP content dominate the taxonomic distribution.

The vertical profiles showed a general relationship between the methylated sulfur species and phytoplankton biomass, in so far as both were present predominantly in the mixed layer, and dropped off sharply in the underlying waters. Initially, this layer was quite thick (ca. 150 m), due to the rapid mixing caused by very high winds in the area. During the last few days on station, the development of a new mixed layer and the formation of stable density stratification some tens of meters below the surface caused a sharp increase in phytoplankton biomass, accompanied by increasing concentrations of methylated sulfur species in the upper layer.

5.2.7.3 Sea-to-air flux of dimethylsulfide and the atmospheric sulfur cycle

(M.O. Andreae, T.W. Andreae)

Air inlets for chemical and physical measurements were mounted on the mast of R/V METEOR. Sampling was controlled by an automatic system to eliminate pollution from the ship's emissions. DMS in the atmosphere was measured during the entire cruise by an automatic system using preconcentration from air on gold wool, followed by thermal desorption, cryogenic trapping and GC/FPD. Ozone, as an indicator of airmass composition and origin, was measured by a UV photometric O_3 analyzer (Thermo Electron Model 49). Total aerosol particle counts were made with a condensation nucleus (CN) counter (TSI Model 3020). The aerosol size/number distribution was determined with a laser-optical particle counter (Royko Model 5120) in six size ranges from 0.2 to > 5.0 micron. The black (soot) carbon content of the aerosol, a tracer for polluted airmasses, was monitored with a Magee Scientific Aethalometer. Aerosol samples for chemical analysis of the soluble aerosol constituents were taken on a daily basis using a two-stage filter pack which collects the large size fraction (> 2 micron) and the small size fraction (< 2 micron) on separate filters. Meteorological data were acquired from the ship's data system (DVS).

The measurements of DMS in seawater were used in conjunction with the wind speed to estimate the sea-to-air flux of DMS. Comparison with the observed atmospheric DMS concentrations (which ranged from ca. 5 to 140 ppt) showed a high degree of correlation between the emission of DMS from the sea and its atmospheric concentration. This relationship has not been previously documented. Its detection was made possible during this cruise by the presence of relatively homogeneous airmasses over an extended period in the area of investigations, and a wide dynamic range of the wind speeds producing a large range of variation in the flux signal.

A pronounced shift in airmass characteristics occurred following a warm front passage on 29 April. Fog developed, accompanied by a sharp decrease in O_3. Simultaneously, the

concentration of very large aerosol particles increased from almost nil to several hundred per liter. Aerosol samples showed the presence of beige-colored dust, which under the microscope had the characteristics of Saharan desert dust. DMS was quite high in this airmass (ca. 100 ppt), consistent with high seawater concentrations south of the study area, and a near-surface inversion in the atmospheric boundary layer.

Condensation nucleus (CN) concentrations showed a wide range of variation, consistent with the origin of the various airmasses. The lowest levels (ca. 30/cm^3) were found in marine polar airmasses, the highest (300-400/cm^3) in airmasses from Europe and Africa. A clear relationship between DMS and CN levels, as had been observed on METEOR cruise no. 15/3 in the South Atlantic, was not evident. Black carbon concentrations ranged from not detectable (< 10ng/m^3) in clean marine air to 200-300 ng/m^3 in air which arrived in advance of the dust episode from Africa.

5.2.7.4 Nitrous oxide and methane in seawater and the overlying atmosphere (S. Rapsomanikis)

There exists an imbalance between known global sources and sinks for the above listed trace gases, which play an important role in the greenhouse effect and in the regulation of stratospheric ozone. Surface waters and the air above them were continuously sampled and analyzed in an effort to establish super- or undersaturation ratios and hence calculate gas fluxes. In the early stages of the cruise, supersaturations of between 101-104% and 103-107% were observed for CH_4 and N_2O respectively. These values are not unusual and fluxes calculated from them would not account for missing global sources. However, for the four days from April 29 to May 2 unusually high supersaturation ratios for CH_4 were observed (120-130%). This observation may be related to high biomass concentrations at the time and place of sampling. The N_2O supersaturation ratio reached values as high as 112% at the same time and location. Although the observations of these four days gave us a glimpse of the probable but spurious production of CH_4 from waters high in biomass activity, production mechanisms remain unknown and speculative. Further treatment of results and comparison with atmospheric physical parameters recorded is taking place and may reveal new trends and explanations.

5.2.7.5 Photochemical production of carbonyl sulfide in seawater (G. Uher)

For COS measurements in air, 400 ml ambient air was passed through an U-tube immersed in liquid argon to trap out trace gases which were separated on a chromatographic column and then analyzed by a flame photometric sulfur detector.

For dissolved COS in seawater, a closed volume of air was cycled through a gas bubbler containing rapidly exchanging seawater from the ship's continuously pumping seawater system. The air was equilibrated with the dissolved gases in the water and analyzed as before. The saturation ratios (SR) of COS in water (that is COS(equil. air)/COS(amb. air)=SR) were calculated from the data obtained. Confirming previous investigations, diurnal variations of the COS saturation ratios were observed with the highest values (SR = 2.3) during mid and late afternoon and the lowest values (SR = 0.7) during the early morning hours. The magnitude of the COS saturation was well correlated to light intensities obtained by the ship's data system (DVS). Low light intensities and decrease of dissolved COS during the night ascribed to hydrolysis resulted in an average SR of approximately 1 indicating that there was no net flux of COS to the atmosphere in the study area. Higher COS supersaturations, up to SR = 5.3, were obtained on 2 May, south of the study area. Although light intensities on this day were high, differences in water mass characteristics probably were responsible for this sharp increase in concentration of dissolved COS.

5.2.7.6 Formation and variability of hydrogen peroxide (H_2O_2)

(O.F.X. Donard, D. Amouroux)

The formation of H_2O_2 in marine waters was mainly thought to be driven by photochemical processes in photic surface waters. Some authors consider that this is a way to measure indirectly the photochemical reactivity of the water masses studied. The general pathways recognized occur via photosensitization of marine "Gelbstoff" leading to secondary reaction products. H_2O_2 is assumed to be the result of disproportionation of radical species photochemically formed (superoxide ion, HO_2, and OH). Some suggestions have been made in the literature of the possible occurrence of H_2O_2 formation by biological phytoplankton cultures.

We determined the concentrations of H_2O_2 in different types of water samples. H_2O_2 measurements have been correlated with fluorescence spectra (both excitation and emission spectra) as well as with other biogeochemical parameters relevant to biological activity such as fluorescence of the chlorophyll from the CTD instrument, and chlorophyll, DMSP and DMS measurements performed in the same samples. Further integration of the results will be performed later with data obtained from other participants.

H_2O_2 concentrations determined in surface waters ranged between 40 and 160 nM during the cruise. Highest values were generally recorded during nighttime. Short- and long-term surface variability studies showed that a diurnal cycle could be observed with maximum concentrations (except for a few values obtained during sunny days) always observed at nighttime. Similar results were observed in tank incubation experiments. The tanks are protected from the direct sunlight flux. Concentrations recorded in the tanks also presented a

diurnal cycle with highest values always observed at nighttime. In general, concentrations detected in the tanks were always slightly higher than values recorded in the ocean.

H_20_2 profiles recorded in the photic zone present a general decrease with depth from ca. 100 to 200 nM for surface waters to 40 nM at 200 m. Depth variability at 10 and 20 m during the grid experiment showed that large fluctuations can be observed on a spatial basis. The diurnal cycle evidenced in surface waters and in the tanks experiment was also observed at 10 and 20 m. In the deep casts, H_2O_2 concentrations were always measurable throughout the whole water column. The 1000 meter samples collected during the grid sampling experiment presented no diurnal effect as seen in surface waters, but concentrations recorded fluctuated between 8 to 40 nM with a medium value of 20 nM. These observations are totally new and should be considered with caution since we were not able to obtain a MilliQ blank level of less of 30 nM on board the ship. The fact that deep water samples had always lower H_2O_2 levels than our blank samples suggests that concentrations recorded in the deep samples may be real. H_2O_2 concentrations were recorded through the whole water column down to 4500 m depth. Concentrations presented very little fluctuations and were mostly equivalent to 20 nM. Higher concentrations (40 to 70 nM) were even observed on well preserved overlying waters collected with the multitube cores.

All biotic incubation experiments presented a slow, but continuous increase of H_2O_2 in the samples studied. These results were also obtained with the incubation of water collected from 1000 m depth. The photochemical irradiation experiments presented a slow increase of H_2O_2 in the samples irradiated. Irradiation of a deep water sample yielded a higher concentration at the end of the experiments. The dark control (filtered water samples) did not present any significant fluctuations during the experiments.

These results suggest that photochemistry is not the only driving factor regulating the concentration of H_2O_2 in marine waters. A biological one, mainly via respiration or other metabolic pathways seems to be an unsuspected factor contributing to the regulation of H_2O_2 in marine waters. Finally, the possible occurrence of H_2O_2 in the whole deep water column (down to 4500 m) and just above the sediment should be confirmed for it could have some major implications in several biogeochemical processes such as the redox speciation of trace metals during the sinking of particulate material and reactions with the refractive dissolved pool of organic carbon in the deep ocean.

5.3 Biological Oceanography

5.3.1 Planktological investigations during the Winter-Spring-Summer transition at 47°N, 20°W (JGOFS) (W. Koeve, S. Podewski, F. Pollehne, B. Zeitzschel, F. Jochem, P. Kähler, A. Dettmer, M. Deckers, O. Haupt, S. Reitmeier, S. Böhm, P. Fritsche, R. Werner, C. Sellmer)

5.3.1.1 Overview (W. Koeve, B. Zeitzschel)

Planktological investigations at the BIOTRANS site (47°N, 20°W) were carried out during legs M 21/1-3 and 6. The following paragraphs will give a short introduction to our first results. Detailed reports on plant nutrients, chlorophyll-a standing stocks, vertical particle flux, primary production, flow cytometric measurements, and measurements of dissolved organic carbon and nitrogen are given below. We refer additionally to the chapters on hydrographic measurements (chapter 5.1.1) and microbiology (chapter 5.3.3).

From the comparison of seasonal nitrate profiles and measurements of accumulated phytoplankton biomass it is obvious that significant phytoplankton growth had already started during March 1992 (Fig. 38). This is in contrast to the existing knowledge of the development of the phytoplankton bloom in the area. High variabilities in mixed layer depth, surface nutrient concentrations and chlorophyll-a concentrations (Fig. 39), and integrated standing stocks (Fig. 40) were observed during March and April. It appears that the development of the phytoplankton spring bloom in 1992 occurred in intermittend phases. Phases with shallow mixed layer depth which enable net phytoplankton growth alternate with stormy periods which are able to mix planktonic matter as deep down as 150-250 m (Fig. 41). These deep mixing events appear to increase both the total new production during spring and the amount of organic matter leaving the productive layer. Whether storm induced mixing increases or decreases deep sedimentation is one important question that arises.

Size fractionated primary production was measured during the drift study in April (leg M 21/2). Integrated rates over the upper 80 m varied between 600 and 800 mg C $m^{-2}d^{-1}$ with no clear trend (Fig. 45), while integrated Chl-a concentrations increased from about 50 mg Chl-a m^{-2} at the beginning of the drift study to 80 mg Chl-a m^{-2} after the storm and to 100 mg Chl-a m^{-2} at the end of the drift study (all values for 80 m integral no graphics shown). This obvious decrease in assimilation numbers (the ratio of primary production vs. Chl-a) is paralleled by a shift in the size structure of the primary producers from a dominance of pico- and nanoplankton at the beginning towards a dominance of microplankton at the end of the drift study (Fig. 45). Evidence from preliminary microscopic analysis on board suggest an increasing importance of (large) diatoms after the storm (DECKERS and POLLEHNE, pers. comm.).

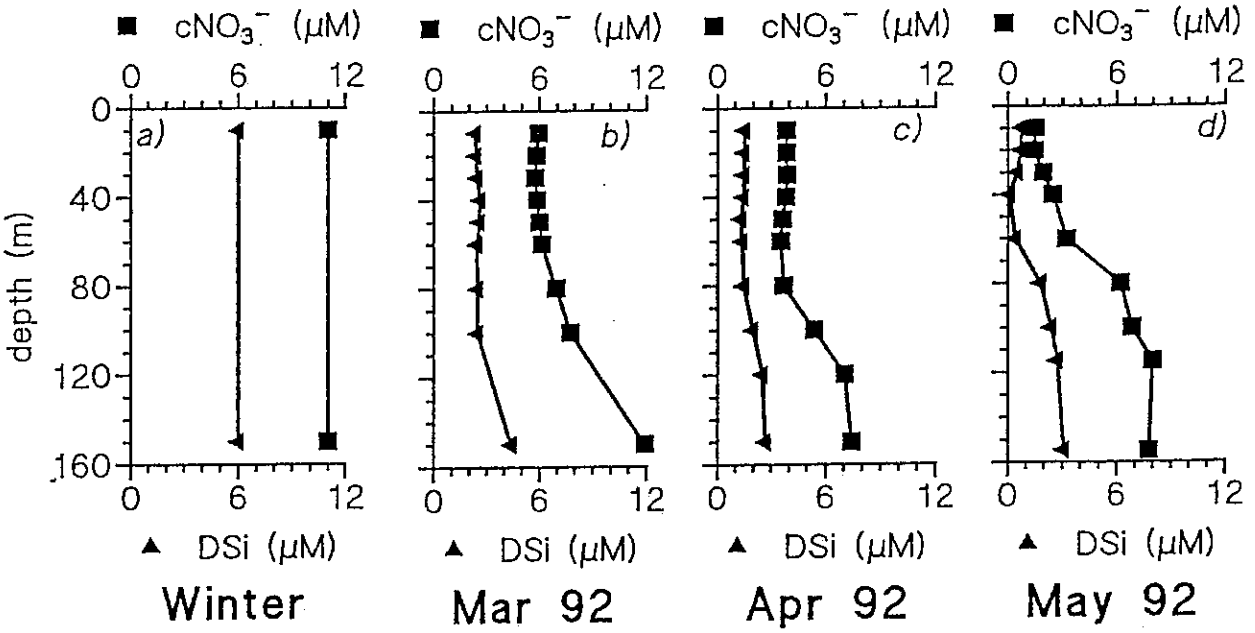

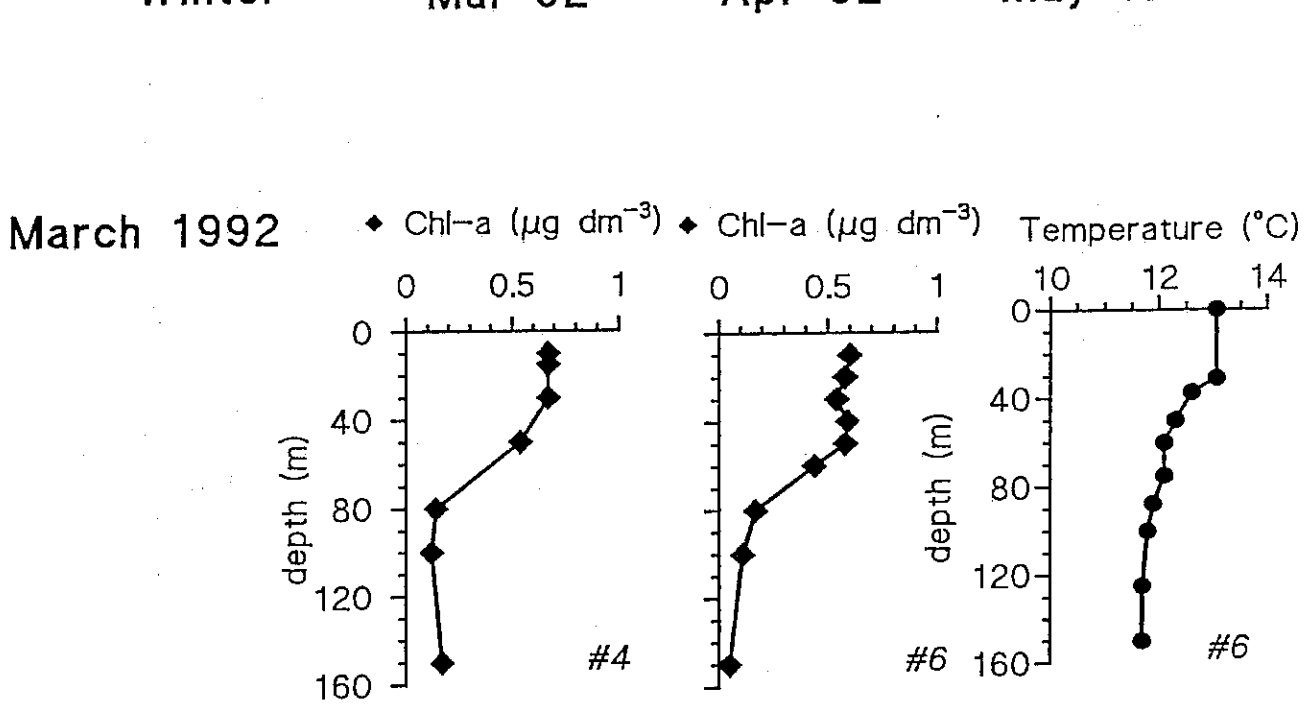

Fig. 38: Seasonal nutrient profiles (a) to (d) from the 47°N, 20°W time series station. The early beginning of the phytoplankton development in 1992 is obvious from nutrient deficiency in the surface layer already in March and from significant chlorophyll-a concentrations during that season.

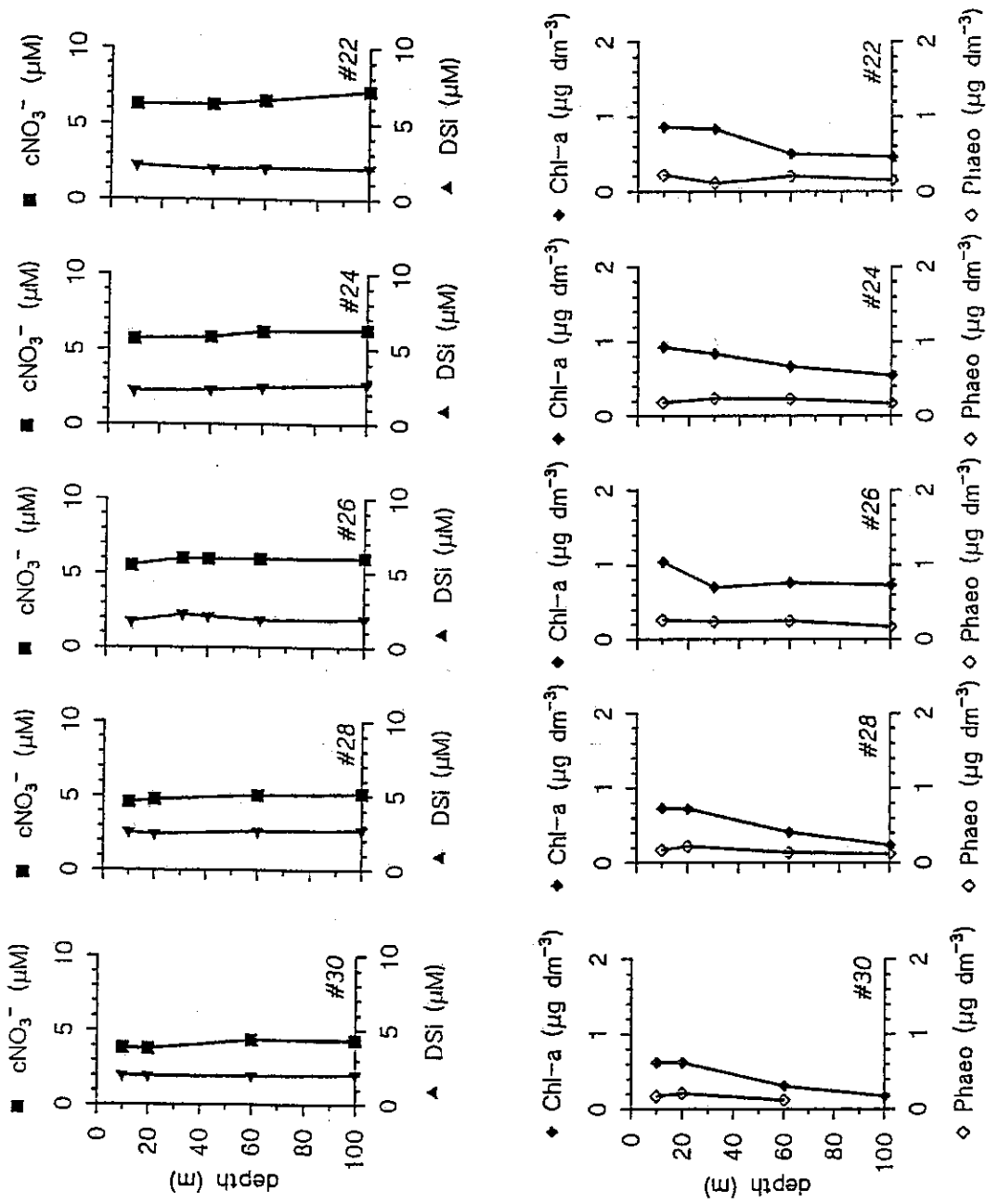

Fig. 39: Nutrient and chlorophyll-a profiles along a west/east transect at 47°N, 20°W. See Fig. 10 for locations of the stations.

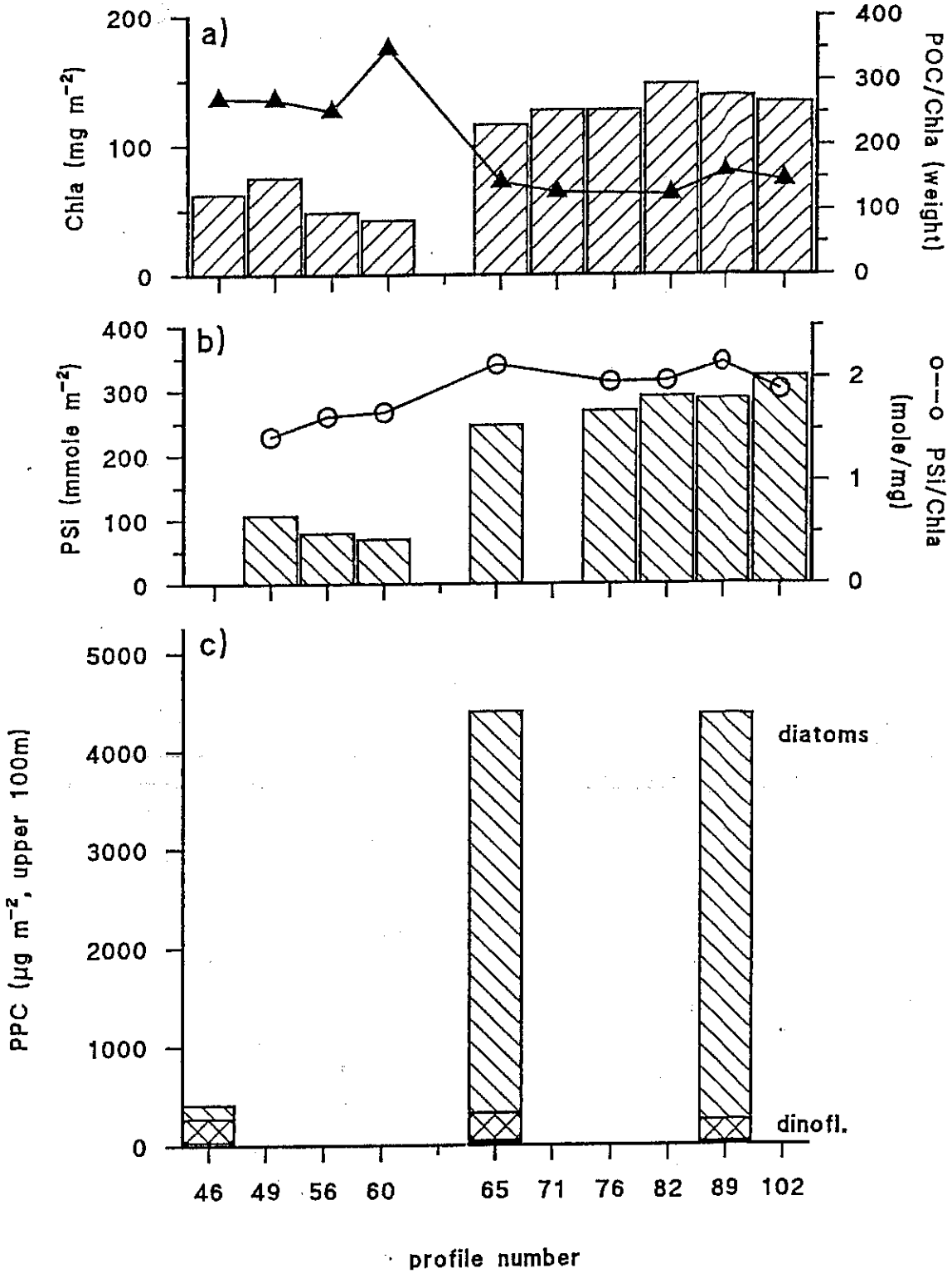

Fig. 40: Integrated standing stocks of chlorophyll-a, particulate silicium (PSi), phytoplankton carbon (PPC) and selected particle ratios during the April drift experiment at 47°N, 20°W. See Fig. 10 for locations of the stations.

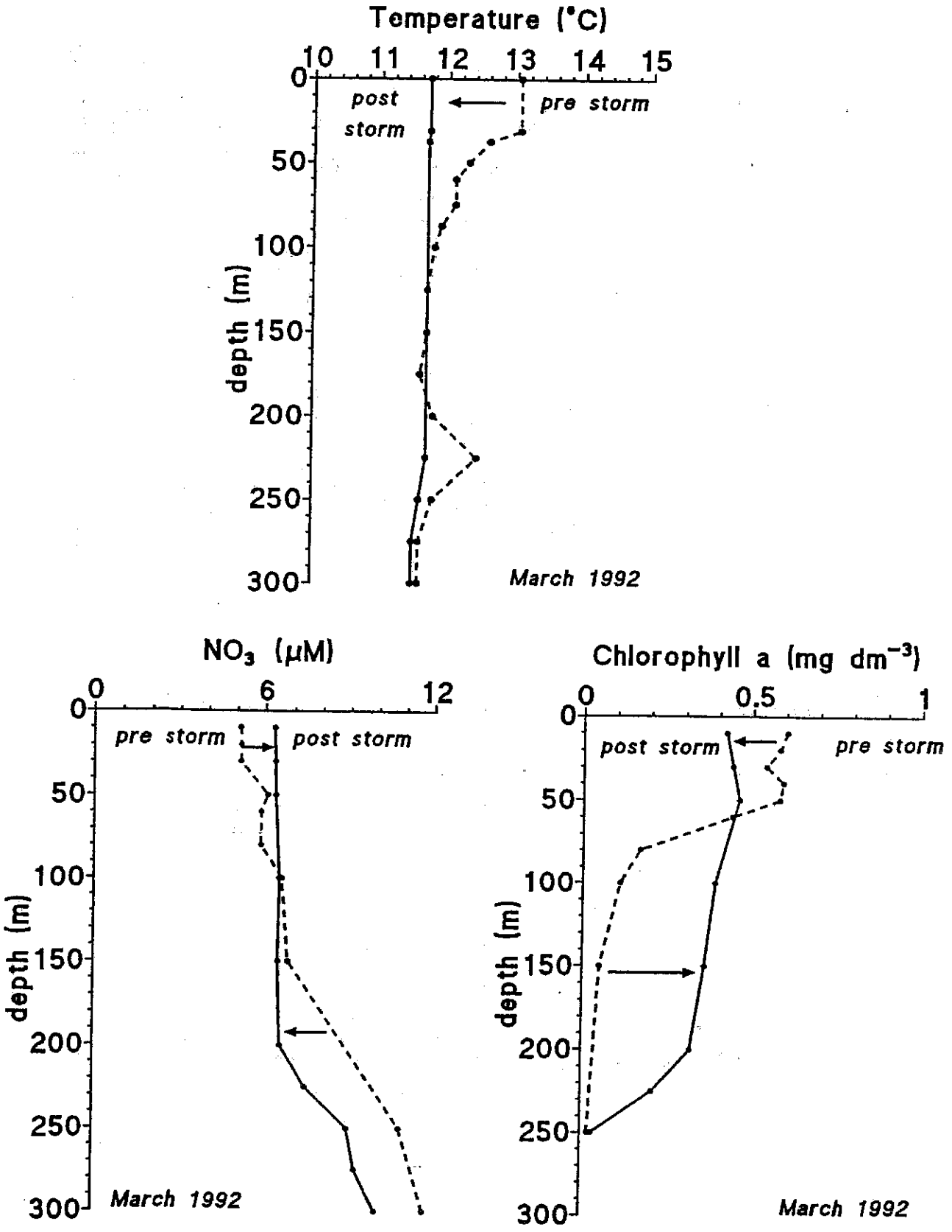

Fig. 41: Storm induced changes in vertical profiles of temperature, nitrate and chlorophyll-a distribution (Observations are from March 1992, 47°N, 20°W).

This change in community structure is further evident from microscopical counts from samples of selected stations and an increase in the PSi/Chl-a rations in the upper 150 m (Fig. 40). A simultaneous decrease in POC/Chl-a (Fig. 40) suggests a change towards a more autotrophic dominated community.

From these observations we conclude that very different phytoplankton communities can coexist during spring at the BIOTRANS site. Together with data from mesoscale hydrographical surveys (data not shown) it appears that much of the observed biological variability is effected by meso-scale hydrographic features and their sensitivity to meteorological perturbations (storms).

One of the major questions arising from this observations concerns the controlling mechanisms that yields these two different communities and the possible importance for vertical flux, particularly deep vertical flux out of the winter mixed layer depth.

First results from drifting sediment traps indicate a sedimentation event just after the drift study in early May, shortly after silicate concentrations had dropped below 0.5 µM.

5.3.1.2 Standing stocks of plant nutrients and chlorophyll-a

(W. Koeve, S. Podewski, R. Werner, P. Fritsche, S. Böhm, S. Reitmeier)

Plant nutrients and the overall seasonal phytoplankton succession

Vertical profiles of plant nutrients, particularly nitrate (NO_3) and silicate (SiO_2), bear important informations on the state of the phytoplankton succession in the course of the seasonal development. A comparison of seasonal nitrate profiles with wintertime nitrate profiles can be used in addition as a first measure of new production of phytoplankton.

Wintertime nitrate concentrations were not measured during this METEOR cruise. While one of our intentions during the first leg was to study the initial and wintertime conditions in the area, low nutrient concentrations in the upper 200 m compared to concentrations at the depth of the winter mixed layer (> 250 m, LEVITUS, 1982 and GLOVER and BREWER, 1988; 400-500 m, ROBINSON et al., 1979) indicate significant nutrient uptake and hence phytoplankton growth already during March (Fig. 38). Wintertime nitrate and silicate concentrations of about 11 and 6 µM, respectively, have been published by GLOVER and BREWER (1988). An independent diagramatical analysis of our data from the first leg indicates wintertime concentrations for 1992 of about 11+-0.9 µM Nitrate and 4.8+-0.6 µM Silicate.

Surface nitrate concentrations during March, April and May were about 5 to 6 µM, below 3 to 6 µM and 1 to 2 µM, respectively (Fig. 38). During August nitrate was depleted in the upper 30 meters. The observations from March and the slow decline of surface nitrate

concentrations indicates that the spring season, which is terminated by a depletion of new nutrients in the surface layer lasted from at least early March to early June. We suggest that the spring development in 1992 appeared in intermittend phases.

Lateral and temporal variability of nutrients and chlorophyll-a

The lateral and temporal heterogeneity in nutrient and chlorophyll profiles which is obvious from the data sets of leg M 21/1 and 2 appears to be strongly related to the hydrographic structure, particularly the variability of the mixed layer depth (see chapter 5.1.1). During leg M 21/1 surface nitrate concentration were between 5 and 6 µM before a storm event but up to 7 µM after the storm had passed (Fig. 41). The same storm caused the mixed layer depth to increase from about 50 m (or even less) to about 240 m. Before the storm event relative high chlorophyll-a concentrations between 0.5 and 0.7 µg dm^{-3} were usually restricted to the shallow mixed layer (Fig. 41) and chlorophyll concentrations decreased rapidly below. After the storm event, however, chlorophyll concentrations were almost homogeneous down to 150 m and significant chlorophyll concentrations were measured even in 225 m depth (Fig. 41).

Mesoscale variability was also evident from pre-drift surveys conducted during the April study. Surface nitrate concentrations along an east/west transect for instance decreased from about 6 µM at profile #22 to 4 µM at profile #30, while silicate concentrations remained at about 2 µM (Fig. 39). Similar differences in surface nitrate concentrations were observed along another transect, surface silicate concentrations along this transect, however, did show some inverse relation to nitrate concentrations (Fig. 42). Variable ratios of nitrate to silicate disappearence relative to wintertime concentrations may indicate varying importance of diatoms vs. non-silicious phytoplankton during the preceeding period at these stations (see KOEVE, 1992). Chlorophyll-a concentrations were below 1 µg dm^{-3} during the east-west pre-survey and surface concentrations decreased from east to west from about 1 to about 0.6µ g dm^{-3}. Although chlorophyll concentrations were usually highest at or near the surface, significant chlorophyll-a concentrations were also observed well below the productive surface layer (about 50 m, see below). Differences in size structure of phytoplankton might emerge from differences in the scatter of in vivo fluorescence as observed for instance along the east-west transect (Fig. 40).

Drift study

The sampling of the mesoscale grid was followed by a drift study where vertical profiles of nutrients, plankton biomass and production parameters were taken twice a day while following a drifting sediment trap which was suspended in 120 m depth. A second independent drift rig carried a trap at 185 m. Both trap systems drifted almost parallel in southeast direction over the whole period of 13 days. The drift tracks are shown in Figure 10.

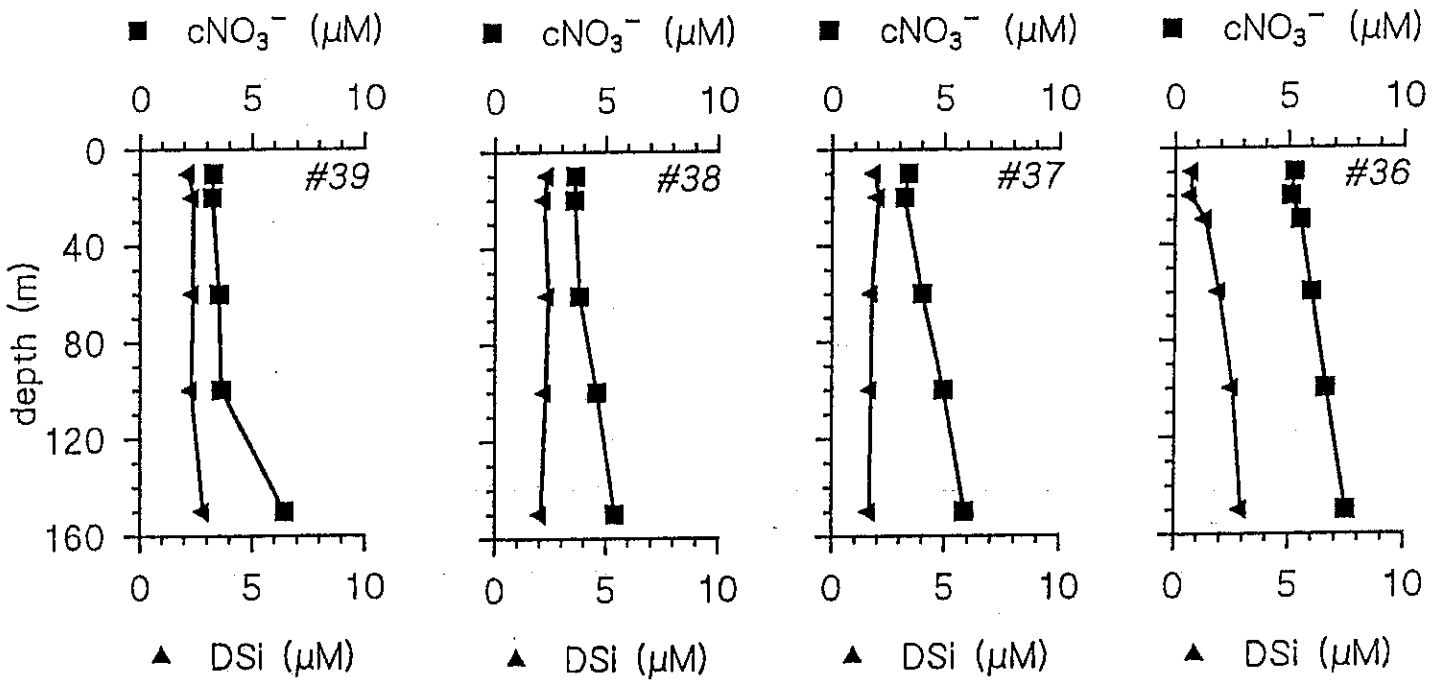

Fig. 42: Vertical profiles of nitrate and silicate along a north-south transect at 47°N, 20°W. See Fig. 10 for locations of the stations

The drift experiment lasted for 13 days, sampling, however, was only possible on 10 days due to a storm event (with windspeeds up to 11 Bft) between 23 and 26 of April. During the four days before the storm, surface nitrate and silicate concentrations were 4 to 5 μM and 1 to 2 μM, respectively. Chlorophyll-a concentrations in the mixed layer (50 to 90 m) were below 0.8 μg dm^{-3}, but at the detection limit (0.1 μg dm^{-3}) at greater depth (Fig. 43). When the sampling started again after the storm, mixed layer depth, nutrient concentrations and chlorophyll concentrations had increased. During the following three days nitrate, silicate and chlorophyll concentrations were homogeneous in the upper 150 m (5-6 μM NO_3, 1-2 μM SiO_2 and about 1 μg dm^{-3} Chl-a). A doubling of Chl-a standing stock integrated over the upper 150 m after the storm compared to the stations sampled before the storm (Fig. 40), questions the Lagrangian character of the drift study, since significant net phytoplankton growth during the stormy period is unlikely. During a following calmer period a shallow mixed layer reestablished quickly giving rise for rapid phytoplankton growth. A surface maximum developed and chlorophyll-a values of almost 2 μg dm^{-3} were recorded. During these days silicate values at the surface dropped below 1 μM. The general decrease of dissolved silica concentrations over the whole period coincides with increasing importance of diatom phytoplankton as documented by microscopical observations. As the silica values, however, were approaching limiting concentrations, a sedimentation event of diatoms and a resulting shift between phytoplankton populations in the near future after the drift experiment could be expected. In order to follow these processes we redeployed our drifting trap system for another period of fourteen days. A sedimentation event during the first half of this period was indeed evident from a first visual inspection of the sampling cups.

Storm events like those observed during leg M 21/1 and 2 will influence both new production and export of organic matter out of the productive layer. Storm induced nutrient inputs will increase spring new production, but storm induced mixing appears to be an important process that transports organic matter out of the euphotic zone (export production). Whether storm induced mixing increases or decreases deep sedimentation (i.e. below the depth of the winter mixed layer) is one important question that arises. Since it dilutes particle concentrations and hence the probability of aggregate formation one might speculate that storm induced sinking favours slow sinking of organic matter and subsequent remineralization in the upper few hundred meters.

5.3.1.3 **Productivity regime and phytoplankton size structure** (F. Jochem)

Primary productivity was measured by daily dawn to dusk in situ incubations along a Lagrangian drift track. Phytoplankton size structure was evaluated by size fractionation of both primary production and chlorophyll measurements. First results of primary production measurements with respect to phytoplankton size structure in the potential spring-bloom period at the investigation site are presented. Incubation experiments on the occurrence and mode of survival of deep-sea phototrophic organisms (namely *Synechococcus*-type coccoid

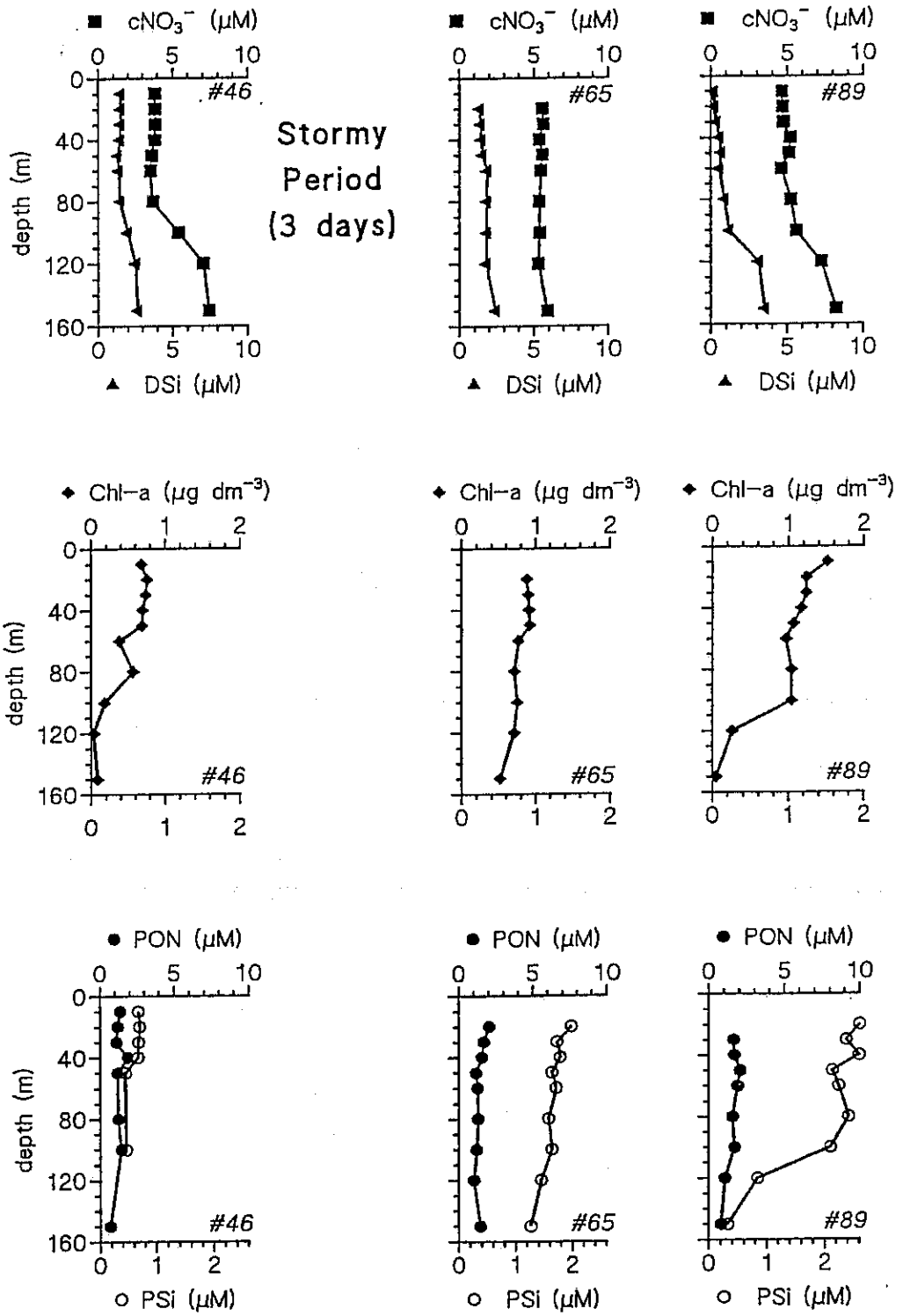

Fig. 43: Typical profiles of nitrite, silicate, chlorophyll-a, particulate organic nitrogen (PON) and particulate silicium (PSi) during the April drift study at 47°N, 20°W. See Fig. 10 for locations of the stations

cyanobacteria; A.E. Detmer) were supplemented by occasional productivity measurements to evaluate the metabolic status of these organisms growing in the dark and under light.

Primary production was measured by in situ $^{14}CO_2$ incubations of 12 hours duration in 250 ml polycarbonate bottles (25 µCi per bottle). 10 to 12 bottles of the upper 80 m were incubated. Two additional bottles treated with 1 x 10^{-5} mol l^{-1} DCMU [3-(3,4-dichlorphenyl)-1,1-dimethylurea] were used as dark correction and substracted from light bottles. After incubation, samples were treated with 1.5 x 10^{-5} mol l^{-1} DCMU to prevent carbon uptake while bottles were processed. Bottle contents subsequently were size-fractionated and filtered onto 0.2 µm membrane filters. ^{14}C-uptake was determined by liquid scintillation measurements in a Packard TriCarb. Due to rough weather conditions, no sampling was possible on days 4 to 7 (April 23 - 27).

For size fractionation "total", "< 20 µm", "< 5 µm", and "< 2 µm", post-screening classes were used. Aliquots of 45 ml were used for fractionation to avoid variance due to different bottles. Estimates for "total" were obtained from untreated aliquots, the other aliquots were filtered through 20 µm net gauze and 25 mm, 5.0 µm, and 2.0 µm Nuclepore filters, respectively.

On one occasion (station 170, April 28), phytoplankton exudation was measured as ^{14}C-accumulation in the 0.2 µm filtrate after removal of inorganic CO_2 by acidification (pH < 2) and 30 minutes airbubbling. ^{14}C in the filtrate of DCMU bottles were used as blanks since no photosynthesis, thus no exudation, should have occurred in these bottles. No exudation was detectable in neither of the samples.

During the first half of the drift study, vertical profiles of primary production (Fig. 44 a) revealed some repression in near-surface samples, leading to a shallow subsurface maximum at 5-15 m depth. During the second half (from station 170, day 9 on), a distinct surface maximum (2 m sample) occurred recurrently, additionally to the shallow subsurface maximum (Fig. 44 b). Maximum production accounted to about 2.4 µg C l^{-1} h^{-1}. At 80 m depth, some productivity (ca. 0.1 µg C l^{-1} h^{-1}) was still detectable. Throughout the whole study period, integrated primary productivity (top 80 m) was about 0.6 to 0.7 g C m^{-2} d^{-1} (Fig. 45).

During the first half of the drift study, phytoplankton productivity was dominated by organisms < 5 µm, the contribution of picoplankton being 40-52%, of small nanoplankton 2-5 µm ca. 30% of total integrated production, respectively. The second half was marked by a significant increase in microplankton (> 20 µm) productivity (from 17% to 43-55% of total) and slightly higher values in the 5-20 µm size fraction, concomitant with the observed increase in diatom abundance. At the same time, pico- and small nanoplankton (< 5 µm) production was lower, contributing only 20% and 10% of total integrated productivity, respectively. Microphytoplankton was restricted, however, to the upper 40 m during the

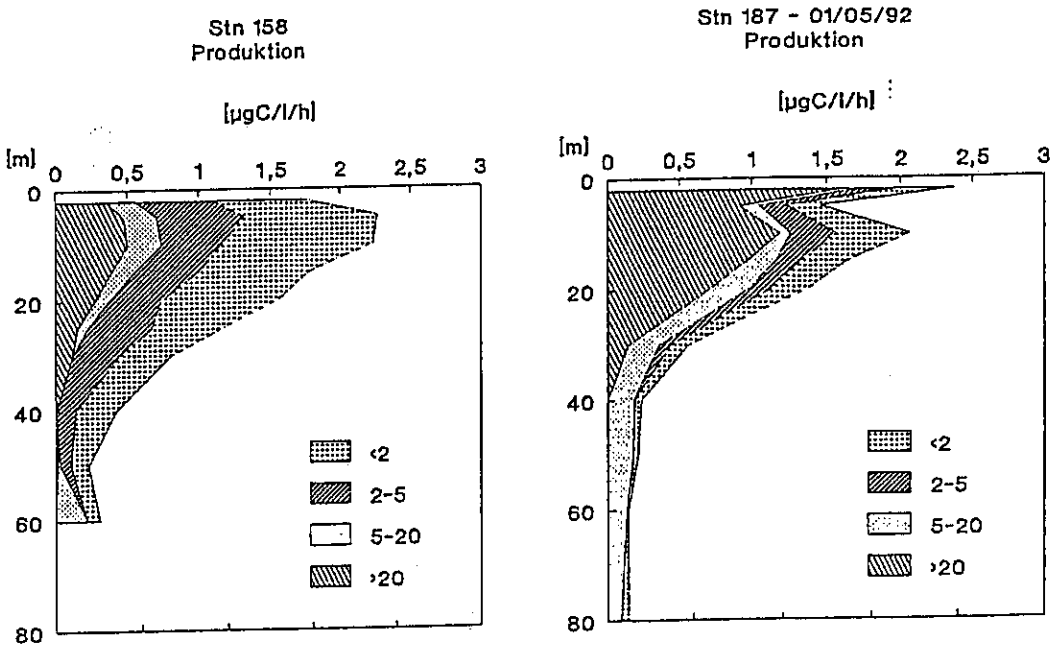

Fig. 44: Vertical profiles of size-fractionated primary production (µg C l^{-1} h^{-1}) at (a) station 158 and (b) station 187

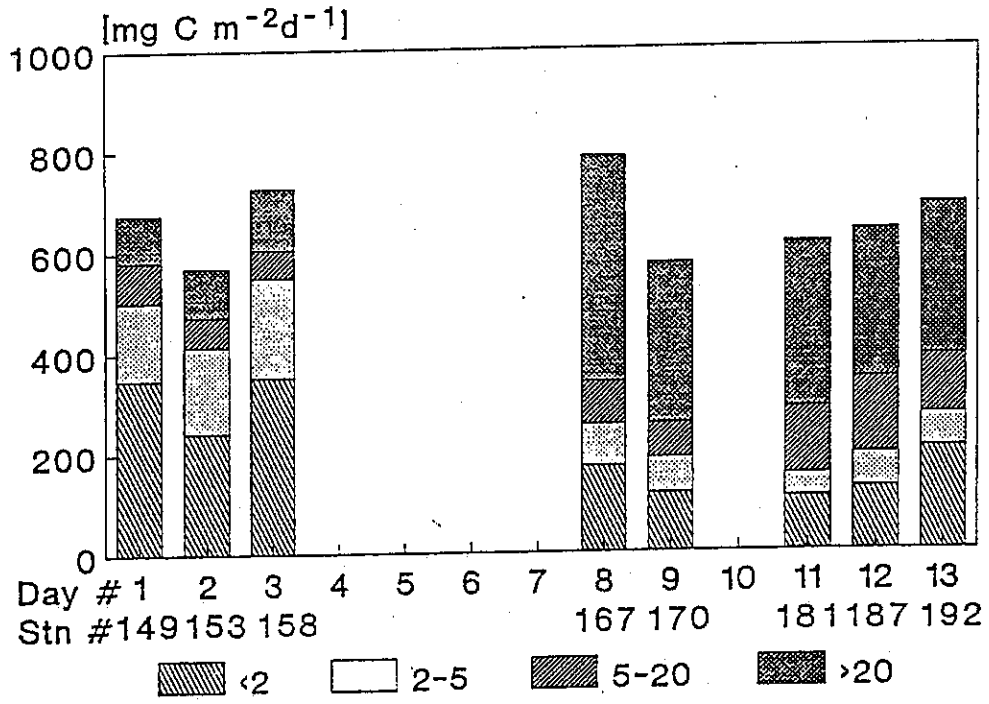

Fig. 45: Size-fractionated integrated primary production (mg C m^{-2} d^{-1}), 80 m water column

whole study period. Whereas 5-20 µm organisms occurred in the upper part of the euphotic zone during the first half of the study, they dominated primary production in the lower part of the euphotic zone during the second half.

Although at first view it may seem that the onset of the diatom spring bloom could be followed along the time-course sampling, there are some doubts as to the drift study being a true time series. Calculations on "new" nutrient concentrations (nitrate, silicate) (Koeve, pers. com.) were done for the upper 150 m water column and their deviation from expected winter concentrations. He comes to the conclusion that, in terms of seasonal succession, the second half of the drift study was an earlier stage, nutrient concentrations being still higher as compared to the first half. The achievement of Lagrangian drifting remains, however, hard to decide upon until detailed analysis of hydrographic data.

Under these presumptions, the second half of the study period may be seen as the onset of the diatom spring bloom, which was not reflected by higher total phytoplankton production as compared to the first half of the study, which then might be interpreted as a "post bloom" situation. In any case, results of this study suggest that the phytoplankton spring bloom at the study site does not appear as a short-term drastic increase in primary production and phytoplankton biomass as seen in textbooks, due to high frequency of strong wind events that prevent accumulation whithin the top meters. Primary production, therefore, seems to be more light- than nutrient-limited during both halves of the study, explaining comparable production rates despite different seasonal stages and different phytoplankton size structure, the latter with a clear shift towards larger cells during the second half of the drift. Whereas the dominance of pico- and small nanoplankton during summer stratification in boreal and temperate waters is well documented, few field studies exist on the transition from the winter to spring system. The key question is whether the picophytoplankton and the "microbial loop" are present throughout the whole year in more or less constant levels, only overruled by larger phytoplankton and grazers during spring and autumn blooms (in terms of contribution to total biomass and productivity). Results of the M 21/2 spring bloom study indicate that pico- and small nanophytoplankton, indeed, decrease during the onset of diatom growth. Physiological reasons for diatoms outcompeting pico- and nanoplankton cells upon the onset of the spring bloom remain to be investigated in view of unexpected high levels of small cells especially during the first half of the study. Since nutrient concentrations and turbulent mixing was still high, this situation can not be seen as the ongoing transition from the spring to the summer situation, thereby explaining the high contribution of picoplankton. These high levels of picoplankton in late winter reveal that high turbulence and high amounts of "new" nutrients, said to favour microphytoplankton growth, may not be the whole explanation of driving the size structure. Despite vigorous vertical mixing throughout the euphotic zone, especially during the time of rough weather on days 4 to 7, microphytoplankton production was only detectable in the upper part of the water column, indicating that this size fraction may not sustain down-mixing better than smaller phytoplankton, as previously thought. This was also reflected by the investigation of phototrophic organisms occurring in deep water (500-

3000 m; see Detmer, below): where dominated by *Synechococcus*-type coccoid cyanobacteria, no larger cells were detectable. ^{14}C-incubations proved these organisms being able of primary production when brought back into the light, which was enhanced by the addition of organics (glucose and amino acids), pointing towards mixotrophy in deep-water *Synechococcus*.

5.3.1.4 Quantitative and qualitative measurements of pico- and nanoplankton by flow cytometry and epifluorescence microscopy (A. Detmer)

Two different methods, flow cytometry and epifluorescence microscopy, were used to investigate cell concentrations of autotrophic pico- and nanoplankton. Furthermore, some qualitative informations of population structure and composition of these size classes were obtained. Flow cytometry enables a simultaneous single cell analysis of multiple parameters as for example cell volume and autofluorescence due to different pigments (chlorophyll, phycoerythrin). It is a rapid way of direct characterization and enumeration of heterogeneous cell populations.

Here a first view on preliminary results from flow cytometry is given. Fluorescence microscopic counts of deep frozen samples have not been done yet.

Field sampling

During processing the grid around the area of the possible drogue stations, samples were taken in the upper 1000 m depth of the water column. Later, during the drogue study, samples from 10 to 150 m depth were taken with a CTD/rosette sampler in the morning (5:00 to 6:30 a.m.); those between 1000 to 3500 m depth in the afternoon (13:00 to 16:30). After prescreening of samples through a 20 µm net to obtain only cells belonging to the pico- and nanoplankton, organisms were fixed with glutaraldehyde (final concentration: 1%). Cytometric analysis was performed on a FLUVO II flow cytometer constructed by Dr. V. Kachel, Max-Planck-Institut, München, using blue excitation (450-490 nm). Chlorophyll was measured as > 615 nm emission and phycoerythrin as 530-585 nm emission. For epifluorescence microscopy, 20 to 50 ml of sample were filtered onto Irgalan-Black prestained 0.2 µm Nuclepore filters. All filters were immediately frozen at -20°C.

First cytometric results of field samples

A great variability of cell concentrations and population structures was observed in the upper 1000 m depth between the different stations of the grid. For example, surface concentrations of chroococcoid cyanobacteria belonging to the genus *Synechococcus* varied between 8 to 38,106 cells l^{-1}. At stations 119 and 120, concentrations between 4 to 18,106 cells l^{-1} were observed at 500 to 1000 m depth, cell numbers, which were not reached in these depths at later stations of the grid (stations 131, 132, 133, and 136).

At all drogue stations in the upper 150 m depth, three different populations of autotrophic pico- and nanoplankton could be detected by flow cytometry based on their different chlorophyll and phycoerythrin features. At stations 149 and 153 a small diatom (not identified) was dominating and *Synechococcus* was a less abundant component. The third population consisted of very small nanoflagellates (diameter: ca. $1.1^{-1}.6$ µm). At stations 158, 162, 167, 181, 182, 187, 188, and 192, *Synechococcus* became the dominating cell type with concentrations of 35.106 cells l^{-1} at 10 m depth.

Below 100 to 200 m depth, the autotrophic pico- and nanoplankton consisted of *Synechococcus* only. Well pigmented cells of this genus were observed up to 4050 m depth (deepest sample) reaching abundances between 8 to 10,106 cells l^{-1}.

Experiments

To get some more informations about the viability of *Synechococcus* populations observed in deeper water, an incubation experiment was processed. Water from 1000 and 10 m depth was prescreened through a 20 µm net to avoid influence of possible grazers. Afterwards eight different incubations, which are listed in Table 5, were carried out in two liter polycarbonate bottles on deck of METEOR. For stimulating possible heterotrophic growth, a mixture of glucose and amino acids was added to four bottles (see Table 5).

Table 5: Conditions of the different incubation bottles

Bottle	Depth [m]	Light	Dark	Glucose/Amino Acids
1000L+	1000	+	-	+
1000L-	1000	+	-	-
1000D+	1000	-	+	+
1000D-	1000	-	+	-
10L+	10	+	-	+
10L-	10+	-	-	+
10D+	10	-	+	+
10D-	10	-	+	-

The experiment was carried out for ten days. From all bottles, subsamples were taken daily and cytometric analysis was done immediately, while filters for fluorescence microscopy were prepared as mentioned above. At irregular intervals, primary productivity was measured by the uptake of radioactive $NaH_{14}CO_3$ (F. Jochem).

First cytometric results showed that *Synechococcus* developed higher cell concentrations in all bottles containing the mixture of glucose and amino acids compared to those without this mixture. Cells from 1000 m depth, incubated in the dark with glucose and amino acids (bottle

1000D+), for example grew slowly up to concentrations of 20,106 cells l^{-1}, whereas cell numbers remained constant (5,106 cells l^{-1}) in the bottle 1000D-. Further calculations (e.g. calculation of growth rates) and microscopic counts still have to be worked out.

First conclusions

From the relative low in situ cell concentrations we infer a typical spring situation of autotrophic pico- and nanoplankton, with a tendency to develop higher abundances during the approaching summer. The occurrence of *Synechococcus* in the deep-sea and the first results of the incubation experiments lead to a variety of questions. Whether these cells get down to these depths by sedimentation or by vertical transport of fecal pellets or whether they are a biological sign of different water masses, still has to be investigated. Furthermore, the possible heterotrophic potential (better growth in the dark after adding glucose and amino acids) of these organisms gives rise to more experiments in the laboratory.

5.3.2 Dissolved organic carbon (DOC) (JGOFS, SFB 313)

(P. Kähler, A. Antia, O. Haupt, C. Sellmer)

Dissolved organic carbon (DOC) was measured during legs M 21/2/3/5 and /6 on board ship, and during all these legs including leg M 21/1 samples were conserved for later measurement. Thus wide stretches of the eastern North Atlantic are covered, and the seasonal development of DOC at a single station (47°N, 20°W) was documented for the first time (Fig. 46). Other parameters measured included particulate matter (C, N, chlorophyll-a), temperature, salinity, nutrients, and oxygen, whenever these were not measured by other groups.

Around a hundred profiles were sampled, most of them with high resolution in the upper 100 m, about one third were sampled down to the sea floor to obtain a survey of DOC in the deep waters of the Atlantic. Deep-water values also served as reference values in each region to secure the reproducability of the method. So far only a third of the samples have been measured and the data processed, but they already reveal a pattern of DOC dynamics which deviates considerably from the picture obtained from currently published information.

At all places and seasons the deep-water value of DOC is at about 80 µmol l^{-1}. Higher concentrations were only measured in some cases and always near the surface, but in many profiles concentrations were homogeneous over the entire water column. In no case we measured concentrations as high as those reported (and now withdrawn) by SUGIMURA and SUZUKI in 1988 (300 µmol l^{-1} for the upper tropical Pacific), although we employed a similar method of platinum-cataly sed high-temperature combustion which yields higher DOC concentrations than conventional wet chemical oxidation. Also values of about 120 µmol l^{-1} (deep-water) and 160 µmol l^{-1} (surface), which where measured by a number of workers and reported by FITZWATER and MARTIN (1993) for 47°N surface waters (May 1989, during a phytoplankton bloom) were not encountered by us there. Our surface values at

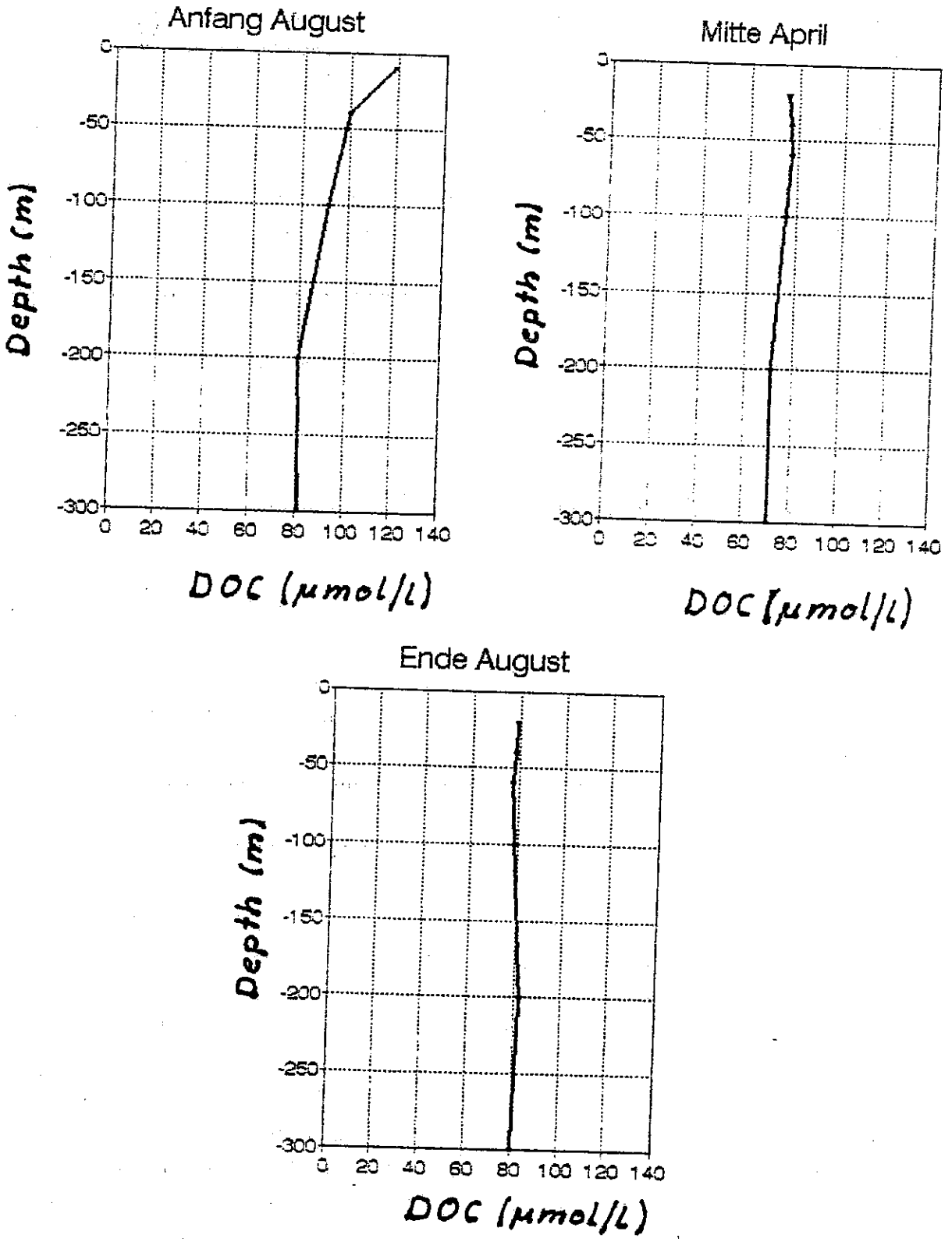

Fig. 46: Seasonal differences in dissolved organic carbon at 47°N, 20°W

this station were around 80 µmol l^{-1} (April), rose to 120 µmol l^{-1} by mid-May, and fell from 120 µmol l^{-1} to 80 µmol l^{-1} during August. At stations north of Iceland, 120 µmol l^{-1} were regularly encountered in surface waters during July and south of Iceland they varied greatly between 150 and 80 µmol l^{-1} (end of July). From these observations we conclude the following:

80 µmol l^{-1} seems to be a basic concentration of DOC in the North Atlantic, which represents either refractory material which behaves conservatively or a concentration below which organisms are not able to concentrate it from so diluted a solution. Above this basic value, DOC builds up in the short term in connection with phytoplankton blooms. The higher concentrations are, however, brought down to the basic 80 µmol l^{-1} by DOC-consuming organisms before the end of the season. Hence, high DOC values in surface waters are due to transient decouplings of DOC production and consumption.

Besides the direct measurement of DOC in samples from the water column we also made incubation experiments with seawater. Their simple setup was to filter a larger seawater sample (10 l) to remove the particulates and then subject the dissolved material to bacterial breakdown at in situ temperature in the dark. Should the DOC be degradeable, a decline of its concentration over time is observed. KIRCHMANN et al. (1991) observed a rapid decrease of a major fraction of DOC in such incubations in water from 47°N, where the initial concentration was high (see above). This means that the material is highly labile and elevated DOC concentrations cannot persist once the supply is shut off. In our experiments, a decrease in DOC was only observed in water with elevated DOC values. Both in deep-water and surface water containing around 80 µmol l^{-1}, no DOC consumption (and no ammonium production) was observed. Where there was DOC consumption, 80 µmol l^{-1} was a lower value not surpassed.

5.3.3 **Microbiology of the upper mixed layer** (B. Karrasch, A. Carstensen, J. deWall)

Preliminary results of the drift experiment carried out during leg M 21/2 for picocyanobacteria counts and bacterial net secondary production (^{3}H-leucine method) are shown in Figures 47 and 48.

At the beginning of the drift experiment, picocyanobacteria numbers up to 20.1 x 109 cells m^{-3} were determined in the mixed layer. After a storm period of three days the abundances of picocyanobacteria in the surface layer decreased to 6.7 x 10^9 cells m^{-3}. To the end of the drift experiment, picocyanobacteria numbers were higher again (14.8 x 10^9 cells m^{-3}). Below 150 m water depth the estimated cell numbers decreased to values below 2.0 x 10^9 cells m^{-3} with minimum abundances of 0.1-0.4 x 10^9 cells m^{-3} at 300 m. For the deep-sea (500-4000 m) cell numbers of < 0.1 x 10^9 m^{-3} were estimated.

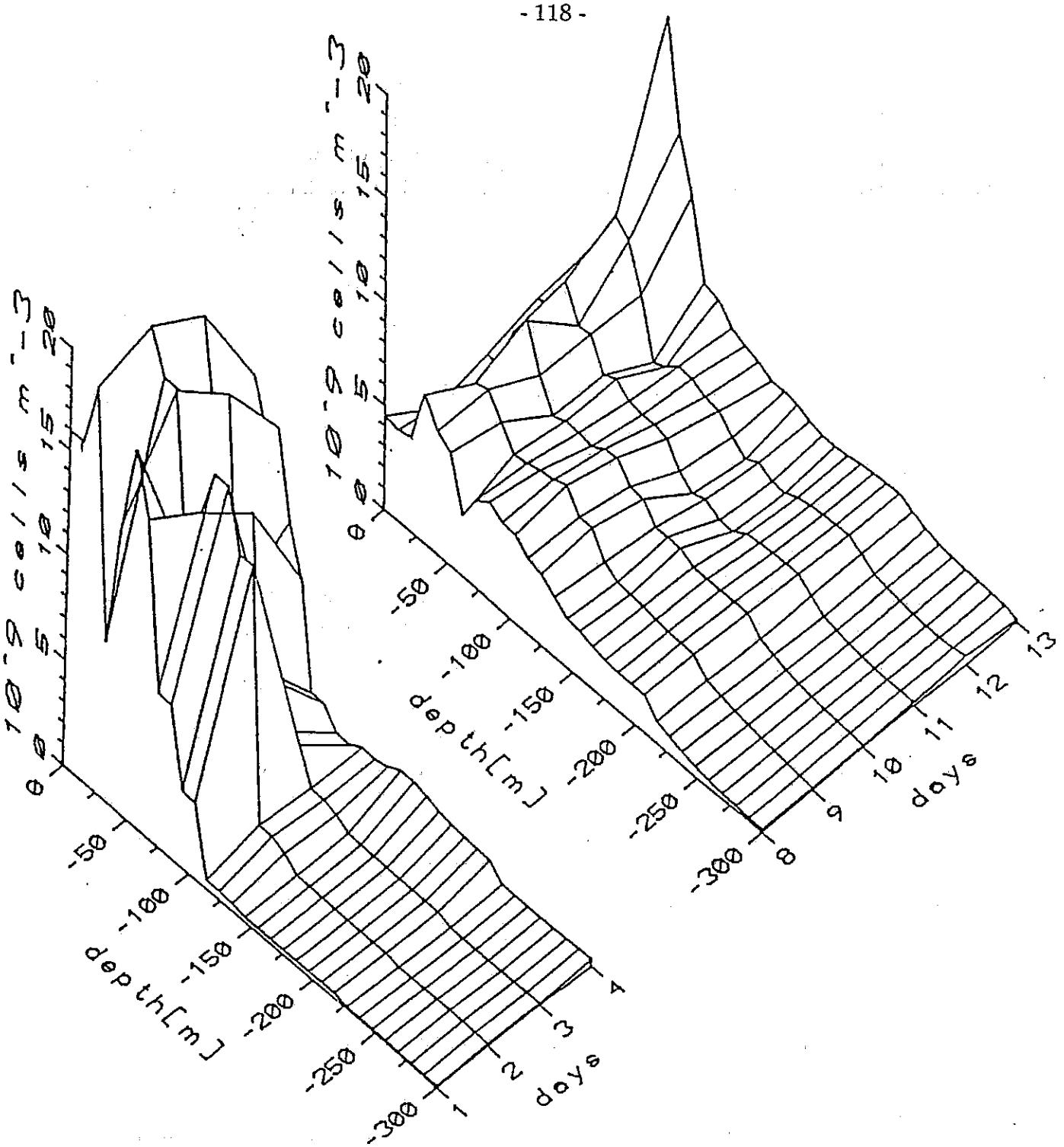

Fig. 47: Vertical and temporal distribution of picocyanobacteria during the drift experiment (M 21/2)

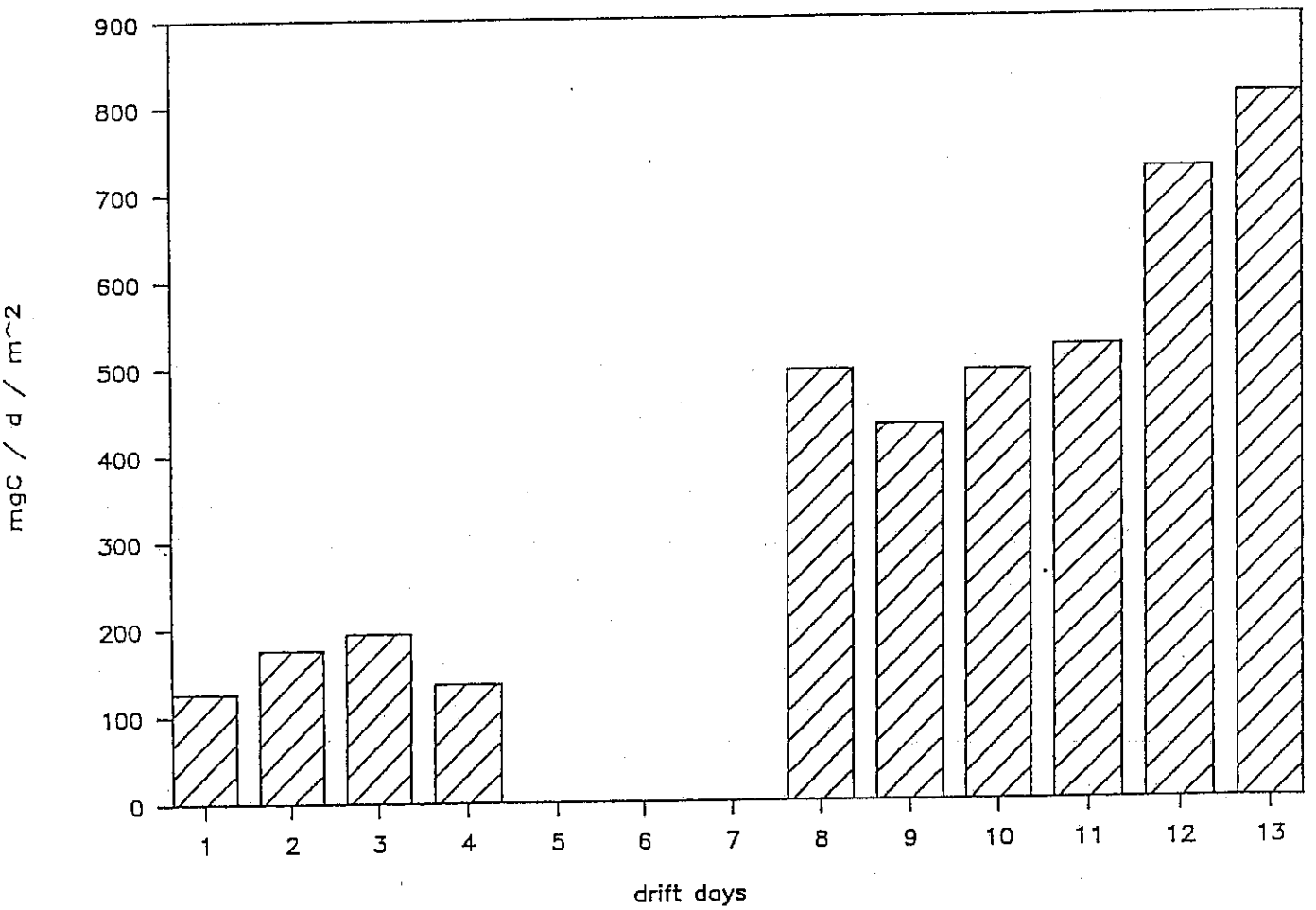

Fig. 48: Integrated (0-300 m) bacterial net secondary production (^{3}H-leucine-method) during the drift experiment (M 21/2)

During the first four days of the drift experiment only low bacterial net secondary production rates (up to 193 mg C/d m^{-2}) were determined (integrated from 0 to 300 m depth). The second phase of this experiment revealed higher production rates with a more or less continuous increase from 495 to 810 mg C/d m^{-2} at the end of the experiment. Highest production rates were always restricted to the upper 50 m of the water column.

During leg M 21/3, stations 199, 202, and 211 were used to investigate the whole water column down to the sediment. Bacterial net secondary production was detected for all sampling depths. The level of production rates in the deep-sea showed a visible relationship to the measured productivity in the euphotic zone for the different investigation areas.

The analyses of the remaining variables (abundance and biomass of bacteria and heterotrophic nanoflagellates, particulate DNA concentration, microbial secondary production derived from the incorporation of ^{3}H-methyl-thymidine, 3H-leucine-microautoradiography and extracellular enzyme activity) and for the water enclosure experiments will be carried out during the next months.

5.3.4 Population dynamics of planktic Foraminifera (JGOFS) (C. Hemleben, J. Bijma, H. Gminder, S. Heller, B. Hiller, W. Kamleiter)

Most planktic foraminifers reproduce in dependence of the lunar phase (population dynamics). As a result, the particle flux of calcium carbonate (sedimentation) is also cyclic. Therefore, these cycles as well as the processes that mark or mask these cycles should be investigated. The latter include primary production, the change of particle transport with water depth, the sediment production at the bottom before, during and after the spring bloom. At the JGOFS stations along 20°W these investigations are part of a long time scale survey. On these legs the emphasis was put on the upper 500 m of the water column, especially the photic zone, but also deeper tows and sediment samples were taken to study the sedimentary processes to the sea floor. Process studies and long time scale surveys are intended to investigate the carbon and calcium cycle in the water column and will finally increase our understanding of climate change during the Late Pleistocene and Early Holocene (Historical Sedimentary Record). Finally, the data will be used to convert the process studies into computer models. Earlier METEOR cruises (M 6, M 10, M 11/1, M 12/3 and M 17/2) are used as a reference for the long time scale surveys.

The sampling procedure for all legs was as follows:
Multiple open and closing net (100 µm mesh size) were used at intervals of 2500-2000-1500-1000-/700-500-300-200-/100-80-60-40-20-0 m. Water samples were taken to investigate the $^{12}C/^{13}C$ ratio in the photic zone (showing various kinds of gradients) and to investigate the relationship with the $\delta^{13}C$ of the calcitic plankton.

Multicorer (MC) and boxcorer (BC) sampling was done to investigate phytodetritus, sediment interface (composition and dissolution at the water sediment interface), and bioturbation by benthic foraminifers. The short MC cores will be used for the examination of thanatocoenosis and taphocoenosis.

Furthermore, several samples were taken to detect the juveniles of planktic foraminifera in restricted layers (thermocline, chlorophyll maximum) for SEM analysis and to investigate the biological niche of benthic foraminifers (culture experiments) from the deep-sea.

Upon arrival (March 22, 1992) in the BIOTRANS area the hydrographic situation reflected the late winter condition. The mixed layer extended down to ca. 100-120 m. Within the following week, a weak thermocline developed. The thermocline caused a concentration of the planktic foraminiferal fauna above it. The living specimens occurred above the thermocline and dead specimens below this level. During the following gale the mixed layer deepened again to more than 200 m, followed by the fauna. In the uppermost 20 m most specimens had not survived the storm (Fig. 49). In addition, many living specimens (plasma filled) did not manage to stay at their main horizon but sank to deeper water. Within the net tows at 700 m we could observe a pronounced increase in plasma-filled specimens right after the storm.

The fauna in the water column consisted of 14 species comprising the spinose species *Globigerina bulloides*, *G. falconensis* and *Turbogloborotalita quinqueloba*, and the non-spinose species *Neogloboquadrina incompta*, (= *N. pachyderma* d) *Globigerinita glutinata*, *G. uvula*, *G. inflata*, *Globorotalia hirsuta* and *G. scitula*. Reproduction of *Globorotalia hirsuta* was noticed during the following two weeks and specimens were observed living down to 500 m. These samples enabled us to study the population structure of this normally deep living species. Rather sporadically, we also observed *Globigerinella siphonifera*, *Globigerinoides ruber*, *G. sacculifer* and *Hastigerina pelagica* in the southern part of the BIOTRANS area. *Neogloboquadrina pachyderma* (left) has not been observed during the first part of the cruise. Rather frequently but at low densities *G. scitula* and *G. falconensis* and *G. uvula* were found. The small size fraction was dominated by *T. quinqueloba* and *N. incompta*. The medium fraction was mostly dominated by *G. glutinata*. The larger fraction consisted of *G. hirsuta* in the deeper tows and of *G. glutinata* or *G. bulloides* in the shallower tows around full moon and of *G. inflata* around new moon.

Depending on their diet, the cytoplasm attains a specific color; yellowish to greenish or brownish cytoplasm is the result of a herbivorous nutrition. The cytoplasm of *G. hirsuta* and *G. glutinata* was greenish, that of *G. bulloides* was generally orange, but that of *N. incompta* reddish. The cytoplasm of *G. inflata* varied strongly (mostly yellowish but sometimes red). Generally, the cytoplasm becomes pale with depth. Only *G. glutinata* is at depth also green. In general, the greenish color is usually due to unicellular green/yellowish algae; the brownish/yellowish color derives from diatoms and the reddish color is due to stored fat.

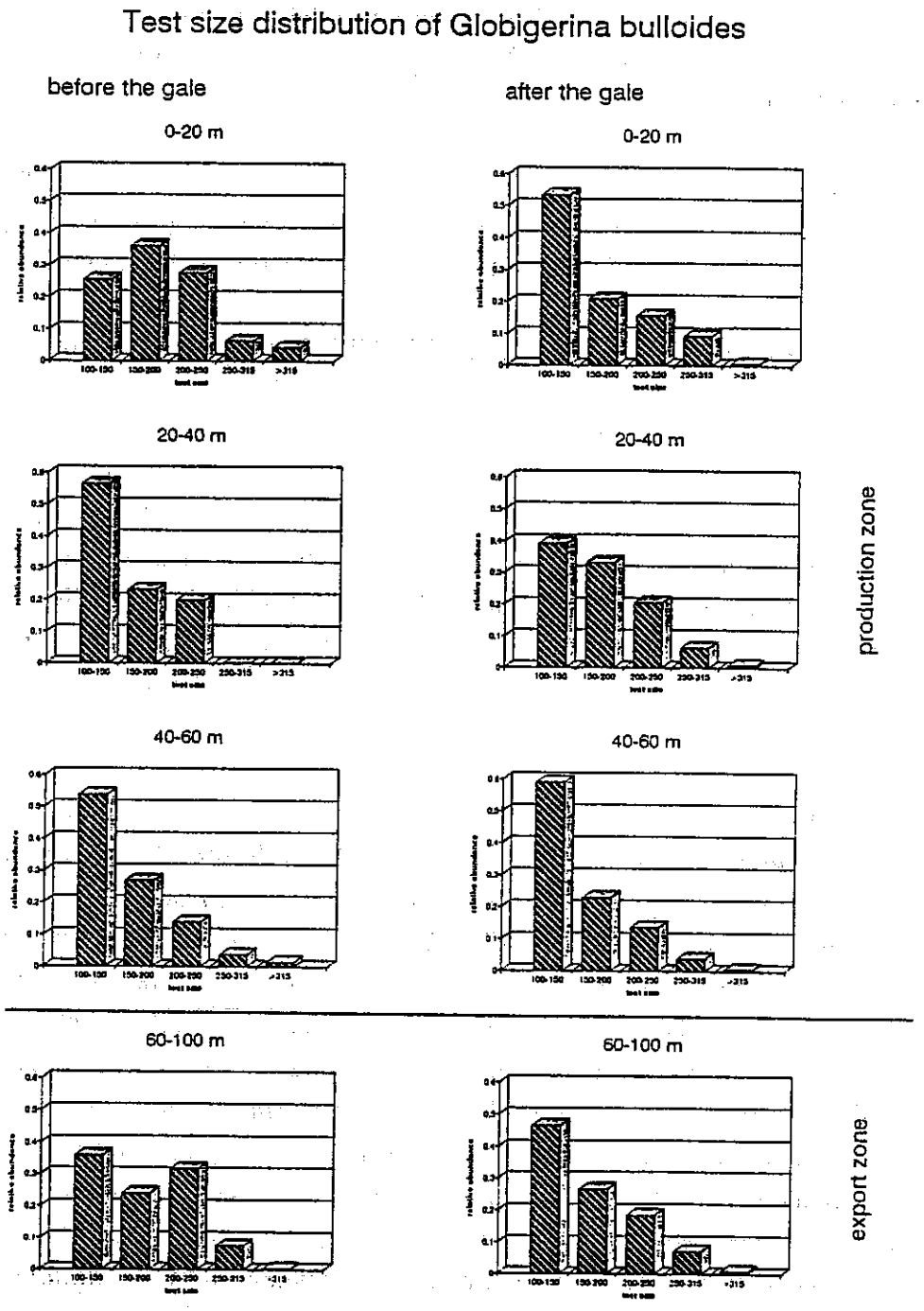

Fig. 49: In March, before the gale, the water column was stratified. *Globigerina bulloides* shows within the reproductive zone in the upper 20 m a size shift towards larger sizes, indicating the growth of specimens. Below this interval, many specimens die, especially the small ones, and sink through the export zone to deeper water. After the gale, the stratified water column is well mixed and the distribution pattern is almost the same over the entire internal. Thus the population structure has been destroyed and will be reestablished only after the formation of a new thermocline.

Despite of the early time of the year (March) samples from the sea floor showed small aggregates of phytodetritus which were still green in color and in part digested by polychaetes. This observation implies that newly settled aggregates had arrived from surface waters.

In April, the standing stock increased and we frequently observed reproduction. *Neogloboquadrina incompta*, *G. glutinata*, *G. inflata* and *G. bulloides* seem to reproduce around full moon. A depth preference was found for the first two species. At full moon, *G. glutinata* was dominant between 20-40 m depth and *G. incompta* was dominant in the upper 20 m. Both depth intervals were separated by a chlorophyll maximum at 20 m depth. Four days after full moon, the juveniles were found in the surface waters. Around the same time, many empty adult *G. inflata* were collected between 200 and 300 m depth. A maximum of empty adult *G. bulloides* was found between 500 and 700 m depth, 2-3 days before new moon. 14 days after full moon many pre-adult *N. incompta* were collected between 20-40 m depth. Many empty adults were found between 200-300 m depth and deeper than 700 m; 15 days after full moon, many of the juveniles were found between 40-80 m depth, below the fluorescence maximum which was between 0 to 40 m. Some adults with pale cytoplasm were still found between 200 to 300 m depth. In summary, lunar reproductive rhythms could be detected but a definitive picture of the reproductive schemes can only be given after the samples have been correctly processed and statistically evaluated.

At the same time the pteropods *Creseis polita* and *C. pyramidata* bloomed between 200-300 m depth, just below the deep thermocline. Stations 167 and 173 were only 45 sm apart but they show completely different water mass properties: The species composition as well as the developmental stage of the two water bodies were also different. At station 167 the bloom was fully developed (at the end of April), thus the foraminiferal fauna was suppressed and occurred below the bloom layer. At station 173 there was no sign of any bloom. Because this situation was found immediately after a storm which lasted for 3 days, it showed again that a storm may destroy vertical gradients (in this case to a depth of ca. 150 m) but leaves horizontal structures mostly intact. After the storm again a greater portion of "living" (plasma-filled) foraminifera was found in deep tows.

Later in the year, in May, the living planktonic foraminiferal fauna was dominated in the southernmost stations at 40°N ,20°W by *Globigerinoides* ruber and *G. sacculifer* in surface waters and *Globorotalia truncatulinoides* in deeper water. Further north, in the BIOTRANS area the well known fauna was observed. *Globorotalia hirsuta* was found deeper than 60 m. *Orbulina universa* decreased in its abundance further north. In total, the fauna south of the BIOTRANS area was very poor although the sediment surface showed a rich species assemblage including juveniles. In the BIOTRANS area itself reproduction took place and was observed around full moon in *G. bulloides*, *T. quinqueloba*, *N. incompta*, and *G. inflata*. During the following days, an increasing amount of adult specimens was found in the tows below 100 m.

At stations 217 and 219 at 54°N a bloom of juvenile pteropods, mainly *Limacina retroversa* was observed in surface waters at 20 m, while dinoflagellates (*Ceratium* sp.) dominated the larger fractions within the phytoplankton.

An interesting observation was made at station 223 (59°N, 20°W) where two thermoclines occurred (at ca. 15 m and ca. 40 m). At the upper one small specimens and at the lower one larger (adult) specimens were observed. This again demonstrates the depth preference of different ontogenetic stages.

In the northern Norwegian Sea, the water column was mostly weakly stratified during June and poor in phytoplankton (except station 227). This suggests that the foraminiferal habitat was rather broad between 80 and almost 0 m. A thermocline occurred sometimes but was poorly developed; the spring bloom was in most cases ongoing or at its end. This implied a nutrient depleted euphotic zone but fully developed zooplankton populations, especially high numbers of planktonic foraminifera and copepods.

The common distribution pattern did not change much between 67°N and 77°N as we stayed inside the Atlantic water mass. The more southern stations (Faeroe Ridge and Aegir Ridge) displayed a "warmer" faunal association compared to the northern stations with a shifting dominance from species like *G. inflata* and *Globigerina bulloides* to *T. quinqueloba* and *N. pachyderma*. The only exception occurred at station 285 when we investigated the mixing zone between the East Greenland Current and the Norwegian Current, west of the Knipovitch Ridge, where we observed a dominance of *N. pachyderma*.

Leg M 21/4 covered the lunar day 22 through 8, this is 8 days before and after full moon (full moon = 0). The days 22 through 27 (stations 224 to 230) were characterized by specimens of *Turborotalita quinqueloba*, *Neogloboquadrina incompta* (= *N. pachyderma*) and *Globorotalia inflata* still growing but starting to show signs of impending reproduction. We could not follow the development of *G. inflata* north of 72°N because of low frequencies. *Turborotalita quinqueloba* and *N. incompta* underwent gametogenesis shortly before and at full moon causing high numbers of large and small empty tests in the deep tows (stations 247 and 250 at 300 through 700 m). At and mainly after full moon (stations 275 and 277) *N. pachyderma* (sinistral) followed while the reproduction of the former species was still in progress. The sinking "population" in the water column was observed in deep tows beyond 700 m down to 2000 m. A first pulse of large specimens was observed in the interval 500 to 700 m at station 284 on lunar day 5. At Station 286 (lunar day 7) the large and rather thick-walled specimens had reached already the interval 1500 m to 2000 m. One to two days later the deep tows contained only very few large specimens but increasing small ones. In addition, the living population showed only very few gametogenic specimens.

During July, the area north of Iceland (Kolbeinsey Ridge) was investigated. The eastern side showed a *N. pachyderma* dominated association whereas on the western flank *T. quinqueloba*,

N. incompta and *N. pachyderma* are common. This does not fit within the normal water mass scheme. Further statistic investigations will evaluate this observation.

During the 4 days of steaming from Island into the BIOTRANS area, the normal North Atlantic planktonic foraminiferal fauna was observed: *G. bulloides*, *T. quinqueloba* and the non-spinose species *N. incompta*, *N. pachyderma* and *G. glutinata*, *G. uvula*, *G. hirsuta*, *G. scitula* and *G. inflata* to a lesser extent. Reproduction was observed in *N. pachyderma* and *G. bulloides*. Further south (54°N, 20°W) *N. pachyderma* dropped out and *N. incompta* dominated together with *G. bulloides* and *T. quinqueloba* the fauna.

Upon arrival in the BIOTRANS area the fauna was very poor in specimens but more diverse compared with the spring investigations: *G. bulloides*, *T. quinqueloba*, *G. falconensis*, *G. siphonifera*, *O. universa*, *G. ruber*, *G. sacculifer* and the non-spinose species *N. incompta*, *G. hirsuta*, *G. scitula* and *G. inflata*.

In summary, METEOR cruise no. 21 was very successful in plankton sampling, and will enable us to compare the various data collected since 1989 to these data. In addition, samples for benthic culture work and further sedimentological studies were taken.

Technical remarks

In total 660 opening/closing tows were taken of which 30 failed by technical and human mistakes; in addition 11 MC liners and 30 various other samples were achieved.

In order to quantify the contaminations in the nets, several "blanks" and additional nets were taken on legs M 21/1 and 2. The "blank" runs showed that there can be significant contamination. Three different runs were made. First, the system was set and all nets were opened before lifted; second, the system was set, but none of the nets were opened; third, the system was not set and the device was lowered and lifted with all nets "opened". These testruns were made to 100 m depth and to 700 m depth. When all nets were opened: No. 1 was most contaminated, No. 2 a bit less, and in Nos. 3-5 almost nothing could be detected, because No. 5 is covered by No. 4, No. 4 by No. 3, etc.; it seems as if the nets that were most susceptible to contamination, namely the one adjacent to the opened one, were indeed most contaminated. However, when all nets were closed the trend was the same, i.e. No. 1 was most contaminated, No. 2 a bit less, and No. 3-4 only very little, although in this situation the order of susceptibility to contamination is reverse. The third run confirmed the first two ones; again No. 1 and No. 2. were most contaminated. On the other hand No. 3 and No. 4 contained more phytoplankton. The only way to explain this is as follows: The phytoplankton in nets 3 and 4 show that indeed the nets closest to the one that is open, is most contaminated. The fact that No. 1 and No. 2 contained most foraminifers may result from the fact that a test run to 100 m was always preceded by a deeper tow to 700 m. In this tow, the first two nets collect a 200 m depth interval and the other nets collect only a 100 m interval. Thus it can be assumed that after rinsing, there are twice as many foraminifers left in the first two nets compared to

the other ones. This is confirmed by two further observations. The testrun made after a 100 m hole showed the opposite trend: nets No. 4 and No. 3 were more contaminated than No. 2 and No. 1. A completely new net, that was used to replace a torn one, was hardly contaminated. This means that contamination may be mainly due to insufficient rinsing.

5.3.5 Deep-sea zooplankton and micronekton (BIO-C-FLUX) (R. Koppelmann)

Zooplankton and micronekton were caught in the BIOTRANS area with three different types of a MOCNESS (Multiple Opening/Closing Net Environmental Sensing System). All systems were equipped with probes for pressure, conductivity and temperature and carried 5-18 dark nets each (see below) which were sequentially opened and closed via conducting cable. The volume filtered by each net was measured by a flowmeter. The distance from the bottom was measured with an altimeter (Simrad Mesotech). During the descent of a MOCNESS, the first net was opened to stabilize the frame. Horizontal samples were taken immediately above the bottom to investigate the benthopelagic fauna, and oblique sampling of the entire water column was carried out to reveal relationships between near-bottom and surface layers. The towing speed of all types of MOCNESS was about two knots.

During leg M 21/1 a $1m^2$-MOCNESS (nine nets of 333 µm mesh size) was employed for 14 successful mesozooplankton hauls. 12 hauls were made throughout the 4000 m water column yielding day and night profiles. 2 near-bottom hauls sampled benthopelagic plankton at discrete distances from the sea floor.

During leg M 21/6, benthopelagic micronekton was obtained by four hauls with a $10m^2$-MOCNESS (five nets of 1600 µm mesh). The first haul failed because the net release mechanism did not work. Three hauls yielded samples at 20, 50, and 100 m above bottom. The last haul caught a cephalopod of about 1 m length, when the MOCNESS was towed at a higher speed of about 3 knots 10 m above the sea floor.

The third type of MOCNESS was a $1m^2$-double-MOC (a double version of the above described $1m^2$-MOCNESS) carrying 2 x 9 nets of 333 µm mesh. It was employed during leg M 21/6 for both water column sampling (7 hauls) and near-bottom investigations (2 hauls with samples at 20, 50 and 100 m above bottom). Since some technical constraints did not allow the altimeter to be used with the double-MOC, its distance above bottom was estimated by foregoing pressure meter readings during bottom contact of the gear. The first deployment of the double-MOC failed by a breakdown of the electronics.

Lists summarizing some relevant station data and presenting an overview of the material sampled is given in chapter 7. The faunistic analysis of the large amount of samples taken on legs M 21/1 and 6 will be very time-consuming and cannot be conducted aboard the ship. A

first semiquantitative result is a distinctly lower zooplankton abundance during leg M 21/6 compared to leg M 21/1. This, however, has to be confirmed by laboratory analyses.

5.3.6 Benthopelagic nekton and megafauna (BIO-C-FLUX) (B. Christiansen)

A free vehicle trap set (RK) was deployed 3 times on leg M 21/1 and 7 times on leg M 21/6. The predominant animal captured in the traps was the lysianassoid amphipod *Eurythenes gryllus*. The bottom traps contained some other amphipod species too, mainly of the genera *Paralicella* and *Orchomene*. Generally, most amphipods were captured in the bottom-near traps. Above 30 m the number of animals declined distinctly. The animals in the bottom traps were of small size, whereas the catch of the pelagic traps also consisted of larger specimens. During two deployments the bait was enclosed in perforated plastic bottles to prevent the amphipods from feeding on the bait. The catch rates were significantly lower than in the deployments where the animals had access to the bait. This may point to an additional attraction by means other than olfaction, e.g. noise generated by chewing mouthparts. Amphipods without access to food appeared to be completely empty.

A free vehicle longline system (FFLL) was deployed once on leg M 21/1. 25 hooks baited with slices of fish were attached to a vertical mooring line of 25 m length. The longline was exposed for 15 hours. After recovery of the system, the bait had disappeared from nearly all hooks, but no fish was caught. Probably the bait had fallen off the hooks or was eaten by lysianassoid amphipods. On leg M 21/6, a modified system was used. 18 hooks were attached to a line of 25 m length which was laid out obliquely from the flotation 7 m above ground to the bottom. This version was deployed twice for 22 and 7 hours, respectively, and each time caught 5 large macrourids of 70 to 85 cm length. Part of the fishes had already been attacked by the amphipod *Eurythenes gryllus*. Some specimens still clinged to the fishes or had already burrowed into the gut space after recovery of the longline.

A single warp ottertrawl (OT) was only used on leg M 21/6. Two hauls each were made in the Iceland Basin at a water depth of about 3000 m and at the BIOTRANS area, water depth about 4500 m. The predominant fishes in the catches of both areas were macrourids and synaphobranchids. Moreover, a number of large invertebrates were caught, for instance decapod crustaceans, holothurians, asteroids and pantopods. Bottom contact of the trawl was only short at the second haul in the BIOTRANS area. Thus the catch consisted mainly of pelagic organisms, as bathypelagic fishes and medusae.

Due to electrical and mechanical failure of METEOR's 18 mm deep-sea cable, the phototrawl (FT) could not be used on leg M 21/1. A transmission of the video signal was not possible, and a trial without video, but with data and command transmission had to be abandoned because the outer strands of the cable broke when 3600 m of wire had been paid out.

On leg M 21/6 a new 18 mm deep-sea cable allowed a transmission of the TV signal in good quality. 4 hauls of the DOS and 5 hauls of the phototrawl could be performed successfully. The TV transmission in real-time proved to be an excellent means to control the phototrawl on the ground and to improve its performance. For example, after bottom contact of the trawl cable had to be paid out and the winch speed adjusted continuously to prevent the trawl from lifting off the bottom. An obstacle in form of a wire stretched out about one meter above the sea floor could be recognized in time for taking steps against a damage or even loss of the gear.

Lebensspuren were abundant on the sea floor in the BIOTRANS area. Holothurian trails, mounds, burrow openings and feeding tracks of echiurids were observed frequently on the TV screen. The recognition of animal life was confined to large forms, like holothurians, fishes, actinarians and hydroids. The fishes, macrourids as well as synaphobranchids, showed distinct escape reactions on the appearance of the phototrawl. Hence, only a few small fishes were caught in the epibenthic net of the phototrawl. Throughout the water column, the density of particles appeared to be high, increasing distinctly in the bottom-near water layer. The nature of the particles could not be recognized, but part of them showed active movements. With lights turned off, bioluminiscence could be observed in the upper 1500 m of the water column.

5.3.7 **Benthic investigations (BIO-C-FLUX)** (O. Pfannkuche)

Benthic investigations at the BIOTRANS site between 1985 and 1990 gave evidence for a close pelago-benthic coupling between processes in the epipelagic zone and processes on the deep seafloor (4550 m depth). Maximum sedimentation rates of particulate organic matter in early summer induced an increase in benthic carbon consumption rates and activity by a factor of 2-5 in comparison to March values (PFANNKUCHE, 1992, 1993). Benthic response to peak sedimentation rates of POM were mainly channeled through the small benthic size groups, mainly bacteria, protozoa and small meiofauna (LOCHTE, 1992). These results, which were obtained from the synthesis of a five years survey, probably describe the general pattern of pelago-benthic coupling for this part of the NE Atlantic, but they contain a range of interannual variability.

Main objectives of the BIO-C-FLUX benthos programme were:

- to follow within one year the reaction of the benthic community to the sedimentation of POM before, during and after the spring phytoplankton bloom at the BIOTRANS station in 47°10'N, 19°33' W;
- to take further samples for long-term studies at two stations already investigated during the JGOFS "North Atlantic Bloom Study" (METEOR cruise no. 10, 1989) and

during METEOR cruise no. 12/3 (1990) at 34°N, 20°W on the Madeira Abyssal Plain and at 59°16'N, 21°W in the Iceland Basin;
- to revisit a benthic station at 48°50'N, 16°30'W on the Porcupine Abyssal Plain which was already sampled during METEOR cruise no. 6/7 (1988).

The following questions were addressed:

- Does the standing stock and activity of benthic organisms follow seasonal variations?
- Can the benthic response to the sedimentation of POM be assayed by measurements of key biochemical parameters?
- Can specific sedimentation events be discriminated and what is the reaction of benthic organisms to such events?
  What are the time lags of benthic reactions to sedimentation events?

Executed work

Samples for macrobenthos (specimens retained on a 1 mm sieve) and larger meiobenthos (specimens retained on a 0.5 mm sieve) were taken with a modified version of the USNEL-spade corer (THIEL, 1980). Samples were analysed down to 20 cm sediment depth. For smaller meiobenthos (specimens retained on a 0.03 mm sieve) and biochemical assays, sediment samples were taken with a multiple corer (BARNETT et al., 1984). Individual cores were subsampled using small piston corers with a surface area of 3.5 cm^2 (5 replicates for each parameter from one multiple corer cast) down to a maximum depth of 10 cm. The piston corers were sectioned horizontally into one-centimeter layers and analyzed separately in the following horizons: 0-1 cm, 1-2 cm, 2-3 cm, 3-4 cm, 4-5 cm, 6-7 cm, 9-10 cm.

At the time series station in 47°10'N, 19°33'W sampling was performed in 5-7 days intervals taking series of 3 multiple corer casts. Benthic samples in the BIOTRANS area were taken during legs M 21/1, M 21/2, M 21/3 and M 21/6. The Madeira Abyssal Plain station was visited during legs M 21/1 and 3, the station in the Iceland Basin during leg M 21/6. The sampling coordinates are listed in Table 6.

Sampling at the BIOTRANS station was performed in an area of 1000 m x 1000 m on an abyssal plain in 4560 m depth. The sampling area was placed in the centre of a transponder array of 3000 m x 3000 m. The sampling gear was tacked with a relay transponder which enables an exact positioning of the sampling gear within the transponder field by interrogation with the array transponders (Fig. 50).

Table 6: Sampling positions of multiple corers (MC) and box grabs (KG) in the transponder field at the BIOTRANS station (sampling positions are given in x/y coordinates).

M 21/1					
	X	Y		X	Y
MC- 373	1706	1530	MC- 386	1471	1502
MC- 374	1600	1483	MC- 387	1087	1142
MC- 375	981	1692	MC- 388	1116	1375
MC- 376	1796	1297	MC- 389	1546	1581
MC- 377	1581	1631	MC- 390	1565	1430
MC- 378	1537	1530	MC- 391	1534	1499
MC- 379	1728	1627	KG-1495	1617	1802
MC- 380	1668	1383	KG-1496	1552	1438
MC- 381	1524	1367	KG-1497	1534	1488
MC- 382	1983	1654	KG-1498	1752	1396
MC- 383	1572	1245	KG-1499	1625	1529
MC- 385	1520	1491			
M 21/2					
MC- 394	1814	988	MC- 398	1512	1416
MC- 395	1605	1560	MC- 399	1470	1496
MC- 396	1423	1468	MC- 400	1507	1533
M 21/3					
MC- 407	1858	1499	MC- 410	1663	1575
MC- 408	1426	1405	MC- 411	1422	1908
MC- 409	1556	1689	MC- 412	1369	2001
M 21/6					
MC- 424	1400	1525	MC- 445	1424	1615
MC- 425	1360	1385	MC- 446	960	1241
MC- 426	1652	1553	MC- 447	1515	1538
MC- 427	1524	1255	MC- 448	1396	1450
MC- 428	1597	1621	MC- 449	1459	1444
MC- 429	1325	1563	MC- 450	1454	1491
MC- 430	1339	1320	MC- 451	1410	1361
MC- 431	1257	1070	MC- 452	1389	1323
MC- 432	1560	1120	MC- 453	1382	1446
MC- 433	1424	639	MC- 454	1138	1491
MC- 434	1453	1362	MC- 455	1383	1509
MC- 435	1575	1373	MC- 456	1723	1768
MC- 436	1416	1467	MC- 457	1356	1361
MC- 437	682	1343	MC- 458	1084	1673
MC- 438	1424	1416	KG-1500	1502	1443
MC- 439	1385	1367	KG-1501	1494	1417
MC- 440	1383	1139	KG-1502	1352	1304
MC- 443	703	1343	KG-1503	1468	1470
MC- 444	1016	1750	KG-1504	1514	1719

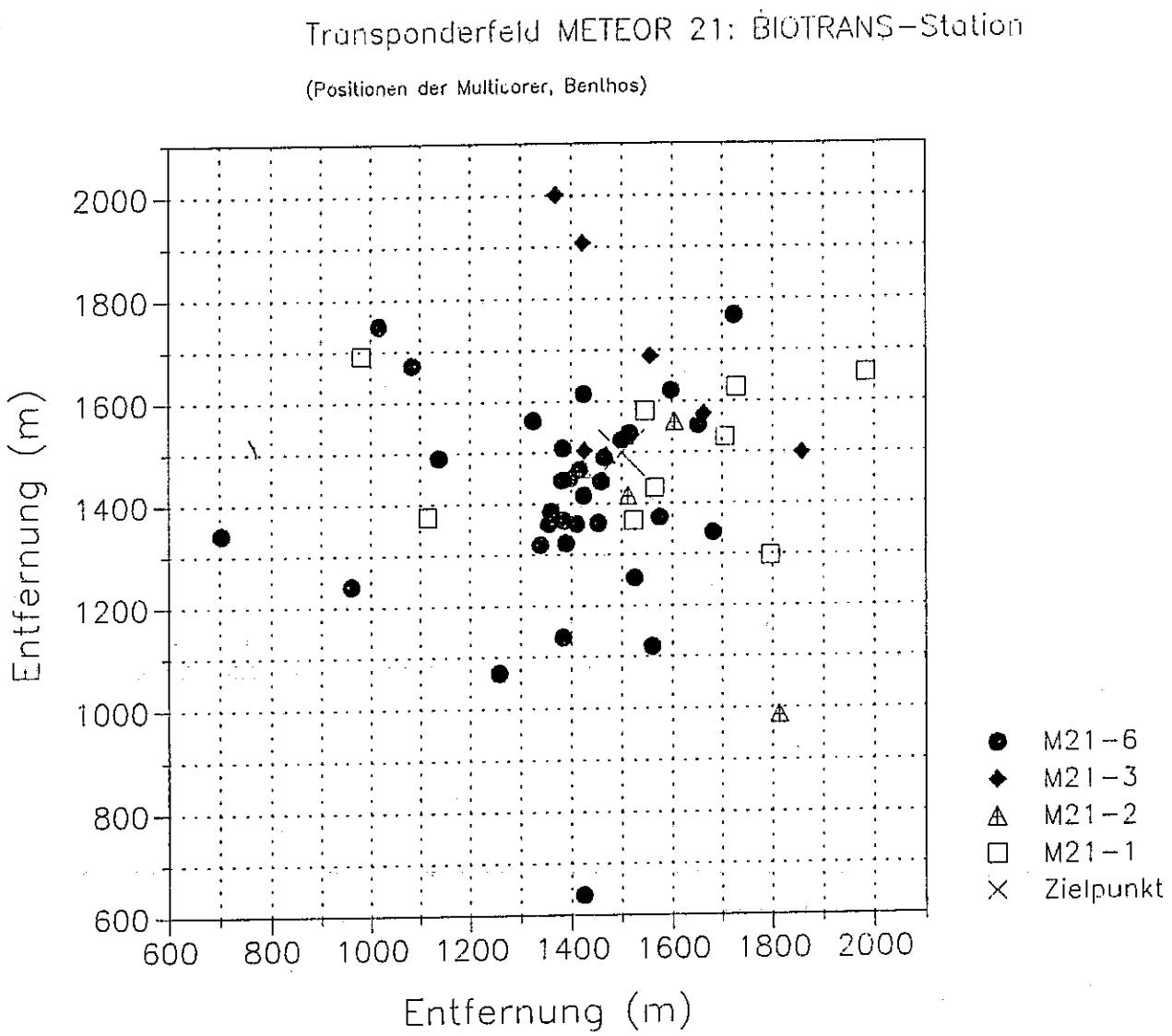

Fig. 50: Sampling positions of multiple corer samples in the transponder array during legs M 21/1, 2, 3, and 6

Samples for the following analyses were taken (measurements marked with an asterisk were carried out in the ship's laboratory):

- Size spectrum analysis of the infauna (macro-, meio-, nanobenthos, bacteria);
- Analysis of the distribution pattern and standing stock of the benthos;
- Measurement of the potential respiratory activity (ETS)*;
- Measurement of ATP activity*;
- Measurement of enzymatic activity (hydrolysis of fluorescein diacetate, FDA)*;
- Measurement of biomass parameters from sediment samples (multiple corer);
  - a) total proteins*;
  - b) phospholipids;
  - c) total adenylates (ATP, ADP, AMP)*;
  - d) DNA;
- Measurement of plant pigments in sediments;
  - a) chlorophyll-a and phaeopigments (TURNER Fluorometer)*;
  - b) chlorophyll-a, b, c and phaeopigments (spectrofluorometer);
- HPLC-analysis of plant pigments in sediments;
- Measurement of total organic carbon;
- Measurement of sediment water content.

Comparison between the investigated sites

Benthic standing stock and activity reflects the export potential of the epipelagic zone which differs greatly between the bio-geochemical provinces of the NE Atlantic. A comparison of the activity potential of hydrolytic enzymes between the areas of investigation demonstrates latitudinal differences. However, this general rule can significantly be modified by a variety of mesoscale biological and physical parameters such as: the development of the phytoplankton bloom, the zooplankton response, degradation rates in the meso- and bathypelagic zone, the meteorological regime, currents, eddies, and lateral advection. A ranking of benthic enzymatic activity in correlation to surface productivity would lead to an increase of activity with higher latitudes. Although enzymatic activity was found to be lowest in the Madeira Basin (Fig. 51), values for the Iceland Basin - where highest activity would be expected - were surpassed by the values from the BIOTRANS station and the Porcupine Abyssal Plain station. The reason for the relatively low activity in the Iceland Basin lies in the physical regime. Strong bottom currents frequently resuspend sedimented POM and thereby reduce the net flux of POM to the seabed.

Seasonal studies at the BIOTRANS station

Although the results from the BIOTRANS station of the period 1985-1990 gave evidence for a close pelago-benthic coupling in the open NE Atlantic with maximum POM flux to the seabed in late spring or early summer in connection with an increase of benthic activity and bacterial as well as protozoan biomass, our results from METEOR cruise no. 21 did not show

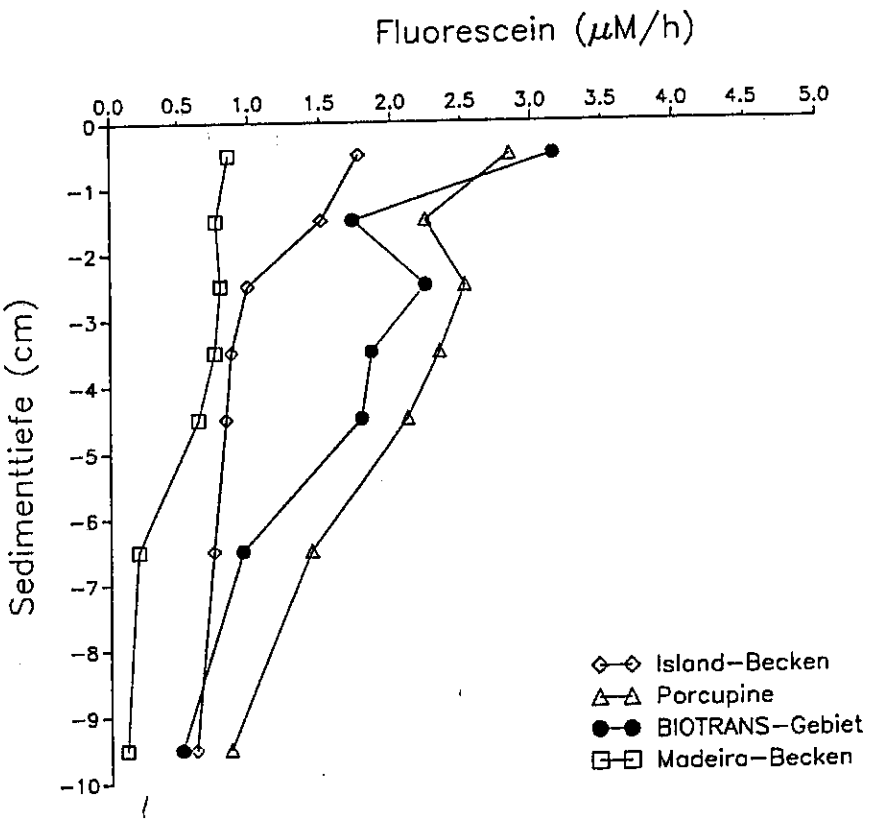

Fig. 51: FDA reduction profiles in the sediment. Comparison of all sites investigated during M 21

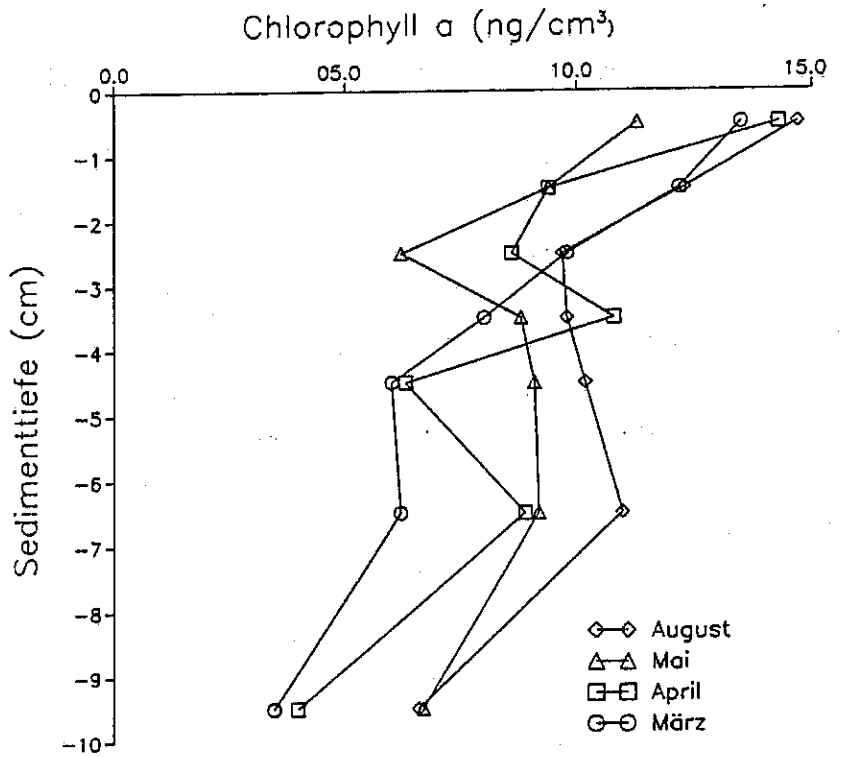

Fig. 52: Seasonal comparison of chlorophyll-a in the sediment profiles at the BIOTRANS station

such a clear tendency. In contrast to previous cruises where a first noticeable sedimentation event on the sea floor was registered in late April and early May (PFANNKUCHE and LOCHTE, 1993), we could recognize a sedimentation event on the sea floor as early as March when green-brownish phytodetrital material was found on top of the sediment in the multiple corer tubes. In consequence a phytoplankton bloom must have taken place some weeks earlier at the end of February, a phenomenon which has not yet been reported from this part of the Atlantic. No traces of substantial sedimentation of detrital matter were found in April and May whereas in August some multiple corer samples contained some whitish, already degraded phytodetritus. Sediment chlorophyll-a and pheopigment did not increase significantly between March and August (Fig. 52), also the activity of hydrolytic enzymes showed no seasonal difference (Fig. 53). In correspondence the values of total adenylates did not show a substantial increase in biomass (Fig. 54). The data suggest that no discrete sedimentation pulse occurred in 1992 which could have caused a substantial effect on the benthic community such as the 1986 pulse (THIEL et al., 1988/89), when a significant increase in benthic standing stock and activity was measured. However, a complete evaluation of the benthic response in 1992 can only be carried out after a detailed analysis of the whole data set.

5.3.8 Differentation between biologically degradable and non-degradable compounds of sedimentary particulate organic matter (BIO-C-FLUX) (S. Scheibe)

Particulate organic matter reaching the deep-sea floor is the only food resource of the benthic community in the deep-sea. It is supposed that only a part of this material is digestable by deep-sea organisms. Another part of the sedimented material is non-digestable by organisms and ends up as the geological record.

Aiming at quantifying the rates of POM recycled or buried in the sediment and its vertical distribution within the sediment, samples were taken for the chemical extraction of total protein contents and for experiments simulating biological digestion by sediment incubation with different common digestive enzymes (proteases, peptidases, amylases, glycosidases, chitinases). For the planned experiments one-cm-layers of sediment were taken out of several (3-5) cores, mixed and transported deep frozen to the home lab.

In order to compare these results with data of the organic input, biomass, activity, and potential respiration of the benthic community, further samples were taken for measuring the contents of chlorophylls and adenylates, for quantification of the electron transport system activity, and for meiofaunal abundance and distribution.

Contents of adenylates and the electron transport system activity were measured on board, both in mixed and in undisturbed cm-layers to compare different subsampling methods.

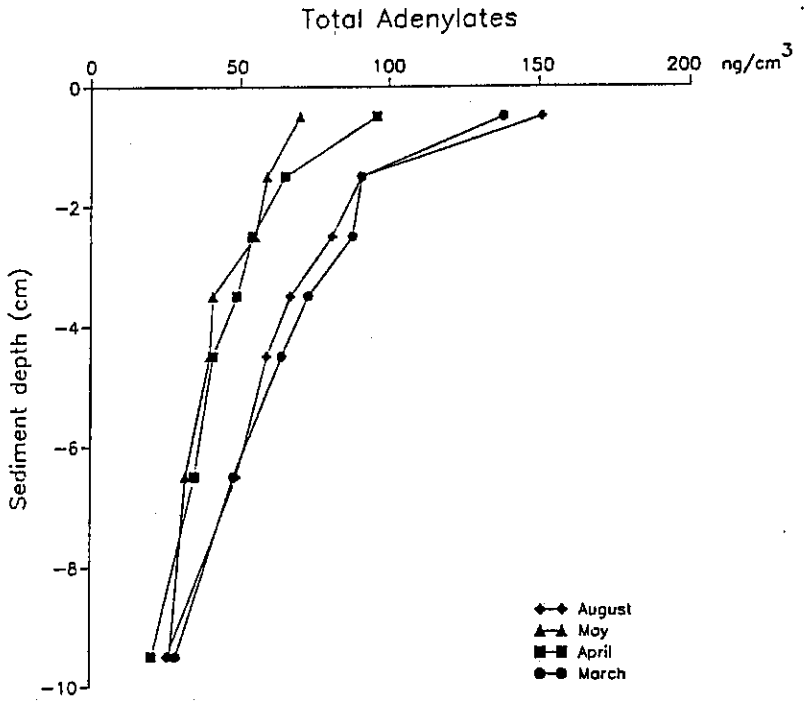

Fig. 53: Seasonal comparison of FDA reduction profiles in the sediment at the BIOTRANS station

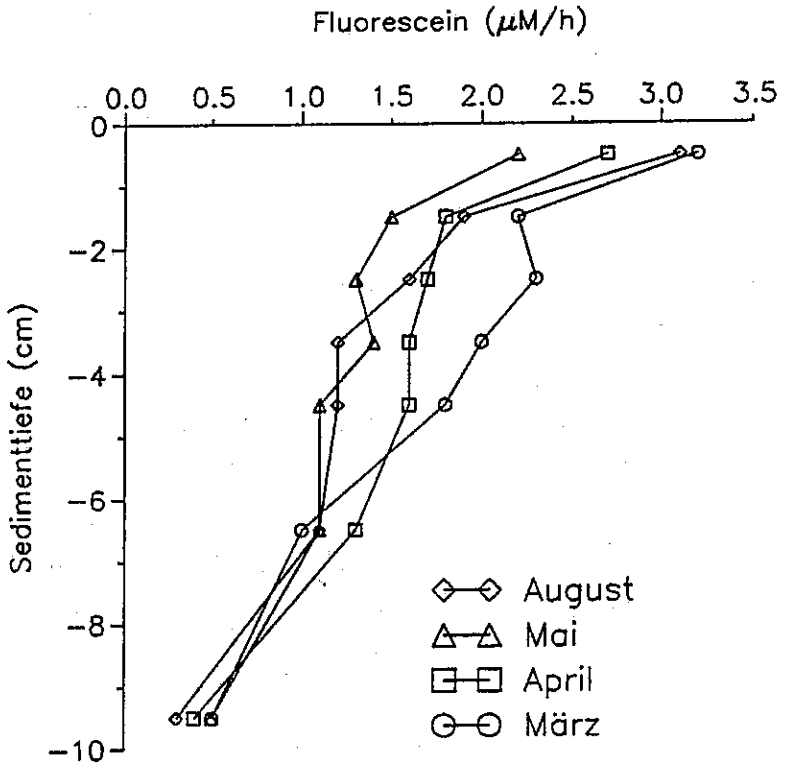

Fig. 54: Seasonal comparison of total adenylate (biomass) in the sediment at the BIOTRANS station

At first view, the not yet completely processed data do not show significant seasonal differences.

Since seasonal as well as large-scale variations under a latitudinal aspect were expected, samples were taken during M 21/1, M 21/3 and M 21/6 on the Madeira Abyssal Plain, the Iberia Abyssal Plain, in the BIOTRANS area and the Iceland Basin.

5.3.9 **Small-scale variability of sedimentary biochemical indicators of biological abundance and activity in the NE Atlantic** (T. Soltwedel)

Changes in standing stock or bioactivity are to be expected in relation to ecological or man induced changes. For the evaluation of man's impact on the environment and the ecosystem the natural variability has to be assessed. The study will focus on the small-scale variability of biochemical indicators.

A number of biochemical sediment compounds are useful to determine the amount of organic matter or the proportion of individual groups of organisms present in the sample. For ecological studies and, in particular, for biomass estimations, it is often advantageous to measure biomass directly rather than indirectly by using abundance values and conversion factors.

Previous investigations showed a great variability for various biochemical compounds measured in subsamples coming from the same box corer or multiple corer or sampling site. For instance, variation coefficients of 3 subsamples per box corer range up to +/- 50%, especially for the pigment content of the sediments.

In order to assess industrial or environmental impacts it seems to be necessary to evaluate the small-scale distribution of biochemical parameters using sets of sediment-subsamples coming from single multicorers or series of multicorers from one station.

During leg M 21/1, sediment samples for biochemical investigations were taken at the BIOTRANS station and at the 'EC-station'/Porcupine Abyssal Plain (49°N/16°W) using a multicorer. Sediment samples will be analyzed at the home lab for adenylates, DNA, particulate proteins and chloroplastic pigments. In addition, measurements of the potential oxygen consumption of the total benthic infauna (electron transport system activity, ETSA) will be done.

This work is part of a MAST II project ("Community structure and processes in the deep-sea benthos") funded by the European Community.

5.3.10 Microbial enzyme activity in deep-sea sediments (BIO-C-FLUX) (A. Boetius)

Before macromolecules and particulate organic material can be used as food, bacteria have to cleave off subunits which they can take up. Therefore, the distribution, quantity and specific activity of microbial hydrolytic enzymes can give information about the amount and the kind of detrital input to an ecosystem.

It is not known to which extend protozoans digest extracellularly.

Using recently developed methods for the investigation of extracellular enzymes with fluorescent substrates, typical gradients of potential activity of different enzymes were found in the sediments of the BIOTRANS area.

Activity was highest in the first centimeter, rapidly decreasing with sediment depth, as was found for chitobiase (Fig. 55), β-glucosidase and also lipase. Fucosidase and a-glucosidase were close to detection limit but could be measured in the first centimeter. This was expected from the usual composition of old, rather degraded detrital material. A yet unexplained phenomenon is the more than fifty times higher activity of aminopeptidase (Fig. 56) compared to the other enzymes. This hydrolase showed a different gradient with a maximum of activity in 2-4 cm sediment depth. This could be interpreted as a different enzyme regulation mechanism, a different substrate distribution or even a change in microbial population.

Further information will be obtained by the analysis of phospholipids as a parameter of microbial biomass in the home laboratory; especially the calculation of specific activity, i.e. enzyme activity per biomass, gives new information about the microbial activity in deep-sea sediments when compared with other areas.

Another question was the seasonality of microbial heterotrophic activity as a response to the input of organic material. This was investigated by the measurement of extracellular hydrolysis of FDA, a nonspecific substrate for esterases. It was expected to find an increase in activity towards summer, when the phytoplankton bloom sediments to the bottom of the ocean as was measured during M 10 (1989). Unfortunately important information was lost, since the summer leg to the BIOTRANS area happened as late as August, and the sediment trap mooring could not be recovered.

Esterase activity decreased rather slowly during the first four centimeters, indicating bioturbation. An increase of potential activity from spring to summer was not found (Fig. 57). This can be explained by our observations of detrital material on top of the cores in March and only little and rather old whitish fluff in August.

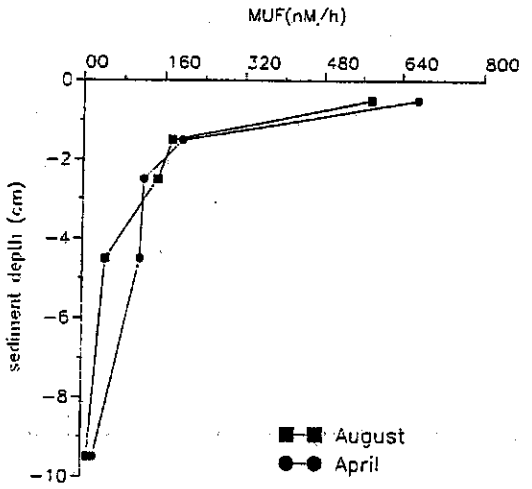

Fig. 55: Activity of chitobiase in the sediment profiles at the BIOTRANS station in April and August 1992

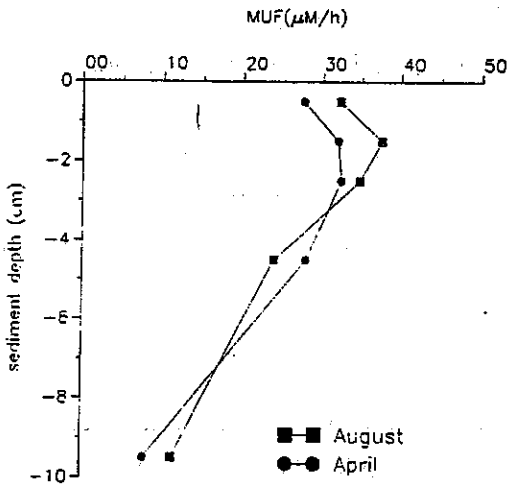

Fig. 56: Activity of aminopeptidase in sediment profiles at the BIOTRANS station in April and August 1992

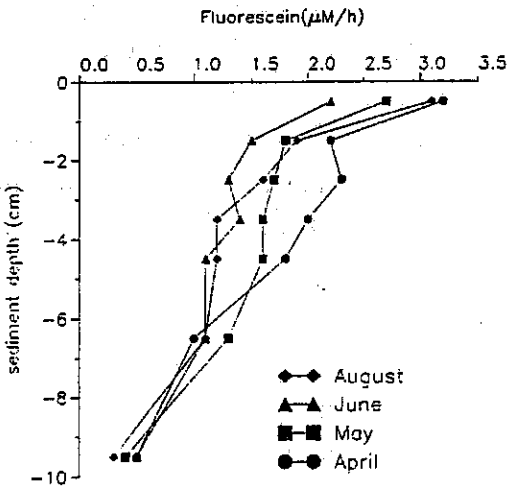

Fig. 57: Activity of esterases in sediment profiles at the BIOTRANS station in April and August 1992

5.3.11 Experiments on microbial breakdown of organic matter (BIO-C-FLUX)

(K. Lochte, A. Boetius)

In deep-sea sediments the key parameter determining bacterial growth is the amount of degradable organic matter present. The annual sedimentation after the spring phytoplankton bloom provides input pulses of organic matter to the sediment. Since the organic material reaching the sea floor is primarily particulate, bacteria have to hydrolyse the macromolecules before mono- or oligomeric subunits can be taken up. In previous work we have shown that the bacterial population in deep-sea sediments is able to quickly degrade fresh inputs of sedimenting phytodetritus and produce biomass.

The main aims of the investigations during leg M 21/6 were a) to determine the growth rates of sediment bacteria under different nutritional conditions, and b) to determine the production of extracellular enzymes when fed with different types of organic matter. At the two stations sampled during the cruise, south of Iceland at 59°N and at the BIOTRANS station at 47°N, experiments were set up with surface sediments diluted by an equal amount of deep-sea water.

For investigation of growth rates, subsamples of the sediment slurries received either no additional organic material or injections of glucose or plankton detritus. For the latter, homogenized and sterilized net plankton which contained a high proportion of zooplankton was centrifuged, and the supernatant was used as dissolved substrate while the washed pellet was used as the particulate substrate. Samples were incubated under simulated in situ conditions. At time intervals subsamples were removed for the determination of bacterial biomass (microscopic direct counts and bulk phospholipids) and bacterial biomass production (incorporation of tritium labelled thymidine and leucine in incubations under in situ conditions). These samples were fixed and stored for later analysis in the home laboratory.

For investigation of stimulation of extracellular enzyme production, subsamples of these slurries were treated similarly and were either not fed or received particulate and dissolved plankton detritus. The samples were incubated under simulated in situ temperature and pressure as well as under 1 atm. At time intervals subsamples were removed and tested for the activity of different enzymes (aminopeptidase, chitobiase, a- and β-glucosidase, fucosidase and lipase by using fluorescence labelled substrates) and for changes in the bacterial biomass (measurement of bulk phospholipids). Occasionally the bacterial uptake of tritium labelled leucine was measured in order to compare it with the hydrolytic activity of aminopeptidase (measured with MCA-leucine). Enzyme activity was determined immediately on board. Samples for biomass and leucine uptake were fixed and stored on board for later analysis in the home laboratory.

Preliminary results of the enzyme production indicate that different enzymes react differently to input of organic matter. Chitobiase increased in activity shortly after addition of dissolved

substrate (Fig. 58 a). The substrate was added in single and double concentrations, producing enzyme activities approximately twice as high in the samples receiving the higher concentration. A similar response of chitobiase activity to the higher concentration was also observed when particulate substrate was added. However, the rise in activity was delayed for a few days. When fed with particulate substrate, the activity of β-glucosidase increased after 4 days of incubation. In the samples with the double substrate concentrations, activities surpassed those of the single-concentration-samples after 15 days (Fig. 58 b). Other extracellular enzymes like fucosidase and lipase decreased with time. Aminopeptidase seems not to be clearly stimulated by the addition of organic matter but could be directly related to bacterial biomass. These observations will have to be seen in context to the changes in bacterial biomass during the experiment.

5.3.12 Microbiology of deep-sea sediments at 47°N, 20°W (BIO-C-FLUX)

(K. Poremba)

The bottom of the deep-sea is known as an extremely oligotrophic environment. This situation changes in summer, when sedimentations of phytodetritus occur as a result of collapsing algae blooms in the euphotic surface layer. In previous studies an extended cover of detritus on the bottom of the BIOTRANS area (47°N, 20°W) was found (THIEL et al., 1988/89). Time-lapse photography in the Porcupine Seabight (50°N, 13°W) showed that the detritus has a short persistence and seems to be biologically degraded very quickly. It could be expected that this short-term richness of organic material is correlated with a simultaneous increase of microbial activity, because microbes are the dominant part of the benthic biomass. The aim of the microbiological investigations during the METEOR cruise no. 21 was the detection of such variations in bacterial abundance and activity between spring and summer.

Sampling site and shipboard handling

The microbiological experiments were performed in March (M 21/1) and August (M 21/6) in the transponder array of the BIOTRANS site to optimize the comparability of results. Water and sediment samples were taken with hydrographic rosette sampler (RS) or multiple corer (MC), respectively. In March 11 MC and 1 RS and in August 10 MC and 1 RS samplings were perfomed.

The collected material was immediately transferred to a 2-4°C cooled experimental container, sectioned, supplemented with flourogenic or radioactive labelled substrates, and partly incubated in pressure vessels for simulating in situ conditions.

Distribution pattern of bacterial standing stock

Samples of the upper mixed layer, the mesopelagial, and the sediment contact zone were taken for the determination of the bacterial standing stock distribution pattern of the whole water column. The bacterial abundance of sediment samples between 0 and 10 cm depth were

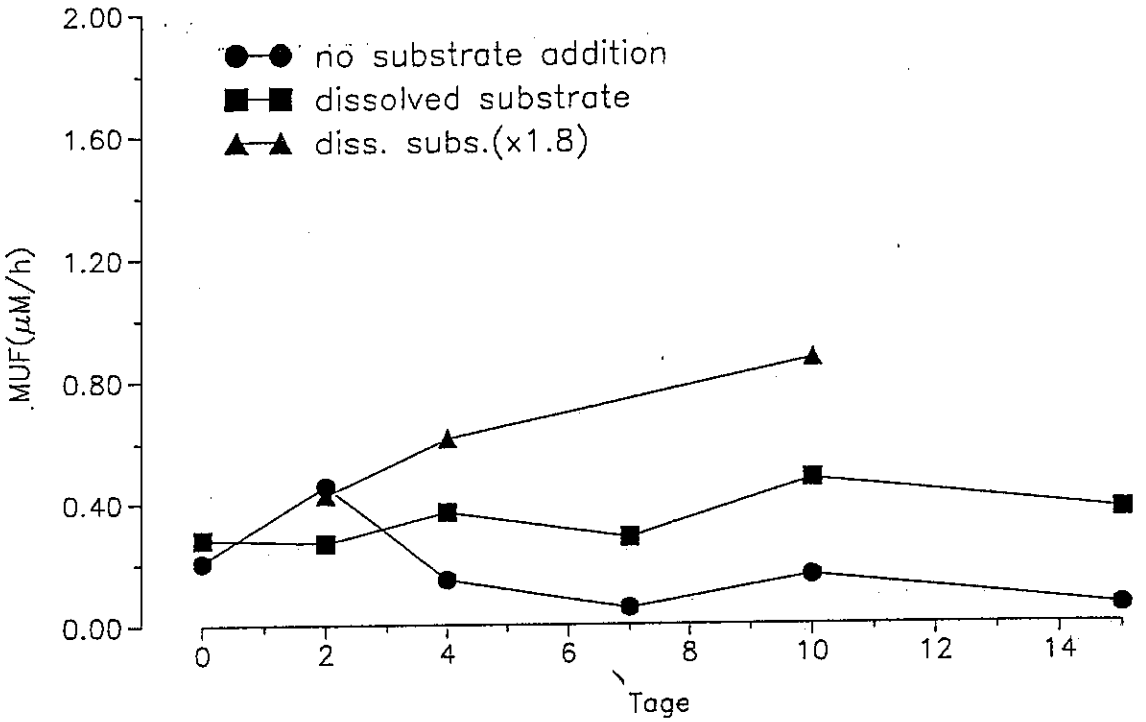

Fig. 58 a: Activity of chitobiase in some series experiments at in situ pressure (450 bar) and in situ temperature (2.5°C)

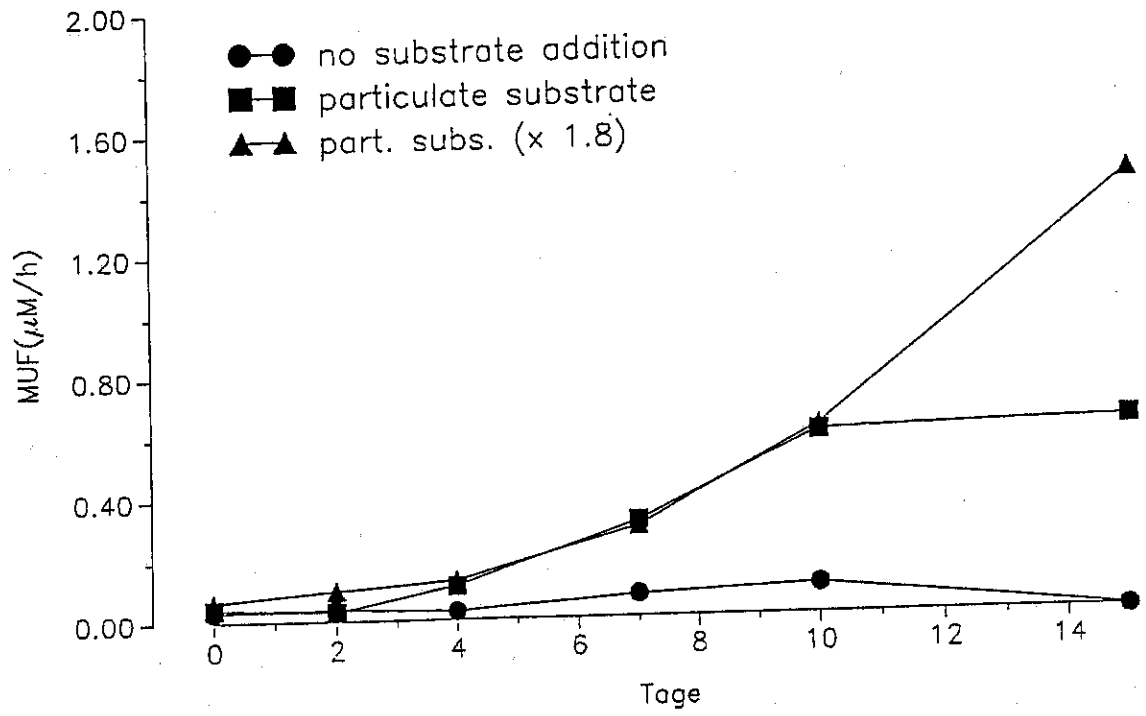

Fig. 58 b: Activity of β-glucosidase in some series experiments at in situ pressure (450 bar) and in situ temperature (2.5°C)

measured and compared with the dry weight of the sediment. The samples were concentrated on Nuclepore filter, stained with Acridine Orange, and the number/size of the organisms determined. This included the measurement of the total bacterial number, the mean cell volume, and the bacterial biomass. Moreover, electron microscopic analysis will enable a morphological view of the material.

Microbial activity

Microbial activity was determined in the benthic boundary layer and the top sediment down to 10 cm depth. A first impression of microbial activity was gained by the cleavage assay of flouresceindiacetate (FDA). A slightly higher FDA activity was found in August in cores containing phytodetritus. Using other flourogenic model substrates the potentials of degrading reactions were determined in more detail. Always the peptidase dominated, while lipase, chitinase, and β-glucosidase had lower levels (Fig. 59). Moreover, the order of the activity rate of these enzymes changed from March to August. Often an adaptation to the elevated pressure was seen. This means that in situ pressure conditions resulted in higher activity rates than incubations at 1 atm. The extent of pressure adaptation partly shifted within the vertical profile.

The benthic mineralization of phytodetritus - the typical carbon source in the deep sea - was determined with ^{14}C-labelled algae (*Anacystis* sp.) and their respiratoric degradation. For this, the formation of labelled CO_2 was measured. The respiratoric activity was higher in summer than in spring, which might be caused by the seasonal richness of organic material sedimented. Moreover, the samples were incubated in a pressure gradient. While in deeper sediment layers an extensive pressure tolerance was found, the organisms of the surface horizon preferred a specific pressure that was situated at 300 atm and not at 450 atm (the in situ conditions) as expected.

Bacterial production was determined with ^{3}H-thymidin. Nearly identical incorporation rates were found in the surface horizon and in the sediment contact water, although both environments harboured different bacterial densities. On the other hand, the production rates found were relatively small compared to shallow aquatic biotops.

Amongst sedimentated phytodetritus an input of carbon into the deep-sea is possible through fixation of CO_2. Not only photosynthesis but also chemoautotrophy and anaplerotic heterotrophy can be responsible for this. This contribution was studied with ^{14}C-labelled bicarbonat according to the measurement of photosynthesis. Ashore the samples will be chemically oxidized and the labelled CO_2 will be collected. Since such microbial autotrophic reactions in sediments often are connected with nitrification processes, the inorganic N-parameters of the pore water of the upper 10 cm were measured in incubation experiments. Indications of denitrification were found in the top horizons, especially in test series with in situ pressure conditions.

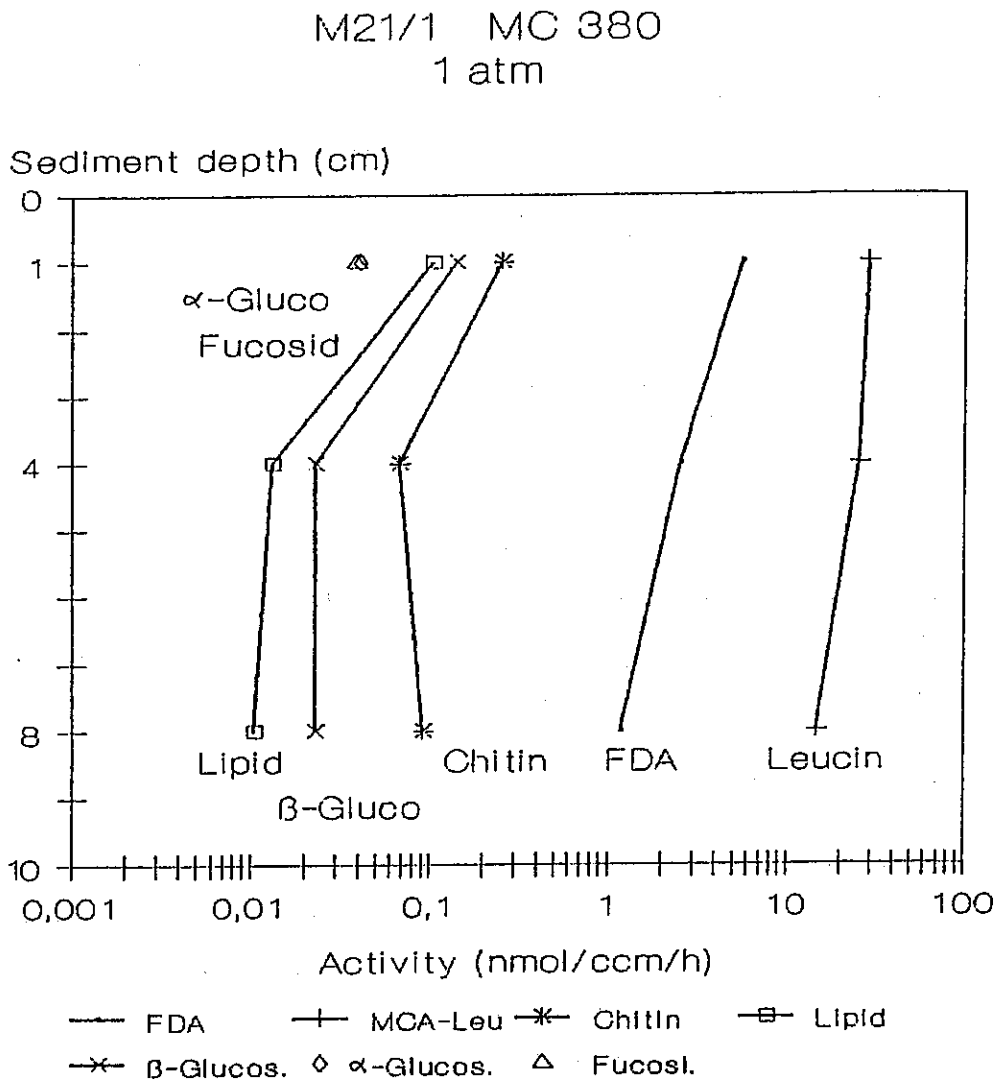

Fig. 59: Vertical profiles of selected cleavage activities in sediment of the BIOTRANS area in March 1992. Conditions: 1 atm, 2°C

Determination of the metabolizing part of the population
Since the main part of the benthic microflora seems to be in a metabolic non-active state (dormancy theory), the portion of active organisms were determined using autoradiographic methods. The sediment samples were supplemented with ^{3}H-labelled leucin or thymidin, respectively. Thus labelled and non-labelled cells could later be distinguished by microscopic observation.

In another experiment the sediment population was fed with ^{14}C-labelled algae and supplemented with antibiotics (sulfonamide, cycloheximide) to differentiate between prokaryotic and eukaryotic mineralization processes. In March up to 30% of the degradation activity in the surface horizon were due to protozoa. With increasing depth the eukaryotic portion on the degradation declined. This is in close correlation with the vertical distribution pattern of these organisms. On the other hand, the eukaryotic degradation part of the surface horizon increased up to 50% in August.

5.3.13 Vertical particle flux - recovery and redeployment of the moorings NB6/NB7 and OG5/OG6 (SFB 313) (B. von Bodungen)

At two sites in the Nordic Seas, in the Norwegian Basin (NB) and in the Jan Mayen Current (OG), vertical particle flux is recorded since 4 years. Each mooring consists of 3 traps, deployed in 500 m, 1000 m and 3000 m above the sediment surface (i.e. 3000 m for the NB- and 2500 m for the OG-site). Both moorings deployed in August 1991 were recovered safely on leg M 21/5. All traps had performed perfectly and from each depth 20 samples were safely recovered. After a short overhaul of traps, releasers and mooring materials both moorings were redeployed for another year's sampling.

Search for the missing mooring NB5
In 1989 the mooring NB5 was deployed and could not be recovered for as yet unknown reasons. During M 21/5 it was tried to locate the mooring by towing a Side Scan Sonar on an eight- shaped track around the mooring position. The sonar was towed between 30 and 50 m above the sea bottom. At the beginning and end of the search track several signals were received which indicated objects of the size of a trap and/or buoyancy packages. The detailed analyses of the track revealed that these objects were located in meter distance from the position where the anchor of the mooring had been dropped in 1989. The attempt to recover the mooring by dredging with the deep-sea wire failed.

5.3.14 Near-bottom particle flux (SFB 313) (G. Graf, P. Linke, W. Ritzrau, W. Queisser)

Since 1991 the project A3 focuses on interactions between the near-bottom Nephloid Layer (BNL) and the particle input into the sediment. For sampling the BNL a specially equipped

bottom water sampler (BWS) was used (THOMSEN et al., in press), which takes samples in 10, 15, 25 and 40 cm distance from the sediment/water interface. During deployment transmission and flowmeter data are transmitted on line and are recorded on board of the ship. By photographing a compass with a current fan, the actual flow direction and small-scale bottom morphology and colonization is documented.

The central working area on leg M 21/5 was the Kolbeinsey Ridge. It can be assumed that this ridge which is situated in an exposed position between two current systems (East Greenland and East Iceland Current) has a strong impact on the near-bottom particle flux. Based on surveys by sedimentologists and micropaleontologists (LACKSCHEWITZ et al., 1990) a profile on 67°55'N including 7 stations was chosen and sampled with an extended working programm. Five stations on the eastern and western flanks of the ridge were sampled with all instruments (CTD, BWS, FS, MUC, GKG, AGT, EPS), whereas the central ridge was documented with CTD profiles and foto system (FS) surveys. The sampling of the BNL (10 and 5 m above sediment surface by CTD and 40, 25, 15 and 10 cm above sediment surface by BWS) included the parameters oxygen, POM, chlorophyll, C/N and bacterial biomass and activity. The sediment cores recovered by the multicorer were used for measurements of oxygen consumption, ATP, DNA and chlorophyll content, meiofauna and foraminifera biomass and activity. Figure 60 shows the transmission and flowmeter data during deployment of the bottom water sampler on station M335. The transmission data are a good indicator for a proper deployment. The decrease in transmission shows the resuspension of particles from the sediment surface when the bottom water sampler is deployed. Already a couple of minutes later, the resuspension cloud had drifted away as indicated by increasing transmission data. The measurements of the flowmeter show the same for the bottom water velocity. After the transmission had reached rather constant values, the pump of the bottom water sampler was triggered to take water samples. Table 7 shows all data received from the bottom water sampler on the Kolbeinsey Ridge profile indicating rather strong currents with a prevailing N/S direction.

Table 7: Mean flow velocity and direction on the Kolbeinsey profile

Station	Mean flow velocity [cm/s]	Height above bottom [cm]	Flow direction
M330	78	28	S
M333	n. d.	-	N to NNE
M335	1.2	17	NNE
	301 to 70	46	
M338	39	46	NEE
M339	1.8	46	NNW

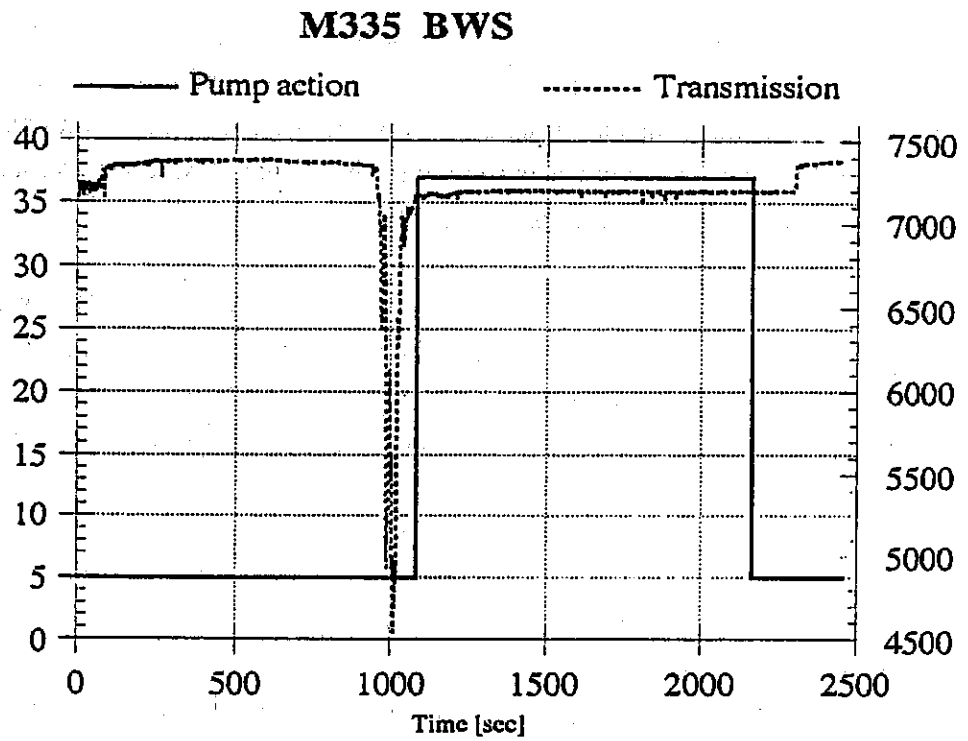

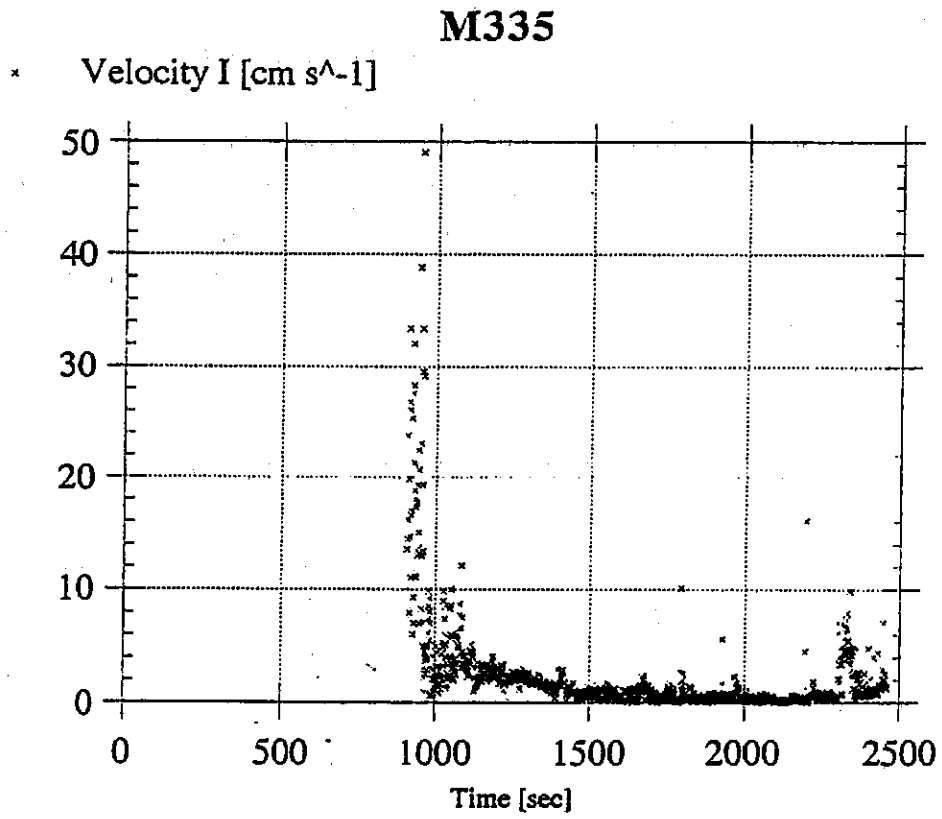

Fig. 60: Transmission and current velocity measured with the bottom water sampler (BWS) at station 335 (M 21/5)

5.3.15 Microbiology of sediments (SFB 313) (M. Ehmcke-Kasch, M. Hollinde, M. Köster, L.-A. Meyer-Reil)

Objectives

Microbiological investigations involved the determination of concentration, enzymatic decomposition and deposition of organic material with special reference to the impact of benthic communities, sediment properties and different water masses. For the purpose of this study, the following parameters were analyzed in sediment profiles: concentration of organic carbon (C) and nitrogen (N), and C/N ratio, enzymatic decomposition potential (total hydrolytic activity, and spectrum of hydrolytic enzymes), and inorganic nutrients (ammonia, nitrite, nitrate). Parallel, intact sediment cores from individual stations were incubated under close to in situ conditions and analyzed for benthic community metabolism (oxygen consumption, carbon dioxide production, and release of nitrogen remineralization products) into the overlying water.

Stations

During the beginning of leg M 21/5, the following three stations visited in earlier years were sampled again: station 317 (Vöring Plateau), station 323 (Lofoten Basin), and station 326 (east of the Island of Jan Mayen). From these stations, the latter was of special interest because of its dense colonization with epibenthic agglutinated foraminiferans observed in previous years.

Along a west-east profile on the Kolbeinsey Ridge, a total of 5 stations (water depth between 450 and 1125 m) were sampled: three stations located on the west side, two on the east side of the ridge. The rocky morphology of the crest did not allow sediment sampling. Information on a geological survey in earlier years implied differences in benthic colonization with a richer fauna on the west side of the Kolbeinsey Ridge.

Methods

Generally, sediments from at least two different cores were dissected with a high resolution at the surface (0.25 cm intervals in the strata 0-1 cm). Subsurface sediments were sliced in 1-2 cm intervals down to a depth of 10 cm. Material from deeper sediment strata was obtained by using plastic syringes (top cut off). Special care was taken to perform all manipulations and treatments of samples at low temperature (0-2°C). The enzymatic decomposition of organic material was investigated by applying fluorescent-labelled model substrates to sediment suspensions. Fluoresceindiace tate (FDA) measures unspecifically the activity of hydrolytic enzymes and serves as a general determinant for the decomposition potential of organic material. For a further differentiation of hydrolytic enzymes, the following Methylumbelliferyl (MUF)-substrates were applied: MUF-phosphate (phosphatase activity), MUF-β-D-glucoside (cellulolytic activity), MUF-N-acetyl-glucosaminide (chitinolytic activity), and MCA-leucine (proteolytic activity). Generally, sediments were suspended in filter-sterilized bottom water from the corresponding station, enriched with the corresponding

substrate at saturation level, and incubated at optimum temperature in time-course experiments. After centrifugation the release of the fluorescent dye in the supernatant was measured within a spectrofluorometer. Enzymatic hydrolysis rates were calculated by linear regression from the slope of the time-dependent activity curves. Additionally, the enzymatic activity was determined in samples collected by the bottom water sampler (10, 15, 20, and 40 cm distance from the sediment surface). To obtain insight into the contribution of epibenthic agglutinated foraminiferans to organic matter decomposition, the enzymatic activity associated with individual foraminiferans was analyzed.

From the dissected sediments, pore water was gained by centrifugation (0°C) and analyzed for inorganic nitrogen compounds (ammonia, nitrite, nitrate) by using standard techniques. Whereas ammonia was determined immediately on board ship, samples for the determination of nitrite and nitrate were frozen until analyzed by chromatography.

For community metabolism, intact sediment cores were incubated under close to in situ conditions. Regularly, subsamples from the bottom water were removed and analyzed for oxygen (Winkler titration), nitrogen compounds (see above), and carbon dioxide (gas chromatography; equilibration of acidified samples with a helium headspeace).

Additional samples from intact cores as well as sediment suspensions were immediately frozen for later analyses of organic carbon (C) and nitrogen (N), and (C/N) ratio, composition of organic material (estimation of available versus refractory carbon), and microbial numbers and biomass.

Results

Up to now, preliminary results are available for the enzymatic decomposition of organic material. The stations along the west-east profile on the Kolbeinsey Ridge were characterized by specific patterns of enzymatic activity which have to be interpreted with special regard to differences in benthic colonization. As it could be shown in a previous investigation (LACKSCHEWITZ et al., 1990), the stations were affected by highly variable sedimentation, transport, and deposition of organic material.

Highest enzymatic activities in surface sediments were observed on the eastern slope of the ridge (Fig. 61: station 333 and 335, water depth 933 and 825 m, respectively). In these sediments, in which enzymatic activity was also elevated in deeper sediment horizons, a rich benthic colonization (ophiuroids, polychaetes, sponges, anthozoans) was documented by photographs. In comparison to these stations, station 330 (water depth 1123 m) located on the foot of the ridge was less colonized, coinciding with lower enzymatic activities. In sediments on the west side (station 331 and 332, water depth 903 and 824 m respectively), gradients in enzyme activities were less pronounced. Generally, enzymatic decomposition of organic material was higher in sediments on the upper slope as compared to sediments in deeper

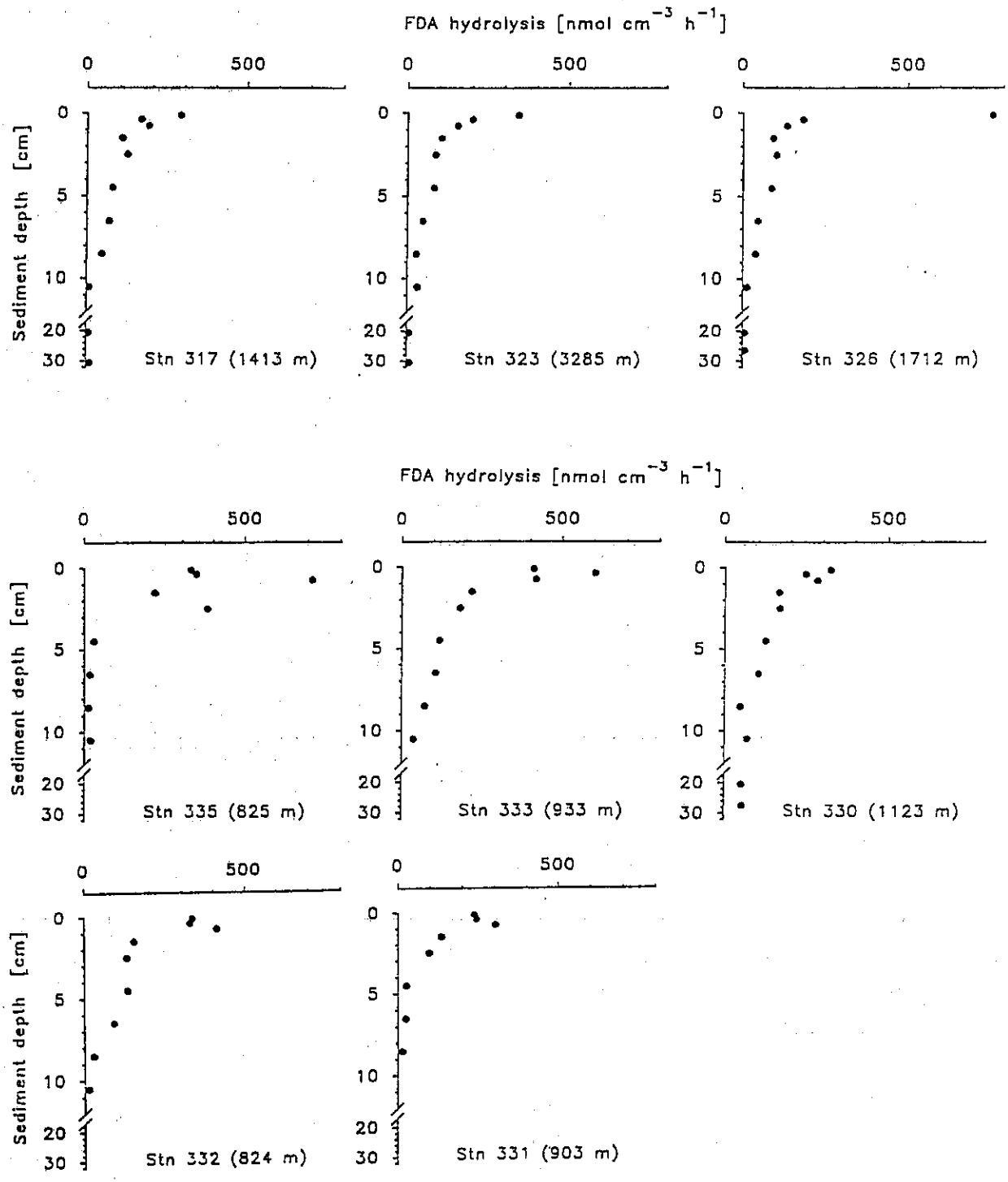

Fig. 61: Enzymatic activity measured by the hydrolysis of fluoresceindiacetate (mol of fluorescein per cm^3 of sediment per h) in sediment profiles of the Norwegian-Greenland Sea: station 317 Vöring Plateau, station 323 Lofoten Basin, station 326 east of the Island of Jan Mayen, station 330, 333, and 335 east side of the Kolbeinsey Ridge, station 331 and 332 west side of the Kolbeinsey Ridge.

waters. Hydrolytic activities in the bottom water revealed different enzymatic decomposition patterns which have to be interpreted considering currents and sediment transport.

Individual living foraminiferans sampled from the station east of the Island of Jan Mayen (station 326, water depth 1712 m) revealed hydrolytic activities dominated by chitin degrading enzymes. This can be taken as an indication that the fraction of the sedimented organic material available for epibenthic foraminiferans is dominated by chitin compounds.

Profiles of inorganic nitrogen compounds (ammonia) revealed generally higher values on the east side as compared to the west side of the Kolbeinsey Ridge. This corresponds to enzyme activity and implies higher organic matter remineralization due to the benthic fauna.

5.3.16 Porifera communities along shelf-basin transects in the Norwegian and Greenland Sea (SFB 313) (J. Reitner, S. Müller-Wille)

Location, samples, and methods

During leg M 21/4 12 large box grabs (GKG), 3 Agassiz trawls, and 8 sediment trap samples in different bathymetric positions and sedimentological situations were taken. In 95% of all samples sponges were present and in 70% they were the dominant macrofaunal elements. Main goals of the study were to pick up living deep water sponges, to keep them in aquaria to study the physiological parameters and to collect the sponge communities from different ecological/bathymetric zones for actuopaleontological, histological, and taxonomic work (see chapter 5.3.17). Additionally, sediment samples from large box grabs were taken to study the spicule record in different sediment depths and to understand the sponge decay and the linked taphonomic processes.

We collected 1-5 specimens from each of the 149 samples. All samples were fixed in buffered 4% glutaraldehyde solution in seawater. 25 selected samples were postfixed with osmium tetroxide and mercury chloride for Scanning Electron Microscopy (SEM) and Transmission Elektron Microscopy (TEM) work.

On board the sponges were examined with a stereomicroscope and press preparates were used to study the spicules and spicule arrangements.

A further goal was to learn something about the fossil documentation of sponge faunas and the record of spicules in the sediment. Therefore, about 200 sediment samples were taken from 14 box cores at 2 cm steps in the upper 10 cm and at 3 cm steps below 10 cm sediment depth. Additionally, one giant piston core (KAL) was sampled, where sponges were present. Some of the samples were already examined on board. Since spicules are fragmented during the production of smear slides, this technique seems not to be adequate. We reached good results by just stirring some sediment in water in a little, flat glass bowl. The spicules were

identified using the nomenclature in use and the spicules found compared with the spicules that should be expected according to the recent sponge fauna.

Transect Iceland-Faeroe Ridge/Aegir Ridge margin/Lofoten Basin
a) Iceland-Faeroe Ridge (station 224, 62°30.31'N, 13°5 9.34'W)
This south-north transect started with a relatively shallow station on the Iceland-Faeroe Ridge (station 224, 62°30.31'N, 13° 59.34'W; large box core) in a water depth of 1484 m. On the sediment surface a lot of small (2 cm) rocks were present which were overgrown mainly by sponges.

The sponge fauna was dominated by poecilosclerid demosponges. Observations were made on thin crusts of *Hymedesmia* sp. (*Hymedesmia* cf. *norwegica*), *Myxilla incrustans*, *Crella* sp., and *Lissodendoryx* sp.. Beside the poecilosclerids hadromerid demosponges were abundant including the taxa Suberites and Polymastia. One calcarean sponge (*Sycon* sp.) and one keratose sponge (*Dysidea*) were collected.

No tetractinellid demosponges and hexactinellids were present. The dominance of Poecilosclerida was clearly reflected in the surface sediments by the dominance of acanthostyles and tylostyles and the rare occurrence of isochelae microscleres. Calcareous spicules were not found at the surface, except one incorporated into the skeleton of an incrusting foraminifer. At a sediment depth of 2-3 cm the diversity of scleres was severely reduced and most spicules were fragmented monaxons. At a depth of 10 cm almost only less characteristic fragments of monaxons appeared. We believe this trend to be the result of bioturbation.

b) Aegir Ridge margin (station 226, 64°28.84'N, 8°18. 74'W)
On this station the sediment surface was collected using an Agassiz trawl in a water depth of 2200 m. The dredged sediment was a sandy mud with some gravels (dropstones). The sponge fauna was dominated by the tetractinellid *Thenea abyssorum* and the large fans of the peocilosclerid *Artemisina foliata* and the hadromerid *"Polymastia" sol.* Minor faunal elements were the typical deep water poecilosclerids *Cladorhiza gelida* and *Asbestopluma furcata*, *Stylocordyla* sp., *Forcepia topsenti*, the tetractinellid *Geodia* sp., the hadromerid *Tentorium semisuberites* and remains of a rigid lyssacine hexactinellid (*Euplectella* ?).

The sponge community was characterized by the first true deep water sponges (*Th. abyssorum, Cladorhiza, Asbestopluma*). The surface sediments contained monaxonic scleres of low diversity, like tylostyles, which are certainly derived from *"Polymastia" sol*, but not exclusively characteristic for this sponge. At 25 cm sediment depth a siliceous ooze overlay an ash layer, identified as the Vedde-layer (10600 a b.p.). This ooze was very rich in diverse monaxonic scleres like oxeas, tylostyles, strongyls and in microscleres like isocheles. It even contained hexactins as common elements, thus documenting a deep water fauna slightly different from that of today, where hexactinellids are very rare. The preservation of the

peculiar calcareous scleres derived from the holothurian *Elpidia glacialis* in the upper 3 cm was remarkable.

c) Lofoten Basin (station 229, 70°47.37'N, 2°40. 52'E)
This deep water station (water depth 3200 m) is located on the abyssal plain of the Lofoten Basin, and the collection was done using an Agassiz trawl. The dredged sediment was a brownish, water-rich mud with some dropstones and abundant *Pyrgo* tests.

The sponge community was dominated by Thenea abyssorum (262 specimens). Only 10 *"Polymastia" sol* and two *Tentorium semisuberites* were collected. The typical deep water peocilosclerids were represented only by *Cladorhiza gelida.* On the dropstones some myxillid and hymedesmid crusts were collected. *Artemisina* and *Stelodoryx* were represented each by two specimens.

Remarkable was the associated benthic community with a dominance of the small sediment feeding holothurian *Elphidia glacialis* (1400 specimens).

The observed sponge fauna was less diverse in contrast to the shallower stations. One controlling factor seemed to be the lower abundance of larger rocks (dropstones?) on which the poecilosclerids usually grow. The deep station was characterized by typical soft bottom adapted sponges.

Leirdjupet (station 232, 74°07.81'N, 21°0 8.85'W; 335 m water depth)
At this station no recent sponges were found. The dominating animals at this site were sedentariid polychaets building chitinous tubes into the organic rich sediment. A remarkable preservation of complete sponges was observed in the giant piston core (KAL) taken at this station (GIK 23428-3). This core consisted of a 6.4 m thick holocene sequence of organic rich shales, in which at three instances (146 cm, 271 cm, 374 cm) whole, but compressed skeletons of *Polymastia cf. kurilensis* were preserved. A similar preservation of sponges is only known from Palaeozoic black shales like the Cambrian Burgess shale or the Devonian Hunsrück Schiefer (RIGBY, 1986; CONWAY MORRIS, 1989).

The surrounding sediments contained spicules of types belonging to *Polymastia* like styles or even orthotriaens and acanthostyles, thus proving the existence of further tetractinellid sponges.

Deep water sponge communities of Knipovitch Rigde
From seven large box cores sponges were collected. Two of these box cores were located on the east side of the Knipovitch Ridge.

a) Knipovitch Ridge E (station 277/1, 76°28.59'N, 8°44. 28'E; station 281/2, 76°45.04'N, 8°11. 63'E)

Both stations were located in water depths of ca. 2000 m (station 277: 1981 m; station 281: 2127 m). The sponge fauna was characterized by relatively abundant small calcareous sponges (*Grantia* sp.) which were growing on large agglutinated foraminifers and small gravels. Sometimes they grew on *"Polymastia" sol* and *Thenea abyssorum. Th. abyssorum* was always present with 1-3 specimens in each box core. Remarkable were many small poecilosclerids (*Hymedesmia* sp., *Forcepia topsenti, Myxilla* sp.) which grew on the larger foraminifers and formed patchy and crusty structures of some centimeters length. They stabilized the sediment surface and were partly covered by sediment. Small *Tentorium semisuberites* adapted to soft bottoms were always present with asexual buds inside the sediment on their root scleres.

Knipovitch Ridge W (station 282/2, 76°52.04'N, 8°24. 31'E, water depth 2362 m; station 284/6, 77°03.98'N, 06°2 1.82'E, water depth 2200 m; station 286/3, 76°38.20'N, 06°2 4.24'E, water depth 2260 m; station 289/3, 75°59.50'N, 06°2 1.42'E, water depth 2192 m; station 291/2, 75°52.54'N, 05°2 8.98'E, water depth 2575 m)

All five stations were located in a mean water depth of ca. 2200 m. No significant differences in the sponge population comparable to those of the eastside were observed. In all box cores *Thenea abyssorum*, *Tentorium semisubrites*, deep water *Grantia* and sediment stabilizing poecilosclerids were found. Occasionally the calcarean taxa *Leucosolenia, Clathrina* and the haplosclerid taxa *Haliclona* and *Gellius* were present.

In all stations of Knipovitch Ridge W and E there was a very good correspondence of living sponge communities and scleres in the sediment. *Thenea abyssorum* was represented by dichotriaens and spined metasters in the upper 3 cm of the sediments and the rich poecilosclerid fauna by diverse monaxonic scleres. The only exception was the record of an ophirhabd in 2-3 cm sediment depth of the core at Station 284, typical for axinellids, which were not found in the area of investigation. But even here the diversity of scleres decreased rapidly in the upper few centimeters of the sediment. The big agglutinating foraminifera which were always found covering the surface incorporated a lot of spicules. To study these, some samples of surface sediment were fixed.

Barents Sea sediment fan (station 292, 75°18.48'N, 09°4 6.23'E)

Box core and AGT samples demonstrated a typical community of deep water/soft bottom sponges. *Thenea abyssorum* was with 60% of the total sponge population the dominant species followed by *"Polymastia" sol* (25%). *Polymastia mammilliaris* was relatively abundant. Poecilosclerids were rare and only represented by a few specimens of *Cladorhiza gelida, Artemisina foliata*, and *Myxilla* sp.. Haplosclerids were represented by Gellius cf. yugosus. Small calcareans (*Grantia*) grew on specimens of *"Polymastia" sol* and *Thenea abyssorum*. Hexactinellids were only represented by dead rigid lyssakine euplectellids.

Results on the distribution of sponges

Except of the shallower stations of the Iceland-Faeroe Ridge the sponge fauna of the deep ocean basins was less diverse. The basins were characterized by muddy, instable soft bottoms, sometimes with a few dropstones or shell remains of bivalves (*Cyclopecten, Veneridae*). On the dropstones, shell debris and larger agglutinated foraminifers small calcareous sponges of the taxon Syconidae/Sycett idae were quite common. Beside the Calcarea a relatively rich Poecilosclerida fauna (*Hymedesmia* div. sp., *Myxilla, Forcepia topsenti*) was observed initially growing on foraminifers. On the soft bottoms *Thenea abyssorum, "Polymastia"sol, Tenttorium semisuberites* and *Cladorhiza gelida* were the dominant faunal elements. Hexactinellids were missing, apart from some dead skeletons of euplectellids. This was in contrast to the East Greenland deep basin in which a rich rosselid lyssakine hexactinellida fauna (*Schaudinnia*) was observed (REITNER and HENRICH, 1991, HENRICH et al., 1992).

The shallower basin areas (1500 m) were dominated by Hadromerida and Poecilosclerida, which were restricted to firm grounds. Within the studied high accumulation zones no living sponges were observed. BARTHEL et al. (1991) had observed different sponges communities in the same area during the METEOR cruise no. 13.

One main factor responsible for the low diversity of the deep water sponge community may be the oceanographic position. The extreme low diverse fauna of the Lofoten Basin may be controlled on the one hand by the very instable soft sediments in the area and on the other hand by the sediment input from the Bear Island Trough via turbidites. This sedimentologial events may destroy the deep benthic communities and the resettlement may be linked to types with a high reproduction rate. Indeed, the dominant sponges *Thenea abyssorum* and *Tentorium semisuberites* exhibit many asexual buds which allow a rapid resettlement of a newly formed sediment surface.

The situation within the Greenland deep basin, including the Vesterisbanken Seamount, is different. This basin is influenced by the cold East Greenland Current and is therefore extremely enriched with oxygen and exhibit a different trophic situation. Sediment input via turbidites from the Greenland shelf areas is of minor significance and probably a rare event. The benthic communities of this area are more stable and consequently exhibit more k-strategists like big rosselid lyssakine (e.g. *Schaudinnia*) and amphidiscophora n (e.g. *Hyalonema*) hexactinellids, as well as the large tetractinellid demosponges (e.g. *Geodia*). All of these sponges bear symbiontic bacteria within their mesohyle in contrast to most of the observed taxa in the Lofoten Basin (REITNER and HENRICH, 1991, HENRICH et al., 1992).

Results of the spicule record

As a rule, sponges are only documented by their scattered spicules. It seems quite probable that these are more or less autochthonous, because in some instances dead sponges could be seen on the sedimentary surface, whose skeletons were not yet fragmented. This may be due

to the fact that spicules tend to form a dense network in the living organism, which stays intact for quite a while after death. In some cases, though, spicules could be found in the sediment surface which did not belong to any of those living sponges found in the box core, e.g. ophirhabd spicules typical for Axinellida. Whether this is due to wider lateral transport or more a problem of sampling, cannot be decided yet. A special case of spicule preservation is the incorporation of spicules into agglutinated tests of benthic foraminifers or polychaete worm tubes. The case of a preservation in whole as in the giant piston core at station 232 seems to be exceptional and due to high sedimentation rates and low bioturbation activity.

The samples of surface sediments exhibited a rich and diverse spicule "fauna", sometimes including characteristic spicule types, like dichotriaenes and metaster derived from *Thenea abyssorum* or chelae of Myxillids. Calcareous spicules were not observed to be preserved in the samples, due to early diagenetic solution. Thus only the main representatives of the deep water siliceous sponge community were documented in the sediment. Most of the spicules, however, are uncharacteristic monaxones like styles, tylostyles, oxeas, very often fragmented. The fragmentation may be due to the activity of sediment feeders like the holothurian *Elpidia glacialis*. Nevertheless, it should be possible to find characteristic spicule associations corresponding to certain sponge communities when using statistical means, like cluster analysis.

5.3.17 Benthic communities of the Greenland Island and Norwegian Sea (SFB 313)

(A. Brandt, K. v. Juterzenka, S. Müller-Wille, D. Piepenburg, J. Reitner, U. Witte)

Background

During legs M 21/4 and M 21/5 investigations on benthic communities were performed at selected sites on continental margins of the Greenland Island and Norwegian (GIN) seas. During leg M 21/4 work focussed on the western Barents Sea, during leg M 21/5 sampling was continued on the Vöring Plateau and on the western side of the GIN seas. The ecology of the eastern GIN region is influenced by the relatively warm Norwegian Current system, and that of the western GIN region by the polar East Greenland Current tranporting extremely cold water masses and sea ice from the Arctic Ocean to the south.

Benthic communities in certain areas on the continental slope off Greenland and on the slopes of the ridges and fracture zones of the GIN seas are surprisingly rich both in biomass and diversity. They are supposed to be fed by the surplus primary production of the relatively near marginal ice zone of the East Greenland Current. The organic material produced there tends to sink out of the euphotic zone in strongly pulsed sedimentation events and is then distributed in the benthic nepheloid layer (BNL) by topography-driven currents, mostly along certain depth zones of slopes, to the areas of potential deposition.

It is hypothesized that along this pathway of lateral matter transport, actually consisting of a series of both physical and biological deposition and resuspension events, benthic colonization is stimulated in certain slope areas characterized by favourable conditions in terms of food supply and bottom morphology. These factors, and hence also the distribution and structure of the benthic communities, are ultimately controlled by the bottom current regime, but vice versa, the physico-chemical properties of the near-bottom water body are modified by biological activity. The quantitative description of the coupling between the communities, inhabiting the upper sediment layers and the BNL, and the abiotic environment is the main goal of the sub-project A3 of the Sonderforschungsbereich 313 of the University of Kiel.

Study programme

To obtain broad information on the various size components of the benthic communities, a set of different sampling gear - box corer (GKG), epibenthic sledge (EBS), Agassiz trawl (AGT), and seafloor photography (UWP) - was employed at each station whenever possible. Box corer samples were analyzed for composition, abundance, biomass and distribution patterns of endo- and epibenthic macrofauna. Catches with the epibenthic sledge provided similar information on the suprafauna community fraction, whereas Agassiz trawl hauls covered the megafaunal components. Seafloor photographies represented in situ views of epibenthic habitats providing both qualitative and quantitative information on benthic biotopes. With regard to epibenthic megafauna organisms the quantitative analysis of the exposures is the most adequate method to evaluate absolute abundances as well as spatial distribution patterns on the 1 m-100 m scale.

Our studies focussed on brittle stars, sponges, and crustaceans - abundant taxa which all are presumed to contribute significantly to the biogenic modification of the particle flux in the BNL. Abundant species from these taxa were investigated in more detail with regard to population structure, trophic relationships, reproduction biology, and metabolic performance.

Sediment samples (or subsamples, if necessary) were sieved through 300 µm or 500 µm meshes. For the community studies all specimens of the species considered (or, when occurring in large numbers, a representative subsample) were sorted out of the catch and preserved for later analyses by freezing at -25°C, in a borax-buffered 4% formalin-seawater solution, in 4% Kohrsolin or in 70% ethanol. The autecological studies on the selected species included 1) the assessment of parameters of population structures (e.g. size frequencies, age structures, sex ratios, fecundities), 2) the biochemical analyses of body compounds with special emphasis to lipid content and composition, and 3) ecophysiological experiments with live specimens kept in cooled aquaria over longer time spans. The live specimens were kept on board in a lab container cooled to 1°C. After the cruise they were transferred to Kiel for further investigations. Their behaviour and metabolic responses to controlled variations of environmental conditions like e.g. temperature and food supply will be studied. This includes the measurement of respiration rates as a parameter of the metabolic activity. Experiments on

feeding behaviour and particle uptake using algae cultures and fluorescent microspheres of different sizes started in part already on board and are continuing in Kiel (flume experiments).

In order to estimate the importance of brittle star larvae, samples were taken from several box cores. Sediment samples were sieved through 200 µm gauze, fixed with filtered and buffered formalin and stained with bengal rose to record the settling of the pelagic ophiurid larvae (*Ophiopluteus*).

In addition to faunistic information on the various sponge assemblages, the biology of the dominant deep water species (the soft bottom specialists *Thenea abyssorum* and *"Polymastia" sol* as well as the generalists *Tentorium semisuberites* and *Grantia* sp.) was studied in more detail. Specimens of these species were counted, measured and checked for presence and number of buds. To study sexual reproduction, undamaged specimens were fixed in Osmiumtetroxyde for histological investigations by light and transmission electron microscopy.

Due to the close cooperation with other working groups of the SFB 313, the results of the community studies can eventually be interpreted in the context of the broad, ecologically significant background informations on the properties of the benthic biotopes, the upper sediment layers and the near-bottom water layer. Especially the data derived from samples taken with near-bottom CTD, multicorer (MUC), and bottom water sampler (BWS) are of great value for the inferential evaluation of our findings (see above).

First results: Leg M 21/4

At the Iceland Faroer Ridge (station 224) a diverse sponge community was dominated by poecilosclerid demosponges (*Hymerdesmia c.f. norvegica, Myxcilla incrustans, Crella* sp., *Lissodendoryx* sp.). Hadromerid demosponges were also abundant (taxa Suberites and Polymastia), whereas no tetractinellids and hexactinellids were found. At the Aegir Ridge in 2200 m depth the sponge fauna was dominated by the deep water tetractinellid *Thenea abyssorum* and the large fans of the poecilosclerid *Artemisina foliata.* The hadromerid *"Polymastia" sol* was also quite common. Minor faunal elements were e.g. the deep water specialists *Asbestopluma furcata* and *Cladorhiza gelida.* In the Lofoten Basin (station 229) a less diverse fauna dominated by *Thenea abyssorum* was found. At all stations at the Knipovitch Ridge the typical deep water soft bottom sponges were present. Strikingly abundant were small calcaroneon sponges (*Grantia* sp.) growing on large agglutinated foraminifera, gravel and other sponges. Remarkable were many poecilosclerids growing on large Foraminifera forming crusts several centimeters big thus glueing Foraminifera together and stabilizing the sediment.

There is evidence from the shipboard investigations in a cooled lab container on sponge life history that only in *Thenea abyssorum* asexual reproduction occurs frequently. Feeding

experiments with algae and microspheres were also carried out already on board and were continued in Kiel.

Box core samples on the continental slope near Bear Island (stations 247, 250) were taken to complete the macrofauna sampling profile of M 17/1. Sediment cores from station 250 where high accumulation rates were recorded during M 17/1 will be used for flume experiments in Kiel. Box core samples from the Kveitehola, a shelf trough in the western Barents Sea, were taken along 3.5 kHz transects (stations 240, 241, 254, 259). These samples showed differences which may be related to estimated bottom currents (see chapter 5.3.15). At station 254 we found coarse sediment and stones, whereas the other samples were characterized by soft bottom (including abundant long black polychaete tubes).

First results: Leg M 21/5

In the sampling area on the Vöring Plateau the epibenthic sledge samples revealed that ophiuroids and small peracarid crustaceans were most abundant. The ophiuroid *Ophiocten* occurred in large numbers. Among the crustacean shrimps (e.g. *Hymenodora, Pandalus*) occurred only occasionally, whereas the smaller peracarids appeared to thrive on the Vöring Plateau as they also did in the area of the Kolbeinsey Ridge. Interestingly the Mysidacea, usually an important component of the suprafauna, were not caught at the Vöring sites during this cruise, and on the Kolbeinsey Ridge also only relatively few were sampled. The most abundant and diverse peracarid taxa were Amphipoda and Isopoda, followed by Cumacea. Tanaids were less frequent in all samples. Both Amphipoda and Isopoda were very speciose, whereas Cumacea and Tanaidacea also seemed to be less diverse. The most important amphipod families have not yet been determined. Of the Isopoda the families Ilyarachnidae, Ischnomesidae, Macrostylidae, Munnidae, Munnopsidae and Paramunnidae - all typical deep-sea asellote isopods - comprised most of the specimens. Leuconidae, Diastylidae and Cucumariidae were likely to be the most abundant cumacean families.

At one location at the Jan Mayen Fracture Zone in 1700 m depth (station 326) the giant Foraminifera *Hyperamina* occurred in very high abundances. A series of 28 seafloor photographies taken at this station showed that at a 100 m-scale a high proportion of the bottom was covered by the characteristic sand shells of *Hyperamina*.

The main benthological sampling area during M 21/5 was the Kolbeinsey Ridge north of Iceland. On a longitudinal transect at 67°55'N across the ridge, sampling focussed on the tracing of a presumed ecological east-west gradient: The eastern slope is probably influenced by water masses of the East Iceland Current, the southern branch of the Greenland Sea Gyre, whereas the conditions on the western slope are shaped by the permanently ice-covered East Greenland Current. The transect consisted of a total of 7 stations ranging in depth from 500 m to 1100 m. At 5 stations the whole set of sampling gear (GKG, EBS, AGT, UWP, MUC, BWS, CTD) could be employed. At two stations on the ridge top, only CTD and UWP were used due to the rough bottom morphology.

At the seven Kolbeinsey transect locations a range of 20 to 33 seafloor photographies per station were taken. First analysis of exposures and samples indicated the existence of the supposed ecological cross-ridge gradient. The ridge top was inhabited by a typical hard bottom fauna dominated by sessile suspension-feeders like sponges and soft corals. Bottom morphology and community properties appeared to be controlled by strong bottom currents. Both ridge slopes were characterized by soft bottom habitats. However, there is evidence from the photographies as well as from the corer samples and trawl catches that at least the megafauna (sea stars, brittle stars, sponges, and crustaceans) was much richer at the western slope both in biomass and diversity. These findings indicate differences in terms of bottom current regimes and, hence, patterns of lateral particle advection.

Small epi- and endobenthic peracarid crustaceans seemed to be frequent on both slopes. However, a brief comparison of the epibenthic sledge samples from stations station 333 (east slope) and station 331 and station 332 (west slope) revealed differences in abundance and composition of the Peracarida. Peracarids were most frequent on the soft and muddy sediment of station 333, which was covered with fluff (and Isopoda Asellota were slightly more frequent than Amphipoda), whereas at station 332 Amphipoda seemed to be more numerous than Asellota. In total, the peracarids seemed to be less frequent on this locality. This sample was characterized by a high percentage of sponge spicules and a more prominent megafauna. The EBS-sample of the outer station of the western slope (station 331) contained fewest peracarids, the sediment was coarse and consisted of a high amount of glass particles. These differences will have to be evaluated when the samples have been sorted and quantitatively analyzed.

Echinoderm distribution across the Kolbeinsey profile showed also significant differences between the eastern and western slope. On the western slope we found species which are known from shelf and slope locations far in the north influenced by the polar East Greenland Current (e.g. the brittle stars *Ophiopleura borealis, Ophioscolex glacialis* and *Gorgonocephalus* sp., and the sea stars *Pontaster tenuispinus* and *Solaster* sp.). On the eastern slope, the ophiuroid Ophiocten was also of importance. For this species, the occurrence of very small specimens (probably only a little older than the settling stage) in box core samples was of interest.

5.3.18 Mammals and Seabirds at 47°N, 20°W (BIO-C-FLUX)

(B. Christiansen, O. Pfannkuche)

The observations on mammals and seabirds were not performed systematically, but only casually on legs M 21/1, 2 and 6 in the BIOTRANS area (47°N, 20°W). Pilot whales (*Globicephala melaena*) were frequently observed on all 3 legs. It seems likely that we observed always the same herd of about 30 specimens. Fin whales (*Balaena physalus*) were

spotted at least five times. In one case we encountered a cow accompanied by her calf. Dolphins were rarely seen, an identification of the species was not possible.

Seabirds were relatively rare in the BIOTRANS area. The ship was frequently accompanied by Kittiwakes (Dreizehenmöwe, *Rissa tridactyla*). Small numbers of Fulmars (Eissturmvogel, *Fulmarus glacialis*), Gannets (Baßtölpel, *Sula bassana*) and Greater black-backed gulls (Mantelmöwe, *Larus marinus*) were sometimes observed around the ship as well as the Pomarine Skua (Spatelraubmöwe, *Stercorarius pomarinus*). Several species of storm petrels were spotted (Bundfüßige Sturmschwalbe, *Oceanites oceanicus*; Sturmschwalbe, *Hydrobates pelegicus*; Wellenläufer, *Oceanodroma leucorhoa*).

5.4 Marine geosciences

5.4.1 Geophysical investigation of the sea floor (SFB 313) (J. Mienert, M. Bobsien, J. Chi, F.-J. Hollender, T. Bergmann)

The working group B1 of the SFB 313 investigates the physical character of sea floor sediments in order to determine the processes moulding high latitude continental margins. The most drastic changes of physical and acoustic properties of the sea floor occur at the water/sediment boundary and in the upper 100 m of sediments. Here, changes in sea floor properties are strongly influenced by sediment composition and grain sizes which in turn are related to climatic changes.

Multi sensor core logger

High resolution compressional wave, gamma ray attenuation (density) and magnetic susceptibility whole core logging proved to be of great value for paleoclimatic studies and inter-core correlations. We measured the three parameters on two up to 6 m long gravity cores located on the western and eastern flank of the Knipovitch Ridge. The average measurement interval was 2 cm. These measurements will be used to investigate the climatic driven sediment cycles at low and high latitudes. Time control for the gravity cores will be derived from oxygen isotope and biostratigraphic data in cooperation with colleagues of the SFB 313.

So far, we anticipate that our results represent time intervals spanning the last climatic cycles to oxygen isotope stages 9 or 11. In the sediment physical record we observed an excellent correlation between compressional wave velocity and density. Figure 62 shows an example of the strong positive correlation (R=0.9) between the two parameters. The observed changes appear to be controlled by the flux in terrigenous material and only to a minor extent by carbonate fluxes. At present, our conclusion pertain only the two cores from the high latitudes.

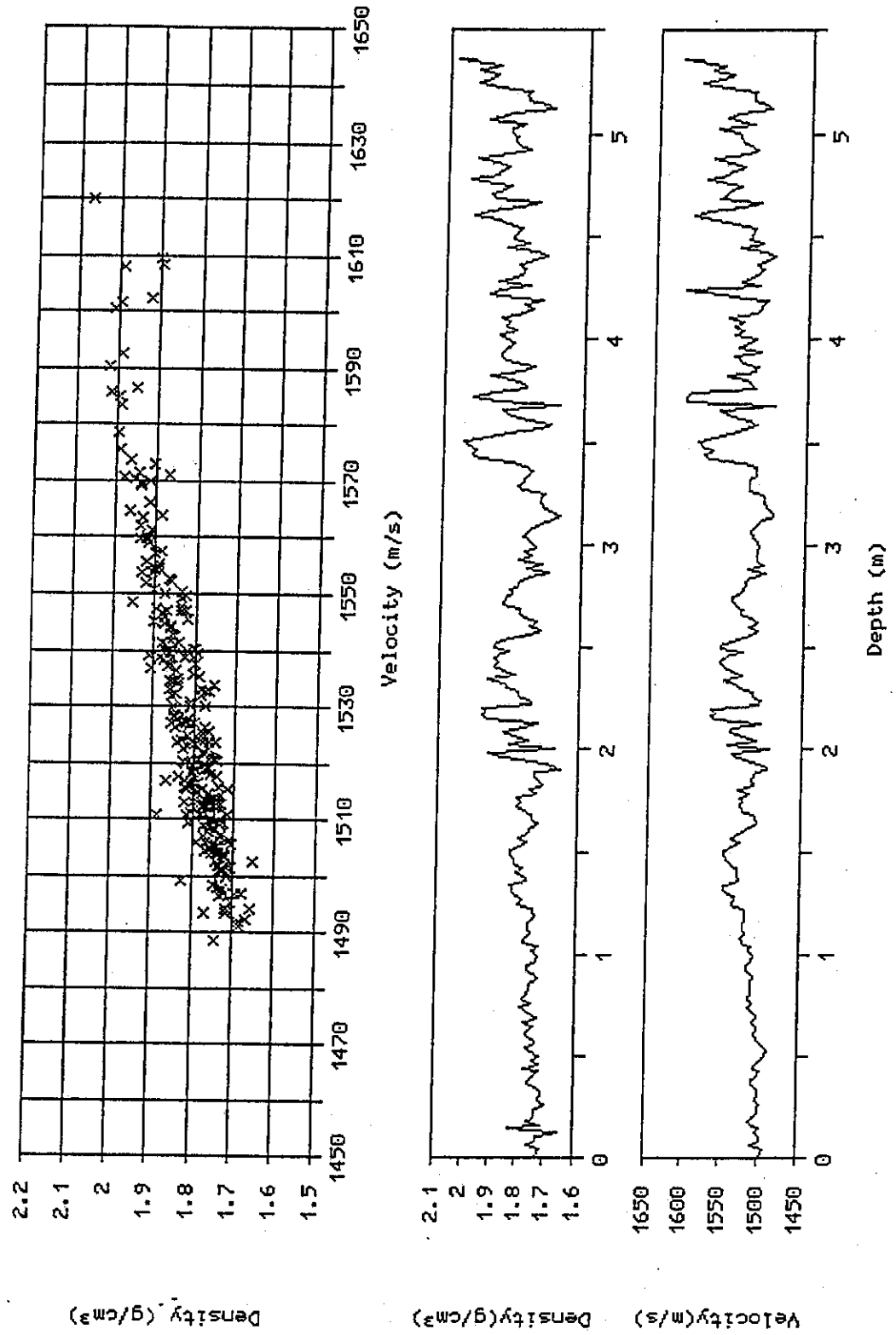

Fig. 62: Measurements of velocity (m/s) and density (g/ccm) versus depth (m) with the Multi Sensor Core Logger. The correlation between velocity and density is shown to the right.

Ocean bottom seismometer

Numerous cruises have shown that conventional gravity coring methods allow to recover up to 20 meter long cores from the sea floor. In order to receive information about physical and acoustical properties of deeper (older) stratigraphic sections we used a remote sensing approach. We varied the technology of low frequency ocean bottom seismometers and developed a High Freqency Ocean Bottom Seismometer (HF-OBS) (Fig. 63). The first tests were carried out in shallow water in the Baltic Sea. After the shallow water tests were passed, we deployed the device in the deep-sea of the North Atlantic at four sites ranging in water depth from 1400 to 2500 m.

Parasound profiling

During leg M 21/5 several profiles were recorded with the Parasound and the Hydrosweep system. The Parasound system is a sediment echosounder (see report M 17/1). In ocean sediments the penetration can reach 100 m. Analogous plots are available for preliminary interpretation on board. In addition, digital data are stored on magnetic tape for seismic processing at a later date. An example of an analogous Parasound profile is shown in Figure 64 which appears to indicate sediment waves on the slope. The maximum depth of penetration is 45 m. Within the sediment column, up to 20 reflectors can be distinguished (Fig. 64).

5.4.2. Analysis of sediment sections and preliminary paleoceanographic results:Norwegian-Greenland Sea deep-sea records (SFB 313)

5.4.2.1 Aegir Ridge, Barents Sea continental margin and northern Knipovitch Ridge

(T. Wagner, M. Antonow, B. Schlünz, K. Michels, S. Schulz, P. Goldschmidt, R. Henrich)

Eight long box cores were taken during leg M 21/4 in the most southern (Aegir Ridge) and the northeastern part (Knipovitch Ridge) of the Norwegian-Greenland Sea. 3.5 to 7.5 meters of the upper sediment layer were obtained, documenting the varying influence of the Norwegian Current along the western coast line of Scandinavia and the Barents Sea on deep-sea sediments as a response to changing climatic and oceanographic conditions.

One box core (42 cm) and a long one (475 cm) were taken on the Aegir Ridge at 65°31'N, 04°0 6'E (2788 mbs). The covered sequence is dominated by silty to sandy silty abundance, recording the two last glacial/interglacial cycles. At 25 cm an ash layer, identified in cores close to Iceland as "Vedde ash", was found. The sedimentary column between 189-249 cm was disturbed by slumping, showing in its upper part a lightbrown sandy silt rich in planktic Foraminifera underlaid by a bioturbated zone leading to a diamicton with an increased Ice Rafted Debris (IRD) content (coal clasts) at its base. A light colored,

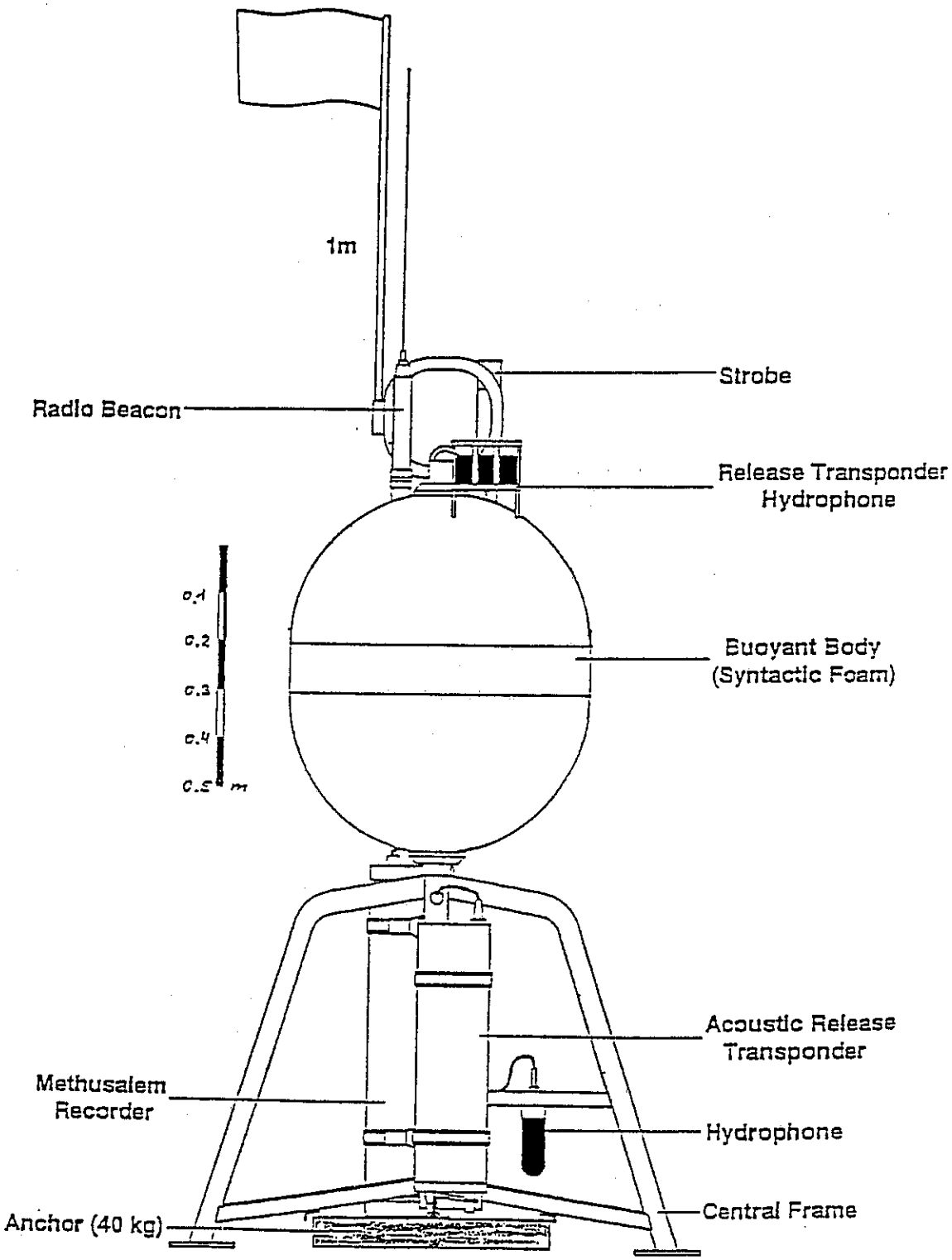

Fig. 63: Schematic diagram of the high Frequency Ocean Bottom Seismometer developed by the SFB 313, project B1 (drawing by P. BERGMANN, GTG). We thankfully acknowledge funding by the DFG.

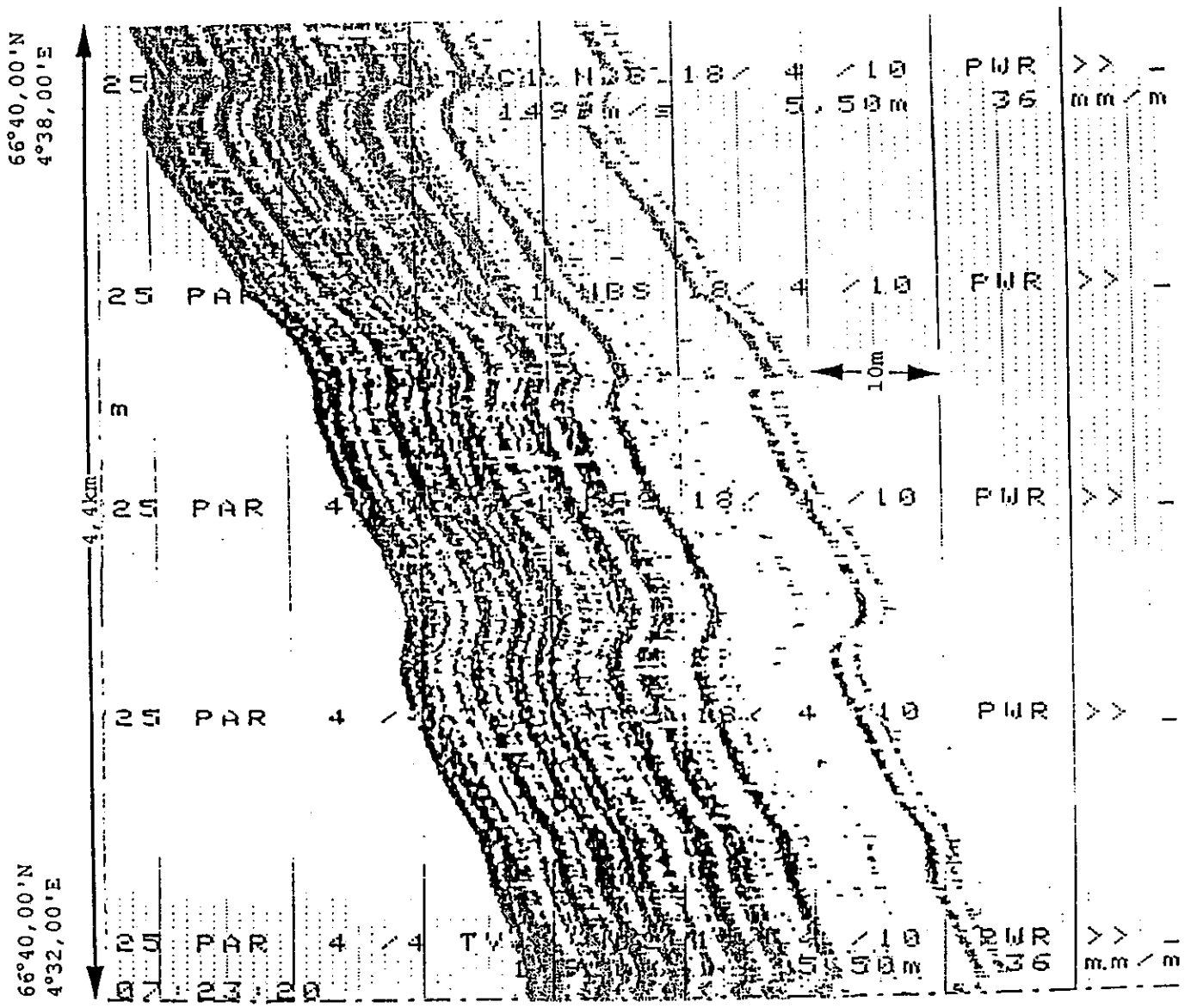

Fig. 64: Example of a Parasound acoustic profile from the Vöring Plateau

Foraminifera-rich sediment horizon was deposited at the deepest part of a second slumped section between 395-475 cm at the base of the core.

Carbonate contents were measured on board using a "carbonate bomb" (Fig. 65). High values between 52-65 wt.% in the upper 20 cm of the box core document high marine productivity caused by an influence of warm water masses in the eastern part of the Norwegian Sea during the Holocene. A sharp decrease in carbonate content further downcore to values around 10 wt.% mark the transition from interglacial to glacial climatic conditions. A pronounced increase in carbonate between 170-210 cm, culminating at 190 cm (34 wt.%) may reflect isotope stage 5.5.

Smear slides were prepared and analyzed on board (Figs. 66 and 67). Semiquantitative data of biogene and lithogene components correlate with the lithological and geochemical data discussed above. In general the sediments are dominated by lithogeneous components ranging between 40 and 95 grain-%, displaying the vicinity of terrigenous source areas. Except for the upper 40 cm of the core the lithogeneous fraction is mainly made up by quarz. The biogenic composition correlates well with the carbonate curve. A sharp decrease in carbonate content at 20 cm from 60 wt.% to value less than 10 wt.% at 40 cm can be related to decreasing amounts of Foraminifera and holothurian spicules. Low carbonate values (10 wt.%) throughout the sediment section between 45-160 cm go together with common or abundant occurring Foraminifera and coccoliths. The pronounced increase in carbonate up to 36 wt.% between 160-210 cm is explained by an increased occurrence of coccoliths, strongly supporting the stratigraphic correlation with isotope stage 5.5.

Seven long box cores (lengths ranged from 350 to 634 cm) and seven box cores were taken between 76°N, 05°E and 77°N, 09°E along two N-S transects east and west of the Knipovitch Ridge in the most northern part of the Norwegian-Greenland Sea. Core positions were located under the western branch of the Norwegian Current where recirculation to the southwest and mixing with polar water masses entering from the Arctic Ocean through the Fram Strait into the northern Atlantic realm take place.

Sedimentological analysis of the obtained sediment cores will give detailed information of the glacial/interglacial history of this oceanographic boundary. All cores show typical sequences of lithological units which can be correlated east and west of the ridge. Silty to sandy silty grain sizes dominate throughout the sediment sequences. Intercalations of homogeneous light to dark gray clay horizons at the base of several cores occur. Changes from light-coloured, Foraminifera-bearing and olive-coloured IRD-rich sediment sections document interglacial and glacial sedimentary processes. In general all sediment types are enriched in sedimentary pellets and rock clasts of grain sizes < 1 mm. Foraminifera are rare, in certain horizons common. First carbonate data from one core east (23454-1) and one west (23456-5) of the ridge are shown in figure 65. Core 23454-1 is characterized by decreasing values from 32 wt.% at the sediment surface to values < 5 wt.% at 30 cm depth. Low carbonate contents

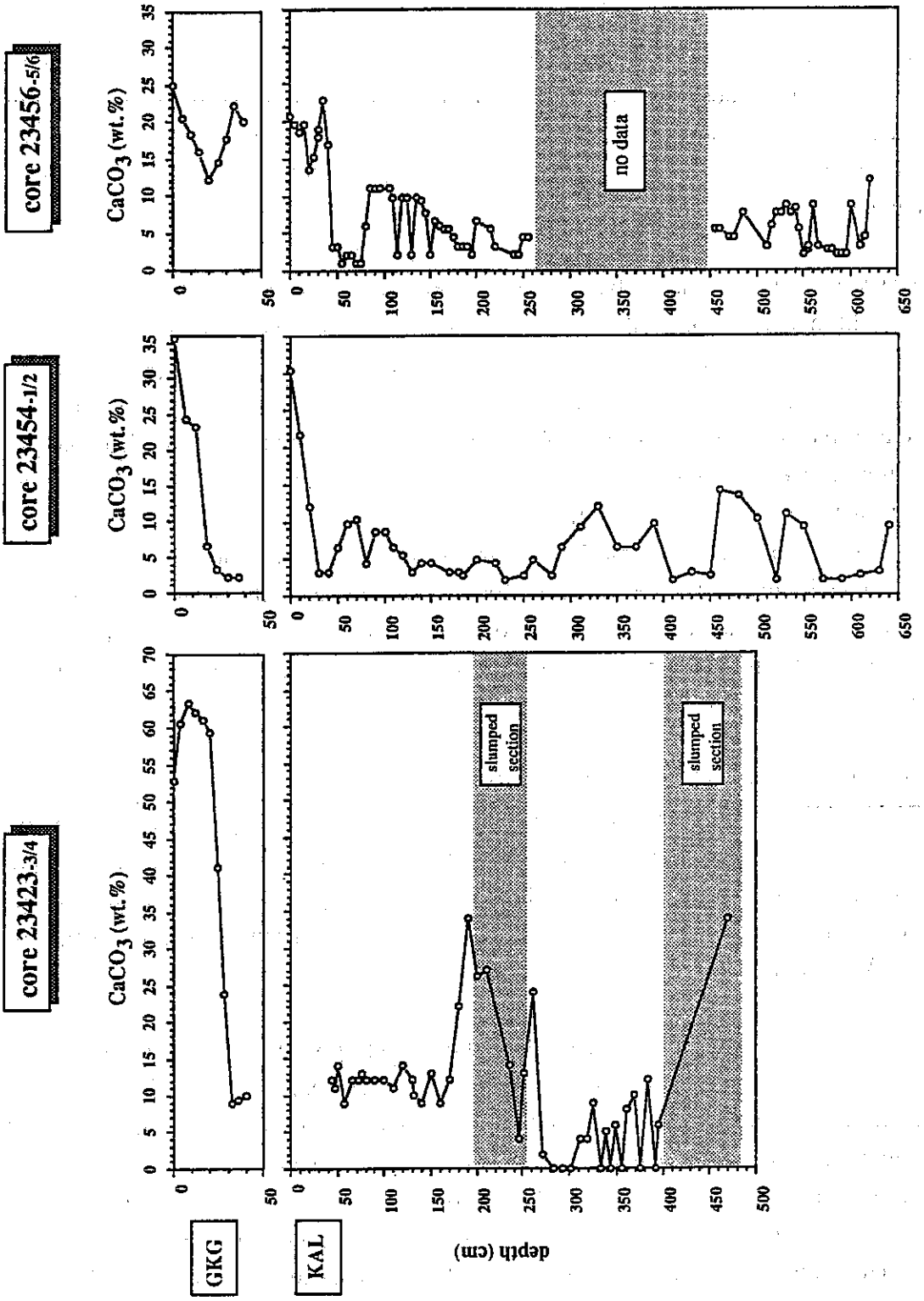

Fig. 65: Carbonate curves of three cores

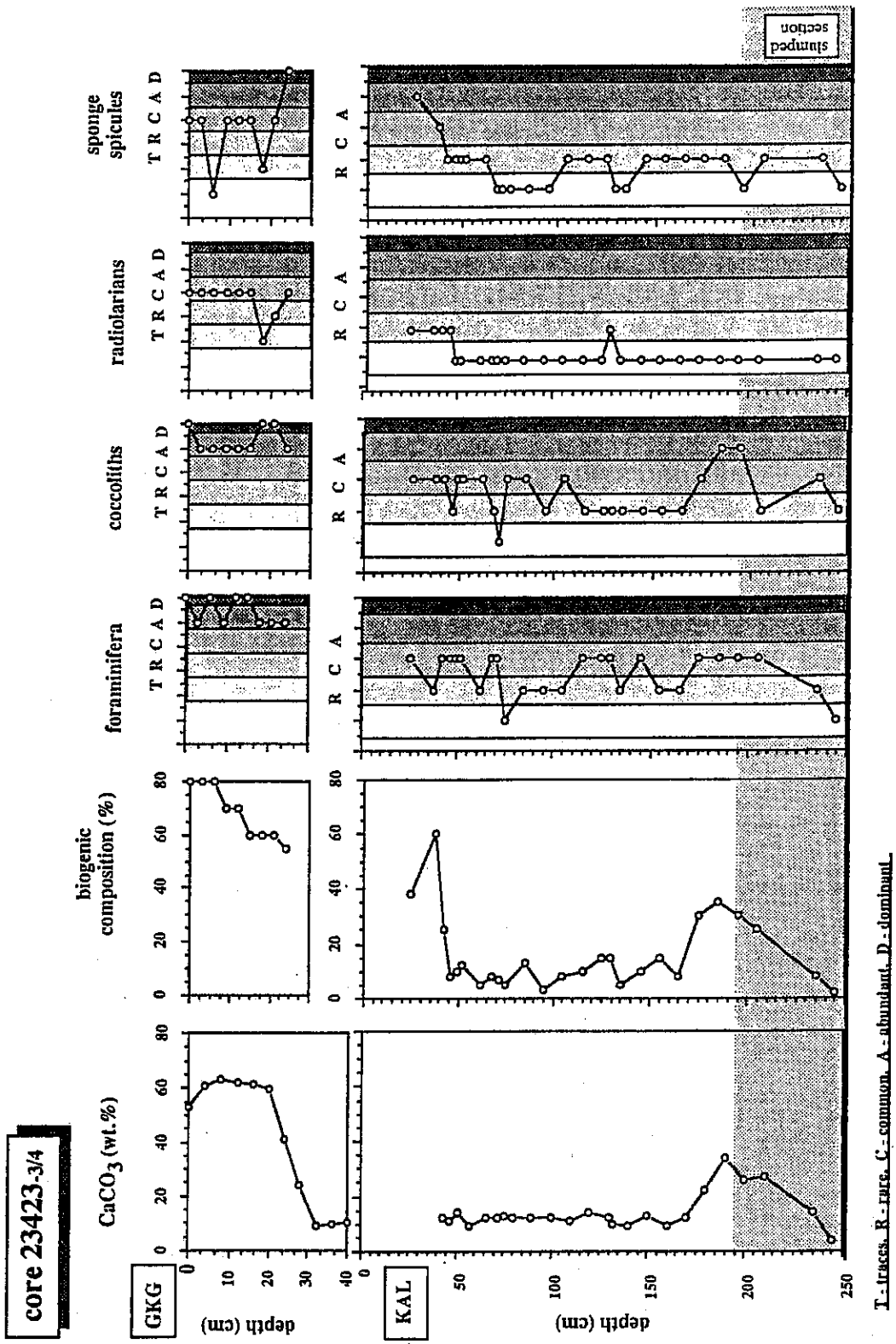

Fig. 66: Smear slide analysis (biogenic components) and carbonate content of the upper 245 cm of core 23423

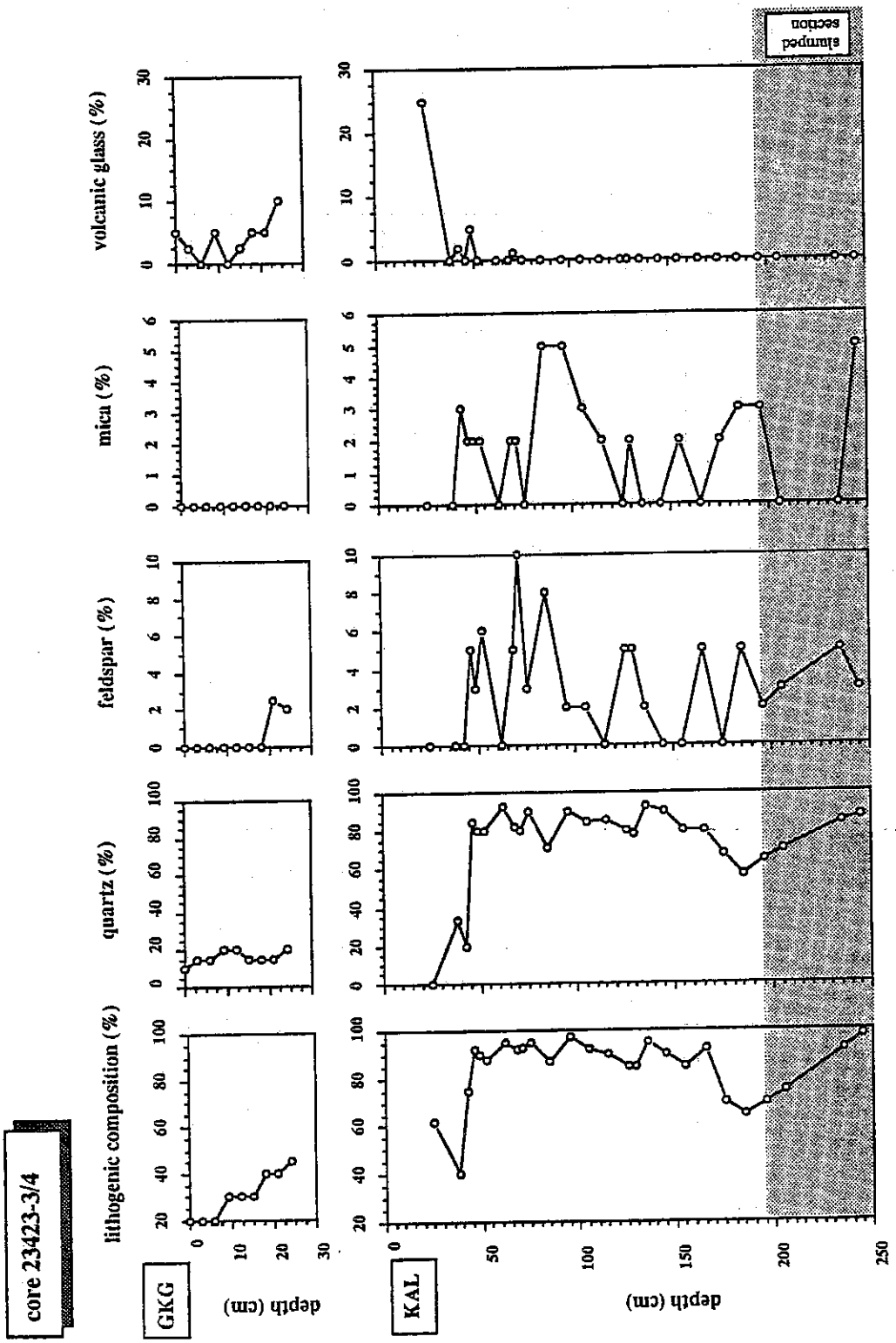

Fig. 67: Smear slide analysis (lithogenic and volcanic components) of core 23423

were measured further downcore up to 300 cm documenting colder climatic conditions. Several increases in carbonate up to 15 wt.% at 460 cm could indicate isotope substages 5.1 to 5.5. The transition to glacial conditions is documented by decreasing carbonate contents from 570 cm to the base of the core. The carbonate record of core 23454-1 shows similarities with core 23423-4 located on top of the Aegir Ridge, displaying the influence of temperated water masses during interglacials even in high latitudes. West of the Knipovitch Ridge the carbonate record of core 23456-5 shows a comparable, but between 90-200 cm a different pattern with core 23454-1 on the eastern side. Alternating carbonate values between 10 wt.% and 2 wt.% reflect multilayered changes between light-coloured, foraminiferous and dark-coloured diamictons.

Sediments from the northern working area are generally lower in carbonate content than those obtained in the southern part of the Norwegian-Greenland Sea. Anyway, similarities between sedimentary records and lithologies obtained further south prove the decreasing influence of the Norwegian Current at the gate to the Polar Ocean.

5.4.2.2 Norwegian Sea, south eastern Greenland and Iceland Sea (SFB 313)

(S. Locker, T. Bohlen, B.Brunssen, S. Jung, A. Kohly, U. Struck)

During leg M 21/5, 8 gravity cores, 2 long kasten cores, 12 box cores, and 1 multicore were taken for geological and paleontological investigations (Fig. 68). In addition, 12 box cores and 17 multicores were drawn solely for investigations devoted to deep-sea biology and geochemistry. Most of the gravity cores were intended to provide data for the interpretation of acoustic profiles (see chapter 5.4.1). They were not opened on board, hence they are not dealt with below.

In order to describe paleontologic al developments in Pleistocene to Holocene plankton communities, four sites were drilled along a SE-NW transect from the Vöring Plateau to the Greenland Basin. At all these sites net and filter samples were also taken from the water column to determine relations between the recent biocoenosis and fossil assemblages. The south eastern anchor point of the transect is marked by box core 23467-2 taken on the Vöring Plateau. This core, recovered from a water depth of 1142 m, displays on top 20 cm of yellowish brown silty clay containing foraminifers and pteropods. Below a sharp contact olive gray silty clay follows. The carbonate content, measured with a "carbonate bomb", drops within the oxygenated top layer from 20 wt.% at the surface to < 10 wt.% below the level of 10 cm (Fig. 69). From base to top, this may represent the initial deglaciation process near the shelf break, followed by the full establishment of the warm Norwegian Current in Holocene time. Indicated by carbonate values which rise continously from < 10 wt.% at the 20 cm level to 40 wt.% at the surface, the postglacial establishment of the Norwegian Current is more clearly shown in multicore 23474-2 from the southern Lofoten Basin. Indicated by rather

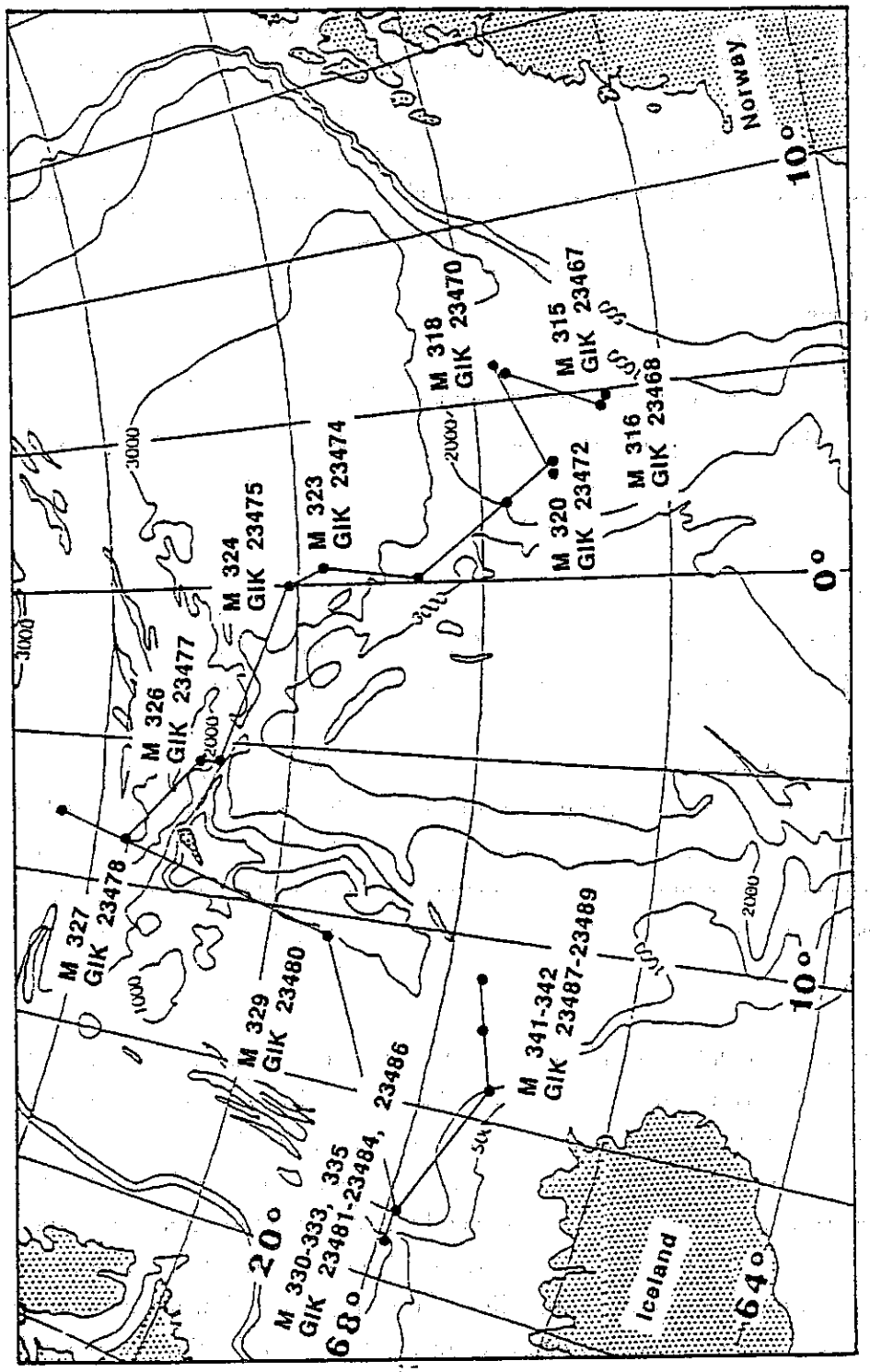

Fig. 68: Position of cores recovered during leg M 21/5

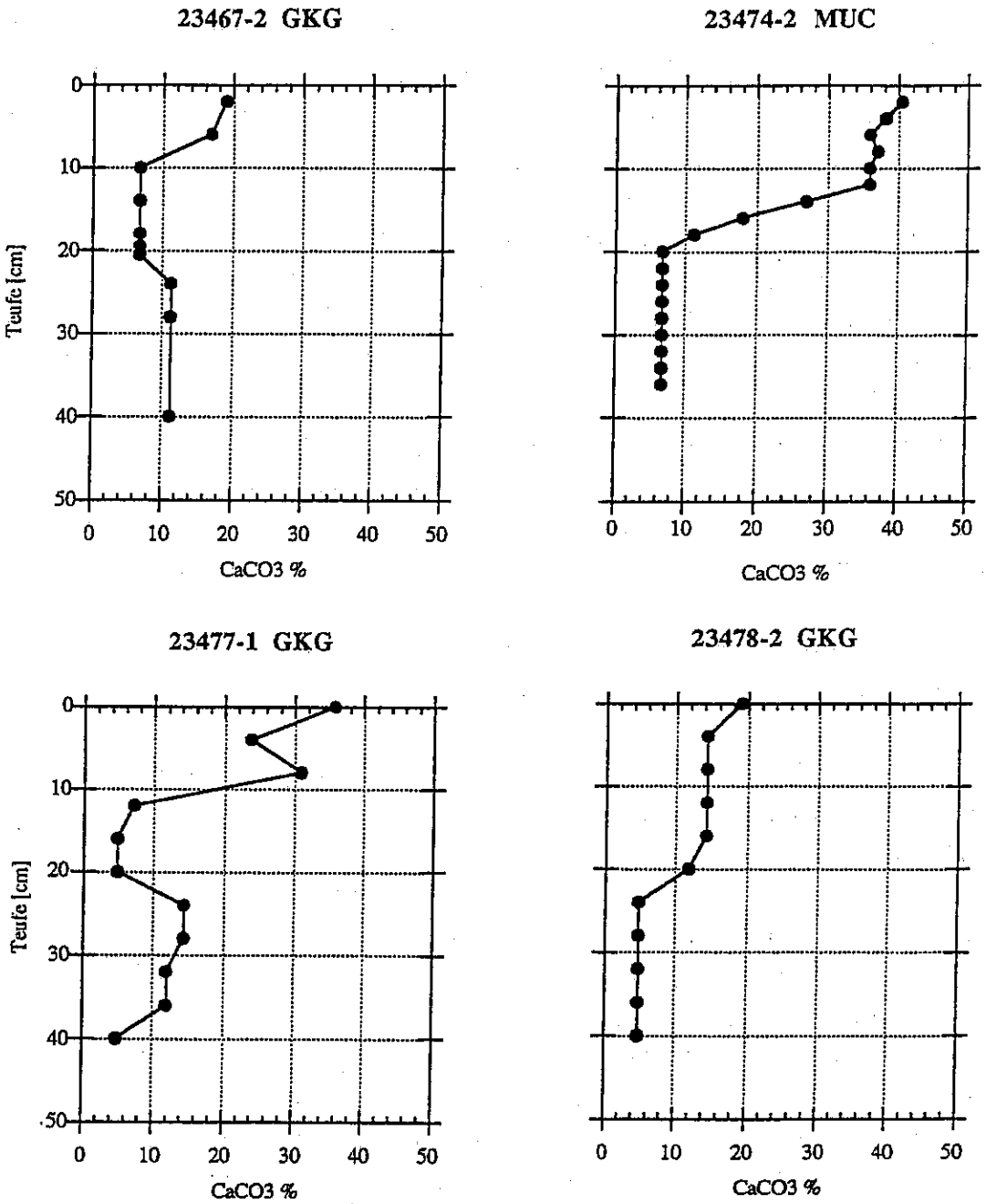

Fig. 69: Carbonate content of cores 23467-2, 23474-2, 23477-1, and 23478-2, representing the paleoecological transect from the Vöring Plateau to the Greenland Basin

variable carbonate values, warm Atlantic water may have also sporadically influenced the area of box core 23477-1 on the Jan Mayen Fracture Zone.

The western point of the paleoecological transect is given by kasten core 23478-3 taken in the southern part of the Greenland Basin. The sediment section recovered from a water depth of 1950 m comprises 252 cm of predominantly yellowish brown silty to sandy clays. Foraminifers are present throughout most of the core, but sponge spicules are visible only down to a depth of 150 cm. Sediment pellets are enriched in several horizons, indicating that environmental conditions have repeatedly changed from glacial to interglacial.

Kasten core 23480-2 was obtained on the central Iceland Plateau where today cool and highly saline deep-water, which leaves the area across the Iceland-Faeroe Ridge, is formed. The core, recovered from a water depth of 1766 m, is intended for detailed paleoceanographic investigations based on oxygen and carbon isotopes, planktic and benthic foraminiferal data. The sediment section contains 323 cm of yellowish brown silty clays to sandy silts which are bioturbated in certain parts. Foraminifers are present throughout most of the core. Several layers having sediment pellets and dropstones may characterize deglaciation phases. Between 262 and 275 cm a distinct ash layer is found above a sharp basal contact. Additionally, in box core 23480-3 covering the disturbed top section of kasten core 23480-2 an ash layer occurs between 21 and 23 cm. Compared to gravity core 23245-1/1984, which has been studied by BIRGISDOTTIR (1991) from nearly the same position, the upper ash may belong into the transition of isotope stages 1/2 and the lower ash into stage 7.

Complementing a biological programme that was started to study the properties of bottom-water masses (see chapter 5.4.4), five box cores were taken along a W-E transect across the Kolbeinsey Ridge to obtain sedimentological and paleoecological data. As in recent time, in latest Pleistocene to early Holocene times cool water masses of the East Greenland Current may have influenced sedimentological and paleoecological conditions on the western side of the ridge crest and warm water masses of the Irminger Current conditions on the eastern side. Both the box cores 23482-2 and 23483-2 from the western side, and box core 23486-3 from the eastern side (898, 818 and 825 m of water depth), display olive brown sandy to silty sediment at the surface, which is densely covered by benthic macro- and microorganisms. In all these cores volcanic glass particles are present whithin the upper centimeters of sediment, and in core 23482-2 a distinct ash layer occurs at a depth of 4 cm. The lower part of all three cores consists of a yellowish to light brown silty clay containing foraminifers. Both easternmost box cores 23484-2 and 23481-2 (930 and 1120 m of water depth) display yellowish brown silty clay at the surface which is sparsely populated by macro- and microorganisms. Even these two cores have volcanic glass particles in the upper sediment layer. In both the latter cores the surface sediment is underlaid by olive gray to light gray silty clay. Finally, all five box cores exhibit distinct burrows in certain parts of the section. The lithologies described clearly indicate that rather drastic paleoceanographic changes developed along the Kolbeinsey Ridge during late Quaternary times.

In order to investigate the pattern of Quaternary deep- and surface-water exchange between the Norwegian-Greenland and Icelandic Seas and the northern North Atlantic, three gravity cores and three box cores were taken along a W-E transect on the southern Iceland Plateau. The gravity cores were left closed, but box cores 23487-2, 23488-2 and 23489-2 were sampled in detail. Despite the differing water depth ranging from 1021 to 1808 m, all three sediment sections are rather uniform. On top yellowish to olive brown silty clay to sandy silt occurs which may exhibit masses of agglutinated foraminifers (*Hyperammina* sp., *Rhizammina* sp.), especially in greater distance from the shelf break. In all these cores a distinct ash layer is found which may be the Vedde ash of 10.6 ka. But regarding long-term paleoceanogra phic developments on the northern flank of the Iceland-Faeroe Ridge, the gravity cores must be examined in more detail.

5.4.3 Near-bottom sediment transport and areas of high Holocene sediment accumulation rates (SFB 313) (J. Rumohr, F. Blaume, H. Beese, M. Seiß)

The research activities of the geological working group in the subproject A2 of SFB 313 focus on the near-bottom sediment transport in the bottom nepheloid layer (BNL) from shallow areas on the shelf along canyons at the outer shelf to high accumulation areas on the continental slope (BLAUME, 1992; RUMOHR, subm.). These mainly near-bottom transport processes feed the allover bottom nepheloid layer (BNL) of the deep sea. A second topic is the accumulation of fine-grained sediments in topographic sediment traps in the deep-sea.

Sediment export from the shelf to the continental slope

The formation of cold and saline bottom water in the shallow western Barents Sea due to brine rejection near the polar front during sea ice formation is well known (SWIFT et al., 1983; MIDTTUN, 1985; BLINDHEIM, 1989). Because of its high density, this "winter water", generated during the freezing process in winter ("near boundary sinking", KILLWORTH, 1983) runs off across the shelf break episodically and spreads over the continental slope until it reaches its in situ density level further downslope ("cascading", NELSON et al., 1973). The contribution of this process to "midwater formation" has become more and more important for the modelling of the Norwegian-Greenland Sea water mass budget since the methods of calculation improved (RUDELS, 1990).

During POSEIDON cruise no. 181, we measured cascading bottom water masses of lower density over the western Barents Sea slope only reaching down to water depths of 600 m (75°N, 15°E, BLAUME, 1992), embedded between the warm and saline northward flowing West Spitsbergen Current (North Atlantic Water: NAW) at the surface and the underlying Norwegian Sea Deep Water. But there is topographical and sedimentological evidence that nowadays Kveitehola, a 100 km long, glacially formed submarine valley northwest of Bear Island, is the outer-shelf gully for the drainage of bottom water masses as well from the shallow western Spitsbergen Bank as from Bear Island Bank with higher densities and

therefore much more kinetic energy. Such cold and sediment loaden plumes might finally sink down to water depths of more than 1.400 m (Storfjord plume deeper than 2.000 m, QUADFASEL et al., 1988).

The east-west orientated Kveitehola valley in its center is 360 m deep and 20 km wide and surrounded by banks ranging between 70 m and 200 m water depth. Two inner basins are separated from the western outer basin by sills with water depths less than 300 m. The innermost basin is filled with a wedge-like postglacial sediment pillow with its maximum thickness of more than 25 m near the northern slope of the valley. This points to a prevailing sediment discharge from the north. At the base of the northern slope of the valley the thickness of the Holocene sediment is reduced to nearly zero in terms of 3,5 kHz sediment echosounding. This asymmetric distribution of sediment thicknesses gives evidence that the sediment load of winter water cascading from the north into Kveitehola settles always after a certain decrease of turbulence further along its pathway in the bottom water and not near the lower slope (Hangfuß). The sediments are mainly made up by sandy silt with little clay content. Clay and part of the fine silt continues the way of sediment transport across the sills and finally across the shelf edge to an area of high clay and silt accumulation in water depths of 1.400 to 2.000 m on the continental slope (GERLACH and GRAF, 1990; BLAUME, 1992).

The activities during leg M 21/4 concentrated on surface sediment sampling (60-80 cm long gravity cores) within the inner Kveitehola Basin for the analyses of regional grain size distribution. Hydrographic data (vertical CTD profiling at 14 stations on the shelf and continental slope around Kveitehola) combined with transmissometer measurements were used to study the regional distribution and thickness of the bottom nepheloid layer and intermediate nepheloid layer (INL). At two N-S sections on the shelf with Kveitehola in their center we found strong differences in the transmission signals between. In water depths of 120 m on shallow banks placed at the endpoints, no near-bottom vertical structure in the signal of transmission was developed. There was a nearly constant signal over the whole area. The only gradient we measured was a maximum of transmisson in the surface layer due to biological activities (typical summer conditions, HONJO et al., 1988), decreasing with water depth. The absence of a BNL in this shallow waters is an argument for well-mixed water masses down to the sea floor - possibly the result of an eddy-like mixing between the Atlantic water and the Polar water at the Bear Island polar front.

However, stations from the inner Kveitehola Basin at water depths down to 360 m showed completely different conditions. From a midwater minimum under the upper layer maximum, the transmission signal increased continuously down to the bottom with a well marked BNL up to 50 m above the sediment surface. Additionally, a 30-50 m thick INL was developed in water depths of 160-210 m. These results are in good agreement with the topography in this area, because we found the BNL and INL structures only near the E-W located small-scaled steaming channel. Comparable situations were measured during summer 1990 and 1991 over

the continental slope west of outer Kveitehola (GERLACH and GRAF, 1990; BLAUME, 1992). Therefore, we interprete the regional thickness and distribution of suspended particles in the nepheloid layers not only as the result of temporary bottom currents flowing down from the shallow banks flanking Kveitehola due to cooling and mixing of NAW in shallow water. They may also result from storm events or as effects of tides and surfing of internal waves over the complex topography in Kveitehola.

Water samples from the BNL, INL and the midwater minimum from each CTD station (10 l rosette sampling) were filtered to correlate the amount of transmission (SEATECH transmissometer) and the weight concentration of suspended particles in specific water masses with high or low particle load (GARDNER, 1989; GARDENER et al. 1990).

Mapping by 3,5 kHz echosounding was completed into the main north-south contributary channel draining the western Spitsbergen Bank. Mapping of the sediment infill at the channel mouth and in the deeper channel revealed that not all the suspended load from the banks gets into the inner basin of Kveitehola but is also piled up in topographic pockets of the glacial morphology with a maximum thickness of more than 30 m in water depths ranging between 180-250 m.

Topographic sediment traps in the deep-sea

Sediment transport in the bottom nepheloid layer on the Vöring Plateau is supposed to be the reason for a ca. 1.000 km^2 wide east-west elongated area between 5°E and 7°E with Holocene sediment thicknesses ranging between 1-3 m (JENSEN et al., 1992). The area is located on top of the northern Vöring Plateau escarpment about 200 m above the general 1.450 m level of the adjacent area in the south. The idea is that during the temporary formation of a topographically controlled anticyclonic vortex (Taylor column, BRECHNER and HOGG, 1980; BIGG, 1984) above the escarpment suspended matter within the bottom nepheloid layer is transported upslope in an oblique direction. Relatively low turbulence in the center of the vortex gives the opportunity of particle settling. As a result of repeated upslope sediment transport during Holocene times a total volume of > 1 km^3 mainly consisting of particles of < 20 µm grain size accumulated. Long-term current meter measurements near the bottom on the southern slope (unpublished data) are in good agreement with the given assumptions.

The normal Holocene sediment thickness on the Vöring Plateau ranges between 15 and 25 cm (VOGELSANG, 1990). A theoretical redistribution of the volume of this high accumulation area over the entire Vöring Plateau (the potential source area) would result in additional 10 cm of sediment thickness. Additional volumes might be stored in other topographic sediment traps on the Vöring Plateau. The obvious amount of long distance deep-sea sediment transport should be considered when bottom sediment particles of grain sizes < 20 µm are used for paleoceanographic reconstructions.

The activity during this cruise leg was the final mapping of sediment thickness and bathymetry and sediment sampling on a profile across the eastern part of the high

accumulation area. Along two N-S sections on 6°00'E and 5°35'E between 67° 35'E and 67°50'E 12 vertical CTD profiles with transmission measurements were carried out across the center of an high accumulation area (JENSEN et al., 1992). There was no evidence for an INL in the midwater. At each station the BNL was very well marked by a more or less slightly increasing gradient up to 200 m above the sea floor. The internal structure of the BNL remained constant. However, it showed no correlation to near-bottom hydrography (temperature and salinity in the Norwegian Sea deep water seemed to be constant in this water depth (1.250m-1.450 m)), but to topography. The BNL thinned out over the southern slope of the Vöring Plateau escarpment with a minimum at the peak (1.250 m water depth) and was best developed with two additionally INL in place of the center of maximum sediment accumulation, north of the Vöring Plateau escarpment. These measurement s in the water column with the result of a maximum load of suspended particles in the bottom water strongly correlated with the geological document (JENSEN et al., 1992), to such extent that our assumption of a topographically controlled sediment transport which built up the high accumulation area in geological times seems to be affirmed.

5.4.4 Cold water shelf carbonates and lag deposits and associated living benthic communities: Spitsbergen Bank (SFB 313) (R. Henrich, J. Reitner, A. Wehrmann)

Geological background

Spitsbergen Bank reveals a very pronounced surface sediment distribution which obviously seems to be controlled by intensive bottom current activity (BJÖRLYKKE et al., 1978; BICKERT and HENRICH, 1989). The top of the bank comprises coarse bioclastic sands, while the typical surface sediment on the upper flanks is a polymixt, residual coquina/gravel deposit which covers an area of almost 80.000 km^2. The formation of the residual lag deposit is a result of a primary enrichment of a postglacial molluscan infauna (almost exclusively *Mya truncata*) excaved by strong bottom currents during early Holocene time (^{14}C datings on *Mya truncata* show a range from 8.7 ka to 6.4 ka). Bottom current vigor progressively increased during the early Holocene due to a glacio-isostatic uplift of the bank causing further intensification of erosional processes. Since about 2.5 ka a secondary hard substrate fauna, predominantly balanids, settled on the coquina/gravel lag deposit providing the prevalent material for the bioclastic sand on the bank top.

Research activities during leg M 21/4

With respect to the above outlined geologic background, it was the major purpose of the research activities during M 21/4 to document the sea floor properties with underwater TV equipment, to study the living benthic communities, and to record the variability of sedimentation processes in situ. The shallow water areas between 40 m and 150 m of the western Spitsbergen Bank were studied with an underwater video camera equipment (Osprey camera with a 300 W halogen lamp), in which the camera was mounted on a frame which could be moved around in a full circle and 90° angle. Viewing direction and focussing was

controlled from an operation desk on board the ship. The survey was completed by using a separate underwater camera system for bottom photography (Undersea Photo System, modified by D. Piepenburg, Kiel). Sampling was executed with a sediment trap.

Results

a. Transect Spitsbergen Bank to Leirdjupet trough NE of Bear Island

Station 233 (74°34,82'N, 21°00,33'E, water depth 104 m)

Sediment: The surface sediments were vast gravel fields formed by large (more than 20 cm) black shale rocks of Jurassic age and coquinas of broken and sometimes complete shells of *Mya truncata, Chlamys islandica* and barnacles. Locally we observed in more protected areas a muddy soft bottom facies. The coquinas and gravel fields formed typical lag deposits. The sediments below the lags were soft, indicated by typical soft bottom dwellers like the endobenthic bivalves.

Living benthic communities: The black shale gravels were mostly overgrown by colonies of large barnacles (balanids), crustose bryozoans, and sedentarid polychaets with agglutinated calcareous tubes. Additionally, orange crustose sponges (*Suberites* sp.), the calcareous sponge *Sycon* sp. and actinid cnidarians (Actinia) were observed. On the mobile coquinas and marly soft bottoms large soft octocorals (*Eunephtya* sp.), regular echinoids, the bivalve Astarte, polyplacophor ans, ophiurid seastars, heavy calcified bryozoans (*Ceriopora* spec.), and bushes of hydrozoans were common. Abundant were the funnel pairs of endobenthic bivales.

Station 234 (74°40,76'N, 20°49,7'E, water depth 80 m)

Sediment: Coquina of large bivalve shells of *Mya truncata, Chlamys islandica* and skeletal elements of relatively large barnacles. The mean size of the components was ca. 5-10 cm. Occasionally, Jurassic black shale clasts were observed. Many of the isolated bivalve shells lay with the concave side on the sediment surface, despite of relatively high bottom currents (ca. 1-2 knots). Beside a prevalent aerial coverage with the typical coquina facies locally patches of basement rock pavements (e.g. black shale cobbles and blocks) were found. These rock pavements were completely overgrown mostly by barnacles associated with hydrozoans forming small reef-like structures. The rock pavement structure may be derived from current winnowed fan-shaped lag deposits.

Benthic communities: On the mobile coquinas regular echinoids, ophiurids, actinids, and sometimes colonial hydrozoans were common. Sea spider crabs were abundant. The rock pavements were extensively overgrown. Main encrusters were barnacles, sponges, bryozoans, and big bushes of hydrozoans. These complex structures were comparable with small initial reefs. Pioneer constructers were barnacles followed by sponges and rigid bryozoan crusts which in turn were dwelled by colonial hydrozoans, and occasionally by actinids. Areas with

muddy soft bottoms were colonized by octocorals (*Eunephtya* sp.), seastars, ophiurids, and regular echinoids.

Station 235 (74°46,49'N, 20°36,43'E, water depth 60 m)
Sediment: Coquina and gravel lag deposits composed of moderately sorted bivalve and barnacle shells with a size of some centimeters. The sediment surface exhibited megaripples. The ripple crests were winnowed demonstrated by an enrichment of larger components.

Benthic communities: On the ripple crests bryozoans, barnacles, and hydrozoans were common. In the ripple valleys seastars and big tentacle feeding colourful holothurians were abundant. Additional faunal elements were a few brachiopods (*Terebratulina*), polyplacophorans, ophiurids, the bivalve Astarte, and regular echinoids. Dead shells of *Mya truncata* and other bivalves were commonly bored by naticid gastropods.

Station 236 (74°51,78'N, 20°24,91'E, water depth 57 m)
Sediment: Coquina of small sized (1-3 cm) barnacle and bivalve debris with an admixture of small-sized pebbles and clasts of Jurassic black shale. This fine gravel exhibited current ripple structures. The observed sediment movements demonstrated rolling and jumping particles.

Organisms: Only a few hydrozoans, tentacle feeding holothurians, and crabs were observed.

Station 237 (75°01,79'N, 20°25,77'N, water depth 44 m)
Sediment: Calcareous sand and fine gravel composed of rolled debris predominantly barnacles and subordinate bivalves admixed with a few bigger (some centimeters) black shale pebbles. The sediment was rapidly moving because of a strong bottom current with a vigor of 2 to 4 knots. As a result megaripples with amplitudes around half a meter were the prevalent structures on the sea floor. On the megaripple crests secondary smaller flat current ripples indicated sediment transport perpendicular to the megaripples. As a result a general smoothing of the megaripple crests was observed. This formation of the megaripple structures may have happened under even stronger current vigors presumably during heavy winter storms.

Organisms: Within little protected areas some rare tentacle feeding holothurians were observed.

Station 238 (74°37,35'N, 20°12,49'E, water depth 82 m)
Sediment: Coquina consisting of large bivale shells (*Mya truncata, Chlamys islandica*) and skeletal elements of relatively large barnacles. The mean size of the components was ca.

5-10 cm. Occasionally black shale clasts were observed. Many of the isolated bivalve shells were found with the concave side up on the sediment surface, despite of relatively high bottom currents (ca. 1-2 knots).

Benthic communities: On the mobile coquinas regular echinoids, ophiuruds, actinids, and sometimes colonial hydrozoans were common. Sea spider crabs, seastars, small ophiurids, and holothurians were further common faunal elements.

b. Transect Kveitehola trough to the top of the Spitsbergen Bank
Station 272-1 (74°59,60'N, 17°52,79'E, water depth 149 m)
Sediment: Rippled calcareous sandy bottom, mainly formed by calcareous benthic foraminifers. The surface exhibited a cover of a light green coloured mat (perhaps of microbial origin, organic fluff). On the mat numerous empty mucoid-gelatinous pockets (ca. 5 cm diameter) of unknown origin were found. These pockets were also quite common within the water mass. In some cases craters of burrowing organisms were seen (crustaceans).

Station 272-2 (75°00,80'N, 17°48,89'E, water depth 118 m)
Sediment: Sediment surface was formed by large Jurassic black shale boulders without any shell debris cover. Between the rocks occasionally a muddy soft bottom facies was present.

Benthic community: The rocks were encrusted by barnacles, hydrozoans, sponges (*Suberites domuncula*), actinids, and bryozoans. This community exhibited again small reef-like structures. Molluscs were rare. On the soft bottoms octocorals were growing.

The organisms found in the sediment trap close to the position of the video run (75°01,13'N, 17°48,80'E; 128 m water depth) were large polychaetes, snow-shoe type agglutinated polychaetes, large agglutinated Foraminifera, bivalves (*Leda*), limped gastropods, polyplacophorans, ascidians, bryozoans, and sedentarid polychaetes.

From a box core with muddy sediment of the same facies close to this position (74°59,59'N, 17°53,33'E, water depth 141 m), sponges (*Suberites domuncula*) and actinids were collected.

Station 273-1 (75°04,69'N, 18°13,70', water depth 71 m)
Sediment: Coquina of barnacle skeletal elements and broken bivalve shells associated with isolated Jurassic black shale lithoclasts. The sediment surface exhibited megaripples. The ripple crests were winnowed and larger clasts were enriched.

Benthic community: On the winnowed rocks and larger calcareous particles barnacles were forming reef-like structures which were encrusted by bryozoans and overgrown by bushes of colonial hydrozoans. On the ripple valley sediments regular echinoids were very common, as well as ophiurids. Sometimes red actinids and living *Chlamys islandica* with overgrown left free moving valves were present.

Station 274-2 (75°08,59'N, 18°34,72'E, water depth 40 m)
Sediment: Calcareous well sorted sandy sediment, formed by barnacle and bivalve debris, occasionally with small clasts of Jurassic black shales. The bottom was structured by large megaripples (amplitude ca. 0.5-1 m). The crests of the megaripples were covered with smaller current ripples with a direction mostly perpendicular to the megaripples. The observed bottom currents were very strong and had a velocity of probably 2-4 knots.

Organisms: Only some lebensspuren on the sediment surface and few tentacle feeding holothurians were observed.

Conclusions

1. The highest diversity of living benthic communities was observed between 80 m and 100 m water depth. This bathymetric zone was characterized by abundant large rock boulders and unsorted coquina and gravel lag deposits. The predominance of hard subtrates provided favourable conditions for encrusting organisms. In some cases small reef-like structures were observed (barnacle-reefs). Colonial hydrozoans, thick branched bryozoans and barnacles were the dominant faunal elements. Tentacle feeding (hydrozoans, barnacles), filter feeding organisms (sponges, bivalves) and decomposers (e.g. some ophiurids) were common. Grazing organisms like regular echinoids, gastropods and polyplacophorans were less commonly represented. Deposit feeders were not observed. The benthic community was controlled by moderate bottom currents, the presence of large rather, stable rock boulders and protected muddy soft bottom areas with a typical infauna.

2. The shallower areas (55 m-40 m) were characterized by very mobile sandy bottoms due to very strong bottom currents. Only few and less diverse organisms are adapted to this facies. If larger rock boulders were present, a few encrusting organisms (bryozoans) and small barnacles settled on the surface. On the unstable sand bottom only tentacle feeding holothurians were seen, standing more or less upright in the current, partly buried in the sediment. Spider crabs were occasionally seen forming traces on the sediment. The major control of organism settlement in this mobile sand environment was exerted by permanently strong bottom currents and rapid sediment movements.

5.4.5 Marine versus terrigenous organic matter fluxes: first considerations from sediment cores along the polar front in the Barents Sea (SFB 313)

(T. Wagner, B. Schlünz, R. Henrich)

One long box core (GIK 23428-3, 757 cm) was obtained at 334 m water depth located in a trough (Leirdjupet) at the slope south of the Spitsbergen Bank. The position was choosen because two different sources of organic matter contribute to the sedimentary organic pool: 1. redeposited organic-rich sediment clasts (black shales) from the Spitsbergen Bank due to lateral downslope sediment transport and 2. vertically through the water column transported marine organic matter from a high-production zone displaying the annual advancing and retreating polar front. Sedimentological investigations from a similar depositional environment nearby have shown that accumulation rates were exceptionally high, giving a good chance to get detailed information on the variability in composition of organic matter during glacial/interglacial cycles.

The sediments of core 23428 were characterized by a uniform lithology throughout the core. At the base of the sequence a darkgray homogenous clay was covered followed by an olive coloured silt containing high amounts of organic rich sediment clasts (Fig. 70). The source of those clasts are most probably jurassic deposits outcroping on the Spitsbergen Bank (Janusfjellet-Fm.). The overlying sedimentary column showed various shell fragments. At 146, 291 and 374 cm almost entire sponges (*Polymastia hurilensis*) up to 5 cm in diameter were incorporated into the sediment. The upper meter of the core was sandy silt with upward increasing amounts of benthic Foraminifera (*Pyrgo*). The uppermost section of the core and the sediment surface were intensively penetrated by polychaete tubes, indicating a suboxic to anoxic depositional environment.

Carbonate contents measured on board (Fig. 71) showed very low values (< 5 wt.%). Smear slide analysis on board displayed a strong dominance of lithogenous, i.e. Quarz, components (Fig. 72). From the base of the core up to 500 cm lithogenous particles dominated the sediment composition. Biogenous components (Fig. 73) increased between 450 and 200 cm and between 100 cm and the sediment surface, reaching maximum values (15%) at the top. Sponge spicules were abundant from 400 cm to the top. Most of the internal canals of the spicule were filled with framboidale pyrite. An increase in diatoms between 450-300 cm was remarkable.

5.5 Actuopaleontological studies of living plankton communities in the North Atlantic and Norwegian-Greenland Sea and their distribution in sediments

(K.-H. Baumann, A. Schröder, A. Kohly, S. Locker)

Planktonic organisms form the basis of marine ecosystems and are ecologically directly dependent on the hydrography of the water masses. Their fossil remains are the most

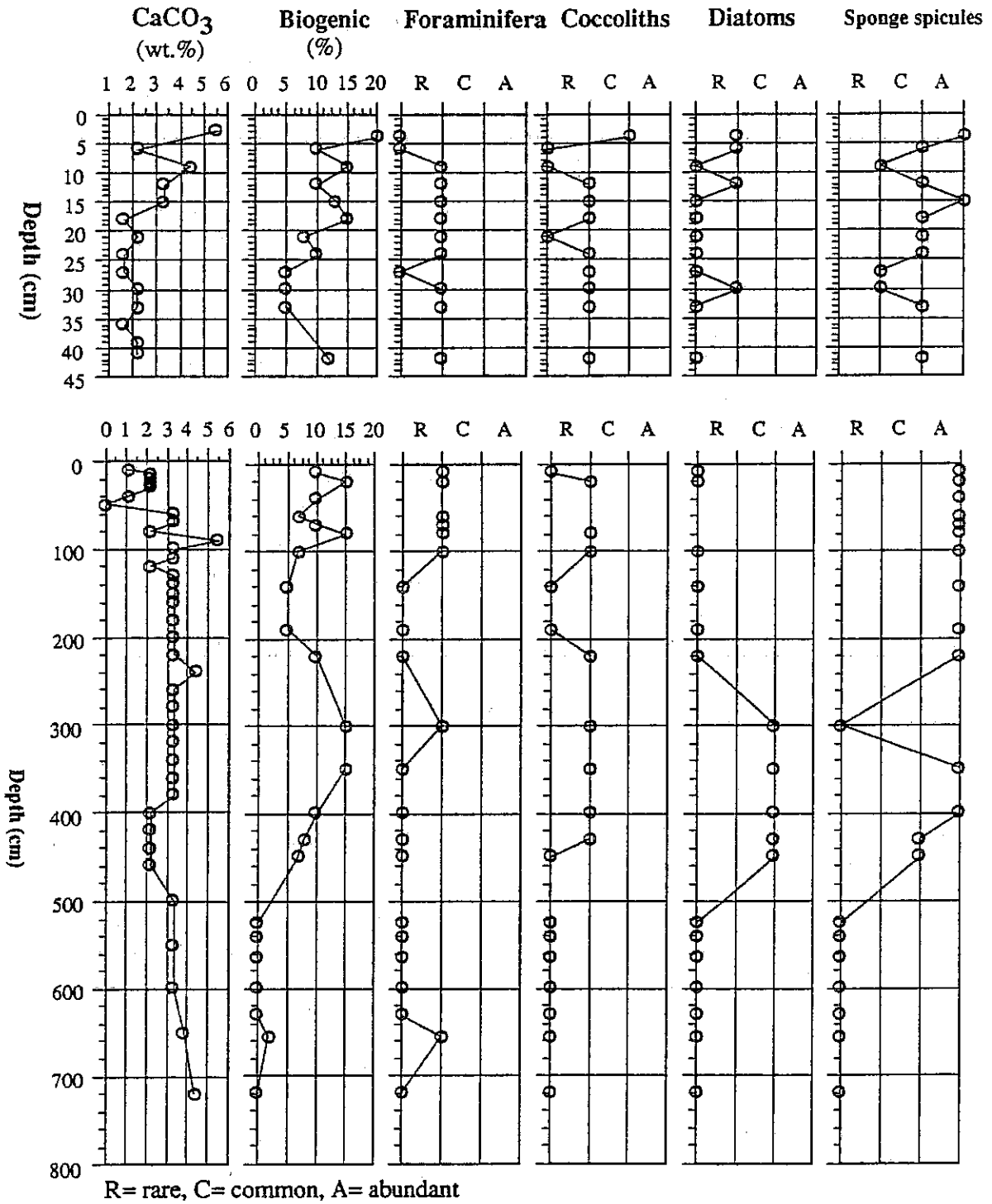

Fig. 70: Smear slide analyses (biogenic components) and carbonate content of core 23428

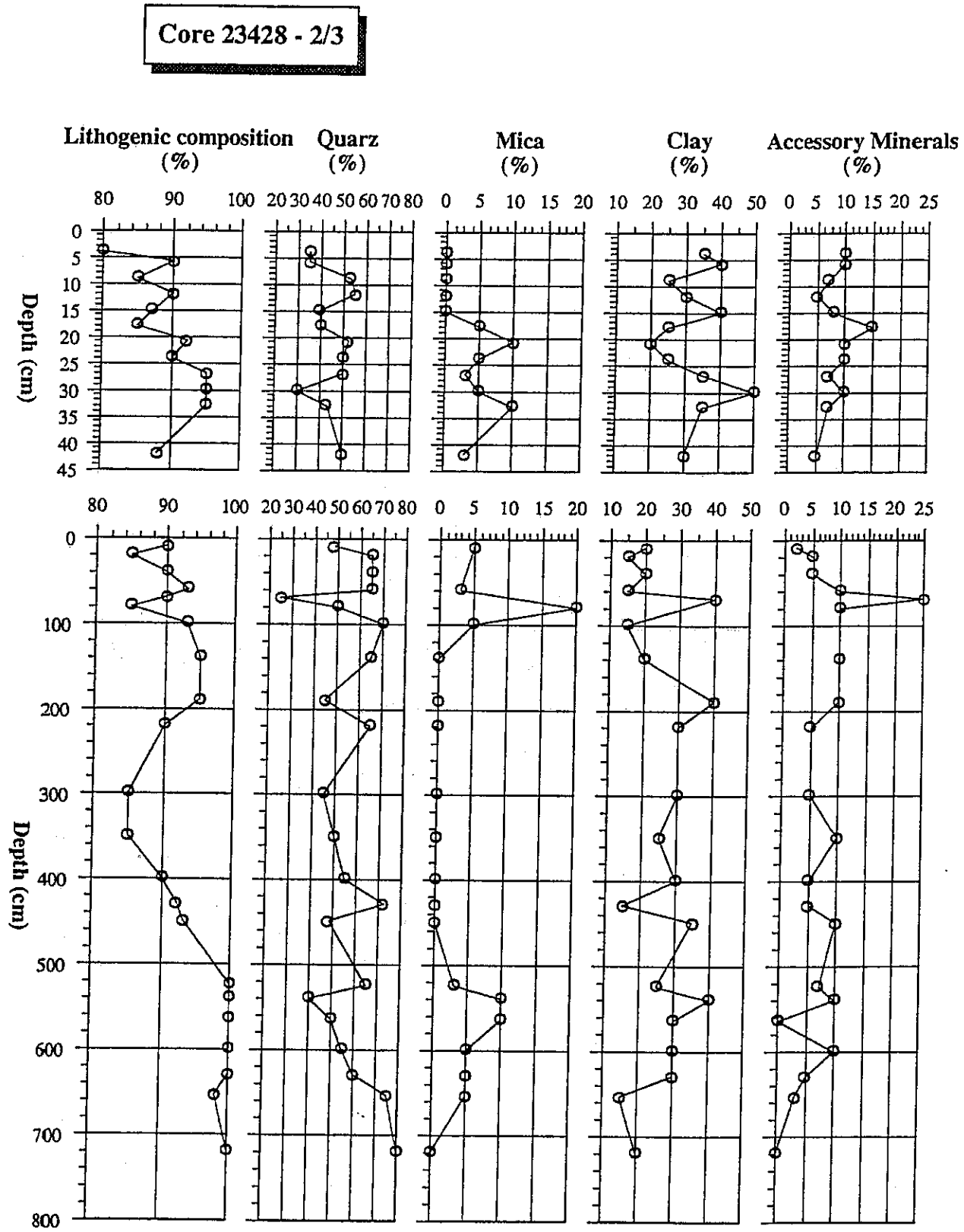

Fig. 71: Smear slides analyses (lithogenic and volcanic components) of core 23428

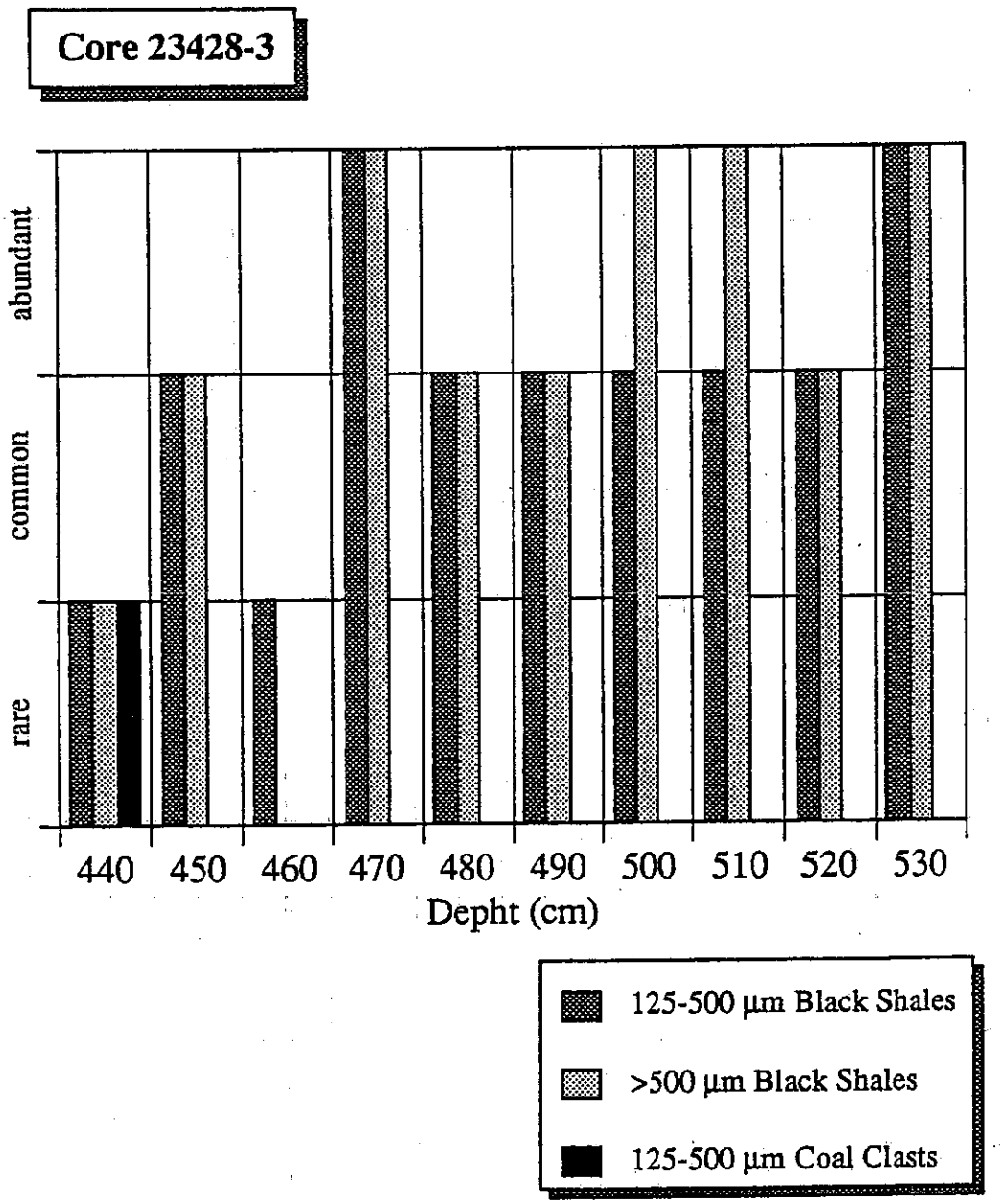

Fig. 72: Coal/black shale-clasts (> 125 µm) in selected sections of core 23428, Leirdjupet

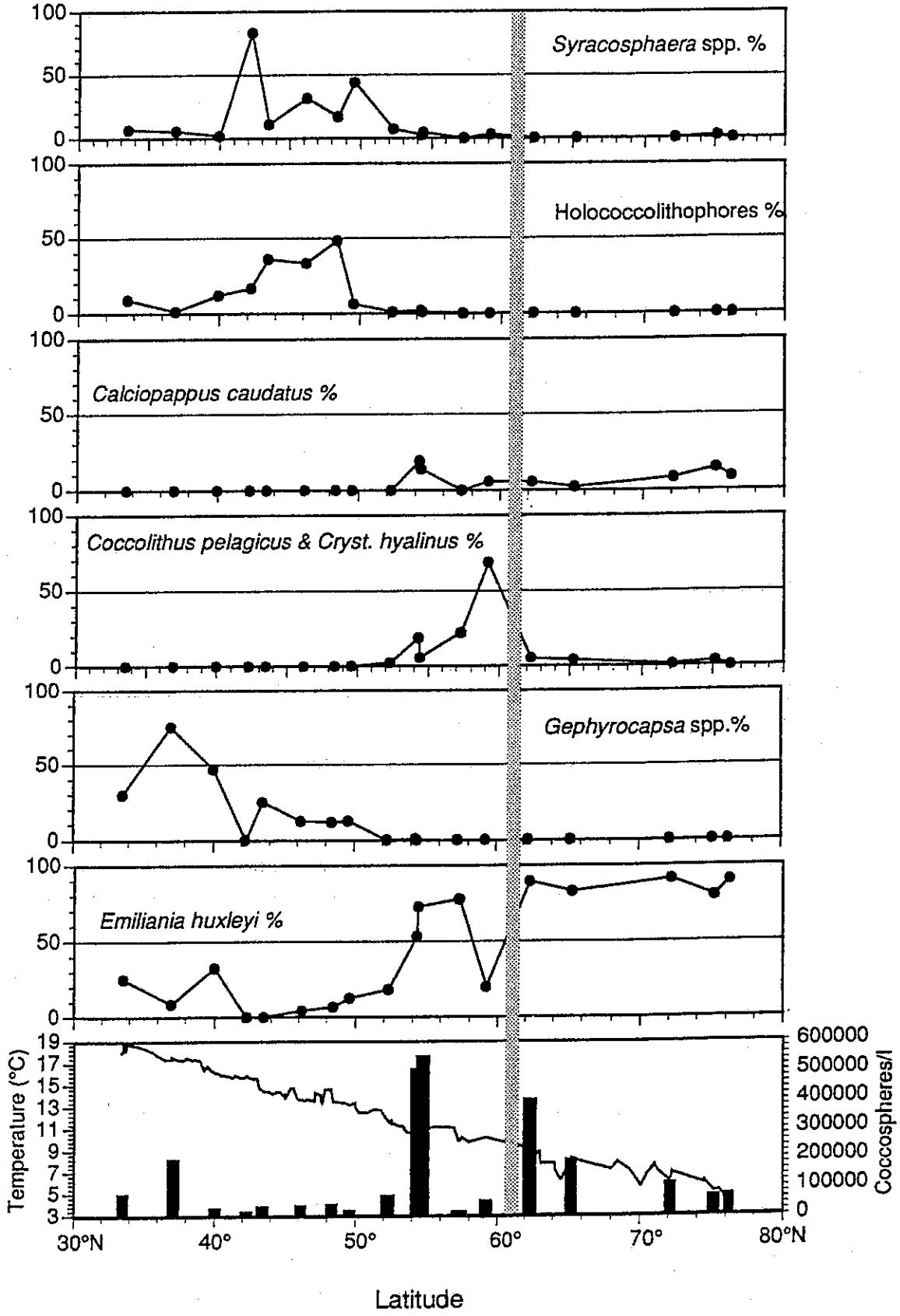

Fig. 73: Absolute amount of coccospheres and relative abundance of species and species groups of investigated surface water samples

important indicators for the reconstruction of previous ecological conditions. The understanding of fossil plankton assemblages requires knowledge of both biogeographical and depth distribution of living communities. Therefore, living and fossil plankton associations from selected stations are studied quantitatively in order to examine

- the distribution and synecology of the plankton groups in the pelagic realm;
- particle transport through the water column and changes in plankton biocoenosis;
- particle sedimentation and changes in the thanatacoenos is of planktonic microfossils, and
- the temporal and spatial distribution of planktoncoenosis from the late Quaternary of the northern North Atlantic.

The focus of research interest during legs M 21/3 to 5 was placed on the horizontal and vertical sampling of water masses. The plankton communities in the North Atlantic and Norwegian-Greenland Sea were sampled on two profiles (NW Madeira-SW Svalbard and from the Vöring Plateau into the Greenland Basin). At 35 stations water samples (2 l) for coccolith and diatom investigations were taken with the rosette sampler (10 l) according to CTD profiles at the following water depths: surface (0-10 m), 10 m, above and below the thermocline, and at 3-6 depth intervals in the deeper water column. Additionally, surface water samples were also gathered with the aid of the "Kiel Sea Water Pump System" on board during leg M 21/3. Plankton samples for the investigation of radiolarian associations were taken with plankton nets (46 µm mesh) at two to four depth intervals (20 m, 100 m, 500 m, 1000 m) at 22 stations. Due to shallower water, depth intervals had to be adjusted to 0-200 m and 200-400 m at the Kolbeinsey Ridge (e.g. 23481-3 and 23482-3, 0-200 m).

The water samples were filtered through cellulose-nitrate filters (45 mm diameter, 0.45 µm pore size) by means of a vacuum pump immediately on board. The filters were dried at 40°C for 12-24 hours and stored, with silica gel, in plastic petri dishes without further washing and conservation.

The net samples were poisoned with formol and stored in the cooling storage.

At most of the stations sampling of the sediment surface and the uppermost sediment column was carried out using GKG or multicorers. At two stations (M92-227, M92-327) longer box cores (see chapter 5.4) were taken for the investigation of the temporal distribution of the above mentioned planktic microfossils and dinoflagellate cysts.

First results on coccolithophore samples

Preliminary, 19 surface water samples have been investigated quantitatively for their contents of coccolithophore species (Tab. 8). Samples have been choosen on the S-N transect in mostly equal distances. The samples were examined with a CamScan Scanning Electron Microscope (SEM) at 10 kV. For SEM investigations, a piece of filter was fixed on a SEM stub with scotch tape and coated with coal and gold. The species composition was determined

by identifying and counting coccospheres on measured transects (1-2 mm^2) at a magnification of 1000x.

Tab. 8: Locations, water depths and hydrographic data of investigated surface water samples

Station	Sample	Position		Water-	Temperatur	Salinity
	No.	Latitude	Longitude	depth	(°C)	(°/oo)
92/199	1	33 56,5 N	21 50,1 W	5m	18,92	36,72
A	10	37 00,0 N	20 57,6 W	7m	17,6	36,51
92/202	12	40 00,2 N	20 00,3 W	5m	16,33	36,02
C	22	42 27,5 N	17 56,0 W	7m	15,9	36,01
D	23	43 50,2 N	16 42,8 W	7m	14,5	35,7
E	24	46 22,8 N	17 40,3 W	7m	13,7	35,62
F	36	48 43,7 N	19 47,8 W	7m	13,5	35,51
92/213	37	49 59,8 N	20 00,2 W	7m	12,67	35,48
92/214	45	52 30,3 N	19 56,6 W	7m	11,52	35,26
92/215	53	54 30,2 N	21 00,1 W	10m	10,25	35,13
92/216	60	54 39,8 N	21 00,1 W	5m	10,5	35,08
92/219	72	57 30,2 N	19 58,8 W	7m	9,83	35,16
92/223	80	59 29,3 N	19 59,5 W	7m	9,48	35,16
92/224	8	62 30,1 N	13 59,6 W	0m	9,2	35,19
92/227	17	65 31,9 N	03 59,0 W	10m	8,5	34,89
92/230	31	72 14,5 N	11 03,6 E	10m	6,3	35,14
92/292	100	75 18,6 N	09 46,2 E	10m	5,1	35,09
92/277	74	76 31,9 N	08 36,8 E	10m	4,3	35,06

Generally, surface water samples yielded between 5000 and 550000 coccolithophorids/l. Highest amounts of coccolithophorids were observed on the Rockall Plateau and north of the Iceland-Faeroe Ridge (Fig. 73), although the sea surface temperature decreased constantly towards the north. However, the number of species gradually decreased to the north as well. More than 20 species were observed at the southernmost station, whereas only 3 species were found at 76°N. In general some of the species and species groups showed a correlation between distribution and water temperature.

South of about 40°N, the community was dominated by individuals of the genus *Gephyrocapsa*. Between 40°N and about 53°N *Syracosphaera* spp. and holococcoliths were mostly observed. However, absolute numbers of coccospheres/l were < 35000 throughout this part of the transect. Coccospheres of the cosmopolitan species *Emiliania huxleyi* were the main components of the coccolithophorid flora in the surface water north of about 53°N. They usually comprised more than 70% of the flora. The cold water form *Coccolithus pelagicus* (non-motile phase as well as its motile phase *Crystallolithus hyalinus*) only dominated at one station (92-223), although it was generally observed north of 52°N. Other species (e.g.) also showed a similar pattern. However, temperature conditions only form a broad ecological framework for their distribution.

First results from plankton net samples
Preliminary investigations of the M 21/4 plankton net samples showed a phytoplankton maximum around the Iceland-Faeroe Ridge and also in parts of the Barent Sea. In between mainly zooplankton (copepodes) and their fecal pellets were abundant. Additionally, high amounts of large Phaeodaria (e.g. *Sagonescena* sp.) were recognized in some of the samples. Further investigations and chemical and preparative treating are now done at the laboratory in Kiel.

First semi-quantitative observations of M 21/5 samples were made on board with a light microscope. The net content displayed highly diverse plankton communities (Tab. 9). In all three listed plankton nets highly abundant diatoms were dominated by different species of vegetative cells of *Chaetoceros* sp. containing spores, indicating a sinking bloom. They occurred together with *Rhizosolenia hebetata f. semispina.* At two stations on the Kolbeinsey Ridge, *Nitzschia* spp. was found in great frequency. Some species, e.g. Thalassiosira *antarctica/ gravida* and *T. anguste-lineata* are characterized as cool adapted species. In all three samples radiolarians were present in minor frequency. All samples were characterized by members of cool-adapted species, especially by *Pseudodictyophimus gracilipes.* The relatively high content of the phaeodarian *Challegeron neptuni* was surprising.

5.6 **Marine optics** (R. Reuter, S. Determann)

From the large number of excitation and emission spectra of fluorescence which were recorded (Table 10), only a few examples are presented here.

Fluorescence close to the surface
Figures 74 to 76 show results of the fluorescence measurements of near-surface samples which were taken either with the "Kiel Pumping System" or with Goflo samplers from deep water. The data are presented as a function of latitude because of the mainly south-north direction of the track.

The distribution of yellow substance fluorescence (Fig. 74) shows strong similarities with the ones of temperature and salinity (Fig. 75): decreasing values of T and S towards the north, parallel an increasing fluorescence. Especially the "blue" water with low content of particles identifies itself with very low concentrations of fluorescing materials up to about 43°N. The fluorescence is typically a factor of 2 higher in the biologically very active "green" water that continues to the north. Signals of chlorophyll at the surface are close to zero in the southern part of the track. The plankton maximum found at the depth stations around 30 m could not be reached by the pumping system. Beginning at 43°N, chlorophyll can be detected well (Fig. 76). The fine structures do not always coincide with the tryptophan fluorescence which also shows much less dynamics in comparison to the distribution of chlorophyll. This might

Table 9: Plankton species from selected net tows

	North of Jan Mayen	Kolbeinsey Ridge E	W
	23479-2	23481-3	23481-3
1.Coccolithophorides:			
Coccolithus pelagicus		C	
2.Diatoms:			
Actinocyclus curvatulus		R	
Chaetoceros spp.	A	A	A
Dactyliosolen tenuis			R
Proboscia alata			R
Rhizosolenia hebetata f. semispina	A	A	A
Rhizosolenia hebetata f. hiemalis		C	
Thalassiosira spp.		C	C
Thalassiosira anguste-lineata		R	
Thalassiosira antarctica/gravida	R	R	
Thalassiosira eccentrica		R	
Thalassiothrix longissima		R	
Pleurosigma sp.		R	
Nitzschia spp.		A	A
3.Silicoflagellates:			
Distephanus speculum		R	R
4.Radiolarians:			
Spumellaria indet.		R	R
Chromyechinus borealis	R		
Echinomma leptodermum		R	R
Nassellaria indet.	C	R	R
Phormacantha hystrix	R		R
Pseudodictyophimus gracilipes	R	R	R
Cycladophora davisiana	R		
Artobotrys borealis	R		
Challengeron neptuni	C	R	R
5.Acantharians:	C		
6.Dinoflagellates:			
Ceratium sp.	R	R	R
Pyrophacus sp.			R
Peridinium sp.		R	
7.Tintinnides:			
Acanthostomella norvegica	R	R	R
Ptychotylis obtusa	R	R	R
Amphorella sp.	R		R
8.Foraminifers:		R	R

Table 10: Spectral regions of the fluorescence measurements with the luminescence spectrometer, and the substance classes which can be identified by these wave lengths

excitation spectra:

emission (nm)	excitation range (nm)	identifiable substance with excitation wave length (nm peak)	
340	230-300	tryptophan	230, 270
420	250-400	yellow substance	
450	250-430	yellow substance	
680	400-670	chlorophyll	400..460

excitation spectra:

excitation (nm)	emission range (nm)	identifiable substance with emission wave length (nm peak)	
230	240-450	tyrosin	290..300
		tryptophan	325..350
		yellow substance	410..460
254	265-500	tyrosin	290..300
		tryptophan	325..350
		yellow substance	410..460
270	280-480	tryptophan	325..350
		yellow substance	410..460
308	315-480	yellow substance	410..460
	650-730	chlorophyll	685
355	370-500	yellow substance	410..460
	650-730	chlorophyll	685
420	440-730	chlorophyll	685
533	570-730	fucoxanthin	685

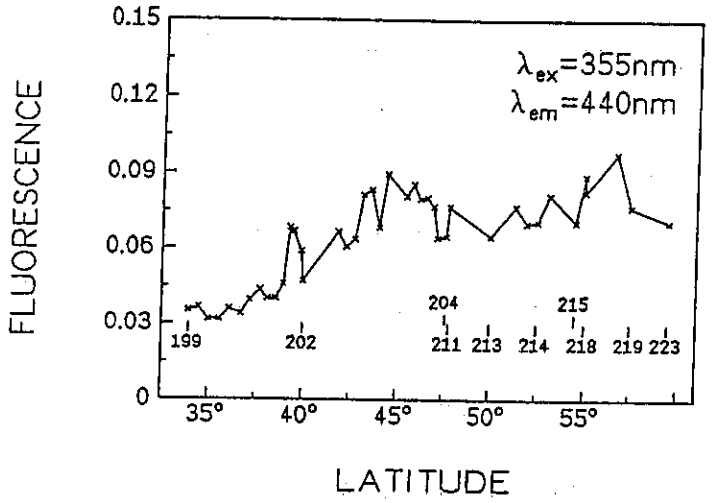

Fig. 74: Fluorescence of yellow substance close to the sea surface

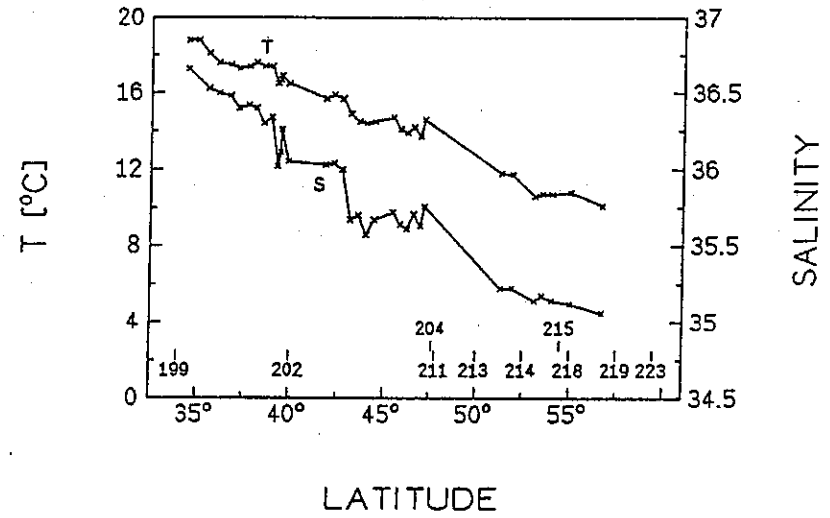

Fig. 75: Temperature and salinity close to the sea surface along the ship track, measured while taking samples with the "Kiel Pumping System", presented as a function of latitude

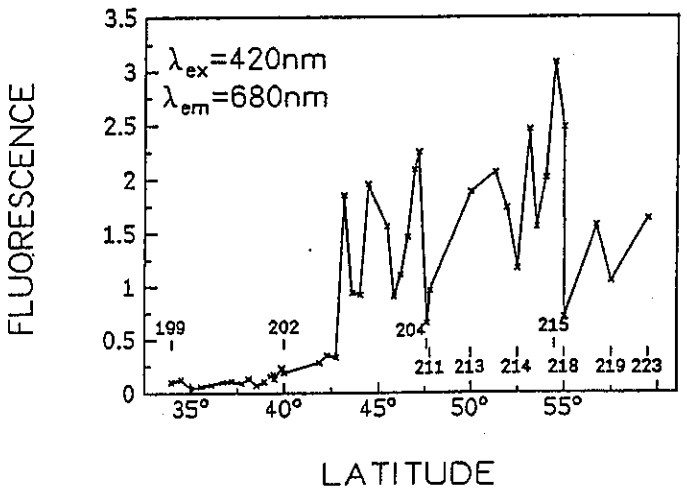

Fig. 76: Fluorescence of chlorophyll close to the sea surface

point out that the tryptophan observed fluorometrically is not derived exclusively from amino acids in the phytoplankton.

Depth profiles of fluorescence

The profiles of the fluorescence at two depth stations are presented as examples: station 202 at 40°N, 20°W in an area of surface water with low plankton content (Fig. 77), and station 214 at 52°30'N, 20°00'W in an area with high biological productivity (Fig. 78). These figures show the fluorescence of yellow substance at 440 nm, the one of tryptophan-like molecules at 330 nm and the one of chlorophyll at 680 nm.

In the surface layer there are relatively low values for the yellow substance which - probably caused by photodegradation - decrease monotonously towards the surface. The tryptophan fluorescence in the surface layer correlates with the one of chlorophyll. At station 214 high plankton concentrations were found. Especially here a deep plankton maximum at 150 m was found which also leads to higher values in the tryptophan signal.

Below the thermocline the distribution of the fluorescence signals is much less variable than in the strongly structured surface layer. Besides the high yellow substance fluorescence also high fluorescence signals of tryptophan were found. A significant increase of the values in the profile of yellow substance at station 214 was observed near the bottom. This may be related to benthic processes.

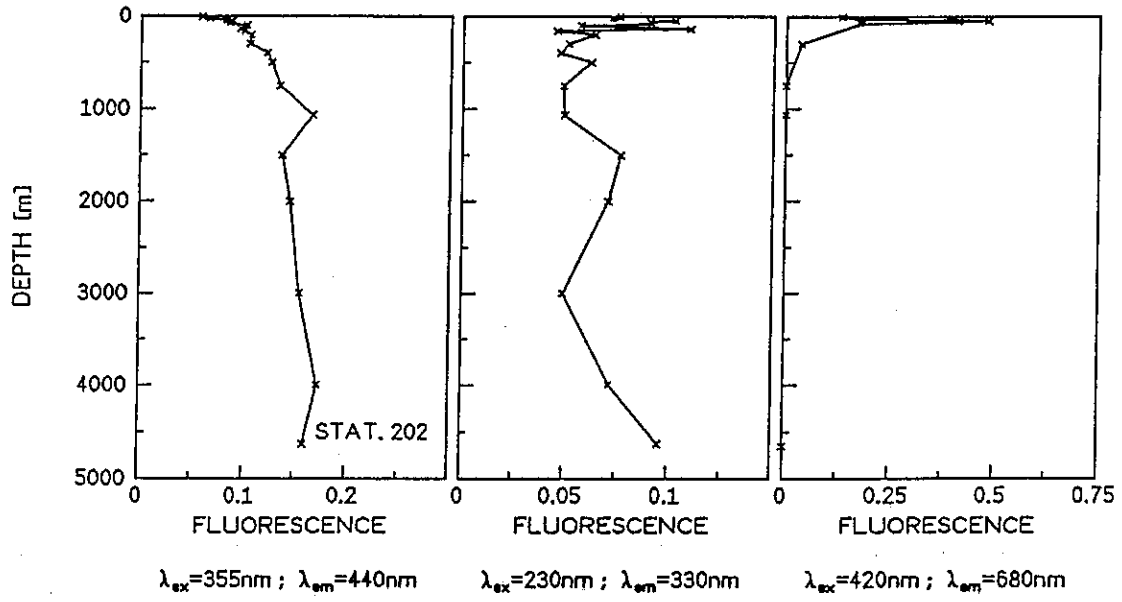

Fig. 77: Station 202, 40°20'N, 20°60'W: Depth profile of yellow substance fluorescence (left), tryptophan (middle), and chlorophyll (right)

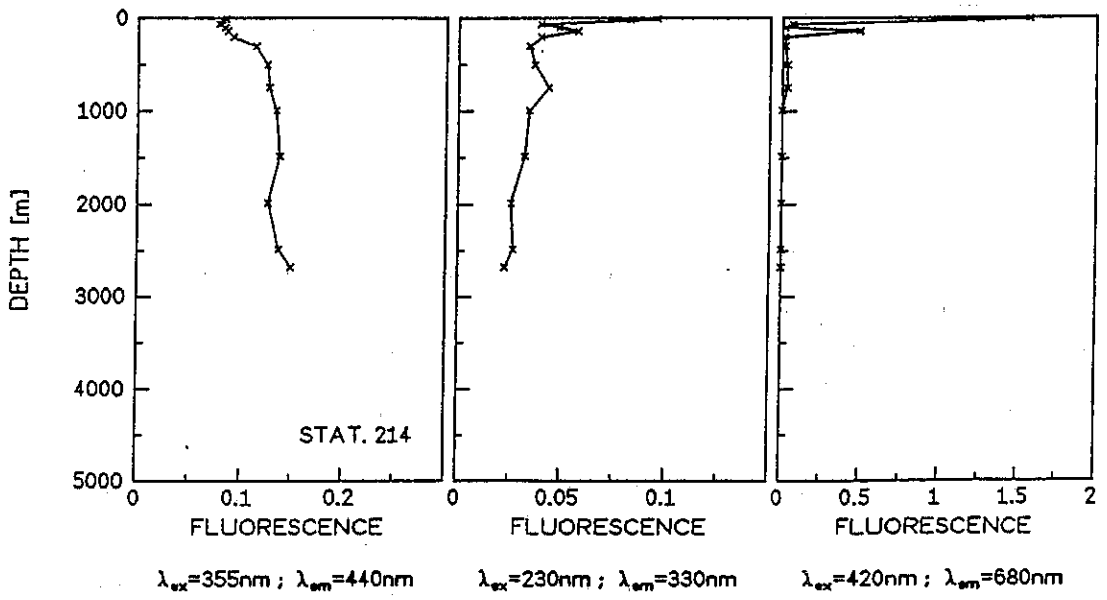

Fig. 78: Station 214, 52°30,4'N, 20°W: Depth profile of yellow substance fluorescence (left), tryptophan (middle), and chlorophyll (right)

6 Bericht der Bordwetterwarte

6.1 Erster Fahrtabschnitt (D. von Bargen)

Am 16.03.1992 verließ METEOR um 19.00 Uhr UTC den Hafen von Las Palmas. Der Kurs führte nach Nordwesten zur Position 34°N, 20°W. Diese lag noch südlich der subtropischen Hochdruckzelle. Entsprechend herrschte auf dem Wege dorthin der Nordostpassat mit Stärken um Bft 5. Am 19.03. morgens ging die Fahrt weiter ins Hauptarbeitsgebiet, dem BIOTRANS-Feld auf 47°N, 20°W. Dabei wurde der Nordostpassat rasch durchquert. Ein Keil des Subtropenhochs schwenkte nach Norden, so daß vorübergehend nur schwache westliche Winde auftraten. Allerdings machte sich ab 40°N eine westliche Dünung bemerkbar, die zunächst nur bei 1,5 m, bald aber bis auf 4 m anstieg und das Schiff mit seinem hochliegenden Gewichtsschwerpunkt in starke Bewegungen brachte. Am 21.03. war das Zielgebiet erreicht und die Messungen wurden am Nachmittag aufgenommen. Auf der Nordseite des erwähnten Hochs wehten mäßige bis frische westliche Winde. Durch starke Tiefdruckentwicklungen im Raum Neufundland verlagerte das Subtropenhoch seinen Schwerpunkt sehr weit nach Norden bis 50°N, 25°W. An seiner Ostflanke lag das Einsatzgebiet dann unter frischen bis starken nördlichen Winden. Die Seegangshöhe betrug um 3 m.

Zum 28.03. änderte sich die großräumige Wettersituation grundlegend. Das Subtropenhoch hatte sich wieder zu den Azoren verlagert. An seiner Nordflanke war ein Tief von Neufundland Richtung Island gezogen und hatte sich dort erheblich vertieft. Das Sturmfeld dieses Tiefs erfaßte METEOR am 28.03. mittags mit West- bis Nordwestwinden Stärke um Bft 9 und Orkanböen. Der Seegang erreichte Höhen bis 7 m. In der einfließenden Kaltluft traten verbreitet Regen- und Graupelschauer auf. Die Forschungsarbeiten mußten für drei Tage unterbrochen werden. Am 30.03. mittags hatte das Sturmtief den Westausgang des Englischen Kanales erreicht, und zum Morgen des 31.03. nahm der Wind allmählich ab. Nachdem die alte Position ereicht war, wurde mittags das Programm bei rasch abnehmender Windsee und Dünung wieder aufgenommen. METEOR lag jetzt zwischen dem nahezu ortsfesten Sturmtief über Südengland und einem umfangreichen Tief südlich von Kap Farvel. Ein Teiltief, das südwestlich an der METEOR Position vorbeigezogen war, hatte den Wind vollständig zum Erliegen gebracht. Erst am Tag darauf gelangte das Einsatzgebiet wieder in den Bereich des ehemaligen Sturmtiefs, wobei zunächst frische, später starke bis stürmische nordöstliche Winde dominierten. In der hochreichend einfließenden Kaltluft traten am 03.04., trotz starken nächtlichen Druckanstieges, noch schwere Sturmböen auf. Am 04.04. hatte sich ein Keil des Subtropenhochs bis Irland vorgeschoben, so daß nur schwache Luftbewegungen registriert wurden. In den Folgetagen gelangte das Einsatzgebiet wieder in die Frontalzone. Tiefs zogen zwischen 50° und 60°N ostwärts. Ihre Ausläufer griffen bis 45°N aus, und es herrschten im Fahrtgebiet frische bis starke Winde aus Südwest bis Nordwest vor. Entlang der Fronten trat zeitweise Nebel auf, so daß das Aufnehmen von Verankerungen in enger Abstimmung mit der Bordwetterwarte geplant wurde. Als abschließende Position wurde 49°9'N, 16°5'W

angelaufen. Von dort lief METEOR am 07.04. nach Dublin, das am 09.04.1992 früh erreicht wurde.

6.2 **Zweiter Fahrtabschnitt** (E. Röd)

Ein vom mittleren Nordatlantik über die Britischen Inseln zur Deutschen Bucht ziehendes Tief brachte Irland zunächst einen lebhaften Wind aus Westsüdwest mit 5-7 Bft, der an der Rückseite in einen stürmischen, sehr böigen Nordwestwind überging. Von Dublin führte die Route nach einem kurzen Zwischenaufenthalt in Cork weiter südwestwärts über eine Station auf Goban Spur ins BIOTRANS-Arbeitsgebiet auf etwa 47°N, 19°W, wo METEOR 17 Tage lang quasi stationär auf Position blieb.

Ein kräftiger Keil des Azorenhochs ließ mit massivem Druckanstieg den Wind hier bald abnehmen. Ein von den Bermudas unter Intensivierung heranziehendes kleines Tief verstärkte an seiner Westflanke die Warmluftadvektion, doch erreichte die Windstärke dabei kaum mehr als Bft 7. Drei einzelne Tiefs begannen am 22.4.92 auf 60°N, 35°W zu einem umfangreichen Zentraltief zu verschmelzen. Am 25.04. hatte es mit 960 hPa seinen niedrigsten Kerndruck erreicht, füllte sich aber anschließend nur sehr langsam auf und zog nur zögernd Richtung Färöer.

Am 28.04. wurde das Island-Tief durch ein neues, von Neufundland kommendes Tief regeneriert. Das Einsatzgebiet blieb dadurch anhaltend in einer scharf ausgeprägten Frontalzone unter einem kräftigen westlichen Jet mit 90-125 Knoten. Dementsprechend schnell überquerten kleine Frontalwellen das Arbeitsgebiet und ließen keine dauerhafte Wetterberuhigung zu. Besonders zwischen dem 23. und 26.04. war der Westsüdwestwind mit 7-8 Bft so stark, daß die wissenschaftlichen Arbeiten mit schwerem Gerät und Drifterbojen unterbrochen werden mußten. Neben der Windsee war besonders die hohe Dünung, die sich bei einem Fetch von mehr als 1000 sm aufbauen konnte, störend und unangenehm. Nach dem Durchzug einer Welle drehte der Wind auf NW und nahm ab, so daß die Arbeiten wieder aufgenommen werden konnten. Bis zum Abschluß des umfangreichen marinbiologischen, marin- und luftchemischen Programmes am 03.05. blieb der Wind zwar anfangs noch ziemlich frisch, verursachte aber keine weiteren Behinderungen. Auf der Strecke nach Funchal durchquerte METEOR nach Verlassen der Westwindzone das Subtropenhoch und profitierte weiter im Süden von der achterlichen Windkomponente des hier lebhaften Nordostpassates. Ein ungewöhnliches Ereignis war am 30.04. zu beobachten: Saharastaub im Warmsektor bei lebhaftem Wind aus Westsüdwest mit Bft 6. Er war offenbar in weitem Bogen um das quasistationäre Azorenhoch herumgeführt worden.

6.3 **Dritter Fahrtabschnitt** (C. Knaack)

Am 09.05.1992, einem Sonnabend, verließ METEOR um 10 Uhr den Hafen von Funchal.

Ein umfangreiches atlantisches Hochdruckgebiet (1033 hPa, 40°N, 50°W) sorgte mit schwachen nördlichen Winden für ruhiges Wetter. Die Haupttiefdrucktätigkeit spielte sich in der Frontalzone nördlich 45°N ab und machte sich durch eine Dünung bis ca. 2 m Höhe im Fahrtgebiet bemerkbar. In der Nacht zum Sonntag erreichten wir bei ca. 33°N den 20. westlichen Längengrad (1. Hauptstation), auf dem nun der nach Norden führende Meridionalschnitt begann.

Bis zum 12.05. blieb der Hochdruckeinfluß und damit das ruhige Wetter erhalten. Am Morgen des 13.05. überquerte eine Kaltfront mit Böen bis Bft 8 unser Fahrtgebiet. METEOR hatte inzwischen 36°5'N erreicht.

Durch den nachfolgenden Kaltluftvorstoß wurde ein weit nach Süden reichender Höhentrog aufgebaut, dessen Achse am 15.05. bei 20°W lag. Zuvor wurde auf seiner Rückseite eine Welle unter Vertiefung genau in unser Forschungsgebiet (2. Hauptstation, 40°N, 20°W) geführt. Dieses Tief wurde hier nahezu stationär, da gleichzeitig an eben dieser Position durch Abtropfung ein Höhentief entstand. Wir lagen also im ruhigen Zentrum eines hochreichenden Tiefs mit senkrechter Achse.

Das ruhige Wetter (meist weniger als Bft 5) blieb uns auf der weiteren Fahrt nach Norden zunächst treu. Auf der 3. Hauptstation (ca. 47°N, 20°W, im BIOTRANS-Gebiet) am 18./19.05. befand sich METEOR in Achsnähe einer meridionalen Tiefdruckrinne zwischen dem Gebiet nordöstlich der Azoren und Island. Da sich das hochreichende Tief östlich der Azoren wieder regenerierte, erreichte der Nordostwind am 21.05. zeitweise Windstärke 7.

Vom Mittelfristmodell des Deutschen Wetterdienstes schon am 20.05. angedeutet und am 22.05. gut erfaßt, beherrschte am 24.05. ein umfangreiches Sturmtief den mittleren Nordatlantik. Es erreichte seinen Höhepunkt mit ca. 970 hPa bei 50°N, 30°W am 24.05. um 06 Uhr UTC. Für uns, inzwischen bei 52°5'N angelangt, bedeutete dies Bft 8 aus Südost bis Ost und einen Seegang von 4 m. Auf der Rückseite des Sturmtiefes wurde sogar Nordwest bis Bft 11 beobachtet. Am Morgen des 25.05. nahm der Wind nach Durchgang einer Okklusion auf Bft 5 ab, und die wetterempfindlichen Forschungsarbeiten - insbesondere eine Verankerung bei 54°6'N, 21°1' W (4. Hauptstation) - konnten ungestört durchgeführt werden.

Das inzwischen hochreichende Tief bewegte sich in den Folgetagen unter allmählicher Auffüllung langsam ostwärts. Am 28.05. befand es sich mit 999 hPa westlich der Biscaya. METEOR hatte inzwischen bei 57°5'N die 5. Hauptstation erreicht. Hier sorgte ein umfangreiches Hoch (1030 hPa) über dem Nordmeer und Skandinavien, an dessen Rand wir uns befanden, für ruhiges und oft sonniges Forschungswetter. Dabei lag wenige Meilen westlich

unseres Fahrtgebietes das Wolkenband einer alten, nahezu stationären Okklusion, verbunden mit ausgedehnten Nebelfeldern. Am Nachmittag des 29.05. war auch METEOR von dichtem Nebel eingehüllt. Dies geschah auf der 6. und letzten Hauptstation der Reise bei 59°5'N.

Im weiteren Verlauf blieb es ruhig. Die Windgeschwindigkeiten lagen meist unter 10 kt, zeitweise herrschte Windstille. So war der Durchgang einer Kaltfront am Nachmittag des 31.05. mit Böen bis Bft 5 für uns alle ein schon fast vergessenes Naturereignis. Am Dienstag Morgen (02.06.) erreichte METEOR den Hafen von Reikjavik - bei ruhigem Wetter.

6.4 **Vierter Fahrtabschnitt** (C. Knaack)

Der 4. Abschnitt der Reise M 21 begann am 05.06. um 18 Uhr in Reikjavik. Auf der Vorderseite eines Sturmtiefes über der Irminger See herrschten südliche Winde Bft 7, zeitweise auch 8. Der Seegang betrug 3 m. Im Bereich einer Okklusion kam es zu Niederschlägen und vorübergehend auch zu Nebel. Im weiteren Verlauf füllte sich das Tief an Ort und Stelle langsam auf und die Front blieb stationär über Südwestisland liegen. Auf der Fahrt nach Osten (1. Meßstation am 07.06. bei 62°5'N, 14°0'W), später nach Nordosten gewann ein stabiles, umfangreiches Hoch über der Norwegischen See und Nordskandinavien zunehmend an Einfluß auf unser Wetter. Der Wind nahm bis zum Abend des 07.06. kontinuierlich auf Bft 3 aus Südost ab.

Mit südöstlichen Winden Bft 4 bis 5 wurde am 08.06. verhältnismäßig milde und feuchte (Taupunkte stromabwärts: > 10°C) Luft advehiert, so daß sich über dem kalten Wasser (ca. 7°C) flache, aber ausgedehnte Nebelfelder bildeten.

Die am gleichen Tage von der Bordwetterwarte auf der Position 64°5'N, 8°0'W aufgenommenen Satellitenbilder (insbesondere russische Meteor-Bilder) sowie Eiskarten (Murmansk) zeigten in den Arbeitsgebieten "Kveitehola-Rinne" und "Barentsseehang" (nahe der Bäreninsel) eisfreie Verhältnisse. Daraufhin wurde der Reiseablauf geändert und statt zum ursprünglich als erstem geplanten Arbeitgebiet, dem Vöring-Plateau (67°5'N, 5°5'E), ging die Fahrt in Richtung Bäreninsel/Spitzbergen.

Auf dem Wege dorthin bestimmten Nebel und meist schwache südliche Winde unser Wetter. Das blockierende Hochdruckgebiet verstärkte sich bis zum 11.06. auf fast 1035 hPa und verlagerte seinen Schwerpunkt in die südliche Barentssee. METEOR hatte inzwischen den 70. Breitenkreis sowie den Nullmeridian überquert.

Starker Druckfall über Ostisland und Jan Mayen zusammen mit einer kräftigen, nordostgerichteten Höhenströmung gaben am 12.06. Hinweise auf eine Wetterumstellung. So nahm der Südwind auf der Vorderseite einer Tiefdruckrinne zwischen Island und Spitzbergen am Nachmittag des 13.06. im Arbeitsgebiet südöstlich der Bäreninsel bis Bft 7 zu. Gleichzeitig

verschwand der Nebel und die (Mitternachts-) Sonne schien vorübergehend - leider nicht bis Mitternacht.

Der isländische Teil der Tiefdruckrinne wurde zur eigenständigen Zyklone und zog in Richtung Bäreninsel. Am Nachmittag des 15.06. befand sich METEOR im Kernbereich (985 hPa), 60 Meilen westnordwestlich der Bäreninsel. Bei entsprechend ruhigem Wetter mit mäßigen bis schlechten Sichten und zeitweiligem Regen herrschte eine Dünung von 3 m, vorherrschend aus Südost. Auf der Rückseite herrschte am 16.06. zeitweise Nordwind Bft 7 bis 8. In der Polarluft sanken die Temperaturen unter den Gefrierpunkt.

Nach Zwischenhocheinfluß (ruhiges Wetter, zeitweise Sonne, sehr gute Sichten) nahm am Nachmittag des 18.06. auf der Vorderseite einer von Grönland unter starker Vertiefung (um 12 Uhr UTC auf Jan Mayen 5.0 hPa Druckfall in 3 Stunden) heranziehenden Zyklone der Südwind auf Bft 6 zu. Der stärkste Wind trat mit Süd 8 in den Frühstunden des 19.06. auf. Am 20.06. - jetzt wurde im Bereich des Knipovitch-Rückens westlich von Spitzbergen gearbeitet - herrschten hier in der Nähe des Tiefdruckzentrums zeitweilig Windstille sowie wieder mäßige bis schlechte Sichten. In den nächsten Tagen bewegte sich das Tief unter Auffüllung etwas nach Süden, so daß zunächst nördliche, später östliche Winde um Bft 4 wieder meist gutsichtige Kaltluft ins Forschungsgebiet brachten.

Am 24.06. wurden die Arbeiten im Gebiet Spitzbergen/Bäreninsel beendet, und METEOR nahm bei ruhigem Wetter Kurs auf das Vöring Plateau bei 67°5'N, 5°5'E vor der mittelnorwegischen Küste. Die Fahrt nach Süden führte zunächst entlang der Achse eines Hochkeils, der zwischen zwei hochreichenden Tiefdruckgebieten östlich von Island und Nordrußland lag.

Am Nachmittag des 26.06. begannen die Forschungsarbeiten auf dem nördlichen Vöring Plateau. Auf der Vorderseite eines von den Faröer Inseln langsam Nordost ziehenden Tiefs wehten südöstliche Winde Bft 5. Bis zum 28.06. zog dieses Tief, verbunden mit einem darüberliegen den Höhentief, auf die Position 59°N 00. In den Frühstunden dieses Tages verließ METEOR das Vöring Plateau mit dem Ziel Trondheim. Dabei wehte ein Süd-, später Südwestwind mit Bft 6 und Schauerböen Bft 8. Ein Wetterschiff bei 66°N, 2°E meldete seit dem 27.06. 12 Uhr UTC beständigen Südwest 7. Dieser Wind verursachte im Fahrtgebiet eine Dünung von etwa 3,5 m. Gegen Abend wurde gemäß dem GEOMAR-Motto "pax optima rerum" das Wetter friedlicher, und METEOR erreichte am Vormittag des 29.06. sicher den Hafen von Trondheim.

6.5 **Fünfter Fahrtabschnitt** (R. Hartig)

Am Donnerstag, den 02.07.1992, abends verließ METEOR Trondheim, wegen einer Reperatur 36 Stunden später als geplant. Über Stationen am Vöring Plateau, dem Lofotbecken und Jan Mayen führte der Fahrtverlauf zum Kolbeinsey Rücken (68°N, 19°W).

Anfangs bestimmte mit 2 bis 4 Bft von Norden einfließende, labile und gutsichtige Meeresluft das Wetter. Die Ausläufer eines Tiefs über der Irminger See sorgten ab 07.07. für eine Umstellung der Großwetterlage. In der Folge dominierte Südwest- bis Westwind der Stärke 4 bis 5Bft und meist starke Sc/St Bewölkung. Über dem nur 1 bis 2°C warmen Wasser kühlte sich die vom Nordatlantik einfließende, relativ milde Luft großräumig ab, so daß vielfach mäßige Sichten, wiederholt auch Seenebel auftraten. Erst im Verlauf des 17.07. sorgte eine Sturmtiefentwicklung südlich Islands für eine neue Großwetterlage. Ostwind 6 Bft, später Nordost und Nord 7 Bft., sowie Regen und Sprühregen wurden in der Folge beobachtet. Mit der Winddrehung auf Nordost vergrößerte sich der Fetch und innerhalb kurzer Zeit entwickelte sich eine 3 m hohe Windsee.

Die Eissituation im Ostgrönlandstrom war zeitweise problematisch. Bei Jan Mayen wurden zwei Growler beobachtet, die vermutlich aus einem Treibeisfeld nordwestlich der Insel abgedriftet waren. Hier konnten die Stationsarbeiten aber fortgesetzt werden. Im Arbeitsgebiet Kolbeinsey-Rücken mußten dagegen zwei Stationen verlegt werden, weil sich Treibeisfelder und zwei Eisberge dem Schiff näherten.

6.6 **Sechster Fahrtabschnitt** (R. Hartig)

Am 26.07.1992 verließ METEOR Reykjavik. Tiefdrucktätigkeit, begleitet von Regen und Schauern mit vorherrschend 7 Bft, bestimmte das Wetter auf der von Stationsarbeiten unterbrochenen Dampfstrecke ins BIOTRANS-Gebiet, das am 02.08. erreicht wurde.

Zwei Großwetterlagen - Hochdruckrandlage und Tief Nordatlantik - waren die beherrschenden Großwetterlagen in diesem Arbeitsgebiet. Zunächst lag das Gebiet in der Randzone des Azorenhochs. Es wurde regelmäßig von den Kaltfronten südlich Islands ziehender Tiefs überquert. Warmfrontduchgänge waren dagegen selten. Daher wurden nahezu ausschließlich westliche Winde mit 4 bis 7 Bft bei meist gute Sichten beobachtet. Lediglich am 06./07.08. sorgte ein SE-wandernder Kaltlufttropfen für eine Unterbrechung des beschriebenen Wetterablaufes. Regen, Schauer, Sichtrückgang und - da er sich zeitweise bis zum Boden durchsetzte - nördliche Windkomponenten begleiteten das Höhentief.

Mitte August sorgte dann ein zur Irminger See ziehendes Sturmtief für die Umstellung der Großwetterlage. Im Zuge dieser Tiefentwicklung bildete sich ein stationärer Höhentrog über dem Nordatlantik, der durch nachfolgende Sekundärtröge immer wieder regeneriert wurde.

Dadurch dominierte ein umfangreiches Zentraltief bis zum Ende der Arbeiten im Forschungsgebiet - zeitweise mit zwei Kernen - das Wetter auf dem Nordatlantik. In der nach Süden verschobenen Frontalzone bildeten sich Wellen und Randtiefs, die entlang etwa 40°N über das BIOTRANS-Gebiet hinweggesteuert wurden. Damit traten jetzt auch Ost- und Nordwindkomponenten auf, und es kam wiederholt zu Nebelbildung im Bereich der durchschwenkenden Warmsektoren. Schönwetterperioden waren nur von kurzer Dauer und beschränkten sich auf den postfrontalen Absinkbereich bei gleichzeitiger Kaltluftadvektion. Das am 22./23.08. durchziehende Randtief bedarf der besonderen Erwähnung. Aufgrund der Analysen und numerischen Vorhersagen war für dieses Tief 4 bis 5 Bft zu erwarten. Eine rasche Intensivierung sorgte in der Nacht etwa 2 Stunden lang für Bft 8, gefolgt von einem ebenso raschen Abflauen des Windes.

Während des gesamten Zeitraumes der Arbeiten im BIOTRANS-Gebiet wurde eine im Mittel 2 bis 3 m, in Spitzenwerten 5 m, hohe Dünung beobachtet.

7 Lists

7.1 Station lists leg M 21/1

7.1.1 List of benthic sampling stations (BIO-C-FLUX)

Date 1992	Ship's Station	Coordinates	Gear-No.	Sounding Depth (m)
18.03.	57	34°00,07'N 20°00,32'W	MC 369	5125
		33°59,92'N 20°00,36'W	MC 370	5125
21.03.	58	46°23,85'N 19°35,58'W	MC 371	4920
23.03.	64	47°10,82'N 19°33,54'W	MC 372	4568
25.03.	73	47°10,83'N 19°33,76'W	MC 373	4568
		47°10,78'N 19°33,52'W	MC 374	4568
	75	47°10,69'N 19°33,37'W	MC 375	4568
		47°10,70'N 19°33,90'W	MC 376	4568
26.03.	79	47°10,71'N 19°33,51'W	MC 377	4568
		47°10,90'N 19°33,71'W	MC 378	4568
27.03.	79	47°10,87'N 19°33,59'W	KG 1495	4568
	84	47°10,82'N 19°33,54'W	MC 379	4568
		47°10,77'N 19°33,48'W	MC 380	4568
		47°10,78'N 19°33,74'W	MC 381	4568
28.03.	86	47°10,99'N 19°33,64'W	MC 382	4568
		47°10,87'N 19°33,57'W	MC 383	4568
	88	47°10,90'N 19°33,10'W	MC 384	4568
31.03.	93	47°10,60'N 19°33,56'W	MC 385	4568
01.04.	93	47°10,86'N 19°33,73'W	MC 386	4568
02.04.	93	47°10,85'N 19°33,66'W	KG 1496	4568
	93	47°10,86'N 19°33,67'W	KG 1497	4568
03.04.	101	47°10,72'N 19°33,70'W	MC 387	4568
	101	47°10,80'N 19°33,69'W	MC 388	4568
04.04.	104	47°10,84'N 19°33,52'W	KG 1498	4568
		47°10,91'N 19°33,56'W	KG 1499	4568
		47°10,82'N 19°33,68'W	MC 389	4568
		47°10,73'N 19°33,64'W	MC 390	4568
	108	47°10,80'N 19°33,63'W	MC 391	4568
06.04.	112	48°50,96'N 16°28,92'W	MC 392	4811

7.1.2 List of water stations (JGOFS)

CTD = Multisonde m. Kranzwasserschöpfer
MSN = Multischließnetz
GFS = Goflow-Wasserschöpfer
APN = Apsteinnetz
SD = Secchi-Disk
RO = Schöpfer-Rosette
FD = Fallen-Drifter
GWS = Großraum-Wasserschöpfer
PN = Planktonnetz
LLV = Langleinenverankerung
DRIFT = Long-Term Drifter and Day Drifter
GRID = CTD-profile on a grid or section

Profile	Station	Date	Time (UTC)	Latitude	Longitude	Notes	Water-depth/m	Wire-cable-length/m
1	57	18-MAR-1992	9:40	34 N 0.00′	20 W 0.00′	CTD,MSN	5124	4600
2	58	18-MAR-1992	11:33	34 N 0.00′	20 W 0.00′	CTD	5124	4600
3	60	22-MAR-1992	9:15	47 N 9.40′	19 W 31.80′	CTD,MSN, APN, SD	4564	4303
4	61	22-MAR-1992	17:30	47 N 11.80′	19 W 34.10′	CTD	4567	250
5	66	23-MAR-1992	17:05	47 N 51.30′	19 W 35.00′	CTD,MSN,RO	4591	500
6	68	24-MAR-1992	6:15	47 N 50.13′	19 W 35.03′	CTD,MSN	4551	500
7	71	25-MAR-1992	3:20	47 N 10.80′	19 W 32.40′	CTD,MSN	4571	500
8	78	26-MAR-1992	6:00	47 N 19.14′	19 W 37.95′	CTD,RO, MSN,APN,SD	4493	2500
9	81	27-MAR-1992	5:28	47 N 1.64′	19 W 30.02′	CTD,MSN, APN,SD	4535	500
10	81	27-MAR-1992	8:15	47 N 1.27′	19 W 28.68′	CTD	4288	500
11	92	31-MAR-1992	18:00	47 N 17.70′	19 W 42.90′	CTD,MSN, APN,RO	4441	700
12	96	1-APR-1992	15:05	47 N 15.92′	19 W 30.96′	CTD,APN,MSN	4559	700
13	99	2-APR-1992	18:20	47 N 17.26′	19 W 30.84′	CTD,APN, MSN,RO,LLV	4542	500
14	103	3-APR-1992	18:10	47 N 5.09′	19 W 24.28′	CTD,APN,SD	4380	2500
15	103	3-APR-1992	20:56	47 N 5.44′	19 W 24.97′	CTD	4450	300
16	106	4-APR-1992	14:54	47 N 12.69′	19 W 29.15′	CTD,MSN, SD,FD	4560	300
17	106	4-APR-1992	16:15	47 N 12.67′	19 W 28.82′	CTD	4562	700
18	111	5-APR-1992	8:50	47 N 29.39′	19 W 9.14′	CTD,MSN, APN,SD	4566	700

7.1.3 List of benthopelagic nekton and megafauna sampling stations (BIO-C-FLUX)

Geräteliste:
DOS = Tiefsee-Beobachtungssystem
FT = Fototrawl
FFLL = Freifall-Langleinensystem
RK = Reusenkette
OT = Ottertrawl
z.W. = zu Wasser
a.D. = an Deck
Positionen sind Aussetzpositionen

Datum 1992	Station Nr.	Gerät	Breite °N	Länge °W	Tiefe m
25.03.	074	RK 110 z.W.	47°09.6'	19°32.5'	4611
26.03.	077	RK 110 a.D.			
27.03.	083	RK 111 z.W.	47°13.3'	19°33.5'	4568
28.03.	087	RK 111 a.D.			
01.04.	095	RK 112 z.W.	47°17.5'	19°30.8'	4540
01.04.	097	FT 029	47°17.0'	19°28.0'	4562
02.04.	098	RK 112 a.D.			
02.04.	099	FFLL 001 z.W.	47°17.3'	19°31.1'	4539
03.04.	102	FFLL 001 a.D.			

7.1.4 1m^2-MOCNESS-hauls during M 21/1

Times of sampling (UTC = local time) and positions refer to the opening and closing of quantitatively sampling nets. N = net, L = left net, R = right net, mab = meters above bottom. Station numbers are BIO-C-FLUX numbers.

Date 1992	Haul	Station No.	Time (UTC)	Position	Depth of sampling	Remarks
21.03.	MOC-1-70 N2	385	22:40	47°00,9'N 19°35,5'W	400 m to	
21.03.	MOC-1-70 N9		23:18	47°01,9'N 19°35,9'W	0 m	
23.03.	MOC-1-71 N2	388	01:29	47°43,1'N 19°30,9'W	4000 m to	
23.03.	MOC-1-71 N9		03:37	47°47,2'N 19°33,2'W	1650 m	
25.03.	MOC-1-72 N2	390	00:15	47°11,1'N 19°32,1'W	400 m to	
25.03.	MOC-1-72 N9		00:45	47°12,1'N 19°31,7'W	0 m	
26.03.	MOC-1-73 N2	398	00:12	47°11,9'N 19°34,1'W	1650 m to	nets twi= sted
26.03.	MOC-1-73 N9		01:29	47°13,4'N 19°35,4'W	400 m	
26.03.	MOC-1-74 N2	399	03:55	47°17,2'N 19°37,3'W	1650 m to	
26.03.	MOC-1-19 N9		05:14	47°18,8'N 19°38,0'W	500 m	
27.03.	MOC-1-75 N2	405	10:50	47°03,7'N 19°28,4'W	1650 m to	
27.03.	MOC-1-75 N9		12:18	47°05,9'N 19°28,5'W	500 m	
28.03.	MOC-1-76 N2	410	02:50	47°15,2'N 19°39,3'W	4000 m to	
28.03.	MOC-1-76 N9		05:07	47°18,7'N 19°41,7'W	1650 m	
31.03.	MOC-1-77 N2	415	13:02	47°11,1'N 19°34,5'W	400 m to	
31.03.	MOC-1-77 N9		13:36	47°11,9'N 19°35,3'W	0 m	
31.03.	MOC-1-78 N2	416	15:51	47°15,4'N 19°38,4'W	1650 m to	
31.03.	MOC-1-78 N9		17:17	47°17,2'N 19°41,8'W	400 m	

7.1.4 Fortsetzung/continued

Date 1992	Haul	Station No.	Time (UTC)	Position	Depth of sampling	Remarks
01.04.	MOC-1-79 N2	421	11:07	47°14,3'N 19°31,9'W	1650 m to	
01.04.	MOC-1-79 N9		12:30	47°17,0'N 19°30,9'W	400 m	
02.04.	MOC-1-80 N2	424	02:59	47°25,9'N 19°34,7'W	4550 m to	2* 20 mab 2* 50 mab
02.04.	MOC-1-80 N9		05:40	47°27,8'N 19°02,2'W	4470 m	2*100 mab
02.04.	MOC-1-81 N2	427	23:07	47°05,1'N 19°38,7'W	1650 m to	
03.04.	MOC-1-81 N9		00:29	47°06,9'N 19°37,2'W	400 m	
04.04.	MOC-1-82 N2	435	10:04	47°11,5'N 19°38,7'W	400 m to	
04.04.	MOC-1-82 N9		10:38	47°12,2'N 19°31,4'W	0 m	
05.04.	MOC-1-83 N2	439	02:32	47°17,0'N 19°38,7'W	4200 m to	2*300 mab 1*400 mab
05.04.	MOC-1-83 N9		06:17	47°23,4'N 19°17,0'W	3000 m	1 cod end bucket lost

7.2 Station lists leg M 21/2

7.2.1 List of benthic sampling stations (BIO-C-FLUX)

Date 1992	Ship's Station	Coordinates	Gear-No.	Sounding Depth (m)
15.04.	117	49°14,60'N 14°12,24'W	MC 393	4484
17.04.	126	47°10,65'N 19°33,52'W	MC 394	4568
	127	47°10,92'N 19°33,51'W	MC 395	4568
	128	47°10,90'N 19°33,90'W	MC 396	4568
22.04.	397	47°10,11'N 19°33,85'W	MC 397	4568
28.04.	171	47°10,84'N 19°33,64'W	MC 398	4568
	172	47°10,88'N 19°33,69'W	MC 399	4568
	173	47°10,96'N 19°33,68'W	MC 400	4568

7.2.2 List of water stations (JGOFS)

CTD = Multisonde m. Kranzwasserschöpfer
MSN = Multischließnetz
GFS = Goflow-Wasserschöpfer
APN = Apsteinnetz
SD = Secchi-Disk
RO = Schöpfer-Rosette

FD = Fallen-Drifter
GWS = Großraum-Wasserschöpfer
PN = Planktonnetz
LLV = Langleinenverankerung
DRIFT = Long-Term Drifter and Day Drifter
GRID = CTD-profile on a grid or section

Profile	Station	Date	Time (UTC)	Latitude	Longitude	Notes	Water-depth/m	Wire-cable-length/m
19	116	15-APR-1992	7:13	49 N 15.98′	14 W 9.50′	CTD,MSN,APN	4464	1000
20	118	15-APR-1992	18:05	48 N 47.61′	15 W 14.39′	CTD GRID	4765	1000
21	119	16-APR-1992	9:38	47 N 23.68′	17 W 41.14′	CTD,MSN,FD	4646	1000
22	120	16-APR-1992	13:40	47 N 22.88′	18 W 0.26′	CTD	4609	1000
23	121	16-APR-1992	16:15	47 N 20.66′	18 W 18.67′	CTD	4613	1000
24	122	16-APR-1992	18:30	47 N 18.13′	18 W 37.64′	CTD	4593	1000
25	123	16-APR-1992	20:40	47 N 15.76′	18 W 55.98′	CTD	4580	1000
26	124	16-APR-1992	23:00	47 N 12.92′	19 W 16.48′	CTD	4306	1000
27	125	17-APR-1992	1:20	47 N 10.83′	19 W 34.70′	CTD	4565	1000
28	131	17-APR-1992	15:58	47 N 8.48′	19 W 52.71′	CTD	4512	1000
29	132	17-APR-1992	18:15	47 N 6.16′	20 W 11.41′	CTD	4246	1000
30	133	17-APR-1992	20:30	47 N 3.85′	20 W 30.11′	CTD	4242	1000
31	134	17-APR-1992	23:00	46 N 55.08′	20 W 12.41′	CTD	4079	1000
32	135	18-APR-1992	1:20	46 N 46.34′	19 W 53.81′	CTD	4562	1000
33	136	18-APR-1992	3:40	46 N 37.60′	19 W 35.53′	CTD	4907	1000
34	137	18-APR-1992	5:54	46 N 49.93′	19 W 22.52′	CTD	4540	1000
35	138	18-APR-1992	8:20	47 N 2.33′	19 W 9.75′	CTD	4567	1000
36	139	18-APR-1992	10:40	47 N 15.23′	18 W 56.93′	CTD,MSN, SD	4579	1000
37	140	18-APR-1992	13:38	47 N 23.68′	19 W 15.18′	CTD	4551	1000
38	141	18-APR-1992	16:12	47 N 32.41′	19 W 33.80′	CTD	4562	1000
39	142	18-APR-1992	18:55	47 N 41.11′	19 W 52.29′	CTD	4535	1000
40	143	18-APR-1992	21:43	47 N 28.67′	20 W 5.07′	CTD,APN	4493	1000
41	144	19-APR-1992	0:55	47 N 15.98′	20 W 18.03′	CTD	4486	1000

7.2.2 Fortsetzung/continued

Profile	Station	Date	Time (UTC)	Latitude	Longitude	Notes	Water-depth/m	Wire-cable-length/m
42	145	19-APR-1992	3:45	47 N 19.67'	19 W 46.50'	CTD	4509	1000
43	146	19-APR-1992	7:55	47 N 2.51'	19 W 9.16'	CTD DRIFT	4556	1000
44	148	19-APR-1992	17:35	47 N 40.93'	19 W 50.25'	CTD,FD, APN,MSN	4535	1000
45	149	20-APR-1992	4:20	47 N 41.08'	19 W 47.88'		4532	1000
46	149	20-APR-1992	6:10	47 N 39.38'	19 W 38.11'	CTD,FD, MSN	4539	300
47	150	20-APR-1992	16:00	47 N 35.65'	19 W 30.76'	CTD,MSN, FD	4548	300
48	151	20-APR-1992	18:00	47 N 34.88'	19 W 29.36'	CTD,FD	4550	4000
49	153	21-APR-1992	4:31	47 N 31.21'	19 W 21.06'	CTD,FD,APN, MSN,RO,SD	4550	1000
50	154	21-APR-1992	11:15	47 N 30.76'	19 W 16.96'	CTD	4566	1000
51	155	21-APR-1992	12:36	47 N 30.53'	19 W 16.87'	CTD	4566	2500
52	156	21-APR-1992	16:51	47 N 31.08'	19 W 15.07'	CTD,MSN,FD	4570	1000
53	157	21-APR-1992	19:20	47 N 30.92'	19 W 14.12'	CTD	4577	2000
54	157	21-APR-1992	21:15	47 N 30.45'	19 W 12.86'	CTD	4570	2000
55	157	21-APR-1992	23:45	47 N 29.52'	19 W 11.16'	CTD	4572	2000
56	158	22-APR-1992	4:30	47 N 29.07'	19 W 8.44'	CTD,FD,RO APN,MSN	4563	1000
57	158	22-APR-1992	11:45	47 N 27.67'	19 W 7.01'	CTD,SD	4573	1000
58	159	22-APR-1992	13:30	47 N 27.71'	19 W 5.67'	CTD,APN	4569	2000
59	159	22-APR-1992	16:18	47 N 27.70'	19 W 3.98'	CTD,FD	4566	1000
60	162	23-APR-1992	4:45	47 N 27.76'	18 W 56.98'	CTD,FD	4570	1000
61	164	23-APR-1992	15:30	47 N 25.59'	18 W 53.92'	CTD,MSN	4576	1000
62	164	23-APR-1992	17:55	47 N 24.62'	18 W 53.88'	CTD,MSN	4574	2500
63	166	26-APR-1992	17:00	47 N 21.67'	18 W 37.02'	CTD	4591	1000
64	166	26-APR-1992	18:34	47 N 21.68'	18 W 36.75'	CTD	4593	300
65	167	27-APR-1992	4:50	47 N 21.44'	18 W 33.34'	CTD	4620	1000
66	167	27-APR-1992	7:15	47 N 20.52'	18 W 33.06'	CTD,FD,MSN	4590	150
67	167	27-APR-1992	9:00	47 N 20.11'	18 W 32.96'	CTD,MSN	4597	4626

70	169	27-APR-1992	21:20	47 N	15.84'	18 W	34.31'	CTD	4580	4500
71	170	28-APR-1992	3: 5	47 N	14.69'	18 W	33.81'	CTD	4580	200
72	170	28-APR-1992	4:15	47 N	14.17'	18 W	33.88'	CTD,APN,FD GRID	4579	300
73	173	28-APR-1992	19:40	47 N	10.94'	19 W	33.95'	CTD,MSN	4564	1000
74	174	28-APR-1992	23:40	47 N	11.20'	18 W	58.55'	CTD	4521	1000
75	175	29-APR-1992	1:50	47 N	12.48'	18 W	42.36'	CTD DRIFT	4581	1000
76	176	29-APR-1992	4:13	47 N	5.23'	18 W	34.30'	CTD,FD	3892	1000
77	176	29-APR-1992	7:10	47 N	3.41'	18 W	35.12'	CTD,APN, MSN,SD	3876	150
78	176	29-APR-1992	10:45	47 N	1.49'	18 W	34.61'		4027	4050
79	177	29-APR-1992	17:30	46 N	59.27'	18 W	34.35'	CTD,SD,MSN GRID	4094	500
80	179	29-APR-1992	21:10	46 N	42.29'	18 W	33.94'	CTD	4624	1000
81	180	30-APR-1992	0: 5	46 N	26.76'	18 W	33.46'	CTD DRIFT	3611	1000
82	181	30-APR-1992	4: 0	46 N	54.97'	18 W	32.33'	CTD,FD	4207	1000
83	181	30-APR-1992	6:30	46 N	53.28'	18 W	32.27'	APN,MSN,SD	4210	1000
84	182	30-APR-1992	9:10	46 N	50.83'	18 W	32.90'	CTD,MSN,APN	4206	2000
85	183	30-APR-1992	17:30	46 N	49.87'	18 W	32.72'	FD GRID	4117	4100
86	184	30-APR-1992	19:35	46 N	57.77'	18 W	34.61'	CTD	4173	1000
87	185	30-APR-1992	22:00	46 N	58.11'	18 W	12.12'	CTD	4310	1000
88	186	1-MAY-1992	0: 5	46 N	43.30'	18 W	12.47'	CTD DRIFT	4421	1000
89	187	1-MAY-1992	4:25	46 N	40.63'	18 W	28.51'	CTD,FD, APN,MSN	4580	1000
90	188	1-MAY-1992	9:00	46 N	38.06'	18 W	27.47'	CTD,SD,MSN	4303	3000
91	188	1-MAY-1992	15: 5	46 N	34.72'	18 W	25.24'	CTD	4103	3000
92	188	1-MAY-1992	17:00	46 N	34.39'	18 W	25.11'	CTD	4080	1000
93	190	1-MAY-1992	19:30	46 N	31.98'	18 W	23.46'	CTD	3833	1000
94	190	1-MAY-1992	20:20	46 N	31.42'	18 W	23.13'	CTD	3770	1000
95	190	1-MAY-1992	21:10	46 N	30.75'	18 W	22.80'	CTD	3740	1000
96	190	1-MAY-1992	22:40	46 N	30.08'	18 W	22.62'	MSN	3651	1000
97	190	1-MAY-1992	23:45	46 N	29.85'	18 W	22.11'	CTD	3651	1000
98	191	2-MAY-1992	0:25	46 N	29.72'	18 W	21.93'	CTD	3664	1000
99	191	2-MAY-1992	1: 5	46 N	29.56'	18 W	21.57'	CTD	3686	1000

7.2.2 Fortsetzung/continued

Profile	Station	Date	Time (UTC)	Latitude	Longitude	Notes	Water-depth/m	Wire-cable-length/m
97	190	1-MAY-1992	23:45	46 N 29.85′	18 W 22.11′	CTD	3651	1000
98	191	2-MAY-1992	0:25	46 N 29.72′	18 W 21.93′	CTD	3664	1000
99	191	2-MAY-1992	1: 5	46 N 29.56′	18 W 21.57′	CTD	3686	1000
100	191	2-MAY-1992	1:45	46 N 29.44′	18 W 21.26′	CTD	3698	1000
101	191	2-MAY-1992	2:26	46 N 29.27′	18 W 20.87′	CTD	3729	1000
102	192	2-MAY-1992	4:00	46 N 27.72′	18 W 18.60′	CTD,FD,MSN	3827	1000
103	193	2-MAY-1992	8:30	46 N 38.26′	18 W 28.23′	CTD,FD	4299	1000
104	194	2-MAY-1992	12:00	46 N 22.84′	18 W 12.27′	CTD,MSN	3990	1000
105	195	2-MAY-1992	15:48	46 N 21.30′	18 W 7.40′	FD	4071	1000
106	195	2-MAY-1992	16:30	46 N 21.12′	18 W 6.63′	CTD,FD TEST	4076	1000
107	197	4-MAY-1992	21:50	36 N 33.00′	16 W 52.00′	CTD	5050	5000
108	197	5-MAY-1992	1:15	36 N 33.69′	16 W 52.31′	CTD	5066	5000
109	197	5-MAY-1992	4:30	36 N 34.36′	16 W 52.88′	CTD	5053	5000

7.3 Station lists leg M 21/3

7.3.1 General list of sampling stations

Station No.	Datum 1992	Koordinaten Breite	Länge	Lottiefe [m]	Geräte
198	10.05.	33°48,3'N	21°55,4'W	5400	2xMC
199	11.05.-12.05	33°56,6'N	21°49,8'W	5400	CTD, 3xMSN, GS, CTD,GFO, ISP, 2xMSN
200	12.05.	33°48,3'N	24°55,2'W	5400	2xMC
201	14.05.	39°51,8'N	20°02,7'W	4700	MC
202	14.05.-15.05.	39°59,5'N	20°01,5'W	4900	CTD, Auslösertest, 2xMSN, GFO, CTD, GS, 3xMSN
203	15.05.	39°59,9'N	20°00,6'W	4900	MC
-	17.05.	44°52,4'N	15°47,0'W	-	Aufnahme eines Drifters von M 21/2
204	18.05.	47°47,0'N	19°45,0'W	4500	CTD
205	18.05.	47°43,8'N	19°54,3'W	4530	Auslegungsversuch der physikalischen Verankerung L2 92PH
206	18.08.-19.05.	47°44,2'N	19°41,8'W	4500	MSN,ISP
207	19.05.	47°43,8'N	19°54,3'W	4530	Auslegung der physikalischen Verankerung L292PH
208	19.05.	47°33,3'N	19°45,5'W	4500	2xMSN, GFO, GS
209	20.05.	47°24'N	19°40'W	4500	2xMC
210	20.05.	47°47,6'N	19°47,0'W	4540	Auslegung der Sinkstoff-fallen-Verankerung L2 92B
211	20.05.-21.05.	47°35'N	19°30'W	4500	CTD, 3xMSN, CTD, ISP, GS, GFO, MSN,PN
212	22.05.	47°24'N	19°40'W	4550	3xMC
213	23.05.	49°59,9'N	20°00,2'W	4380	CTD, PN, CTD
214	24.05.	52°30,2'N	19°59,8'W	2700	CTD, 2xPN, 3xMSN, GFO
215	25.05.	54°32,0'N	21°04,4'W	3004	CTD + Auslegung der Sinkstoffallen-Verankerung L3 92

7.3.1 Fortsetzung/continued

Station No.	Datum 1992	Koordinaten Breite	Länge	Lottiefe [m]	Geräte
216	25.05.-	54°37,3'N	21°05,6'W	3000	2xMSN, ISP,
	26-05	54°42,0'N	21°14,0'W	3080	CTD, Auslegung der physikalischen Verankerung L3 92PH
217	26.05.-	54°41,5'N	20°43,1'W	2800	3xMSN,
	26.05.	54°46,4'N	20°44,4'W		3xPN, GFO, 3xMC
218	27.05.	55°00,4'N	19°59,5'W	1750	CTD
219	28.05.	57°30,3'N	19°55,5'W	1150	2xMSN, 3xPN, CTD, ISP
220	29.05.	59°15,5'N	19°59,0'W	2800	MC
221	29.05.-	59°29,8'N	19°59,9'W	2800	ISP
	30.05.				
222	30.05.	59°15,5'N	19°55,5'W	2800	MC
223	30.05.-	59°30,0'N	20°00,1'W	2800	2xMSN, CTD,
	31.05.				GFO, 3xPN, CTD, 3xMSN, ISP

List of gears:

CTD = Kranzwasserschöpfer (12 bzw. 24 Flaschen) mit CTD-Sonde
MSN = Multi-Schließnetz
PN = Plankton-Netz
GFO = Goflo-Wasserschöpfer
GS = 400 L-Gerard-Schöpfer
ISP = In-situ-Pumpen
MC = Multicorer

7.3.2 List of water stations (JGOFS)

CTD = Multisonde m. Kranzwasserschöpfer
MSN = Multischließnetz
GFS = Goflow-Wasserschöpfer
APN = Apsteinnetz
SD = Secchi-Disk
RO = Schöpfer-Rosette

FD = Fallen-Drifter
GWS = Großraum-Wasserschöpfer
PN = Planktonnetz
LLV = Langleinenverankerung
DRIFT = Long-Term Drifter and Day Drifter
GRID = CTD-profile on a grid or section

Profile	Station	Date	Time (UTC)	Latitude	Longitude	Notes	Water-depth/m	Wire-cable-length/m
110	199	10-MAY-1992	23:22	33 N 56.03′	21 W 50.14′	CTD,MSN,GWS	5408	5360
111	199	11-MAY-1992	10:15	33 N 56.56′	21 W 51.29′	CTD,GFO,MSN	5409	5000
112	202	14-MAY-1992	10:50	40 N 0.07′	20 W 0.19′	CTD,MSN,GFO	4706	4651
113	202	15-MAY-1992	10:20	40 N 0.03′	20 W 1.52′	CTD,GWS,MSN	4789	300
114	204	18-MAY-1992	7:45	47 N 47.18′	19 W 45.00′	CTD	4541	4563
115	211	20-MAY-1992	16:30	47 N 35.06′	19 W 29.85′	CTD,MSN	4545	4620
116	211	21-MAY-1992	0:10	47 N 40.20′	19 W 29.20′	CTD,GWS,GFO, MSN	4539	500
117	213	23-MAY-1992	8: 5	49 N 59.92′	20 W 0.26′	CTD,PN	4383	500
118	213	23-MAY-1992	10:55	50 N 0.17′	19 W 59.91′	CTD	4377	4389
119	214	24-MAY-1992	3:33	52 N 30.14′	20 W 0.04′	CTD,PN,SD, MSN,GFO	2781	2676
120	215	25-MAY-1992	5:10	54 N 30.16′	21 W 0.13′	CTD	2966	2941
121	216	26-MAY-1992	4:55	54 N 39.82′	21 W 8.79′	CTD,MSN	3040	2995
122	218	27-MAY-1992	13:10	55 N 0.09′	19 W 59.98′	CTD	1622	1581
123	219	28-MAY-1992	6:45	57 N 30.37′	19 W 57.93′	CTD,MSN,PN	1146	1126
124	223	30-MAY-1992	12:10	59 N 29.25′	19 W 59.50′	CTD,MSN,GFO	2775	2748
125	223	31-MAY-1992	6:00	59 N 18.82′	19 W 42.31′	CTD,PN,MSN, GFO	2765	2500

7.3.3 **List of benthic sampling stations** (BIO-C-FLUX)

Date 1992	Ship's Station	Coordinates	Gear-No.	Sounding Depth (m)
10.05.	198	33°48,23'N 21°55,51'W	MC 401	5287
		33°47,91'N 21°56,97'W	MC 402	5339
12.05.	200	33°48,75'N 21°55,56'W	MC 403	5408
		33°48,31'N 21°57,40'W	MC 404	5312
14.05.	201	39°51,64'N 20°02,55'W	MC 405	4679
15.05.	202	39°59.84'N 20°00,55'W	MC 406	4725
20.05.	209	47°10.79'N 19°33,46'W	MC 407	4568
		47°10,91'N 19°33,86'W	MC 408	4568
22.05.	212	47°10,88'N 19°33,68'W	MC 409	4568
		47°10,99'N 19°33,53'W	MC 410	4568
		47°10,93'N 19°33,67'W	MC 411	4568
		47°11,05'N 19°33,61'W	MC 412	4568
27.05.	217	54°46,38'N 20°44,36'W	MC 413	2751
		54°47,06'N 20°43,90'W	MC 414	2758
29.05.	220	59°15,01'N 19°58,61'W	MC 415	2777
		59°13,56'N 19°57,19'W	MC 416	2771
30.05.	222	59°15,37'N 19°59,59'W	MC 417	2779
		59°14,18'N 19°57,55'W	MC 418	2779

7.4 Station list leg M 21/4

List of gear and abbreviations:

AG	Agassis-Trawl	Profil	Profilfahrt
BG	Backengreifer	MN	Multinetz
WS	Bodenwassergreifer	OBS	Ocean Bottom Seismograph
CTD	Sonde mit Trübungssensor und Kranzwasserschöpfer	PS	Parasound Sedimentecholot
		RL	Rumohr-Lot
DRG	Dredge, meist Dreiecksdredge	RN	Radiolarien-Netz
EBS	Epibenthos-Schlitten	UW-Fo.	Unterwasser-Foto
GKG	Großkastengreifer	UW-Ka.	Unterwasser-Kamera
HS	Hydrosweep Fächerlot	Video	Video
KAL	Kastenlot	WS	Wasserschöpfer
KOL	Kolbenlot		

GIK Proben-Nummer des Geologisch-Paläontologischen Instituts und Museums der Universität Kiel

UTC+2h Bordzeit=Mitteleuropäische Sommerzeit

Stations-Nos. M21	GIK	Datum 1992	Gerät	Zeit UTC	Geograph. Positionen Breite °N	Länge °E/W*	Wasser-tiefe (m)	Seil-länge (m)	Bemerkungen Eindr./Gewinn (cm) / (cm)
224	23420-1	07.06	CTD	04:07	62°30.10	13°59.56*	1488	1450	25,50,100,150, 200,300,500, 1000,1450m
	23420-2		MN	05:09	62°30.16	13°59.54*	1483		
			MN	05:50	62°30.69	13°59.69*	1480		100,700
	23420-3		RN	07:42	62°31.27	14°00.47*	1000		1000-500m,
	23420-4		GKG	10:20	62°30.31	13°59.34*	1475		18/18
225	23421-1	08.06	CTD	00:06	63°59.80	09°59.50*	662	666	20,40,60,80m, 100,150,200m, 250,300,400m, 500,600,630m
	23421-2		MN	01:04	64°00.14	09°59.23*	664.9		100,700m

7.4 Fortsetzung/continued

Stations-Nos. M21	GIK	Datum 1992	Gerät	Zeit UTC	Geograph. Positionen Breite °N	Länge °E/W*	Wassertiefe (m)	Seillänge (m)	Bemerkungen Eindr./Gewinn (cm) / (cm)
	23421-3		RN	02:45	64°00.20	09°58.02*	600		50,300,600m
	23421-4		GKG	04:39	64°00.19	09°5.793*	658		20/20, nicht vollständig geschlossen
226	23422-1	09.06	AGT	13:05	64°28.36	08°14.63*	2201		
227		09.06	Profil	00:55	65°25.50	04°10.30*			Beginn Profil
				01:40	65°30	04°00*			Ende Profil
		09.06	Profil	01:48	65°30	04°00*			Fortsetzen d. Profilfahrt
				02:23	65°31.60	04°08.80*			Ende Profil
	23423-1		CTD	05:05			3131	3136	keine Proben, da nur 4 geschlossen und unklar welche
	23423-2		MN	07:10	65°30.93	03°58.30*	3117		
			MN	07:45	65°31.17	03°58.08*	3111		
	23423-3		GKG	09:45	65°31.75	04°06.33*	2788		47/47
	23423-4		KAL	12:11	65°31.07	04°06.03*	2717		500/475
	23423-5		CTD	17:12	65°31.88	03°59.04*	3110		10,15,20,50m, 100,200,400m, 600,800m
228	23424-1	10.06	CTD	20:22	70°00.09	00°00.08*	3291		nur 2 Behälter geschlossen
	23424-2		MN	23:09	70°01.17	00°03.65*		3290	
			MN	23:38	70°01.38	00°04.01*		3291	
	23424-3	11.06	GKG	01:17	70°02.14	00°03.95*		3247	65/65
			Profil	02:28	70°02.60	00°01.90			Beginn Profil 21-1
				10:10	70°42	03°49			Kursänderung 056°

				10:20	70°44	03°44		Kursänderung 281°
				12:28	70°48.90	02°44.91		Ende Profil 21-1
229	23425		AGT					
230	23426-1	12.06	RN		72°14.84	11°00.15	2139	500,1000m
	23426-2		MN	12:21	72°14.32	11°01.24	2137	
			MN	12:57	72°14.35	11°01.46	2136	700m
	23426-3		CTD		72°14.37	11°01.47	2130	10,25,40,60, 600,800, 1000,1500, 2000,2084
	23426-4		GKG	16:08	72°14.62	11°04.47	2075	55/47
231	23427	13.06	CTD		73°51.10	21°37.58	490	10,15,20,30, 40,50,60,80, 100,20,300, 350,400,450, 481
			MN	08:42	73°37.98	20°09.17	485	
232		13.06	Profil	12:30	73°51	21°38.70		Beginn Such profil
				13:56	74°07.80	20°53.30		Kursänderung auf 270°
				14:57	74°08.00	20°53.30		Ende Such-profil
	23428-1		CTD		74°07.92	21°08.55	349	10,20,40,60
	23428-2		GKG		74°07.88	21°08.85	335	47/45
	23428-3		KAL	17:12	74°07.81	21°08.85	334	790/757
233	23429-1	13.06	Video		74°34.80	21°00.05	102	
	23429-2		UW-Fo.		74°34.80	21°00.05		
	23429-3		BG	22:08	74°34.82	21°00.18	100	
	23429-4		BG	22:14	74°34.84	21°00.33	104	

7.4 Fortsetzung/continued

Stations-Nos. M21	GIK	Datum 1992	Gerät	Zeit UTC	Geograph. Positionen Breite °N	Länge °E/W*	Wassertiefe (m)	Seillänge (m)	Bemerkungen Eindr./Gewinn (cm) / (cm)
234	23430-1	13.06	UW-Ka.	23:18	74°40.95	20°48.09		80	
	23439-2	14.06	Video	00:17	74°40.76	20°49.98		89	
	23430-3		BG	00:35	74°40.67	20°49.98		80	
	23430-4		BG	00:42	74°40.63	20°50.23		81	
235	23431-1	14.06	UW-Fo.	01:50	74°46.49	20°36.43	61	58	
	23431-2		BG	02:03	74°46.20	20°37.13		60	
	23431-3		BG	02:07	74°46.20	20°37.30		59	
	23431-4		Video						
236	23432-1	14.06	Video	03.35	74°51.98	20°24.59	54		
	23432-2		BG	03:52	74°51.78	20°24.91		57	
	23432-3		BG						Gerät defekt
237	23433-1	14.06	BG	05:17	75°01.85	20°15.77		43	
	23433.2		BG	05:21	75°01.79	20°15.77		44	
	23433-3		BG	05:26	75°01.70	20°15.55		43	
238	23434-1	14.06	Video	08:20	74°37.09	20°12.36		81	
	23434-2		BG	08:54	74°37,35	20°12.49		82	
	23434-3		BG						
			Profil	09:15	74°37	20°12			Beginn Profil 21-6
				12:29	74°42	18°20			Ende Profil 21-6
239		14.06	Profil	12:29	74°42	18°20			Beginn Profil 21-7
				13:22	74°42.10	17°47			Ende Profil 21-7
240	23435-1	14.06	GKG	14:19	74°49.60	17°47.90	309	310	Biologie, GKG-Einsatz

241	23436-1	14.06	GKG		74°49.51	17°48.04		Biologie, GKG-Einsatz
242		14.06	Profil	15:42	74°54	17°41.50		Beginn Profil 21-8
				16:36	74°54	18°20		Ende Profil 21-8
243		14.06	Profil	16:49	74°54	18°20		Beginn Profil 21-9
				17:49	74°55.50	17°40		Ende Profil 21-9
244		14.06	Profil	18:04	74°57	17°40		Beginn Profil 21-10
				19:03	74°57	18°20		Ende Profil 21-10
245		14.06	Profil	19:03	74°57	18°20		Beginn Profil 21-11
				19:43	74°52.50	18°40		Ende Profil 21-11
246		14.06	Profil	19:48	74°52.50	18°40		Beginn Profil 21-12
		15.06		00:45	74°52.60	15°30.20		Ende Profil 21-12
247	23437-1	15.06	UW-Fo.		74°	15°		
	23437-2		CTD	04:06	74°55.52	15°22.44	860	10,20,35,45, 400,500,600, 700,800,857
	23437-3		MN	04:59	74°55.84	15°24.15	841	
			MN	05:32	74°55.99	15°24.75	833	
	23437-4		GKG	06:45	74°54.97	15°20.14	899	Biologie, GKG-Einsatz

7.4 Fortsetzung/continued

Stations-Nos. M21	GIK	Datum 1992	Gerät	Zeit UTC	Geograph. Positionen Breite °N	Länge °E/W*	Wasser-tiefe (m)	Seil-länge (m)	Bemerkungen Eindr./Gewinn (cm) / (cm)
248		15.06	OBS	10:20	74°41.30	14°00			
249		15.06	Profil	17:55	74°57	14°51			Beginn Profil 21-13a
				18:40	75°03	14°31.50			Ende Profil 21-13a
				18:45	75°02.70	14°49.50			Beginn Profil 21-13b
				19:32	74°56.40	14°53.50			Ende Profil 21-13b
				19:41	74°57	14°53.50			Beginn Profil 21-13c
				20:45					Profil 21-13c abgebrochen
250	23438-1	15.06	CTD	21:00	74°59.28	14°47.26	1281		10,20,30,40, 50, 100,250, 500,800, 1266
	23438-2		MN	22:22	75°00.07	14°45.05		100	
	23438-3		UW-Fo.						
	23438-4	16.06	GKG	02:35	75°00.43	14°41.25		1269	
	23438-5		GKG	03:40	75°00.51	14°42.03		1264	
251		16.06	Profil	06:30	74°55	15°20			Beginn Profil 21-14
				07:36	74°57	15°56			Ende Profil 21-14
252		16.06	Profil	07:36	74°57	15°56			Beginn Profil 21-15

				09:15	74°50	15°47			Ende Profil 21-15
253		16.06	CTD	09:02					
			Foto	09:26					
254	23439-1	16.06	CTD	10:55	74°54.42	15°52.29		372	1 Probe bodennah
	23439-2		UW-Fo						
	23439-3		GKG	12:25	74°54.32	15°52.29		390	
255	23440-1	16.06	CTD	13:15	74°54.83	15°52.93	361	360	1 Probe bodennah
	23440-2		UW-Fo.	13:45					
256		16.06	Profil	14:30	74°51.80	15°53.60			Beginn Profil 21-16
				15:49	74°46.50	16°40.50			Ende Profil 21-16
257		16.06	Profil	15:49	74°46.50	16°40.50			Beginn Profil 21-17
				16:50	74°46.50	17°20			Ende Profil 21-17
258		16.06	Profil	17:00	74°45	17°26			Beginn Profil 21-18
				18:10	74°54.10	17°25.80			Ende Profil 21-18
259	23441-1	16.06	CTD	18:50	74°52.47	17°25.72	321	300	1 Probe bodennah
	23441-2		UW-Fo.	19:05					
	23441-3		GKG	20:01	74°52.39	17°25.06		317	nicht geschlossen
	23441-4		GKG	20:15	74°52.34	17°24.84		315	
260	23442-1	16.06	CTD	21:00	74°50.43	17°27.07		304	1 Probe bodennah

7.4 Fortsetzung/continued

Stations-Nos. M21	GIK	Datum 1992	Gerät	Zeit UTC	Geograph. Positionen Breite °N	Länge °E/W*	Wassertiefe (m)	Seillänge (m)	Bemerkungen Eindr./Gewinn (cm) / (cm)
	23442-2		RL						80/64
261	23443-1	16.06	CTD	23:55	74°46.52	17°24.61		304	1 Probe bodennah
	23443-2		RL		74°46.45	17°25.06	301	301	27/17
262		17.06	Profil	00:35	74°45	17°27.40			Beginn Profil 21-19
				01:16	74°45.50	17°27.20			Ende Profil 21-19
263	23444-1	17.06	CTD	01:22	74°45.31	17°47.28		260	1 Probe bodennah
	23444-2		RL	02:44	74°45.69	17°46.73	260	80	
264	23445-1	17.06	CTD	03:18	74°47.46	17°47.00		297	1 Probe bodennah
	23445-2		RL	04:40	74°47.62	17°46.36	299.9		/60
265		17.06	CTD	05:15	74°44.54	17°47.01		315	1 Probe bodennah
266	23446-1		CTD	05:50	74°50.73	17°47.22		315	1 Probe bodennah
	23446-2	RL		06:32	74°50.71	17°47.57	318	317	/25 Kernverlust durch Ausrutschen des Sediments, obere cm stark wassergesättigt
267	23447-1	17.06	CTD	06:57	74°51.33	17°46.93		324	1 Probe bodennah
			RL	07:26	74°51.32	17°46.76	325	319	/60
268	23448-1	17.06	CTD	08:12	74°52.27	17°46.91		318	

			RL	08:18	74°52.30	17°46.87	313	313	/60, Ton siltig sandig
269		17.06	Profil	08:50	74°53	17°40			Beginn Profil 21-20
				09:25	74°53	18°03			Ende Profil 21-20
270		17.06	Profil	09:25	74°53	18°03			Beginn Profil 21-21
				10:05	75°00	18°03			Ende Profil 21-21
271		17.06	Profil	10:15	74°59.50	20°18.10			Beginn Profil 21-22
				10:50	74°59.50	17°45			Ende Profil 21-22
272	23449-1	17.06	CTD	11:06	74°59.58	17°53.68		147	
	23449-2		Video	11:51	74°59.60	17°52.79	149	149.3	
	23449-3		Video	12:16	75°00.89	17°48.55		118.2	
	23449-4		BG	12:58	75°01.13	17°48.80		127.9	
	23449-5		BG	13:18	75°01.14	17°48.81		127.7	
	23449-6		BG	13:21	75°01.04	17°48.40		117.7	
	23449-7		BG	13:27	75°00.99	17°48.29		114.8	
	23449-8		GKG	14:02	74°59.59	17°53.33		141	27/27
	23449-9		UW-Fo						
	23449-10		RL	15:09	74°59.37	17°58.27		157	90/70
273	23450-1	17.06	Video	16:19	75°04.69	18°13.70	75	71	
	23450-2		BG	16:47	75°04.70	18°14.28	74.5		
	23450-3		BG	16:54	75°04.72	18°14.38			
274	23451-1	17.06	BG	17:46	75°08.55	18°34.47		39	
	23451-2		Video						
275	23452-1	18.00	CTD	03:30	75°45.42	12°17.39	1804	1804	10,30,55, 65,80,100, 200,300,400, 500,800,1200, 1800

7.4 Fortsetzung/continued

Stations-Nos. M21	GIK	Datum 1992	Gerät	Zeit UTC	Geograph. Positionen Breite °N	Länge °E/W*	Wassertiefe (m)	Seillänge (m)	Bemerkungen Eindr./Gewinn (cm) / (cm)
	23452-2		MN	05:11	75°54.99	12°12.84		1856	
			MN	05:44	75°55.10	12°11.73		1863	
276		18.06	Profil	11:10	76°20	8°39			Beginn Profil 21-23
				12:59	76°32.50	8°47.20			Ende Profil 21-23
277	23453-1	18.06	GKG	14:36	76°28.59	8°44.25	2016	2016	51/43
	23453-2		KAL	16:39	76°28.60	8°44.72		2094	610/361
	23453-3		CTD	18:45	76°31.98	8°36.87		2310	10,20,40,55, 70,80,100, 200,300,400, 500,600,800, 1000,1500, 2000,2260
	23453-4		MN	21:30	76°32.14	8°37.39		2310	
			MN	23:08	76°32.29	8°37.55		2311	
			MN	23:43	76°32.41	8°37.38		2311	
	23453-4	19.06	RN	0:52	76°32.84	8°37.88		2312	0-500,500-1000
278		19.06	Profil	04:04	76°48.5	8°54			Beginn Profil 21-24
				05:18	76°48.5	8°54			Ende Profil 21-24
279		19.06	Profil	05:18	76°48.5	8°54			Beginn Profil 21-25
				06:22	76°52.50	8°23.50			Ende Profil 21-25
280		19.06	Profil	06:22	76°52.50	8°23.50			Beginn Profil 21-26
				07:30	76°45.50	8°12.70			Ende Profil

								21-26
281	23454-1	19.06	KAL		76°45.10	8°92.60	2144	675/361
	23454-2		GKG	11:06	76°44.98	8°11.75	2126	41/41
	23454-3		SL		76°45.10	8°12.00	2130	
	23454-4		CTD					Sonde nicht ausgesetzt, da kein "clean ship" möglich
282	23455-1	19.06	CTD	15:23	76°51.19	8°22.15	2495	10,20,40,60, 80,100,200, 300,400,500, 600,800, 1000,1250, 1500,2000
	23455-2		GKG	17:49	76°52.04	8°24.31	2362	44/44
	23455-3		KAL	20:16	76°50.90	8°21.68	2497	650/592
283		20.06	Profil	00:54	77°13.20	6°26.80		Beginn Profil 21-27
				03:22	76°53.80	6°18.80		Ende Profil 21-27
284	23456-1	20.06	CTD	05:02	77°03.85	6°22.11	2196 2199	10,20,30,40, 50,60,70,80, 90,100,200, 300,400,500, 600,800,1000, 1250,1500,2000
	23456-2		MN	05:50	77°03.65	6°22.11	2199	700-0, 100-0
			MN	06:33	77°04.71	6°20.86	2149	
	23456-3		RN	07:05	77°03.85	6°22.11	2199	1000-500,500-0
	23456-4		RN	09:01	77°03.85	6°22.11	2199	500-0
	23456-5		KAL	11:31	77°04.02	6°20.47	2182	650/634
	23456-6		GKG	13:30	77°04.00	6°21.80	2200	54/42
	23456-7		GKG		77°04.18	6°21.52	2140	Biologie, GKG-Einsatz
	23456-8		SL					
			Profil	19:18	77°06	6°20		Beginn Profil

7.4 Fortsetzung/continued

Stations-Nos. M21	Stations-Nos. GIK	Datum 1992	Gerät	Zeit UTC	Geograph. Positionen Breite °N	Länge °E/W*	Wassertiefe (m)	Seillänge (m)	Bemerkungen Eindr./Gewinn (cm) / (cm)
									OBS A
				19:41	77°02	6°20			Ende Profil OBS A
			Profil	19:45	77°02	6°22			Beginn Profil OBS B
				20:08	77°06	6°22			Ende Profil OBS B
			Profil	21:12	77°06	6°24			Beginn Profil OBS C
				21:45	77°02	6°24			Ende Profil OBS C
			Profil	22:00	77°03	6°30			Beginn Profil OBS D
				22:18	77°04.50	6°15			Ende Profil OBS D
285			Profil	12:48	76°33.50	6°24.60			Beginn Profil 21-28
				13:26	76°26.60	6°23.90			Kursänderung auf 135°
				14:50	76°38	6°24			Ende Profil 21-28
286	23457-1	21.06	KAL	15:57	76°38.12	6°23.84	2250	2252	leer
	23457-2		KAL	18:08	76°38.20	6°23.80		2253	775/658
	23457-3		GKG	20:01	76°38.20	6°24.30		2259	44/40
	23457-4		CTD	21:28	76°39.12	6°42.73		2600	10,30,45,55,60 80,100,250,500, 750,1000,1500, 2000
		22.06	MN	01:39	76°40.97	6°46.66		2547	
			MN	02:15	76°41.25	6°47.35		2526	

287			Profil	05:10	76°13	6°21			Beginn Profil 21-29
				06:39	76°00	5°38			Ende Profil 21-29
288			Profil	06:39	76°00	5°38			Beginn Profil 21-30
				07:41	76°00	6°25			Ende Profil 21-30
289	23458-1	22.06	CTD	08:40	75°59.91	6°21.99	2199	2199	80,90,100,200, 300,400,500, 600,800,1000, 1250,1500,2000
	23458-2		MN	09:38	75°59.49	6°23.65		2159	
	23458-3		GKG	11:52	75°59.50	6°21.42		2192	44/44
	23458-4		KAL	13:54	75°59.67	6°21.35		2197	
290		22.06	Profil	17:00	75°50.50	4°59.60			Beginn Profil 21-31
				17:10	75°50	4°51.80			
				17:50	75°45.80	4°48.20			Ende Profil 21-31
291	23459-1	22.06	KAL	20:13	75°52.44	5°30.63		2622	705/593
	23459-2		GKG	22:18	75°52.54	5°28.98		2574	56/56
292		24.06	Profil	00:00	74°54	10°45			Beginn Profil 21-32a
				00:40	74°54	11°10			Ende Profil 21-32a
			Profil	00:47	74°53	11°10			Beginn Profil 21-32b
				01:24	74°53	10°45			Ende Profil 21-32b
294	23461-1	26.06	RL	15:42	67°48.10	6°50.23			100/20, Sedi ment z.T. rausgerutscht

7.4 Fortsetzung/continued

Stations-Nos. M21	GIK	Datum 1992	Gerät	Zeit UTC	Geograph. Positionen Breite °N	Länge °E/W*	Wasser-tiefe (m)	Seil-länge (m)	Bemerkungen Eindr./Gewinn (cm) / (cm)
295	23462-1	26.06	RL	17:17	67°43.10	6°50.64	1283	1282	100/90
	23462-2		KAL		67°43.50	6°51.30		1277	700/425
296	23463-1	26.06	RL	20:55	67°35.90	6°53.05	1229	1228	100/90
297	23464-1	26.06	RL	21:51	67°32.94	6°50.05	1253	1253	100/90
298	23465-1	26.06	RL	22:46	67°30.92	6°59.45	1304	1304	
299		26.06	Profil	23:30	67°30	7°00			Beginn Profil 21-33
		27.06		01:49	67°54.90	7°00			Ende Profil 21-33
300		27.06	Profil	02:00	67°54.80	7°04.90			Beginn Profil 21-34
				04:05	67°33	7°05			Ende Profil 21-34
301		27.06	Profil	04:05	67°33	7°05			Beginn Profil 21-35
				06:25	67°33	6°00			Ende Profil 21-35

7.5 Station list leg M 21/5

List of gear and abbreviations:

AG	Agassis-Trawl	Profil	Profilfahrt
BG	Backengreifer	MN	Multinetz
WS	Bodenwassergreifer	OBS	Ocean Bottom Seismograph
CTD	Sonde mit Trübungssensor und Kranzwasserschöpfer	PS	Parasound Sedimentecholot
		RL	Rumohr-Lot
DRG	Dredge, meist Dreiecksdredge	RN	Radiolarien-Netz
EBS	Epibenthos-Schlitten	UW-Fo.	Unterwasser-Foto
GKG	Großkastengreifer	UW-Ka.	Unterwasser-Kamera
HS	Hydrosweep Fächerlot	Video	Video
KAL	Kastenlot	WS	Wasserschöpfer
KOL	Kolbenlot		

GIK Proben-Nummer des Geologisch-Paläontologischen Instituts und Museums der Universität Kiel

UTC+2h Bordzeit=Mitteleuropäische Sommerzeit

Zeitangaben:

Bodenkontakt	GKG, KAL, MC, SL, UWP, BWS
Beginn des Einsatzes	CTD, MSN, ISP, RN, GWS
Anfang und Ende des Einsatzes	PS+HS+SBP, EBS, AGT

Anmerkung: Profile vorn als zweistellige Zahl, hinten mit Leg-Nummer, Stationen vorn als dreistellige Zahl.

Stations-Nos. M21	GIK	Datum 1992	Gerät	Zeit UTC	Geograph. Positionen Breite °N	Länge °E/W*	Wasser-tiefe (m)	Seil-länge (m)	Bemerkungen Eindr./Gewinn (cm) / (cm)
315	23467-1	03.07.	CTD	19:08	66°40.0	04°54.8	1143	1100	
	23467-2		GKG	20:25	66°40.2	04°55.0	1142	1133	--/49
316	23468-1	03.07.	SL	22:15	66°40.7	04°34.6	1223	1218	1250/650
36		03.07.	PS,HS	23:35	66°39.0	04°38.0			Profil 21-36

7.5 Fortsetzung/continued

Stations-Nos. M21	Stations-Nos. GIK	Datum 1992	Gerät	Zeit UTC	Geograph. Positionen Breite °N	Geograph. Positionen Länge °E/W*	Wassertiefe (m)	Seillänge (m)	Bemerkungen Eindr./Gewinn (cm) / (cm)
		04.07.		01:50	66°39.0	04°32.0			Profil-Ende
317	23469-1	04.07.	CTD	08:15	67°37.2	05°46.9	1408	1377	
			MSN	09:35	67°37.5	05°46.3	1410	100	
			MSN	09:55	67°37.5	05°46.3	1409	700	
			GKG	11:19	67°39.1	05°44.9	1415	1405	--/40
			MC	12:36	67°39.2	05°45.1	1411	1424	--/15
			MC	13:48	67°39.2	05°45.5	1412	1412	--/15
			UWP	14:57	67°39.1	05°45.3	1416	1152	
			BWS	16:50	67°39.2	05°43.3	1425	1443	
			EBS	18:08	67°39.3	05°41.7	1353	2001	
				20:35	67°41.1	05°39.0			
37		04.07.	PS,HS	21:40	67°44.0	05°58.0			Profil 21-37
				24:00	67°50.0	05°58.0			Profil-Ende
318		05.07.	ISP	00:35	67°46.3	05°55.5	1286	1120	
	23470-1		CTD	05:52	67°46.2	05°55.2	1282	1000	
	23470-2		RN	07:00	67°46.2	05°55.3	1278	1000	
			RN	09:30	67°46.3	05°55.6	1291	500	
	23470-3		SL	11:11	67°46.4	05°55.5	1291	1274	1300/707
319	23471-1	05.07.	CTD	19:06	67°13.5	02°55.5	1307	1200	
			MSN	20:05	67°13.4	02°54.7	1307	100	
			MSN	20:20	67°13.4	02°54.7	1307	700	
			MSN	21:20	67°13.4	02°54.7	1309	100	
	23471-2		RN	21:40	67°13.2	02°57.7	1309	1000	
			RN	23:45	67°13.2	02°55.1	1308	500	
38		06.07.	PS,HS	01:15	67°10.0	03°00.0			Profil 21-38
				03:19	67°16.0	03°00.0			Profil-Ende
320	23472-1	06.07.	SL	04:27	67°13.2	02°56.2	1299	1293	1250/607
321		06.07.	AGT	08:20	67°44.0	02°09.5	1843	3000	
				11:10	67°43.4	01°58.5			
322	23473-1	06.07.	CTD	18:05	68°43.8	00°09.8	2435	2300	
	23473-2		RN	19:44	68°43.8	00°09.9	2395	1000	

			RN	21:45	68°43.3	00°07.0	2401	500	
			MSN	22:40	68°43.2	00°07.0	2401	100	
			MSN	23:00	68°43.1	00°06.9	2400	700	
323	23474-1	07.07.	CTD	05:14	69°41.3	00°27.8	3291	3200	
			GWS	07:40	69°40.7	00°27.7	3290		Gerät defekt
			LB-6	11:05	69°41.9	00°25.5			Verankerung a.D.
			MSN	11:30	69°41.3	00°27.7	3290	100	
			MSN	11:50	69°41.2	00°27.9	3290	700	
			MC	13:47	69°41.4	00°27.6	3290	3255	--/37
	23474-2		MC	15:58	69°41.5	00°28.0	3308	3260	--/42
			GKG	17:58	69°41.2	00°27.6	3285	3234	>60/--
			UWP	20:25	69°40.9	00°27.5	3284	3283	
	23474-3		RN	22:30	69°41.0	00°26.9	3290	1000	
		08.07.	RN	00:27	69°41.0	00°26.7	3284	500	
			RN	01:18	69°41.2	00°26.6	3286	500	
			ISP	02:12	69°41.1	00°26.6	3289	2500	
			MSN	08:55	69°41.5	00°26.7	3285	2500	
			GWS	12:03	69°40.5	00°24.3	3283	1500	
			RN	13:14	69°40.4	00°24.5	3285	500	
			LB-7	18:20	69°41.4	00°28.9	3278		Verankerung i.W.
			SSS	20:50	70°01.3	00°25.4			Suche LB-5
				23:40	69°57.2	00°11.4	3282	6000	Bodensicht
		09.07.		08:00	69°57.1	00°19.9	3284	8195	maximale SL
				10:55	69°54.1	00°39.9			SSS a.D.
323		09.07.	Suchg.	13:00	69°58.9	00°19.3			Suchgeschirr v.D.
				14:40	diverse Kurse		3289	3650	maximale SL
				19:00					Suche Ende
324		09.07.	MSN	19:45	70°03.5	00°02.9	3273	100	
			MSN	20:15	70°03.5	00°02.9	3273	700	
	23475-1		SL	21.55	70°04.4	00°01.2	3272	3258	1200/787
39		10.07.	PS,HS	00:00	70°00.0	00°06.0			Profil 21-39
				01:46	70°06.0	00°06.0			Profil-Ende
325	23476-1	10.07.	CTD	12:47	70°45.2	05°29.5*	2407	1700	

7.5 Fortsetzung/continued

Stations-Nos. M21	GIK	Datum 1992	Gerät	Zeit UTC	Geograph. Positionen Breite °N	Länge °E/W*	Wassertiefe (m)	Seillänge (m)	Bemerkungen Eindr./Gewinn (cm) / (cm)
	23476-2		RN	14:13	70°45.6	05°30.1*	2383	1000	
			RN	16:06	70°46.3	05°31.0*	2385	500	
326		10.07.	MSN	18:12	70°57.4	05°33.3*	1710	100	
			MSN	18:30	70°57.3	05°33.0*	1713	700	
	23477-1		GKG	19:54	70°57.3	05°33.4*	1713	1690	--/48
			MC	21:35	70°57.4	05°32.9*	1711	1704	--/27
			UWP	22:50	70°57.6	05°32.7*	1700	1669	
			BWS	23:45	70°57.5	05°32.9*	1713	1740	
327	23478-1	11.07.	CTD	07:45	71°38.1	08°26.9*	1954	1815	
			MSN	09:07	71°38.1	08°26.7*	1950	100	
			MSN	09:23	71°38.0	08°26.7*	1951	700	
	23478-2		GKG	10:45	71°38.0	08°27.0*	1949	1927	--/46
	23478-3		KAL	12:07	71°38.5	08°27.3*	1950	1936	600/252
328		11.07.	OG-5	18:55	72°23.0	07°42.0*			Verankerung a.D.
	23479-1		CTD	19:15	72°22.7	07°42.1*	2595	2500	
			GWS	21:10	72°22.5	07°41.7*	2599	2200	
			MSN	23:00	72°22.8	07°43.3*	2612	2500	
		12.07.	ISP	02:02	72°22.6	07°41.8*	2589	2230	
	23479-2		RN	08:50	72:22.3	07°41.4*	2593	1000	
			RN	11:10	72°22.5	07°41.4*	2587	500	
			MSN	12:22	72°21.8	07°40.9*	2586	100	
			MSN	12:39	72°21.6	07°40.6*	2588	700	
			OG-6	15:46	72°21.6	07°36.1*	2626		Verankerung i.W.
			GWS	16:36	72°23.0	07°42.6*	2693	100	
	23479-3		MC	17:46	72°22.7	07°41.5*	2627	2567	--/34
			GKG	19:28	72°22.7	07°41.3*	2627	2582	--/32
			AGT	20:30	72°22.7	07°41.6*	2629	4300	
				23:50	72°19.5	07°55.1*			
40		13.07.	PS,HS,	17:36	69°27.5	10°37.0*			Profil 21-40
			SBP	18:12	69°22.9	10°47.1*			Profil-Ende

329		13.07.	MSN	18:12	69°22.9	10°47.1*	1768	100	
			MSN	18:32	69°23.0	10°47.0*	1771	700	
	23480-1		KAL	19:50	69°22.8	10°46.7*	1768	1741	250/0
	23480-2		KAL	20:35	69°22.7	10°46.7*	1766	1742	600/323
	23480-3		GKG	22:10	69°22.9	10°46.6*	1773	1735	--/46
41		13.07.	PS,HS,	22:45	69°23.0	10°47.0*			Profil 21-41
			SBP	23:20	69°21.0	11°00.0*			Profil-Ende
330	23481-1	14.07.	CTD	16:09	67°55.1	17°55.9*	1116	1085	
			MSN	17:04	67°55.1	17°56.7*	1111	100	
			MSN	17:24	67°55.1	17°56.7*	1112	700	
			BWS	19:20	67°54.7	17°58.0*	1122	1092	
			GKG	20:52	67°55.2	17°55.3*	1118	1097	--/51
	23481-2		GKG	21:35	67°53.5	17°55.2*	1120	1098	--/50
			GKG	22:20	67°55.6	17°55.2*	1135	1098	--/36
			MC	23:05	67°54.6	17°54.5*	1116	1094	--/33
			MC	24:00	67°54.9	17°54.1*	1119	1095	--/32
		15.07.	UWP	00:44	67°54.9	17°54.5*	1113	1086	
			ISP	01:28	67°54.6	17°54.9*	1105	1030	
	23481-3		RN	07:30	67°54.5	17°55.9*	1101	500	
			RN	08:50	67°54.5	17°56.1*	1103	200	
			EBS	09:25	67°54.6	17°56.1*	1127	1800	
				11:35	67°54.2	18°01.5*			
330		15.07.	AGT	12:08	67°54.7	17°55.7	1124	1800	
				13:51	67°53.7	18°01.3			
42		15.07.	PS,HS,	14:18	67°55.0	17°55.0			Profil 21-42
			SBP	15:40	67°55.0	18°30.0			Profil-Ende
331	23482-1	15.07.	CTD	16:42	67°54.9	18°45.9	920	911	
			MSN	17:33	67°54.5	18°46.2	915	100	
			MSN	17:50	67°54.3	18°46.3	918	700	
			BWS	18:49	67°54.0	18°46.3	906	515	Gerät defekt
			GKG	19:45	67°53.7	18°46.2	895	894	--/46
	23482-2		GKG	20:25	67°53.4	18°45.8	898	905	--/46
			GKG	21:20	67°54.1	18°44.4	907	912	--/47
			MC	22:05	67°53.8	18°43.9	904	903	--/10
			MC	22:50	67°53.5	18°43.4	910	912	--/12
			MC	23:25	67°53.0	18°42.6	848	885	--/10

7.5 Fortsetzung/continued

Stations-Nos. M21	Stations-Nos. GIK	Datum 1992	Gerät	Zeit UTC	Geograph. Positionen Breite °N	Länge °E/W*	Wassertiefe (m)	Seillänge (m)	Bemerkungen Eindr./Gewinn (cm) / (cm)
		16.07.	MC	00:20	67°53.0	18°43.4	894	908	--/10
			UWP	01:02	67°52.6	18°43.4	895	882	
			EBS	01:53	67°51.6	18°44.9	856	1250	
				03:27	67°50.9	18°46.8			
			AGT	03:55	67°51.9	18°44.4	876	1300	
				05:00	67°51.0	18°48.8			
	23482-3		RN	06:06	67°50.6	18°49.6	868	500	
			RN	07:20	67°50.5	18°49.5	863	200	
			GWS	07:54	67°50.2	18°49.4	858	800	
332	23483-1	16.07.	CTD	09:40	67°53.6	18°38.5	866	844	
			MSN	10:35	67°53.2	18°37.8	850	100	
			MSN	12:32	67°52.6	18°36.9	785	700	
			GKG	13:51	67°52.2	18°36.8	778	774	--/21
			GKG	14:51	67°51.8	18°36.9	801	787	--/0
	23483-2		GKG	15:22	67°51.6	18°36.9	818	818	--/50
			GKG	15:59	67°51.7	18°37.0	820	820	--/49
			MC	16:54	67°51.9	18°37.5	822	817	--/0
			MC	17:30	67°52.0	18°38.5	833	822	--/10
			MC	18:16	67°52.0	18°38.6	836	824	--/25
			UWP	19:03	67°52.0	18°39.1	839	831	
			AGT	19:45	67°51.3	18°39.4	835	1200	
				20:45	67°51.1	18°39.5			
			EBS	21:10	67°50.9	18°39.6	840	843	
				22:35	67°50.1	18°40.1			
43		16.07.	PS,HS,	22:55	67°50.7	18°38.0			Profil 21-43
		17.07.	SBP	04:15	67°50.4	18°38.0			Profil-Ende
333		17.07.	GWS	06:12	67°55.1	18°03.0	949	900	
	23484-1		CTD	06:57	67°55.1	18°02.7	947	936	
			MSN	08:05	67°55.5	18°02.1	939	100	
			MSN	08:30	67°55.6	18°02.1	930	700	
			GKG	09:40	67°55.8	18°02.0	929	915	--/51
	23484-2		GKG	10:20	67°56.1	18°02.4	930	917	--/51

			GKG	10:55	67°56.0	18°02.0	928	917	--/51
			MC	12:14	67°56.3	18°02.3	933	943	--/22
			MC	12:54	67°56.3	18°02.5	935	963	--/17
			EBS	14:17	67°56.2	18°02.8	931	1250	
				15:55	67°55.6	17°59.7			
			AGT	16:25	67°56.7	18°03.0	888	1304	
				17:38	67°57.5	17°59.6			
			BWS	18:27	67°56.4	18°02.4	935	918	
			EBS	19:17	67°56.4	18°02.4	993	1352	
				20:55	67°56.8	17°57.5			
			UWP	21:35	67°56.6	18°02.3	948	962	
			GWS	22:15	67°56.9	18°01.7	901	100	
44		17.07.	PS,HS,	23:00	67°54.5	17°55.0			Profil 21-44
		18.07.	SBP	02:55	67°54.1	17°55.0			Profil-Ende
45		18.07.	PS,HS	03:18	67°54.6	17°51.0			Profil 21-45
			SBP	05:23	67°55.8	17°51.0			Profil-Ende
334	23485-1	18.07.	SL	06:16	67°54.9	17°52.4	1120	1114	1200/926
335	23486-1	18.07.	CTD	08:00	67°55.0	18°07.4	818	803	
			MSN	08:50	67°54.9	18°07.3	820	100	
			MSN	09:15	67°55.1	18°07.5	823	700	
	23486-2		RN	10:15	67°55.2	18°07.4	832	500	
			RN	11:25	67°55.2	18°07.2	816	200	
			GKG	12:19	67°55.0	18°07.4	826	822	--/36
	23486-3		GKG	12:55	67°54.9	18°07.1	825	822	--/44
			GKG	13:34	67°55.1	18°07.3	819	818	--/0
			GKG	14:06	67°55.0	18°07.6	828	830	--/0
			GKG	14:41	67°55.0	18°07.2	823	821	--/48
			MC	15:22	67°54.9	18°07.3	821	837	--/15
			MC	16:05	67°54.9	18°07.3	818	807	--/15
			EBS	16:42	67°55.0	18°09.0	884	1200	
				18:12	67°54.9	18°02.8			
			AGT	18:36	67°54.9	18°07.2	810	1200	
				19:45	67°55.0	18°03.5			
			BWS	20:30	67°54.9	18°08.0	882	927	
			UWP	21:50	67°55.0	18°06.8	834	837	
			GWS	22:25	67°54.9	18°06.8	825	770	
336		19.07.	UWP	00:24	67°55.2	18°24.5	495	496	

7.5 Fortsetzung/continued

Stations-Nos. M21	Stations-Nos. GIK	Datum 1992	Gerät	Zeit UTC	Geograph. Positionen Breite °N	Geograph. Positionen Länge °E/W*	Wassertiefe (m)	Seillänge (m)	Bemerkungen Eindr./Gewinn (cm) / (cm)
			CTD	00:54	67°55.2	18°24.4	429	416	
337		19.07.	CTD	02:19	67°55.1	18°29.8	600	572	
			UWP	03:11	67°55.0	18°29.8	578	556	
338		19.07.	BWS	05:02	67°53.4	18°45.8	898	896	
			CTD	06:03	67°53.5	18°46.0	900	880	
339		19.07.	CTD	07:45	67°51.6	18°37.0	823	805	
			BWS	09:10	67°51.6	18°37.6	826	817	
340		19.07.	CTD	11:50	67°56.3	18°01.6	930	200	
			MSN	12:14	67°56.4	18°01.7	943	910	
			AGT	13:32	67°56.4	18°01.1	1126	1700	
				14:51	67°56.9	17°55.3			
46		20.07.	PS,HS,	01:06	67°19.1	14°22.8			Profil 21-46
			SBP	02:03	67°20.9	14°05.2			Profil-Ende
341		20.07.	GWS	02:57	67°20.2	14°11.7	1035	970	
	23487-1		CTD	04:05	67°20.1	14°11.4	1036	990	
			MSN	05:05	67°20.0	14°12.0	1036	100	
			MSN	05:20	67°20.3	14°12.4	1036	700	
	23487-2		GKG	06:42	67°20.3	14°11.8	1036	1006	--/48
	23487-3		KAL	08:05	67°20.2	14°11.5	1035	1008	540/98
	23487-4		SL	10:20	67°20.3	14°11.8	1035	1021	1250/704
47		20.07.	PS,HS,	11:00	67°20.0	14°14.0			Profil 21-47
			SBP	21:10	67°40.0	11°00.0			Profil-Ende
342	23488-1	20.07.	SL	22:25	67°39.5	11°04.7	1841	1808	1350/696
	23488-2		GKG	23:40	67°39.5	11°04.6	1841	1796	--/47
343	23489-1	21.07.	CTD	03:37	67°30.2	12°30.2	1775	1700	
			GWS	05:06	67°30.3	12°30.3	1777	1100	
	23489-2		GKG	06:35	67°30.3	12°30.1	1774	1727	--/41
	23489-3		SL	07:43	67°30.5	12°30.1	1775	1718	550/373

7.6. Station lists leg M 21/6

7.6.1 List of water stations (JGOFS)

CTD = Multisonde m. Kranzwasserschöpfer
MSN = Multischließnetz
GFS = Goflow-Wasserschöpfer
APN = Apsteinnetz
SD = Secchi-Disk

RO = Schöpfer-Rosette
FD = Fallen-Drifter
GWS = Großraum-Wasserschöpfer
PN = Planktonnetz
LLV = Langleinenverankerung

Profile	Station	Date	Time (UTC)	Latitude	Longitude	Notes	Water-depth/m	Wire-cable-length/m
126	345	28-JUL-1992	10:50	59 N 16.40′	21 W 4.50′	CTD,MSN	2877	2869
127	349	30-JUL-1992	23:15	54 N 59.90′	19 W 59.80′	CTD,MSN	1649	1630
128	350	31-JUL-1992	17:51	52 N 29.70′	20 W 0.00′	CTD,MSN	2796	2800
129	351	2-AUG-1992	4:29	47 N 10.90′	19 W 33.70′	CTD,MSN	4598	4567
130	358	3-AUG-1992	2:23	47 N 10.90′	19 W 33.60′	CTD,MSN	4566	1000
131	359	3-AUG-1992	13: 5	47 N 13.80′	20 W 8.80′	CTD	4501	1000
132	368	5-AUG-1992	22:25	47 N 7.90′	19 W 33.70′	CTD	4607	4563
133	373	7-AUG-1992	3:43	47 N 4.70′	19 W 40.90′	CTD,MSN	4480	2800
134	381	9-AUG-1992	15:12	47 N 14.60′	19 W 34.90′	CTD,MSN	4560	100
135	387	11-AUG-1992	17:47	47 N 12.60′	19 W 35.40′	CTD,MSN	4563	2500
136	396	13-AUG-1992	23:10	47 N 12.60′	19 W 35.10′	CTD,MSN	4563	2500
137	403	15-AUG-1992	21:30	47 N 20.70′	19 W 48.50′	CTD	4514	500
138	404	15-AUG-1992	23:25	47 N 20.60′	19 W 34.00′	CTD,MSN	4499	500
139	405	16-AUG-1992	1:35	47 N 20.50′	19 W 19.10′	CTD	4553	500
140	406	16-AUG-1992	3:21	47 N 10.50′	19 W 19.10′	CTD,MSN	4419	500
141	407	16-AUG-1992	5: 7	47 N 0.50′	19 W 19.00′	CTD	4552	500
142	408	16-AUG-1992	6:46	47 N 0.60′	19 W 33.90′	CTD,MSN	4552	500
143	409	16-AUG-1992	8:55	47 N 0.60′	19 W 48.60′	CTD	4163	500
144	410	16-AUG-1992	10:35	47 N 10.60′	19 W 48.50′	CTD,MSN	4492	500
145	416	17-AUG-1992	11:45	47 N 10.10′	19 W 33.80′	CTD	4569	4500
146	421	19-AUG-1992	11:20	47 N 43.30′	19 W 55.00′	CTD	4473	4380
147	424	19-AUG-1992	23:30	47 N 10.60′	19 W 34.60′	CTD,MSN	4565	2500
148	431	21-AUG-1992	5:55	47 N 9.90′	19 W 34.00′	CTD,MSN	4564	1000
149	442	22-AUG-1992	23:50	47 N 10.20′	19 W 33.10′	CTD,MSN	4567	2500

7.6.1 Fortsetzung/continued

Profile	Station	Date	Time (UTC)	Latitude	Longitude	Notes	Water-depth/m	Wire-cable-length/m
150	453	24-AUG-1992	11:15	47 N 10.80′	19 W 35.90′	CTD	4563	100
151	456	24-AUG-1992	15:53	47 N 10.20′	19 W 34.60′	CTD,MSN	4564	2500
152	459	25-AUG-1992	12:35	47 N 10.20′	19 W 33.30′	CTD	4564	100
153	461	25-AUG-1992	23:25	47 N 32.60′	19 W 57.00′	CTD,MSN	4505	1500

7.6.2 List of benthic sampling stations (BIO-C-FLUX)

Date 1992	Ship's Station	Coordinates		Gear-No.	Sounding Depth (m)
28.07.	345	59°16,13'N	21°04,84'W	MC 419	2880
		59°16,23'N	21°04,80'W	MC 420	2879
		59°16,06'N	21°04,91'W	MC 421	2878
29.07.	347	59°16,02'N	21°04,99'W	MC 422	2880
		59°16,12'N	21°04,77'W	MC 423	2879
02.08.	352	47°10,88'N	19°33,67'W	MC 424	4568
		47°10,81'N	19°33,79'W	MC 425	4568
	355	47°10,82'N	19°33,59'W	MC 426	4568
		47°10,72'N	19°33,68'W	MC 427	4568
03.08.	361	47°10,95'N	19°33,71'W	MC 428	4568
		47°10,88'N	19°33,78'W	MC 429	4568
05.08.	365	47°10,82'N	19°33,71'W	MC 430	4568
		47°10,59'N	19°33,92'W	MC 431	4568
08.08.	379	47°10,81'N	19°33,57'W	KG 1500	4568
		47°10,87'N	19°33,64'W	KG 1501	4568
		47°10,65'N	19°33,62'W	MC 432	4568
		47°10,39'N	19°33,72'W	MC 433	4568
09.08.	383	47°10,80'N	19°33,82'W	KG 1502	4568
		47°10,79'N	19°33,65'W	MC 434	4568
		47°10,87'N	19°33,58'W	MC 435	4568
10.08.	385	47°10,80'N	19°33,82'W	MC 436	4568
		47°10,77'N	19°33,53'W	MC 437	4568
11.08.	385	47°10,81'N	19°33,72'W	MC 438	4568
	388	47°10,76'N	19°33,77'W	MC 439	4568
12.08.	388	47°10,66'N	19°33,75'W	MC 440	4568
	390	47°24,01'N	19°46,77'W	MC 441	4568
		47°24,25'N	19°46,70'W	MC 442	4568
15.08.	399	47°10,77'N	19°34,25'W	MC 443	4568
		47°10,99'N	19°34,02'W	MC 444	4568
	401	47°10,83'N	19°33,68'W	KG 1503	4568
		47°10,83'N	19°33,78'W	MC 445	4568
17.08.	415	47°10,78'N	19°34,19'W	MC 446	4568
	417	47°10,80'N	19°33,64'W	MC 447	4568
		47°10,98'N	19°33,66'W	KG 1504	4568
		47°10,84'N	19°33,67'W	MC 448	4568
19.08.	423	47°10,76'N	19°33,68'W	MC 449	4568
		47°10,85'N	19°33,69'W	MC 450	4568
20.08.	427	47°10,78'N	19°33,73'W	MC 451	4568
		47°10,86'N	19°33,60'W	KG 1505	4568
22.08.	439	47°10,86'N	19°33,74'W	MC 452	4568
		47°10,81'N	19°33,74'W	MC 453	4568
	441	47°10,85'N	19°33,93'W	MC 454	4568
		47°10,86'N	19°33,75'W	MC 455	4568
		47°11,00'N	19°33,50'W	MC 456	4568
24.08.	445	47°10,78'N	19°33,77'W	MC 457	4568
25.08.	458	47°10,95'N	19°33,97'W	MC 458	4568

7.6.3 List of benthopelagic nekton and megafauna sampling stations (BIO-C-FLUX)

Geräteliste:
DOS = Tiefsee-Beobachtungssystem
FT = Fototrawl
FFLL = Freifall-Langleinensystem
RK = Reusenkette
OT = Ottertrawl
z.W. = zu Wasser
a.D. = an Deck
Positionen sind Aussetzpositionen

Datum 1992	Stat. Nr.	Gerät	Breite °N	Länge °W	Tiefe m
27.07.	344	OT 003	59°18.5′	20°35.2′	2850
28.07.	346	OT 004	59°16.5′	21°05.3	2880
02.08.	353	RK 113 z.W.	47°08.6′	19°34.4′	4571
03.08.	360	RK 113 a.D.			
04.08.	363	OT 005	47°33.1′	19°02.6′	4477
05.08.	366	RK 114 z.W.	47°04.6′	19°40.2′	4511
06.08.	370	RK 114 a.D.			
06.08.	372	DOS 005	48°10.8′	19°33.5′	4563
07.08.	374	DOS 006	47°19.1′	19°33.1′	4532
07.08.	375	DOS 007	47°24.9′	19°39.9′	4515
07.08.	375	DOS 008	47°24.3′	19°41.2′	4518-3880
08.08.	377	RK 115 z.W.	47°15.3′	19°34.4′	4560
09.08.	381	RK 115 a.D.			
10.08.	384	OT 006	47°10.9′	19°35.3′	4566
12.08.	391	RK 116 z.W.	47°18.9′	19°38.9′	4460
13.08.	394	RK 116 a.D.			
13.08.	395	FT 030	47°18.8′	19°12.7′	4555
14.08.	397	FT 031	47°25.8′	19°02.7′	4560
15.08.	400	RK 117 z.W.	47°10.9′	19°27.7′	4554
16.08.	412	RK 117 a.D.			
19.08.	422	RK 118 z.W.	47°17.9′	19°29.5′	4556
20.08.	426	FFLL 002 z.W.	47°10.1′	19°34.1	4565
20.08.	428	RK 118 a.D.			
20.08.	430	FT 032	47°24.0′	19°21.0	4554
21.08.	431	FFLL 002 a.D.			
21.08.	436	FT 033	47°23.3′	19°24.9′	4544-4220
23.08.	444	FFLL 003 z.W.	47°12.9′	19°33.9′	4562
23.08.	445	RK 119 z.W.	47°11.1′	19°35.7′	4569
23.08.	450	FFLL 003 a.D.			
24.08.	453	RK 119 a.D.			
25.08.	460	FT 034	47°32.0′	19°40.4′	4533

7.6.4 1m^2 double-MOCNESS-hauls during M 21/6

Times of sampling (UTC = local time) and positions refer to the opening and closing of quantitatively sampling nets. N = net, L = left net, R = right net, mab = meters above bottom. Station numbers are BIO-C-FLUX numbers.

Date 1992	Haul	Station No.	Time (UTC)	Position	Depth of sampling	Remarks
02.08.	MOC-D-01	480	20:55	47°11,5'N 19°35,1'W		electronics crashdown
04.08.	MOC-D-02 L2	484	01:20	47°09,5'N 19°37,4'W	1450 m to	left nets twisted
04.08.	MOC-D-02 L9,R9		03:43	47°06,3'N 19°42,0'W	0 m	
05.08.	MOC-D-03 L2	486	04:48	47°21,1'N 20°01,7'W	1450 m to	
05.08.	MOC-D-03 L9,R9		06:43	47°24,3'N 20°05,7'W	0 m	
09.08. bottom	MOC-D-04 L2,R2	505	06:08	47°24,5'N 19°22,8'W	4534 m to	L2+R2 2*20 mab
09.08.	MOC-1-82 L9,R9		08:40	47°27,0'N 19°26,6'W	4434 m	4*50 mab 4*100 mab
11.08.	MOC-D-05 L2	515	09:55	47°16,1'N 19°17,1'W	4500 m to	
11.08.	MOC-D-05 L9,R9	14:17		47°15,7'N 19°30,9'W	1050 m	
17.08.	MOC-D-06 L2	535	00:14	47°25,9'N 19°31,9'W	4500 m to	
17.08.	MOC-D-06 L9,R9		03:34	47°27,2'N 19°31,2'W	1050 m	
20.08.	MOC-D-07 L2	550	17:39	47°15,4'N 19°32,4'W	1450 m to	
20.08.	MOC-D-07 L9,R9		19:54	47°11,6'N 19°36,1'W	0 m	
23.08.	MOC-D-08 L2	564	07:30	47°12,4'N 19°33,6'W	1450 m to	
23.08.	MOC-D-08 L2,R9		09:52	47°17,4'N 19°33,6'W	0 m	
24.08.	MOC-D-09 L2	572	05:15	47°15,1'N 19°38,7'W	4500 m to	
24.08.	MOC-D-09 L9,R9		08:50	47°12,6'N 19°47,8'W	1050 m	
25.08.	MOC-D-10 L2,R9	575	03:04	47°16,5'N 19°29,5'W	4532 m to	4*20 mab 4*50 mab
25.08.	MOC-D-10 L9,R9		06:38	47°17,9'N 19°36,8'W	4452 m	4*100 mab

7.6.5 $10m^2$-MOCNESS-hauls during M 21/6

Times of sampling (UTC = local time) and positions refer to the opening and closing of quantitatively sampling nets. N = net, L = left net, R = right net, mab = meters above bottom. Station numbers are BIO-C-FLUX numbers.

Date 1992	Haul	Station No.	Time (UTC)	Position	Depth of sampling	Remarks
06.08.	MOC10-15	492	03:07	47°12,5'N 19°17,8'W		net release failed
08.08.	MOC10-16 N2	498	05:28	47°27,0'N 19°32,4'W	4509 m	4*20 mab
08.08.	MOC10-16 N5		07:28	47°27,6'N 20°00,1'W		
13.08.	MOC10-17 N2	523	02:38	47°15,6'N 19°20,1'W	4508 m	3*50 mab 1 cod end
13.08.	MOC10-17 N5		04:20	47°13,9'N 19°23,3'W		bucket lost
14.08.	MOC10-18 N2	528	20:48	47°22,3'N 19°55,6'W	4428 m	4*100 mab
14.08.	MOC10-18 N5		22:45	47°21,7'N 20°00,8'W		
21.08.	MOC10-19 N2	555	15:01	47°17,9'N 19°31,1'W	4526 m	3*10 mab 1 net bar
21.08.	MOC10-19 N5		16:35	47°21,5'N 19°32,9'W		cable torn

7.7 Kernbeschreibungen M 21/4 und M 21/5 (SFB 313)

Core Descriptions Legend

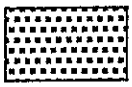
Sand

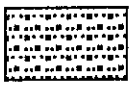
Silty Sand

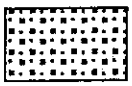
Sandy Silt

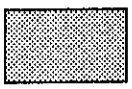
Silt

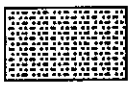
Silty Clay

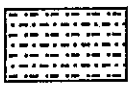
Clayey Silt


Clay

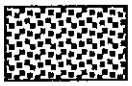
Ash


Continuous Laminae

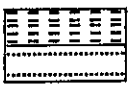
Stripes
Streaks


Tilted Layering

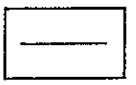
Horizontal sharp contact

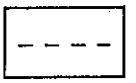
Horizontal gradational contact

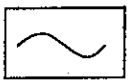
Uneven sharp contact

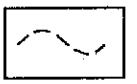
Uneven gradational contact

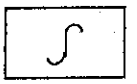
Weakly bioturbated

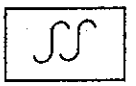
Bioturbated

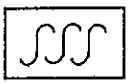
Strongly bioturbated


Grading
coarsening / fining upward


Sediment Pellets


Dropstones


Foraminifera


Coal/Black Shale


Shell

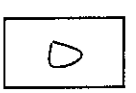
Chalk

Sediment colors according to Rock Color Chart (Geological Society of America)

Meteor 21/4	05.06.1992 -29.06.1992
Station: M 224/92	Date: 07.06.1992
Position: 62° 30´ 31 N ; 13° 59´ 34 W	Water Depth: 1475 m

Core: GIK 23420-4, GKG — Core Recovery: 18 cm
Section: 0 - 18 cm

Depth (cm)	Lithology	Structure	Colour	Description
			2.5 Y 4/3	0-2 cm: lag deposit*, densely colonised by benthic life**
			2.5 Y 4/3	2-8 cm: olive brown, weakly bioturbated, silty fine sand with rock and shell fragments 3 cm: 2 cm Ø rounded quartz dropstone 5 cm: sed. pellet
10			2.5 Y 4/3	8-15.5 cm: olive brown, weakly bioturbated clayey silt 10 cm: sed. pellet
		@ @ @	2.5 Y 5/4	15.5-18 cm: light olive brown Foraminifera layer with Pyrgo
20				EOC: 18 cm
30				*rock fragments (up to 2 cm Ø): basalt, reddish granite, some very rounded **Dead: coarse Balanides fragments, Pteropoda, Globigerina; living: chalk sponges (*Sycon*), Hadromerida, Demospargia, many Ophiuriden, 1 regular Edrinide, 1 Ascidie; agglutinated Polychaeta
40				

Meteor 21-4	05.06.1992 - 29.06.1992
Station: M 225/92	Date: 08.06.1992
Position: 64° 00´ 19 N ; 09° 5´ 79 W	Water Depth: 658 m

Core: GIK 23421-4, GKG — Core Recovery: 20 cm
Section: 0 - 20 cm

Depth (cm)	Lithology	Structure	Colour	Description
			5Y4/4	0-0.5 cm: olive silty clay with dropstones*, disturbed surface **
			5Y 3/1	0.5-17 cm: dark grey ash layer (silty clay); dropstones increasing toward bottom
10				10 cm: reddish dropstone (1-2 cm Ø), sed. pellets
				16-17 cm: dropstone-rich layer
		@ @	5Y 7/1	17-20 cm: light grey silt; foram-rich layer with ash particles and dropstones
20				EOC: 20 cm * Surface, dead: mussel fragments, large agglutinated Polychaeten tubes; living: small solitary Actinien on dropstones
30				**** GKG face strongly disturbed because scoop did not close completely -> partial sediment loss and disturbance of the surface**
40				

Meteor 21-4	**05.06.1992 - 29.06.1992**
Station: M 227/92	**Datum: 09.06.1992**
Position: 65° 31´ 75 N ; 04° 06´ 33 W	**Water Depth: 2788 m**

Core: GIK 23423-3, GKG **Core Recovery: 44 cm**
Section: 0 - 44 cm

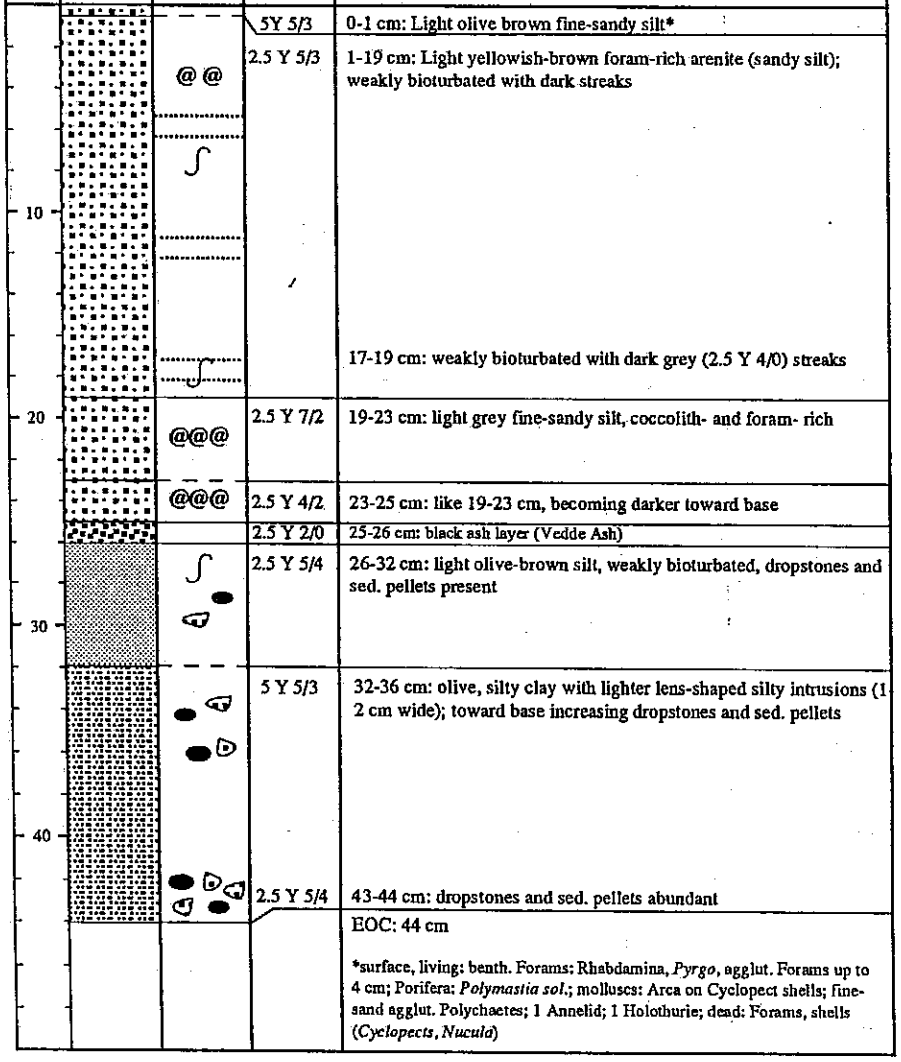

Meteor 21-4	**5.6.1992 - 29.6.1992**
Station: M 227/92	**Date: 9.6.1992**
Position: 65° 31´ 07 N ; 04° 06´ 03 W	**Water Depth: 2717 m**

Core: GIK 23423-4, KAL **Core Recovery: 475 cm**
Section: 0 - 150 cm

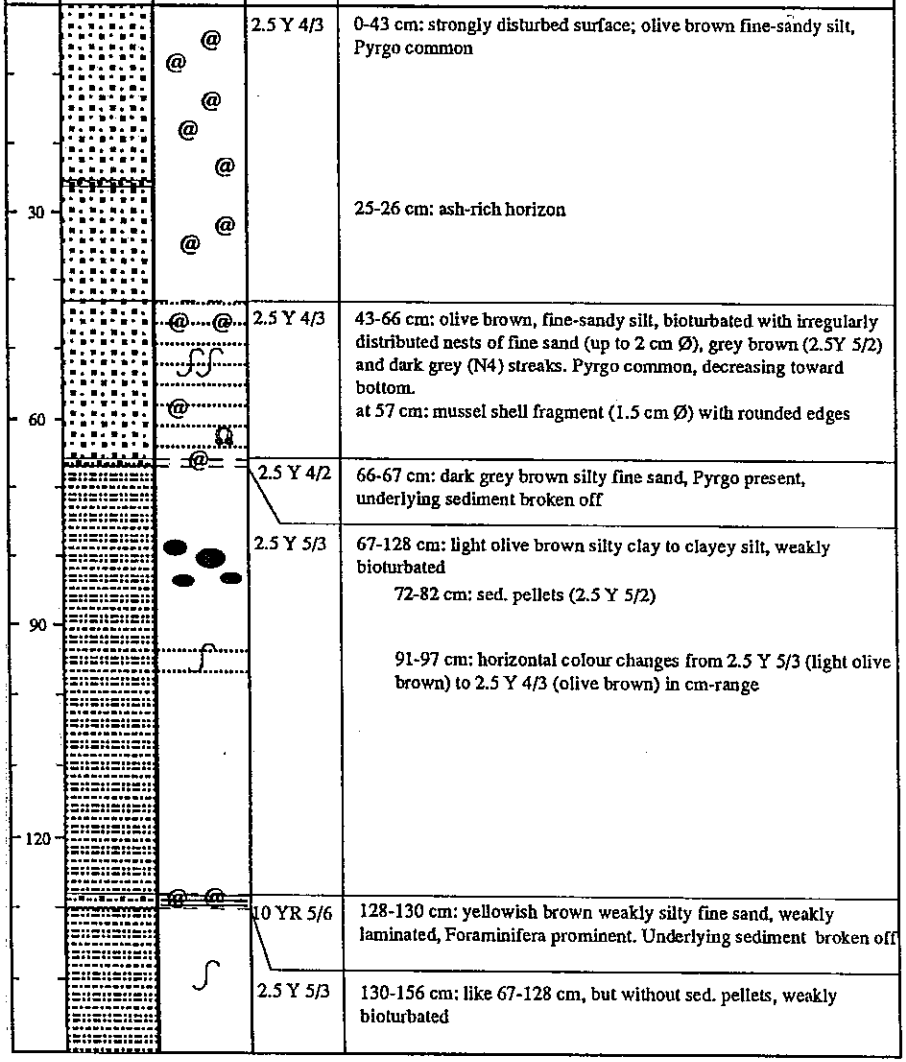

Meteor 21-4	5.6.1992 - 29.6.1992
Station: M 227/92	Date: 9.6.1992
Position: 65° 31´ 07 N ; 04° 06´ 03 W	Water Depth: 2717 m

Core: GIK 23423-4, KAL — Core Recovery: 475 cm
Section: 150-300 cm

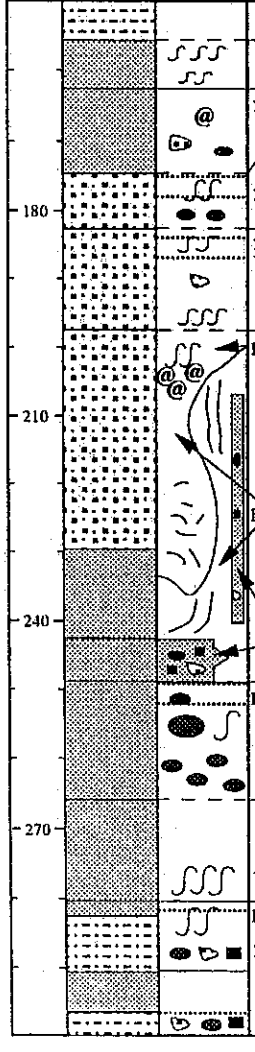

Depth (cm)	Colour	Description
		(130-156 cm: see above)
	5 Y 4/1	156-163 cm: dark grey silt, strongly bioturbated in upper part, decreasing toward bottom
	2.5 Y 5/3	163-175 cm: light olive brown silt with fine-sandy wedges to 0.5 mm thick, Foraminifera, sed. pellets and scattered dropstones (mm size) present.
	2.5 Y 4/4	175-183 cm: olive brown weakly fine-sandy silt, bioturbated, at top light olive brown (2.5 Y 5/6) diffuse streaks to 1 cm thickness with dark yellow brown (10 YR 4/6) fine-sandy sed. pellets
	2.5 Y 4/4	183-198 cm: olive brown fine-sandy silt, bioturbation increasing toward base, streaks of overlying sed. material, in lower part distinct pale brown bioturbation structures (10 YR 6/3) at 188 cm: consolidated worm burrow relict, 1 cm long 191 cm: basaltic dropstone 1 cm Ø
	10 YR 4/4	198-249 cm: slumped 198-230 cm: dark yellowish brown fine-sandy silt, bioturbated with irregularly distributed light and dark brown streaks, Foraminifera common.
	10 YR 6/3	230-243 cm: dark yellow brown silt, bioturbated with dark streaks (10 YR 4/2), sed. pellets to mm size
	5 Y 4/2	243-249 cm: olive brown silt, weakly bioturbated, with streaks from overlying material, dark sed. pellets and dropstones common, coal particles to 2 mm Ø
	10 YR 4/4	249-266 cm: dark yellowish brown silt, sed. pellets (up to mm size) toward base increasingly common; irregularly distributed wedges of fine sand, at top weakly bioturbated with light streaks 254-257 cm: sed. pellet (8x2 cm)
	5 Y 5/3	266-281 cm: olive silt, in upper part somewhat fine-sandy, in lower part strongly bioturbated, spotty 271-272 cm: yellowish red (5 YR 5/6) layer
	10 YR 5/3 2.5 Y 4/2	281-395 cm: alternating layers of brown silt and dark greyish brown clayey silt, each with nests and streaks of the other material. Transition to underlying sed. more sharply defined than to overlying sed. Darker layers rich in Sed. Pellets, coaly particles and dropstones (weakly rounded edges, to 1 cm Ø)

Meteor 21-4	5.6.1992 - 29.6.1992
Station: M 227/92	Date: 9.6.1992
Position: 65° 31´ 07 N ; 04° 06´ 03 W	Water Depth: 2717 m

Core: GIK 23423-4, KAL — Core Recovery: 475 cm
Section: 300-450 cm

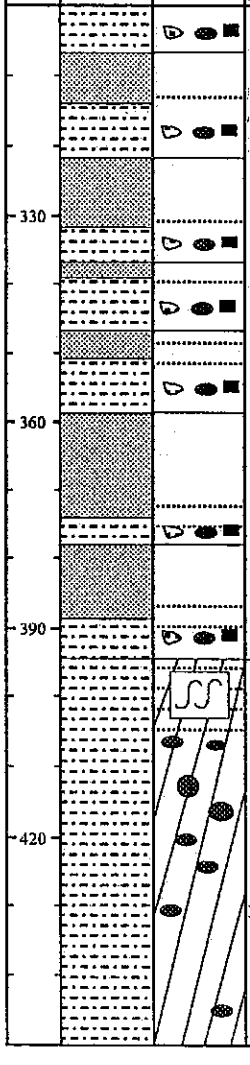

Depth (cm)	Colour	Description
		(281-395 cm: see above)
	2.5 Y 5/4	395-475 cm: slump with diagonal layers of light olive brown clayey silt, in upper part bioturbated with dark horizontal streaks (5 YR 4/2). sed pellets present
	10 YR 5/4	in middle part colour change to yellowish brown (10 YR 5/4), sed. pellets rare.

Meteor 21-4	**5.6.1992 - 29.6.1992**
Station: M 227/92	**Date: 9.6.1992**
Position: 65° 31´ 07 N ; 04° 06´ 03 W	**Water Depth: 2717 m**

Core: GIK 23423-4, KAL **Core Recovery: 475 cm**
Section: 450-475 cm

Depth (cm)	Lithology	Structure	Colour	Description
				(395-475 cm: see above) at base change to dark grey brown (10 YR 4/2) silty fine sand in 90° angle to upper part of slump with 1 cm thick brownish yellow (10 YR 6/8) horizon and mm-thick dark grey bands; Foraminifera common
480				475 cm: EOC
510				
540				
570				

Meteor 21-4 | 5.6.1992 - 29.6.1992
Station: M 228/92 | Date: 11.6.1992
Position: 70° 02`14 N ; 00° 03` 95 W | Water Depth: 3247 m

Core: GIK 23424-3, GKG | Core Recovery: 65 cm*
Section: 0 - 65 cm

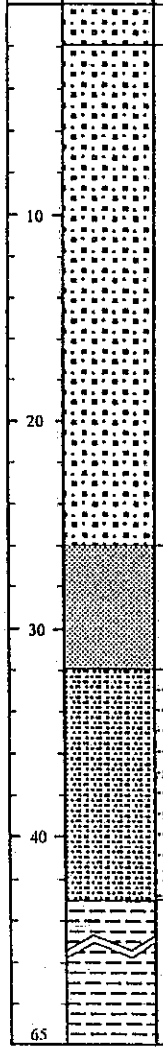

Depth (cm)	Colour	Description
	2.5 Y 5/3	0-2 cm: light olive brown fine-sandy silt with Pyrgo and few agglutinated Polychaet tubes
	2.5 Y 5/4	2-26 cm: light olive brown fine-sandy silt, Pyrgo and smaller Foraminifera abundant, weakly bioturbated with light and dark spots
	5 Y 4/2	26-32 cm: olive grey silt, bioturbated in upper part with dark spots
	2.5 Y 4/2	32-43 cm: dark grey brown silty clay with <1 mm thick dark stripes, abundance increasing toward bottom; down to 40 cm brown (10 YR 4/3) streaks at 38.5 cm: brownish yellow (10YR 6/6) horizon at 42 cm: brownish yellow (10YR 6/6) horizon
	5 Y 4/1	43-65 cm: dark grey, water-saturated, plastic clay (distal turbidite - "quick clay") * The portion of the GKG face beneath 43 cm could not be sampled precisely because the clay was pressed out of the GKG by the overlying Sediment. EOC: 65 cm

Meteor 21-4 | 5.6.1992 - 29.6.1992
Station: M 230/92 | Date: 12.6.1992
Position: 72° 14´ 62 N ; 11° 04´ 47 E | Water Depth: 2075 m

Core: GIK 23426-4, GKG | Core Recovery: 47 cm
Section: 0 - 47 cm

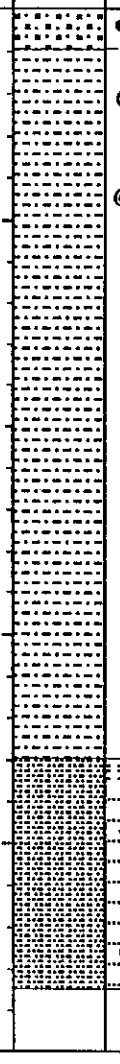

Depth (cm)	Colour	Description
	2.5 Y 5/3	0-2 cm: light olive brown fine-sandy silt with living Polychaetes, sea cucumbers, Pyrgo, Actinia; flat clay aggregate (sed. pellet) ca. 20 x 15 x 1mm; crab burrows (Chondrites)
	2.5 Y 6/3	2-17 cm: light yellowish brown clayey silt, foram-rich; bioturbated with light olive-coloured spots; Pyrgo abundant from 17 cm: Pyrgo distinctly decreasing toward bottom
	10 YR 3/3	36-47 cm: silty clay with fine dark brown bands and streaks; bioturbated; rich in plankt. Forams, especially in lower part 36-37cm: distinctly bordered dark brown band
		EOC: 47 cm

Meteor 21-4	**5.6.1992 - 29.6.1992**
Station: M 232/92	**Date: 13.6.1992**
Position: 74° 07′ 88 N ; 21° 08′ 85 E	**Water Depth: 335 m**

Core: GIK 23428-2, GKG **Core Recovery: 45 cm**
Section: 0 - 45 cm

Depth (cm)	Lithology	Structure	Colour	Description
		∫∫ @	5 Y 4/4	0-4 cm: olive clayey silt, bioturbated, scattered Forams; chitinous Polychaet tubes very abundant to 25 cm
10		∫∫	5 Y 3/2	4-11 cm: dark olive grey clayey silt, bioturbated; black streaks and spots very abundant
20		∫∫	5 Y 4/3	11-39 cm: olive clayey silt, bioturbated with black spots; very strongly decomposed C_{org}-rich particles
30				
40		∫	5 Y 3/2	39-45 cm: dark olive grey clayey silt, weakly bioturbated; black streaks and spots abundant
				45 cm: EOC

Meteor 21-4	**5.6.1992 - 29.6.1992**
Station: M 232/92	**Date: 13.6.1992**
Position: 74° 07′ 81 N ; 21° 08′ 85 E	**Water Depth: 334 m**

Core: GIK 23428-3, KAL **Core Recovery: 757 cm**
Section: 0-150 cm

Depth (cm)	Lithology	Structure	Colour	Description
		@@@ ∫∫∫ @	5 Y 4/2	0-20 cm: olive grey fine-sandy silt, strongly bioturbated, Polychaeten tubes very common, 1 cm long black tissue fragment, Foraminifera common
30		@ ∫∫ @ @ @	5 Y 4/2	20-59 cm: olive grey fine-sandy silt, bioturbated with dark grey (7.5 YR N3) spots; Foraminifera predominant, increasing to base (53-59 cm)
60		∫∫∫ @	5 Y 4/2	59-71 cm: olive grey fine-sandy silt, strongly bioturbated with dark grey (7.5 YR N3) streaks and spots, increasing distinctly toward base; org. films and Forams present; burrow (ca. 2 cm wide) filled with overlying sediment
		∫∫	7.5 YR N3	71-72.5 cm: dark grey fine-sandy silt, partly bioturbated
		∫∫∫	5 Y 3/2	72.5-92 cm: dark olive grey fine-sandy silt, strongly bioturbated, commonly with black streaks and spots in cm range. Black tissue fragments present discordant layering toward underlying sed.
90		Ω	5 Y 4/2	92-415 cm: olive grey, homogenous clayey silt, very weakly bioturbated with indistinct dark grey streaks; black tissue fragments, mussel shell and *Scaphopoda* fragments (<1 mm) present
120		∫		
		∫∫		at 146 cm: sponge, 2 x 1 cm (*Polymestia hurilensis*)

Meteor 21-4	5.6.1992 - 29.6.1992
Station: M 232/92	Date: 13.6.1992
Position: 74° 07´ 81 N ; 21° 08´ 85 E	Water Depth: 334 m

Core: GIK 23428-3, KAL — Core Recovery: 757 cm
Section: 150-300 cm

Depth (cm)	Lithology	Structure	Colour	Description
				(92-415 cm: see above)
				153-167 cm: strongly bioturbated with dark streaks
				at 158 cm: mussel shell, 1 cm Ø
				at 172 cm: 2 mussel shells,weakly bioturbated
180				
				188-210 cm: strongly bioturbated area with dark streaks and spots; mussel shell and *Scaphopoden* fragments present
210				210-221 cm: weakly bioturbated, colour increasingly darker
				221-387 cm: bioturbated with dark streaks, shell and *Scaphopoden* fragments common
240				
270				291 cm: sponge (*Polymestia hurilensis*)

Meteor 21-4	5.6.1992 - 29.6.1992
Station: M 232/92	Date: 13.6.1992
Position: 74° 07´ 81 N ; 21° 08´ 85 E	Water Depth: 334 m

Core: GIK 23428-3, KAL — Core Recovery: 757 cm
Section: 300-450 cm

Depth (cm)	Lithology	Structure	Colour	Description
				(92-415 cm: see above)
330				
360				
				374 cm: sponge (*Polymestia hurilensis*)
390				387-403 cm: shell fragments rare, bioturbated
				403-415 cm: bioturbated, large shell fragment
420			5 Y 4/2	415-532 cm: olive grey clayey silt, weakly bioturbated, black rock fragments increasing toward base (coal/black shale) up to 1.5 cm Ø, pyrite; mussel fragments (up to 2 cm) irregularly distributed , coal fragments

Meteor 21-4	5.6.1992 - 29.6.1992
Station: M 232/92	Date: 13.6.1992
Position: 74° 07´ 81 N ; 21° 08´ 85 E	Water Depth: 334 m

Core: GIK 23428-3, KAL — Core Recovery: 757 cm
Section: 450-600 cm

Depth (cm)	Lithology	Structure	Colour	Description
480				(415-532 cm: see above)
510				at 512 cm: dropstone (2 cm Ø)
				at 532 cm: mussel shell
540			5 Y 4/2	532-588 cm: olive grey silty clay, dropstones (up to 5 cm Ø) very common, irregularly distributed nests filled with dark sandy material 541-545 cm: olive (5 Y 4/4) horizon at 552 cm: mussel fragment
570				
			5 Y 4/2	588-642 cm: olive grey clayey silt, bioturbated with sed. pellets and distinctly fewer and smaller dropstones than in overlying horizon

Meteor 21-4	5.6.1992 - 29.6.1992
Station: M 232/92	Date: 13.6.1992
Position: 74° 07´ 81 N ; 21° 08´ 85 E	Water Depth: 334 m

Core: GIK 23428-3, KAL — Core Recovery: 757 cm
Section: 600-757 cm

Depth (cm)	Lithology	Structure	Colour	Description
630				(588-642 cm: see above)
660			5 Y 4/1	642-757 cm: dark grey weakly silty clay, indistinctly laminated with dark and olive-coloured (5 Y 4/4) horizons 645-649 cm: dropstone, 6 cm Ø, light colour 647-665 cm: dropstone, 19 x 14.5 cm, black shale
690				
720				
757				757 cm: EOC

Meteor 21-4	**5.6.1992 - 29.6.1992**
Station: M 272/92	**Date: 17.6.1992**
Position: 74° 59` 59 N ; 17° 53` 33 E	**Water Depth: 149 m**

Core: GIK 23449-8, GKG **Core Recovery: 27 cm**

Section: 0 - 27 cm

Depth (cm)	Lithology	Structure	Colour	Description
		Ω	5 Y 4/3	0-2 cm: olive fine-sandy silt; Hyas, large rock with Bryozoa growth, Actinea; 1 sponge, mussel shell fragments, Polychaeten
10		∫∫∫ Ω	5 Y 4/3	2-27 cm: olive fine-sandy silt, strongly bioturbated, with black (N2) and light (5 Y 4/3, 5 Y 3/2) spots; shell and snail fragments abundant; Polychaeten tubes
20				27 cm: dark grey tough clay with purple tinge
30				EOC: 27 cm
40				

Meteor 21-4 — **5.6.1992 - 29.6.1992**
Station: M 277/92 — **Date: 18.6.1992**
Position: 76° 28´ 59 N ; 08° 44´ 25 E — **Water Depth: 2016 m**

Core: GIK 23453-1, GKG — **Core Recovery: 43 cm**
Section: 0 - 43 cm

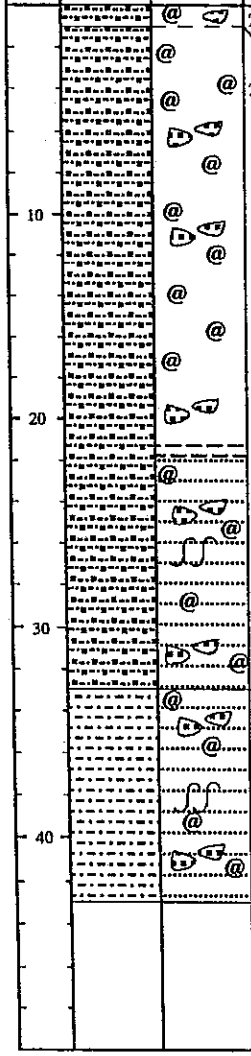

Lithology	Structure	Colour	Description
		2.5 Y 4/3	0-1 cm: olive brown weakly silty sand with dark, reddish rock fragments; sponges and *Thenaea sp.* present, agglut. Forams and Pyrgo abundant
		2.5 Y 4/3	1-33 cm: olive brown weakly silty sand, abundant dropstones (weakly rounded) up to 5 cm Ø, Forams very abundant
			21-22 cm: reddish band 21-43 cm: increasing bioturbation with grey streaks
		2.5 Y 4/3	33-43 cm: olive brown clayey silt, abundant dropstones (weakly rounded) up to 5 cm Ø, Forams very abundant, Pyrgo scattered; bioturbated with sandy streaks
			EOC: 43 cm

Meteor 21-4 — **5.6.1992 - 29.6.1992**
Station: M 277/92 — **Date: 18.6.1992**
Position: 76° 28´ 60 N ; 08° 44´ 72 E — **Water Depth: 2094 m**

Core: GIK 23453-2, KAL — **Core Recovery: 361 cm**
Section: 0-150 cm

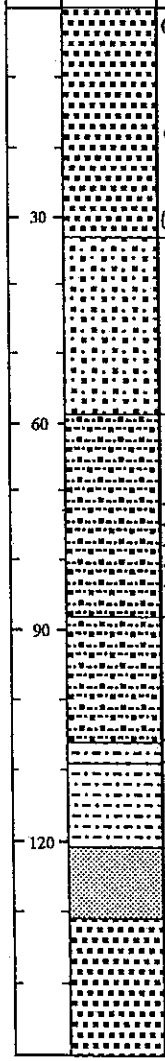

Lithology	Structure	Colour	Description
		2.5 Y 5/4	Core slid approximately 2 m out of the KAL because the core catcher failed to close 0-33 cm: light olive brown fine sand, strongly disturbed surface, very foram-rich, Pyrgo common; with black rock fragments to 1 cm Ø
		2.5 YR 5/4	33-59 cm: light olive brown, weakly fine-sandy silt, in middle part broken off from underlying sediment; strongly bioturbated with olive grey and brownish spots; light grey sed. pellets present; scattered Pyrgo and dropstones (up to 3 cm Ø)
		2.5 Y 5/3	59-88 cm: light olive brown silty fine sand with sandy lenses 70-84 cm: bioturbated with light streaks at 73, 88-90 cm: dropstone- (up to 1 cm Ø) rich layer
		2.5 Y 4/3	88-106 cm: olive brown silty fine sand; distinct increase in dropstones and sed. pellets toward base; increase in grain size of matrix 97-100 cm: sandy strong brown (7.5 YR 5/6) spots up to 1 cm Ø
		N 3	106-109 cm: very dark grey, strongly clayey silt, spotty; dropstones common; scattered sandy lenses up to 1 cm Ø
		2.5 Y 4/3	109-121 cm: olive brown strongly clayey silt, bioturbated; scattered dropstones and sed. pellets 109-112 cm: orange (7.5 Y 5/6) sandy spot 112-115 cm: light olove brown (2.5 Y 5/3) silty horizon with 2 cm Ø Dropstones
		10 YR 6/4	121-131 cm: light yellow brown silt, weakly bioturbated, at base dark (N3) sed. pellets (up to 1.5 cm Ø)
		10 YR 6/4	131-162 cm: foram-rich sand with dropstones (<1 cm Ø, weakly rounded edges) 143-148 cm: dark grey distinct streaks

Meteor 21-4	**5.6.1992 - 29.6.1992**
Station: M 277/92	**Date: 18.6.1992**
Position: 76° 28´ 60 N ; 08° 44´ 72 E	**Water Depth: 2094 m**

Core: GIK 23453-2, KAL **Core Recovery: 361 cm**
Section: 150-300 cm

Depth (cm)	Lithology	Structure	Colour	Description
				(131-162 cm: see above)
			2.5 Y 4/4	162-170 cm: olive brown silty fine sand, weakly bioturbated with dark indistinct spots; foram-rich
			2.5 Y 4/3	170-177 cm: olive brown silt; toward base colour change to 2.5 Y N5 (grey); black dropstone (8 cm Ø, possibly black shale) pressed into underlying horizon
			N5	170-170.5 cm: strong brown (7.5 YR 5/6) sandy discontin. bands
			5 Y 6/1	177-179 cm: light grey fine-sandy silt with lightly distributed black rock fragments (<1mm); strong brown (7.5 YR 5/6) oval spot (1 cm Ø)
180			5 Y 4/2	179-186 cm: olive grey clayey silt, in upper part strongly bioturbated; spotty; scattered sed. pellets; 0.5 cm Ø red dropstone
			2.5 Y 6/3	186-193 cm: light yellowish brown silt, Forams predominant; scattered dropstones; fine-sandy nests up to 1 cm Ø
			2.5 Y 4/3	193-207 cm: olive brown fine-sandy silt, weakly bioturbated; at base indistinct red colour 193-201 cm: accumulation of sandy nests; black dropstones (coal?)
210			2.5 Y 6/2	207-211 cm: light brown grey clayey silt, Forams predom., dropstns.
			2.5 Y 4/2	211-224 cm: dark grey brown fine-sandy silt with clayey parts; dropstones and sed. pellets (<1 mm) present; large dropstone at 211 cm
			(see descrip.)	224-233 cm: as above, but colour change: 224-226 = 5 Y 6/1; 226- 229 = 2.5 Y 6/2; 229-233 = 5 Y 4/2. Middle layer sandy, Forams common; in lower part bioturbated with dark spots
240			2.5 Y 6/3	233-247 cm: light yellow brown silt with dropstones (up to 1 cm Ø) and sandy nests; in lower part more clayey and darker at 241 cm:1 cm thick sandy band, discontinuous, Forams and dropstones common
			2.5 Y 5/3	
			2.5 Y 6/3	247-265 cm: light yellow brown silty fine sand, grain size strongly variable; at top sed. pellet layer with coal fragments; sandy wedges; sed. pellets increasing toward bottom; at base black dropstone (5 cm Ø), pressed approximately 2 cm into underlying sed. below 256 cm: brown yellow (10 YR 6/6) areas
270			N6	265-271 cm: grey silty clay, weakly bioturbated with dark spots at 266 cm: reddish dropstone
			2.5 Y 5/3	271-303 cm: light olive brown clayey silt; bioturbation increasing toward base; dark spots; scattered dropstones 282-283 cm: grey (2.5 Y 6/1) band running diagonally through the sediment 293-296 cm: orange aureolae around dropstones

Meteor 21-4	**5.6.1992 - 29.6.1992**
Station: M 277/92	**Date: 18.6.1992**
Position: 76° 28´ 60 N ; 08° 44´ 72 E	**Water Depth: 2094 m**

Core: GIK 23453-2, KAL **Core Recovery: 361 cm**
Section: 300-361 cm

Depth (cm)	Lithology	Structure	Colour	Description
				(271-303 cm: see above)
			N4	303-323 cm: dark grey sandy clay with sandy wedges; dropstones (up to 2 cm Ø) and sed. pellets common
330				323-361 cm: Core Catcher; see 303-323 cm
360				EOC: 361 cm
390				
420				

Meteor 21-4	**5.6.1992 - 29.6.1992**
Station: M 281/92	**Date: 19.6.1992**
Position: 76° 44′ 98 N ; 08° 11′ 75 E	**Water Depth: 2126 m**

Core: GIK 23454-2, GKG **Core Recovery: 41 cm**
Section: 0 - 41 cm

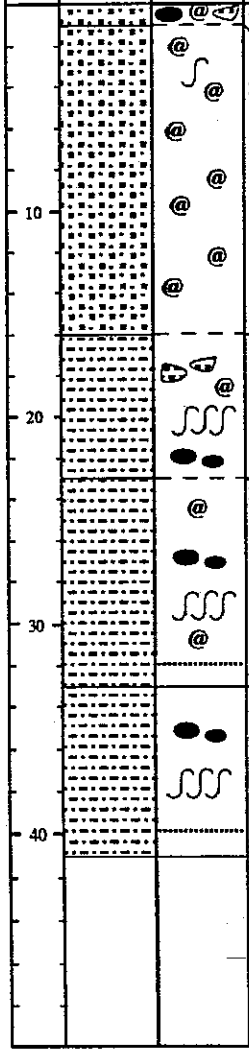

Lithology	Structure	Colour	Description
		2.5 Y 5/4	0-1 cm: light olive brown sandy silt; agglut. Forams, Pyrgo, chalk sponges; white and black dropstones; sed. pellets; funnel-shaped burrow openings
		2.5 Y 5/4	1-16 cm: light olive brown fine-sandy silt; weakly bioturbated; Pyrgo very abundant
		2.5 Y 5/3	16-23 cm: light olive brown clayey silt, strongly bioturbated; dropstones, sed. pellets; rare Forams
		10 YR 5/4	23-33 cm: yellowish brown clayey silt, strongly bioturbated; scattered Forams; sed. pellets: N4 2 cm Ø, red 1 cm Ø 32-33 cm: dark yellowish brown (10 YR 3/4) band
		10 YR 5/2	33-41 cm: greyish brown clayey silt with sed. pellets and brownish streaks in lower part, strongly bioturbated
			EOC: 41 cm

Meteor 21-4	**5.6.1992 - 29.6.1992**
Station: M 281/92	**Date: 19.6.1992**
Position: 76° 45′ 1 N ; 08° 12′ 6 E	**Water Depth: 2144 m**

Core: GIK 23454-1, KAL **Core Recovery: 361 cm**
Section: 0-150 cm

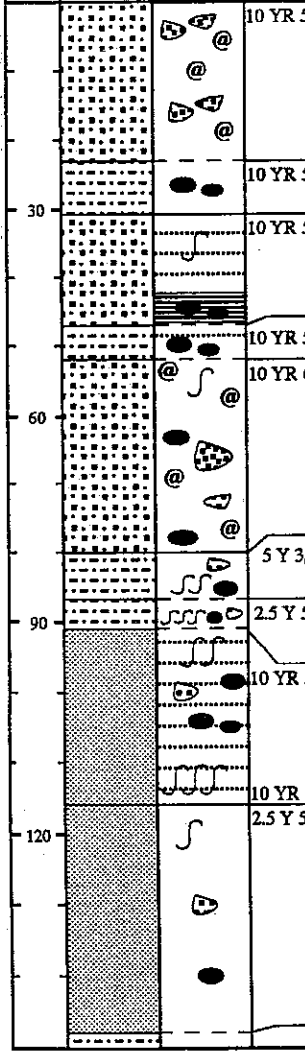

Lithology	Structure	Colour	Description
		10 YR 5/4	0-23 cm: yellowish brown fine-sandy silt with Pyrgo (very abundant), scattered Polychaeten tubes and black dropstones present
		10 YR 5/4	23-31 cm: yellowish brown weakly clayey silt with scattered grey sed. pellets
		10 YR 5/4	31-47 cm: fine-sandy silt with reddish brown (5 YR 4/4) stripes, laminated at bottom; weakly bioturbated; abundant dark grey sed. pellets in lower part
		10 YR 5/1	47-52 cm: grey clayey silt with brown streaks; sed. pellets present
		10 YR 6/1	52-80 cm: light yellowish brown fine-sandy silt, weakly bioturbated with dark grey spots; foram-rich; sed. pellets and dropstones up to 1.5 cm Ø at 66 cm: 7 x 4 cm black dropstone
		5 Y 3/1	80-87 cm: very dark grey clayey silt, bioturbated with light spots; scattered dark sed. pellets 80-81 cm: dropstone layer
		2.5 Y 5/2	87-91 cm: greyish brown clayey silt, strongly bioturbated; scattered dropstones 90-5-91 cm: sed. pellet layer
		10 YR 5/4 10 YR 6/4	91-116 cm: yellowish brown silt; bioturbation increasing toward base; streaks, becoming darker toward base; light and dark grey sed. pellets; dropstones present
		2.5 Y 5/2	116-148 cm: greyish brown homogenous silt with light grey diffuse spots; distinct colour change from above; dropstones and dark sed. pellets rare, weakly bioturbated
			148-176 cm: see next page

Meteor 21-4	**5.6.1992 - 29.6.1992**
Station: M 281/92	**Date: 19.6.1992**
Position: 76° 45´ 1 N ; 08° 12´ 6 E	**Water Depth: 2144 m**

Core: GIK 23454-1, KAL **Core Recovery: 361 cm**

Section: 150-300 cm

Depth (cm)	Lithology	Structure	Colour	Description
			10 YR 5/4	148-176 cm: yellowish brown clayey silt, strongly bioturbated; spotty; sed. pellets present; at bottom darker streaks
180			2.5 Y 5/3	176-185 cm: layey silt, in upper part bioturbated with dark spots, with abundant small black sed. pellets
			2.5 Y 3/3	185-187 cm: clayey silt
			2.5 Y 5/2	187-228 cm: greyish brown fine-sandy silt, weakly bioturbated 193-199 cm: bioturbated dark streaks; scattered grey sed. pellets (Ø mm-range, larger toward base)
210				
			5 Y 4/1	228-232 cm: dark grey fine-sandy silt, strongly bioturbated; alternating light and dark streaks 231-232 cm: olive yellow horizon
			2.5 Y 4/3	232-254 cm: fine-sandy silt, in lower part bioturbated with dark grey spots; dropstones and dark grey sed. pellets (Ø mm-range) abundant
240				
			5 Y 3/1	254-258 cm: clay, at base mm-sized coal particles
			(see descript.)	258-281 cm: silt, alternating between 5 Y 6/2 (258-260, 261- 266, 270-273) and 5 Y 4/2 (260-261, 266-270, 273-281); dark grey sed. pellets; occasional sandy layers
270				
			2.5 Y 5/2	281-340 cm: greybrown silt, Foram-dominant (Pyrgo), partially bioturbated 294-296 cm: dark grey-black horizon with coal (1.5 cm Ø) and sed. pellets

Meteor 21-4	**5.6.1992 - 29.6.1992**
Station: M 281/92	**Date: 19.6.1992**
Position: 76° 45´ 1 N ; 08° 12´ 6 E	**Water Depth: 2144 m**

Core: GIK 23454-1, KAL **Core Recovery: 361 cm**

Section: 300-450 cm

Depth (cm)	Lithology	Structure	Colour	Description
				(281-340 cm: see above) 308-309 cm: dark grey-black horizon with coal (1.5 cm Ø) and sed. pellets
330				323-329 cm: strongly bioturbated with grey-black spots at 331 cm: Corg-rich rock fragment (black shale?) 2 cm Ø
			2.5 Y 5/3	340-370 cm: fine-sandy silt, foram-rich; small sandy sed. pellets abundant; dropstones present, in lower part abundant, bioturbated 350-355 cm: strongly bioturbated spotty black horizon 350-363 cm: large light distinctly rounded dropstone (quarzite)
360			2.5 Y 5/2	
			10 YR 5/4	370-412 cm: yellowish-brown silt, weakly bioturbated with dark and light grey spots; in upper and lower parts dropstone- and sed. pellet-rich 386-401 cm: foram-rich layer
390				
			2.5 Y 6/2	412-431 cm: silt, distinct bioturbation with colour (2.5 Y 6/2) streaks; sed. pellets very abundant
420				431-601 cm: alternation of (1) dark sandy and light fine-sandy silt horizons with (2) strongly bioturbateed parts; darker horizons usually sharply bordered, lighter ones, Forams dominant; sed. pellets present throughout
			N4	431-437 cm: dark grey layer with abundant sed. pellets and dropstones; olive yellow oxidised band (2.5 Y 6/8)
			N6	437-446 cm: light grey layer; Forams, dropstones and sed. pellets scattered
			2.5 Y 5/3	446-454 cm: strongly bioturbated horizon

Meteor 21-4	**5.6.1992 - 29.6.1992**
Station: M 281/92	**Date: 19.6.1992**
Position: 76° 45′ 1 N ; 08° 12′ 6 E	**Water Depth: 2144 m**

Core: GIK 23454-1, KAL — **Core Recovery: 361 cm**
Section: 450-600 cm

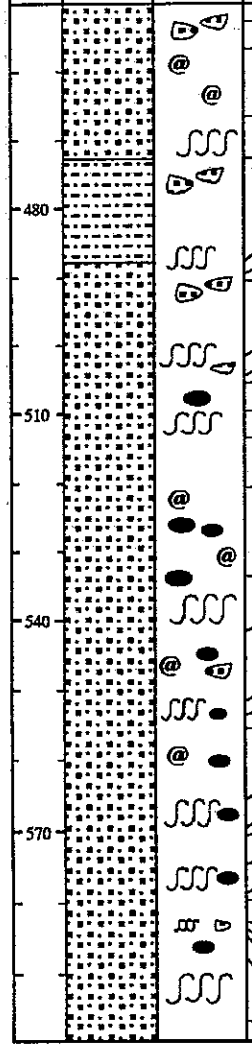

Depth (cm)	Colour	Description
		(431-601 cm, 446-454 cm: see above)
	N3	454-458 cm: dark layer; scattered dropstones
	N5	458-468 cm: light layer, Forams present
	5 Y 3/2	468-474 cm: strongly bioturbated, dropstones present
	10 YR 5/4	474-489 cm: light clayey homogenous silt; dropstones present
	5 Y 3/2	489-491cm: strongly bioturbated region
	5 Y 3/2	491-492 cm: dark layer; dropstones present
	5 Y 5/1	492-503 cm: light layer; dropstones abundant
	5 Y 4/4	503-506 cm: strongly bioturbated; dropstones present
	N4	506-507 cm: dark horizon
	N6	507-511 cm: light; scattered sed. pellets
	2.5 Y 5/3	511-515 cm: strongly bioturbated region
	5 Y 4/3	515-522 cm: dark layer
	2.5 Y 6/3	522-535 cm: light layer; sed. pellets and Forams present
	5 Y 3/1	535-543 cm: strongly bioturbated region; sed. pellets present
	5 Y 6/1	543-553 cm: light layer; sed. pellets present; scattered dropstones and Forams 543-545 cm: increasingly sandy
	2.5 Y 5/3	553-555 cm: strongly bioturbated region; sed. pellets present
	5 Y 4/2	555-557 cm: dark layer; sed. pellets present
	5 Y 6/1	557-567 cm: light layer; scattered sed. pellets and Forams
	5 Y 4/2	567-571 cm: strongly bioturbated region; scattered sed. pellets
	5 Y 4/2	571-572 cm: dark layer; scattered sed. pellets
	5 Y 6/1	572-576 cm: light layer; rusty spots
	5 Y 4/1	576-580 cm: strongly bioturb. region; sed. pellets abundant
	5 Y 4/1	580-581 cm: dark layer; sed. pellets abundant
	5 Y 6/1	581-584 cm: light layer
	5 Y 4/1	584-585 cm: strongly bioturbated region; scattered dropstones
	5 Y 4/1	585-586 cm: dark layer; scattered dropstones
	5 Y 6/1	586-589 cm: light layer; scattered sed. pellets
	5 Y 4/2	589-598 cm: strongly bioturbated region; rusty spots
	5 Y 4/1	598-601 cm: dark layer; sandy stripe

Meteor 21-4	**5.6.1992 - 29.6.1992**
Station: M 281/92	**Date: 19.6.1992**
Position: 76° 45′ 1 N ; 08° 12′ 6 E	**Water Depth: 2144 m**

Core: GIK 23454-1, KAL — **Core Recovery: 361 cm**
Section: 600-675 cm

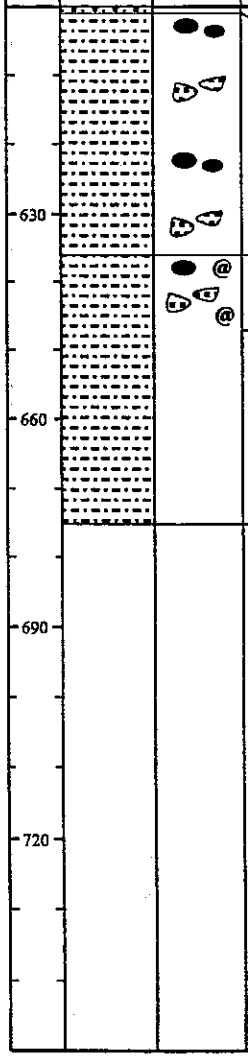

Depth (cm)	Colour	Description
		(431-601, 598-601 cm: s. oben)
	N3	601-636 cm: clayey silt with sandy layers; dropstone- and sed. pellet-rich
	N5	636-647 cm: like 601-636 cm; Forams present
		647-675 cm: Core Catcher
		675 cm: EOC

Meteor 21-4	**5.6.1992 - 29.6.1992**
Station: M 282/92	**Date: 19.6.1992**
Position: 76° 52′ 04 N ; 08° 24′ 31 E	**Water Depth: 2362 m**

Core: GIK 23455-2, GKG **Core Recovery: 44 cm**
Section: 0 - 44 cm

Depth (cm)	Lithology	Structure	Colour	Description
		@	2.5 Y 5/4	0-1 cm: light olive brown fine-sandy silt with coarse sand fraction; Pyrgo and agglut. Forams present, scattered Polychaetes and Pteropods; angular and rounded black dropstones, up to 1 cm Ø
		@	2.5 Y 5/4	1-10 cm: light olive brown fine-sandy silt; Pyrgo abundant, Forams and dropstones present, decreasing toward base; Corg- rich rock fragments up to 0.5 cm Ø (weathered black shales)
10		∫∫	5 Y 5/1	10-15 cm: grey silty clay, strongly bioturbated; Corg- rich rock fragments (weathered black shales)
			5 Y 6/1	15-16 cm: light grey silty clay, increasingly fine-sandy towards base, partially in lenses
			N5	16-27 cm: grey clayey silt
20		∫∫	5 Y 6/1	20-27 cm: silty clay with dropstones up to 1 cm Ø; bioturbated
		∫∫	N5	at 25 cm: 5 cm Ø Dropstone
30		∫∫	10 YR 5/2	27-34 cm: greyish brown silty clay; scattered dropstones, bioturbated
			10 YR 6/4	34-44 cm: light yellowish brown clayey silt
40		∫∫		at 39 cm: small yellow band 40-44 cm: scattered dropstones; in upper part bioturbated
				44 cm: EOC

Meteor 21-4	**5.6.1992 - 29.6.1992**
Station: M 282/92	**Date: 19.6.1992**
Position: 76° 50′ 90 N ; 08° 21′ 68 E	**Water Depth: 2497 m**

Core: GIK 23455-3, KAL **Core Recovery: 592 cm**
Section: 0-150 cm

Depth (cm)	Lithology	Structure	Colour	Description
		@	2.5 Y 4/3	0-4 cm: surface sed. slumped in KAL. Olive brown Foramsand; Pyrgo very common; dark flat rock fragments common
		@	10 YR 5/4	4-8 cm: yellow brown fine-sandy silt, Forams very common; scattered dropstones
		@	10 YR 5/3	8-23 cm: brown silt, Forams predominant (increasing toward base); dark grey sed. pellets; bioturbated at base
			2.5 Y 5/2	23-31 cm: grey brown silty clay with dark brown (7.5 YR 4/4) streaks; dark sed. pellets up to 1 cm Ø
30			7.5 YR 4/4	31-32 cm: brown laminated band
		@	2.5 Y 5/2	32-34 cm: grey brown clayey silt; dropstones up to 2 cm Ø
		@	10 YR 4/4	34-56 cm: dark yellow brown foram-rich fine-sandy silt, weakly bioturbated with darker spots; dropstones and sed. pellets (up to 1 cm Ø), increasing toward bottom
60			5 Y 3/1 10 YR 6/1	56-62 cm: very dark grey sandy clay, weakly bioturbated with light spots; 1 cm thick sed. pellet layer at top
		@	10 YR 5/4	62-138 cm: dark yellow brown clayey silt, weakly bioturbated with indistinctly bordered darker and lighter bands; Forams present
				at 73 cm: dark grey sed. pellets, up to 4 cm Ø
90		@		
		@		100-103 cm: sed. pellet layer
		@		
120		@		116-117 cm: sed. pellet layer
		@		124-125 cm: sed. pellet layer
		@		at 133 cm: dropstone (1.5 cm Ø)
			10 YR 3/1	138-139 cm: very dark grey clayey sand; sed. pellets common
		@	10 YR 5/4	139-161 cm: yellowish brown weakly Foram-dominant clayey silt, bioturbated streaks (3-4 cm Ø) predominantly in upper part

Meteor 21-4	**5.6.1992 - 29.6.1992**
Station: M 282/92	**Date: 19.6.1992**
Position: 76° 50´ 90 N ; 08° 21´ 68 E	**Water Depth: 2497 m**

Core: GIK 23455-3, KAL **Core Recovery: 592 cm**

Section: 150-300 cm

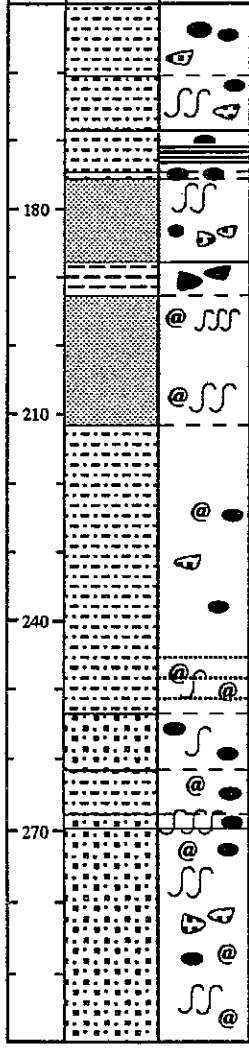

Depth (cm)	Colour	Description
		(139-161 cm: see above) at 157 cm: 2 cm Ø dropstone, randomly scattered sed. pellets (mm-size)
	10 YR 5/4	161-169 cm: yellowish brown homogenous clayey silt; dropstones rare, sed. pellets common
	10 YR 5/4	169-175 cm: yellowish brown clayey silt, middle part laminated 169-171 cm: bioturbated, sed. pellets common
180	10 YR 3/1	175-176 cm: ver dark grey sandy silt; accumulations of sed. pellets (rather like weathered black shales); partly with orange oxydisation aureolae
	2.5 Y 5/2	176-188 cm: grey brown silt, in middle part darker 182-184 cm: accumulations of sed. pellets and black dropstones (up to 1 cm Ø)
	5 Y 3/1	188-193 cm: very dark grey sand-clay diamict with dropstones up to 1 cm Ø
	2.5 Y 5/2	193-212 cm: alternations of fine-sandy silty lighter (2.5 Y 5/2) horizons (Forams common) at 193-196, 197-199, 202-205 cm and silty darker (10 YR 5/4) horizons (distinctly more bioturbated) at 196-197, 199-202, 205-212 cm
210	10 YR 5/4	
	2.5 Y 5/3	212-254 cm: light olive brown, more clayey silt; coloured (10 YR 5/6) streaks 212-215 cm; dropstones and sed. pellets rare 224-225 cm: dark grey (10 YR 4/1) layer with many sed. pellets and Forams 232-234 cm: dark spots (sandy, Pyrgo present)
240		increasing Forams (Pyrgo)toward base; weakly bioturbated with coloured (5 Y 6/1) streaks
	2.5 Y 4/3	254-262: olive brown fine-sandy silt, spottily bioturbated; accumulations of dark sed. pellets up to 1.5 cm Ø
	2.5 Y 5/4	262-268 cm: light olive brown homogenous clayey silt, toward base increasingly bioturbated; Pyrgo present; dark sed. pellets present
	5 Y 3/1	268-270 cm: very dark grey fine-sandy silt, strongly bioturbated with streaks in upper part; sed. pellets common
270	10 YR 5/4	270-313 cm: yellow brown Foram-predominant fine-sandy silt, mm-sized sed. pellets and dropstones; colour at base lighter; transition to underlying sed. disturbed by bioturbation at 274-275 and 280-290 cm: olive (2.5 Y 4/3) horizon at 287 cm: strongly weathered black rock fragments

Meteor 21-4	**5.6.1992 - 29.6.1992**
Station: M 282/92	**Date: 19.6.1992**
Position: 76° 50´ 90 N ; 08° 21´ 68 E	**Water Depth: 2497 m**

Core: GIK 23455-3, KAL **Core Recovery: 592 cm**

Section: 300-450 cm

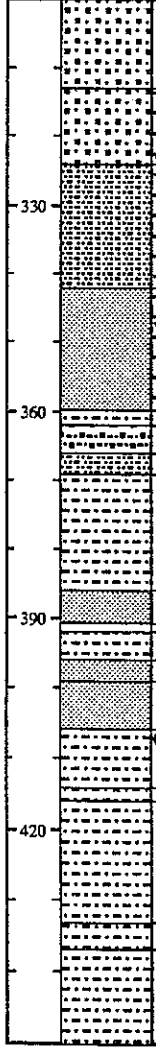

Depth (cm)	Colour	Description
		(270-313 cm: see above)
	10 YR 4/3	313-324 cm: brown fine-sandy silt, bioturbated with dark streaks; dark grey sed. pellets at 318 cm: dark brown (7.5 YR 4/3) streaks; underneath, strongly bioturbated with dark brown sed. pellets and brownish grey streaks
330	10 YR 4/1	324-342 cm: dark grey silty clay with brown streaks at 329 cm: brown (7.5 YR 4/4) band; underneath, bioturbated with sed. pellets up to 1 cm Ø
	2.5 Y 4/2	342-360 cm: dark greyish brown silt with sandy lenses, strongly bioturbated with lighter and dark grey spots and streaks; colour gradually darker toward base at 345 cm: black weathered rock fragment
	N3	360-362 cm: very dark grey homogenous clayey silt
360	N5	362-366 cm: grey homogenous silty-sandy layer with common dropstones up to 0.5 cm Ø
	2.5 Y 4/2	366-369 cm: dark greyish brown silty clay; dropstones present
	10 YR 5/2	369-386 cm: greyish brown clayey silt with darker spots, in lower part bioturbated; dropstones common; colour becoming darker toward bottom at 371 cm: chalk fragment
	2.5 Y 4/2	386-391 cm: dark greyish brown silt, strongly bioturbated with 0.5 cm sand lenses
390	N6	391-392 cm: grey homogenous clayey silt
	10 YR 5/4	392-396 cm: yellowish brown clayey silt, weakly bioturbated; at base sandier
	5 YR 5/4	396-399 cm: reddish brown silt with dropstones
	2.5 Y 4/3	399-406 cm: olive brown silt, bioturbated; dropstones present
	10 YR 6/2	406-414 cm: light brownish grey Foram-dominant clayey silt with dropstones; at base dark grey sed. pellets
	2.5 Y 5/3	
	10 YR 4/3	414-416 cm: brown clayey silt, bioturbated; dropstones
420	2.5 Y 5/3	416-433 cm: light olive brown clayey silt; dropstones common; Forams present; toward base increasingly sandy and distinct increase in Foraminifera
	2.5 Y 4/2	433-437 cm: dark greyish brown clayey silt with sandy lenses; dropstone-rich
	10 YR 5/3	437-466 cm: brown clayey silt, at top grey sandy lenses up to 2 cm thick; toward base increasingly bioturbated with dark spots; dropstones present at 441 cm: yellow dropstone

Meteor 21-4	**5.6.1992 - 29.6.1992**
Station: M 282/92	**Date: 19.6.1992**
Position: 76° 50´ 90 N ; 08° 21´ 68 E	**Water Depth: 2497 m**

Core: GIK 23455-3, KAL **Core Recovery: 592 cm**
Section: 450-592 cm

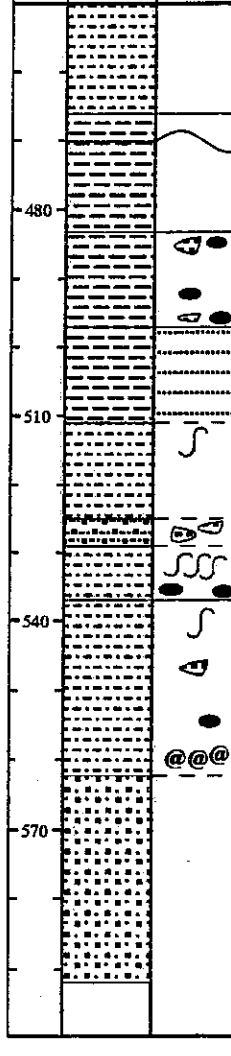

Lithology	Structure	Colour	Description
			(437-466 cm: see above)
		N4	466-470 cm: dark grey homogenous clay with coarser wedges
		2.5 Y 6/3 2.5 Y 4/2 N4	470-483 cm: homogenous clay with continuous colour change: light yellowish brown -> dark greyish brown -> dark grey
		N6	483-497 cm: grey homogenous clay with coarser wedges 484-485, 493-494, 496-497 cm: dark grey (10 YR 4/1) bands with dropstones and sed. pellets (<1 mm)
		5 Y 5/2	497-511 cm: olive grey homogenous clay with scattered darker streaks 510-511 cm: darkgrey (10 YR 4/1) horizon with weathered black shale
		2.5 Y 5/2	511-525 cm: greyish brown clayey silt, bioturbated with dark grey spots and streaks 514-517 cm: sandy nests (<1 cm Ø)
		5 Y 5/1	525-529 cm: grey foram-rich fine-sandy silt with dark dropstones (<1 mm)
		2.5 Y 6/2	529-537 cm: light brownish grey clayey silt, very strongly bioturbated with dark olive streaks; weathered black shales; at base accumulations of sed. pellets
	@@@	2.5 Y 5/3	537-562 cm: light olive brown clayey silt, weakly bioturbated with dark grey spots; scattered dropstones and sed. pellets; at base transition to very foram-rich fine-sandy silt
			562-592 cm: Core Catcher; foram-rich fine-sandy silt
			592 cm: EOC

Meteor 21-4	**5.6.1992 - 29.6.1992**
Station: M 284/92	**Date: 20.6.1992**
Position: 77° 04´ 0 N ; 06° 21´ 8 E	**Water Depth: 2200 m**

Core: GIK 23456-6, GKG **Core Recovery: 42 cm**
Section: 0 - 42 cm

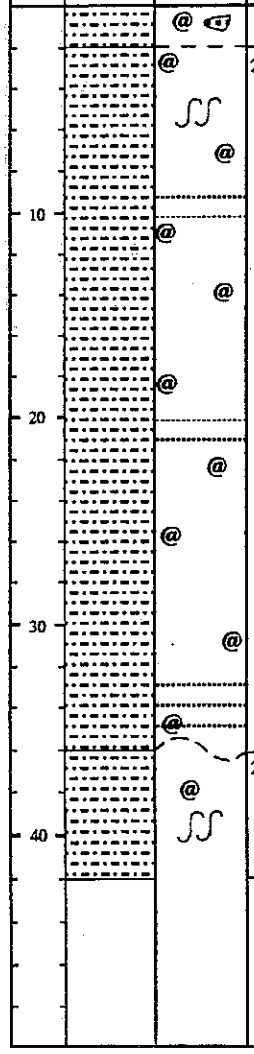

Depth (cm)	Colour	Description
	5 Y 5/4	0-2 cm: olive clayey silt; Pyrgos, agglut. Forams and dropstones rare
	2.5 Y 5/4	2-36 cm: light olive brown foram-rich homogenous clayey silt; scattered light sandy nests (up to 3 cm Ø, greyish), bioturbated; few dark brown streaks; abundant grey streaks between 33 and 36 cm.
	2.5 Y 5/2	36-42 cm: greyish brown clayey silt, bioturbated; scattered Forams
		42 cm: EOC

Meteor 21-4	**5.6.1992 - 29.6.1992**
Station: M 238/92	**Date: 20.6.1992**
Position: 77° 04´ 02 N ; 06° 20´ 47 E	**Water Depth: 2182 m**

Core: GIK 23456-5, KAL **Core Recovery: 634 cm**
Section: 0-150 cm

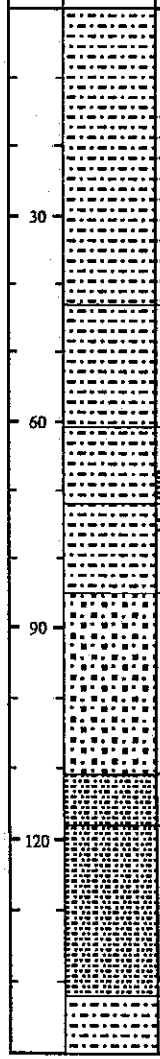

Depth (cm)	Colour	Description
	10 YR 5/4	0- 43 cm: surface slightly disturbed. Yellowish brown homogenous clayey silt, foram-rich; sed. pellets (mm-size) from 15 cm: bioturbated with light spots and horizontal streaks; Forams (Pyrgo) very abundant
	2.5 Y 4/3	43-61 cm: olive brown clayey silt; scattered dropstones (up to 1 cm Ø) and sed. pellets, weakly bioturbated 53-57, 59-61 cm: very dark greyish brown (10 YR 3/2) indistinct horizontal bands
	10 YR 3/1	61-72 cm: very dark grey clayey silt with dropstones 61-63 cm: dark bioturbated horizons 67-72 cm: laminated with accumulation of dropstones and sed. pellets
	10 YR 5/1	72-85 cm: grey clayey silt, in lower part accumulation of bioturbation structures at 74 cm: yellowish brown (10 YR 5/6) sed. pellet layer 74-77 cm: scattered dark colour stripes at 80 cm: dark grey spots up to 2 cm Ø
	10 YR 5/4	85-111 cm: yellowish brown fine-sandy silt; Pyrgo and light grey sed. pellets (up to 1 cm Ø) abundant
	2.5 Y 3/1	111-118 cm: homogenous weakly silty clay 111-114 cm: sandy; abundant coal and sed. pellets, bioturbated
	10 YR 5/1	118-142 cm: grey silty clay, bioturbated with colour changes (10 YR 5/1, 2.5 Y 5/3); sed. pellets present 124-125, 141-142 cm: layered accumulations of sed. pellets 124-125, 130-132 cm: 2.5 Y 3/1 125-130 cm: Pyrgo present
	2.5 Y 4/2	142-152 cm: dark greyish brown clayey silt, bioturbated with light spots; scattered dark grey sed. pellets (up to 1 cm Ø)

Meteor 21-4	**5.6.1992 - 29.6.1992**
Station: M 238/92	**Date: 20.6.1992**
Position: 77° 04´ 02 N ; 06° 20´ 47 E	**Water Depth: 2182 m**

Core: GIK 23456-5, KAL **Core Recovery: 634 cm**
Section: 150-300 cm

Depth (cm)	Lithology	Structure	Colour	Description
				(142-152 cm: see above)
			(see descrip.)	152-311 cm: clayey silt with continuous colour darkening toward bottom; sed. pellets rare, in middle more common; Forams abundant in upper part (to 220 cm)
				152- 213: 2.5 Y 6/3
				159-160 cm: dark bioturbated layer with accumulations of sed. pellets
180				176-181 cm: dark bioturbated layer with accumulations of sed. pellets
				187-188 cm: dark bioturbated layer with accumulations of sed. pellets
				195-201 cm: dark bioturbated layer with accumulations of sed. pellets
210				213-243: 5 Y 5/2; 5 Y 5/1
240				at 241 cm: thin, partially indistinct colour bands (2.5 Y 5/5) up to 1 cm thick
				243-311: 5 Y 5/1
270				at 276 cm: thin, partially indistinct colour bands (2.5 Y 5/5) up to 1 cm thick
				at 280 cm: dark grey partially elongated horizontal spots
				at 291 cm: dark grey partially elongated horizontal spots
				at 295 cm: thin, partially indistinct colour bands (2.5 Y 5/5) up to 1 cm thick
				at 298 cm: dark grey partially elongated horizontal spots

Meteor 21-4	**5.6.1992 - 29.6.1992**
Station: M 238/92	**Date: 20.6.1992**
Position: 77° 04´ 02 N ; 06° 20´ 47 E	**Water Depth: 2182 m**

Core: GIK 23456-5, KAL **Core Recovery: 634 cm**
Section: 300-450 cm

Depth (cm)	Lithology	Structure	Colour	Description
				(152-311 cm: see above)
				at 307 and 311 cm: thin, partially indistinct colour bands (2.5 Y 5/5) up to 1 cm thick
			2.5 Y 5/1	311-324 cm: clayey silt, from 313 cm strongly bioturbated with dark grey spots, in lower part scattered sed. pellets
			2.5 Y 3/1	
330			5 Y 5/1 ⇕ 5 Y 4/2	324-346 cm: alternation between grey and olive-grey clayey silt
				327-328, 334-337: strongly bioturbated
				340-346 cm: coaly dropstones up to 1 cm Ø; weathered rock fragment (7.5 YR 5/8)
360			2.5 Y 5/3	346-557 cm: foram-dominant clayey silt with indistinct colour patterns
				346-363 cm: foram-rich with 1.5 cm Ø sed. pellets; indistinct colour bands (2.5 Y 5/5) at 350, 354, 357 and 360 cm; in lower part bioturbated with darker spots
			10 YR 5/1	363-393 cm: foram-rich (Pyrgo); bioturbated with dark grey spot; dark strongly disturbed horizon at 376-378 cm
390				393-401 cm: indistinct colour banding (2.5 Y 5/5); Foram-rich
			5 Y 5/1	401-438 cm: bioturbated with light spots and stripes; in lower part Pyrgo abundant, underneath present; at 409 cm 0.5 cm wide colour horizon (2.5 Y 5/5); 416-438 cm: abundant small sed. pellets; at 415 cm 8x4 cm Ø coal clast
420				
			2.5 Y 5/3	438-447 cm: small sed. pellets and dropstones; in lower part bioturbated
			2.5 Y 3/1	447-449 cm: dark sed. pellets; bioturbated with distinct boundary to underlying sediments

Meteor 21-4	**5.6.1992 - 29.6.1992**
Station: M 238/92	**Date: 20.6.1992**
Position: 77° 04´ 02 N ; 06° 20´ 47 E	**Water Depth: 2182 m**

Core: GIK 23456-5, KAL **Core Recovery: 634 cm**
Section: 450-600 cm

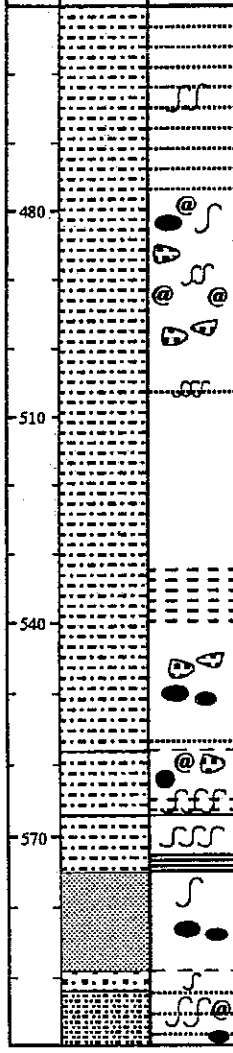

Depth (cm)	Colour	Description
	10 YR 5/1	(346-558 cm: see above) 449-479 cm: bioturbated with darker and lighter spots and streaks
480	10 YR 5/1	479-487 cm: accumulation of dropstones and sed. pellets (up to 2 cm Ø); weakly bioturbated, from 487 cm bioturbated; foram-rich
	10 YR 5/1	
510		505-507 cm: strongly bioturbated with dark grey spots and streaks
540	2.5 Y 5/1	531-541 cm: indistinct stripes and spots (2.5 Y 5/5) 541-558 cm: dark, small dropstones and sed. pellets; at base indistinct streaks (5 Y 5/5)
	2.5 Y 6/2	558-567 cm: light brownish grey foram-rich clayey silt with dropstones and sed. pellets (< 1 mm Ø) 564-566 cm: strongly bioturbated with dark olive spots and stripes
570	2.5 Y 4/2	567-575 cm: dark grey brown clayey silt, strongly bioturbated with sandy areas; at base indistinct lamination
	2.5 Y 5/1	575-589 cm: silt with darker sandy areas; sed. pellets (up to 1 cm Ø) present; weakly bioturbated
	2.5 Y 3/1	589-592 cm: very dark grey fine-sandy silt; in upper part weakly bioturbated
	2.5 Y 6/1	592-617 cm: silty clay, bioturbated with darker streaks and spots; scattered Pyrgo; dark grey sed. pellets present

Meteor 21-4	**5.6.1992 - 29.6.1992**
Station: M 238/92	**Date: 20.6.1992**
Position: 77° 04´ 02 N ; 06° 20´ 47 E	**Water Depth: 2182 m**

Core: GIK 23456-5, KAL **Core Recovery: 634 cm**
Section: 600-634 cm

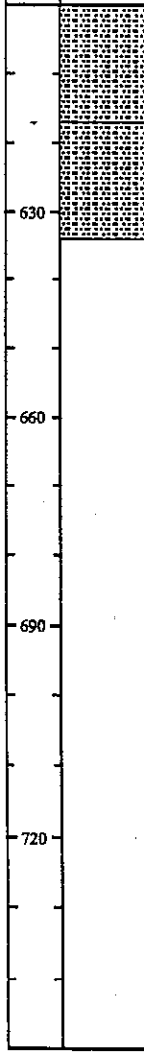

Depth (cm)	Colour	Description
		(592-617 cm: see above) 612-613 cm: dark grey (N4) discontinuous band
630	10 YR 6/1	617-624 cm: grey silty clay, weakly bioturbated with dark spots; rare Pyrgo 624-634 cm: Core Catcher; see 617-624 cm
		634 cm: EOC

Meteor 21-4	5.6.1992 - 29.6.1992
Station: M 286/92	Date: 21.6.1992
Position: 76° 38´ 2 N ; 06° 24´ 3 E	Water Depth: 2259 m

Core: GIK 23457-3, GKG — Core Recovery: 40 cm
Section: 0 - 40 cm

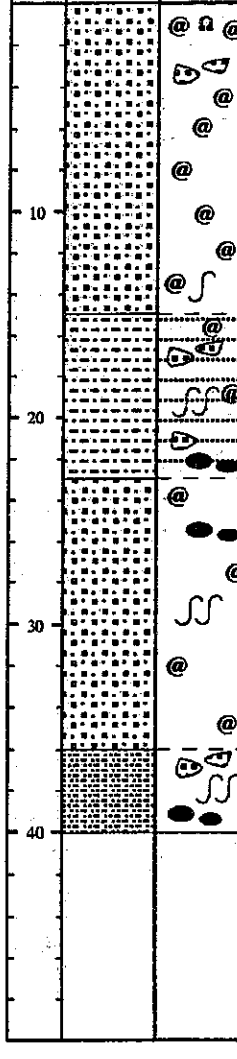

Depth (cm)	Colour	Description
0	10 YR 5/4	Surface: olive sandy silt, very foram-rich (Pyrgo); dropstones present, agglut. Forams abundant; chalk sponges, snail shells, Thenea, agglut. Polychaets present 0-15 cm: yellowish brown very foram-rich (Pyrgo) fine-sandy silt; at base weakly bioturbated with light spots; scattered dropstones
15	2.5 Y 5/3	15-23 cm: light olive brown clayey silt, in upper part foram- rich (Pyrgo), decreasing toward base; bioturbated with grey and, in lower part, brownish streaks and spots; small dark grey/black (7.5 YR 4/4) sed. pellets, dropstones abundant; down to 19 cm scattered sandy lenses
23	10 YR 6/3	23-36 cm: pale brown fine-sandy silt, bioturbated with brownish and grey spots, partly laminated; foram-rich (Pyrgo); sed. pellets up to 1 mm Ø present
36	N4	36-40 cm: dark grey weakly silty clay, commonly with sed. pellets and dropstones; bioturbated
40		EOC: 40 cm:

Meteor 21-4	5.6.1992 - 29.6.1992
Station: M 286/92	Date: 21.6.1992
Position: 76° 38´ 2 N ; 06° 23´ 8 E	Water Depth: 2253 m

Core: GIK 23457-2, KAL — Core Recovery: 573 cm
Section: 0-150 cm

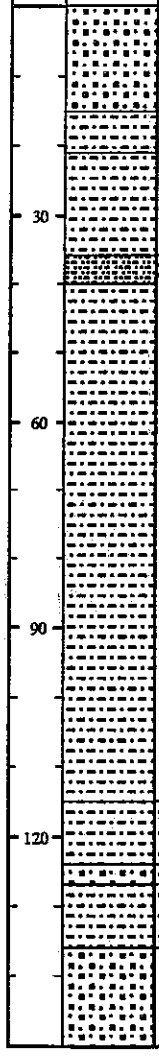

Depth (cm)	Colour	Description
0	2.5 Y 5/4	Topmost 175 cm slid out of the core. 0-15 cm: surface strongly disturbed. Light olive brown foram- rich (Pyrgo) fine-sandy silt with scattered black dropstones up to 1 cm Ø
15	2.5 Y 4/3	15-21 cm: olive brown clayey silt, bioturbated with dark spots; sandy layers; dropstones up to 1 mm Ø; scattered Forams
21	10 YR 6/4	21-36 cm: light yellowish brown clayey silt, weakly bioturbated with brown spots; foram-rich (Pyrgo); scattered dark grey sed. pellets up to 1 cm Ø; dropstones up to 1 mm Ø abundant
36	N3	36-40 cm: very dark grey strongly bioturbated weakly silty clay with light spots and stripes
40	10 YR 5/4	40-115 cm: yellowish brown foram-rich clayey silt 40-49 cm: weakly bioturbated 55-56 cm: accumulation of sed. pellets and dropstones 71-79 cm: accumulation of sed. pellets and dropstones 80-88 cm: weakly bioturbated 97-102 cm: accumulation of sed. pellets and dropstones; weakly bioturbated
115	2.5 Y 5/3	115-124 cm: light olive brown clayey silt, strongly bioturbated with dark grey (N4) spots and streaks (darker portion coarser); abundant light sed. pellets and dropstones
124	10 YR 3/1	124-127 cm: very dark grey weakly bioturbated sandy silt with abundant dark sed. pellets and dropstones
127	2.5 Y 4/4	127-136 cm: olive brown clayey silt, bioturbated with light streaks and spots; abundant sed. pellets and dropstones, decreasing toward base 130-132 cm: light brownish grey, not bioturbated
136	10 YR 5/4	136-153 cm: yellowish brown foram-rich (Pyrgo) sandy silt; from 143 cm scattered sandy nests 136-143 cm: greater fine sediment fraction 146-153 cm: weakly bioturbated with darker spots at 148 cm: 3 cm Ø black shale clast

Meteor 21-4 — **5.6.1992 - 29.6.1992**
Station: M 286/92 — **Date: 21.6.1992**
Position: 76° 38´ 2 N ; 06° 23´ 8 E — **Water Depth: 2253 m**

Core: GIK 23457-2, KAL — **Core Recovery: 573 cm**
Section: 150-300 cm

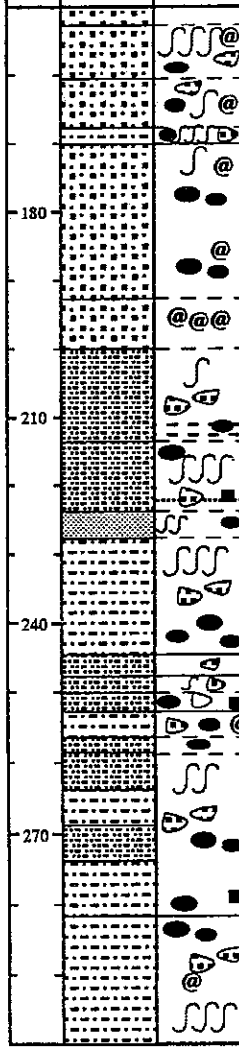

Depth (cm)	Colour	Description
		(136-153 cm: see above)
	2.5 Y 4/3	153-162 cm: olive brown sandy silt, strongly bioturbated; sed. pellets and dropstones abundant; Forams (Pyrgo) present; dark spots present, at Basis more common
	10 YR 5/4	162-168 cm: yellowish brown foram-rich weakly sandy silt, weakly bioturbated, in upper part abundant small sed. pellets and dropstones
	N3	168-170 cm: very dark grey clayey silt, strongly bioturbated; sed. pellets and dropstones abundant
	10 YR 5/4	170-193 cm: yellowish brown foram-richer fine-sandy silt, weakly bioturbated; Pyrgo abundant 170-177 cm: sed. pellets < 1 mm 188-189 cm: sed. pellets < 1 mm
	10 YR 6/4	193-200 cm: light yellowish brown very foram-rich sandy silt; Pyrgo very abundant, sandy nests present
	2.5 Y 5/3	200-214 cm: light olive brown silty clay, in upper part bioturbated with sandy nests filled with underlying sediment; from 204 cm sed. pellets and dropstones abundant, light spots present; at base 10 YR 3/3 band
	2.5 Y 5/2	214-224 cm: greyish brown strongly bioturbated silty clay; sed. pellets very abundant; dropstones present; scattered brownish streaks at base at 222 cm: 1 cm Ø coal clast
	10 YR 6/4	224-228 cm: light yellowish brown bioturbated silt; mm-Ø sed. pellets abundant
	5 Y 4/4	228-245 cm: olive strongly bioturbated clayey silt; sed. pellets and dropstones abundant; becoming darker toward base
	7.5 YR 5/6	233-239 cm: sed. pellet layer
	N3	at 245 cm: very dark grey bioturbated clayey silt with abundant sed. pellets
	N4	245-248 cm: dark grey homogenous weakly silty clay, dropstones rare
	N6	248-250 cm: grey silty clay, toward base increasingly bioturbated; dropstones abundant; boundary with overlying sediment marked by sed. pellet layer
	2.5 Y 3/2	250-253 cm: very dark greyish brown silty clay, in upper part strongly bioturbated; scattered sed. pellets; chalk clast; oxidation aureola(up to 1 mm Ø) abundant; dropstones up to 1 cm; well rounded black shales
	2.5 Y 6/2	253-257 cm: light brownish grey clayey silt, at bas strongly bioturbated; Forams very abundant; sed. pellets and dropstones (1 cm Ø) increasing toward base
	2.5 Y 3/2	257-259 cm: like 250-253 cm
	2.5 Y 5/2	259-282 cm: alternation between bands of light silty clay and of dark clayey silt; bioturbated; spotty; sed. pells and dropstones present, at base dark grey sed. pellets up to 1 cm Ø
	5 Y 4/3	259-264, 269-274 cm: light; 264-269, 274-282: dark
	2.5 Y 6/2	277-282 cm: scattered coaly dropstones
		282-300 cm: light brownish grey clayey silt, foram-rich (Pyrgo abundant); < 1 mm sed. pellets and dropstones presrent (1 cm "Trochitenkalk", rounded) 286-289 cm: dark strongly bioturbated layer with accumulation of sed. pellets, some with rust-coloured aureola

Meteor 21-4 — **5.6.1992 - 29.6.1992**
Station: M 286/92 — **Date: 21.6.1992**
Position: 76° 38´ 2 N ; 06° 23´ 8 E — **Water Depth: 2253 m**

Core: GIK 23457-2, KAL — **Core Recovery: 573 cm**
Section: 300-398 cm

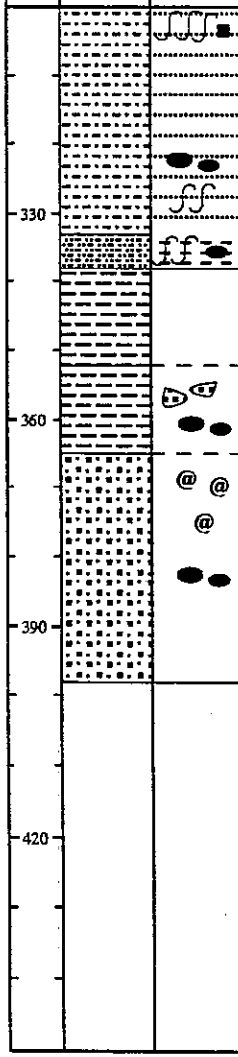

Depth (cm)	Colour	Description
	2.5 Y 5/2	300-333 cm: greyish brown clayey silt, strongly bioturbated with dark grey streaks and spots 303-307 cm: coal clasts; oxidised aureola (7.5 Y 5/8)
	2.5 Y 4/4	323-333 cm: distinct increase in sandy sed. pellets; oxidised aureola (10 YR 5/6); bioturbated
	2.5 Y 3/2	333-338 cm: very dark greyish brown weakly silty clay, bioturbated; laminated; sed. pellets present
	N4	338-352 cm: dark grey homogenous clay with few fine-sandy nests
	N3	352-365 cm: very dark grey clay; dark sed. pellets and dropstones (up to 2 cm Ø, sandstone) abundant
		365-398 cm: Core Catcher: greyish brown fine-sandy silt, foram-rich with Pyrgo; dark dropstones up to 0.2 cm Ø)
		398 cm: EOC

Meteor 21-4	**5.6.1992 - 29.6.1992**
Station: M 289/92	**Date: 22.6.1992**
Position: 75° 59´ 50 N ; 06° 21´ 42 E	**Water Depth: 2192 m**

Core: GIK 23458-3, GKG **Core Recovery: 44 cm**
Section: 0 - 44 cm

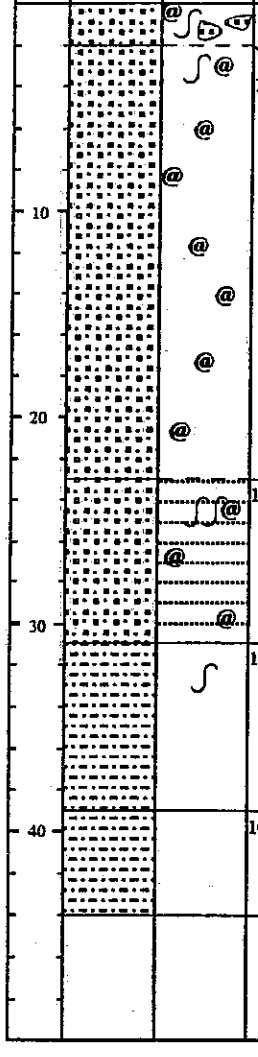

Lithology	Structure	Colour	Description
		2.5 Y 5/3	0-2 cm: light olive brown sandy silt with Pyrgo, Thenea, agglut. Forams, funnel-shaped burrow openings, angular dropstones, weakly bioturbated
		10 YR 5/4	2-23 cm: yellow brown foram-rich bioturbated sandy silt; Pyrgo very common
		10 YR 5/4	23-31 cm: yellow brown foram-rich bioturbated sandy silt; Pyrgo very common; greyish streaks
		10 YR 4/3	31-39 cm: brown clayey silt, scattered bioturbation
		10 YR 5/3	39-44 cm: brown homogenous clayey silt
			EOC: 44 cm

Meteor 21-4	**5.6.1992 - 29.6.1992**
Station: M 289/92	**Date: 22.6.1992**
Position: 75° 59´ 67 N ; 06° 21´ 35 E	**Water Depth: 2197 m**

Core: GIK 23458-4, KAL **Core Recovery: 547 cm**
Section: 0-150 cm

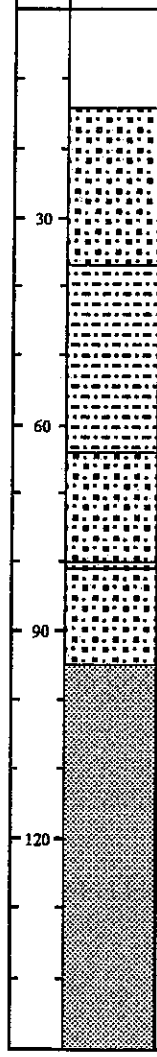

Lithology	Structure	Colour	Description
			0-14 cm: surface disturbed
		2.5 Y 5/4	14-37 cm: light olive brown foram-rich fine-sandy silt with scattered sandy lenses; Pyrgo abundant from 34 cm: toward base increasingly bioturbated with lighter parts
		10 YR 5/3	
		2.5 Y 4/4	37-64 cm: olive brown clayey silt with scattered Forams and clayey sed. pellets 50-58 cm: weakly bioturbated; sed. pellets and dropstones (up to 1 cm Ø) abundant
		10 YR 5/4	64-80 cm: yellowish brown foram-rich fine-sandy silt, weakly bioturbated with darker spots; scattered sed. pellets and dropstones
		N3	80-81 cm: very dark grey bioturbated weakly fine-sandy silt, scattered sed. pellets
		10 YR 6/3	81-95 cm: pale brown foram-rich bioturbated fine-sandy silt, sed. pellets abundant
		10 YR 5/4	95-196 cm: yellowish brown foram-rich silt, to 103 cm bioturbated with abundant sandy sed. pellets (1 cm Ø); scattered dropstones 103-108 cm: strongly bioturbated with dark grey (10 YR 5/8) spotty bands; sed. pellet-dominant

Meteor 21-4	**5.6.1992 - 29.6.1992**
Station: M 289/92	**Date: 22.6.1992**
Position: 75° 59´ 67 N ; 06° 21´ 35 E	**Water Depth: 2197 m**

Core: GIK 23458-4, KAL **Core Recovery: 547 cm**
Section: 150-300 cm

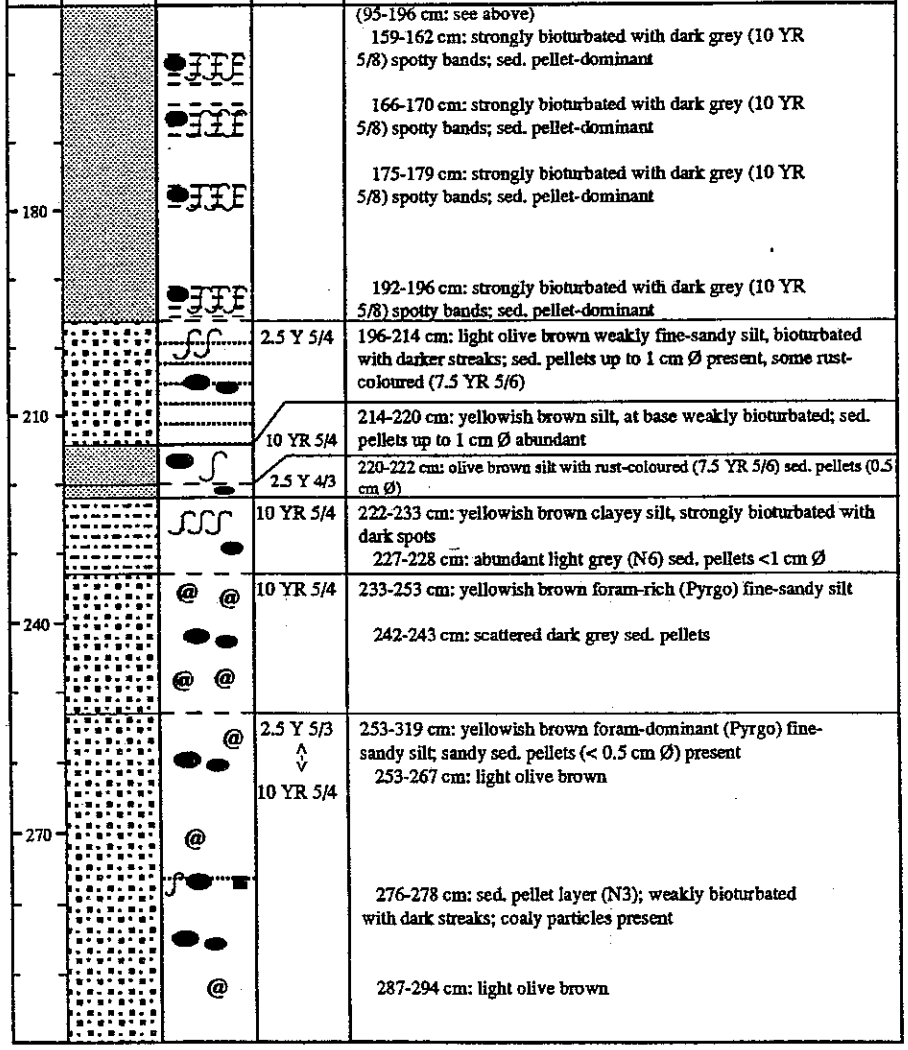

Depth (cm)	Structure	Colour	Description
			(95-196 cm: see above) 159-162 cm: strongly bioturbated with dark grey (10 YR 5/8) spotty bands; sed. pellet-dominant 166-170 cm: strongly bioturbated with dark grey (10 YR 5/8) spotty bands; sed. pellet-dominant 175-179 cm: strongly bioturbated with dark grey (10 YR 5/8) spotty bands; sed. pellet-dominant 192-196 cm: strongly bioturbated with dark grey (10 YR 5/8) spotty bands; sed. pellet-dominant
180		2.5 Y 5/4	196-214 cm: light olive brown weakly fine-sandy silt, bioturbated with darker streaks; sed. pellets up to 1 cm Ø present, some rust-coloured (7.5 YR 5/6)
210		10 YR 5/4	214-220 cm: yellowish brown silt, at base weakly bioturbated; sed. pellets up to 1 cm Ø abundant
		2.5 Y 4/3	220-222 cm: olive brown silt with rust-coloured (7.5 YR 5/6) sed. pellets (0.5 cm Ø)
		10 YR 5/4	222-233 cm: yellowish brown clayey silt, strongly bioturbated with dark spots 227-228 cm: abundant light grey (N6) sed. pellets <1 cm Ø
240	@ @	10 YR 5/4	233-253 cm: yellowish brown foram-rich (Pyrgo) fine-sandy silt 242-243 cm: scattered dark grey sed. pellets
	@	2.5 Y 5/3 ∧∨ 10 YR 5/4	253-319 cm: yellowish brown foram-dominant (Pyrgo) fine-sandy silt; sandy sed. pellets (< 0.5 cm Ø) present 253-267 cm: light olive brown
270	@		276-278 cm: sed. pellet layer (N3); weakly bioturbated with dark streaks; coaly particles present
	@		287-294 cm: light olive brown

Meteor 21-4	**5.6.1992 - 29.6.1992**
Station: M 289/92	**Date: 22.6.1992**
Position: 75° 59´ 67 N ; 06° 21´ 35 E	**Water Depth: 2197 m**

Core: GIK 23458-4, KAL **Core Recovery: 547 cm**
Section: 300-450 cm

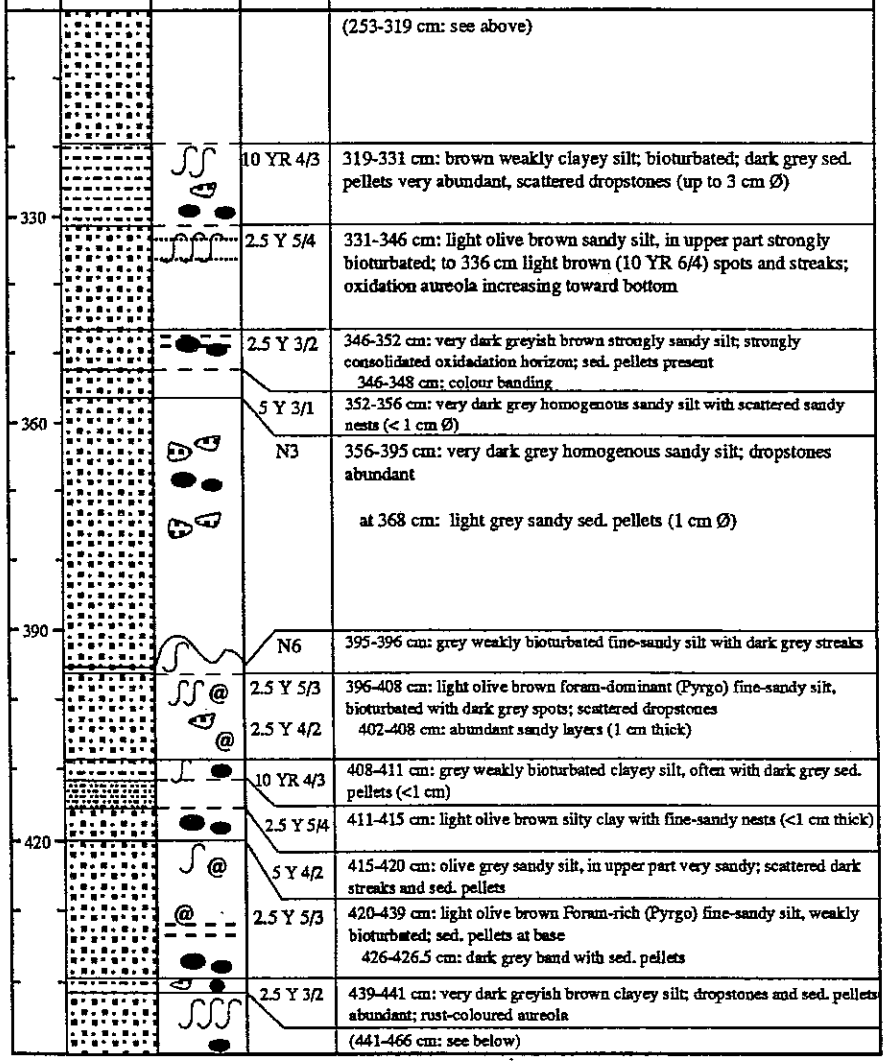

Depth (cm)	Structure	Colour	Description
			(253-319 cm: see above)
330		10 YR 4/3	319-331 cm: brown weakly clayey silt; bioturbated; dark grey sed. pellets very abundant, scattered dropstones (up to 3 cm Ø)
		2.5 Y 5/4	331-346 cm: light olive brown sandy silt, in upper part strongly bioturbated; to 336 cm light brown (10 YR 6/4) spots and streaks; oxidation aureola increasing toward bottom
		2.5 Y 3/2	346-352 cm: very dark greyish brown strongly sandy silt; strongly consolidated oxidadation horizon; sed. pellets present 346-348 cm: colour banding
360		5 Y 3/1	352-356 cm: very dark grey homogenous sandy silt with scattered sandy nests (< 1 cm Ø)
		N3	356-395 cm: very dark grey homogenous sandy silt; dropstones abundant at 368 cm: light grey sandy sed. pellets (1 cm Ø)
390		N6	395-396 cm: grey weakly bioturbated fine-sandy silt with dark grey streaks
	@ @	2.5 Y 5/3 2.5 Y 4/2	396-408 cm: light olive brown foram-dominant (Pyrgo) fine-sandy silt, bioturbated with dark grey spots; scattered dropstones 402-408 cm: abundant sandy layers (1 cm thick)
		10 YR 4/3	408-411 cm: grey weakly bioturbated clayey silt, often with dark grey sed. pellets (<1 cm)
		2.5 Y 5/4	411-415 cm: light olive brown silty clay with fine-sandy nests (<1 cm thick)
420	@	5 Y 4/2	415-420 cm: olive grey sandy silt, in upper part very sandy; scattered dark streaks and sed. pellets
	@	2.5 Y 5/3	420-439 cm: light olive brown Foram-rich (Pyrgo) fine-sandy silt, weakly bioturbated; sed. pellets at base 426-426.5 cm: dark grey band with sed. pellets
		2.5 Y 3/2	439-441 cm: very dark greyish brown clayey silt; dropstones and sed. pellets abundant; rust-coloured aureola
			(441-466 cm: see below)

Meteor 21-4	**5.6.1992 - 29.6.1992**
Station: M 289/92	**Date: 22.6.1992**
Position: 75° 59´ 67 N ; 06° 21´ 35 E	**Water Depth: 2197 m**

Core: GIK 23458-4, KAL **Core Recovery: 547 cm**

Section: 450-513 cm

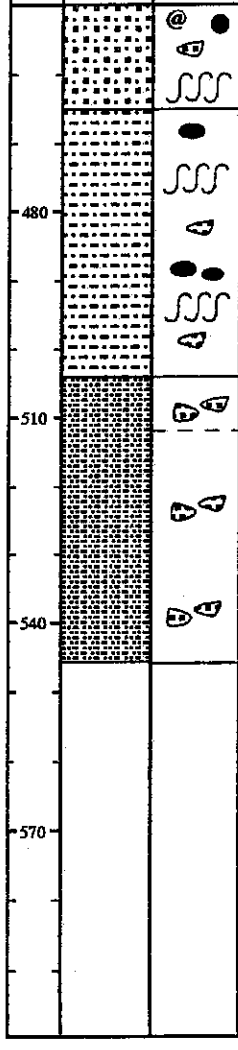

Depth (cm)	Lithology	Structure	Colour	Description
			2.5 Y 5/3 ⇕ 10 YR 5/4	441-466 cm: light olive brown foram-rich (Pyrgo) fine-sandy silt; at top of base small (mm-range) dropstones; 3-4 cm Ø dark grey sed. pellet sunk into underlying sediment 447-451, 456-460, 463-466 cm: darker bands; strongly bioturbated; sed. pellets abundant
			2.5 Y 5/4 ⇕ 5 Y 4/3	466-505 cm: interlayering of lighter (466-471, 474-478, 483- 487, 489-493 cm) and darker (strongly bioturbated; 471- 474, 478-483, 487-489, 493-505 cm) layers of clayey silt; sed. pellets and dropstones (Ø mm- range) abundant, more common in darker layers; rust-coloured sandy nests, more common at 474-483; at base oxidised horizon
				505-513 cm: homogenous weakly silty clay with scattered dropstones
				Core Catcher: see 505-513 cm
				547 cm: EOC

Meteor 21-4	**5.6.1992 - 29.6.1992**
Station: M 291/92	**Date: 22.6.1992**
Position: 75° 52´ 54 N ; 05° 28´ 98 E	**Water Depth: 2574 m**

Core: GIK 23459-2, GKG **Core Recovery: 56 cm**
Section: 0 - 56cm

Depth (cm)	Lithology	Structure	Colour	Description
0		@ @ @	5 Y 5/4	Surface: abundant Pyrgo and aggl. Forams; Cyclopects, Gastropods, and Dropstones (weathered black shales?) present 0-20 cm: olive fine-sandy silt; foram-rich (Pyrgo)
20				20-56 cm:
56				56 cm: EOC

Meteor 21-4	**5.6.1992 - 29.6.1992**
Station: M 291/92	**Date: 22.6.1992**
Position: 75° 52´ 44 N ; 05° 30´ 63 E	**Water Depth: 2622 m**

Core: GIK 23459-1, KAL **Core Recovery: 593 cm**
Section: 0-150 cm

Depth (cm)	Lithology	Structure	Colour	Description
0		@ @	2.5 Y 4/4	0-13 cm: **Strongly disturbed** Olive brown fine-sandy silt, Pyrgo abundant, weakly bioturbated
			2.5 Y 5/2	13-21 cm: grey brown weakly fine-sandy silt; sed. pellets (mm-Ø) abundant, dropstones up to 1 cm Ø present, edges weakly rounded, weakly bioturbated
30		@ @	10 YR 4/3 10 YR 3/2	21-35 cm: brown fine-sandy silt; sed. pellets (10 YR 4/2) up to 2 mm Ø; Pyrgo present; bioturbated streaks in boundary to underlying sediment, weakly bioturbated
		@	10 YR 4/3	36-40 cm: brown strongly silty fine sand; sed. pellets (1 cm Ø) abundant; Pyrgo present
			10 YR 5/3	40-52 cm: brown fine-sandy silt with bioturbated streaks, layered up to 2 cm long; sed. pellets present 42-47 cm: weak colour layering due to darker (10 YR 4/4) stripes
60			10 YR 4/3	52-104 cm: brown homogenous fine-sandy silt; in upper part sed. pellets (up to 1.5 cm Ø) abundant, weakly bioturbated 70-71 cm: 10 YR 4/2 70-80 cm: Pyrgo common 76-78 cm: 10 YR 4/2; sed. pellets (2.5 Y 4/3) distinctly layered 85-87 cm: 10 YR 3/3
90			10 YR 4/3	104-114 cm: brown weakly fine-sandy silt; sed. pellets (up to 8 mm Ø) rare 104-106 cm: bioturbated spots up to 4 mm large 106-114 cm: large bioturbation streak (2.5 Y 3/2)
120		@ @	7.5 YR 4/2	114-126 cm: brown relatively homogenous foram-dominant fine-sandy silt, in upper part darker (10 YR 3/3); sed. pellets up to 6 mm Ø rare, weakly bioturbated
		@ @ @	10 YR 4/3	126-153 cm: brown fine-sandy silt, Forams dominant; sed. pellets 2-3 mm Ø 126-134 cm: strongly bioturbated (2.5 Y 3/2) 139-143 cm: strongly bioturbated (2.5 Y 3/2) 146-152 cm: strongly bioturbated (2.5 Y 3/2) 143-153 cm: sed. pellets increasingly larger

Meteor 21-4	**5.6.1992 - 29.6.1992**
Station: M 291/92	**Date: 22.6.1992**
Position: 75° 52´ 44 N ; 05° 30´ 63 E	**Water Depth: 2622 m**

Core: GIK 23459-1, KAL **Core Recovery: 593 cm**
Section: 150-300 cm

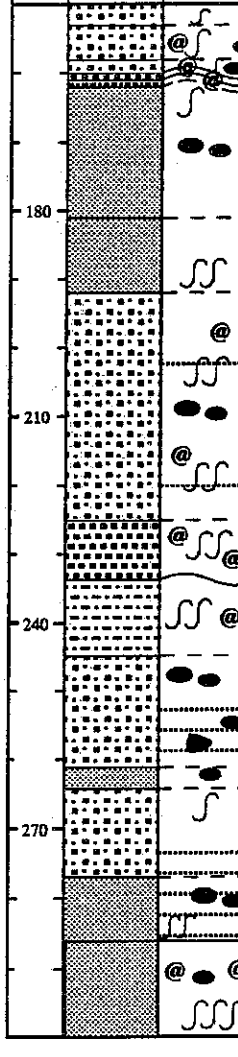

Lithology	Structure	Colour	Description
			(126-153 cm: see above)
		2.5 Y 4/3	153-158 cm: olive brown weakly fine-sandy silt; oval sed. pellets up to 1 cm Ø; scattered Pyrgo, weakly bioturbated
		2.5 Y 4/2	158-160 cm: dark grey brown strongly fine-sandy silt; 1 sed. pellet (7.5 YR 5/8); weakly bioturbated
		2.5 Y 7/2	160-161 cm: light grey fine-sandy Foram-rich layer, at base darker (N4) horizon (2 mm thick)
		2.5 Y 5/4	161-162 cm: light olive brown strongly silty fine sand, foram-dom.
		2.5 Y 5/6	162-181 cm: light olive brown foram-dominant silt, in upper part common dark bioturbation spots; sed. pellets up to 2 mm Ø present
		5 Y 4/3	181-192 cm: olive silt, bioturbated streaks at base
		2.5 Y 5/4	192-225 cm: light olive brown fine-sandy silt; Pyrgo common; sed. pellets up to 6 mm Ø; streaks with black layering 203-204 cm: dark (N4) bioturbation horizons 219-221 cm: dark (N4) bioturbation horizons
		2.5 Y 6/3	225-234 cm: light yellow brown strongly foram-dominant fine sand, in lower part coarse to middle-sandy; Pyrgo common; in upper part bioturbated
		2.5 Y 4/4	234-245 cm: olive brown clayey silt, in upper part (to 239 cm) streaks with foram-dominant fine sand; round to oval burrows, bioturbated
		2.5 Y 4/3	245-261 cm: olive brown fine-sandy silt; sed. pellets up to 5 mm Ø common 247-248, 252-253, 257-258, 260-261 cm: dark (N4) colour stripes 255-257 cm: black decomposed Dropstone (black shale?)
		2.5 Y 6/3	261-264 cm: light yellow brown homogenous silt, at base sed. pellets (up to 1.5 cm Ø) common
		5 Y 4/2	264-277 cm: olive grey fine-sandiy Silt, in lower half colour transition from 7.5 YR 5/6) to (5 Y 4/4), weakly bioturbated 271-272 cm: ochre-coloured clayey layer
		5 Y 5/2 5 Y 4/1	277-286 cm: olive grey silt with streaks and bands 283-286 cm: bioturbation horizon; sed. pellets (mm-Ø) common; orange spots
		5 Y 5/4	286-306 cm: olive silt, Forams dominant; scattered sed. pellets (mm-Ø) 286-290 cm: lightening (2.5 Y 6/4); weakly bioturbated 290-299 cm: strongly bioturbated

Meteor 21-4	**5.6.1992 - 29.6.1992**
Station: M 291/92	**Date: 22.6.1992**
Position: 75° 52´ 44 N ; 05° 30´ 63 E	**Water Depth: 2622 m**

Core: GIK 23459-1, KAL **Core Recovery: 593 cm**
Section: 300-450 cm

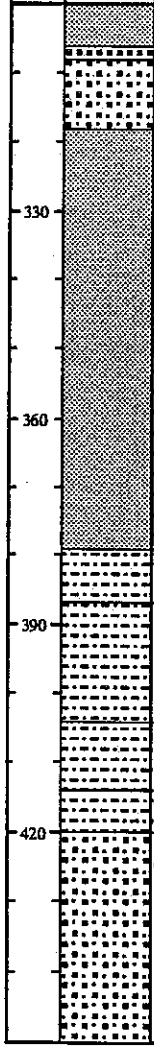

Lithology	Structure	Colour	Description
		N5	(286-306 cm: see above) 305-306 cm: weakly bioturbated
		2.5 Y 6/3	306-308 cm: light yellow brown foram-dominant fine sand with darker (2.5 Y 4/2) clayey base (1 cm thick)
		2.5 Y 4/2	308-318 cm: dark grey brown fine-sandy silt; weakly bioturbated 308-312 cm: distinctly lighter (2.5 Y 5/4); oxidised
		5 Y 5/3	318-379 cm: olive fine-sandy silt; Pyrgo in fine- sandy streaks; weakly bioturbated 324-324.5, 329-331, 348-351, 356-358, 360-365, 368-369, 371-377 cm: dark (5 Y 4/1) (bioturbated) banding, with some distinct colour changes
		2.5 Y 4/3	377-387 cm: olive brown clayey silt, bioturbated; horizontal oxidation horizons (10 YR 6/8); sed. pellets present
		N4	387-404 cm: dark grey homogenous clayey silt with sandy parts; sed. pellets present
		N6	404-414 cm: grey clayey silt, spotty 407-409 cm: bioturbated dark grey (N5) band 409-410, 413-414 cm: dark grey sed. pellet layers; scattered dropstones
		N6	414-420: grey clayey silt; toward base increasing colour darkening with sed. pellets; diffuse yellowish (2.5 Y 6/8) streaks
		10 YR 5/4	420-527 cm: yellow brown foram-dominant fine-sandy silt, spottily bioturbated; Pyrgo present 424-437 cm: strongly bioturbated; accumulation of sed. pellets 436-442 cm: coaly dropstones

Meteor 21-4	**5.6.1992 - 29.6.1992**
Station: M 291/92	**Date: 22.6.1992**
Position: 75° 52´ 44 N ; 05° 30´ 63 E	**Water Depth: 2622 m**

Core: GIK 23459-1, KAL **Core Recovery: 593 cm**
Section: 450-593 cm

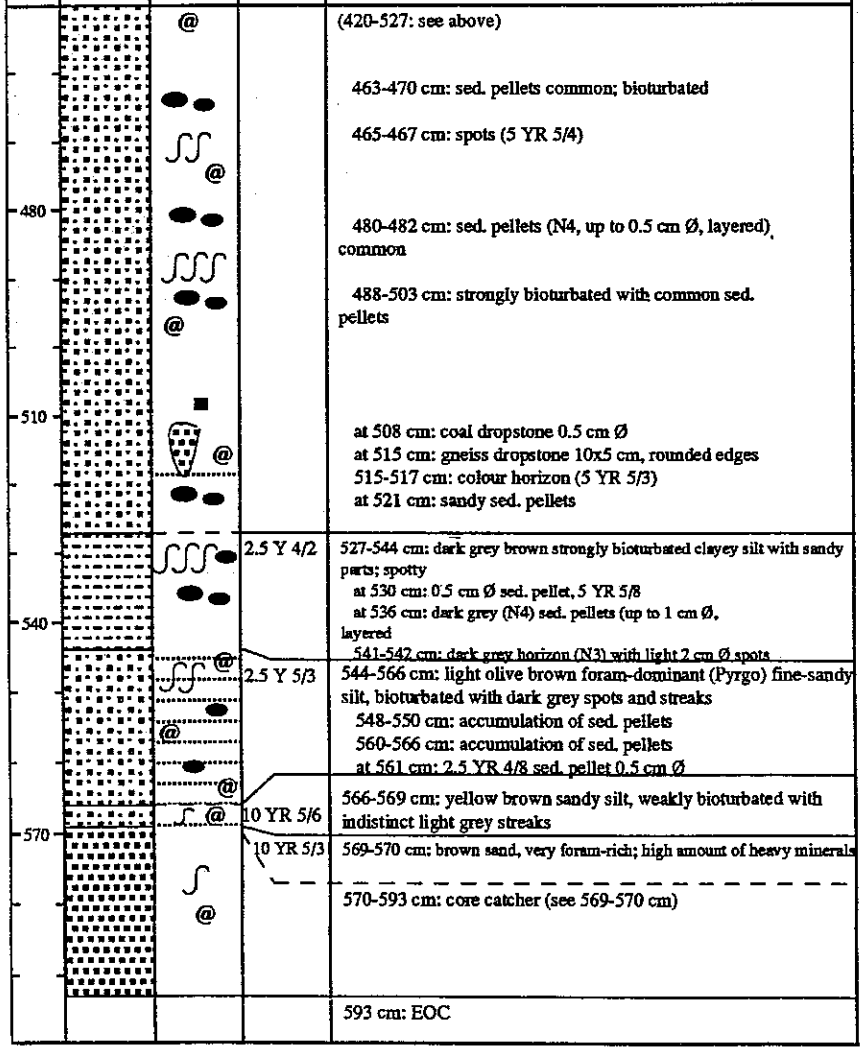

Colour	Description
	(420-527: see above)
	463-470 cm: sed. pellets common; bioturbated
	465-467 cm: spots (5 YR 5/4)
	480-482 cm: sed. pellets (N4, up to 0.5 cm Ø, layered) common
	488-503 cm: strongly bioturbated with common sed. pellets
	at 508 cm: coal dropstone 0.5 cm Ø at 515 cm: gneiss dropstone 10x5 cm, rounded edges 515-517 cm: colour horizon (5 YR 5/3) at 521 cm: sandy sed. pellets
2.5 Y 4/2	527-544 cm: dark grey brown strongly bioturbated clayey silt with sandy parts; spotty at 530 cm: 0.5 cm Ø sed. pellet, 5 YR 5/8 at 536 cm: dark grey (N4) sed. pellets (up to 1 cm Ø, layered 541-542 cm: dark grey horizon (N3) with light 2 cm Ø spots
2.5 Y 5/3	544-566 cm: light olive brown foram-dominant (Pyrgo) fine-sandy silt, bioturbated with dark grey spots and streaks 548-550 cm: accumulation of sed. pellets 560-566 cm: accumulation of sed. pellets at 561 cm: 2.5 YR 4/8 sed. pellet 0.5 cm Ø
10 YR 5/6	566-569 cm: yellow brown sandy silt, weakly bioturbated with indistinct light grey streaks
10 YR 5/3	569-570 cm: brown sand, very foram-rich; high amount of heavy minerals
	570-593 cm: core catcher (see 569-570 cm)
	593 cm: EOC

Meteor 21-4	**5.6.1992 - 29.6.1992**
Station: M 295/92	**Date: 26.6.1992**
Position: 67° 43.10´ N ; 6° 51.30´ E	**Water Depth: 1277 m**

Core: GIK 23462-2, KAL **Core Recovery: 425 cm**

Section: 0-150 cm

Depth (cm)	Lithology	Structure	Colour	Description
30		@ @ @ @ @ @	10 YR 4/3	0-100 cm: silty clay, weakly fine-sandy; scattered Pyrgo, few Pogo 0-20 cm: disturbed; at base irregular brown layer, 2-4 cm thick; diagenetically and biologically not sedimentary
			10 YR 3/4 ⇩ 2.5 Y4/4 ⇩ 2.5 Y 5/2	20-34 cm: streaky colour change: Colour -> olive brown -> greyish brown from 34 cm: homogenous
90				
120			5 Y 4/2	100-117 cm: olive green (with reddish parts) silty fine-sandy clay, bioturbated; sed. pellets (greenish, 2-10 mm Ø) present
			5 Y 3/1	117-134 cm: silty clay, weakly layered; scattered very dark grey sed. pellets (2-3 mm Ø); bioturbated base
			5 Y 5/2	134-152 cm: silty fine-sandy clay, bioturbated (burrows 10-30 mm Ø, some filled with clay [2.5 Y 4/2]); abundant brownish (5 Y 4/2) clay pellets (2-20 mm Ø); large (20 cm) clay block with diffuse boundary with matrix

Meteor 21-4	**5.6.1992 - 29.6.1992**
Station: M 295/92	**Date: 26.6.1992**
Position: 67° 43.10´ N ; 6° 51.30´ E	**Water Depth: 1277 m**

Core: GIK 23462-2, KAL **Core Recovery: 425 cm**

Section: 150-300 cm

Depth (cm)	Lithology	Structure	Colour	Description
				(134-152 cm: see above)
180			2.5 Y 4/2	152-251 cm: dark greyish brown silty clay with sed. pellets (5 mm Ø); relatively homogenous; bioturbated; at base streaky layering, sed. pellets larger at 164 cm: diagenetic band (1-2 cm thick, 10 YR 4/4), partially consolidated
210				
240				
270				251-424 cm: silty clay, bioturbated; clay pellets, especially at 310-322 and 340-347 cm 278-289 cm: brown diagenetic band

Meteor 21-4	**5.6.1992 - 29.6.1992**
Station: M 295/92	**Date: 26.6.1992**
Position: 67° 43.10´ N ; 6° 51.30´ E	**Water Depth: 1277 m**

Core: GIK 23462-2, KAL **Core Recovery: 425 cm**

Section: 300-424 cm

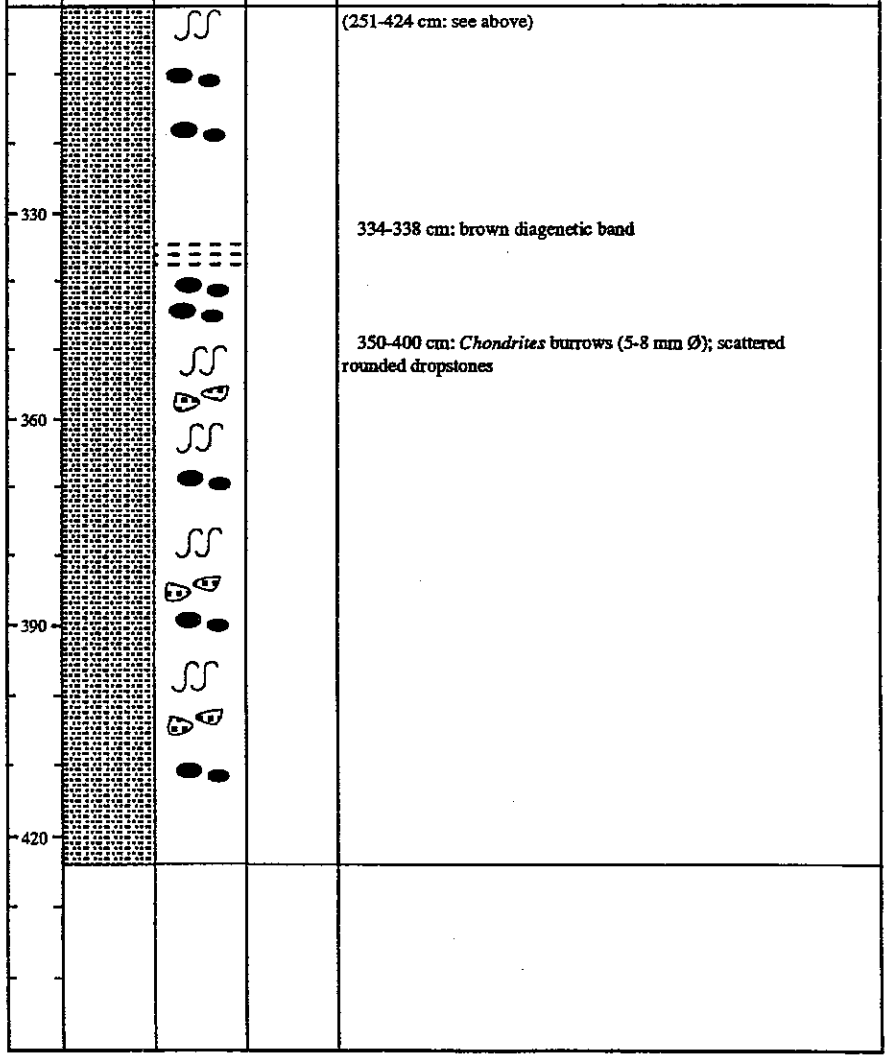

8 Schlußbemerkung

Im Namen aller wissenschaftlichen Teilnehmer bedanken wir uns herzlich bei den Kapitänen Müller und Wagener und der Besatzung von METEOR für die ausgezeichnete Zusammenarbeit, für technische Hilfeleistungen und die gute Atmosphäre an Bord. Unser Dank gilt auch den Mitarbeitern der Leitstelle "METEOR", der Deutschen Forschungsgemeinschaft, dem Bundesministerium für Forschung und Technologie und dem Auswärtigen Amt, die mitgeholfen haben, daß diese Expedition ein Erfolg werden konnte. Danken möchten wir ferner den Helferinnen und Helfern in den Heimatinstitutionen für die vor und während der Reise geleistetete Unterstützung. Dies gilt auch für Frau Weigert vom Contiways Reisebüro in Hamburg und Herrn Bohn von der Transportfirma Lehnkering Montan in Hamburg. Frau Berghahn leistete wertvolle Hilfe im Koordinationsbüro am Institut für Hydrobiologie und Fischereiwissenschaft der Universität Hamburg.

Die Expedition wurde gefördert mit Mitteln der Deutschen Forschungsgemeinschaft im Vorhaben Pf 248/2-1 sowie im Rahmen der Einzelvorhaben von JGOFS, SFB 313 und BIO-C-FLUX durch die Deutsche Forschungsgemeinschaft und den Bundesminister für Forschung und Technologie.

9 Literatur

ALMGREN, T., D. DYRSSEN and S. FONSELIUS (1983): Determination of alkalinity and total carbonate. In: K. GRASSHOFF, M. EHRHARDT and K. KREMLING (Eds.) Methods of Seawater Analysis. Verlag Chemie, Weinheim; Deerfield, Florida; Basel, 99-123.

ARHAN, M (1990): The North Atlantic Current and Subarctic Intermediate Water. J. Mar. Res., **48**, 109-144.

ARHAN, M., A. COLIN DE VERDIERE and H. MERCIER (1989): Direct Observations of the Mean Circulation at 48°N in the Atlantic Ocean. J. Phys. Oceanogr., **19**, 161-181.

BARNETT, P.R.O., J. WATSON, AND D. CONELLY (1984): A multiple corer for taking virtually undisturbed samples from shelf, bathyal and abyssal sediments. Oceanol. Acta 7, 399-408.

BARTHEL, D., O.S. TENDAL und U. WITTE (1991): Faunistik, Biologie, Ökologie und Spicula-Lieferung von Schwämmen. In: S.A. GERLACH und G. GRAF (Eds.) Europäisches Nordmeer; Reise Nr.13, 6.Juli-24.August 1990. METEOR-Ber., Univ. Hamburg, 91-2, 37-47.

BICKERT, T. und R. HENRICH (1989): Karbonate nahe der Arktis: Rezente Flachwasserkarbonate auf der Spitzbergenbank (Barentsschelf). Geol. Paläont. Mitt., **16**, 4.

BIGG, G.R. (1984): A note on the temporal evolution of Taylor columns over topography. Dyn. Atmos. Oceans., **8** (1), 87-94.

BIRGISDOTTIR, L. (1991): Die paläo-ozeanographische Entwicklung der Islandsee in den letzten 550000 Jahre. Ber. Sonderforschungsber. 313, **34**, 1-112. Appendix.

BJÖRLYKKE, K., B. BUE and A. ELVERHÖI (1978): Quaternary sediments in the northwestern part of the Barents Sea and their relation to the underlying Mesozoic bedrock. Sedimentology (25): 227-246.

BLAUME, F. (1992): Hochakkumulationsgebiete am norwegischen Kontinentalhang: Sedimentologische Abbilder Topographie-geführter Strömungsmuster. Ber. Sonderforschungsber. 313, **36**, 1-150.

BLINDHEIM, J. (1989): Cascading of Barents Sea bottom water into Norwegian Sea. Rapp. P.-v. Réun. Cons. int. Explor. Mer, **188**, 49-58

BRADSHAW, A.L. and P.G. BREWER, (1988): High precision measurements of alkalinity and total carbon dioxide in seawater by potentiometric titration: 1. Presence of unknown proteolyte(s)? Mar. Chem., **23**, 69-86.

BRECHNER, W.O. and N.G. HOGG, (1980): Oceanic observations of stratified Taylor columns near a bump. Deep-Sea Res., **27**, 1029-1045.

BREWER, P.G., A.L. BRADSHAW and R.T. WILLIAMS (1986): Measurements of total carbon dioxide and alkalinity in the North Atlantic Ocean in 1981. In: J.R. TRABALKA and D.E. REICHLE (Eds.) The Changing Carbon Cycle. Springer Verlag, 348-370.

BROECKER, W.S. and T.-H. PENG (1982): Tracers in the Sea. Eldigio Press, 1-690.

CHEN, C.T.A. (1982): On the distribution of anthropogenic CO_2 in the Atlantic and Southern oceans. Deep-Sea Res., **29**, 563-580.

CHEN, R.F. and BADA J.L. (1992): The fluorescence of dissolved organic matter in seawater. Mar. Chem., **37**, 191-221.

COLIN DE VERDIERE, A., H. MERCIER and M. ARHAN (1989): Mesoscale variability transition from the Western to the Eastern Atlantic along 48°N. J. Phys. Oceanogr., **19**, 1149-1170.

CONWAY MORRIS, S. (1989): The persistence of Burgess Shale-type faunas: implications for the evolution of deeper-water faunas. Trans. Royal Soc., Edinburgh: Earth Sciences, **80**, 271-283.

DETERMANN, S., R. REUTER, P. WAGNER and R. WILLKOMM (1993): The horizontal and vertical distribution of fluorescent matter in the eastern Atlantic Ocean. (Submitted to Deep-Sea Res.)

DICKSON, A.G. (1981): An exact definition of total alkalinity and a procedure for the estimation of alkalinity and total inorganic carbon from titration data. Deep-Sea Res., **28A** (6), 609-623.

DICKSON, A.G. and C. GOYET (eds, 1991): Handbook of Methods for the Analysis of the Various Parameters of the Carbon Dioxide System in Sea Water. U.S. DOE, SRGP 89-7A.

DIETRICH, G., K. KALLE, W. KRAUSS and G. SIEDLER (1975): Allgemeine Meereskunde, Bornträger, Berlin, 593 pp.

FITZWATER, S.E. and J.H. MARTIN (1993): Notes on the JGOFS North Atlantic Bloom Experiment - dissolved organic carbon intercomparison. Mar. Chem., **41**, 179-185.

GARDNER, W.D. (1989): Baltimore Canyon as a modern conduit of sediment to the deep sea. - Deep-Sea Res., **36** (3), 323-358.

GARDNER, W.D. and I.D. WALSH (1990): Distribution of macroaggregates and fine-grained particles across a continental margin and their potential role in fluxes. Deep-Sea Res., **37** (2), 401-411.

GERLACH, S.A. and G. GRAF, (1990): Europäisches Nordmeer, Reise Nr. 13, 6. Juli - 24. August 1990. - METEOR-Ber. Univ. Hamburg, 91-2, 217 S.

GLOVER, D.M. and P.G. BREWER (1988): Estimates of wintertime mixed layer nutrient concentrations in the North Atlantic. Deep-Sea Res., **35**, 1525-1546.

GOYET, C. and POISSON, A. (1989): New determination of carbonic acid dissociation constants in seawater as a function of temperature and salinity. Deep-Sea Res., **36**, 1635-1654.

GRASSHOFF, K. (1976): Methods of Seawater Analysis. Verlag Chemie, Weinheim, New York, 317 pp.

HARVEY, J. and M. ARHAN (1988): The water masses of the Central North Atlantic in 1983-84. J. Phys. Oceanogr., **18**, 1855-1875.

HAYASE, K., H. TSUBOTA and I. SUNADA (1988): Vertical distribution of fluorescent organic matter in the North Pacific. Mar. Chem., **25**, 373-381.

HENRICH, R., M. HARTMANN, J. REITNER, P. SCHÄFER, S. STEINMETZ, A. FREIWALD, P. DIETRICH and J. THIEDE, J. (1992): Facies belts, biocoenoses, volcanic structures and assocoated sediments of the Arctic seamount Vesterisbanken (Central Greenland Sea). Facies, **27**, 71-104.

HOGG, N.G. (1973): On the stratified Taylor column. J. Fluid Mech., **58**, 517 - 537.

HONJO, S., S.J. MANGANINI and G. WEFER (1988): Annual particle flux and a winter outburst of sedimentation in the northern Norwegian Sea. Deep-Sea Res., **35** (8), 1223-1234.

JENSEN, P., J. RUMOHR and G. GRAF (1992): Sedimentological and biological differences across a deep-sea ridge (Vöring Plateau escarpment, Norwegian Sea) exposed to advection and accumulation of fine-grained particles. (Oceanologica Acta: in press)

JOHNSON, K.M., P.J.LeB. WILLIAMS, L. BRÄNDSTRÖM and J.McN. SIEBURTH (1987): Coulometric total carbon dioxide analysis for marine studies: Automatization and calibration. Mar. Chem., **21**, 117-133.

KILLWORTH, P.D. (1983): Deep convection in the world ocean. Reviews on Geophysics and Space Physics, **21** (1), 1-26.

KIRCHMANN, D.L., Y. SUZUKI, C. GARSIDE and H.W. DUCKLOW (1991): High turnover rates of dissolved organic carbon during a spring phytoplankton bloom. Nature, **352**, 612-614.

KOEVE, W., R.W. EPPLEY, S. PODEWSKI and B. ZEITZSCHEL (1993): An unexpected nitrate distribution in the tropical North Atlantic at 18°N/30°W - implications for new production. Deep-Sea Res. II, **40**, 521-536.

KRAUSS, W. and R. KÄSE (1984): Mean circulation and eddy kinetic energy in the Eastern North Atlantic. J. Geophys. Res., **89**, C3, 3407-3415.

KUPFERMANN, S.L., G.A. BECKER, W.F. SIMMONS, U. SCHAUER, M.G. MARIETTA and H. NIES (1986): An intense cold core eddy in the North-East Atlantic. Nature, **319**, 474-477.

LACHSCHEWITZ, K.S., R. OEHMIG und H.-J. WALLRABE ADAMS (1990): Der aktive mittelozeanische Rücken als Sedimentationsraum - Zusammensetzung und Dynamik der Sedimente am Kolbeinsey-Rücken (N'Island). Zbl. Geol. Paläont. Teil 1, **11**, 1727-1738.

LEVITUS, S. (1982): Climatological Atlas of the World Ocean. NOAA Technical Paper No. 3, US Dept. of commerce, Rockville, MD., 173 pp.

LOCHTE, K. (1992): Bacterial standing stock and consumption of organic carbon in the benthic boundary layer of the abyssal North Atlantic. In: G.T. Rowe and V. Pariente (Eds.) Deep-sea food chains and the global carbon cycle. Kluwer Academic Publishers, Dordrecht, The Netherlands, 1-10.

MIDTTUN, L. (1985): Formation of a dense bottom water in the Barents Sea. Deep-Sea Res., **32**, 1233-1241.

MITTELSTAEDT, E. (1987): Cyclonic cold core eddy in the eastern North Atlantic. I. Physical description. Mar. Ecol. Progr. Ser., **39**, 145-152.

NELSON, D.D., J.W. PIERCE and D.D. COLQUHOUN (1973): Sediment dispersal by cascading coastal water. Geol. Soc. Am. Abstr. Programs (8), 423-424.

NYFFELER, F. and C.-H. GODET (1986): The structural parameters of the benthic nepheloid layer in the northeast Atlantic. Deep-Sea Research, **33**, 195-207.

PFANNKUCHE, O. (1993): Benthic response to the sedimentation of particulate organic matter at the BIOTRANS station, 47°N, 20°W. Deep-Sea Res. II, **40**, 135-149.

PFANNKUCHE, O. (1992): Organic carbon flux through the benthic community in the temperate abyssal northeast Atlantic. In: G.T. Rowe and V. Pariente (Eds.) Deep-sea food chains and the global carbon cycle, Kluwer Academic Publishers, Dordrecht, The Netherlands, 183-198.

PFANNKUCHE, O. and K. LOCHTE, (1993): Central oceanic bentho-pelagic coupling: cyanobacteria as tracers of sedimenting salp feacal pellets. Deep-Sea Res., **40**, 727-737.

PFANNKUCHE, O. and K. LOCHTE, (1992): Central oceanic bentho-pelagic coupling: cyanobacteria as tracers of sedimenting salp feacal pellets. Deep-Sea Res., (in press).

PODEWSKI, S., G. SAURE, R.W. EPPLEY, W. KOEVE, R. PEINERT and B. ZEITZSCHEL (1993): The Nose: a characteristic inversion within the salinity maximum water in the tropical northeast Atlantic. Deep-Sea Res. II, **40**, 537-557.

QUADFASEL, D., B. RUDELS and K. KURZ (1988): Outflow of dense water from a Svalbard fjord into the Fram Strait. Deep-Sea Res., **35** (7), 1143-1150.

REITNER, J. und R. HENRICH (1991): Benthos-Gemeinschaften des Vesterisbanken-Seamount in der NE-Grönland-See (FS "Polarstern"-Expedition ARK VII/1, 1990). Verh. Deutsch. Zool. Ges., **84**, 507-508.

RIGBY, J.K. (1986): Sponges of the Burgess Shale (Middle Cambrian) British Columbia. Palaeont. Can., **2**, 1-105.

ROBINSON, A.R., D.J. MCGILLICUDDY, J. CALMAN, H.W. DUCKLOW, M.J.R. FASHAM, F.E. HOGE, W.G. LESLIE, J.J. MCCARTHY, S. PODEWSKI, D.L. PORTER, G. SAURE, J.A. YODER (1993): Meso-scale and upper ocean variabilities during the 1989 JGOFS Bloom Study. Deep-Sea Res. II, **40**, 9-35.

ROBINSON, C. and P.G.LeB. WILLIAMS (1991): Development and assessment of an analytical system for the accurate and continual measurement of total dissolved inorganic carbon. Mar. Chem., **34**, 157-175.

ROBINSON, M.K., R.A. BAUER and E.H. SCHROEDER (1979): Atlas of the North Atlantic - Indian Ocean monthly mean temperatures and mean salinities of the surface layer. U.S. Naval Oceanographic Office Ref. Pub. 18, Washington D.C.

RUDELS, B. (1990): Haline convection in the Greenland Sea. Deep-Sea research, **37**, 1491-1511.

RUMOHR, J. (1993): A high accumulation area on the continental slope off northern Norway and the conception of winter water cascades. Deep-Sea Res. (subm.)

SAVIDGE, G., D.R. TURNER, P.H. Burkill, A.J. WATSON, M.V. ANGEL, R.D. PINGREE, H. LEACH and K.J. RICHARDS (1992): The BOFS 1990 Spring Bloom Experiment: Temporal evolution and spatial variability of the hydrographic field. Progr. Oceanogr., **29**, 235-281.

SCHAUER, U. (1989): A deep saline cyclonic eddy in the West European Basin. Deep-Sea Res., **36**, 1549-1565.

SCHÜSSLER, U. and K. KREMLING (1993): A pumping system for underway sampling of dissolved and particulate trace elements in near-surface waters. Deep-Sea Res., **40** (2), 257-266.

SUGIMURA Y. and Y. SUZUKI (1988): A high-temperature catalytic oxidation method for determination of non-volatile dissolved organic carbon in seawater by direct injection of a liquid sample. Mar. Chem., **24**, 105-131 .

SWIFT, J.H., T. TAKAHASHI and H.D. LIVINGSTON (1983): The contribution of Greenland and Barents Seas to the deep water of the Arctic Ocean. J. Geophys. Res., **88**, 5981-5986.

SY, A. (1988): Investigation of large-scale circulation patterns in the central North Atlantic: the North Atlantic Current, the Azores Current, and the Mediterranean Water plume in the area of the Mid-Atlantic Ridge. Deep-Sea Res., **35**, 383-413.

SY, A., U. SCHAUER and J. MEINCKE (1992): The North Atlantic Current and its associated hydrographic structure above and eastwards of the Mid-Atlantic Ridge. Deep-Sea Res., **39**, 825-853.

THIEL, H. (1980): Benthic investigations of the deep Red Sea. - Cour. Forsch.-Inst. Senckenberg, **40**, 1-35.

THIEL, H., O. PFANNKUCHE, G. SCHRIEVER, K. LOCHTE, CH. HEMLEBEN, R.F.G. MANTOURA, C.M. TURLEY, J.W. PATCHING and F. RIEMANN (1988/89): Phytodetritus on the deep-sea floor in a central oceanic region of the northeast Atlantic. Biol. Oceanogr., **6**, 203-239.

THOMSEN, L., G. GRAF, V. MARTENS and E. STEEN (1993): An istrument for sampling water from the benthic boundary layer. Continental Shelf Research (in press).

THURMAN, E.A. and R.L. MALCOLM (1981): Preparative isolation of aquatic humic substances. Environ. Sci. Technol., **15**, 463-466.

VOGELSANG, E. (1990): Paläo-Ozeanographie des Europäischen Nordmeeres an Hand stabiler Kohlenstoff- und Sauerstoffisotope. Ber. Sonderforschungsber. 313, **23**, 136 S.

WOODS, J.D. (1984): The warm watersphere of the Northeast Atlantic - A Miscellany -. Ber. Inst. Meereskunde Kiel, 128, 39 pp.

WORTHINGTON, L.V. (1976): On the North Atlantic circulation. John Hopkins Univ. Oceanogr. Studies, **6**, 110 pp.

YENTSCH, C.S. and A.D. PHINNEY (1985): Spectral fluorescence: a taxonomic tool for studying the structure of phytoplankton populations. J. Plankton Res., **7**, 617-632.

Veröffentlichungen zu METEOR-Expeditionen
in anderen Berichtsreihen

Gerlach, S.A., J. Thiede, G. Graf und F. Werner (1986): Forschungsschiff Meteor, Reise 2 vom 19. Juni bis 16. Juli 1986. Forschungsschiff Poseidon, Reise 128 vom 7. Mai bis 8. Juni 1986. Ber. Sonderforschungsbereich 313, Univ. Kiel, 4, 140 S.

Siedler, G., H. Schmickler, T.J. Müller, H.-W. Schenke und W. Zenk (1987): Forschungsschiff Meteor, Reise Nr. 4, Kapverden - Expedition, Oktober - Dezember 1986. Ber. Inst. f. Meeresk., 173, Kiel, 123 S.

Wefer, G., G.F. Lutze, T.J. Müller, O. Pfannkuche, W. Schenke, G. Siedler und W. Zenk (1988): Kurzbericht über die Meteor - Expedition Nr. 6, Hamburg - Hamburg, 28. Oktober 1987 - 19. Mai 1988. Berichte, Fachbereich Geowissenschaften, Universität Bremen, 4, 29 S.

Müller, T.J., G. Siedler und W. Zenk (1988): Forschungsschiff Meteor, Reise Nr. 6, Atlantik 87/88, Fahrtabschnitte Nr. 1 - 3, Oktober-Dezember 1987. Ber. Inst. f. Meeresk., 184, Kiel, 77 S.

Lutze, G.F., C.O.C. Agwu, A. Altenbach, U. Henken-Mellies, C. Kothe, N. Mühlhan, U. Pflaumann, C. Samtleben, M. Sarnthein, M. Segl, Th. Soltwedel, U. Stute, R. Tiedemann und P. Weinholz (1988): Bericht über die "Meteor"-Fahrt 6-5, Dakar - Libreville, 15.1.-16.2.1988. Berichte - Reports, Geol. Paläont. Inst., Univ. Kiel, 22, 60 S.

Wefer, G., U. Bleil, P.J. Müller, H.D. Schulz, W.H. Berger, U. Brathauer, L. Brück, A. Dahmke, K. Dehning, M.L. Duarte-Morais, F. Fürsich, S. Hinrichs, K. Klockgeter, A. Kölling, C. Kothe, J.F. Makaya, H. Oberhänsli, W. Oschmann, J. Posny, F. Rostek, H. Schmidt, R. Schneider, M. Segl, M. Sobiesiak, T. Soltwedel und V. Spieß (1988): Bericht über die Meteor - Fahrt M 6-6, Libreville - Las Palmas, 18.2.1988 - 23.2.1988. Berichte, Fachbereich Geowissenschaften, Universität Bremen, 3, 97 S.

Hirschleber, H., F. Theilen, W. Balzer, B. v. Bodungen und J. Thiede (1988): Forschungsschiff Meteor, Reise 7, vom 1. Juni bis 28. September 1988, Ber. Sonderforschungsbereich 313, Univ. Kiel, 10, 358 S.

METEOR-Berichte
Verzeichnis der veröffentlichten Arbeiten

89-1 (1989) Meincke, J., Quadfasel, D.
GRÖNLANDSEE 1988-Expedition, Reise Nr. 8, 27. Oktober 1988 - 18. Dezember 1988. Universität Hamburg, 40 S.

89-2 (1989) Zenk, W., Müller, T.J., Wefer, G.
BARLAVENTO-Expedition, Reise Nr. 9, 29. Dezember 1988 - 17. März 1989. Universität Hamburg, 238 S.

90-1 (1990) Zeitzschel, B., Lenz, J., Thiel, H., Boje, R., Stuhr, A., Passow, U.
PLANKTON '89 - BENTHOS '89, Reise Nr. 10, 19. März - 31. August 1989. Universität Hamburg, 216 S.

90-2 (1990) Roether, W., Sarnthein, M., Müller, T.J., Nellen, W., Sahrhage, D.
SÜDATLANTIK-ZIRKUMPOLARSTROM, Reise Nr. 11, 3. Oktober 1989 - 11. März 1990 Universität Hamburg, 169 S.

91-1 (1991) Wefer, G., Weigel, W., Pfannkuche, O.
OSTATLANTIK 90 - EXPEDITION, Reise Nr. 12, 13. März - 30. Juni 1990. Universität Hamburg, 166 S.

91-2 (1991) Gerlach, S.A., Graf, G.
EUROPÄISCHES NORDMEER, Reise Nr. 13, 6. Juli - 24. August 1990. Universität Hamburg, 217 S.

91-3 (1991) Hinz, K., Hasse, L., Schott, F.
SUBTROPISCHER & TROPISCHER ATLANTIK, Reise Nr. 14/1-3, Maritime Meteorologie und Physikalische Ozeanographie, 17. September - 30. Dezember 1990. Universität Hamburg, 58 S.

91-4 (1991) Hinz, K.
SUBTROPISCHER & TROPISCHER ATLANTIK, Reise Nr. 14/3, Geophysik, 31. Oktober - 30. Dezember 1990. Universität Hamburg, 94 S.

92-1 (1992) Siedler, G., Zenk, W.
WOCE Südatlantik 1991, Reise Nr. 15, 30. Dezember 1990 - 23. März 1991. Universität Hamburg, 126 S.

92-2 (1992) Wefer, G., Schulz, H.D., Schott, F., Hirschleber, H.B.
ATLANTIK 91 - EXPEDITION, Reise Nr. 16, 27. März - 8. Juli 1991, Universität Hamburg, 288 S.

92-3 (1992) Suess, E., Altenbach, A.V.
EUROPÄISCHES NORDMEER, Reise Nr. 17, 15. Juli - 29. August 1991, Universität Hamburg, 164 S.

93-1	(1993) Meincke, J. Becker, G.	WOCE-NORD, Reise Nr. 18, 2. September - 26. September 1991. NORDSEE, Reise Nr. 19, 30. September - 12. Oktober 1991. Universität Hamburg, (in Vorbereitung)
93-2	(1993) Wefer, G. Schulz, H.D.	OSTATLANTIK 91/92 - EXPEDITION, Reise Nr. 20, M 20/1 und M 20/2, 18. November 1991 - 3. Februar 1992. Universität Hamburg, 248 S.
93-3	(1993) Wefer, G. Hinz, K. Roeser, H.A.	OSTATLANTIK 91/92 - EXPEDITION, Reise Nr. 20, M 20/3, 4. Februar 1992 - 13. März 1992. Universität Hamburg, 145 S.
93-4	(1993) Pfannkuche, O. Duinker, J.C. Graf, G. Henrich, R. Thiel, H. Zeitzschel, B.	NORDATLANTIK 92, Reise Nr. 21, 16. März - 31. August 1992. METEOR-Berichte, Universität Hamburg, 93-4, 281S.